Towards the Total Synthesis of Salvinorin A:

An Access to Decalones by Rearrangements of Epoxyazulenes

Dissertation

der Mathematisch-Naturwissenschaftlichen Fakultät

der Eberhard Karls Universität Tübingen

zur Erlangung des Grades eines

Doktors der Naturwissenschaften

(Dr. rer. nat.)

vorgelegt von

Tamer Kocakaya

aus Kirchheim unter Teck

Tübingen

2025

Gedruckt mit Genehmigung der Mathematisch-Naturwissenschaftlichen Fakultät der Eberhard Karls Universität Tübingen.

Tag der mündlichen Qualifikation:	28.11.2025
Dekan:	Prof. Dr. Thilo Stehle
1. Berichterstatter/-in:	Prof. Dr. Martin E. Maier
2. Berichterstatter/-in:	Prof. Dr. Thomas Ziegler

“Think left and think right and think low and think high.

Oh, the thinks you can think up if only you try!”

– Dr. Seuss

Acknowledgements

I am deeply grateful to everyone who has accompanied me on this academic and personal journey. My sincere apologies to those whose names I may have overlooked; please know that your support has been just as meaningful. A special thanks goes to my close friend Habib Doğanay, with whom my journey at the University of Tübingen began, and to my longtime roommates Tobias Brenner and Michael Kittelberger, who quickly became two of my dearest friends. Your companionship has meant the world to me.

During my B.Sc. and M.Sc. studies, I had the privilege of working as a research assistant in the groups of Prof. Dr. Martin E. Maier, Prof. Dr. Lars Wesemann, Prof. Dr. Andreas Schnepf, and Prof. Dr. Pierre Koch. These experiences provided me with invaluable practical insights across organic, inorganic, and medicinal chemistry. Thank you for giving me these opportunities.

My deepest gratitude goes to Prof. Dr. Martin E. Maier, whose mentorship has been instrumental throughout my academic journey. He offered me the opportunity to pursue my bachelor's, master's, and doctoral theses under his guidance, providing a perfect balance of support, expertise, and independence – giving me the freedom to explore and pursue my own ideas. He furthermore enabled me to attend conferences and to undertake a research stay in Porto Alegre, Brazil, where I was warmly welcomed by Prof. Dr. Cesar Petzhold and his group. I am likewise grateful to Prof. Dr. Thomas Ziegler for kindly serving as my second supervisor.

I am grateful to all former members of the Maier group. It was a privilege to work with you and to get to know you both as colleagues and as friends. Being the 'last man standing' of the group, I had the pleasure of meeting many wonderful people over the years – far too many to list in full. Among them, I would especially like to thank the following for their work, support, and the good times we shared in and outside the lab: our secretary Magdalena Muresan; our technical assistants Maria Murani, Claudia Braun, and Florian Herrmann; and my former supervisors and doctoral colleagues: Dr. Alexander Riefert, Dr. Alexander Zhdanko, Dr. Marius Morkunas, Dr. Lena Kämmler, Dr. Max Wohland, Dr. Sarah Müller, Dr. Stefan Heß, Dr. Lea-Marina Rudek, Dr. Sibylle Riedel, Dr. Rathi Krishnan Rengarasu, Dr. Michael Wormann, Dr. Khoa Linh Pham, Dr. Marc Halang, Dr. Frank Schmidt, Dr. Marvin Wenninger, Dr. Jessica Jünger, Dr. Andreas Paul, and Dr. Csaba Szabó. I also wish to thank the teams supporting us in analytical work: Dr. Markus Kramer and his NMR team, Dr. Norbert Grzegorzek and his MS team, and Dr. Hartmut Schubert for X-ray analysis.

My gratitude extends to those I had the pleasure of supervising in lab courses and during their bachelor's theses, whose enthusiasm made this part of my work very rewarding: Fotios Fotakis, Samuel Fisser, Johannes Walz, Çiğdem Oğuz, Dilan Ehrlich, Dr. Annika Stetter, and Felix Vöhringer.

Finally, I want to express my deepest love and appreciation to my family and my partner, Francesca Wannenwetsch. Your unwavering support, patience, and faith in me have carried me through the most challenging moments of this journey. Your support means everything to me, and I am blessed to have you in my life.

TABLE OF CONTENTS

List of Abbreviations

Ac	acetyl
acac	acetylacetone/acetylacetonate
addn.	addition
AIBN	2,2'-azobis(2-methylpropionitrile)
APF	allyl diethylphosphonoformate
approx.	approximately
aq.	aqueous
b.p.	boiling point
b.r.s.m.	based on recovered starting material
BHT	butylated hydroxytoluene
BINOL	1,1'-bi-2-naphthol
Bn	benzyl
Boc	*tert*-butyloxycarbonyl
BTAF	benzyltrimethylammonium fluoride
BTSE	1,2-bis(trimethylsiloxy)ethane
Bu	butyl
CAS	Chemical Abstracts Service
cat.	catalyst(s), catalytic
CDI	carbonyldiimidazole
cf.	'see/compare' (from Latin *confer/conferatur*)
conc.	concentrated
cond.	conditions
COSY	correlation spectroscopy
d.r.	diastereomeric ratio
d.s.	diastereoselecitivity
DABCO	1,4-diazabicyclo[2.2.2]octane
dba	dibenzylideneacetone
DBAD	di-*tert*-butyl azodicarboxylate
DBN	1,5-diazabicyclo[4.3.0]non-5-ene
DBU	1,8-diazabicyclo[5.4.0]undec-7-ene
DCC	*N*,*N*'-dicyclohexylcarbodiimide
DCE	1,2-dichloroethane
DCM	dichloromethane
DDQ	2,3,-dichloro-5,6-dicyano-1,4-benzoquinone
DEAD	diethyl azodicarboxylate
DHP	(3,4)-dihydropyran(yl)
DIAD	diisopropyl azodicarboxylate
DIPEA	*N,N*-diisopropylethylamine (Hünig's base)
DMAP	4-dimethylaminopyridine
DMAPP	dimethylallyl pyrophosphate
DMF	dimethylformamide
DMP	Dess-Martin periodinane
DMPS	dimethylphenylsilyl
DMPU	*N,N'*-dimethylpropyleneurea
DMS	dimethyl sulfide
DMSO	dimethyl sulfoxide
DOR	δ-opioid receptor(s)
dppf	1,1'-bis(diphenylphosphino)ferrocene
dppp	1,3-bis(diphenylphosphino)propane
DS	diastereomer
e.g.	'for example' (from Latin exempli gratia)
EA	ethyl acetate
ee	enantiomeric excess
EMDO	2-ethyl-2-methyl-1,3-dioxolane
eq	(molar) equivalent(s)
et al.	et alii
Et	ethyl
FGA	functional group addition
FGI	functional group interconversion
GC	gas chromatography
GGPP	geranylgeranyl pyrophosphate
HFIP	hexafluoroisopropanol
HMBC	heteronuclear multiple bond correlation
HMDS	hexamethyldisilazane (KHMDS/LHMDS: lithium/potassium hexamethyldisilazide)
HMPA	hexamethylphosphoramide
HPLC	high performance liquid chromatography
HSQC	heteronuclear single quantum coherence
i.e.	'that is' (from Latin *id est*)
IMDA	intramolecular DIELS-ALDER reaction
IPP	isopentenyl pyrophosphate

IUPAC	International Union of Pure and Applied Chemistry
KOR	κ-opioid receptor(s)
L	ligand (as in Pd**L**$_n$)
LDA	lithium diisopropylamide
LSD	lysergic acid diethylamide (from German ***L**ysergs**s**äure**d**iethylamid*)
***m*-CPBA**	*meta*-chloroperoxybenzoic acid
MDMA	3,4-methylenedioxymethamphetamine
Me	methyl
MEM	methoxymethyl ether
MEP	methylerythritol
MNBA	2-methyl-6-nitrobenzoic anhydride
MOA	mechanism of action
MOR	μ-opioid receptor(s)
MPM	(4-methoxyphenyl)methyl/ *p*-methoxybenzyl (PMB)
MS	mass spectrometry
MS	molecular sieves (as in 4 Å **MS**)
Ms	mesyl (as in mesylates, ROMs)
MTBE	methyl *tert*-butyl ether
MVA	mevalonic acid
NBS	*N*-bromosuccinimide
NMO	4-methylmorpholine *N*-oxide
NMP	*N*-methyl-2-pyrrolidone
NMR	nuclear magnetic resonance
NOE(SY)	nuclear OVERHAUSER effect (spectroscopy)
NOP	nociception opioid peptide receptor
***o*-DCB**	*ortho*-dichlorobenzene
PDC	pyridinium dichromate
PE	petroleum ether
Ph	phenyl
PIDA	phenyliodine(III) diacetate/ (diacetoxyiodo)benzene
PIFA	phenyliodine(III) bis(trifluoroacetate)/ (bis(trifluoroacetoxy)iodo)benzene
PMB	*p*-methoxybenzyl/ (4-methoxyphenyl)methyl (MPM)
PP	pyrophosphate
PPTS	pyridinium *para*-toluenesulfonate
Pr	propyl
***p*-TSA**	*para*-toluenesulfonic acid (*p*-TsOH)
py	pyridine
qNMR	quantitative NMR (spectroscopy)
Red-Al	trade name for sodium bis(2-methoxy-ethoxy)aluminum hydride
resp.	respectively
R_f	retention factor (in TLC)
rt	room temperature
Sal	salvinorin (as in SalA = salvinorin A)
SAR	Structure–Activity Relationship
sat.	saturated (in the context of solutions)
Selectride (L- or K-)	trade name for (lithium or potassium) tri-*sec*-butylborohydride
SET	single electron transfer
sln.	solution
TBAF	tetra-*n*-butylammonium fluoride
TBDPS	*tert*-butyldiphenylsilyl
TBS	*tert*-butyldimethylsilyl
TES	triethylsilyl
Tf	triflyl (as in triflates, ROTf)
TFAA	trifluoroacetic anhydride
THBP	*tert*-butyl hydroperoxide
THF	tetrahydrofuran
THP	tetrahydropyran(yl)
TIPS	tri-*iso*-propylsilyl
TLC	thin-layer chromatography
TMOB	1,3,5-trimethoxybenzene
TMP	2,2,6,6-tetramethylpiperidine
TMS	trimethylsilyl
tol	tolyl
TPAP	tetrapropylammonium perruthenate
Ts	tosyl (as in tosylates (ROTs)
vs.	versus

CHAPTER 1: INTRODUCTION

Having refined its biochemical repertoire over billions of years, nature's ability to synthesize intricate bioactive compounds continues to inspire and challenge chemists dedicated to natural product synthesis. Plants and fungi, in particular, contain secondary metabolites with diverse biological properties, which humans have made use of for different purposes. Since millennia, such natural products have been used as drugs, whereas neither the chemical structures, nor the reasons for the observed effects of these drugs were known for the longest time.

While the opium poppy has been used medicinally or in religious rituals for about 8000 years,[1] its main active ingredient was first isolated by SERTÜRNER in 1804, who evaluated its sedative effects in self-experiments.[2] Yet, the structure of morphine (**I-1**, **Figure 1**), named after the mythological god of dreams, Morpheus, was only revealed over a century later.[1]

The isolation of natural products such as morphine (**I-1**) and quinine (**I-2**) ushered in the era of modern medicine and therapeutics.[3] Quinine remains an indispensable anti-malarial drug over 400 years after its effectiveness was recognized by Native Peruvians.[4] Opioids like morphine marked milestones in the treatment of pain and 'everyday ailments' like coughing or diarrhea. In the late 1800s, cocaine (**I-3**) was added to the portfolio of pharmacies as a harmless stimulant, which was claimed to be "no more habit-forming than coffee or tea."[5]

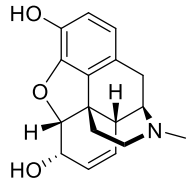

morphine (**I-1**)

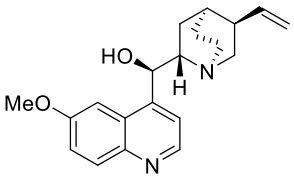

quinine (**I-2**)

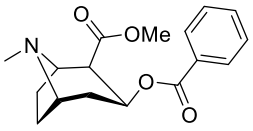

cocaine (**I-3**)

Figure 1. Chemical structures of selected natural products.

As we know today, such and similar claims about opioids did not stand the test of time. Leading to tolerances, dependencies, and serious adverse effects, these drugs were strictly regulated starting from the early 1900s. Still, drug abuse involving *stimulants* such as cocaine or *sedatives* such as opioids remains an unsolved problem world-wide,[6,7] and overdose deaths, mainly attributed to the illicit opioid fentanyl, continue to rise in the 'opioid epidemic.'[8] Nevertheless, opioids are still the most commonly used and often the most effective class of analgesics.[9]

By modifying the structures of drugs, their effects can be dramatically altered. For instance, synthetic opioids like loperamide (**I-4**) or fentanyl (**I-5**) share very little similarity with classical opioids like morphine (**Figure 2** on the next page). Due to these differences, loperamide

selectively activates μ-opioid receptors in the gastrointestinal tract instead of those in the brain, making it a non-narcotic opioid used against diarrhea and inflammatory bowel diseases.[10,11] Similarly, introducing a fluorine atom into fentanyl diminishes its extreme narcotic effects. Its fluorinated analogs NFEPP (**I-6**) and FF3 (**I-7**) are currently examined as non-toxic and non-narcotic pain killers, which seem to act only in inflamed tissue and not in the brain.[9,12,13]

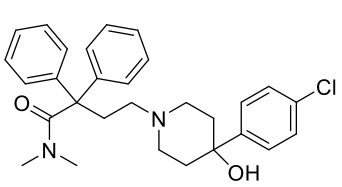

loperamide (**I-4**)

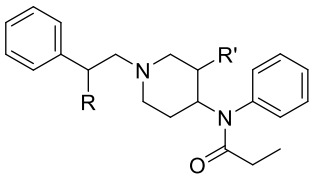

fentanyl (**I-5**), R = R' = H
NFEPP (**I-6**), R = H, R' = F
FF3 (**I-7**), R = F, R' = H

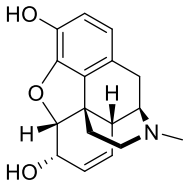

morphine (**I-1**)

Figure 2. Structures of synthetic opioids in comparison to that of morphine (**I-1**).

Starting in the 1940s, psychoactive compounds such as LSD (**I-8**, **Figure 3**), psilocybin (**I-9**) and MDMA (**I-10**) were introduced to a broad audience by the chemists HOFMANN[14] and SHULGIN.[15] These and similar 'psychedelics' had a big impact on science and society – and, next to the problems and risks associated with them, their potential in psychotherapy became evident. In his book "*The Psychedelic Explorer's Guide – Safe, Therapeutic, and Sacred Journeys*," FADIMAN summarized both the recreational use (*and misuse*) of psychedelics and their early applications in psychotherapy.[16] After decades of illicit use and underground therapy following the 'war on drugs' in the 1970s, psychedelics are experiencing a renaissance in scientific research,[17–19] which includes re-emerging studies into the treatment of drug addiction,[20,21] post-traumatic stress disorder (PTSD),[22,23] and treatment-resistant depression.[24] Notably, the introduction of a bromine atom into LSD makes its derivative, 2-Br-LSD, devoid of hallucinogenic effects while maintaining the potential for therapeutic use, e.g., for pain and mood disorders.[25–27]

While further research and trials in psychedelic therapy are warranted, Australia became the first country to allow MDMA and psilocybin for the treatment of PTSD and depression in 2023.[28] European countries, Canada and the United States are poised to follow.[29]

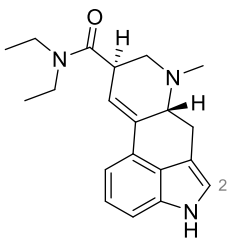

LSD (**I-8**)

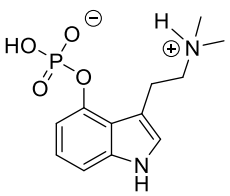

psilocybin (**I-9**)

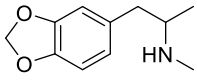

MDMA (**I-10**)

Figure 3. Examples for drugs of interest in the 'psychedelic renaissance.'

Another remarkable psychoactive natural product is salvinorin A (SalA, **I-11**, **Figure 4**), which exerts 'similar' hallucinogenic effects to those of LSD and psilocybin. Acting as a highly selective nonalkaloidal κ-opioid receptor agonist, salvinorin A falls in the gap between opioids and psychedelics, combining some biological effects of both, while sharing structural similarity with neither. Consequently, the unique properties of the diterpenoid salvinorin scaffold are considered a promising lead for novel therapeutics with potential in the treatment of pain, mental disorders, and addiction.[30,31] In the present thesis, these aspects will be discussed further in the context of our studies towards a novel total synthesis of salvinorin A.

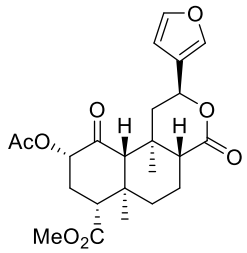

salvinorin A (**I-11**)

Figure 4. Structure of salvinorin A, a hallucinogenic diterpenoid.

The broached developments in psychedelic therapy hold an exceptional potential for the fight against various mental disorders. Next to the promising psychopharmacological applications, the reemerging interest in psychoactive natural products also fosters the discovery and exploration of non-psychoactive derivatives. Those, in turn, often represent promising drug candidates for the directed treatment of physiological disorders such as pain and inflammation. However, to prevent a premature end to this era of psychedelic therapy – similar to the abrupt end in the 1970s – and the accompanying discovery of non-psychoactive derivatives, both the scientific community and society must learn from past mistakes. Unbiased and agenda-free research, as well as reasoned and responsible use of these drugs have to be implemented for a sustainable progress in order to keep this psychedelic renaissance from "going off the rails."[32]

1.1 PROPERTIES OF SALVINORIN A AND ITS ANALOGS

1.1.1 Natural Source, Biological Properties and Biosynthesis of Salvinorins

With nearly a thousand species, the *salvia* genus of plants has found wide use as culinary and medicinal herbs for millennia. Next to common species like *salvia officinalis* ('common sage') and *salvia rosmarinus* ('rosemary'), rare species such as *salvia divinorum* were recognized for their effects on the human body and mind. Being indigenous to Oaxaca, Mexico, *salvia divinorum* has a long tradition in Mazatec culture, in which it has been used for the treatment of gastrointestinal diseases, headaches, inflammations, and as an herbal tonic for the sick and dying. Furthermore, the herbal extracts were used in shamanic rituals, inducing an altered state of consciousness in the healers during spiritual healing sessions. *Salvia divinorum* seems to have been employed as a initiation plant (or 'training herb') for prospective healers, which then proceeded their training with even more powerful psychedelics: morning glory seeds containing ergine, a natural analog of LSD (**I-8**), and 'magic mushrooms' containing psilocybin (**I-9**). This mind-altering property of *salvia divinorum* – revealing the healers both the origins of the patients' illnesses and the remedies best used to alleviate those illnesses – can also be deduced from its name, which translates to *diviner's* or *seer's sage*.[33,34]

This link from *salvia divinorum* to LSD and psilocybin persuaded the 'inventor of LSD,' ALBERT HOFMANN, to examine these psychoactive compounds from a chemist's perspective. Achieving the synthesis of psilocybin and its metabolite, psilocin,[35] he later stated, with some regret: "Thus, with the isolation and synthesis of the active principles, the demystification of the magic mushrooms was accomplished. The compounds whose wondrous effects led the Indians to believe for millennia that a god was residing in the mushrooms had their chemical structures elucidated and could be produced synthetically in flasks."[36]

The 'psychoactive principle' of *salvia divinorum*, however, eluded HOFMANN's endeavors of isolation and synthesis. In 1982, this psychoactive principle was isolated, characterized, and named *salvinorin* by ORTEGA *et al*.[37] In the following years, other chemists including the groups of VALDÉS and PRISINZANO identified dozens of similar compounds,[38–41] renaming the principal constituent responsible for the hallucinogenic effects to *salvinorin A*.[1] While the sage plants are generally rich in terpenes and terpenoids, those of *salvia divinorum* caught the attention of chemists, ethnopharmacologists, and recreational drug users alike.

[1] A detailed discussion of the salvinorin analogs (including salvinorin B–J, divinatorin A–F, salvidivin A–D, and salvinicin A & B) would, arguably, add limited value and goes far beyond the scope of the present thesis. Some particular (natural and synthetic) analogs, which are deemed important for structure-activity relationship (SAR) or represent intermediates in the reported total syntheses of salvinorin A, will be shown in the following chapters.

VALDÉS *et al.* reported that some recreational use was observed in young Mexicans using dried *salvia divinorum* leaves as a mild marijuana substitute in the 1980s.[42] Recreational use was first recognized as problematic in the early 2000s, when young adults across the world used 'high' doses for "intense, but short-lived, psychedelic-like changes in mood and perception, with concomitant hallucinations and disorientation."[43] With effective doses of as little as 0.2 mg (*when inhaled/smoked*), salvinorin A is often described as "the most potent naturally occurring hallucinogen".[44] However, oral or sublingual administrations of salvinorin A were reported to not induce hallucinations even in higher doses (up to 4 mg) due to pharmacokinetic effects which hamper bioavailability and metabolize the drug into non-hallucinogenic metabolites.[45]

A direct comparison with other psychoactive drugs is also impeded by the subjective perception of the barely tangible, and even less expressible, psychotropic effects of such drugs. Studies by ALBERTSON[46] and PRISINZANO[47] questioned the comparisons of salvinorin A with psychedelics such as LSD or psilocybin, stating that drug-experienced participants compared the effects of salvinorin A more to *dreaming* than to drugs like LSD, psilocybin or marijuana.

While the full spectrum of physiological and psychotropic effects of SalA – which also depend on several factors such as dose, 'dosage form' (SalA vs. *salvia divinorum* plants or extracts), and routes of administration – is difficult to evaluate, the 'incomparability' with other drugs becomes apparent when their mechanisms of action (MOA) are examined. 'Classical' psychoactive drugs like LSD, psilocybin, MDMA, and many others, exert their 'main' effects by complex interactions with neurotransmitters in the brain. Next to *direct interactions with neurotransmitter receptors* [either by mimicking ligands (*agonism*) or blocking the receptors and preventing ligands from activating them (*antagonism*)], *indirect interactions* increasing extracellular neurotransmitter levels play an essential role [either by inducing their release from or by inhibiting their reuptake into pre-synaptic neurons].

Most psychoactive drugs affect several neurotransmission pathways mainly through serotonergic and/or dopaminergic actions, often resulting from a combination of direct and indirect interactions.[48,49] In particular, hallucinogenic and psychedelic effects are mainly attributed to the activation of the serotonin receptor subtype 5-HT_{2A} (5-HT = 5-hydroxy-tryptamine or serotonin).[50,51] Not coincidentally, LSD and psilocybin can be considered serotonin derivatives, whereas MDMA is based on the structure of dopamine.

In stark contrast to monoaminergic drugs, salvinorin A lacks key structural features common to neurotransmitters, such as a nitrogen atom, and does not activate serotonin receptors. Instead, SalA, a non-alkaloidal diterpenoid derived from *trans-neo*-clerodane (**I-12**, **Figure 5**), acts as a potent and highly selective κ-opioid receptor agonist.[52] Yet, some more recent investigations suggest that the endocannabinoid system and an unexpected involvement of dopaminergic pathways may also play a role in some of the unique pharmacological effects of SalA.[53–56]

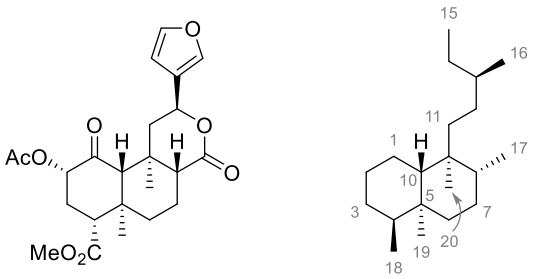

salvinorin A (**I-11**) *trans-neo*-clerodane (**I-12**)

Figure 5. SalA and its parent terpene *trans-neo*-clerodane, including their numbering system.

While some aspects of opioids and their receptors have been broached so far, a detailed discussion goes far beyond the scope of this work. Some central aspects of the **μ-**, **δ-**, and **κ-opioid receptors** (**MOR**, **DOR**, and **KOR**), distributed throughout the central nervous system and within peripheral tissue of neural and non-neural origin, can be summarized as follows:

- **MOR**: Being the primary targets for most opioids, activation of MOR results in analgesia, euphoria, and sedation. As important as MOR agonists like morphine and other opioids are, they have great potential for severe side effects such as respiratory depression. Endogenous MOR peptide ligands, the endorphins, are positive reinforcers. Activation of MOR is considered to be responsible for the addictive potential of opioids.[57]
- **DOR**: DOR also contribute to pain relief but are less involved in addiction development. They seem promising in modulating mood and have been a target for novel opioids that treat mental disorders such as depression and anxiety.[56]
- **KOR**: As with MOR and DOR, KOR are involved in modulating pain and mood. In contrast to those, KOR activation can result in intense mind-altering effects such as hallucinations. Endogenous KOR peptide ligands, the dynorphins, are negative reinforcers, producing dysphoria instead of euphoria – thus, KOR activation is presumed to be the body's "addiction control mechanism".[57,58] KOR regulate "numerous intracellular signaling pathways and a myriad of physiological processes," making novel KOR agonists promising drug candidates for treating pain, addiction, and various other physiological or neurological disorders.[59]

While the research into the therapeutic potential of KOR agonists is not yet as advanced as that of the much earlier introduced MOR agonists, a better understanding of the interactions of salvinorin A and its derivatives with the KOR is believed to pave the way for developing safer drugs that could, one day, be remedies to a wide range of maladies.[30,60–62]

In recent years, the body of research on salvinorin A grew – answering some questions while also raising new ones. The following sections will briefly cover the biosynthesis of salvinorin A, its binding mode and structure–activity relationship at the KOR (**Chapter 1.1.2**), before the total syntheses of SalA and some of its analogs will be discussed in **Chapter 1.2**.

Terpene biosynthesis in plants proceeds via two independent pathways involving mevalonic acid (MVA) or methylerythritol (MEP), which both give isopentenyl pyrophosphate (IPP) and dimethylallyl pyrophosphate (DMAPP). By coupling these C_5 building blocks, the precursor of C_{20} diterpenes and diterpenoids, geranylgeranyl pyrophosphate (GGPP), is obtained.[63]

In 2007, ZJAWIONY *et al.* showed that the salvinorin biosynthesis proceeds via the MEP pathway.[64] Enzymatic conversion of GGPP (**I-13**) by the class II diterpene synthase SdKPS, via cyclization and a series of 1,2-H and -methyl shifts, gives kolavenyl PP (**I-15**) (**Scheme 1**). With the elucidation of SdKPS in 2017, GANG *et al.* proposed a pathway to salvinorin A (**I-11**) via the precursors salvinorin H (**I-17**) and salvinorin B (**I-18**).[65] Other possible pathways proceeding from the central precursor hardwickiic acid **I-16**, the 'interconversion' of the salvinorin analogs salvinorin A–J and divinatorin A–F, and the structures of these analogs are summarized in a 2020 review from MARTINEZ-MAYORGA *et al.*[30]

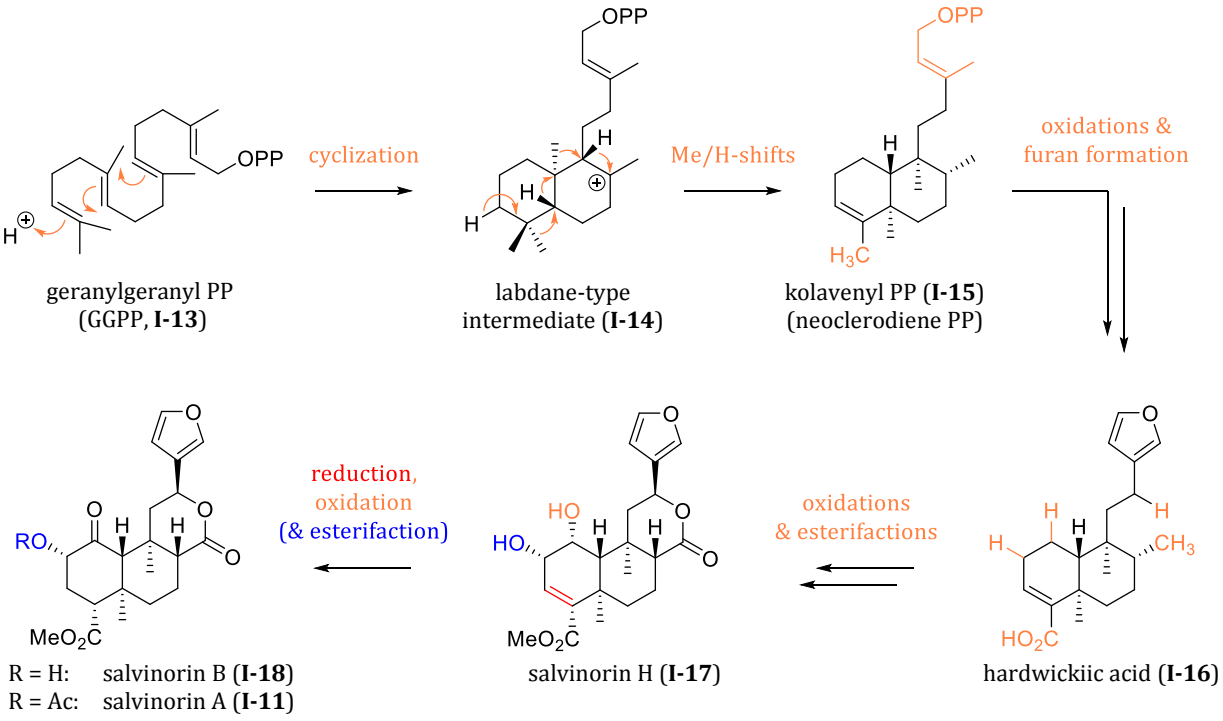

Scheme 1. Simplified overview of salvinorin A biosynthesis starting from GGPP.

1.1.2 KOR Binding Mode & Structure–Activity Relationship (SAR) of SalA

The recognition of salvinorin A (SalA) as a highly selective κ-opioid receptor agonist has persuaded numerous researchers to investigate its structure–activity relationship (SAR). In these endeavors, salvinorin analogs proved invaluable in examining the KOR and advancing the development of novel KOR ligands. As stated by SHENVI *et al.* in a 2018 review of salvinorin analogs and their KOR activity, a set of about 600 analogs has been prepared, in which nearly all of the analogs are semi-synthetic modifications of the isolated natural product, and thus, do not offer a particularly high diversity.[66] There have already been four total syntheses of SalA at that point – however, those routes were deemed suboptimal for analog generation and no activity data for any analogs from those routes were reported. While some aspects of the salvinorin scaffold's SAR were elucidated, several crucial aspects remained unsolved: a consensus binding model was not yet established, little pharmacology besides agonism had been observed in the tested analogs, and consequently, an adequate predictive model could not be developed. Still, SHENVI *et al.* concluded that the "future of the SalA scaffold is bright, illuminated largely by innovations in chemical synthesis and close ties with advanced pharmacology."[66]

Especially since 2017/2018, some of those innovations in synthesis and pharmacology were achieved. On the one hand, the groups of PRISINZANO[67] and SHENVI[68] coincidingly synthesized analogs with more deep-seated structural changes in the salvinorin scaffold (discussed below). On the other hand, the nanobody-stabilized active-state KOR crystal structure was published by WACKER & ROTH *et al.,* which postulated a binding mode for SalA.[69] This paved the path for PULS & WOLBER which claimed to have finally solved an "old puzzle" by elucidating and evaluating the binding mode of SalA at the KOR in 2023.[70] Before, conflicting and opposing theories of binding modes at the KOR were published by several groups, relying on docking studies using 'similar' receptors (homology models based on receptors like MOR or rhodopsin), 'active-like' KOR structures, or mutagenesis studies (see PULS & WOLBER[70] for further details and references).

The binding mode of SalA at the KOR presented by PULS & WOLBER is shown in **Figure 6** on the next page. Most notably, SalA adopts a vertically binding mode within the KOR binding site. The furan moiety points towards the receptor center, while the two ester moieties are orientated towards the extracellular site. Crucial interactions in the SalA-KOR complex are hydrogen bonds with the vicinal tyrosines Y312 and Y313 in the transmembrane helix 7 (TM7), as well as with cysteine C210 in the extracellular loop 2 (ECL2). Furthermore, hydrophobic interactions with different residues of the transmembrane helices 2, 3, 6, and 7 are seen. These interactions with several non-conserved residues in the KOR binding site (especially with V118, Y312 and Y313) are thought to be responsible for SalA's excellent opioid receptor subtype selectivity with no binding to MOR, DOR, and NOP (NOP = nociception opioid peptide receptor).

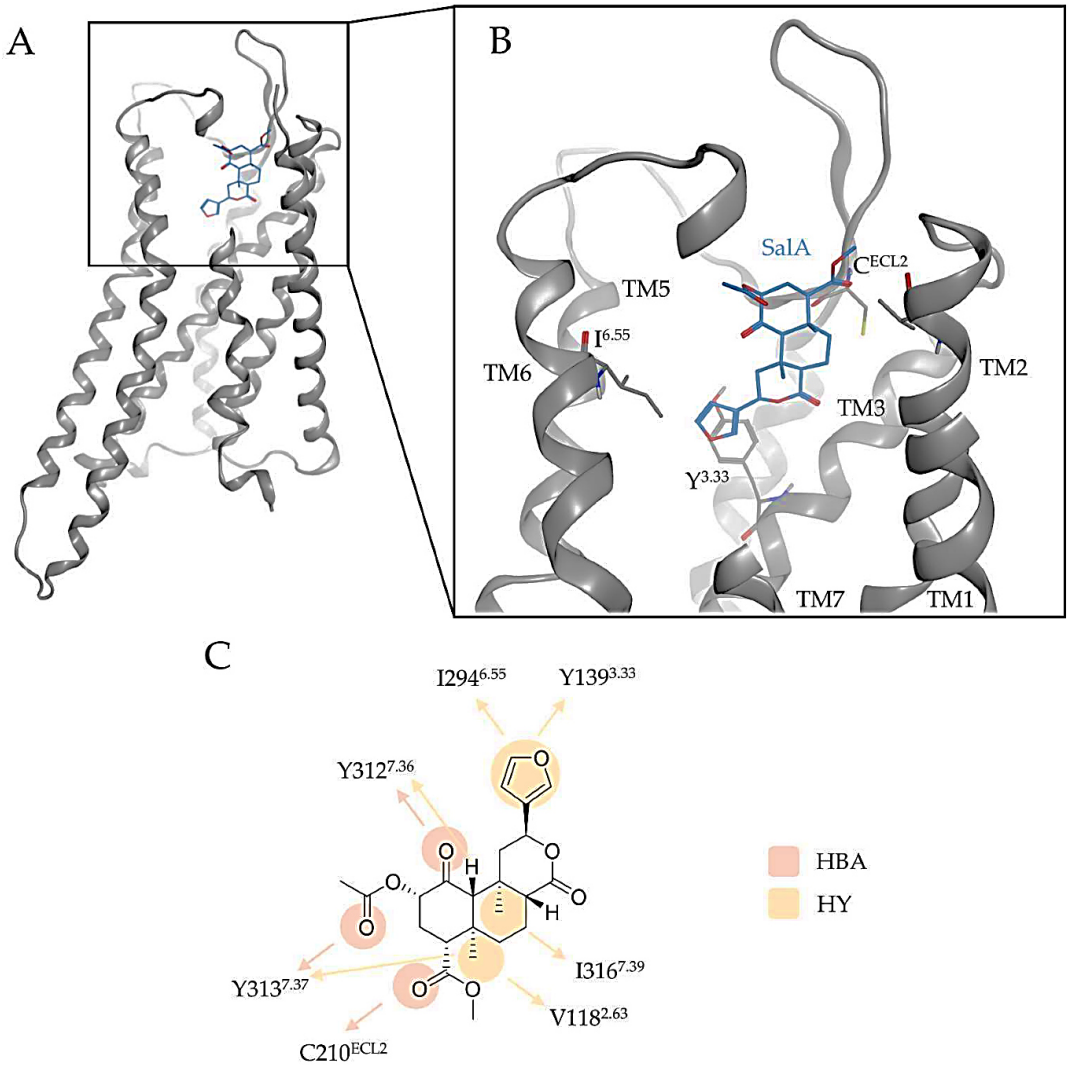

Figure 6. Binding mode of SalA at the KOR (from PULS & WOLBER,[70] edited for better visibility).

(**A**) shows the overall architecture of KOR bound to SalA while (**B**) highlights the binding pocket of SalA at the KOR. (**C**) depicts the protein-ligand interactions between SalA and KOR. $Y^{3.33}$ denotes to $Y139^{3.33}$, C^{ECL2} to $C210^{ECL2}$, and $I^{6.55}$ to $I294^{6.55}$. TM denotes to transmembrane helices, HBA to hydrogen bond acceptor, and HY to hydrophobic contact. **Notes:** The residues **$Y312^{7.36}$** and **$Y313^{7.37}$** are referred to as **$Y312^{7.35}$** and **$Y313^{7.36}$** in the body text of the article and seem to have been mislabeled in the figure. Superscripts of residues denote BALLESTEROS-WEINSTEIN numbering.[71]

As mentioned, the SAR of SalA has been difficult to generalize due to a rather non-diverse set of analogs, missing data for many analogs, and inconsistent binding mode theories. Nevertheless, important insights were accumulated from many studies of various groups. These have been summarized in reviews such as those of PRISINZANO & ROTHMAN (2008)[72] LI & LEE (2016), which also covered the diverse 'non-KOR-related' biological activities of various clerodanes,[73] and SHENVI (2018).[66] The latter noted that the comparison of SalA analogs is complicated by (i) variation of biological assays between reports, (ii) incomplete data sets, and (iii) often-neglected measurements of reference compounds. To paint a more complete picture, a standardization of the data was attempted by assembling raw data from the original literature for a "more comprehensive summary of all the analogs that have been reported."[66] Several of those analogs were also evaluated by PULS & WOLBER in order to validate their proposed binding mode.[70]

The central aspects of the SAR of SalA are indicated in **Figure 7**. Some of these aspects will be condensed by showcasing several notable analogs. The wordings (e.g., affinity, potency, activity, and efficacy), even if ambiguous in some cases, are taken from the cited authors.<2> Values for K_i and EC_{50} will be omitted to the mentioned incomparability issue, focusing instead on 'qualitative' assessments. Details and other analogs can be seen in the cited reviews and references therein.

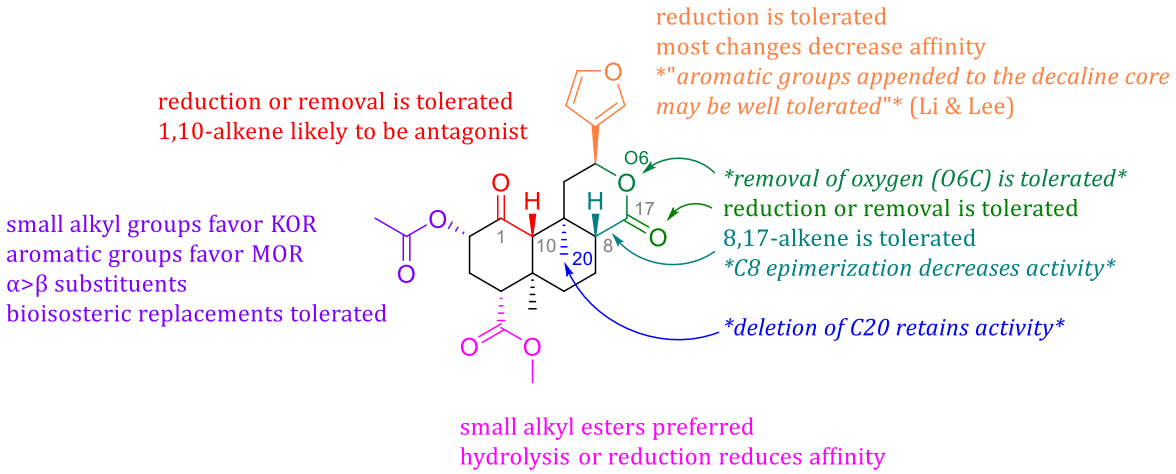

Figure 7. Summary of the SAR of SalA, from PRISINZANO & ROTHMAN (2008).[72] Adapted with some newer insights (quote from LI & LEE[73] and our own additions in **italics and asterisks**).

Remarkably, SalA (K_i = 1.3 ± 0.5 nM, EC_{50} = 4.5 ± 1.2 nM)[75] is similar in efficacy to (i) the endogenous KOR ligand dynorphin A, and (ii) the KOR-selective alkaloid U50,488 (**I-19**), which is often used as the reference KOR agonist (**Figure 8** on the next page).[72] Blood esterases rapidly deacetylate SalA to SalB (**I-18**). SalB, generally accepted as the inactive metabolite, showcases the issues in comparing quantitative values among publications, since inconsistent experimental data were reported (K_i = 111 to >10,000 nM, EC_{50} = 2.4–492 nM, omitting standard errors).[70]

<2> To 'pure chemists,' the terms and measurements of pharmacology can be rather confusing due to inconsistent or vague use, as also criticized by pharmacology committees.[74] Below is a brief summary for better comprehension:
Agonists/antagonists/partial & **biased (ant)agonists**: agonists induce a receptor response by interacting at its active site ('binding site'). Antagonists block receptor activation through various mechanisms: (i) improper interactions at the active site, leading to an inactive receptor conformation, (ii) blocking the active site and preventing agonists from binding, or (iii) allosteric interactions at sites other than the active site. Partial agonists produce a weaker response than full agonists, while biased agonists selectively activate specific signaling pathways (e.g., favoring the G-protein pathway over β-arrestin recruitment in opioid receptors).
Affinity/selectivity: a ligand's affinity for a receptor is expressed as the 'binding constant' $\mathbf{K_i}$ (for agonists) or less commonly as K_e (for antagonists), with low values reflecting high affinities. Selective ligands exhibit high affinity for one receptor and low affinities for others. K_i values can vary, e.g., due to measurements using different radioligands.
Activity/potency: potent (or 'active') agonists induce high receptor activity, while potent antagonists deactivate a receptor. Potency is measured as $\mathbf{EC_{50}}$ (for agonists) or IC_{50} (for antagonists). These values can differ based on the assay used (e.g., Ca^{2+} mobilization, GTP-binding, or cAMP inhibition assays for KOR).
Efficacy/effectiveness: Efficacy refers to the maximum response a drug can produce when it fully activates a receptor, while effectiveness factors in pharmacokinetics (absorption, distribution, metabolism, excretion), patient variability et cetera. In simple terms, a drug may be *efficacious in the lab* but *not effective in clinical practice* due to issues like poor bioavailability or side effects. Conversely, a drug can be effective in real-world use without necessarily being highly potent, selective, or even fully efficacious. Drugs that target multiple receptors (sometimes referred to as 'dirty drugs') can offer therapeutic benefits by modulating several pathways simultaneously.

In general, most structural modifications of SalA lead to decreased affinity or potency – or both. Changes at C2 can increase both while improving metabolic stability, as seen for alkoxymethyl ether **I-18.a** and thiocyanate RB64 (**I-18.b**). Aryl ester analogs were found to favor MOR over KOR.[66] RB64, on the other hand, proved to be a selective G protein-biased KOR agonist, eliciting a long-lasting analgetic effect with no or little sedation, dysphoria, or anhedonia in mice.[76–78]

Other modifications of the **A ring**, such as changes at the C4 methyl ester, lead to a decrease in, or complete loss of, activity. Yet, alanine derivative **I-20** only lost affinity (K_i) by a factor of 21 and potency (EC_{50}) by a factor of 10. Similarly, removal of the C1 ketone (**I-21**) caused only a modest loss in affinity (4.5-fold) and potency (3–6.2-fold).[66] The susceptibility to changes in activity resulting from modifications at the A ring seems consistent with the postulated interactions in the active site (*cf.* binding mode of PULS & WOLBER, **Figure 6**).

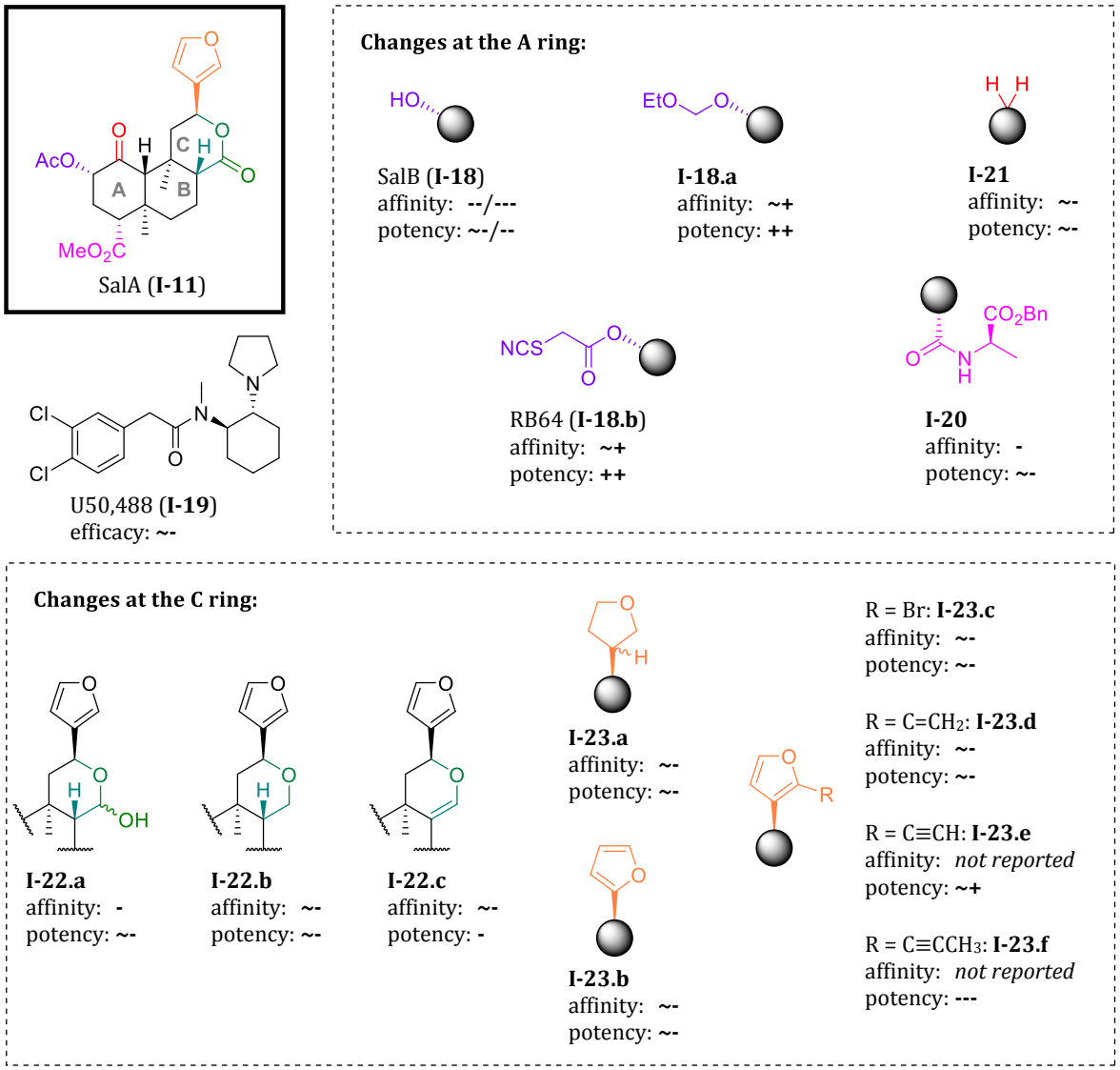

Figure 8. SAR of SalA involving structural modifications at the A and C rings.

Some qualitative assessments of affinity and potency are added (compared to SalA), denominated with: **~-** for similar or *slightly decreased* (1–10-fold loss), **-** for *decreased* (10–100-fold loss), **--** for *strongly decreased* (100–1000-fold loss), and **---** for a >1000-fold or *complete loss*; increasements are denoted with **~+** to **+++**.

Changes at the **C ring** – which shows no direct interactions in the postulated binding mode – are generally tolerated and result in only modest loss of activity [e.g., reductions of the lactone moiety (**I-22.a**–**I-22.c**)]. Modifications of the furan moiety dampened activity in most cases. Yet, reduction of the 3-furyl (**I-23.a**), replacement with 2-furyl (**I-23.b**), or substitution at the furan C2 (**I-23.c**–**I-23.f**) was tolerated. While bromination, vinylation, and ethynylation retained activity, propynylation reduced potency immensely (affinities for **I-23.e** & **I-23.f** not reported).[66,79] Substitution of the furan with bioisosteric aryl groups, benzene or thiophene,[80,81] gave analogs that retained high affinity, potency, and selectivity for the KOR.[82]

Next to quick metabolic inactivation by esterases, and fast elimination from the central nervous system, another factor adds to the unfavorable pharmacokinetic properties impairing a potential clinical usefulness of SalA and its direct analogs: an epimerization at C8, favoring the less active, *trans*/*cis*-fused epimer, 8-*epi*-**I-11**.[83] SHENVI *et al.* identified the driving force as a steric clash due to a double 1,3-diaxial strain involving the C20 methyl group (indicated in the conformation style shown in **Figure 9**), as well as a more favorable lactone geometry in 8-epi-**I-11**.[84]

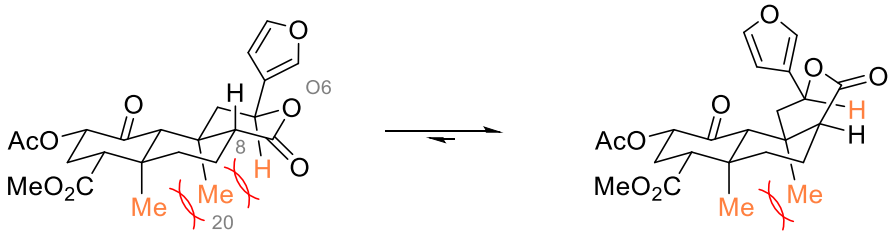

Figure 9. C8 epimerization of SalA, favoring the *trans*/*cis*-fused epimer 8-*epi*-**I-11**.

In 2009, PERLMUTTER *et al.* noted that "no studies have evaluated the importance, if any, of the C20 methyl group," without associating it to C8 epimerization.[85] Unfortunately, their planned synthesis of 20-*nor*-SalA (**I-24**, **Figure 10**) was not finalized. In 2017, SHENVI *et al.* achieved the synthesis of **I-24** and examined the C8 epimerization in more detail: treating SalA with DBU favors the less potent, *trans*/*cis*-fused, 8-*epi*-**I-11** by a factor of 2.5. The deletion of the C20 methyl group 'reverses the equilibrium,' favoring the more potent, *trans*/*trans*-fused, 20-*nor*-SalA (**I-24**) by the same factor (2.5).[68] In 2018, they also prepared O6C-20-*nor*-SalA (**I-25**), in which the lactone-oxygen within the C ring was replaced by a carbon atom. In this analog, the undesired C8 epimerization is completely suppressed, which further corroborated that the C8 epimerization is driven by reduced 1,3-diaxial strain and more favorable lactone geometry in the unnatural epimers.[86] In 2017, before these insights were brought about by SHENVI *et al.*, PRISINZANO *et al.* prepared another 20-*nor*-analog: the "*pseudo*-neoclerodane" **I-26**.

Not yet associating the C20 methyl group with C8 epimerization, this analog was instead "*rationally designed* by careful analysis and generalization of previous semisynthesis data."[67] Thus, it combined several of the previously broached modifications, as well as deletion of both methyl groups (C19 and C20) for an easier synthetic access. The authors stated that **I-26** *maintained* KOR activity with a low nanomolar EC_{50} of 9 nM ± 2 nM,[67] which certainly can still be considered an impressively low value. Yet, comparing this value to the exceptionally high potency of SalA (EC_{50} = 0.08 nM ± 0.02 nM)[67] indicates a 110-fold loss – as was emphasized in SHENVI's 2018 review, noting that "it is difficult to infer what causes this potency decline" since several modifications were included at once.[66]

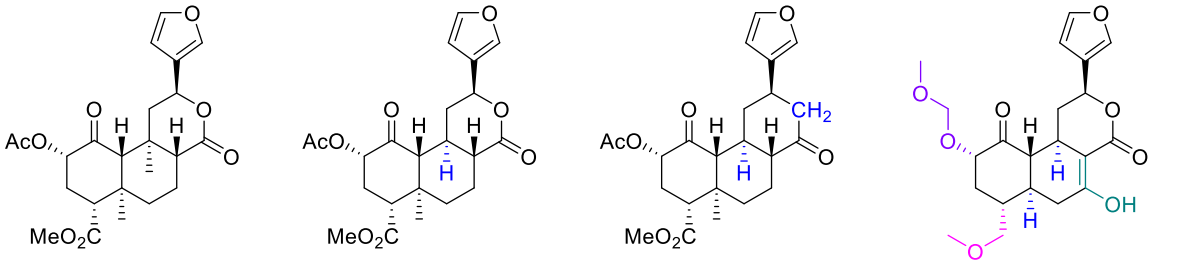

SalA (**I-11**)

20-*nor*-SalA (**I-24**)
affinity: ~-
potency: ~-

O6C-20-*nor*-SalA (**I-25**)
affinity: *not reported*
potency: ~-

I-26
affinity: *not reported*
potency: --

Figure 10. Affinities and potencies of 20-*nor*-SalA analogs.

An arguably more rational design of KOR ligands was reported very recently, in August 2024, by PULS & WEBER *et al*.[87] Utilizing their previously postulated binding mode (**Figure 6** on page **9**), they conducted a *virtual screening* of around 3 million compounds with a *3D pharmacophore* similar to that of SalA bound to the KOR. The best 1821 virtual hits were then subjected to *molecular docking* experiments.[88] Experimental testing of a selection of 13 virtual hits revealed two compounds with nanomolar affinity and potency, high KOR selectivity, and fully G protein-biased agonist activity *in vitro*. These compounds, SalA-VS-07 and SalA-VS-08 (**I-27** and **I-28**, **Figure 11**), share a spiro-piperidine scaffold novel for opioid receptor modulation. The authors concluded that "this is the first time that new nonbasic opioids have been rationally rather than serendipitously discovered."[87]

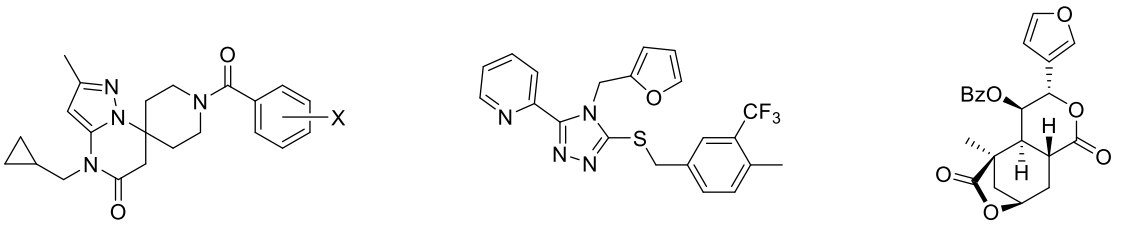

X = *para*-Cl: SalA-VS-07 (**I-27**)
X = *meta*-F: SalA-VS-08 (**I-28**)

I-29

collybolide (**I-30**)

Figure 11. Other scaffolds examined in association with KOR ligand research.

An example for serendipitous discovery of KOR agonists is triazole **I-29**, which was identified and optimized within a *high throughput screening* (HTS) campaign. This campaign, in which four scaffolds of KOR agonist and antagonists were discovered, represents a highly interdisciplinary collaboration involving several research groups such as those of AUBÉ and PRISINZANO.[89,90] Triazole **I-29** was found to be a promising analgetic with limited side effects, most likely due to a limited capacity to cross the blood-brain barrier and a selective targeting of peripheral KOR.[91]

From a *chemist's perspective*, the nitrogen-containing scaffolds of **I-27/I-28** and **I-29** share as little, or even less, similarity with salvinorin A than the scaffolds of synthetic opioids share with morphine (as exemplified in **Figure 2** on page **2**). On the other hand, the fungal metabolite collybolide (**I-30**) arguably resembles SalA in many structural features and had attracted attention as a new non-nitrogenous KOR agonist with potent antipruritic activity in mice, a known effect of KOR activation.[92] With the total synthesis of collybolide by SHENVI *et al.,* however, its KOR activity was reexamined and ultimately refuted.[93] From the *κ-opioid receptor's perspective*, SalA does indeed seem to share more similarity with the nitrogen-containing scaffolds of **I-27**–**I-29**. Therefore, a more holistic approach to drug design and development has to consider the "*view from inside the receptor*"[94] and its recognition of a ligand's molecular features, which can be abstractly described by, for instance, pharmacophore models.[95]

To conclude, the accumulating insights into the KOR, the signaling pathways it mediates, and SARs of different KOR ligands have led to promising advances in developing novel therapeutics. The current strategies of KOR modulation encompass the whole spectrum of full, partial, or biased agonists and antagonists. A plethora of novel KOR ligands are investigated for their therapeutic potential in various diseases and conditions such as pain, pruritus, depression, anxiety, and addiction.[77,87,96] Within these endeavors, salvinorin A and its analogs have proven as promising drug candidates and contributed invaluably to the understanding of the KOR.

The non-nitrogenous scaffold of SalA remains both the most extensively studied one[87] and one of only a few acting as opioid receptor ligands.[97] Yet, this unique scaffold comes with certain drawbacks and uncertainties. While the synthetic accessibility, and thus the SAR of SalA and its analogs have advanced over the years, there still is limited information about the *in vivo* pharmacology of SalA analogs. Furthermore, the pharmacokinetics and psychoactive effects of SalA have hindered its clinical utility – however, the generally unwanted psychoactive effects "might actually be therapeutic for neuronal circuit function and brain health," as stated by LIU & LE *et al.,* which summarized the therapeutic potentials of SalA and some of its analogs.[98] The potential of these and many other novel therapeutics may be further unveiled by modern advancements in the highly interdisciplinary field of drug development, leveraging synergies from refined synthetic approaches, modern computational techniques, and new insights into complex receptor mediated pathways associated with physiological and psychological disorders.

1.2 TOTAL SYNTHESES OF SALVINORIN A

To date, several total syntheses of salvinorin A (**I-11**) and its derivatives have been reported by various research groups. A review of the published syntheses up to the year 2020 was published by SHENVI *et al.*[99] These, and the more recently reported total syntheses will be summarized in this chapter. Within the scope of this work, this does not encompass a fully detailed treatment of every aspect. Instead, crucial transformation steps, as well as observed obstacles, in the respective approaches will be highlighted. Some unsuccessful attempts will also be briefly covered to emphasize the various challenges towards SalA and its derivatives.

1.2.1 ROOK's Approach to SalA (2007)

The first synthetic approach to (–)-salvinorin A is represented by the work of ROOK *et al.,* in which they examined a retrosynthetic disconnection of its scaffold between C6–C7 and C9–C10 (**Scheme 2**).[100] Accordingly, a MICHAEL addition of fragment **I-31** to α,β-unsaturated 3-furyl lactone **I-32** was planned as a central step to link these two fragments, whereas an olefin cross-metathesis should then establish the C6–C7 bond of **I-11**. Fragment **I-31** should in turn be prepared from cyclohexenone **I-33**. However, an efficient synthesis of **I-33** could not be achieved by the route involving a DIELS-ALDER reaction of methyl acrylate and the furan compounds **I-34**, which represent enamines of the chiral auxiliaries (–)-ephedrine or (+)-pseudoephedrine. The desired *exo*-stereoisomer of the hydrolyzed cycloadduct **I-35** could be prepared with moderate enantiomeric excess (60% *ee*), but the route to **I-33** was further impeded by epimerization of the ester group. Thus, the following steps were not pursued.

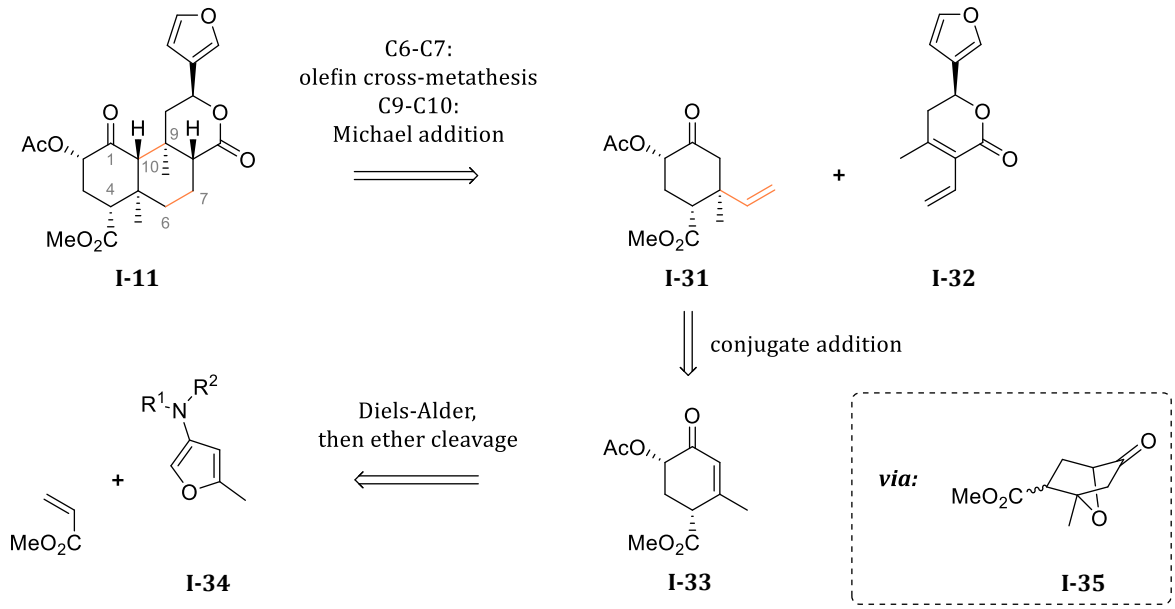

Scheme 2. ROOK's approach to SalA (2007).[100]

1.2.2 EVANS' Total Synthesis of SalA (2007)

In 2007, EVANS *et al.* reported the first total synthesis of salvinorin A (**Scheme 3**).[101] The key step in this achievement represents a transannular cyclization cascade (from **I-37** to **I-36**). The convergent route to macrolactone **I-37** was approached by the chelate-controlled coupling of vinyl iodide **I-38** (prepared in 3 steps) with aldehyde **I-39** (prepared in 14 steps) to allyl alcohol **I-40**. Protection, deprotection, and ester hydrolysis revealed seco-acid **I-41**. After SHIINA macrolactonization[102], double deprotection, and double oxidation, the stage was set for the cyclization of macrolactone **I-37** to the tricyclic framework **I-36**. A concerted *exo*-DIELS-ALDER reaction of the *E*-enolate (of the β-keto ester) could not be ruled out entirely, but a stepwise *bis*-MICHAEL reaction, initiated by the *Z*-enolate, seems to be the more plausible mechanistic pathway. With this cyclization, the salvinorin framework with its two quaternary stereocenters (C5 and C9) was installed with the correct 1,3-diaxial relation of the methyl groups.

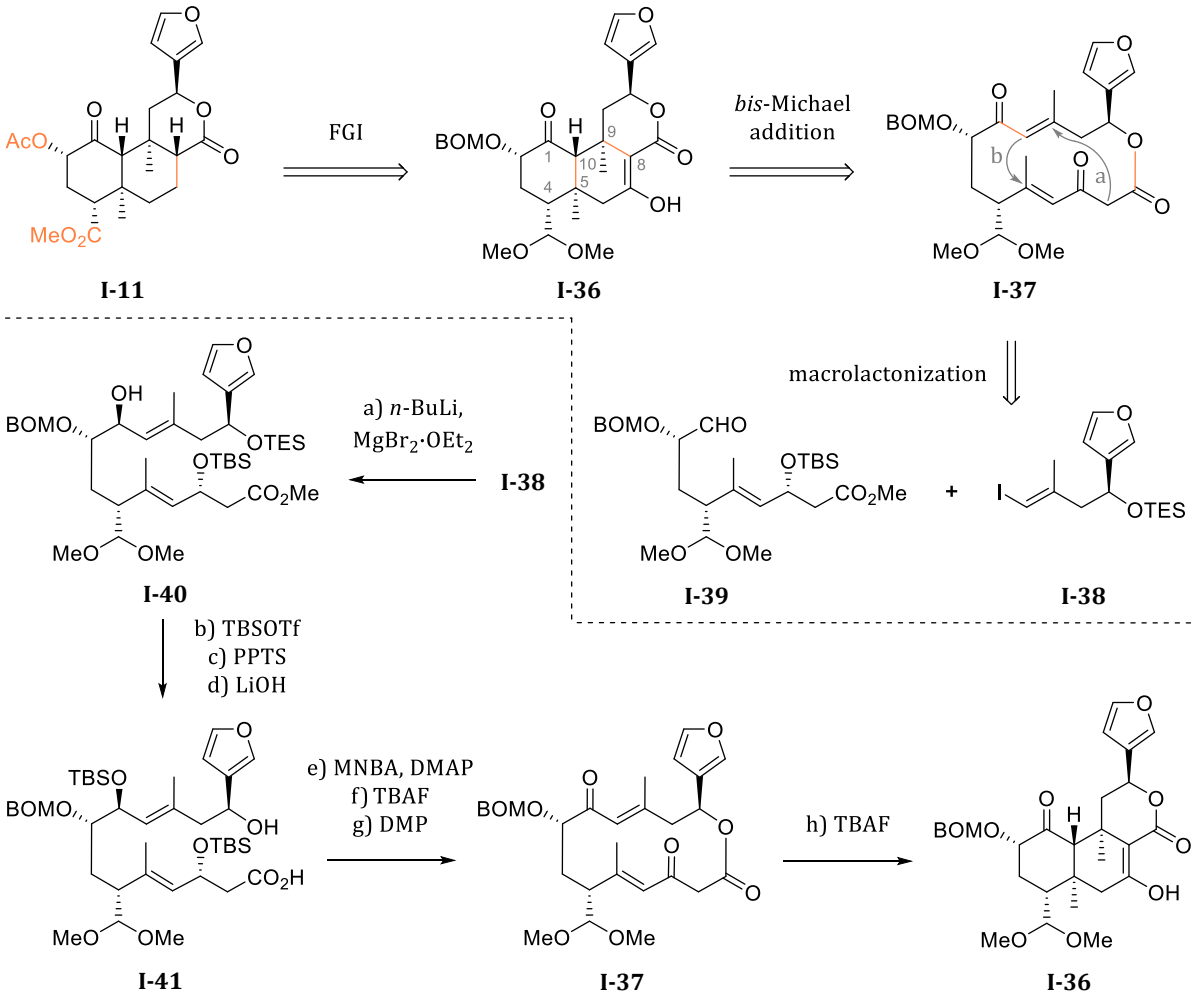

Scheme 3. EVANS' total synthesis of SalA (**I-11**).[101] *Continuation in **Scheme 4**.*

Reagents and conditions: **a)** *n*-BuLi, $MgBr_2 \cdot OEt_2$, −78 °C, then **I-39**, $MgBr_2 \cdot OEt_2$, DCM, −78 °C to 0 °C; **86%**. **b)** TBSOTf, 2,6-lutidine. **c)** PPTS, MeOH. **d)** LiOH, *i*-PrOH/H_2O; **75%** over 3 steps. **e)** MNBA, DMAP. **f)** TBAF. **g)** DMP; **85%** over 3 steps. **h)** TBAF, −78 °C to 5 °C; **99%**.

The late-stage transformation (**Scheme 4**) of *trans*-decalin **I-36** included an enol triflate formation and subsequent reduction of both the triflate and the resulting α,β-unsaturated lactone. Saturated lactone **I-42** was deprotected to its α-hydroxy ketone (acyloin) and oxidized to 8-*epi*-salvinorin B (8-*epi*-**I-18**). This epimer could be equilibrated to **I-18**, whereas the 'wrong' isomer predominated (8-*epi*-**I-18**/**I-18** = 2.5:1). By acetylation of **I-18**, the enantioselective total synthesis of salvinorin A (**I-11**) was accomplished in 29 steps with 1% overall yield.[99]

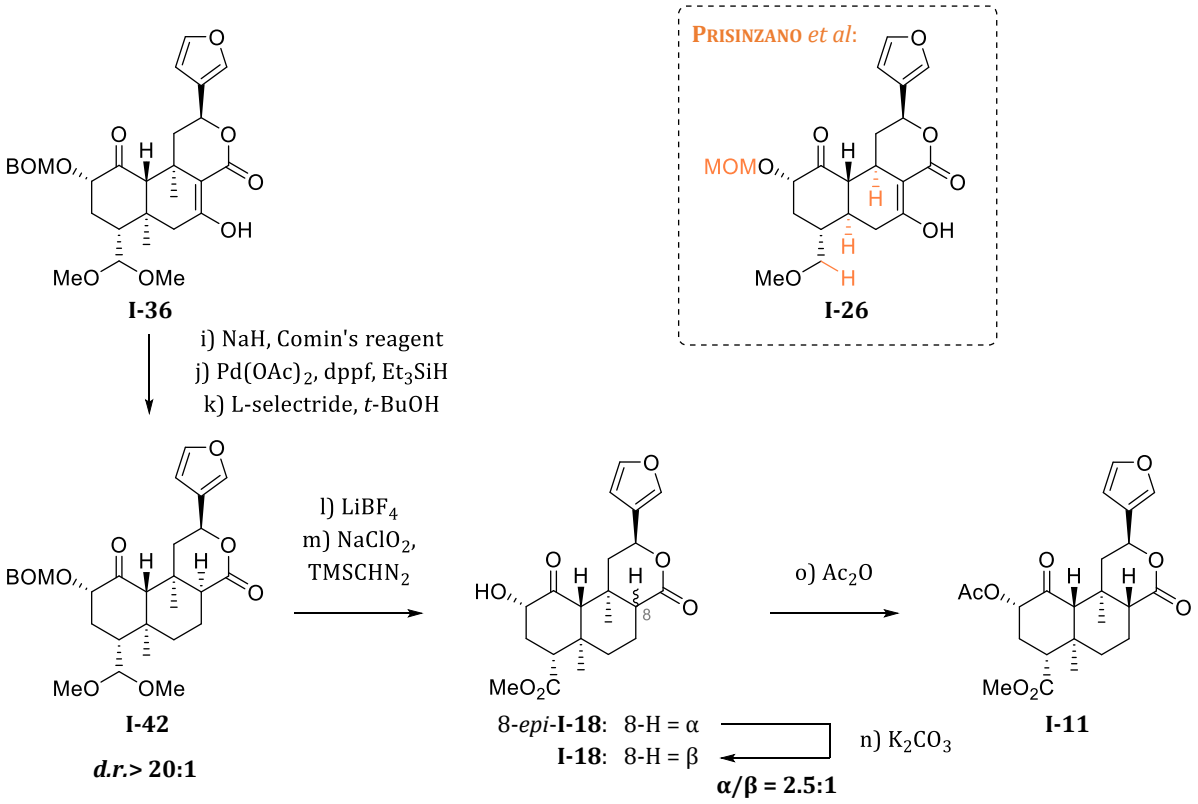

Scheme 4. Late-stage transformations to SalA (**I-11**) by EVANS *et al.*[101] Additionally, the "*pseudo*-neoclerodane" **I-26** synthesized by PRISINZANO *et al.*[67] is shown.

Reagents and conditions: **i)** NaH, COMIN's reagent. **j)** Pd(OAc)$_2$, dppf, Et$_3$SiH. **k)** L-Selectride, *t*-BuOH, –78 °C to –55 °C; **64%** over 3 steps. **l)** LiBF$_4$, MeCN/H$_2$O. **m)** NaClO$_2$, then TMSCHN$_2$; **83%** over 2 steps (*d.r.* = 2.5:1) **n)** K$_2$CO$_3$, MeOH; **quant. mass recovery** (*d.r.* = 2.5:1). **o)** Ac$_2$O, py, DMAP; **78%**.

In 2017, PRISINZANO *et al.* synthesized "*pseudo*-neoclerodane" **I-26**, which was mentioned in **Chapter 1.1.2**.[67] Their synthetic strategy incorporated EVANS' transannular cyclization cascade as the last step, affording **I-26** as a simplified derivative of EVANS' cyclization product **I-36**. The structural differences, shown in orange, allowed for a relatively short[<3>] synthetic access to this modified salvinorin scaffold while retaining nanomolar potency at the KOR (*cf.* **Chapter 1.1.2**).

[<3>] Without going too much into detail, the number of steps were either reported as 9 (PRISINZANO *et al*)[67] or 16 (SHENVI *et al*).[99] Counting the longest linear sequence from (*R*)-glycidol indicates 13 steps. While this is shorter than EVAN's sequence to **I-36**, amounting to 22 steps, a direct comparison of **I-26** and **I-36** does not seem adequate.

1.2.3 PERLMUTTER's Approach to 20-*nor*-SalA (2009)

As also mentioned in **Chapter 1.1.2**, PERLMUTTER *et al.* approached the synthesis of 20-*nor*-SalA (**I-24**).[85] Their rationale for this goal was to further examine the, at that time unknown, effect of the C20 methyl group on the SAR of SalA. Including several functional group interconversions (FGI) in their retrosynthetic considerations, 1,4-diketone **I-43** was aimed for as a key intermediate towards (±)-**I-24**. The DIELS-ALDER cycloaddition of quinone **I-44** and known diene[103] **I-45** resulted in a 'modest yield' but enabled the simultaneous formation of three stereogenic centers in **I-46**. After epimerization of C10 and conjugate reduction of the C2–C3 alkene, the synthesis of **I-43** was achieved. In 2011, an enantioselective variation of this approach was published by HANQUET *et al.,* in which chiral sulfinyl-derivatives of **I-44** were employed.[104] However, no further pursuits proceeding from **I-43** were published.

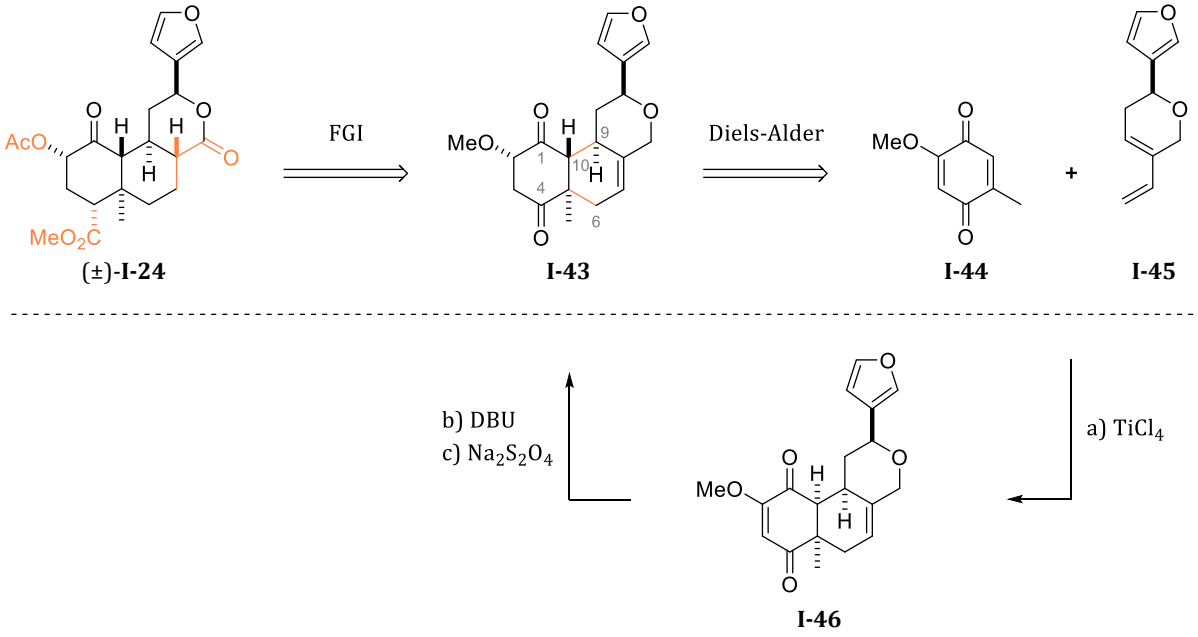

Scheme 5. Synthesis of 20-*nor*-SalA precursor **I-43** by PERLMUTTER *et al.* (2009).[85]<4>

Reagents and conditions: **a)** toluene, $TiCl_4$ (*precomplexation of* **I-44**), –78 °C to –45 °C; 5 h; **37%**. **b)** DCM, DBU (10 mol%), 1 h; **87%**. **c)** toluene/H_2O, $Na_2S_2O_4$, $NaHCO_3$, Adogen 464, 14 h; **73%**.

<4> Within the present thesis, the **relative stereochemistry** of racemic compounds is indicated by ***bold block bonds*** *or* ***hashed bonds*** and thus is distinguished from **absolute stereochemistry** indicated by **(*hashed*) *wedged bonds***.

1.2.4 HAGIWARA's Total Syntheses of SalA (2008 & 2009)

An alternative approach was pursued by HAGIWARA *et al.,* who reported their 1st generation total synthesis of SalA in 2008 (**Scheme 7**),[105] later complemented by a 2nd generation synthesis in 2009.[106] Starting from WIELAND-MIESCHER ketone derivative **I-47**, reductive alkylation and hydrolysis gave diketone **I-48**. Subjecting diketone **I-48** to WITTIG conditions resulted in the concomitant formation of the lactone, which was reduced to the diol and orthogonally protected (**I-49**). A hydroboration/oxidation sequence of the methylidene groups to aldehydes followed. After epimerization, the thermodynamically favored *bis*-aldehyde was protected as *bis*-dioxolane **I-50**. Selective deprotection of the primary TBS ether, oxidation, and 3-furylation yielded diastereomeric 3-furyl alcohol **I-51** (desired/undesired isomer = 2:3). Deprotection of the aldehydes and the secondary alcohol afforded a 3-furyl hemiacetal. A threefold oxidation with subsequent esterification then afforded 2-deacetoxysalvinorin A (**I-52**).

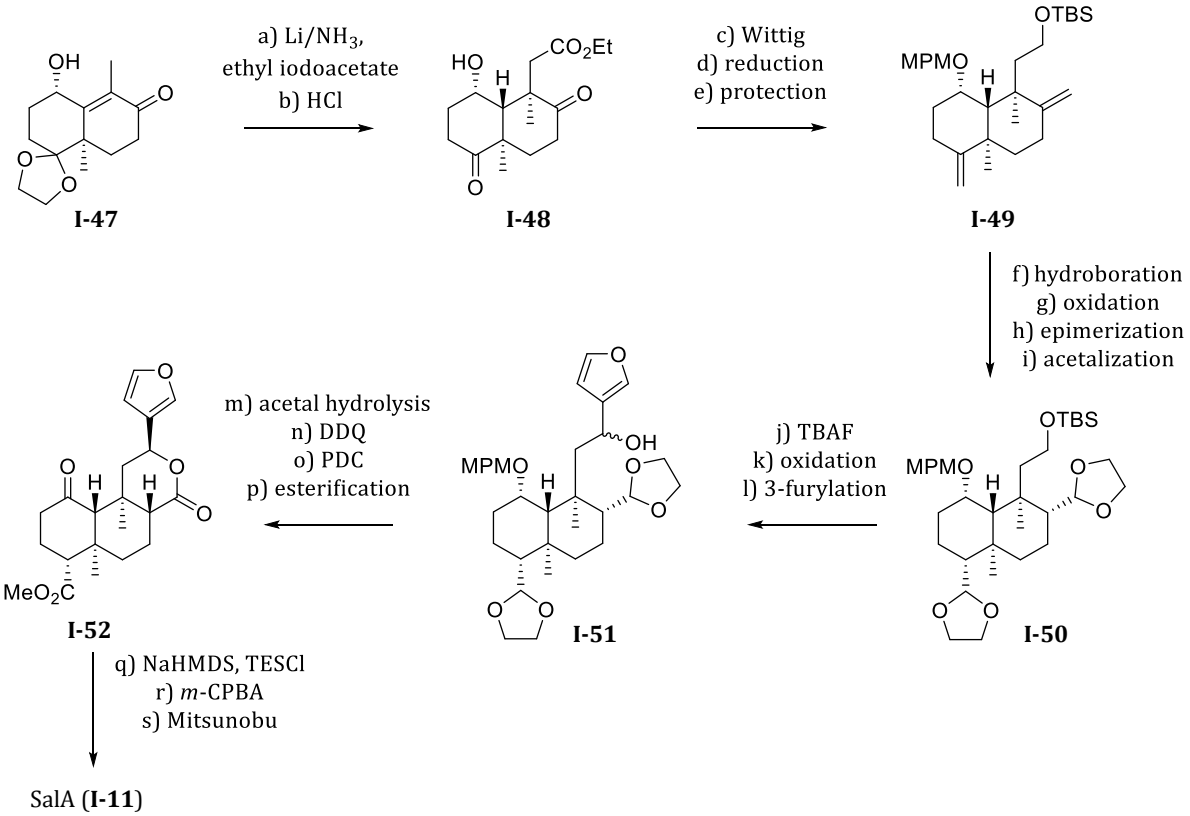

Scheme 6. HAGIWARA's total synthesis (1st gen., 2008) of salvinorin A (**I-11**).[105]

Reagents and conditions: **a)** Li/NH_3, THF, −78 °C, ethyl iodoacetate; **51%**. **b)** 3 M HCl, EtOH, rt, 3 h; **quant**. **c)** NaHMDS, Ph_3PCH_3Br, THF, rt, 4 h. **d)** LAH, Et_2O, 0 °C, 0.5 h; **57%** over 2 steps. **e)** TBSCl, DMAP, Et_3N, DCM, rt, 1.5 h; **99%**; NaH, MPMCl, DMF, rt, 3 h; **94%**. **f)** BH_3·THF, THF, then 3 M NaOH, H_2O_2. **g)** PDC, NaOAc, MS 4 Å, DCM. **h)** NaOMe, MeOH, rt, 2 h; **85%** over 3 steps. **i)** ethylene glycol, 2-ethyl-2-methyl-1,3-dioxolane, *p*-TSA, 40 °C, 7.3 h; **99%**. **j)** TBAF, THF; **quant**. **k)** same as **g)**; **78%**. **l)** 3-bromofuran, *t*-BuLi, THF, −78 °C, 1 h; **66%** (*d.r.* = 2:3). **m)** *p*-TSA, acetone/H_2O, reflux, 4 h. **n)** DDQ, H_2O/DCM, 0 °C, 1 h. **o)** PDC, 2-methyl-2-butene, DMF, rt, 22 h; **40%** over 3 steps. **p)** DCC, DMAP, MeOH/DCM, rt, 2 h; **90%**. **q)** NaHMDS, TESCl, THF, −78 °C, 1 h; **quant**. **r)** *m*-CPBA, $NaHCO_3$, toluene/H_2O, 0 °C, 1.5 h, then AcOH; **70%**. **s)** PPh_3, DIAD, AcOH, DCM, rt, 1.6 d; **86%**.

The final steps involved RUBOTTOM oxidation[107] of the silyl enol ether, affording the 2-epimer of salvinorin B (2-*epi*-**I-18**). Inversion at C2 by MITSUNOBU reaction[108] then gave SalA (**I-11**). With this sequence, HAGIWARA *et al.* minimized C8 epimerization, an unsolved issue in EVANS' work. Furthermore, this route proved to be shorter, amounting to 20 steps with 0.5%[99] overall yield.

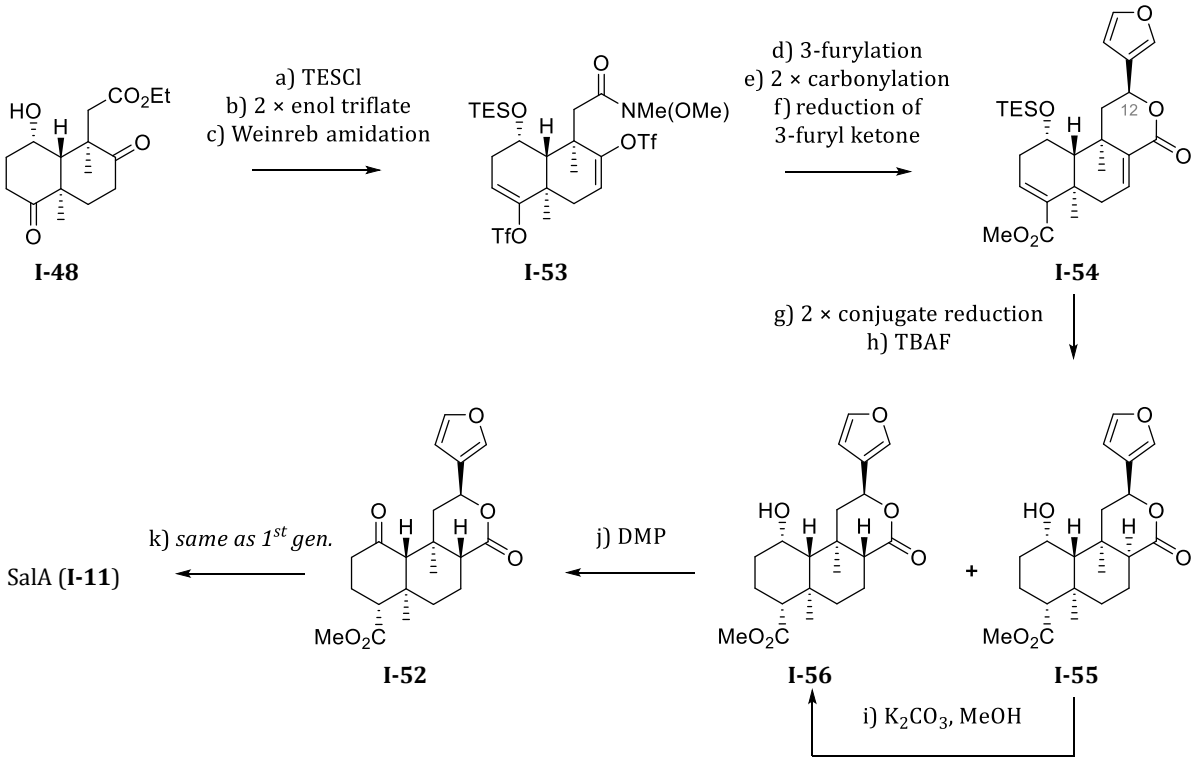

Scheme 7. HAGIWARA's total synthesis (2nd gen., 2009) of salvinorin A (**I-11**).[106]

Reagents and conditions: **a)** TESOTf, py, DMAP, DMF, 100 °C; **93%**. **b)** COMIN's reagent, NaHMDS, THF; **66%**. **c)** *i*-PrMgCl, THF, (MeO)NHMe·HCl; **quant**. **d)** 3-bromofuran, *t*-BuLi, THF; **70%**. **e)** $Pd(PPh_3)_4$, dppf, Et_3N, CO, MeOH/DMF (3:1), 60 °C; **69%**. **f)** K-Selectride, *t*-BuOH, THF; **95%**. **g)** SmI_2, Et_3N, AcOH, toluene, O_2 quench; **64%**. **h)** TBAF, THF; **64%** of **I-55** & **27%** of desired **I-56** (~2.5:1). **i)** K_2CO_3, MeOH; **66%** of **I-55** & **28%** of desired **I-56** (~7:3). **j)** DMP, DCM; **98%**. **k)** same as q)–s) in **Scheme 6**.

In HAGIWARA's 2nd gen. synthesis (**Scheme 7**),[106] some previously unresolved aspects were addressed to further improve yield. Central key steps were a double carbonylation of a *bis*-enol triflate and 3-furylation of a WEINREB amide.[109] For this purpose, δ-hydroxy ester **I-48** was first protected as TES ether, before double triflation to the *bis*-enol triflate and WEINREB amidation afforded **I-53**. A sequence of 3-furylation, double palladium-catalyzed carbonylation, and reduction of the 3-furyl ketone with K-Selectride and *t*-BuOH yielded *bis*-unsaturated (lactonic) ester **I-54**. The latter reduction gave the desired C12 isomer in 95% yield and proved superior to methods using L-Selectride or other reducing agents. With this 3-furylation approach, a higher stereoselectivity at C12 was achieved than in the 1st gen. synthesis. After "multiple attempts," conditions suited for the double conjugate reduction of **I-54** could be found (SmI_2, NEt_3, AcOH). This afforded a single diastereomer with the undesired (*S*)-configuration at C8. Desilylation with

TBAF gave a mixture of the C8 epimers **I-55** (*undesired*) and **I-56** (*desired*) in a ratio of ~2.37:1. Base-catalyzed isomerization of **I-55** resulted in the same mixture with a ratio of 7:3 (~2.33:1). The desired stereoisomer **I-56** was then oxidized to 2-deacetoxysalvinorin A (**I-52**), from which SalA (**I-11**) was prepared using the sequence reported in the 1st gen. synthesis.

Thus, the route from the central building block **I-48** to **I-11** was improved. Compared to the 1st gen. synthesis, the 2nd gen. synthesis also amounts to a 20-step route but with higher yield (up to 1.4% instead of 0.5%, when isomerization steps from **I-55** to **I-56** are included).[99] As in EVANS' work, C8 epimerization posed a central obstacle in this approach. This seemed to be less problematic in HAGIWARA's 1st gen. synthesis, in which 2-deacetoxySalA (**I-52**) was apparently prepared without epimerization (*cf.* **Scheme 6**).

1.2.5 HAGIWARA's Total Synthesis of SalF (2011)

HAGIWARA *et al.* also reported a route to salvinorin F (**I-60**) in 2011, starting from their *bis*-unsaturated ester **I-54** (**Scheme 8**).[110] A selective conjugate reduction of the C7–C8 double bond, which left the C3–C4 double bond intact, was achieved with SmI_2 only "*under the right conditions*." The major diastereomer **I-57**, with the undesired (*S*)-configuration at C8, was deprotected and isomerized to SalF (**I-60**). The *minor diastereomer* **I-58** could be deprotected to **I-60** without epimerization by combining TBAF and acetic acid.

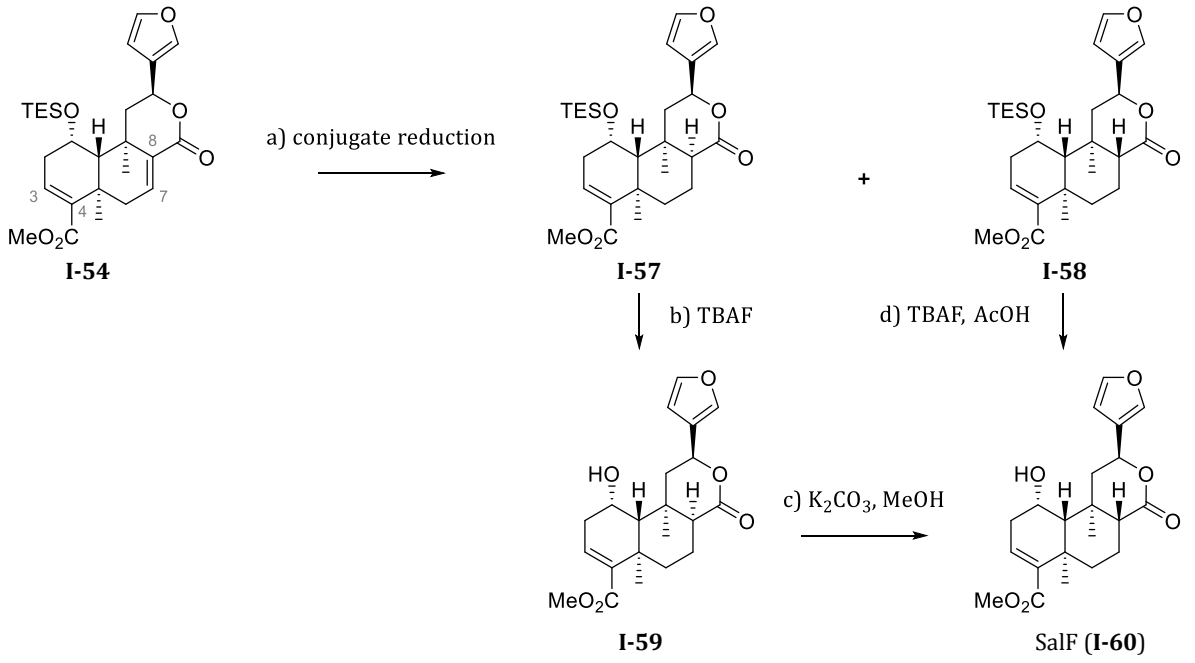

Scheme 8. HAGIWARA's synthesis of SalF (**I-60**).[110]

Reagents and conditions: **a)** SmI_2 (8 eq), pivalic acid (31 eq), toluene, 0 °C, then O_2; **62%** of **I-57** & **21%** of **I-58**. **b)** TBAF, THF, rt; **68%** of **I-59** & **14%** of **I-60**. **c)** K_2CO_3, MeOH, rt; **75%** of **I-59** & **25%** of **I-60**. **d)** TBAF, AcOH, THF, 60 °C; **81%**.

1.2.6 FORSYTH's Total Synthesis of SalA (2016)

In 2016, FORSYTH *et al.* reported a total synthesis of SalA (**I-11**) which incorporated an intramolecular DIELS-ALDER reaction (IMDA) as key step (**Scheme 9**).[111] Starting from dithiane **I-61** and tartaric acid derivative **I-62**, trienyl allyl carbonate **I-63** was prepared in five steps (55% yield). Subjecting **I-63** to heat enabled the IMDA reaction in high yield, giving *trans*-decalin **I-64** after dethioketalization. The quaternary center at C9 was installed by a substrate-controlled stereoselective TSUJI-TROST allylation of the allyl enol carbonate to diketone **I-65**. After a double enol triflate formation/carbonylation sequence, which was inspired by HAGIWARA's 2nd gen. synthesis (*cf.* **Scheme 7**), and oxidative cleavage of the allyl group, aldehyde **I-66** was obtained.

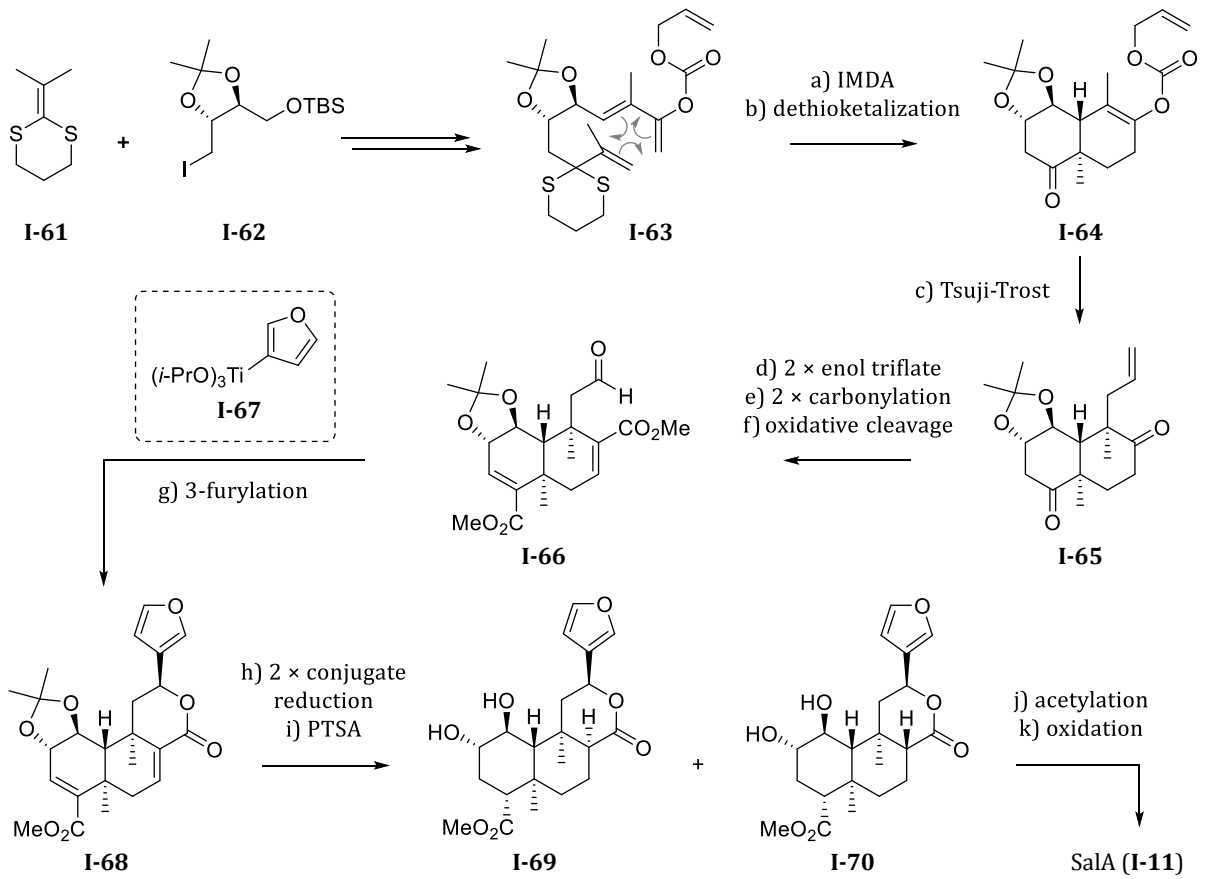

Scheme 9. FORSYTH's total synthesis (2016) of SalA (**I-11**).[111]

Reagents and conditions: **a)** *o*-DCB, reflux, 16 h; **90%**. **b)** PIFA, MeCN, aq. $NaHCO_3$; **67%**. **c)** $[Pd(PPh_3)_4]$, toluene, 30 min; **94%**. **d)** KHMDS, COMIN's reagent, THF, –78 °C; **72%**. **e)** $[Pd(PPh_3)_4]$, dppf, Et_3N, MeOH/DMF, 60 °C; **73%**. **f)** (i) OsO_4, NMO·H_2O, 2,6-lutidine, acetone/H_2O (10:1); (ii) PIDA; **75%** over 2 steps. **g)** **I-67** (1.25 eq), (*R*)-BINOL-Ti(O*i*-Pr)$_2$ (10 mol%), THF, 0 °C; **74%** (*d.r.* = 8:1). **h)** SmI_2, Et_3N, MeOH, THF. **i)** *p*-TSA, MeOH; **51%** over 2 steps (**I-69**/**I-70** = 2.5:1). **j)** Ac_2O, 2,6-lutidine, DCM. **k)** TPAP, NMO, DCM, **72%** over 2 steps.

Another key step was the stereoselective introduction of the 3-furyl moiety at C12, a previously unsolved issue in the syntheses of SalA (**I-11**). For this purpose, 3-furyl titanium complexes were considered, which were successfully employed in the groups of SIBI in 2004[112] and BOUKOUVALAS in 1998[113]. Additionally, GAU *et al.* published several papers on the *enantioselective* addition of 3-furyl titanium complexes to aldehydes and ketones from 2010 onwards.[114,115]

Thus, FORSYTH *et al.* continued their work towards salvinorin A with (3-furyl)Ti(O*i*-Pr)$_3$ (**I-67**), which enabled the asymmetric addition to aldehyde **I-66** with concomitant lactonization to give 3-furyl lactone **I-68** in good yield and selectivity (84%, *d.r.* = 8:1). A double conjugate reduction was achieved with SmI_2, as also employed in HAGIWARA's 2nd gen. synthesis, but with some variations to the reaction conditions in this case. As might be expected, a mixture of C8 epimers resulted, again in a 2.5:1 ratio favoring the undesired epimer. These were liberated of the acetonide protecting group, revealing the diols **I-69** and **I-70**. The minor epimer **I-70** was acetylated selectively at the less hindered C2 hydroxy group. A LEY-GRIFFITH oxidation[116] at C1 finalized this total synthesis of SalA (**I-11**) in 16 steps, starting from dithiane **I-61**, with an overall yield of ~0.85% (without epimer recycling of **I-69**).

1.2.7 SHENVI's Total Syntheses of 20-*nor*-SalA Analogs (2018 & 2019)

To expand insights into the SAR of SalA, SHENVI *et al.* carried out the racemic syntheses of 20-*nor*-SalA (**I-24**) in 2018[68] and O6C-20-*nor*-SalA (**I-25**) in 2019[86] (**Scheme 10**). The effects of these derivatizations – favoring the natural salvinorin C8-configuration while still retaining high affinity and potency for KOR – have been discussed in **Chapter 1.1.2**.

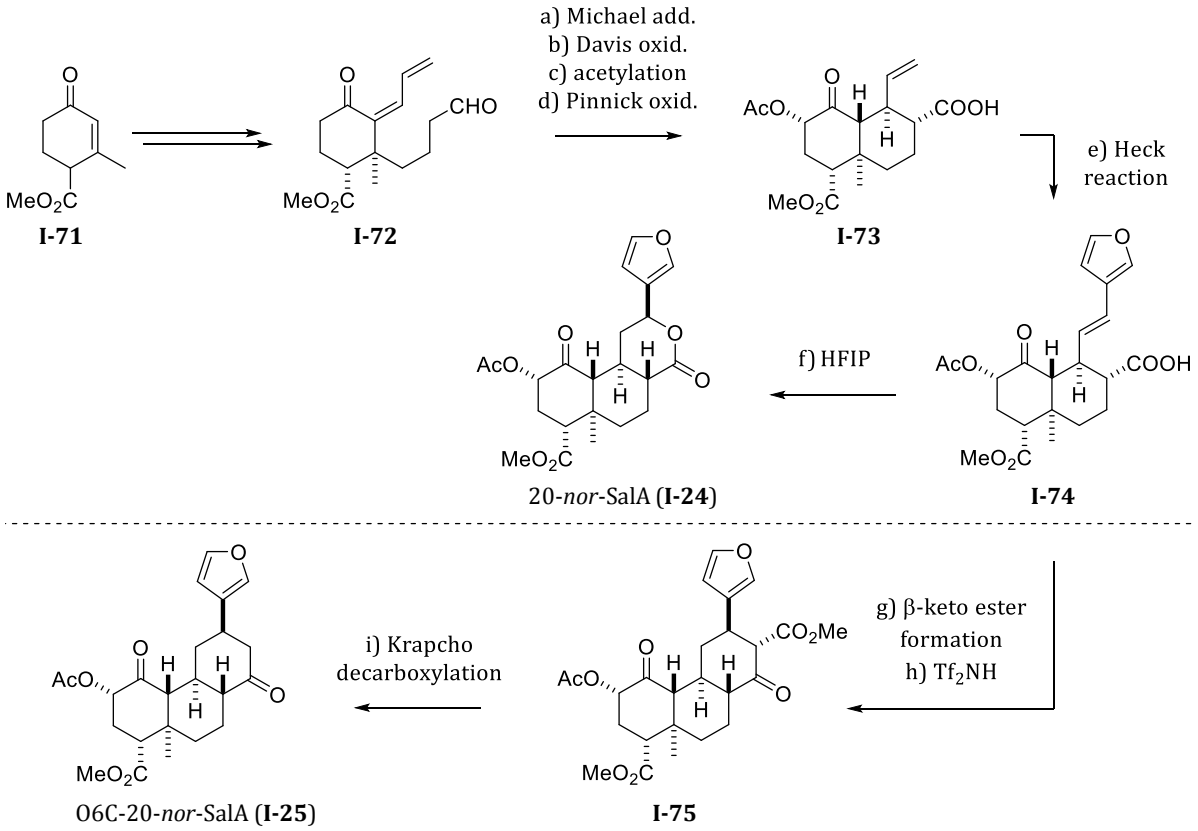

Scheme 10. SHENVI's syntheses of 20-*nor*-SalA (**I-24**) and O6C-20-*nor*-SalA (**I-25**).[68,86]

Reagents and conditions: **a)** pyrrolidine, AcOH, THF/MeOH, 65 °C; K_2CO_3, 65 °C; **53%** (*d.r.* > 15:1). **b)** LDA, –78 °C, DAVIS oxaziridine; **60%** (*d.r.* > 10:1). **c)** Ac_2O, DMAP, DBU, rt to 80 °C; **84%** (*d.r.* = 5:1). **d)** $NaClO_2$, NaH_2PO_4, *t*-BuOH, 2-methyl-2-butene; **91%**. **e)** 3-bromofuran, $Pd(OAc)_2$ (10 mol%), XPhos (20 mol%), K_2CO_3, DMF, 80 °C; **81%**. **f)** HFIP, 50 °C, 48 h; **63% conv.** (*d.r.* = 4:1). **g)** (i) CDI, THF; (ii) $MgCl_2$, Et_3N, $MeO_2C(CH_2)COOK$, MeCN, 80 °C; **76%** over 2 steps. **h)** Tf_2NH (20 mol%), toluene, 60 °C; **86%** (*d.r.* = 2:1). **i)** NaCl, DMSO/H_2O, 170 °C; **53%**.

Commencing from HAGEMANN's ester **I-71**, dienone aldehyde **I-72** was prepared and subjected to a MICHAEL addition to generate the *trans-decalin* core. After α-acetoxylation at C2 and oxidation of the aldehyde, carboxylic acid **I-73** was obtained. A HECK arylation with 3-bromofuran yielded 3-vinyl furan **I-74**, from which 20-*nor*-SalA (**I-24**) was obtained by lactonization of the acid and alkene moieties in hexafluoroisopropanol (HFIP). Alternatively, the acid group of 3-vinyl furan **I-74** could be transformed to a β-keto ester, enabling the cyclization to **I-75** and subsequent KRAPCHO decarboxylation to O6C-20-*nor*-SalA (**I-25**).

1.2.8 METZ's Total Syntheses of SalA (2018 & 2021)

Similar to the group of FORSYTH, METZ *et al.* relied on the IMDA reaction in their total synthesis of racemic SalA (**I-11**), published in 2018,[117] which was complemented by an asymmetric version in 2021.[118] In the latter 2nd gen. synthesis, they delved into some alternative approaches in the 'mid-game' to little avail. Thus, the route was kept basically the same as in the 1st gen. synthesis, now implementing improvements and a shortening of the route by two steps. In their work, they employed not only one, but *two* IMDA key steps to build the salvinorin framework (**Scheme 11**). Starting from 3-furaldehyde (**I-76**), practically enantiomerically pure dienyl enoate **I-77** was prepared and then subjected to the first IMDA reaction, affording 3-furyl lactone **I-78**. After oxidative cleavage, the resulting keto aldehyde was transformed to triene **I-79**, epimerizing 'C8' to the desired configuration along the way. In the second IMDA reaction, triene **I-79** gave rise to *trans*-decalin **I-80** with all carbon centers of the salvinorin framework in place.

Dihydroxylation of **I-80** afforded *cis*-diol **I-81**, albeit as the undesired diastereomer. Regioselective inversion by MITSUNOBU esterification at C2 and subsequent C1 oxidation gave SalA (**I-11**) in 16 steps from **I-76** with a 1.4% overall yield. To date, METZ' 2nd gen. synthesis stands as the shortest, and *only protection group-free*, asymmetric total synthesis of SalA.

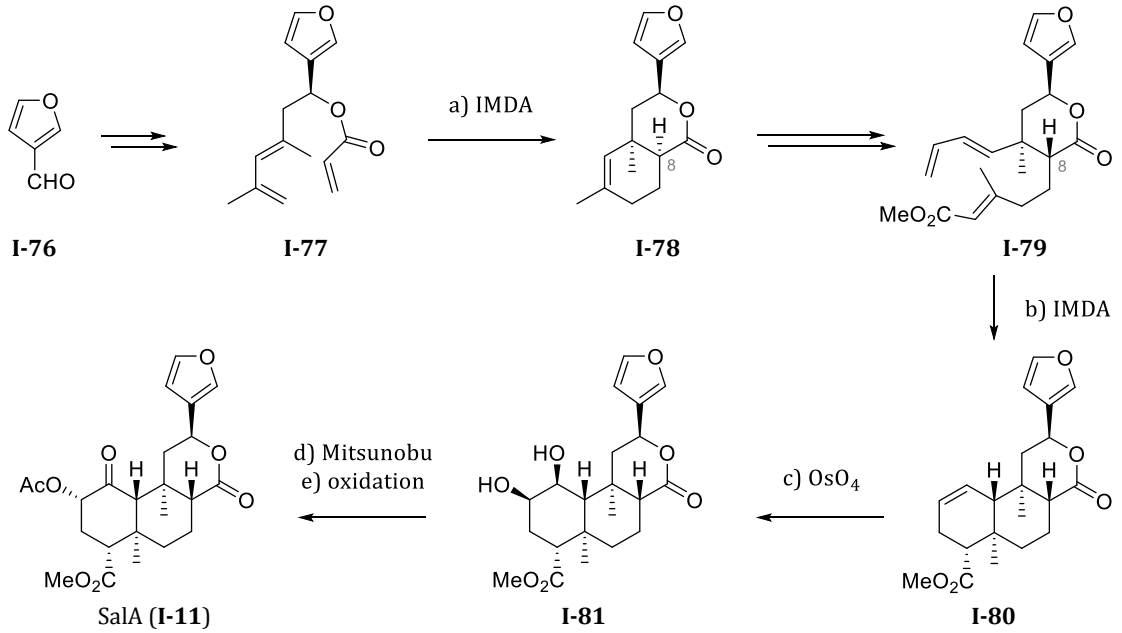

Scheme 11. METZ's asymmetric synthesis (2nd gen.) of SalA (**I-11**).[118]

Reagents and conditions: **a)** BHT (10 mol%), PhCl, 183 °C, 3 d, then rt, 19 h; **94%** (91% *d.s.*). **b)** BHT (1.2 eq), PhCl, 200 °C, 88 h; **66%** (88% *b.r.s.m.*) (94% *d.s.*). **c)** OsO_4 (1 eq), 3,5-lutidine (2 eq), THF, toluene, 0 °C to rt, 24 h; **95%**. **d)** PPh_3, DBAD, HOAc, THF, 60 °C, 47 h; **50%** (61% *b.r.s.m.*). **e)** TPAP, NMO, DCM, MS 4 Å, 2 h; **92%**.

1.2.9 MAIER's Formal Total Synthesis of SalA (2022)

In our group, the total synthesis of SalA was pursued by L.-M. RUDEK[119] (*formerly* L.-M. MEHL) and M. HALANG.[120] As central intermediates, *trans*-decalones such as **I-82** were aimed for, which were to be obtained from a CLAISEN rearrangement of allyl alcohol **I-83** (**Scheme 12**).

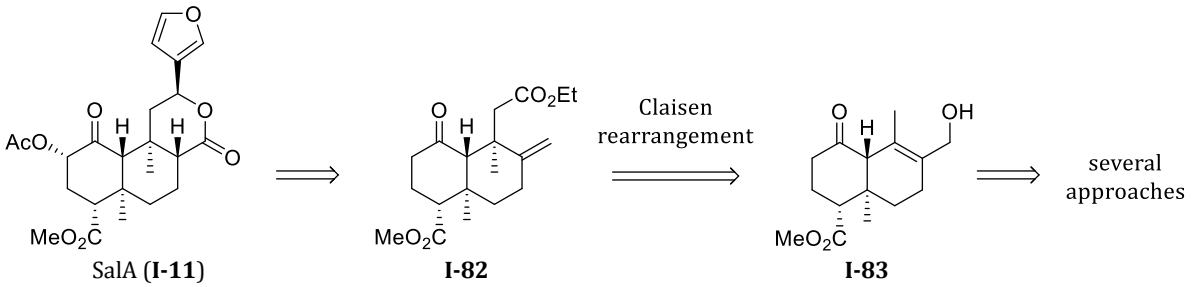

Scheme 12. MAIER's approaches to **I-11** via a central CLAISEN rearrangement.

Several approaches from different substrates resulted in dead-ends or inconclusive results. One of those approaches will briefly be summarized on the next page. The insights from the different approaches allowed for the elaboration of a successful CLAISEN rearrangement, and thus a formal total synthesis by MAIER & HALANG.[121] Starting from **I-84**, hydroxy enoate **I-47** was prepared, which was also used in HAGIWARA's syntheses[105,106] (*cf.* pages **19–20**). From **I-47**, allyl alcohol **I-85** was obtained in 6 steps. CLAISEN rearrangement of **I-85** installed the quaternary C9 and yielded the desired ester **I-86** with some C9 epimer. Ozonolysis and deketalization then gave *bis*-keto ester **I-87**, a central intermediate in HAGIWARA's 2nd gen. synthesis.[106] This alternative route contributes to insights into stereochemical aspects of rearrangements on decalin systems, and opens up routes to salvinorin analogs with alkyl groups at C5, C9, or C10.

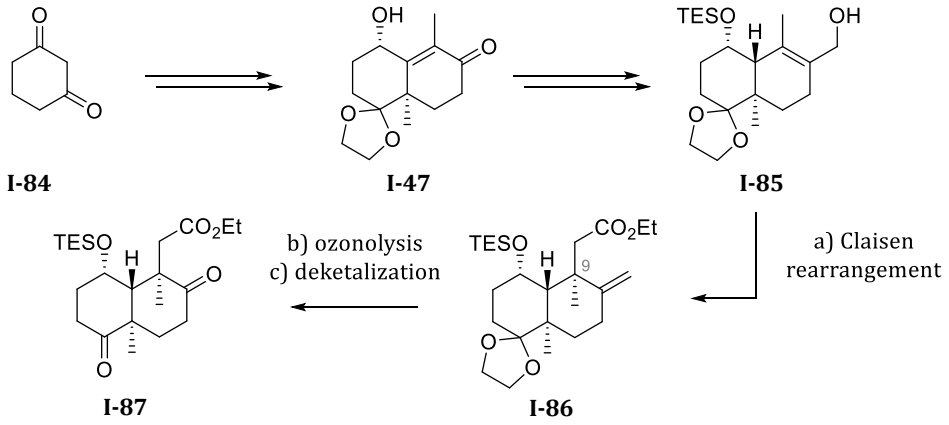

Scheme 13. Formal total synthesis of salvinorin A (**I-11**) by MAIER & HALANG.[121]

Reagents and conditions: **a)** $MeC(OEt)_3$, hydroquinone, *o*-DCB, 180 °C, 19 h; **53%** (& **20%** of C9 epimer). **b)** O_3, DCM/MeOH, –78 °C, 1 h; **68%**. **c)** 3 M HCl, EtOH, 3 h; **82%**.

MAIER & HALANG also devised other routes with allylic alcohols similar to **I-85**, which would involve an early incorporation of the C4 methyl ester, as well as an alternative to the CLAISEN rearrangement. For this purpose, allylic alcohol **I-88** was to be obtained by a PRINS reaction of alkene **I-89** (**Scheme 14**). A gold(I)-catalyzed 6-*endo*-dig cyclization of alkyne-substituted silyl enol ether **I-91** was planned as key step to decalone **I-90**. Starting from HAGEMANN's ester **I-71** (also used in SHENVI's syntheses, *cf.* page **24**), silyl enol ether **I-91** was to be prepared by 1,4-addition of an alkynyl tether with subsequent enolate trapping by silylation.

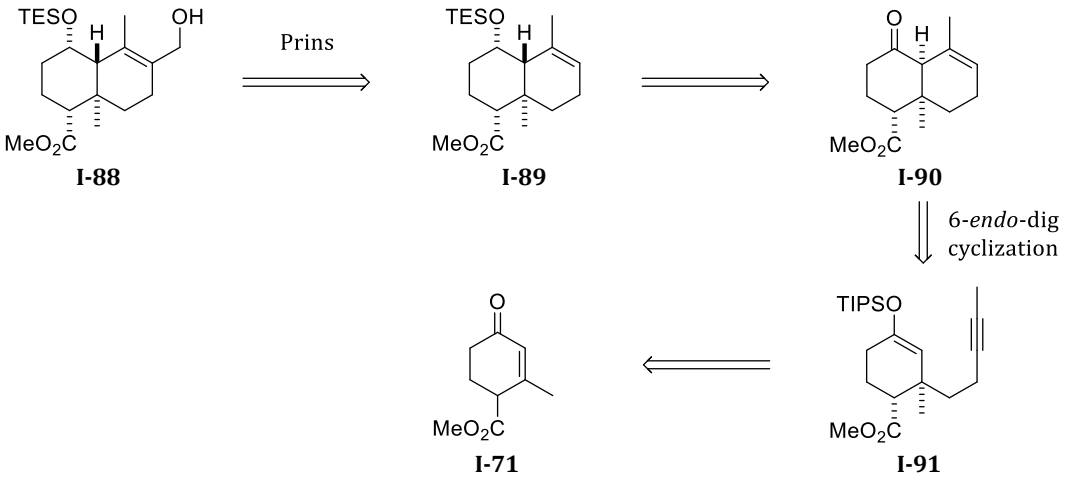

Scheme 14. MAIER & HALANG's approach to allyl alcohol **I-88** involving a 6-*endo*-dig cyclization.

In the literature, similar 6-*endo*-dig cyclization reactions proved challenging in several reported instances, often leading to 5-*exo*-dig or other cyclization products instead. Yet, BARRIAULT *et al.* developed a highly selective 6-*endo*-dig cyclization method for the synthesis of decalones,[122] which made this envisioned route promising.

To briefly summarize the results detailed in HALANG's doctoral thesis,[120] the planned enolate trapping with TIPSOTf did not succeed, and a regioselective formation of TIPS enol ether **I-91** from the isolated ketone proved difficult. This impeded the search for conditions which would allow for a selective 6-*endo*-dig cyclization of **I-91** to decalone **I-90**. However, the TMS enol ether could successfully be prepared by enolate trapping with TMSCl. With this, conditions for the desired cyclization to **I-90** could be found, albeit resulting in moderate yield and selectivity (33% 6-*endo*-dig & 23% 5-*exo*-dig). These findings, however, were only reported in HALANG's doctoral thesis and not published in a journal article.

Coinciding with the thesis defense of HALANG, BARRIAULT *et al.* published the most recent total synthesis of SalA – employing the very same TIPS enol ether **I-91** in a 6-*endo*-dig cyclization, as shown below. Leveraging the experience with this cyclization method developed in their group, BARRIAULT *et al.* succeeded in finding more suitable conditions for this purpose.

1.2.10 BARRIAULT's Formal Total Synthesis of SalA (2023)

In their formal total synthesis of SalA, BARRIAULT *et al.* first transformed vinyl iodide **I-92** to silyl ether diene **I-93** in 3 steps (**Scheme 15**).[123] After DIELS-ALDER reaction with methyl acrylate, TIPS enol ether **I-91** was obtained and then subjected to 6-*endo*-dig cyclization, affording *cis*-decalone **I-90** with high yield and selectivity after optimization of the conditions. Incidentally, very similar conditions were tried in HALANG & MAIER's approach using either a regioisomeric mixture of TIPS enol ether **I-91** or the desired regioisomer of the respective TMS enol ether. While HALANG & MAIER used either DCM *or* acetone as solvent, a *solvent mixture* of DCM *and* acetone proved best in the work of BARRIAULT *et al.,* showcasing how 'little' details can lead to profoundly different outcomes in some reactions.

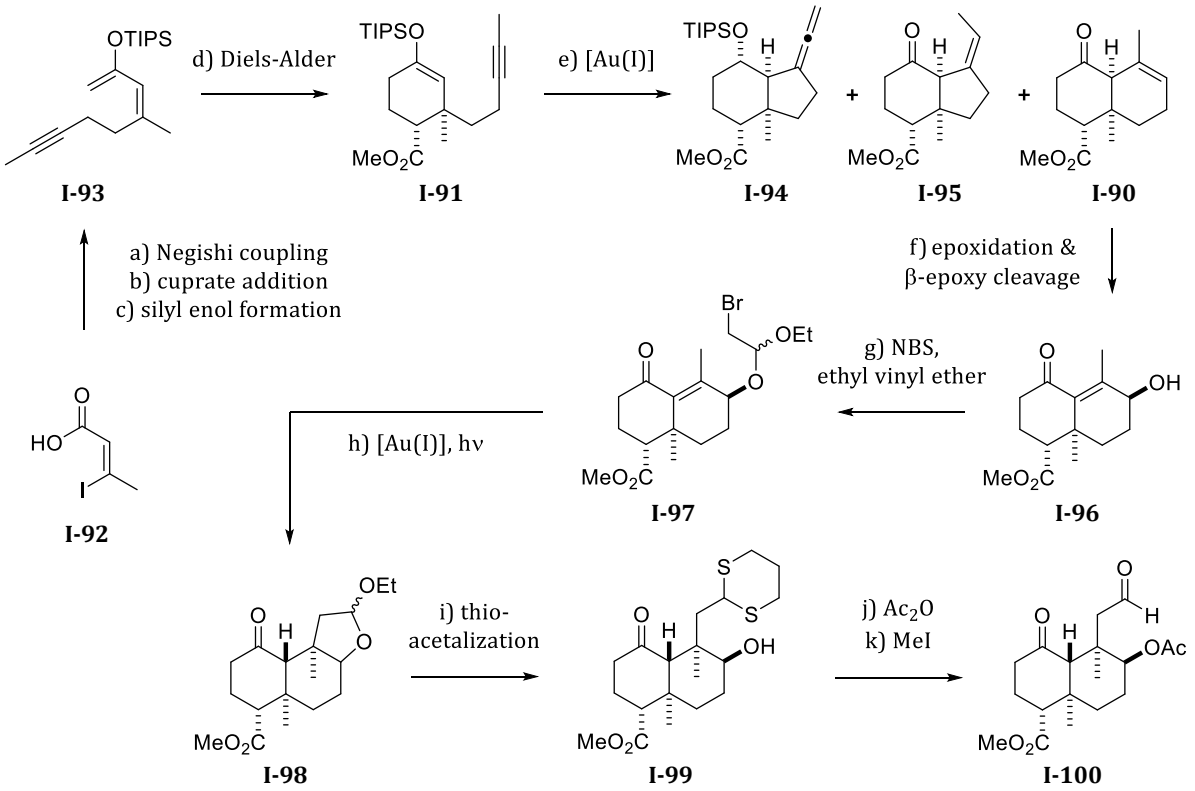

Scheme 15. BARRIAULT's synthesis of (±)-SalA (**I-11**).[123] *Continuation in **Scheme 16**.*

Reagents and conditions: **a)** (pent-3-yn-1yl)zinc iodide, $Pd(PPh_3)_4$ (5 mol%), THF, 40 °C, 18 h; **60%**. **b)** MeLi, CuCN, Et_2O, 0 °C to rt, 1 h; **70%**. **c)** TIPSOTf, Et_3N, DCM, 0 °C to rt, 2 h; **88%**. **d)** methyl acrylate (5 eq), Et_2AlCl (1.2 eq), DCM, –78 °C, 1 h; **70%** (*d.r.* > 20:1). **e)** [JohnPhosAu(MeCN)]SbF_6 (10 mol%), DCM/acetone (20:1), rt, 16 h; **2%** of **I-94** & **18%** of **I-95** & **80%** of **I-90** (**76%** isolated). **f)** HCO_2H, H_2O_2, DCM/H_2O, rt, 18 h, *then* DBU, 40 °C, 24 h; **62%** (one-pot) (*d.r.* = 5:1). **g)** ethyl vinyl ether, NBS, DCM, 0 °C to rt, 18 h; **83%**. **h)** $Au_2(dppm)_2Cl_2$ (10 mol%), DIPEA, UV-A LED, rt, 18 h; **98%**. **i)** propane-1,3-dithiol, $BF_3{\cdot}OEt_2$, DCM, 0 °C to rt, 1.5 h; **80%**. **j)** Ac_2O, Et_3N, DMAP, DCM; **98%**. **k)** MeI, $CaCO_3$, MeCN/H_2O, **99%**.

The *cis*-fused decalone **I-90** was then transformed to allylic alcohol **I-96** via epoxidation and β-epoxy cleavage. After α-bromo acetalization to **I-97**, *trans*-decalone acetal **I-98** was obtained in a 5-*exo*-dig radical cyclization by utilizing Au(I) photoredox conditions. Notably, de- or trans-

acetalization reactions of **I-98** were unsuccessful, and thus dithioacetal **I-99** was prepared. A planned substitution of the hydroxy group of **I-99** with a nitrile group, intended as a lactone building block, also proved unsuccessful. Therefore, **I-99** was transformed to γ-acetoxy aldehyde **I-100**. Proceeding from **I-100**, several steps were incorporated which were used on other substrates in previous total syntheses of SalA (**Scheme 16**).

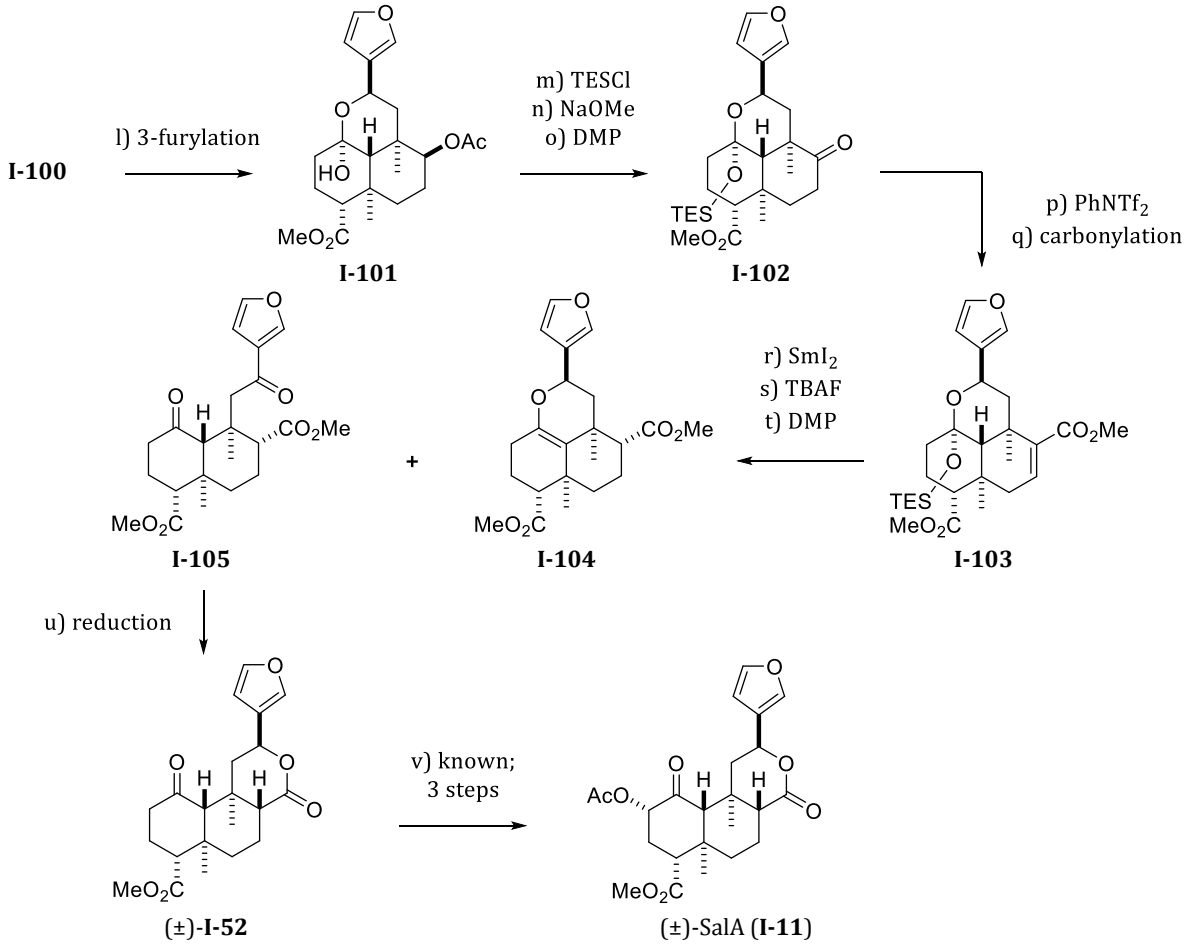

Scheme 16. BARRIAULT's synthesis of (±)-SalA.[123] *Continuation of* ***Scheme 15***.

Reagents and conditions: **l)** (3-furyl)Ti(O*i*-Pr)$_3$ (**I-67**) (2 eq), THF, 0 °C to rt, 1 h; **63%** (*d.r.* > 20:1). **m)** NaHMDS, TESCl, THF, **77%**. **n)** NaOMe, MeOH; **94%**. **o)** DMP, $NaHCO_3$, DCM; **98%**. **p)** $PhNTf_2$, KHMDS, THF; **95%**. **q)** $Pd(PPh_3)_4$, dppf, Et_3N, CO (1 atm), MeOH/DMF, 60 °C, 18 h; **66%**. **r)** SmI_2 (8 eq), Et_3N (15.8 eq), THF/MeOH (9:1), –78 °C, 1 h; **61%** (*d.r.* = 7:1). **s)** TBAF, THF, 0 °C. **t)** DMP (1.5 eq), $NaHCO_3$, DCM, rt, 18 h; **16%** of **I-104** & **55%** of **I-105** (over 2 steps). **u)** K-Selectride, *t*-BuOH, THF, –78 °C to –30 °C, 6 h; **19%** of **I-104** & **57%** of (±)-**I-52**. **v)** reported by HAGIWARA *et al*;[105] shown in **Scheme 6** on page **19** – not performed in this synthesis.

Aldehyde **I-100** was subjected to 3-furylation with (3-furyl)Ti(Oi-Pr)$_3$ (**I-67**). FORSYTH *et al.* used **I-67** in combination with (*R*)-BINOL-Ti(O*i*-Pr)$_2$, resulting in high selectivity for the desired diastereomer (*d.r.* = 8:1) (*cf.* **Scheme 9** on page **22**). For BARRIAULT *et al.,* however, the racemic addition afforded the undesired diastereomer (*d.r.* > 20:1). Addition of (*R*)-BINOL-Ti(O*i*-Pr)$_2$ did not affect selectivity and also led to the undesired C12 configuration, which was presumed to be a result of intramolecular chelation involving the acetoxy group. Furthermore, a concomitant

hemiketalization with the C1 ketone was observed, giving rise to hemiketal **I-101**. After silylation of hemiketal **I-101**, the C8 hydroxy group was revealed and oxidized to ketone **I-102**. A palladium-catalyzed carbonylation reaction via its enol triflate afforded unsaturated ester **I-103**, which was reduced with SmI_2, establishing the desired C8 configuration in good diastereoselectivity (7:1). This sequence was also used by HAGIWARA *et al.* and FORSYTH *et al*. In the latter syntheses, the reduction was conducted on unsaturated lactones, resulting in a preference for the undesired C8 epimer. For **I-103**, a reduction to the desired epimer with an *equatorial* ester group is preferred. These observations are in accordance with the previously discussed driving forces of C8 epimerization in the salvinorin scaffold (*cf.* **Figure 9** on page **12**).

After desilylation of the TES group, the labile hemiketal was oxidized at the 3-furyl alcohol moiety to give 3-furyl ketone **I-105** along with some dehydration product, enol ether **I-104**. Reduction of 3-furyl ketone **I-105** with K-Selectride/*t*-BuOH led to the correct configuration of C12, affording 2-deacetoxySalA (**I-52**). Notably, no epimerization at C8 was observed during this reduction – however, some enol ether **I-104** was formed. At this point, merely α-acetoxylation of **I-52** was pending, which was not performed by BARRIAULT *et al*.[124] This concluded their racemic formal synthesis of SalA, culminating in 21 steps to **I-52** with an overall yield of about 0.3%. In 2024, BARRIAULT *et al.* published a review of the total syntheses of SalA and its analogs, not including some of the approaches covered in this present thesis.[106]

As demonstrated by the diverse approaches discussed in this chapter, each new synthesis provided deeper insights into the salvinorin scaffold. The primary distinctions between the approaches lie in the construction of the core structure: while HAGIWARA *et al.* employed a bicyclic precursor, other researchers developed or adapted elaborate cyclization strategies using acyclic or monocyclic precursors. In the later stages towards SalA and its analogs, several steps were inspired by previous approaches, though some outcomes were unexpected from prior observations with other substrates. In many cases, even minor variations in reaction conditions proved critical. For example, late-stage reactions involving a potential C8 epimerization could be addressed more adequately in later approaches. Another notable example is the 6-*endo*-dig cyclization utilized by HALANG & MAIER and BARRIAULT *et al.,* where small tweaks in conditions significantly influenced outcomes. This also highlights how similar approaches can be pursued in parallel within particular research areas, often unbeknownst to the individual researchers. Furthermore, this underscores the importance of publishing 'unsuccessful' results, as these can complement and inspire other research efforts (*or prevent unpromising attempts*), as will be illustrated by other examples throughout this thesis.

1.3 PLANNED SYNTHESIS OF SALVINORIN A

In the work discussed in this thesis, another potential synthetic access to salvinorin A (**I-11**) was identified and pursued. Central to the synthetic route were insights gained during the author's master's thesis[125] and early doctoral research project which aimed at a synthetic access to englerin A. These pursuits will be briefly summarized to bridge the gap between our work on englerin A and salvinorin A, in which similar synthetic rationales were applied. To elucidate this rationale – leveraging cycloadditions to construct the respective core structures of natural products – special types of (3+2) and (5+2) cycloadditions will be discussed.

1.3.1 Summary of the Attempted (3+2) Cycloaddition Towards Englerin A

In our approach towards englerin A, alkenynones such as **I-108** represented central precursors (**Scheme 31**). The route proceeding from 4-pentynol (**I-106**) involved a low-yielding alkylation of a labile alkenyne aldehyde [step e)], affording **I-108** with low overall yield. However, starting from 3-butynol (**I-109**) and incorporating the alkenyne moiety *in the nucleophile instead of the electrophile* allowed for an efficient alkylation of aldehydes such as isobutyraldehyde [step k)], improving overall yield of alkenynone **I-108** significantly (38% vs. 18% over 6 steps).

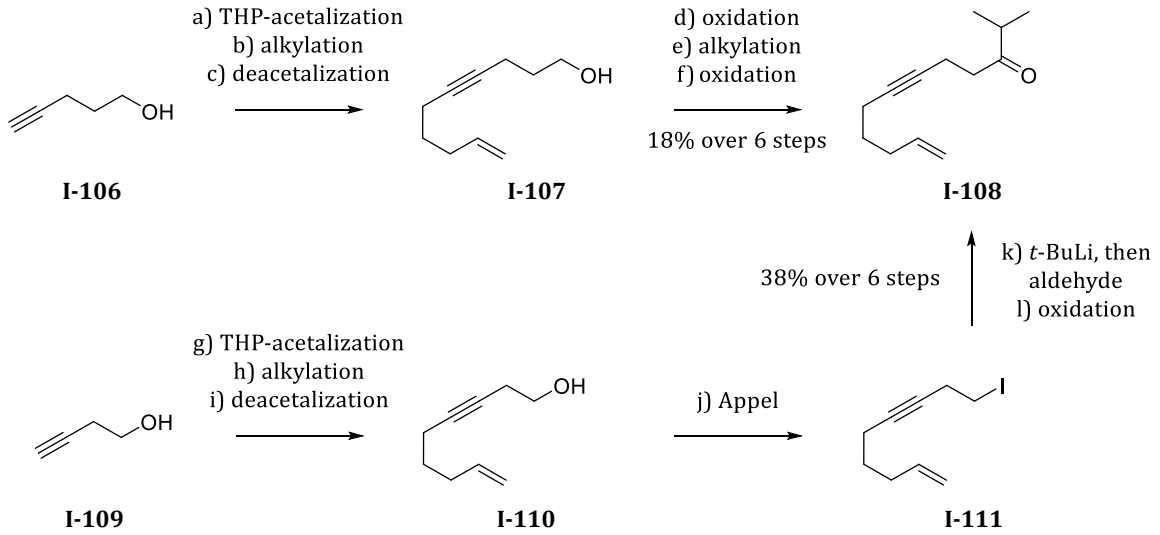

Scheme 17. Preparation of alkenynone **I-108** from 4-pentynol (**I-106**) or 3-butynol (**I-109**).

Reagents and conditions: **a)** DCM (0.8 M), *p*-TSA (0.25 mol%), DHP (1.2 eq), rt, 4 h; **95%**. **b)** THF (0.4 M), *n*-BuLi (2.5 M in hexane, 1 eq), 0 °C, 1 h, then 5-bromopentene (1.2 eq) & DMPU (2 eq), rt, 23 h; **74%**. **c)** MeOH (0.11 M), *p*-TSA (2.5 mol%), rt, 17 h; **96%**. **d)** DCM (0.16 M), DMP (1.2 eq), 0 °C to rt, 1 h; **e)** THF (0.11 M), *i*-PrMgCl (1.8 M, 1.35 eq), 0 °C to rt, 1.5 h; **34%** over 2 steps. **f)** same as d); **77%**. **g)** same as a); **91%**. **h)** same as b); **65%**. **i)** same as c); **91%**. **j)** DCM (0.48 M), PPh_3 (1.5 eq), imidazole (1.4 eq), I_2 (1.25 eq), then **I-110**, 0 °C, 1 h; **89%**. **k)** hexane/Et_2O (3:2, 0.1 M), *t*-BuLi (1.7 M in pentane, 2.1 eq), –78 °C to rt, 1 h; then *i*-PrCHO (2 eq), –78 °C, 45 min; **77%**. **l)** DCM (0.2 M), $(COCl)_2$ (1.1 eq), DMSO (2.2 eq), –78 °C; then substrate, NEt_3 (5 eq), –78 °C to rt, 1 h; **96%**.

From alkenynone **I-108**, oxabicyclo[3.2.1]octene **I-112** was to be obtained by intramolecular (3+2) cycloaddition (**Scheme 32**).[5] Sharing high similarity with the guaiane core, a synthesis of **I-112** and its derivatives may enable access to englerin A (**I-113**) and related natural products. These pursuits hinged on cycloadditions of *differently tethered* alkenynones such as **I-114** (*1-en-9-yn-6-ones* instead of *9-en-4-yn-1-ones*), as reported by IWASAWA *et al.*[126–128] Depending on the catalyst, the platinum-containing carbonyl ylide **I-114.I** afforded different cycloadducts: with neutral Pt(II) catalysts, the (3+2) cycloaddition was followed by a 1,2-alkyl migration to give **I-116**, whereas cationic Pt(II) catalysts obviated this migration and gave **I-115** instead.

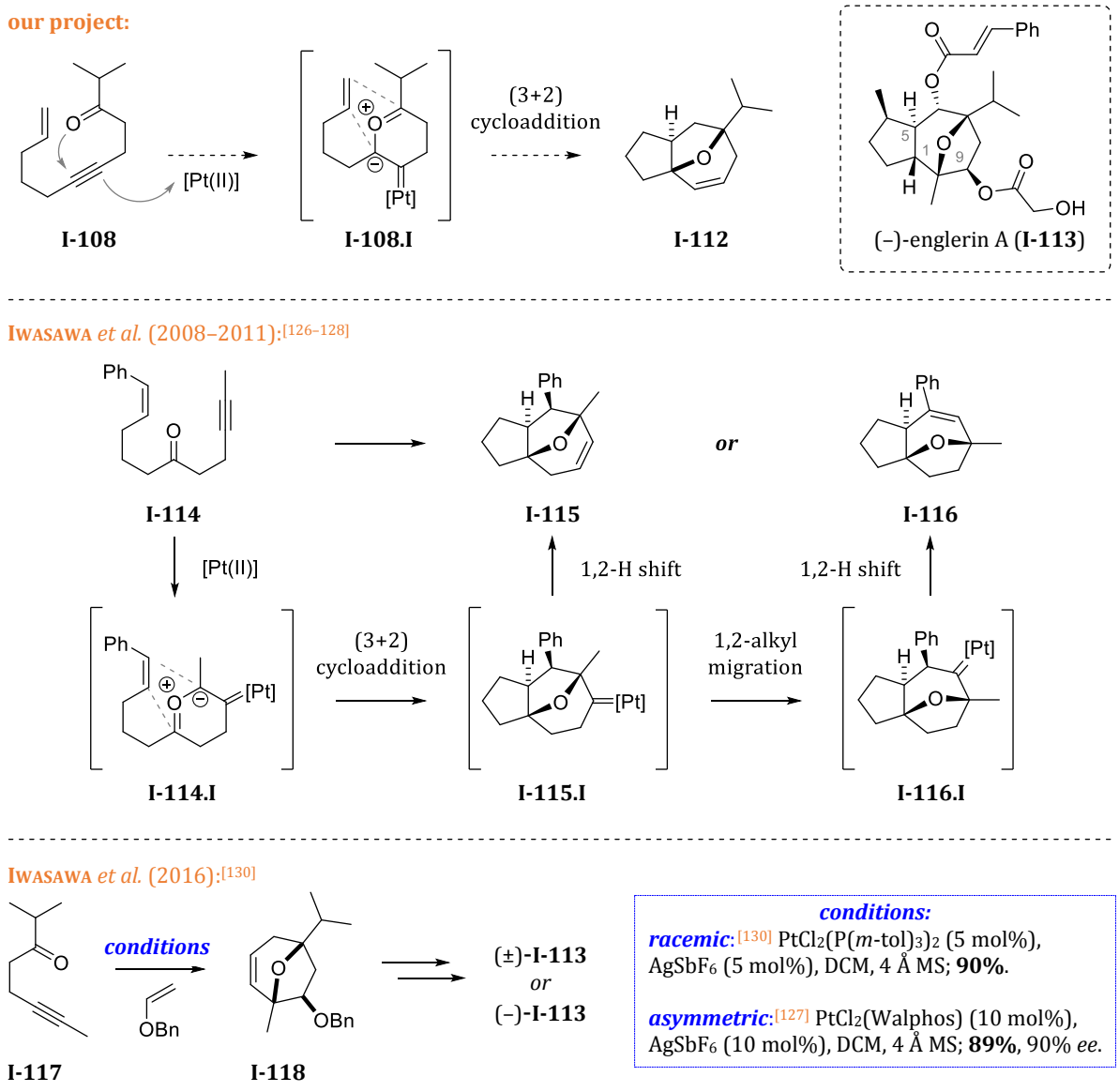

Scheme 18. Inter- and intramolecular (3+2) cycloadditions of alk(en)ynones.

[5] The notation '(x+y)' indicates the *numbers of atoms* involved in a respective cycloaddition. Most often, the notation '[x+y]' is used in the literature. We opted to use parentheses instead of brackets, which should be reserved for the *numbers of involved electrons*, as recommended by IUPAC.[129]

Later, IWASAWA *et al.* employed their methodology in an *intermolecular* cycloaddition from **I-117** to **I-118**, which was subsequently transformed to (±)-englerin A (**I-113**).[130] This also represented a formal asymmetric synthesis of (–)-**I-113**, since **I-118** was previously prepared by their enantioselective cycloaddition with chiral Walphos ligands.[127]

Other (3+2) cycloadditions of alkenynones, tethered analogously to our substrate **I-108** or those of IWASAWA *et al.* (e.g., **I-114**), were reported by METZ *et al.* (**Scheme 19**).[131] Using alkenynones such as **I-119** or **I-121** in a *domino cycloaddition/oxidation sequence* involving gold catalysts and pyridine-*N*-oxides (e.g., **I-122**), they obtained either cycloadduct **I-120** or **I-123**.

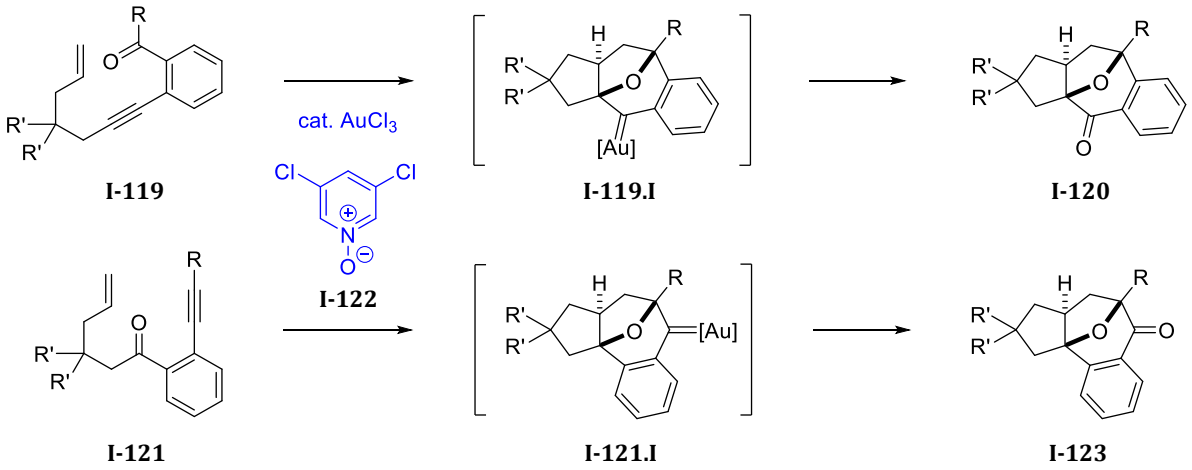

Scheme 19. Domino cycloaddition/oxidation of differently tethered alkenynones.[131]

Similar aryl-fused substrates can also be used for yet another cycloaddition, which was recently used in the synthesis of steroids such as estrone (**I-126**) by HO *et al.* (2022 and 2023).[132,133] This method, introduced by YAMAMOTO *et al.* for aldehyde analogs (*9-en-4-yn-1-als*),[134] generates *cis*-decalones such as **I-125** by a gold- or copper-catalyzed (4+2) cycloaddition (**Scheme 20**).

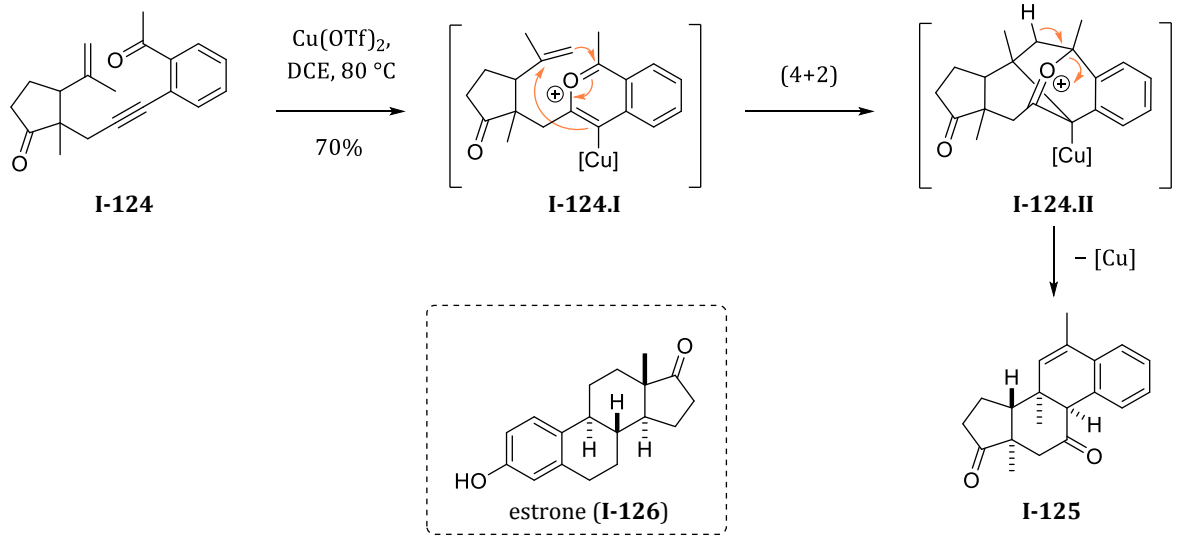

Scheme 20. Copper-catalyzed (4+2) cycloaddition of alkenynones to *cis*-decalones.[133]

Alternatively tethered alkenynones with 'switched' en/yne-positioning (*4-en-9-yn-1-ones*) also proved suitable for two other total syntheses of (–)-englerin A (**I-113**), published back to back by ECHAVARREN *et al*[135] and MA *et al*[136]. These approaches, the former of which is shown in **Scheme 21**, involved using similar substrates in an intriguing gold-catalyzed domino reaction developed in previous work of ECHAVARREN *et al.*[136,137] This is initiated by the reaction between the en- and yne-moieties, generating a cyclopropyl gold carbene intermediate **I-127.I**. While this mechanism only shares little similarity with the previously shown (3+2) or (4+2) cycloadditions, it further showcases the versatile use of alkenynones in different cyclization reactions.

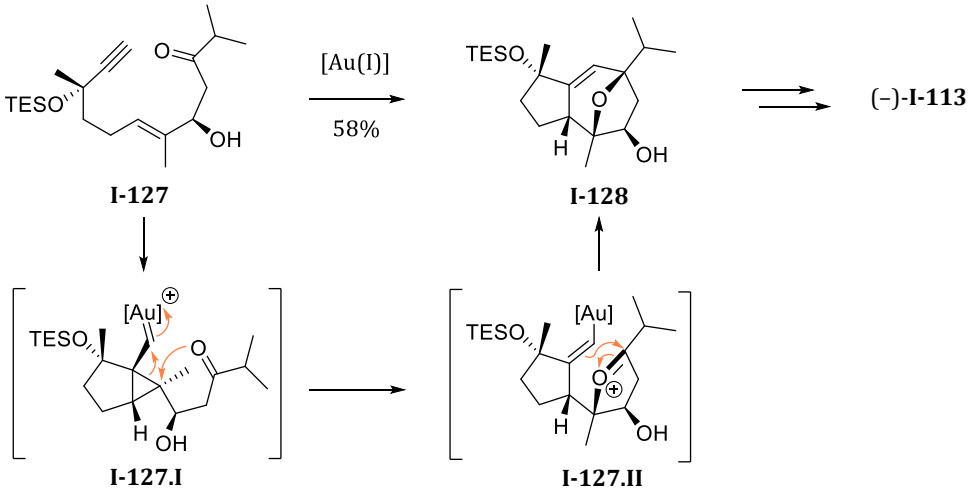

Scheme 21. Gold-catalyzed domino reaction of alkenynone **I-127** to oxatricycle **I-128**.[135]

The methodologies of IWASAWA, METZ, and YAMAMOTO & HO were applied to our substrates. Treating alkenynone **I-108** or its phenyl analog **I-129** with different platinum-, gold- or copper-catalysts merely led to low conversions, complex mixtures, or decomposition,[<6>] with no significant formation of the desired cycloadducts being evident. These attempts encompassed 27 variations using the catalysts listed in **Scheme 22** on the next page. This included experiments with or without additives such as $AgSbF_6$, pyridine-*N*-oxide, or ethyl vinyl ether. In some cases, precipitated AgCl, formed by a preformation of a solution of catalyst and $AgSbF_6$, was filtered off. While this lessened the extent of decomposition, it did not aid in product formation.

In one attempt, furan **I-131** was obtained under relatively forcing conditions (*yield not determined*). The formation of **I-131** can be explained by a 5-*exo*-dig attack of the carbonyl oxygen at the alkyne activated by the cationic Au(III) complex. Similar cycloisomerizations to furans from alkynones (*alk-4-yn-1-ones* or *alk-3-yn-1-ones*) are known to occur with (*either neutral or cationic*) Au(I), Au(III) or Pd(II) catalysts.[138,139] However, neutral Au(III) complexes (i.e., using $AuCl_3$ without $AgSbF_6$) did not facilitate cycloisomerization to furan **I-131**.

[<6>] Generally, the use of the term 'decomposition' in this thesis indicates 'very complex mixtures' in which little remaining substrate and only insignificant amounts of distinctive and identifiable compounds were discernible.

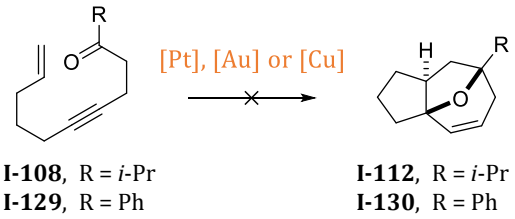

I-108, R = *i*-Pr
I-129, R = Ph

I-112, R = *i*-Pr
I-130, R = Ph

used catalysts, additives & solvents:

catalysts: **[Pt(II)]:** $PtCl_2(P(m\text{-tol})_3)_2$, $PtCl_2$(dppp), $PtCl_2(MeCN)_2$, $PtCl_2(dmso)_2$, $PtCl_2$(1,2,3,4-tetraethylcyclobutadiene); **[Au(I)]:** $AuClPPh_3$, $(AuCl)_2$dpppf; **[Au(III)]:** $AuCl_3$; **[Cu(II)]:** $Cu(acac)_2$
additives: $AgSbF_6$ (in 1:1 ratio to [Pt] or [Au]); 4 Å MS; ethyl vinyl ether (in 4 cases); pyridine-*N*-oxide (in 2 cases).
solvents: DCM, DCE, MeCN, $CDCl_3$.

Generally, 1–10 mol% catalyst was used. The reactions were run at temperatures ranging from –10 to 84 °C (reflux in DCE).

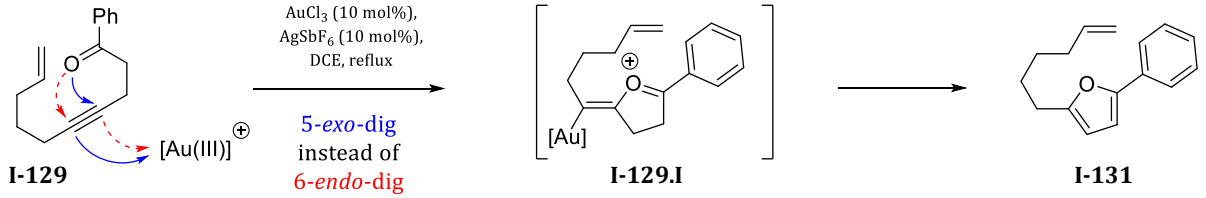

I-129 **I-129.I** **I-131**

Scheme 22. Overview of the attempted (3+2) cycloadditions of alkenynones **I-108** and **I-129**.

With these results, our cycloaddition attempts were discontinued. Why this cycloaddition did not proceed still lacks a conclusive explanation.[7] Seemingly, alkenynones tethered in this fashion (i.e., **9-en-4-yn-1-ones**) do not allow for the desired cycloaddition in a significant amount. It may be presumed that different competing pathways led to the formation of complex mixtures (e.g., 6-*endo*-dig attack to carbonyl ylides with subsequent (3+2) or (4+2) cycloaddition vs. 5-*exo*-dig attack to furan precursors vs. initial cyclopropane formation from the linked en/yne-moieties). To the best of our knowledge, cycloaddition reactions of similar alkenynones were reported only for *aryl-fused substrates* such as those of METZ *et al.* and HO *et al.* (page **33**). However, a central aspect of these two approaches, which stands in stark contrast to our approach, is the formation of carbonyl ylides which can be considered *aromatic pyrylium ions*, as indicated for **I-124.I**. Presumably, the aromatic nature of these intermediates may direct the preferred pathway towards cycloaddition reactions.

[7] This project was discontinued ~6 months after beginning the doctoral research. The experimental details are omitted in the present doctoral dissertation. Some of the details can be seen in the preceding master's thesis (synthesis of alkenynone **I-108** from 4-pentynol & first cycloaddition attempts).[125] The optimized route to **I-108** from 3-butynol was reported in the bachelor's thesis of F. FOTAKIS,[140] which was supervised as a part of this project.

Other syntheses of englerin A were approached via related cycloadditions, as was also treated in a recent review of CHANDRA & ANDERSON *et al.* (2023).[141] These include the generation of *carbonyl ylides* from α-diazo-β-ketoesters in rhodium-catalyzed (3+2) cycloadditions, which were used in a former project within our group (MAIER *et al.,* 2010)[142] and in a total synthesis of (–)-**I-113** by HASHIMOTO *et al.* (2015)[143] (**Scheme 23** on the next page). Next to these (3+2) cycloadditions, two syntheses by the groups of NICOLAOU & CHEN (2010)[144] and TCHABANENKO (2019)[145] relied on related intermolecular (5+2) cycloadditions of *oxidopyrylium ylides*.

While the yields of these oxidopyrylium–alkene (5+2) cycloadditions were rather moderate, they facilitated another access to the englerin core. In their approach, NICOLAOU & CHEN *et al.* achieved an asymmetric *intermolecular* version by using an acrylate incorporating a bornyl sulfonamide auxiliary. Notably, TCHABANENKO *et al.* isolated side-products stemming from an isomerization of the oxidopyrylium ylide **I-139.I** to the conjugated dienone **I-139.II**.
The formation of dienone **I-139.II** and dimer **I-140**, resulting from an cycloaddition of oxidopyrylium **I-139.I** with the *exo*-methylidene moiety of dienone **I-139.II**, was obviated when 2,6-di-*tert*-butylpyridine was added. However, the regio- and diastereoselectivity resulting from the addition of *vinyl acetate* was still subpar, affording the desired cycloadduct **I-143** in 30% yield with their optimized conditions. Yet, these observations contribute additional insights into oxidopyrylium (5+2) cycloadditions, which will be treated in the following subchapter.

MAIER *et al.* (2010):[142]

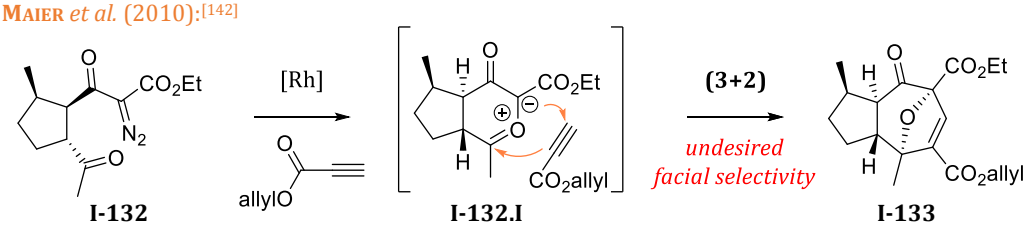

I-132 **I-132.I** **I-133**

HASHIMOTO *et al.* (2015):[143]

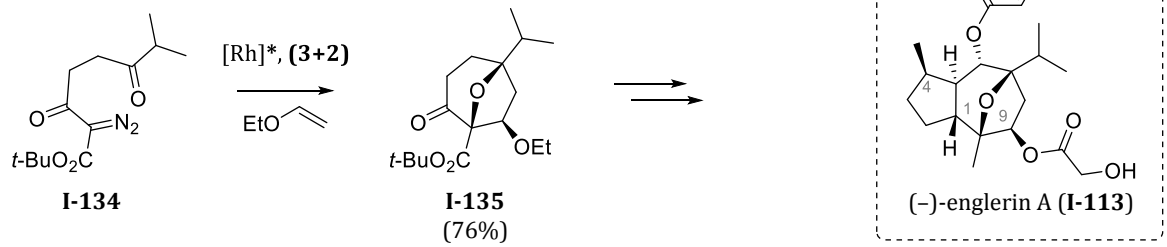

I-134 **I-135** (76%)

(–)-englerin A (**I-113**)

NICOLAOU & CHEN *et al.* (2010):[144]

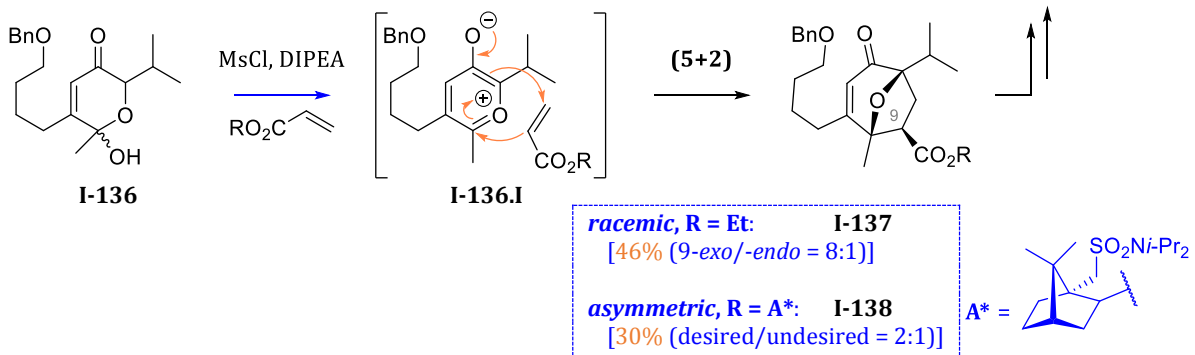

I-136 **I-136.I**

TCHABANENKO *et al.* (2019):[145]

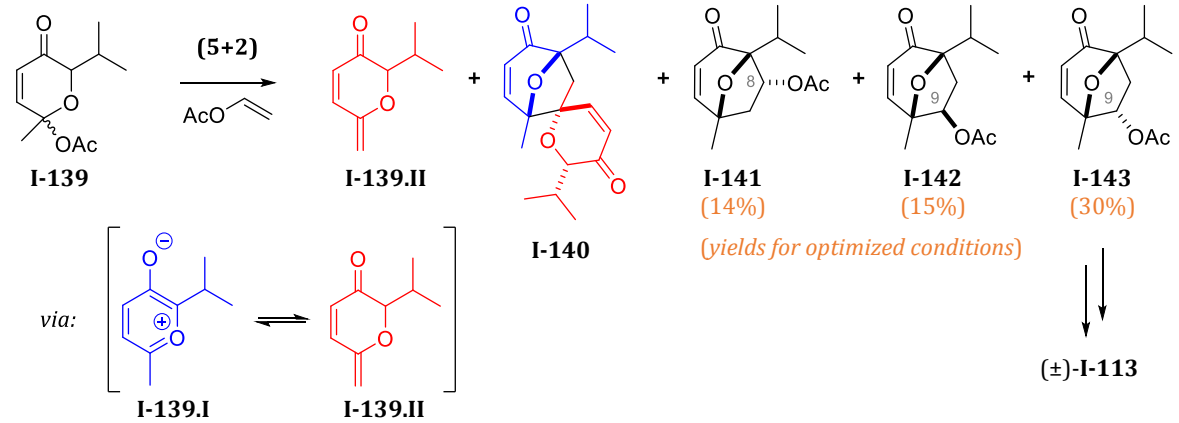

I-139 **I-139.II** **I-140** **I-141** (14%) **I-142** (15%) **I-143** (30%)

(*yields for optimized conditions*)

I-139.I **I-139.II**

(±)-**I-113**

Scheme 23. Other *carbonyl ylide* (3+2) and *oxidopyrylium* (5+2) cycloadditions towards **I-113**.

1.3.2 Planned Route to SalA via (5+2) Cycloaddition and Rearrangement

In 1980, HENDRICKSON *et al.* disclosed (5+2) cycloadditions using pyranulose acetate **I-144** as a precursor for *oxidopyrylium ylide* **I-144.I** (**Scheme 24**).[146,147] Such ylides can be considered a type of *carbonyl ylides*, as indicated from one of their various resonance structures (**I-144.III**). Shortly thereafter, this cycloaddition was examined in more detail by SAMMES *et al.*[148–156]<8> In general, addition of olefinic dienophiles affords oxabicyclo[3.2.1]octenes (**I-145** or **I-146**) by (5+2) cycloaddition, while (5+3) ylide dimerization to **I-147** or (4+3) cycloaddition (e.g., to **I-148**) can predominate with unsuitable dienophiles.

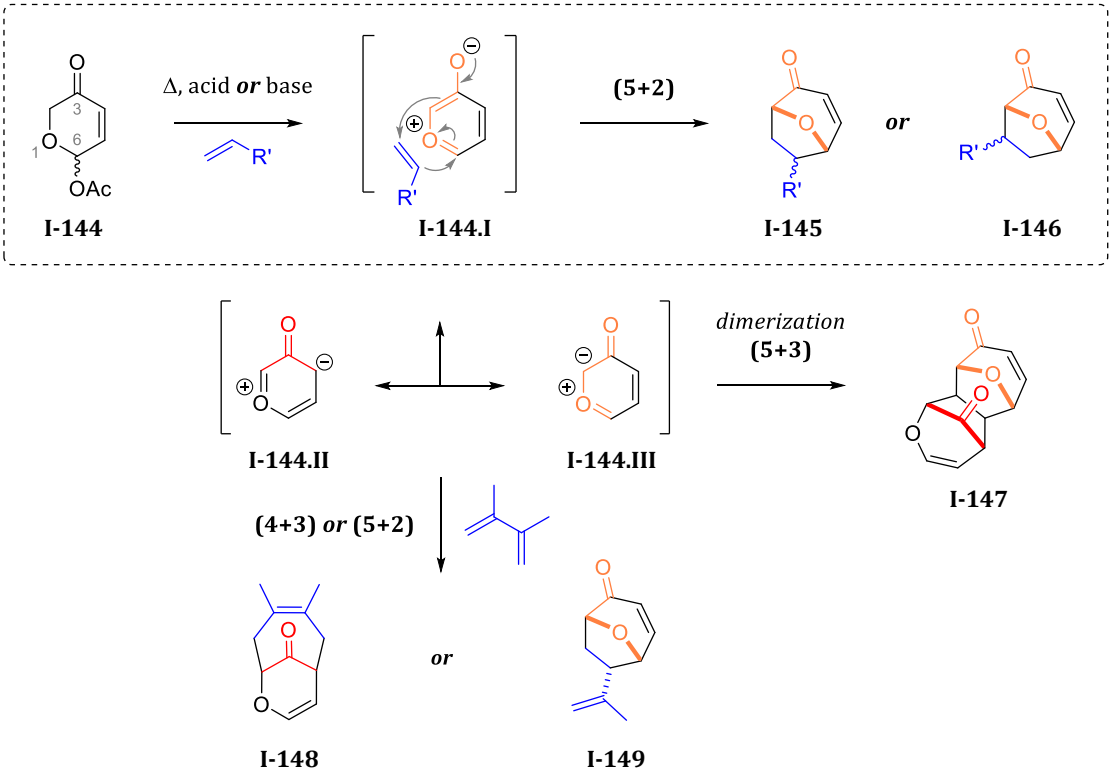

Scheme 24. General overview of different cycloadditions involving oxidopyrylium ylides.

These observations showcase the ambivalent character of these ylide intermediates, which can also react as dienophiles themselves, allowing for cycloadditions across C2–C4, as indicated from resonance structure **I-144.II**. In *intermolecular* (5+3) cycloadditions, *vinyl ethers* or *styrene* proved especially suitable dienophiles allowing for good regio- and diastereoselectivity, whereas "attempted reaction[s] with *vinyl acetate* failed".[150] This observation also concurs with the subpar yield and selectivity for TCHABANENKO's cycloadduct **I-143** (*cf.* **Scheme 23** on page **37**).

<8> The articles "Recent Studies on 3-Oxidopyrylium and its Derivatives" (P. G. Sammes, *Gazz. Chim. Ital.* **1986**, *116*, 109–114)[153] and "An Unusual LEWIS-acid-catalysed Addition of Acetonitrile to a Perhydroazulene" (P. G. Sammes, A. G. Swanson, R. J. Whitby, *J. Chem. Research (S)* **1988**, 162–163)[156] could not be found as online resources. However, physical copies of these journals were present in the faculty library of the University of Tübingen.

SAMMES *et al.* soon focused on *intramolecular* variations of this cycloaddition, which obviated undesired side-reactions such as dimerization. Some of their examples are summarized in **Scheme 25**. By using alkenyl and alkynyl tethers varying both in length and position on the pyranulose moiety, different cycloadducts (**I-155**–**I-162**) could be accessed, whereas the main focus was laid on *epoxyazulene*-based frameworks (**I-155**–**I-157** and **I-160**–**I-162**). Generally, oxidopyrylium ylides were generated by heating the pyranulose acetates, most often – but not always – in the presence of amine bases (NEt_3, DBU or DBN). Notably, *pyranulose* **I-152** was subjected to the cycloaddition under 'acidic' conditions (cat. AcOH). Similar to their oxygen analogs, *oxidopyridinium ylides* gave amine-bridged cycloadducts (e.g., **I-164**).

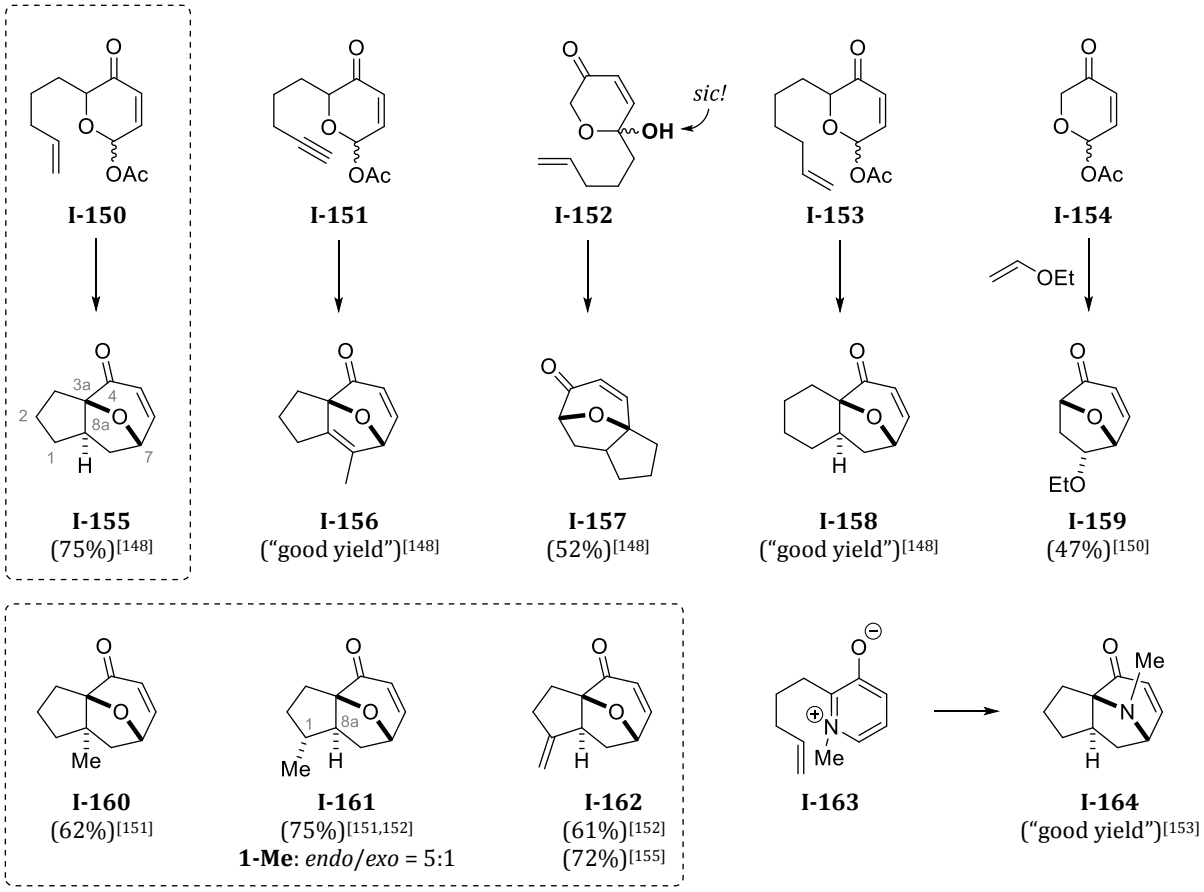

Scheme 25. Overview of the (5+2) cycloadditions reported by SAMMES *et al*. The substrates for **I-160**–**I-162** are not shown for a better overview.

As seen in these and the following examples, *intramolecular* oxidopyrylium–alkene (5+2) cycloadditions proceed in a highly regio- and stereocontrolled fashion, often affording the depicted *endo*-cycloadducts as single isomers.[9] Substituents *on or adjacent to the alkene moiety* are also incorporated preferentially in an *endo*-orientation, as seen for the 1-Me group in **I-161** or the ethoxy ether in the intermolecular example of **I-159**.

Over the decades, this entry to oxabicyclo[3.2.1]octenes has been leveraged to access a wide variety of different natural product scaffolds, including the intermolecular approaches to englerin A (*cf.* **Scheme 23** on page **37**). Some notable intramolecular cycloadditions are shown in **Scheme 26**.[157–161] While many other impressive examples were reported, a further discussion goes far beyond the scope of this thesis. For further reading, reviews treating both the previously discussed (5+2) and (3+2) cycloadditions (until 2018) are recommended.[162–165]

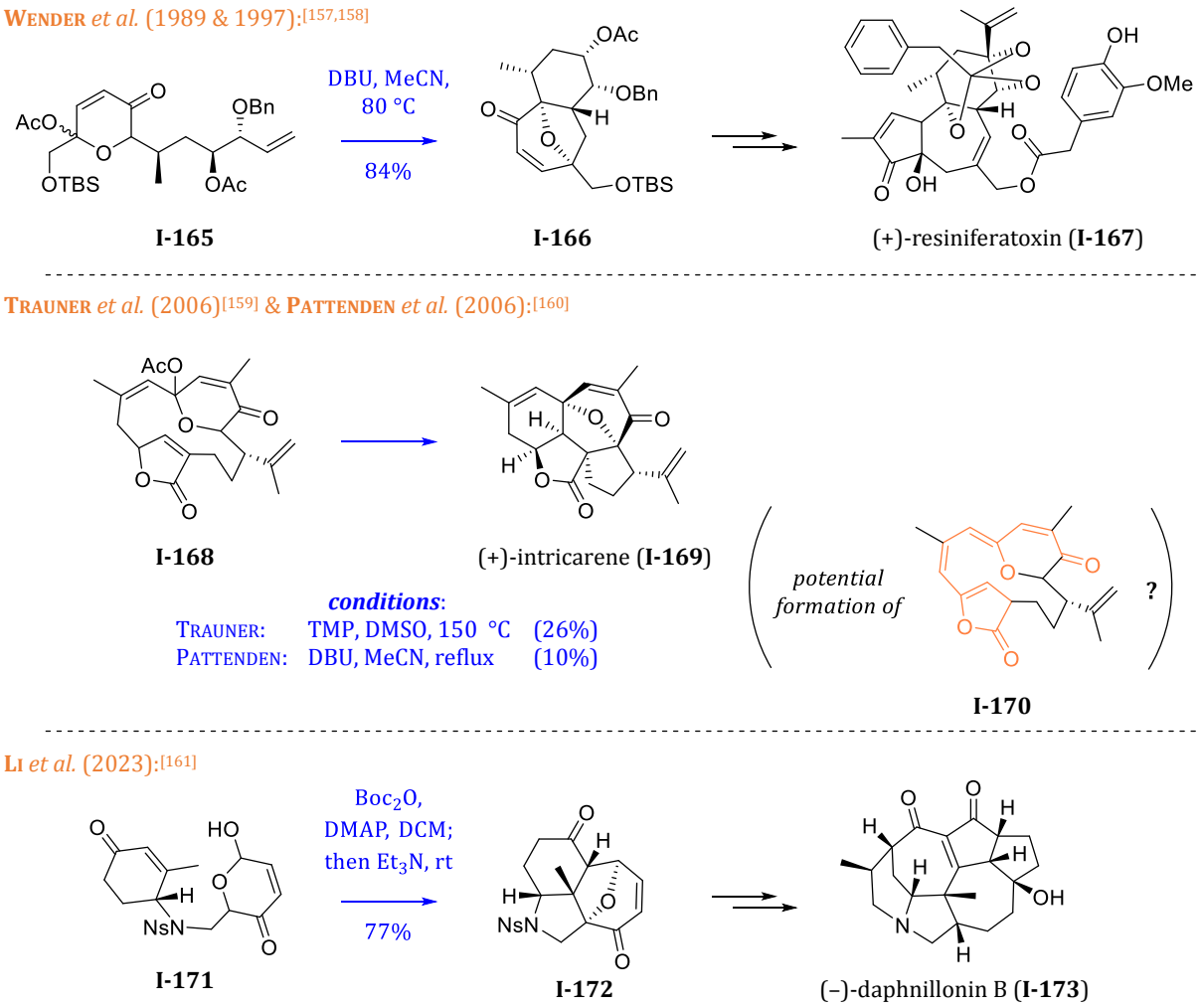

Scheme 26. Examples of oxidopyrylium cycloadditions applied in natural product synthesis.

[9] Substituents are designated as ***exo-*** or ***endo-*** according to their position **relative to the ether bridge**: on the 'same side' as the ether bridge (*exo-*) or 'opposed' to it (*endo-*).

These *intramolecular* cycloadditions proceeded with high regio- and stereoselectivity, affording the desired cycloadducts as single enantiomers. Furthermore, good yields were achieved – with the example of (+)-intricarene (**I-169**) being an exception barely lessening the impressiveness of generating multiple ring-connections and stereocenters in such an *intricate* polycycle, which was coincidingly published in 2006 by the groups of TRAUNER and PATTENDEN.[159,160] While neither of these authors elaborated further on yield or observed side products, it *may be surmised* that an undesired isomerization of the respective oxidopyrylium to the *exo*-methylidene could have occurred. Such an isomerization, as reported by TCHABANENKO *et al.* for a simpler *para*-alkyl oxidopyrylium ylide (*cf.* **Scheme 23** on page **37**), could give **I-170**, which would exhibit an extensive conjugated system (indicated in orange).

While WENDER *et al.* started their work on the first total synthesis of (+)-resiniferatoxin (**I-167**) back in 1989,[157,158] they published syntheses of related daphnane diterpenes relying on the (5+2) cycloaddition up until 2011.[166,167] These examples, as well as the very recent synthesis of (–)-daphnillonin B (**I-173**) by LI *et al.*,[161] stand testament to the ongoing relevance and versatility of the oxidopyrylium–alkene (5+2) cycloaddition in natural product synthesis.

For the sake of completeness, some *general enantioselective methodologies* for such inter- and intermolecular cycloadditions must be mentioned, which include both (i) *substrate-controlled approaches* by MASCAREÑAS *et al*[168] or MITCHELL *et al*[169] and (ii) *external asymmetric induction* through a dual thiourea catalyst system, introduced by JACOBSEN *et al*.[170,171] A further discussion of these examples, however, will be omitted, since no asymmetric synthesis was pursued in our work. Furthermore, some mechanistic details on oxidopyrylium formation from pyranulose acetates will be discussed in **Chapter 2.1.2**, linking these details with our experimental findings.

In our group, similar approaches to englerin A (**I-113**) were considered, which would integrate an *intramolecular* oxidopyrylium–alkene (5+2) cycloaddition instead of intermolecular approaches published by NICOLAOU & CHEN *et al.* and, later, TCHABANENKO *et al*. Upon examination of the discussed literature, a special 'use-case' of (5+2) cycloadducts piqued our interest: SAMMES *et al.* reported a LEWIS-acids catalyzed rearrangement of epoxyazulenes[10] to decalones, shown on the example from **I-174** to **I-175**/**I-176** in **Scheme 27** on the next page.[151] Extending this method to other epoxyazulene substrates later on, they gained access to several sesquiterpene-based natural products and their derivatives, as will be discussed in more detail in **Chapter 2.3**.

[10] In this thesis, compounds such as (3a*R**,4*R**,6*R**,7*R**,8a*R**)-6-methyloctahydro-1*H*-3a,7-epoxyazulen-4-ol (**I-174**) are addressed as '(3a,7)-*epoxyazulenes*' or 'tricyclic compounds' for brevity.

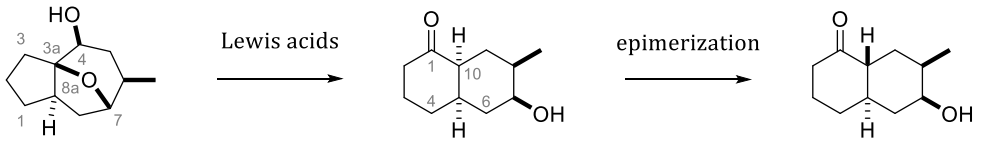

I-174 **I-175** **I-176**

Scheme 27. An example of the LEWIS acid-induced epoxyazulene to decalone rearrangement.

We eventually opted to refrain from further pursuits towards englerin A and, instead, investigate whether this rearrangement could be leveraged to gain access to salvinorin A (**I-11**). While other approaches were concurrently pursued in our group, as briefly mentioned in **Chapter 1.2.9**, this rearrangement promised a potentially viable synthesis of the salvinorin *trans*-decalone core.

Since the rearrangement of 3a,7-epoxyazulenes such as **I-174** has, to the best of our knowledge, only been reported by SAMMES *et al.* for a rather small number of mostly 'unfunctionalized' substrates, the (retro-)synthetic planning involved some uncertainties. Especially the functional group tolerance of the rearrangement under rather harsh LEWIS-acidic conditions could not be assessed assuredly. A general retrosynthetic analysis of salvinorin A (**I-11**) incorporating this rearrangement at different 'levels of functionalization' can be seen in **Scheme 28** on the next page. The *fully functionalized epoxyazulene* **2** would – after reduction of the C4 ketone, successful rearrangement of the thus generated tricyclic alcohol, and isomerization – afford the 7-hydroxyl analog (**1**) of 2-deacetoxysalvinorin A (**I-52**).

However, it seemed reasonable to examine the rearrangement on *less functionalized substrates* first. The 3-furylation of an aldehyde with subsequent lactonization, as well as methyl ester formation should be feasible on the decalone core, as was previously shown on some examples within already published total syntheses of salvinorin A (**Chapter 1.2**). For these purposes, alkene moieties seemed suitable precursors. Incorporating a nitrile group as a potential C_1 building block for the lactone ring, the *minimally functionalized epoxyazulene* would be *bis*-alkenyl ketonitrile **7**.

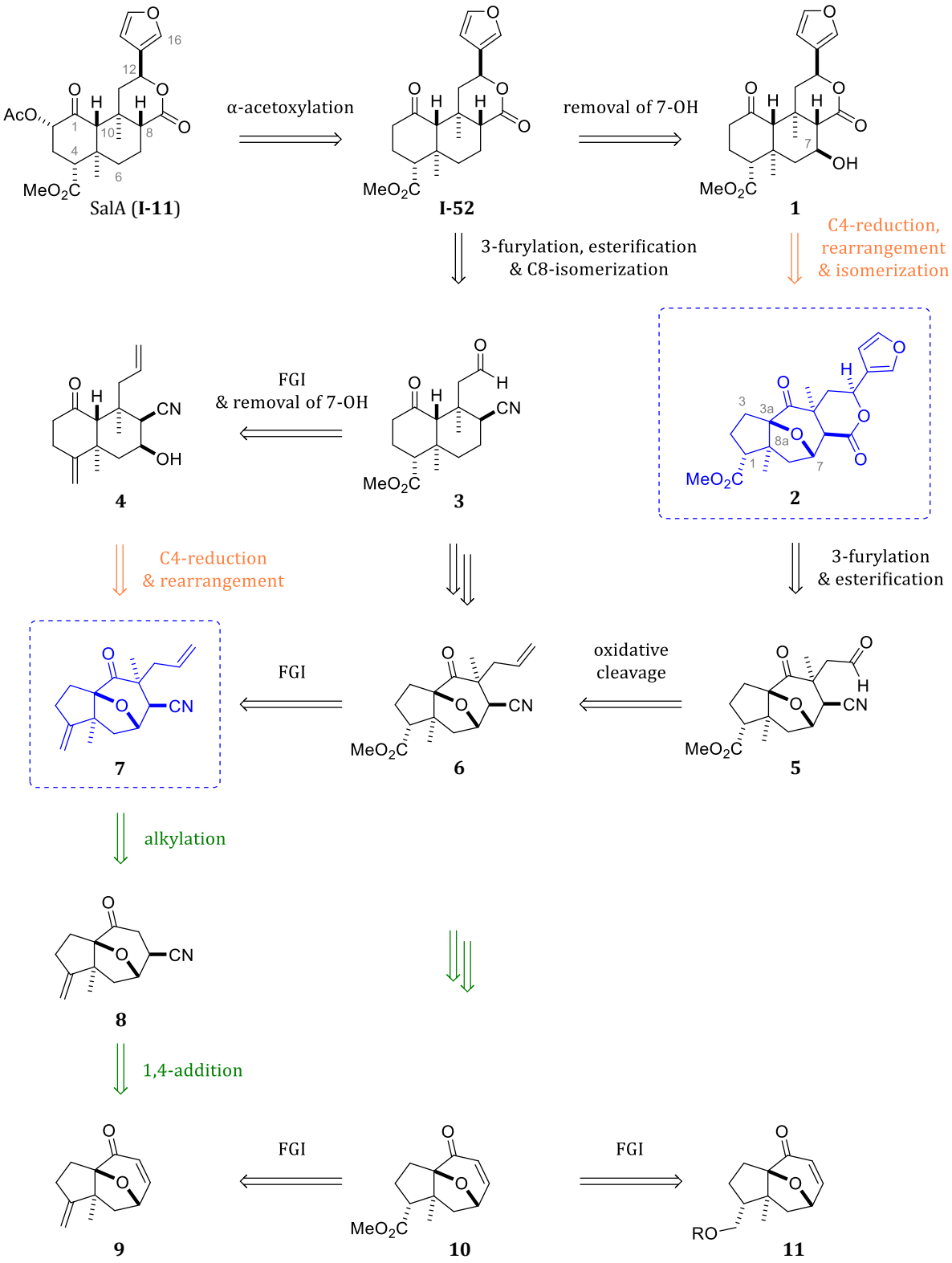

Scheme 28. Retrosynthetic analysis of salvinorin A (**I-11**) in search of suitable epoxyazulenes for a rearrangement to decalones. The *fully* and *minimally functionalized* substrates (**2** and **7**, respectively) are shown in blue.[11]

[11] To improve readability, *compounds pursued, employed, or synthesized in our work* are henceforth numbered anew, starting from '**1**'. The prefix '**I-**' will, however, still be used for (i) compounds treated in discussed literature, (ii) some reagents, or (iii) structures in general discussions, such as in mechanistic considerations.

Tricyclic enones functionalized at C1, such as 1-*endo*-methyl ester **10** or ester precursors **11**, may be accessible by oxidopyrylium–alkene (5+2) cycloaddition in a diastereo- or even enantioselective fashion. Yet, the early introduction of an ester moiety may give rise to isomerization issues before, during, or after the cycloaddition stage. The cycloaddition precursor **15** would most likely not be viable due to isomerization of the terminal alkene, which would give conjugated α,β-enoates (**Scheme 29**). Assuming a selective cycloaddition to **10** could be realized, epimerization at the ester α-carbon C1 may ensue during functionalization reactions on the tricyclic core. This potential epimerization to 1-*exo*-esters would be 'reversable' after successful rearrangement to the *trans*-decalone core, in which 4-esters are known to assume the depicted *equatorial* configuration. For tricyclic systems, however, a definite prediction of the preferred configuration is less straightforward.

To obviate these issues, as well as a potential incompatibility of esters with the highly LEWIS-acidic rearrangement conditions, we opted to aim for tricyclic enone **9** as the first key intermediate. The preparation of **9** seemed feasible, since it represents a 'combination' of two similar cycloadducts bearing either the 8a-methyl or the 1-*exo*-methylidene[12] group (**I-160** and **I-162**, respectively), which were previously prepared by SAMMES *et al.*

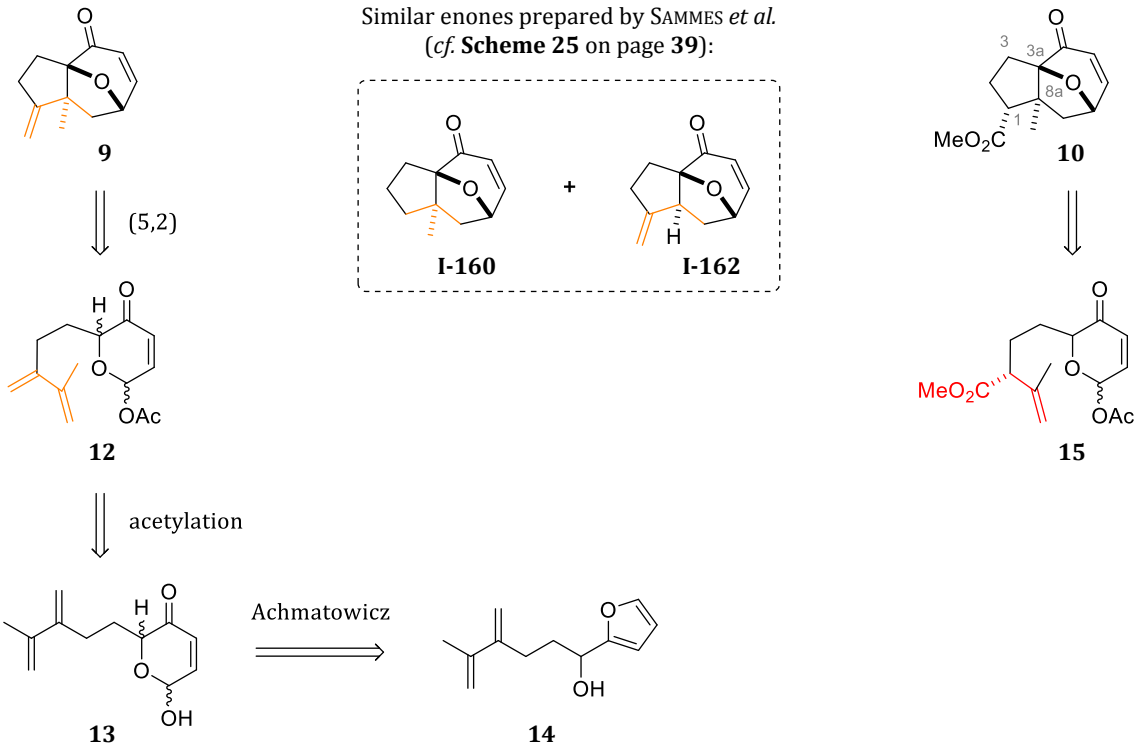

Scheme 29. Retrosynthetic analysis of tricyclic enone **9**.

[12] This *exo(cyclic)*-prefix indicates the olefinic connection between C1 to the CH_2-group '*outside of the ring*' and should not be confused with the *exo*-prefix indicating substituent configuration. Furthermore, the preferred IUPAC name 'methylidene' is used instead of the also commonly encountered '(*exo*)-methylene'.[172]

The cycloadduct precursor, dienyl-tethered pyranulose acetate **12**, was to be prepared via ACHMATOWICZ reaction of dienyl furfuryl alcohol **14** and subsequent acetylation of the resulting pyranulose **13**. In this sequence, however, the dienyl moiety of **14** was expected to cause a potential issue in the ACHMATOWICZ reaction, as will be elaborated on later.

Next to the broached uncertainties regarding the rearrangement of epoxyazulenes to decalones, two other questions remained en route to the *minimally functionalized epoxyazulene* **7**: how could dienyl furfuryl alcohol **14** be prepared efficiently, and how would the tricyclic compounds proceeding from enone **9** behave in functionalization reactions?

While SAMMES *et al.* generally prepared their alkenyl-tethered furfuryl alcohols by alkylating furfural (**16**) with readily available alkenyl building blocks, the dienyl furfuryl alcohol en route to **I-162** proved quite challenging (**Scheme 30**). In their optimized route, which was "more than twice as efficient as the [previous] one," furfuryl alcohol **I-180** was obtained from chloroprene (**I-177**) in 28% over four rather laborious steps.[152,155]

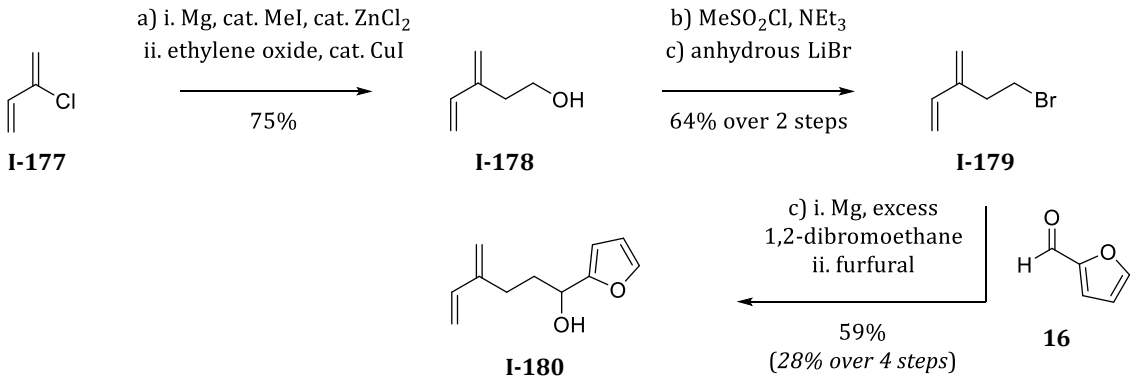

Scheme 30. Overview of the 'optimized' preparation of **I-180** by SAMMES *et al.*[155]

Assuming that an adequate route to tricyclic enone **9** could be achieved, the question of stereoselectivity in subsequent functionalization reactions was to be clarified. With their epoxyazulenes, SAMMES *et al.* reported *exo*-selective alkylations at C6 and C4. To this day, however, no C5-functionalization was reported on 3a,7-epoxyazulenes. Based on these limited results and without having definite proof at hand, we presumed potential *exo*-selectivity for both the (i) 1,4-addition of a nitrile moiety at C6 and (ii) subsequent alkylations for the installment of the quaternary C5 center of *bis*-alkenyl ketonitrile **7**.

Bearing these aspects in mind, we set out to investigate these intriguing 3a,7-epoxyazulenes and our goal to leverage their potential aptitude for rearrangements to decalones, which may ultimately facilitate an alternative access to salvinorin A (**I-11**).

CHAPTER 2: RESULTS AND DISCUSSION

2.1 SYNTHETIC ROUTE TO TRICYCLIC ENONE 9

2.1.1 Carbocupration and Synthesis of Dienyl Furfuryl Alcohol 14

The retrosynthetic analysis of furfuryl alcohol **14** reveals that several approaches involving different C–C-bond forming reactions can be considered for its preparation (**Scheme 31**). The furyl moiety may be introduced by classic organometallic reactions, either by (i) adding the furyl building block as a nucleophile to a *dienyl-substituted electrophile* (e.g., dienyl aldehyde **17**) or (ii) adding a *dienyl-substituted nucleophile* to a furyl-substituted electrophile [e.g., furfural (**16**) or 2-furyloxirane (**25**)]. Following these rationales, the dienyl compounds required in the respective approaches would share a common 2-methyl-1,3-butadiene unit substituted at C3 with either a C_1 (**24**), C_2 (**28**) or C_3 (**19**) building block.

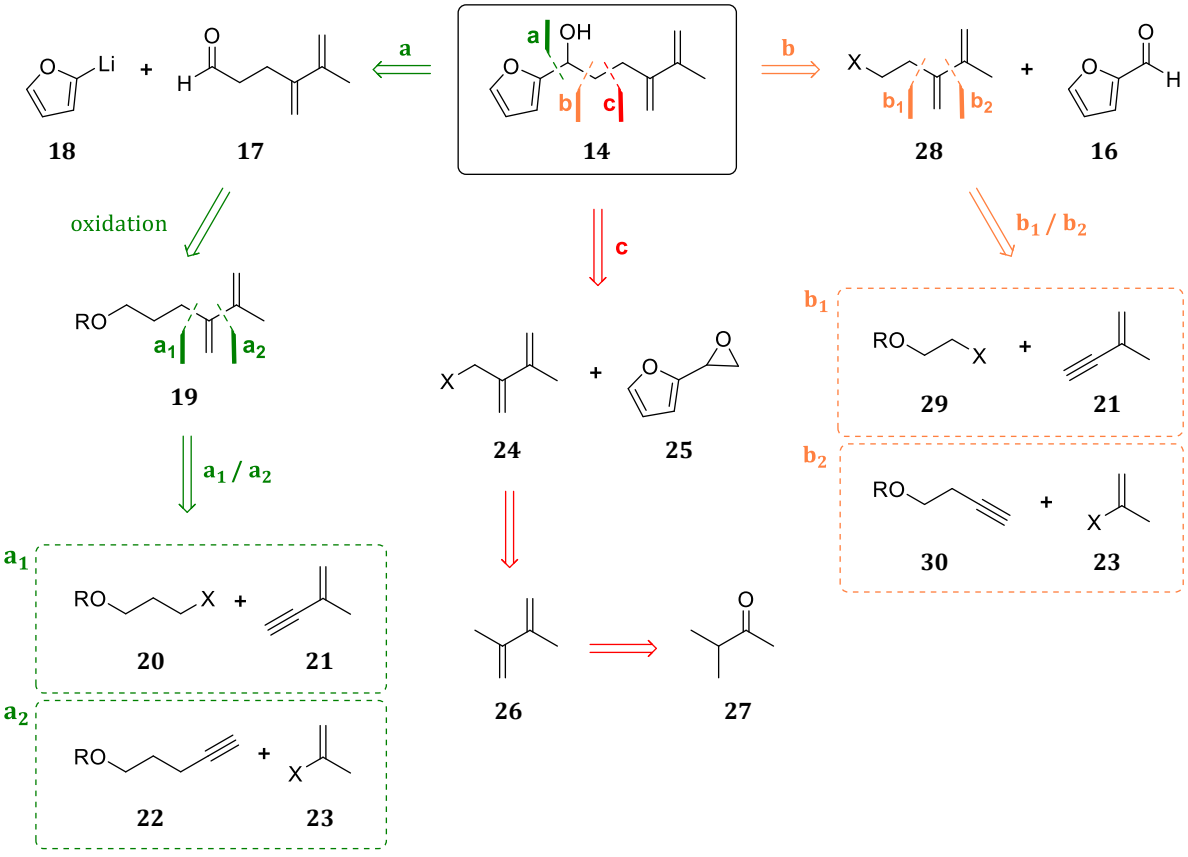

Scheme 31. Retrosynthetic analysis of furfuryl alcohol **14**.

First, an allylic bromination of 2,3-dimethyl-1,3-butadiene (**26**) was approached to test whether a preparation of **24** would be feasible (**Scheme 32**). In our hands, the reaction of **27** to **26** proceeded with only low yields (28% yield; literature yield:[173] 73%). Subsequent WOHL-ZIEGLER bromination of **26**, which is reported in the literature only sparingly with no yield given,[174] resulted in complex mixtures. In general, allylic bromination of conjugated dienes such as **26** can prove challenging.[175] A radical polymerization of **26**, representing 3-methylated isoprene, to a caoutchouc derivative called *methyl rubber* seems very likely under these conditions.[176] Subsequently, this route did not seem promising and was not pursued further.

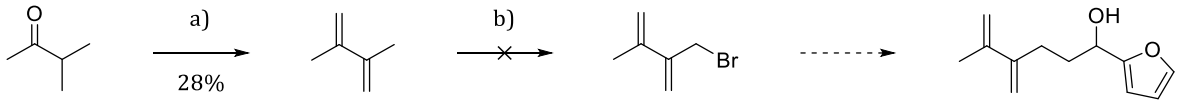

27 **26** **24** **14**

Scheme 32. Synthetic approach to **14** starting from methyl isopropyl ketone (**27**).

Reagents and conditions: **a)** Addition of **27** (45 min) to KO*t*-Bu (1 eq), DMSO (2 M), 140 °C; **28%**. **b)** NBS (1 eq), AIBN (5 mol%), CCl_4, reflux, 2 h.

For C_2- and C_3-substituted dienes **28** and **19**, the carbocupration of alkynes was envisioned to be a suitable approach. Generally, the 2,3-butadiene moiety common in both synthetic targets can be approached by *carbocupration of alkynes* with a retrosynthetic cut *adjacent to* (route a_1 and b_1) or *in between* (route a_2 and b_2) the conjugated diene. Subsequently, alkenyne **21** and a C_3 or C_2 cuprate (from **20** or **29**) would have to be employed in case of a retrosynthetic cut adjacent to the diene. A retrosynthetic cut in between the diene would require adding a vinyl cuprate [e.g., from 2-bromopropene (**23**)] to substrates such as 4-pentynol (**22**) or 3-butynol (**30**).

While both these routes were investigated, many early attempts resulted in mostly inconclusive results and complex mixtures with little or no formation of the desired products. Nevertheless, critical insights into the carbocupration reaction could be obtained, which then allowed for an exceptionally high-yielding synthesis of dienyl alcohol **19** starting from 3-chloro-1-propanol (**20**). For the sake of conciseness, failed approaches are only summarized briefly before some mechanistic considerations, as well as the required conditions for a successful carbocupration of alkynes are discussed in more detail.

The first carbocupration reactions aimed at using a vinyl cuprate (from GRIGNARD reagent **23.I**) for the addition to THP-protected 3-butynol **30.a** (**Scheme 33**). For this purpose, 2-bromopropene (**23**) was treated with magnesium, followed by the addition of CuBr or CuBr·DMS (or the addition of GRIGNARD reagent **23.I** to CuBr or CuBr·DMS) to generate the respective cuprates. In some cases, these cuprates were stabilized with stochiometric amounts of $MgBr_2$, formed by the addition of 1,2-dibromoethane. As reported in the literature, such a complexation can improve the yield of carbocupration reactions, especially with branched alkyl cuprates.[177] In neither of these attempts, an indication of product formation (THP ether **28.b** or dienyl alcohol **28.a**) was evident. Consequently, the addition of dienyl halide **28** – via APPEL reaction of **28.a** and subsequent halogen-metal exchange – to furfural (**16**) could not be investigated.

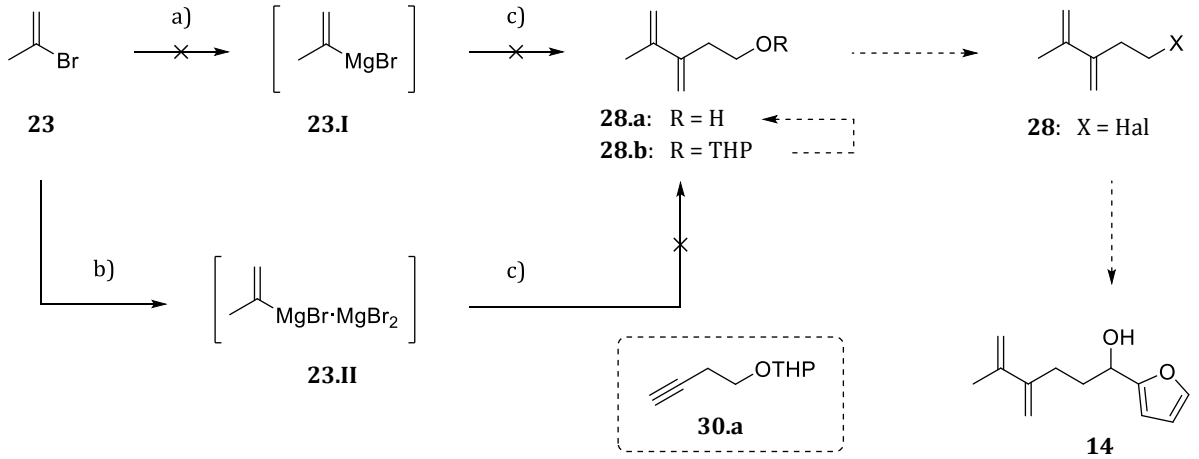

Scheme 33. Attempted synthesis of **14** via alcohol **28.a** starting from 2-bromopropene (**23**).

Reagents and conditions: **a)** Mg (1-5 eq), THF or Et_2O, rt or reflux. **b)** Mg (3 eq), 1,2-dibromoethane (1 eq), THF, 0 °C to rt. **c)** CuBr or CuBr·DMS (1 eq), cooled or rt; then **30.a**, –60 °C to rt.

Ensuing these and some other failed carbocupration reactions, we opted to focus on the carbocupration of alkenyne **21**. Such carbocuprations of alkyne systems were examined since the 1970s and are subject of a plethora of publications, including mechanistic studies, synthetic examples, and reviews. Some of the observations and claims regarding cuprate chemistry in general – as well as the carbocupration of alkynes and alkenynes in particular – seem increasingly inconclusive after examining an increasing number of publications. Therefore, the following mechanistic considerations are not aimed to fully discuss every possibility and oddity, but instead focus on an examination of the carbocupration of alkynes which eventually allowed us to find a pragmatic synthesis of our desired product. For additional information, some more recent reviews on the carbocupration of alkenynes and alkynes can be considered.[178–180]

Some mechanistic considerations will be discussed based on our successful carbocupration of alkenyne **21** with cuprate **20.II** derived from 3-chloro-1-propanol (**20**) (**Scheme 34**), a sequence for which a literature precedent (with moderate yields) was also found.[181] Treating **20** with *i*-PrMgCl affords a magnesium alcoholate, which then undergoes a GRIGNARD reaction by oxidative insertion of magnesium into the C–Cl bond to give the NORMANT-GRIGNARD reagent **20.I**.[182] This also renders a previous protection of the hydroxy group (e.g., as THP-ether) unnecessary. After addition of CuBr·DMS complex, cuprate **20.II** is generated, which in turn affords vinyl cuprate **20.III** after addition of alkenyne **21**. In this case, this addition proceeds (i) with high regioselectivity favoring the 1,2-adduct, presumably by preferential orbital interaction of the cuprate with the C1–C2 π-system perpendicular to the conjugated butadienyl π-system, as well as (ii) in a stereospecific *syn*-fashion, and (iii) in "the MARKOWNIKOW way", both of which is explicable by steric considerations.[183,184] Hydrolysis then affords dienyl alcohol **19**.

It is evident that other products would be possible. In fact, exceptions to the mentioned aspects can result from (i) changes in substrates (e.g., conjugated dienyls or enones resulting in 1,4-addition, the latter being a wide-spread use case of cuprates),[183–185] (ii) functional groups which facilitate a chelation of the cuprate,[178] or (iii) depending on the nature of the cuprate, both regarding the 'counter' ion and the introduced alkyl group (e.g., tertiary or secondary alkyl groups can favor the *anti*-MARKOWNIKOW product).[183]

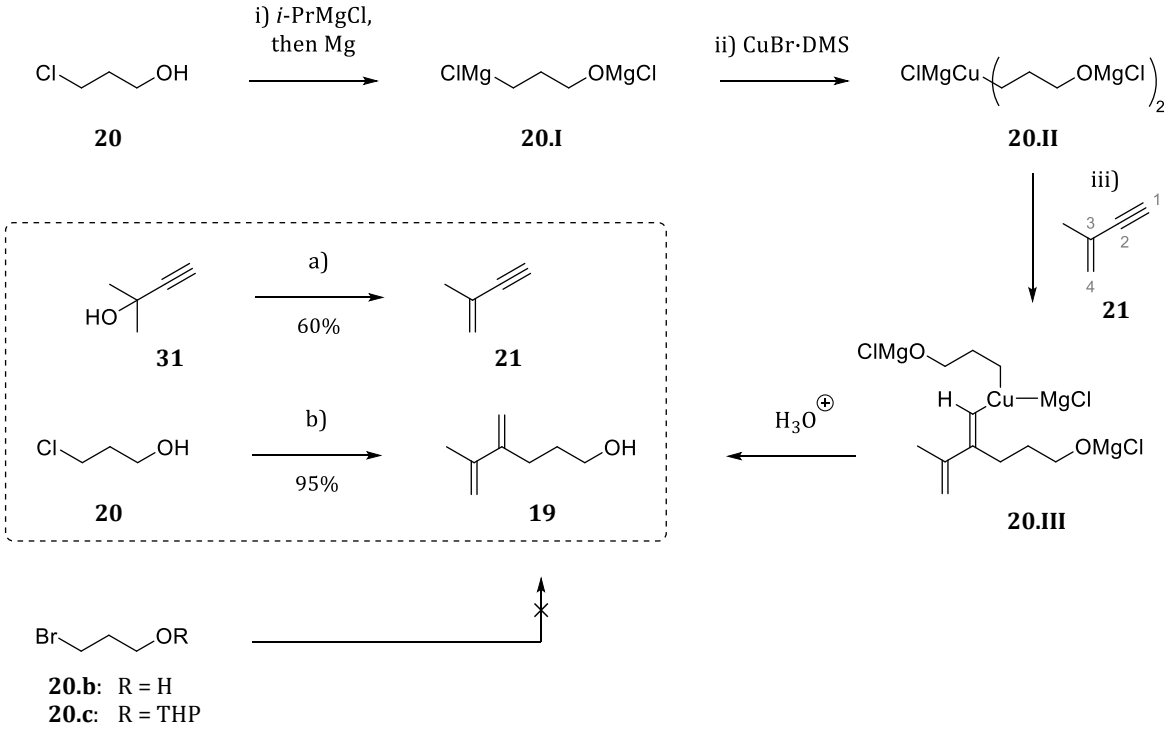

Scheme 34. Successful synthesis of dienyl alcohol **19** by carbocupration of alkenyne **21**.

Reagents and conditions: **a)** Ac_2O (1.25 eq), H_2SO_4 (96% aq., 5 mol%), 80 °C, 1.5 h; **60%**. **b) (i)** *i*-PrMgCl (1.35 M in THF, 1 eq), THF (up to 0.4 M), 0 °C, 30 min, rt, 30 min; then Mg (1.07 eq) and 1,2-dibromoethane (5 mol%), rt, 19 h; **(ii)** CuBr·DMS (0.5 eq), –55 °C, 2 h; **(iii)** alkenyne **21** (0.5 eq), –55 °C to rt, 17 h; **95%**.

With the conditions listed in **Scheme 34**, a reproducible carbocupration method was achieved, affording desired dienyl alcohol **19** in high yields of 89–98% even after distillation. Since this carbocupration reaction is highly dependent on multiple factors, and variations of reaction conditions incorporated several small alterations, a methodological analysis pinpointing specific factors is only possible within certain limits. Nevertheless, critical insights are summarized below and details regarding preparation and purification of reagents are elucidated further in the Experimental Section (**Chapter 4.1.1**).

Choice of reagents:

As indicated in **Scheme 34**, early approaches used 3-bromo-1-propanol or its THP-acetal (**20.b** and **20.c**, respectively), resulting in inhomogeneous reactions mixtures and complex mixtures with only traces of **19**. Explanation for this could be the lower solubility of bromo NORMANT-GRIGNARD reagents, which tend to precipitate at low temperatures. Comparisons of the solubilities of both *chloro* and *bromo magnesium alcoholates* of **20.I** led NORMANT *et al.* to conclude that the preparation of chloro magnesium alcoholates is necessary to ensure homogeneous solutions.[182] Furthermore, the presence of a THP-ether was reported to lead to sticky, low soluble cuprates in some cases.[186] Subsequently, we refrained from using bromo or THP-ether substrates, focusing on 3-chloro-1-propanol (**20**) as substrate instead.

For the deprotonation of the hydroxy group of **20**, self-prepared *i*-PrMgCl solutions *seemed somewhat superior* to commercially obtained solutions. In early attempts, the concentration of the (NORMANT-)GRIGNARD reagents was determined by titration of an aliquot with the method introduced by PAQUETTE *et al*.[187] However, a much simpler titration with 0.1 M HCl against phenolphthalein as indicator proved equally suitable and was thus preferred.

Magnesium turnings were activated extensively before use by the dry-stirring method published by BROWN *et al*.[188] Doing so, the formation of the NORMANT-GRIGNARD reagent **20.I** could be achieved at room temperature, which seemed to have a major impact on yield (*vide infra*).

CuBr·DMS was selected as the copper reagent of choice for cuprate formation. The complexation of Cu(I) salts with dimethyl sulfide is known to be accompanied by major advantages compared to respective non-complexed cuprous salts, allowing for an efficient purification of Cu(I) salts by preparation of highly stable Cu(I) complexes.[189,190] Commercial samples of CuBr most often display a turquoise to greenish color due to Cu(II) impurities. DMS forms highly colored complexes with those impurities (e.g., dark red complex with $CuBr_2$), which can be separated from colorless CuBr·DMS readily. The iodide complex CuI·DMS loses DMS spontaneously,

whereas CuBr·DMS is stable to storage in inert atmosphere and can be handled routinely in air.[191] In many examples, cuprates generated with CuBr·DMS give rise to better results than those generated by CuBr, especially when alkyl lithium reagents are used.[186,189,191]

CuBr·DMS was prepared from CuBr which was previously purified by washing first with acetic acid and then with methanol. A DMS solution of purified CuBr was treated with hexane according to the procedure of HOUSE *et al.,* precipitating CuBr·DMS as a small grained and nearly colorless solid.[191,192] Alternatively, purified CuBr was dissolved in DMS and cautiously overlayed with hexane, allowing exceptionally large colorless crystals (prisms of up to ~10 cm) to form over several days. The complex prepared by trituration afforded CuBr·DMS with much smaller grain size but also stronger discoloration due to residual impurities. Some of the brownish impurities could be washed off with methanol and acetone, but a completely colorless complex like that from slow crystallization could not be obtained.

It is crucial to note that for a high-yielding and reproducible carbocupration, large crystals of CuBr·DMS must be finely powdered before utilization due to its inherently poor solubility in THF (and generally most other solvents without additional DMS). Disregard of previous grinding, while keeping all other factors the same, dramatically lowered the yield of the carbocupration from >89% to 55–65%. Generally, the grain size of CuBr·DMS had a much greater influence on yield than most other factors, including a discoloration of the complex.

Alkenyne **21** was prepared by acetylation and concomitant β-elimination of acetic acid using 2-methyl-3-butyn-2-ol (**31**) as described in literature,[193] yielding 60% of **21** and thus being comparable to published results (55–72%).[193–195]

Choice of reaction conditions:

Other crucial factors, including optimal temperatures were discerned especially for both the first and the last step of the carbocupration reaction: the formation of NORMANT-GRIGNARD reagent **20.I** and the hydrolysis procedure of cuprate **20.III** to dienyl alcohol **19**.

The preparation of **20.I** at high temperatures (reflux) led to an inhomogeneous mixture with grey cloudy precipitate, which resulted in promising yields for early attempts (39–44%) but was soon determined to be significantly detrimental to yield. The use of activated magnesium turnings (*vide supra*) enabled complete conversion of **20** to **20.I** at ambient temperatures, as determined by titration. Both the alkoxy and the carbanionic center are detected in titrations with hydrochloric acid, providing a value of *normality* (N), which is divided by two for the determination of *molarity* (M). In early attempts, using activated magnesium turnings and

omitting heating resulted in higher conversions of **20** to **20.I** [87% conversion (rt, 16 h, self-prepared *i*-PrMgCl solution) vs. 52% (reflux, 2 h, commercial *i*-PrMgCl sln.) and 64% (reflux, 2 h, self-prepared *i*-PrMgCl sln.)] and consequently, higher yields of dienyl alcohol **19** (69% vs. 44% and 39%). Additionally, the inhomogeneous mixture after heating tended to interrupt stirring after addition of CuBr·DMS and alkenyne **21**, contributing to irreproducibility (52% conversion to 44% yield vs. 64% conversion to 39% yield). Properly activated magnesium turnings also allowed for nearly stochiometric amounts, so that practically no excess of magnesium had to be used (e.g., 1.07 eq Mg and 5 mol% 1,2-dibromethane, leaving only 2 mol% Mg). As a consequence, CuBr·DMS *could be added to the solution* of **20.I**, omitting the often-employed transfer of the GRIGNARD solution into a suspension of copper reagent.

The hydrolysis of the carbocuprated intermediate **20.III** proved to be another critical factor. As reported by HOUSE *et al.,* an optimal hydrolysis of cuprate reactions can be exceptionally dependent of temperature.[191] In their specific case, a conjugated addition of Me_2CuLi (prepared from MeLi and CuBr·DMS) to an enone (1-cyclohexenyl methyl ketone) was found to result in dramatically higher yields when the reaction mixture was allowed to warm to room temperature before hydrolysis: dropwise addition of AcOH and MeOH at –60 °C resulted in merely 1.3% yield, while addition of aqueous NH_4Cl at –60 to –70 °C resulted in 11% yield; however, addition of aqueous NH_4Cl at 20 °C raised the yield to 70%. This pronounced difference was explained by precipitation of polymeric $(MeCu)_n$ at temperatures above –20 °C.

Consequently, our carbocupration mixture was also slowly hydrolyzed with aqueous NH_4Cl at room temperature after formation of the cuprate reagent **20.III** [from **20.I** with CuBr·DMS at low temperatures (–60 to –40 °C, 2 h) and addition of alkenyne **21** (–60 °C)], allowing the reaction mixture to slowly warm to room temperature overnight (15–18 h). After hydrolysis, insoluble copper and magnesium precipitates were filtered off, enabling a clean separation of the copper-containing aqueous phase (*intense blue coloration indicating copper amine complexes*) from the organic phase. Earlier attempts with hydrolysis by aqueous HCl or H_2SO_4 solutions at low temperatures resulted in complex mixtures.

Since carbocupration reactions are generally run in ethereal solution (diethyl ether or THF), with THF being able to dissolve/complex cuprates more efficiently, THF was used as solvent. Initially, a molarity of 0.15 M was aimed for because NORMANT *et al.* determined the solubility of **20.I** to be 0.3 N in THF.[182] In the process of optimization, the molarity could be increased considerably to 0.4 M without influence on yield (concentrations higher than 0.4 M were not tested). Presumably, NORMANT *et al.* falsely determined a low solubility due to heating at reflux, which should have resulted in similar inhomogeneous mixtures as observed in our case.

To summarize, the synthesis of dienyl alcohol **19** could be optimized excellently, resulting in yields of up to 98%. This specific example of carbocupration was also published by SHEA *et al.* (46% yield), however similar executions of the reported conditions did not seem promising in our hands and proved less reproducible and efficient (e.g., preparation of 0.24 M **20.I** with MeMgBr and heating at reflux, transfer of **20.I** into a solution of uncomplexed CuBr, hydrolysis with 6 N HCl).[181] Critical factors for reproducible results in our carbocupration were determined to be the use of properly activated magnesium, omitting reflux conditions, the purity and especially grain size of CuBr·DMS, as well as a slow hydrolysis at room temperature.

These results may play a role in contributing more insights into the generally often low- or moderately yielding carbocupration reactions, further increasing the appeal of this extraordinarily versatile C–C-bond forming reaction.

Dienyl alcohol **19** was then transformed to dienyl aldehyde **17** by SWERN oxidation[196] with yields of approx. 70% (**Scheme 35**). One detrimental factor to yield was found to be the relatively high volatility of **17**, which noticeably evaporated during concentration of the crude product by rotary evaporator. This effect seemed to be even more pronounced at lower heating bath temperatures, presumably due to prolonged duration of the concentration process. An adequate purification by distillation was not feasible, since residual DMSO was co-distilled at the high temperatures required for distillation (100 °C at 25 mbar), which seemed to be contradictory to the apparent volatility of **17** even at low temperatures.

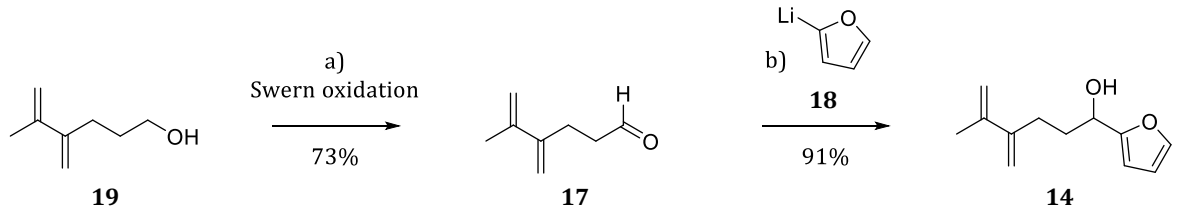

Scheme 35. Transformation of dienyl alcohol **19** to dienyl furfuryl alcohol **14**.

Reagents and conditions: **a)** DCM (0.2 M), $(COCl)_2$ (1.1 eq), DMSO (2.2 eq), –60 °C, then **19** (–75 °C to –60 °C), NEt_3 (5 eq), –75 °C to rt, 50 min; **73%**. **b)** THF (0.16 M), **18** (1 eq, 0.84 M in THF), –78°C to –40 °C, 30 min; **91%**.

Interestingly, the problem of volatility was less noticeable after purification by flash chromatography using a low-polarity eluent (PE/DE, 15:1), indicating a tendency of **17** to *co-evaporate* with polar solvents like DCM instead of a '*true volatility*'. Other observations made later in the doctoral research strongly suggested that many of our compounds tend to retain even volatile solvents like DCM or Et_2O in an unusual extent or, in fact, co-evaporate partially with those solvents. Both effects were found to be especially pronounced in the cases of dienyl alcohol **19** and dienyl aldehyde **17**.

As a general practice, dilution with hexane and co-evaporation of residual polar solvents proved to be highly beneficial and allowed for an efficient removal of solvents even in a comparably weak vacuum. In many cases, this afforded solid products from otherwise oily compounds retaining minute amounts, barely discernible in NMR, of residual solvents such as DCM or EA.

Presumably, the 'volatility' issue of dienyl aldehyde **17** may also be addressed by such a co-evaporation, which should have a somewhat positive effect on the yield. An extraction process using petroleum ether or hexane instead of DCM seems conceivable, which – based on experiences in other reactions – may also facilitate the removal of DMSO, which should 'prefer' the aqueous phase, from crude **17**.

Next, the furylation of dienyl aldehyde **17** was performed with 2-lithiofuran (**18**) to give dienyl furfuryl alcohol **14** in 91% yield (**Scheme 35** on the previous page). This furylation was conducted at temperatures below –60 °C with either (i) slow addition of 2-lithiofuran to aldehyde **17** or (ii) rapid addition of aldehyde **17** to 2-lithiofuran, both of which resulting in similar yields. An excess of 2-lithiofuran, however, proved slightly detrimental to yield.

The slow addition of an equimolar amount of 2-lithiofuran to aldehyde **17** was chosen as the preferred procedure since potential incomplete conversions could be compensated for by further addition of 2-lithiofuran. This was, however, only the case once and could be traced back to a partially degraded solution of *n*-BuLi (2.25 M instead of 2.5 M). Generally, an occasional titration of stored *n*-BuLi solutions is highly advised, even though an adequate determination of organolithium reagents is more laborious than a 'simple titration' of organomagnesium reagents (aq. HCl & phenolphthalein). For organolithium compounds, GILMAN's double titration method[197] was used, which uses two 'simple titrations' of both an untreated aliquot (determining total base content) and an aliquot treated with an excess of organic halides such as 1,2-dibromoethane (determining base content *without* alkyl lithium reagent). Subtraction of the second titer from the first indicates the concentration of *active alkyl lithium reagent*.

The solubility of 2-lithiofuran was determined to be approx. 0.85 M in THF at room temperature. The slightly yellow solution should be used immediately. A change of color to orange was observed upon prolonged standing, generally resulting in slightly lower yields of **14**.

2.1.2 ACHMATOWICZ Reaction and Cycloaddition to Tricyclic Enone 9

With furfuryl alcohol **14** in hands, we focused our attention on examining the key intramolecular (5+2) cycloaddition of pyranulose acetate **12** to tricyclic enone **9**. For this purpose, furfuryl alcohol **14** had to be transformed to pyranulose **13** first, for which a variation of the ACHMATOWICZ reaction was investigated.

The general, *and partially simplified*, mechanism of the ACHMATOWICZ reaction, also termed ACHMATOWICZ rearrangement, is shown in **Scheme 36**. In 'short,' this reaction represents an oxidative ring cleavage of a furfuryl alcohol **I-181**, generating a hydroxy dicarbonyl **I-183**, which in turn reacts in a ring-closing hemiacetal formation to afford a pyranulose **I-186**. The original method reported by ACHMATOWICZ *et al.* made use of bromine in methanol for the oxidation to **I-183** via a formal 'diacetal' **I-182**.[198] Since then, several alternative oxidative conditions were reported, including those generating intermediate epoxides **I-184** using *m*-CPBA or a combination of TBHP and metal catalysts such as $VO(acac)_2$.[199,200] Notably, the latter combination, representing the classical SHARPLESS epoxidation of allylic alcohols,[201–203] emerged as a well-suited method for an efficient ACHMATOWICZ reaction when other oxidation-sensitive functional groups are present, as discussed below. Mechanistically, this vanadium-catalyzed epoxidation is thought to involve several equilibria, catalytic species and intermediates,[204,205] the discussion of which is omitted in this work. Generally, the hydroxy group of the furfuryl alcohols **I-181**, formally representing allylic alcohols, allows for interactions with the vanadium catalyst and thus directs the epoxidation in a highly regio- and diastereoselective fashion.

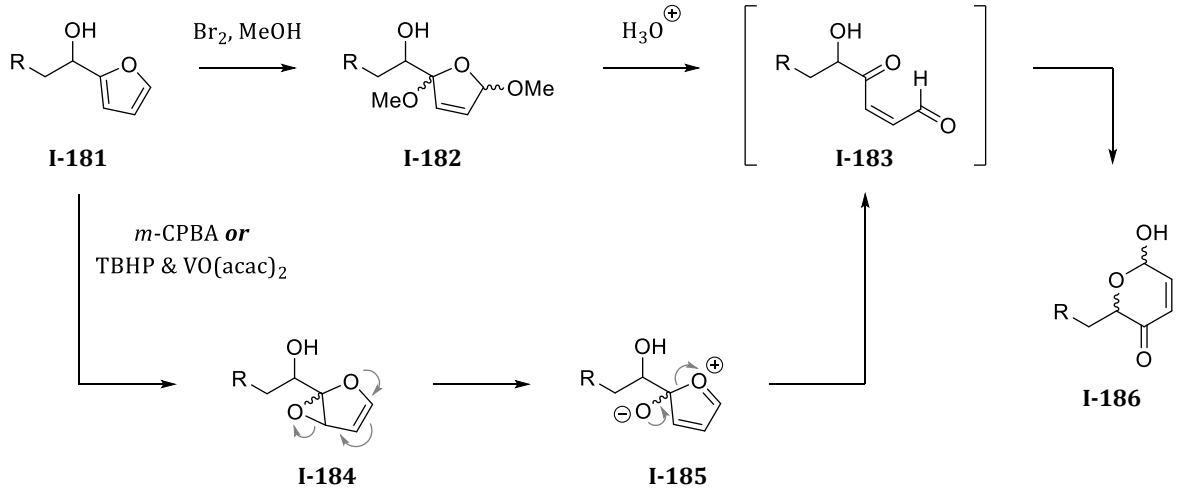

Scheme 36. ACHMATOWICZ reaction of a furfuryl alcohol **I-181** to a pyranulose **I-186**.

SAMMES *et al.* reported that their furfuryl alcohol substrates with electron-rich alkenes or dienes (such as **I-187** or **I-188** in **Figure 12**) led to selectivity problems and poor yields due to concomitant oxidation of the alkene moieties, when 'classic variations' of the ACHMATOWICZ reaction were used (Br_2 in MeOH or *m*-CPBA in DCM). Subsequently, they employed the alternative of a photosensitized oxygenation using *in situ*-generated singlet oxygen, which allowed for a selective oxidative cleavage of the furan moiety.[152,154,155,206]

Due to the laborious procedure of such an oxidation, we opted to apply the variation using TBHP/$VO(acac)_2$ instead, which also proved successful for substrates used in a previous project within our group (**I-189**)[207] or by FERINGA & MINNAARD *et al.* (**I-190**).[208]

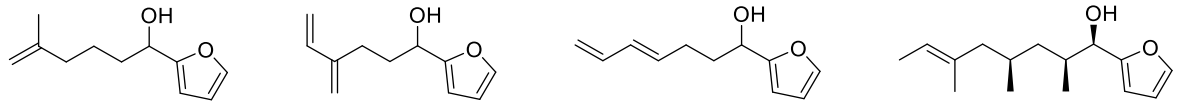

I-187 **I-188** **I-189** **I-190**

Figure 12. Selection of furfuryl alcohols with electron-rich alkenes, requiring more selective variations of the ACHMATOWICZ reaction.

To ensure an efficient oxidation, commercially obtained $VO(acac)_2$ was recrystallized from chloroform[209] and a *3 M solution of TBHP in DCM* was prepared by extraction of aqueous TBHP,[210,211] subsequently drying the extract by storing it over 4 Å MS. For determination of peroxide concentration, iodometric titration was carried out by reducing an aliquot of the peroxide solution with 1 M $Na_2S_2O_3$ until the dark-blue color, resulting from addition of potassium iodide and starch, dissipated. In some cases, additional catalytic amounts of $(NH_4)_6Mo_7O_{34}\cdot 4H_2O$ and sulfuric acid were added to facilitate the oxidation process of iodide to iodine – this, however, seemed unnecessary in the present case of iodometric titration. The determined titer confirmed a concentration of 3.0 M in all cases. More meticulous methods of drying the peroxide solution or determining the concentration, both described by SHARPLESS *et al.*,[203,212] were not deemed necessary, since this variation of the ACHMATOWICZ reaction is known to be not overly sensitive to water or small deviations of peroxide equivalents.

Early attempts of the ACHMATOWICZ reaction with our substrate **14,** as well as the subsequent acetylation of the obtained pyranulose **13** to its acetate **12**, could be realized in moderate yields of 40–60% and 56–76%, respectively (**Scheme 37**). The two diastereomers of **12** could be separated to an extent, but no efforts were made to assign the spectra to the respective *syn*- or *anti*-diastereomer. The lack of diastereoselectivity was deemed inconsequential for the following cycloaddition reaction, as discussed later.

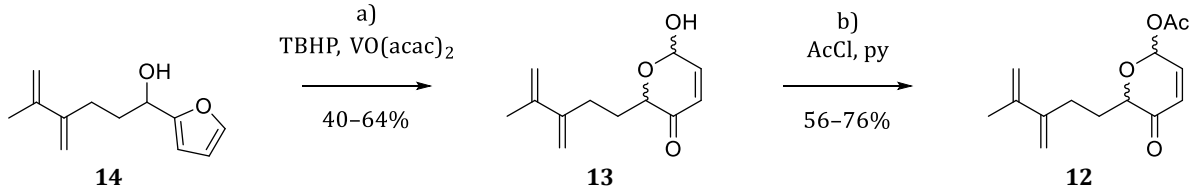

Scheme 37. Two-step synthesis of pyranulose acetate **12** via isolated pyranulose **13**.

Reagents and conditions: **a)** DCM (0.1 M), $VO(acac)_2$ (≤5 mol%), TBHP (3 M in DCM, 1.2–1.5 eq), 0 °C to rt, 3.5–16 h; **40–64%**. **b)** DCM (0.15 M), py (1.5 eq), acetyl chloride (1.3 eq), 0 °C to rt, 1 h; **56–76%**.

Alongside moderate yields, a pronounced irreproducibility was evident, which was soon identified to stem from the lability of both the acetylated and, especially, the 'unprotected' pyranulose. This became increasingly obvious as stored samples of **12** and **13** degraded over time. This was observed both in solution (TLC analysis solutions stored at room temperature) and with purified samples (stored at –28 °C). Especially pyranulose **13** was found to poly- or oligomerize, resulting in mostly insoluble, inhomogeneous mixtures. Consequently, we examined procedures which would minimize this undesired polymerization and allow for an efficient transformation of **14** to **12**.

When *crude* pyranulose **13** was acetylated, the yield of **12** improved to 52–57% (over 2 steps), which also proved more reproducible than prior yields of 22–49% (over 2 steps) via *isolated* pyranulose **13**. Still, this improvement was not yet satisfactory.

Further improvements were ensured by developing a *one-pot synthesis* of **12**. This approach was also inspired by a one-pot procedure by BENKOVICS & BLACKMOND *et al*[205] which was reported alongside mechanistic studies of the vanadium-catalyzed ACHMATOWICZ reaction. Therein, an acetylation reaction was conducted directly after *in situ* generation of pyranulose **I-192** and quenching excess peroxide with trimethyl phosphite, giving the products in good yields (75% of **I-193.a** *or* 70% of **I-193.b**; **Scheme 38** on the next page). This procedure was adapted in our work with minor adjustments, most notably using $VO(acac)_2$ instead of $VO(O\textit{i}\text{-}Pr)_3$, as well as adding pyridine in the acetylation step. BENKOVICS & BLACKMOND *et al.* claimed $VO(O\textit{i}\text{-}Pr)_3$ superior to $VO(acac)_2$, explained by the weaker inhibitory effect of the formed *t*-BuOH on the former vanadium catalyst. In our work, no comparison of these catalysts was pursued.

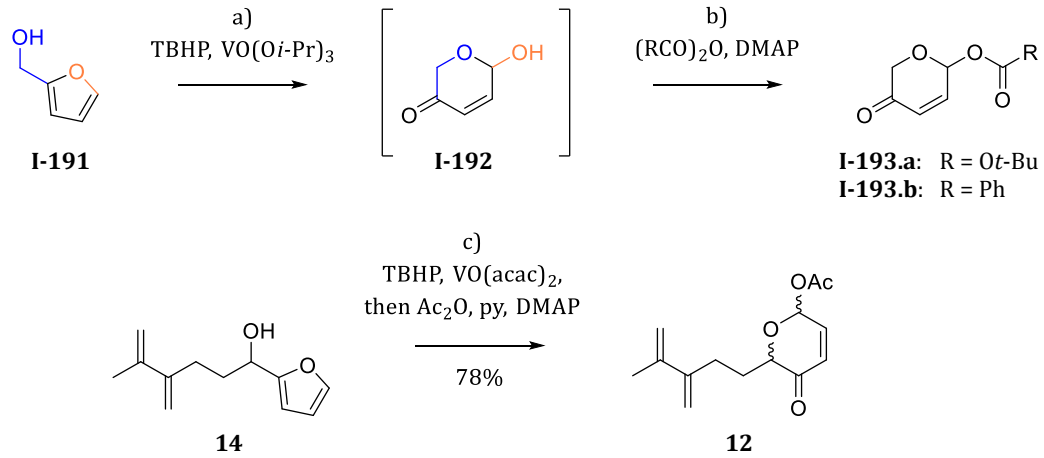

Scheme 38. One-pot synthesis of **I-194.a** and **I-194.b** reported by BENKOVICS & BLACKMOND *et al*[205] and our adaption of this procedure for a *one-pot synthesis* of pyranulose acetate **12**.

Reagents and conditions: **a)** DCM (0.46 M), $VO(O\textit{i}\text{-}Pr)_3$ (2 mol%), TBHP (~5.5 M in decane, 1.25 eq), 10 °C to rt, 4 h; $P(OMe)_3$ (0.4 eq). **b)** Boc_2O ***or*** $(PhCO)_2O$ (1.2 eq), DMAP (3 mol%), 5 °C, 15 min; **I-194.a** (**75%**) ***or*** **I-194.b** (**70%**). **c)** DCM (0.09 M), $VO(acac)_2$ (4.4 mol%), TBHP (~5.5 M in nonane, 1.3 eq) 0 °C to rt, 5.5 h; $P(OMe)_3$ (0.4 eq), 0 °C, 1 h; then 1,4-hydroquinone (trace), DMAP (5 mol%), py (1.3 eq), Ac_2O (1.2 eq), 0 °C, 30 min; **78%**.

Early attempts of this one-pot synthesis of **12** were conducted as a part of F. VÖHRINGER's B. Sc. thesis[213], during which an initial yield of 45% was increased to 73% (from **14**), likely resulting from minimizing stirring time before acetylation (5.5 h vs. 17 h).

In later experiments, adding a 'trace' amount of hydroquinone (<5 mol%) proved both to slightly raise yield (78%) and also allow for prolonged stirring before acetylation (up to 21 h) without significant detriment to yield. Hydroquinone was also used to stabilize purified **12** and did not affect the following cycloaddition in either a negative or positive way.

To conclude, combining the ACHMATOWICZ and acetylation reactions in a one-pot procedure enabled a much more efficient synthesis of **12** from **14** by minimizing polymerization, resulting in 78% yield (one-pot, *effectively over 2 steps with an average yield of 88%*) instead of the initial yield range of 22–49% (over 2 steps). Additionally, this one-pot synthesis was found to be reproducible even in larger scales (77% from 71 mmol (13.66 g) **14**), while consecutive reactions tended to give lower yield with increasing scale.

En route to tricyclic enone **9**, only the cycloaddition of pyranulose acetate **12** remained. Generally, both *pyranuloses and pyranulose acetates* such as **13** and **12** can undergo cycloaddition reactions – in some cases, however, with *pronouncedly different outcomes* depending on a potential ambivalent nature of the (di)enophile and the rate of oxidopyrylium formation. In a former project within our working group, heating pyranulose **I-194** gave *cis*-decalone **I-196** by an *intramolecular DIELS-ALDER (IMDA) reaction*[214,215] and subsequent acetal opening of **I-195** (**Scheme 39**). Higher substituted and 'shorter' (pentadienyl- instead of hexadienyl-tethered) substrates gave similar [4+2] cycloadducts (i.e., **I-197** and **I-198**).[207]

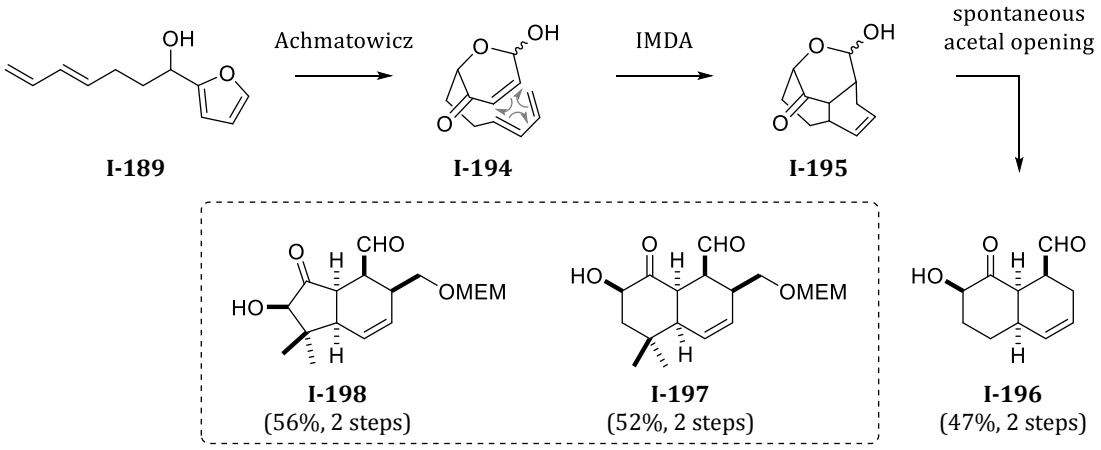

Scheme 39. IMDA reaction of pyranuloses to *cis*-decalones by RICHTER & MAIER *et al.*[207]

On the other hand, *pyranulose acetates* generally do not undergo [4+2], but (5+2) cycloadditions instead, as was covered in detail in **Chapters 1.3.1** and **1.3.2**. When pyranulose acetate **12** was heated with triethylamine in acetonitrile, tricyclic enone **9** was obtained as a single diastereomer in 74% yield (**Scheme 40** on the next page). Falling in the yield range reported by SAMMES *et al.* for similar products (61–75%, *cf.* **Scheme 25** on page **39**), alternative reagents and conditions were only investigated sparingly. Without heating, the cycloaddition proceeded slowly (~80% conversion after 7 d). With the stronger amidine base DBU, complex mixtures were obtained, which may be attributed to using *excess* DBU (2 eq).

MITCHELL *et al.* emphasized the importance of using DBU in only an equimolar amount to avoid complex mixtures.[216] Furthermore, they found quinuclidine (4 eq) to be superior to other bases. The second-best base proved to be NMP (4 eq), which was also used in their more recent publications.[217]

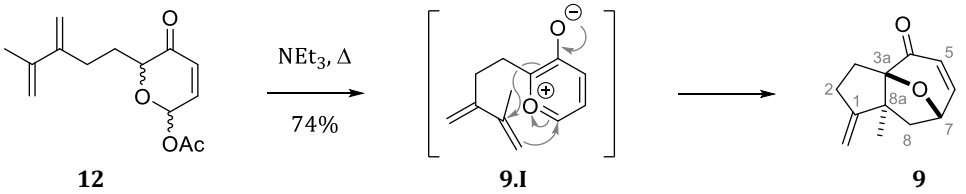

Scheme 40. Intramolecular oxidopyrylium (5+2) cycloaddition to tricyclic enone **9**.

Reagents and conditions: MeCN (0.09 M), NEt_3 (4 eq), 90 °C, 17 h; **74%**.

Using a *diastereomeric mixture* of pyranulose acetate **12** was expected to be inconsequential to the cycloaddition due to the formation of the planar oxidopyrylium **9.I**. While the yield did not differ significantly within experiments in which the diastereomers were used separately, it was observed that the *syn*- and *anti*-diastereomers of **12** did require different reaction times. With the *minor, more polar diastereomer*, full conversion proved noticeably faster than with the *major, less polar diastereomer*. The exact time required was not determined, but after heating for 2 h, the *minor diastereomer* was no longer discernible by NMR, while additional heating for 4 h was still insufficient to fully convert the *major diastereomer* (**9**/**12** = 1:0.11).

TANTILLO & MITCHELL *et al.* identified the rate determining step in this cycloaddition to be the deprotonation of the carbonyl α-H, which is followed by a fast elimination of acetate to generate the aromatic oxidopyrylium.[218] Previous mechanistic studies by MITCHELL *et al*[216] indicated a faster deprotonation for *syn*-pyranulose acetates, explained by steric repulsion between relatively bulky amine bases and the *pseudo*-axial acetate group in the *anti*-diastereomer. Their proposed mechanistic pathway, adapted for *syn*- and *anti*-**12**, is depicted in **Scheme 41**. Consequently, the major, slower-reacting, diastereomer should correspond to *anti*-**12**, while the minor, faster-reacting, diastereomer should correspond to *syn*-**12**.

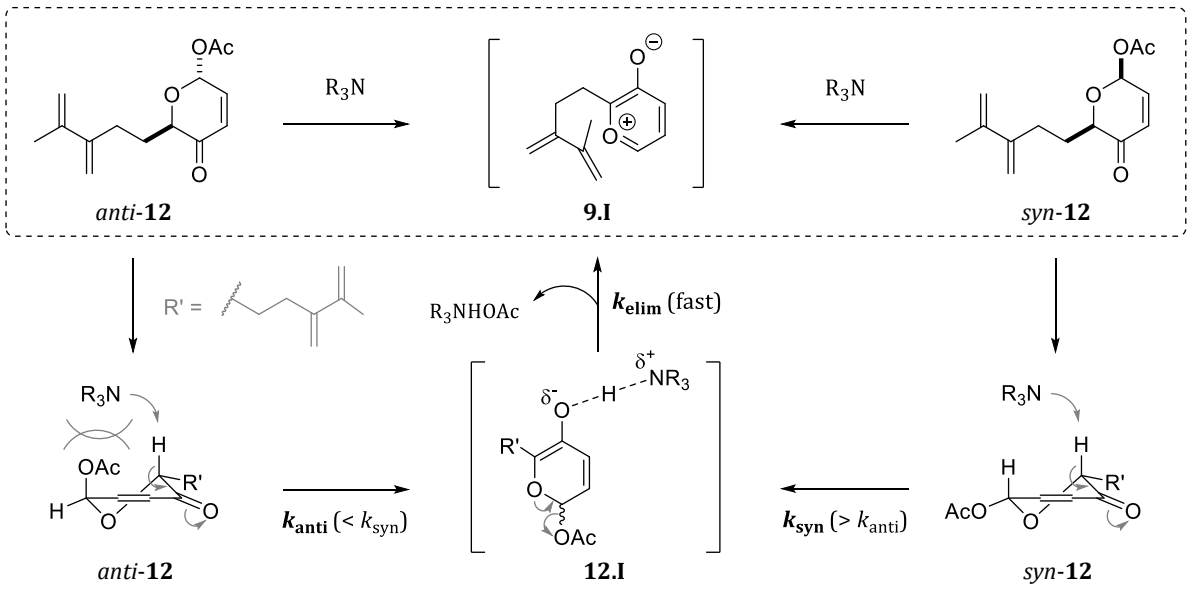

Scheme 41. Proposed pathway,[216] adapted for oxidopyrylium **9.I** from *anti*- and *syn*-**12**.

According to the stereoselectivity observed by SAMMES *et al.,* the methyl group on C8a was expected to assume the depicted *endo*-orientation. The confirmation of this configuration was not trivial but was affirmed unequivocally by X-ray analysis of higher-substituted compounds, as shown later (e.g., **Figure 22** on page **102**). In NOESY-NMR, no cross-peak between the 8a-CH_3 and 7-H was evident. While both are assigned as *endo*-substituents, more precise descriptions would be *pseudo*-axial (8a-CH_3) and *pseudo*-equatorial (7-H). The bent structure of such tricyclic compounds leads to a geometrical relation of these substituents resembling more of an 1,3-*anti*- than an 1,3-*syn*-relationship, and, thus, no NOE is observed.

The analysis of **9** also revealed that the R_f value of **9** coincided with that of the *less polar diastereomer* of **12**. An adequate resolution in TLC was only achieved by eluting the same TLC plate repeatably (e.g., 2–3 times in PE/DE, 3:1), a practice which also proved helpful in several other cases. Furthermore, the methylene protons of **9** appeared as relatively inconclusive multiplets due to superimposition in ^{1}H NMR. Measurements in C_6D_6 instead of $CDCl_3$ resulted in better separation of the signals, allowing for an easier assignment. This solvent effect was observed in several tricyclic compounds and can be seen in **Figure 13**.

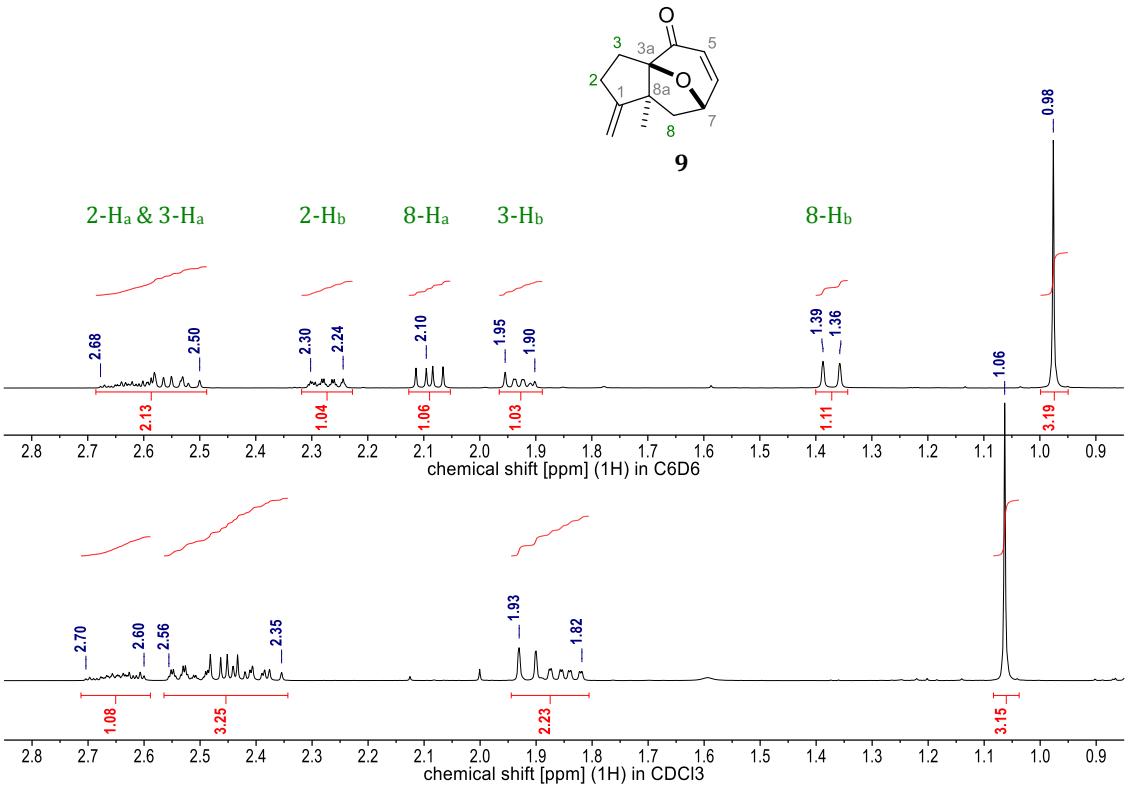

Figure 13. Section of methylene protons in the ^{1}H NMR spectra of tricyclic enone **9** (400 MHz; upper: C_6D_6; lower: $CDCl_3$). The full spectra can be seen in the **Appendix**.

In general, the diastereotopic protons of the tricyclic compounds lead to other noticeable effects, such as:

- large chemical shift differences between protons bound to the same carbon atom [e.g., 8-H_a (1.38 ppm) and 8-H_b (2.09 ppm)],
- dissimilar couplings of protons to neighboring protons in ^{1}H-^{1}H COSY spectra [*e.g.*, 8-H_a couples to 8-H_b, but not to 7-H (d, ^2J = 12 Hz); 8-H_b couples to both 8-H_a and 7-H (dd, ^2J = 12 Hz, ^3J = 7.3 Hz],
- often strong one-bond artifacts[219] ($^1J_{CH}$) in ^{1}H-^{13}C HMBC spectra despite of commonly used suppression methods, strong $^2J_{CH}$ couplings, and weak or missing $^3J_{CH}$ couplings [e.g., 3-H_a couples to C1, but not to C4; 3-H_b does not couple to C1, but to C4].

Some of these effects can be attributed to the aforementioned structural properties of the tricyclic compounds, resulting in geometrical relationships which allow or prevent a coupling of the respective nuclei. Additionally, some protons show rather complex signals resulting from higher-order spin systems and superimposition.

This (5+2) cycloaddition concluded the preparation of tricyclic enone **9** in an overall satisfying synthetic route, especially after optimizing the ACHMATOWICZ/acetylation sequence by employing the one-pot method. The route to tricyclic enone **9** will be summarized in **Chapter 3**.

Incidentally, approaches to optimize the cycloaddition may include a more thorough screening of bases like NMP and utilizing other pyranulose esters (e.g., trifluoroacetates or Boc-esters). Furthermore, more recent developments such as the *palladium-catalyzed* method developed by SUGA *et al.* seem promising for a more efficient generation of oxidopyrylium ylides from pyranulose acetates, potentially allowing for higher-yielding cycloadditions.[220,221]

2.2 FUNCTIONALIZATION OF THE EPOXYAZULENE CORE

After the successful synthesis of tricyclic enone **9**, suitable tricyclic precursors for the key skeletal rearrangement to the decalone core structure of salvinorin A (**I-11**) were sought for. The results of the rearrangement reactions will be treated collectively in **Chapter 2.3** but some aspects will be summarized briefly to clarify the build-up of the next chapters.

The epoxyazulene-to-decalone rearrangement reported by SAMMES *et al.* proved a highly challenging endeavor accompanied by several issues with our substrates. A vast portion of our work was dedicated to gaining insights into the LEWIS acid-induced rearrangement, investigating various different routes and substrates as potential answers to these challenges. The presence of the nitrile group, which was to provide a C_1 building block for the lactone in our initial synthetic plan (*cf.* **Chapter 1.3**), was identified as a central problem in the rearrangement. Consequently, compounds without the 6-nitrile group were also synthesized.

For a better overview, the functionalization of the tricyclic core structure will be merged in the following chapters according to *which carbon centers were to be modified*, summarizing central aspects and potential issues for each reaction. Both nitrile-functionalized compounds and compounds lacking the nitrile group will be treated collectively in these subchapters. For a better comparison and a better readability, those two compound classes will be referred to by the prefixes 'cyano' (or suffix '-nitrile') and 'decyano,' where applicable and deemed necessary. Furthermore, compounds which differ only by the presence or absence of the nitrile group will be designated with the same number, adding an '**-H**' as suffix for decyano compounds [e.g., ketonitrile **8** and (*decyano*) ketone **8-H**].

As mentioned in **Chapter 1.3.2**, functionalization reactions on the epoxyazulene core were expected to proceed in an *exo*-selective fashion. Indeed, **exclusive *exo*-selectivity** of newly introduced substituents, preferring to approach from the less-hindered *exo*-face of the tricyclic system, was observed for most reactions. While the configuration of some compounds could not be determined *unambiguously* by (NOESY-)NMR initially (as mentioned for tricyclic enone **9**), X-ray analysis of higher-functionalized analogs corroborated the *exo*-selectivity in all cases. Similar observations were reported by SAMMES *et al.* for functionalization of C6 or C4 – with one important exception within their published work, as will be discussed in **Chapter 2.3**.

Next to the summaries within the respective chapters, **Chapter 3** will provide a condensed summary which collectively covers (i) the synthesis of tricyclic enone **9**, (ii) the functionalization of this epoxyazulene core, and (iii) the rearrangement of epoxyazulenes to decalones.

2.2.1 Functionalization Reactions at C5 and C6

En route to functionalized cyano and decyano substrates, tricyclic enone **9** was first transformed to either ketonitrile **8** (**Scheme 42**) or ketone **8-H** (**Scheme 43** on the next page). For the 1,4-hydrocyanation, we opted for the LEWIS acid-mediated 1,4-addition of TMSCN to enone **9** since initial synthesis plans included using silyl enol ether **33** as an enolate equivalent of ketonitrile **8**. According to UTIMOTO *et al.,* this 1,4-addition is thought to proceed via the initially formed 1,2-adduct (i.e., **32**) and a subsequent 'replacement' of the introduced nitrile group by another equivalent of TMSCN to give the thermodynamically favored 1,4-adduct (i.e., **33**).[222]

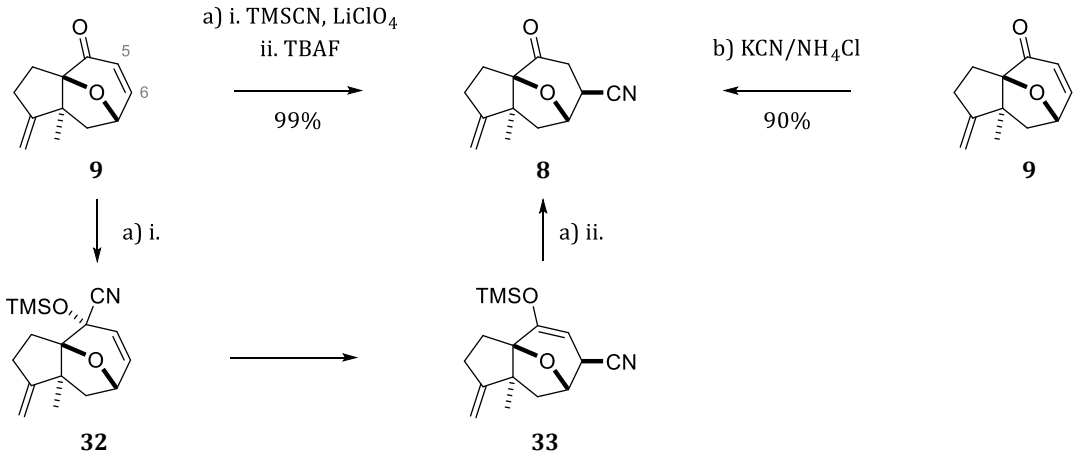

Scheme 42. 1,4-Hydrocyanation of tricyclic enone **9** to ketonitrile **8**.

Reagents and conditions: **a) i.** *no solvent*, TMSCN (4 eq), $LiClO_4$ (5 mol%), 80 °C, 4 h; removal of TMSCN in vacuo; **ii.** THF (0.21 M), TBAF (1 M in THF, 0.33 eq), –78 °C to –30 °C, 45 min; **99%**. **b)** DMF/H_2O (9:1, 0.1 M), NH_4Cl (1.2 eq), KCN (1.6 eq), rt, 25 h; **8** (**90%**) & remaining **9** (**5%**).

A crucial aspect of the 1,4-addition of TMSCN to enone **9** was the exclusion of solvents, which are known to be detrimental to yield.[222,223] With optimized conditions, only silyl enol ether **33** was discernible in TLC and NMR. Removal of excess TMSCN using the vacuum pump connected to the Schlenk line, co-evaporating residual TMSCN with THF, yielded an off-white solid of practically pure **33**. In initial attempts, the surprisingly stable adducts **32** and **33** were isolated by chromatography with little hydrolysis. Incidentally, even the addition of water in the presence of $LiClO_4$ or iodine did only partially hydrolyze the adducts.

Yet, even 0.33 equivalents of TBAF were sufficient for a fast and clean desilylation at –50 °C, affording ketonitrile **8** in quantitative yield. The use of *substochiometric* amounts was prompted by reports on the desilylation of alkynes,[224,225] indicating that the generally employed (over-)stoichiometric amounts of TBAF might be unnecessary and even disadvantageous in some cases. It has to be considered that commercially obtained TBAF solutions do not contain anhydrous TBAF, which is known to be highly unstable.[226] Instead, such solutions contain water (~5 w-%) and most certainly consist of TBAF·$3H_2O$, which can further promote desilylation.

Another 'more classical' 1,4-hydrocyanation method was briefly investigated in later phases of the project. Using KCN and NH_4Cl in aqueous DMF[227,228] afforded a colorless solid, which consisted of ketonitrile **8** (90% yield) and remaining enone **9** (5%), as indicated by quantitative NMR.<13> This much simpler method, which was not optimized, represents a suitable alternative, when ketonitrile **9** instead of silyl enol ether **33** is aimed for.

For the conjugated reduction of enone **9**, diphenylsilane with catalytic amounts of palladium(0) and zinc chloride was used (**Scheme 43**). This procedure, originally reported by KEINAN *et al.*,[229,230] was also used by SAMMES *et al.* on the similar tricyclic enone lacking only the 8a-methyl group (**I-162** in **Scheme 25** on page **39**; 86% yield).[155] With our enone **9**, ketone **8-H** was obtained in quantitative yields with traces of arylsilicon species co-eluting with **8-H**. The yield seemed to be only limited by minor impurities, generally resulting in yields of over 95%.

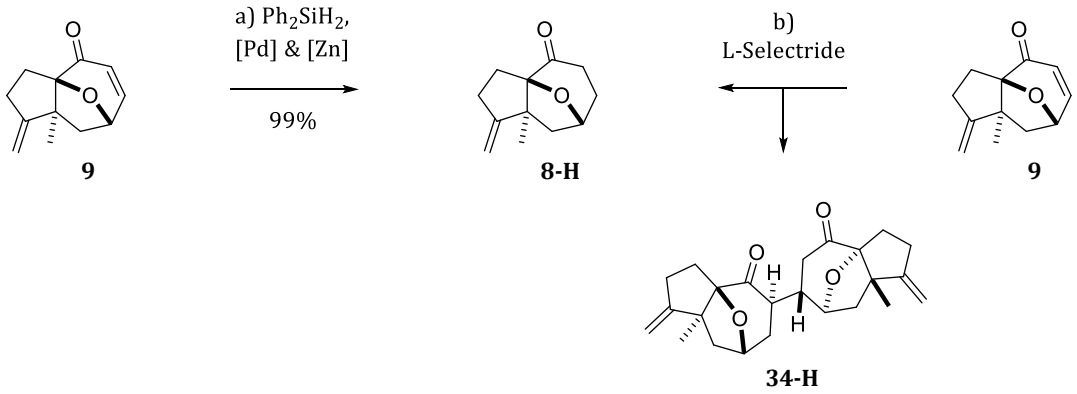

Scheme 43. Conjugated reduction of tricyclic enone **9** to ketone **8-H**.

Reagents and conditions: **a)** $CHCl_3$ (0.17 M), $ZnCl_2$ (25 mol%), Ph_2SiH_2 (1.2 eq), $Pd(PPh_3)_4$ (2 mol%), rt, 15 min; **99%**. **b)** THF (0.06 M), L-Selectride (1.05 eq), –78 °C to –65 °C, 15 min; **8-H** (**49%**) & **34-H** (**33%**).

Highest yields were obtained with $CHCl_3$ as solvent and when $ZnCl_2$ (25 mol%; superior to 10 or 50 mol%) was *allowed to become slightly wet*. KEINAN *et al.* highlighted that this reduction does not have to be conducted in an inert atmosphere and with dry reagents, with completely anhydrous conditions being detrimental to yield.[229–231] Similarly, $CHCl_3$ was claimed the best solvent, as was also observed in our case: using DCM instead led to unclean and much slower conversion (1 d instead of 15 min), presumably due to poor solubility of $ZnCl_2$ in DCM.

The conjugate reduction was also attempted with L-Selectride[232] earlier, but resulted in only 49% yield of ketone **8-H** – accompanied by formation of the dimer **34-H** (33% yield) resulting from MICHAEL addition of the lithium enolate to enone **9**. Dimer **34-H** presumably adopts the depicted configuration due to *exo*-selective functionalization on the tricyclic core.

<13> Quantitative NMR (qNMR), identified as a very useful analysis method in later stages of our research, was conducted with 1,3,5-trimethoxybenzene (abbreviated as TMOB) as internal standard (*cf.* **Chapter 4.0.4**).

Next, we investigated functionalization at C5 with the overall goal of establishing an *endo*-methyl and an *exo*-2-(3-furanyl)-2-ethanol group (**Scheme 44**). Considering the mentioned *exo*-face selectivity, the methyl group would have to be introduced first (**35**). Using the enolate of **35** to open (3-furyl)-oxirane (**36**) should then afford δ-hydroxy nitrile **37** which may either spontaneously form lactone **38** or be converted to it readily. Alternatively, introducing an *exo*-allyl group, subsequent oxidative cleavage to aldehyde **39**, and 3-furylation to **37** or **38** seemed conceivable. The relative configuration of the hydroxy moiety of the furfuryl group was disregarded in the initial planning, since stereoselective methods of 3-furylation have been reported in previous syntheses of salvinorin A (**Chapter 1.2**).

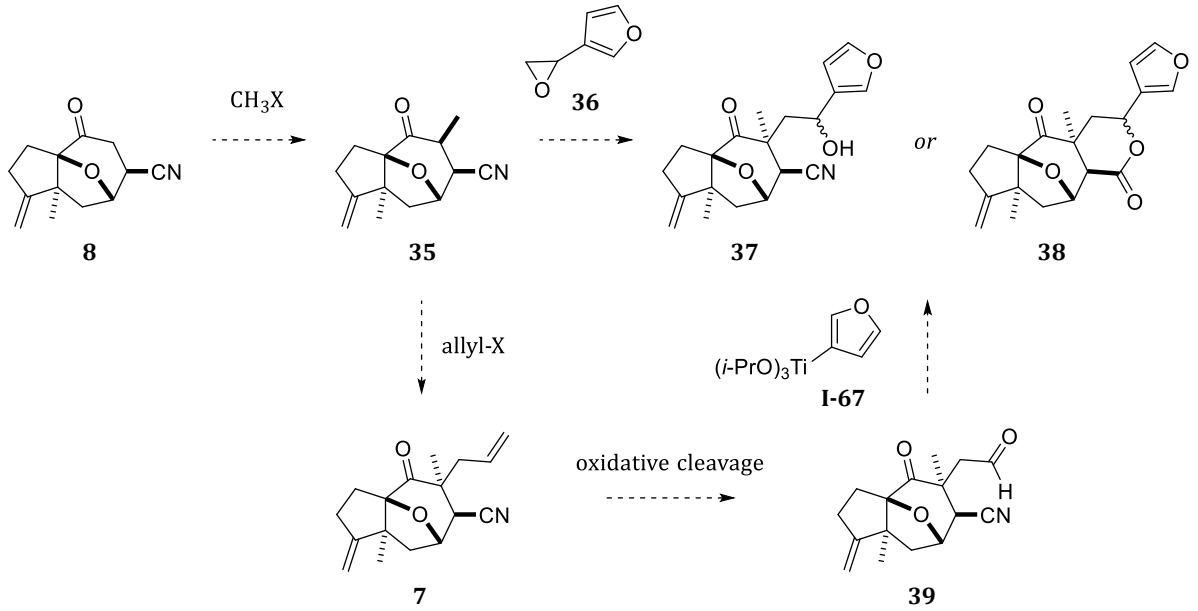

Scheme 44. Initial strategy proceeding from ketonitrile **8** via initial monomethylation.

First examinations of the general reaction behavior of the nucleophiles – i.e., silyl enol ether **33** and enolate **8.M** (generated either from ketonitrile **8** or from silyl enol ether **33**) – with different electrophiles led to rather discouraging results, which are summarized in **Scheme 45** and **Table 1** on the next pages. Nevertheless, constructive insights could be obtained from those attempts, elucidating some interesting traits of the tricyclic core structure.

Simple methylation or allylation attempts using enolate **8.M** (M = Li or K) led to the undesired dialkylated products **35.a** and **35.b**, respectively. Two selective monomethylation methods, using manganese enolates[233] or silyl enol ethers,[234] resulted in no conversion.

Epoxide opening reactions using silyl enol ethers, or their enolates generated by treatment with MeLi,[235] are reported to be especially efficient in the presence of $LiClO_4$.[236–238] To investigate these methods, several variations were tried on 5-unsubstituted substrates first. However, treating silyl enol ether **33** or ketonitrile **8** with strong bases (MeLi or LDA) led to complex mixtures, even before addition of electrophiles (**Table 1**, entries A5, B3, C2). NMR analysis of minor compounds from these complex mixtures indicated a cleavage of the ether bridge, which *ultimately* turned out to be a very serendipitous 'side reaction' for our goals, as will be discussed in detail in **Chapter 2.4**.

Functionalization attempts of the 'naked' enolate by treating silyl enol ether **33** with TBAF, even with only catalytic amounts and addition of molecular sieves, in presence of electrophiles (entries A4 + C1) led to clean desilylation to ketonitrile **8**. For this purpose, other fluoride sources like BTAF may be better alternatives due to the previously mentioned residual water content of TBAF solutions.[239] However, a general prediction of 'best choice reagent' seems not feasible. For instance, aldol reactions with silyl enol ethers were reported to be more efficient when TBAF was used instead of BTAF.[240]

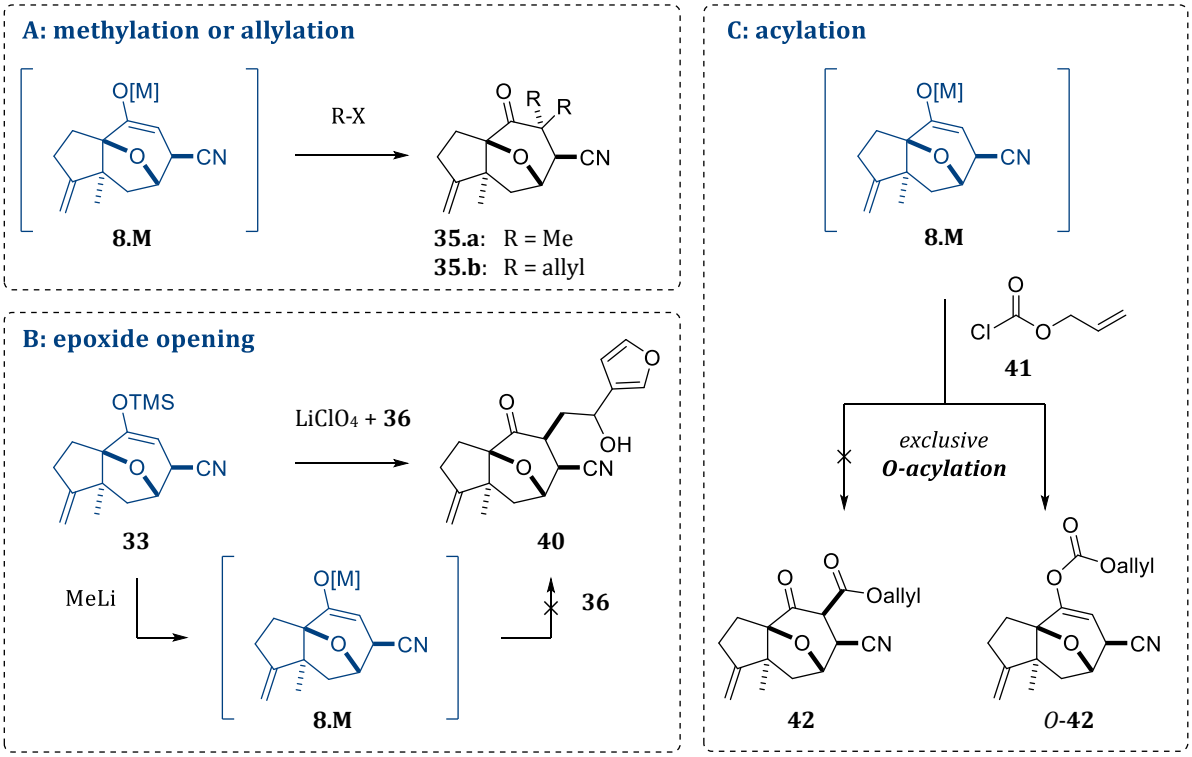

Scheme 45. First attempts of functionalization at C5 including (**A**) methylation or allylation, (**B**) epoxide opening and (**C**) acylation. Details in **Table 1** on the next page.

Table 1. Summary of reactions depicted in **Scheme 45**. Generally, the enolate formation was conducted at –78 °C and the resulting mixture allowed to warm to room temperature. THF was used as solvent if not stated otherwise.

Entry	nucleophile	electrophile (+ additives)	results & remarks
A1	Li-enolate **8.M** (**8** + LHMDS)	MeI (1.3 eq)	**dimethylation** (**35.a**) & recovered **8**
A2	silyl enol ether **33**	MeI (1.05 eq) + CF_3COOAg (1.05 eq)	no conversion
A3	Mn-enolate **8.M** (**8** + LHMDS + $MnBr_2$)	MeI (1.1 eq) or allyl bromide (1.1 eq)	no conversion
A4	silyl enol ether **33**	allyl bromide (1.5 eq) + TBAF (1.1 eq)	**desilylation** to ketonitrile **8**
A5	Li-enolate **8.M** (silyl enol ether **33** + MeLi)	allyl bromide (3 eq)	**cleavage of ether bridge** after addition of MeLi, complex mixture after addition of allyl bromide
A6	K-enolate **8.M** (**8** + KHMDS)	allyl bromide (1 eq)	**diallylation** (**35.b**) & recovered **8**
B1	silyl enol ether **33**	(3-furyl)oxirane (**36**) (1 eq) + $LiClO_4$ (0.05 eq or 3 eq)	complex mixture
B2	Li-enolate **8.M** (silyl enol ether **33** + MeLi)	(3-furyl)oxirane (**36**) (1 eq) + $LiClO_4$ (3 eq)	complex mixtures (tried three times), **cleavage of ether bridge**
B3	Li-enolate **8.M** (silyl enol ether **33** + MeLi)	–	**cleavage of ether bridge**
B4	K-enolate **8.M** (**8** + KHMDS)	(3-furyl)oxirane (**36**) (2 eq) + $LiClO_4$ (3 eq)	recovered ketonitrile **8** (**70%**; after 24 h)
C1	silyl enol ether **33**	allyl chloroformate (**41**) (1.1 eq) + MS 4 Å + TBAF (0.1 eq)	**desilylation** to ketonitrile **8**
C2	Li-enolate **8.M** (**8** + LDA)	allyl chloroformate (**41**) (1.1 eq)	complex mixture, **cleavage of ether bridge**
C3	Li-enolate **8.M** (**8** + LHMDS)	allyl chloroformate (**41**) (1.1 eq)	*O*-acylation (*O*-**42**) (**62%**, 78% *b.r.s.m.*)
C4	Li-enolate **8.M** (**8** + LHMDS)	allyl chloroformate (**41**) (1.1 eq)	solubility problems (in toluene instead of THF), low conversion to *O*-**42**
C5	K-enolate **8.M** (**8** + KHMDS)	allyl chloroformate (**41**) (1.3 eq)	*O*-acylation (*O*-**42**) (**51%**, 83% *b.r.s.m.*)

With these results, the ***initial monomethylation*** of ketonitrile **8** with subsequent *allylation* or *epoxide opening* en route to lactone **38** seemed complicated to ensure, prompting us to investigate more promising approaches. An '***acylation first***' approach was devised with the goal of incorporating a TSUJI-TROST reaction, as will be discussed in the following subchapter. Central to this approach was the preparation of allyl β-ketoester **42**, which initially proved similarly challenging as the other approaches, albeit for other reasons. As summarized in entries C1–C5, acylation of ketonitrile **8** with allyl chloroformate (**41**) proceeded, as one would expect, with monosubstitution. However, only *O-acylation* was observed, affording the undesired allyl enol carbonate *O*-**42** instead of allyl β-ketoester **42**. Consequently, we set out to find alternative reagents and conditions which would allow for a *C-selective acylation* at C5.

2.2.1.1 *C*-Acylation & Methylation at C5 and subsequent TSUJI-TROST Allylation

By finding a selective *C*-acylation method for ketonitrile **8**, the synthesis of allyl β-ketoester **42** was to be achieved (**Scheme 46**). The latter should be methylated readily at C5, affording α-methyl β-ketoester **43** which was to be subjected to TSUJI-TROST allylation. This would effectively 'invert' the C5-configuration by (re-)introducing the allyl group in an *exo*-face selective manner, thus giving rise to the desired 5-*exo*-allyl,*endo*-methyl ketonitrile **7**.

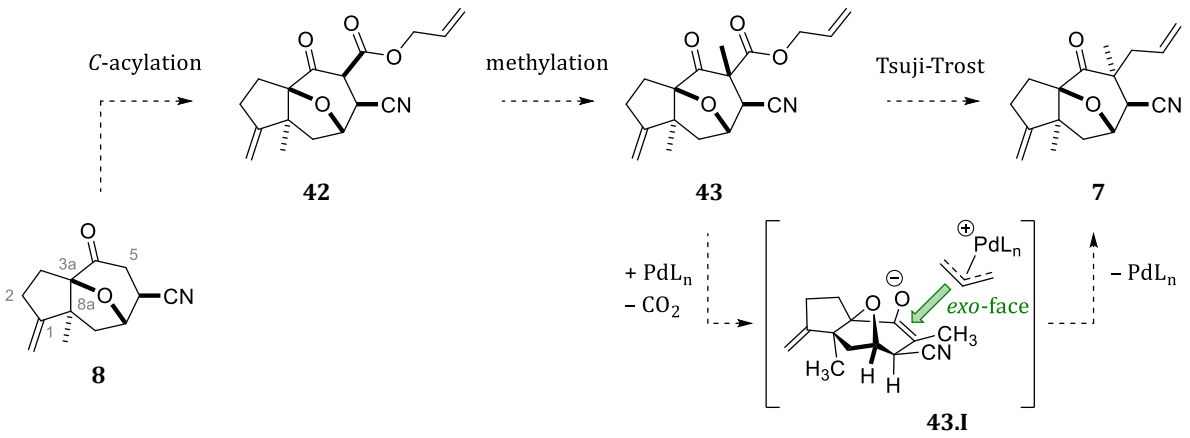

Scheme 46. '*Acylation first*' approach to **7** via TSUJI-TROST allylation. Each reaction should proceed with *exo*-selectivity, affording the desired diastereomer of **7** in the last step.

Coinciding with our quest for reagents which would allow selective *C*-acylation, STOLTZ *et al.* reported such a *C*-acylation with allyl diethylphosphonoformate[241] [APF (**41.a**), **Scheme 47** on the next page]. In their previous work, derivatives of MANDER's reagent (methyl cyanoformate),[242] such as allyl cyanoformate (**41.b**), also proved suitable reagents for this purpose.[243] Another reagent was introduced by TROST *et al.,* incorporating imidazole as the 'leaving group' (**41.c**), which could be used to 'switch' regioselectivity as desired, resulting in selective *O*-acylation *with* $BF_3{\cdot}Et_2O$, and selective *C*-acylation *without* $BF_3{\cdot}Et_2O$.[244]

We were most intrigued by APF (**41.a**), since it represented the STOLTZ group's reagent of choice for the *C*-acylation of cyclohex-2-en-1-one (72% yield)[241] and was, to the best of our knowledge, only used in one previous publication by HANESSIAN *et al.* (same substrate, 61%).[245]
APF, readily prepared by ARBUZOV reaction of allyl chloroformate and triethyl phosphite,[246] was found to be stable to storage without loss of quality for at least several months, allowing for a convenient preparation in advance.

Gratifyingly, only *C*-acylation was observed for both ketonitrile **8** and decyano ketone **8-H** when APF (**41.a**) was employed as acylating reagent (**Scheme 47** and **Table 2** on the next page). For ketonitrile **8**, however, an *efficient* acylation proved to be a formidable challenge which will be discussed integrating both a selection of experiments (7 of 22 reactions, **Table 2**) as well as retrospective insights that elucidated some previously inconclusive aspects.

First attempts at acylating ketonitrile **8** led to rather inconsistent results. Switching the solvent from THF to Et_2O or MTBE *seemed* to give better results, but in all cases most of the substrate remained unchanged (e.g., entries CN-1 to CN-3). Prolonged reaction times or warming the reaction mixture (40–60 °C) were unproductive, leading to decreasing product/substrate ratios (entry CN-3). The addition of $ZnCl_2$ or HMPA led to no or low conversion, respectively. In general, some similarly conducted runs gave P/S ratios ranging from 1:0.35 to 1:7 (not listed).

Considering a *seemingly* reversible product formation (entry CN-2), assumed to be mediated by a retro-CLAISEN addition, the effect of the counter ion (Li or K) was investigated. Concurrently, NMR analysis of APF (**41.a**), which was used without further purification until this point, indicated that the liquid APF retained significant amounts of the formed chloroethane (approx. 0.5 eq), which was henceforth removed in vacuo.

Using KHMDS and 'purified' APF, a more reproducible *C*-acylation of **8** could be ensured. However, a precise evaluation was further complicated by keto-enol tautomerism: β-ketoester **42** showed a strong tendency to isomerize to its enol tautomer *OH*-**42**, which predominates in solution. This was also evident in NMR spectra in which only the enol tautomer was evident (4-OH: δ = 12.4 ppm). As a consequence of this tautomerism, a chromatographic purification proved tedious. Next to excessive broadening of the product fraction, a complete separation from remaining ketonitrile **8**, *eluting amidst the product fraction*, was not feasible within a single column. Using a ternary eluent of PE and a 100:1 mixture of DCM/MeOH (*increasing the eluent polarity gradually*), which enables efficient H-bond interactions between the compounds and the mobile phase, alleviated the separation issue to an extent.

Four acylation reactions with **8** gave (*OH*)-**42**[<14>] in *isolated* yields of 55–64%, whereas a more fitting yield of 80% (85% *b.r.s.m.*) can be asserted, when the mixed fraction is included (entry CN-5). Even higher yields were obtained in the acylation of *decyano* ketone **8-H**, which also provided additional information for the acylation of ketonitrile **8** (entries CN-6 to CN-8) that will be discussed below. In the first attempt (not listed), decyano ketone **8-H** was acylated with the 'optimized' conditions for **8** (entry CN-5), resulting in similar results for (*OH*)-**42-H** (53% isolated yield, additional mixed fraction).

[<14>] The keto and enol tautomers **42** and *OH*-**42** are addressed collectively as (*OH*)-**42**.

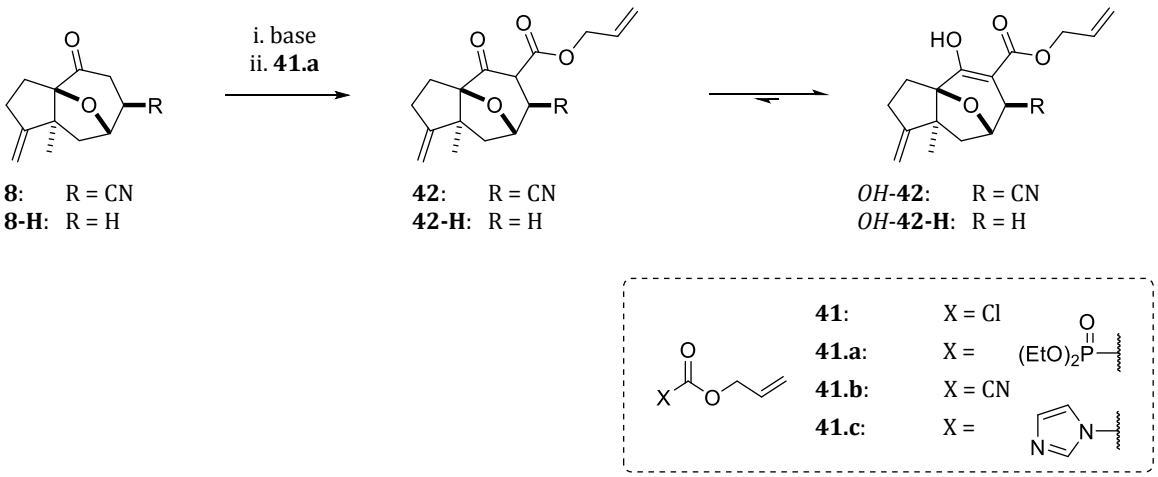

Scheme 47. *C*-selective acylation of ketonitrile **8** and ketone **8-H.** Details in **Table 2**.

Table 2. Selection of reagents and conditions for *C*-acylation of **8** (entries **CN-1–8**) and **8-H** (entry **H-1**). Bases and APF were used as solutions (LHMDS/KHMDS: 1 M in THF, addition over 4–5 min; APF: 25 vol% in the used solvent, addition over 1–3 min). Unless stated otherwise, the quenched mixtures were **extracted with diethyl ether**. The **product/substrate ratios** of crude products, or aliquots taken at the indicated time points, are listed as **P/S** (determined by NMR).

entry	reagents and conditions	results and remarks
CN-1	0.230 mmol, **THF**, **LHMDS** (1.1 eq), –78 °C to 5 °C (2 h); **APF** (1.2 eq), –78 °C to –15 °C (2 h), rt (18 h), 60 °C (3.5 h)	**38%** yield (isolated, 91% *b.r.s.m.*)
CN-2	0.288 mmol, **Et_2O**, **LHMDS** (1.1 eq), –78 °C to –20 °C (1 h), rt (2 h); **APF** (1.5 eq), –60 °C (10 min), rt (42 h)	**55%** yield (isolated, 77% *b.r.s.m.*)
CN-3	0.230 mmol, **MTBE**, **LHMDS** (1.2 eq), –78 °C (30 min), rt (1.5 h); **APF** (1.5 eq), –78 °C (1 h), –78 °C to rt (23 h), 40 °C (5 h), rt (69 h)	low conversion, NMR ratio worse with time: **P/S** = 1:2.13 (after rt, 23 h, aliquot), **P/S** = 1:1.89 (after 40 °C, 5 h, aliquot), **P/S** = 1:5 (crude product); ***extraction with EA***
CN-4	0.460 mmol, **MTBE**, **KHMDS** (1.2 eq), –78 °C to –15 °C (1.25 h), rt (20 min); **APF** (1.5 eq), –78 °C to rt (13 h)	**60 %** yield (isolated); **APF purified** in vacuo from here on
CN-5	0.953 mmol, **MTBE**, **KHMDS** (1.05 eq), –78 °C to –15 °C (1.25 h), rt (20 min); **APF** (1.2 eq), –78 °C to rt (15 h)	**P/S** = 1:0.08; **59%** yield (isolated); **80 %** (85% *b.r.s.m.*), when mixed fraction is included
CN-6	10.444 mmol, **MTBE, KHMDS** (1.1 eq), –78 °C to –45 °C (1 h), rt (30 min); **APF** (1.2 eq), –78 °C to rt (14 h)	**P/S** = 1:0.07; **43%** yield (qNMR)
CN-7	9.219 mmol, **MTBE**, **KHMDS** (1.05 eq), –78 °C to –20 °C (1.5 h), rt (20 min); **APF** (1.2 eq), –78 °C to rt (11 h)	**P/S** = 1:0.16, additional substrate in aqueous phase; **62%** yield (qNMR) from impure **8**; ***extraction with PE***
CN-8	9.942 mmol, same as in entry **CN-7**	**15%** yield (qNMR) from pure **8**; ***extraction with EA***
H-1	2.601 mmol, **MTBE**, **KHMDS** (1.1 eq), –78 °C to –40 °C (1 h), rt (30 min); **APF** (1.2 eq), –78 °C to rt (22 h)	methylated without isolation, good and reproducible yields, even with substrate **8-H** (5–10%) remaining: (**75–78%** over 2 steps, **87% yield for *C*-acylation**); ***extraction with EA***

To omit a tedious chromatographic purification, bulb-to-bulb distillation (*Kugelrohr* distillation) was implemented to remove phosphorous-based impurities from the crude acylation product. This enabled an acylation/methylation sequence, as discussed below. For decyano ketone **8-H**, this sequence resulted in satisfying yields of 75–78% over 2 steps (79–87% *b.r.s.m.*). Calculating back with the methylation yield for isolated (*OH*)-**42-H** (86%), the *C-acylation was determined to effectively result in 88% yield* (entry H-1). This yield, especially when the additionally recovered substrate is factored in, highlights the efficiency of *C*-acylation with APF.

In later runs, the *C*-acylation conditions optimized for **8-H** (entry H-1) were applied to ketonitrile **8** in higher-scale experiments. Doing so, however, led to noticeably lower yields than in earlier, smaller-scale runs (entry CN-6 vs. entry CN-5). With these or similar conditions several higher-scale acylations of ketonitrile **8** resulted in rather moderate yields of 42–53% (determined by qNMR, not listed) with up to 35% of remaining substrate.

Meticulous reexamination of the results from previous *C*-acylation reactions raised the suspicion that firstly, and more obviously, the *enolate mixture* would have to be allowed to warm for a longer period of time. Secondly, *extraction with ethyl acetate* was a common factor in less successful acylations and was suspected to, somehow, have led to low yields (*e.g.*, entry CN-3).

Consequently, the last two experiments were conducted simultaneously, repeating the procedure listed in entry CN-5 – then, one was extracted with petroleum ether, and the other with ethyl acetate. In fact, this led to an unexpectedly striking difference in yield [62% with PE (from impure **8**), entry CN-7 vs. 15% with EA (from fractionally crystallized **8**), entry CN-8], even though the TLC plates *before* work-up were practically indistinguishable from each other. In the latter crude product, only 15% of (*OH*)-**42**, 7% of ketonitrile **8**, and no indication of *distinct* side products were evident in the complex mixture. In hindsight, the often observed 'low conversion,' initially thought to have resulted from retro-CLAISEN addition can be attributed to *decomposition* of the product instead.

This drastic decomposition 'effectuated by ethyl acetate' lacks a conclusive explanation. Yet, it was evident that the crude product from the extraction with PE was barely contaminated with phosphorus-based impurities, exhibiting only small peaks at $\delta = 28$ and -10 ppm in ^{31}P NMR. The crude product from extraction with EA, however, revealed large amounts of *other* impurities with primarily one intensive signal at $\delta = 8$ ppm in ^{31}P NMR. The latter impurities were also evident in crude products of decyano analog (*OH*)-**42-H**, which were extracted with EA in most cases – however, the presence of these impurities did not seem detrimental to the yield of (*OH*)-**42-H** judging by the high two-step yield after removal of the impurities by *Kugelrohr* distillation and subsequent methylation.

Another crucial aspect, the *incomplete conversion* of the *C*-acylation reaction, is explicable by incomplete formation of the respective enolates of **8** and **8-H**. This becomes especially apparent when comparing entries CN-5 and CN-7, which were essentially conducted in the same manner. Nevertheless, a higher amount of unreacted substrate was present in the latter crude product. Additionally, some substrate remained in the aqueous phase due to the incomplete extraction of the considerably polar ketonitrile **8** with petroleum ether.

This comparably lower conversion most likely was a consequence of the larger scale (entry CN-5: 0.953 mmol, entry CN-7: 9.219 mmol) and the decision to limit the period of time for which the enolate mixture was allowed to warm to ambient temperatures after removing the cooling bath. However, the tenfold increase in scale logically necessitates a longer warming time to effectively reach the same internal reaction temperature. This strongly suggests that the enolate mixture should be allowed to stir at room temperature until *full enolate formation* is achieved, which incidentally seems to be slower for ketonitrile **8** than for decyano ketone **8-H**.

Throughout most of our work, we kept this period as short as possible to prevent the previously broached side reactions resulting from base-induced cleavage of the ether bridge, which will be discussed in more detail in **Chapter 2.4**. In retrospect, it became successively evident that this cleavage does not pose a significant problem when KHMDS or LHMDS, even in small excess (≤1.2 eq), is used instead of stronger bases like LDA. Therefore, it is advised to stir the enolate mixture at room temperature for about 1–1.5 h in higher-scale acylations of ketonitrile **8**.

To conclude briefly, the *C*-acylation with APF (**41.a**) proved very satisfactory considering the prior challenges of C5-functionalization. Integrating the detailed findings, decyano ketone **8-H** could be acylated to (*OH*)-**42-H** with 87% yield, whereas ketonitrile **8** was acylated to (*OH*)-**42** with a slightly lower yield of 80%. In both cases, some substrate remained and was recoverable, which was pronouncedly easier after the methylation since a chromatographic separation after acylation was impeded by keto-enol tautomerism. For high yields in the acylation step, ensuring adequate enolate formation and refraining from using ethyl acetate for the extraction proved crucial, especially for the acylation of ketonitrile **8**. Instead, extractions with diethyl ether or petroleum ether are strongly advised. While petroleum ether proved suitable for limiting phosphorous-based impurities promoting a decomposition of (*OH*)-**42**, petroleum ether alone is not able to fully extract unreacted ketonitrile **8**. Therefore, an extraction with diethyl ether or a mixture of PE/DE should be considered for acylations experiments with potentially incomplete conversions resulting from an inadequate enolate formation.

The *C*-methylation of β-ketoesters (*OH*)-**42** and (*OH*)-**42-H** with Cs_2CO_3 and methyl iodide resulted in good yields (**Scheme 48**).[<15>] However, some *O*-methylation was observed for cyano β-ketoester (*OH*)-**42**, giving both **43** (75% yield) and *OMe*-**43** (11% yield). With decyano β-ketoester (*OH*)-**42-H** afforded **43-H** in 85% yield with no discernible *O*-methylation. Changes in reagents and conditions for (*OH*)-**42**, such as using DMF instead of acetone, K_2CO_3 or DBU instead of Cs_2CO_3, or conducting the reaction at different temperatures (0 °C or 50 °C) did not result in significantly different outcomes. While addition of HMPA (e.g., NaH, HMPA & MeI in THF) can shift the selectivity towards *C*-methylation in some cases,[247,248] such optimization attempts were not pursued in our work.

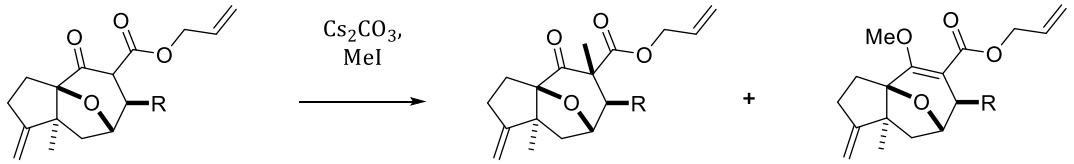

(*OH*)-**42**: R = CN
(*OH*)-**42-H**: R = H

43: R = CN
43-H: R = H

OMe-**43**: R = CN
OMe-**43-H**: R = H

Scheme 48. *C*-Methylation of cyano or decyano β-ketoesters **42** or **42-H**.

Reagents and conditions: acetone (0.2–0.3 M), Cs_2CO_3 (1–2 eq), rt, 30 min, then MeI (2–3 eq), 3–15 h;
with (*OH*)-**42**: **43** (**75%**) & *OMe*-**43** (**11%**); with (*OH*)-**42-H**: **43-H** (**85%**).

As mentioned before, the methylation was later conducted as a two-step sequence with crude acylation products purified by *Kugelrohr* distillation. This much more convenient sequence had no significant impact on the yield of methylation in either way.

However, the required amounts of reagents depended on the amount of residual phosphorus-based impurities from the prior acylation reaction. Especially the impurities extracted with ethyl acetate seemed to efficiently inhibit the methylation reaction even in small amounts, making higher equivalents of both reagents and a prolonged reaction time necessary for complete conversion. While *Kugelrohr* distillation was sufficient to obviate this problem, the best approach is to *simply refrain from using ethyl acetate* altogether. Doing so, less equivalents of Cs_2CO_3 could be used and, consequently, more ketone substrate (**8** or **8-H**) remaining from incomplete acylations could be recovered.

[<15>] These 'β-ketoesters' are intended to also represent their respective enol tautomers. Furthermore, the relative stereochemistry at C5 is not depicted, as tautomerism could result in epimerization.

For the last step of our '*acylation first*' approach, the TSUJI-TROST reaction was examined. In general, this reaction leverages the readiness of palladium catalysts to form cationic allyl complexes, as already indicated in **Scheme 46** on page **69**. These allyl palladium complexes can be generated from several olefinic substrates and can be attacked by a variety of nucleophiles. This versatility, combined with excellent regio- and stereocontrol, established the TSUJI-TROST reaction as a powerful method incorporated in a plethora of both racemic and asymmetric total syntheses.[249–252] One variation of this reaction uses allyl β-ketoesters (**I-199**) or allyl enol carbonates (**I-200**) in a *decarboxylative allylic alkylation*<16> in which both the nucleophile and the electrophile originate from the substrate (**Scheme 49**).[253] Both substrates generate enolate **I-203** via decarboxylation, which recombines with the π-allylpalladium complex to give allylated ketone **I-204** and regenerate the catalyst. Notably, both Pd(0) and Pd(II) (pre-)catalysts can be used in the TSUJI-TROST allylation. For STOLTZ *et al.,* $Pd(OAc)_2$ proved superior to $Pd_2(dba)_3$ in their asymmetric method, explained by "the lack of dba in the reaction mixture, which would likely result in trapped Pd(0)-olefin species that lie outside of the catalytic cycle."[254,255]

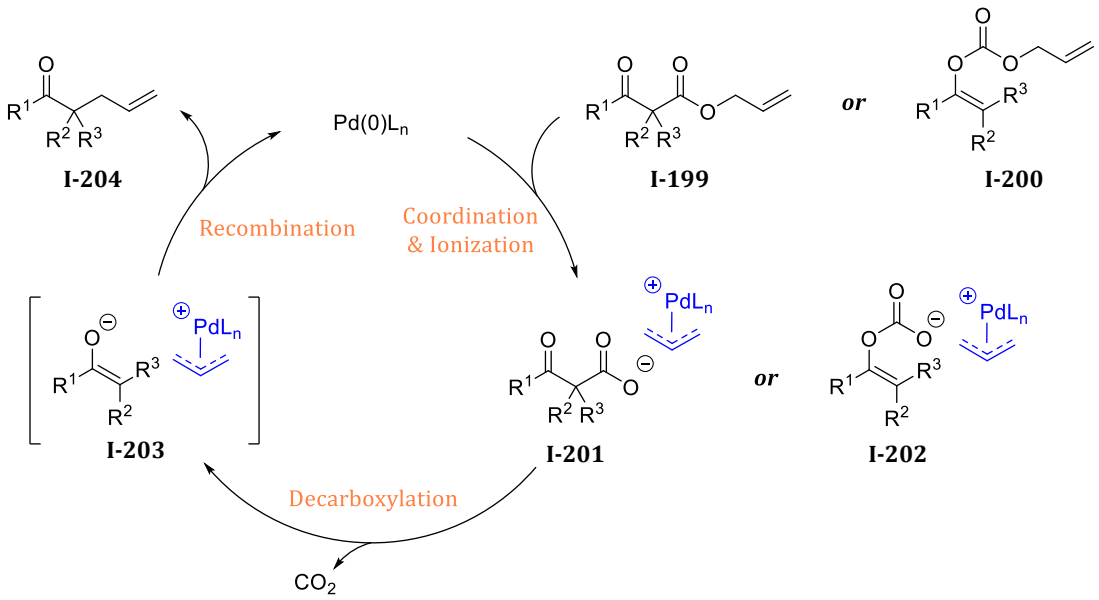

Scheme 49. Mechanism of the TSUJI-TROST allylation; from TROST *et al.*[253]

As evident, *O*-acylation of ketones to allyl enol carbonates – as was initially observed with our substrates – generally poses no hindrance for subsequent TSUJI-TROST allylation. In some cases, *O*-acylation is even preferred since using allyl enol carbonates instead of allyl β-ketoesters can result in better selectivity and yield, as reported by both TSUJI *et al*[256] and TROST *et al.*[257]

<16> This *decarboxylative allylic alkylation* is also called TSUJI allylation or, as in this thesis, TSUJI-TROST allylation.

Before achieving *C*-selective acylation, we considered a potential route to 5-allyl-5-methyl-substituted ketone **7** via TSUJI-TROST allylation of allyl enol carbonate **44** (**Scheme 50**). This approach was soon abandoned, as α-monomethylation of ketonitrile **8** proved unsuccessful and only dialkylation was observed. Similarly, subjecting allyl enol carbonate *O*-**42** to TSUJI-TROST allylation gave 5-diallyl ketonitrile **35.b** and ketonitrile **8**, without formation of monoallylated ketonitrile **45** [**8**/**35.b** ≈ 1:0.7 (NMR); *yields not determined*]. Moreover, **45** is not considered a suitable precursor for **7**, since methylation of **45** would most likely give undesired 5-*epi*-**7**.

The allylic dialkylation to **35.b** in the TSUJI-TROST allylation can be explained by a rather rare 'enolate scrambling,' which TROST *et al.* and STOLTZ *et al.,* among others, examined in mechanistic studies.[251,253,258] A detailed discussion involving solvent effects, different ion pairs, inner and outer sphere mechanisms, which also seem to depend on the used ligand classes, *et cetera* is omitted, as that would go far beyond the scope of this thesis.

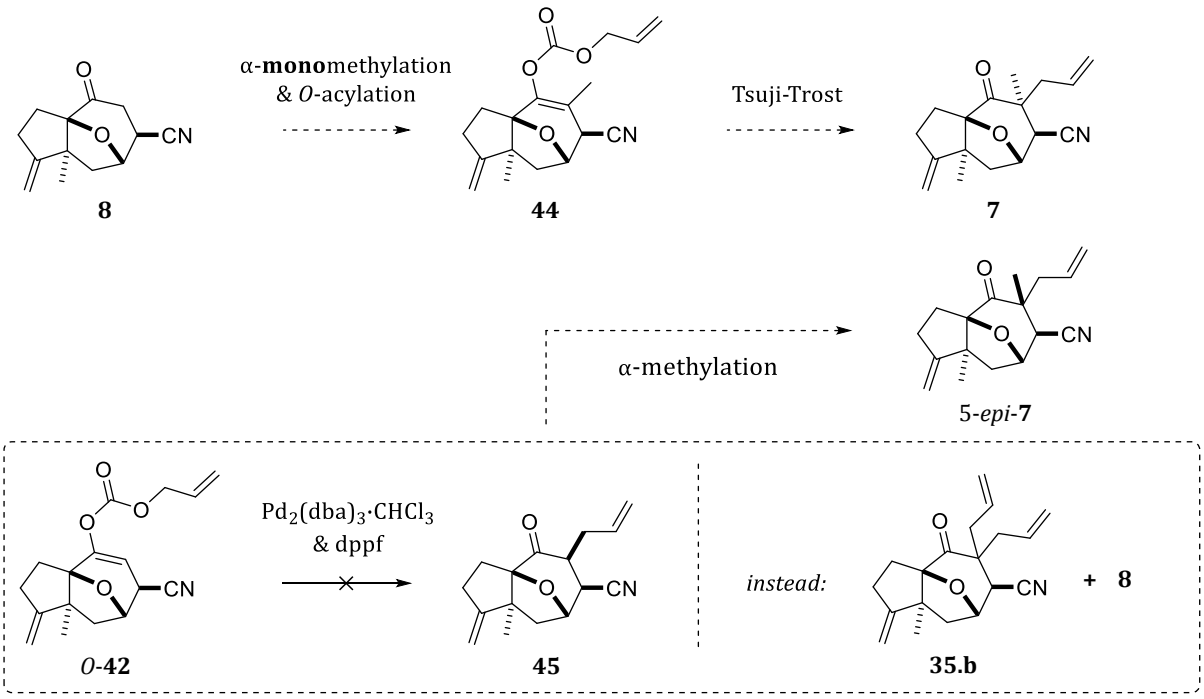

Scheme 50. First investigations involving TSUJI-TROST allylation of allyl enol carbonates.

With our allyl β-ketoesters (*OH*)-**43** and (*OH*)-**43-H**, TSUJI-TROST allylation gave the desired 5-*exo*-allyl,*endo*-methyl products as single diastereomers and in high yield (**Scheme 51**). While using $Pd(PPh_3)_4$ with very low catalyst loadings (as low as 1 mol%) gave **7** with 98% yield, using $Pd_2(dba)_3{\cdot}CHCl_3$ with either dppp or dppf (x mol% $Pd_2(dba)_3{\cdot}CHCl_3$, 2.5x mol% ligand; x = 1–5) resulted in lower yields (~80% of **7**). Latter catalyst system also had the disadvantage of the displaced dba ligand co-eluting with **7** in chromatography. Additionally, the preformation of the catalyst-ligand solution made this combination less convenient than a simple addition of solid $Pd(PPh_3)_4$ to the substrate solution. For the preparation of the decyano analog **7-H**, only the combination of $Pd_2(dba)_3{\cdot}CHCl_3$/dppf was used, resulting in 90% yield without dba co-elution.

In contrast to the previously mentioned observations by STOLTZ *et al.,*[254,255] using $Pd(OAc)_2$ and PPh_3 resulted in slow conversion and low yield (41% of **7**). It has to be noted that STOLTZ *et al.* did not use PPh_3, but chiral phosphinooxazoline ligands. In the original reports of TSUJI *et al.,* however, the combination of $Pd(OAc)_2$ and PPh_3 was used.[256,259] Moreover, coinciding with the reports of TSUJI *et al.,* SAEGUSA *et al.* reported basically the same decarboxylative allylic alkylation of allyl β-ketoesters using $Pd(Ph_3)_4$ (both in 1980).[260]

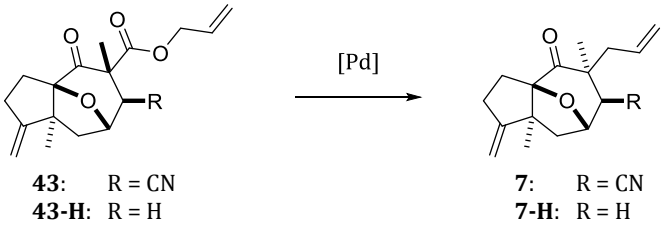

43: R = CN
43-H: R = H

7: R = CN
7-H: R = H

Scheme 51. TSUJI-TROST allylation of α-methyl β-ketoesters **43** and **43-H**.

Reagents and conditions: with **43**: DCM (~0.05 M, degassed), $Pd(PPh_3)_4$ (1 mol%), 2.5 h; **98%**;
with **43-H**: DCM (0.06 M, degassed), $Pd_2(dba)_3{\cdot}CHCl_3$ + dppf (1 mol% + 2.5 mol%, preformed solution), 2 h; **90%**.

In later experiments, with $Pd(PPh_3)_4$ being the rather obvious catalyst of choice, DCM was used as preferred solvent, replacing THF which was used in initial allylations. This resulted from establishing an efficient one-pot TSUJI-TROST allylation/MEINWALD rearrangement sequence, which was not successful in THF, as discussed in the following chapter. The used solvents were degassed by the *'pump-freeze-thaw'* method or – much more conveniently – by briefly applying vacuum and removing a small amount of the solvent along with the gases and subsequent flushing with inert gas (repeated 3 times).

2.2.2 Transformation of the *exo*-Methylidene to a Methyl Ester

To examine the compatibility of methyl esters in the pending rearrangement to decalones, several methyl esters were prepared from *exo*-methylidene substrates, as exemplified on the reaction sequence from *exo*-methylidene **7-H** to methyl ester **6-H** in **Scheme 52**. This included epoxidation, rearrangement to an aldehyde, oxidation to a carboxylic acid, and methylation.

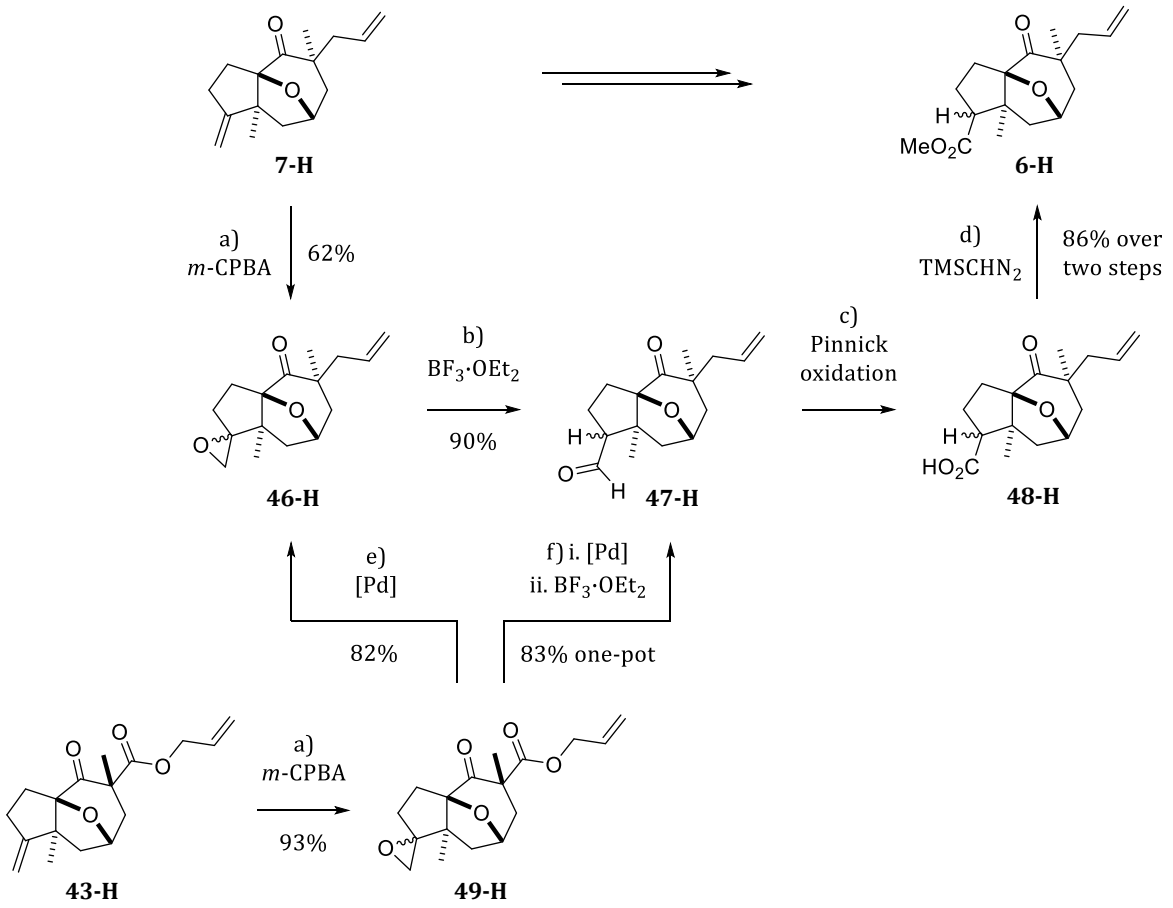

Scheme 52. Synthesis of methyl ester **6-H** starting from 5-allyl-5-methyl-substituted ketone **7-H** or from α-methyl β-ketoester **43-H**.

Reagents and conditions: **a)** DCM (0.2 M), *m*-CPBA (1.2 eq, in portions), 0 °C to rt, 19 h; **46-H** (**62%**) ***or*** **49-H** (**93%**). **b)** DCM (0.05 M), $BF_3{\cdot}OEt_2$ (10 mol%), 45 min; **90%**. **c)** *t*-BuOH/H_2O (5:2, 0.05 M), 2-methyl-2-butene (15 eq), NaH_2PO_4 (1.2 eq), $NaClO_2$ (1.2 eq), 3 h. **d)** toluene/MeOH (3:2, 0.1 M), $TMSCHN_2$ (2 M in Et_2O, 1.4 eq), **86%** over 2 steps. **e)** THF (0.05 M), $Pd_2(dba)_3{\cdot}CHCl_3$ + dppp (2 mol% + 5 mol%, preformed solution in THF), 3 h; **82%**. **f)** DCM (0.06 M), $Pd_2(dba)_3{\cdot}CHCl_3$ + dppf (1 mol% + 2.5 mol%, preformed solution in DCM), 1.75 h; then $BF_3{\cdot}OEt_2$ (10 mol%), 15 h (full conversion in <2 h); **83%** (one-pot).

The initial epoxidation of ketone **7-H** with *m*-CPBA proved the limiting factor in this sequence, resulting in a moderate yield of epoxide **46-H** (63%). It was *assumed* that the allyl group may have limited yields due to regioselectivity issues, even though no epoxidation of the allyl group was clearly evident. A more regioselective epoxidation was presumed to be feasible with allyl

β-ketoester substrates, which were expected to lead to less undesired epoxidation due to lower electron density of the allylic olefin '*incorporated in the ester moiety*.'
Indeed, epoxidation of allyl β-ketoester **43-H** selectively gave the desired epoxide **49-H** in an excellent yield of 93%, before the epoxide was subjected to TSUJI-TROST allylation (82% of **46-H**) and subsequent MEINWALD rearrangement to aldehyde **47-H** (90% yield). These two reactions were later combined in a one-pot sequence, which improved the yield of aldehyde **47-H** (83% one-pot vs. 74% over 2 steps). After PINNICK oxidation, crude acid **48-H** was then alkylated to methyl ester **6-H** using trimethylsilyldiazomethane (86% yield over 2 steps).

The preparation of methyl esters was conducted on substrates (i) both with and without the nitrile group and (ii) bearing ketones, and secondary or tertiary alcohols on C4. The alcohol substrates were obtained from the respective ketones by reduction or methylation, as will be discussed in **Chapter 2.3**. The syntheses of the different methyl esters are summarized in **Scheme 53** and **Table 3** on the next pages. For the sake of brevity, the reaction sequences will be discussed collectively. General insights will be elucidated on the collection of these methyl esters, highlighting issues with specific substrates and caveats within each step of the sequence.

The diastereomeric nature of the products within this reaction sequence complicated analysis by both TLC and NMR. The NMR signals were assigned only in cases, where an assignment was unambiguous. The NMR spectra of the diastereomeric mixtures or the separated diastereomers are attached. However, the separation of most diastereomeric mixtures proved challenging.

As mentioned in **Chapter 1.3.2**, a potential epimerization of the diastereomeric esters either before, after, or even during the epoxyazulene-to-decalone rearrangement was assumed. In the decalone core, the undesired diastereomer should be readily epimerized to the desired ester with the preferred equatorial configuration. Therefore, diastereoselective epoxidation methods were not attempted. Moreover, the separation of ester diastereomers was only pursued partially, mostly for analytical purposes. The focus was concentrated on gaining qualitative insights first – that is, whether an ester group would tolerate the rearrangement conditions.

Generally, these compounds were prone to retain solvents, especially DCM or EA, even with excessive evaporation. This was most pronounced for the comparatively polar products proceeding from 5-unsubstituted ketonitrile **8**. As already noted in the discussion of aldehyde **17**, a co-evaporation procedure proved very useful for removal of residual solvents: dissolving the often viscous oils in a small amount of DCM, adding some hexane, and co-evaporating the solvents by rotary evaporator gave products which generally were free of residual solvents and, in some cases, even solidified after or during this process due to insolubility in hexane.

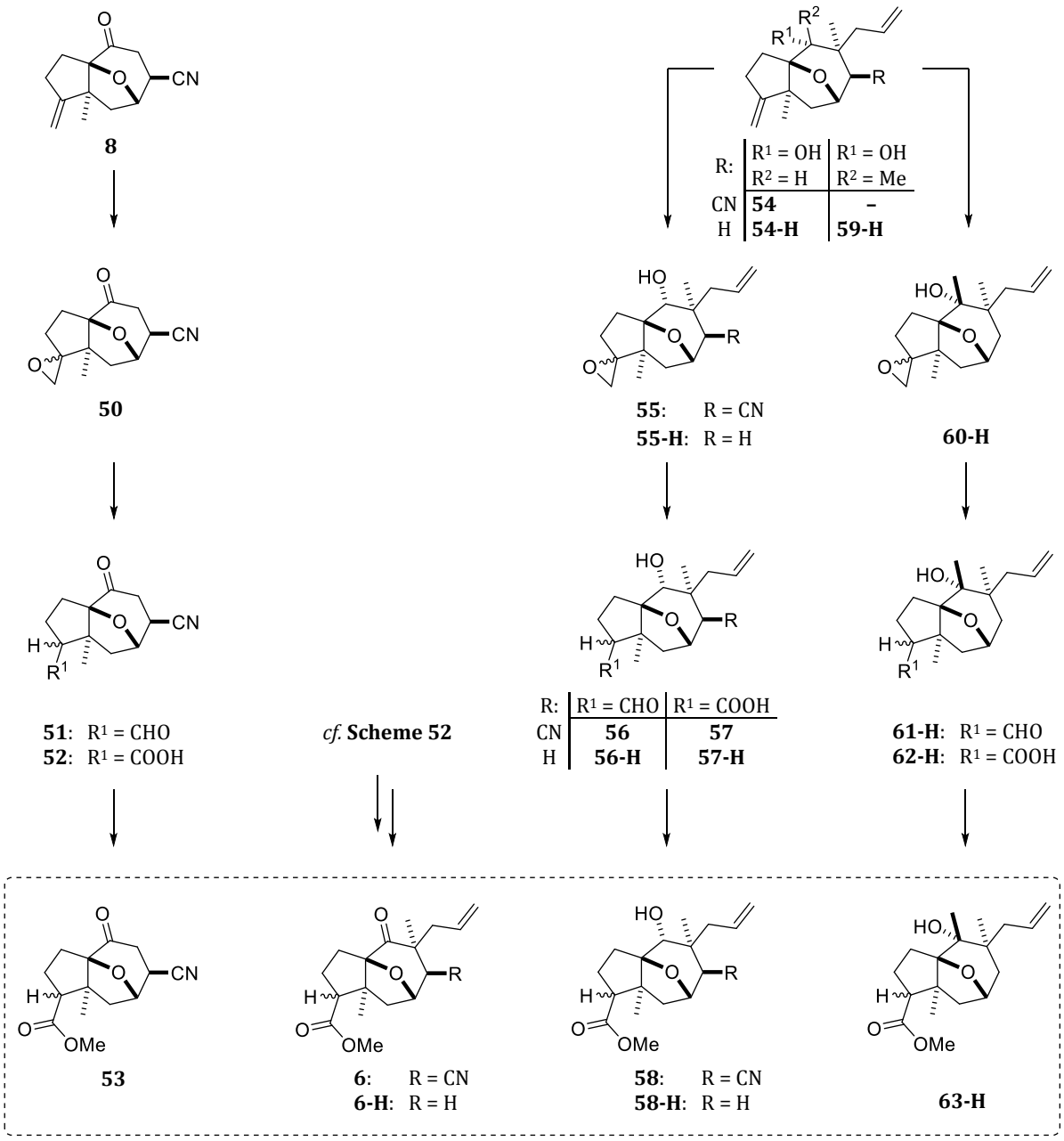

Scheme 53. Summary of prepared methyl esters. Details in **Table 3** on the next page.

Table 3. Employed reaction sequences, as well as results and remarks, for the preparation of the methyl esters.

Product	reaction sequence	results and remarks
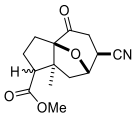 **53**	i. epoxidation (87%, *d.r.* ≈ 2:1), ii. MEINWALD, iii. PINNICK (67% over 2 steps, 'purified' by acid-base extraction), iv. MeCN (0.075 M), DBU (1.1 eq), MeI (1.2 eq), 1 h; <78%	**<45%** over 4 steps (**Ø ≤ 82%**), *significant amounts of residual solvents*
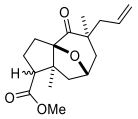 **6-H**	**reaction sequence A**: i. TSUJI-TROST (90%), ii. Epoxidation (62%, *d.r.* ≈ 1:1), iii. MEINWALD (90%) , iv. PINNICK, v. $TMSCHN_2$ (86% over 2 steps) **reaction sequence B**: i. epoxidation (93%, *d.r.* ≈ 1.5:1), ii&iii. TSUJI-TROST/MEINWALD (83% one-pot), iv. PINNICK, v. $TMSCHN_2$ (86% over 2 steps)	**reaction sequence A**: **43%** over 5 steps (**Ø = 85%**) **reaction sequence B**: **66%** over 5 steps (**Ø = 92%**)
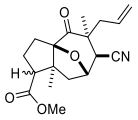 **6**	**reaction sequence B**: i. epoxidation (91%, *d.r.* ≈ 1.5:1), ii&iii. TSUJI-TROST/MEINWALD (64% one-pot), iv. PINNICK, v. $TMSCHN_2$ (57% over 2 steps) **alternative methods of esterification** (each 57% over 2 steps): a) TMSCl in MeOH; b) H_2SO_4 in MeOH; c) Cs_2CO_3 & MeI in MeCN	**reaction sequence B**: **33%** over 5 steps (**Ø = 80%**) *formation of **side-products*** ***yields for esterifications determined by qNMR***
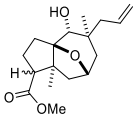 **58-H**	i. epoxidation (79%, *d.r.* ≈ 3:1), ii. MEINWALD (85%), iii. PINNICK, iv. $TMSCHN_2$ (97% over 2 steps)	**68%** over 4 steps (**Ø = 91%**)
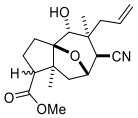 **58**	i. epoxidation (*addn. of **$NaHCO_3$** (2 eq) crucial*, 77% (87% *b.r.s.m.*), *d.r.* ≈ 2.3:1), ii. MEINWALD, iii. PINNICK, iv. $TMSCHN_2$ (77% over 3 steps)	**59%** over 4 steps (**Ø = 88%**)
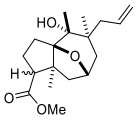 **63-H**	i. epoxidation (83%, *d.r.* ≈ 5.5:1), ii. MEINWALD (85%), iii. PINNICK, iv. $TMSCHN_2$ (88% over 2 steps)	**62%** over 4 steps (**Ø = 89%**), ***d.r.* ≈ 5.5:1** after epoxidation, **9:1** after MEINWALD

2.2.2.1 Epoxidation of the *exo*-Methylidene

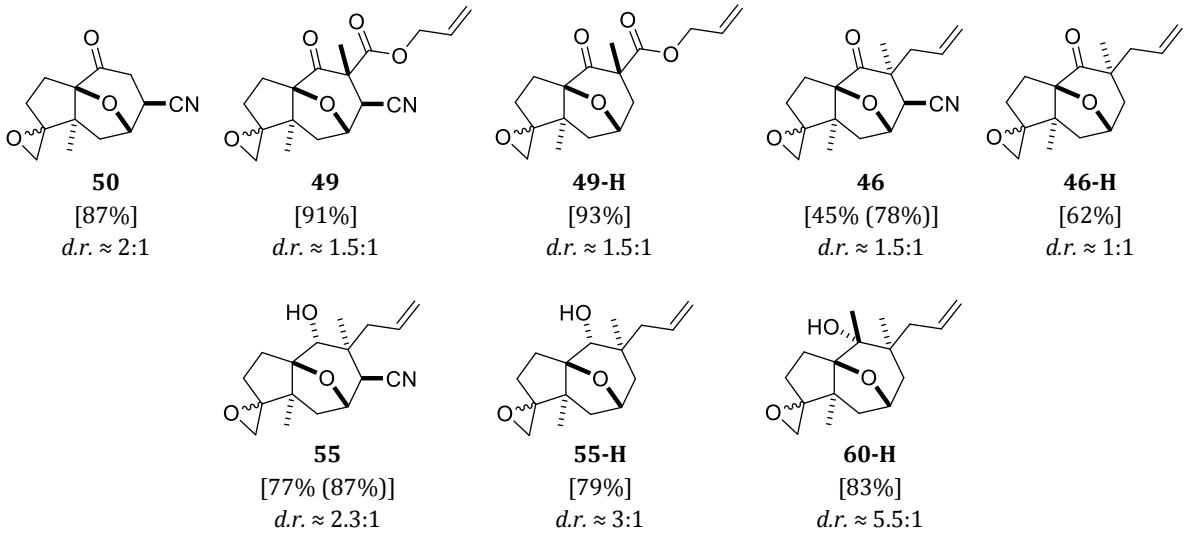

Figure 14. Prepared epoxides with yields [(*b.r.s.m.*) in parentheses] and diastereomeric ratios.

The epoxidation of the *exo*-methylidene group generally resulted in high yields in the range of 80–90%. However, the epoxidation of the ketones **7** and **7-H** proceeded with only moderate yields. Initial epoxidation of the allyl β-ketoesters (**43**/**43-H** to **49**/**49-H**) and a subsequent TSUJI-TROST allylation gave the desired epoxides **46** and **46-H** more efficiently, as covered below. With these allyl β-ketoesters, the epoxidation step gave yields of 91%/93% (**49**/**49-H**) instead of 45%/62% with the allyl-substituted ketones **46**/**46-H**.

Good yields were also obtained with 5-unsubstituted ketonitrile **50** and with 5-allyl-5-methyl substrates bearing secondary or tertiary alcohols at C4. The addition of $NaHCO_3$ during epoxidation proved crucial for secondary alcohol **54** (to **55**), since without such an addition a complex mixture was obtained. This was not the case for its decyano analog **54-H** (to **55-H**).

Evidently, the epoxidation of *allyl-substituted alcohols* was less problematic than that of *allyl-substituted ketones*. This somewhat contradicts our previous assumption of regioselectivity issues due to the presence of the allyl group. Furthermore, the diastereoselectivity was found to be higher for substrates with secondary and, especially, tertiary alcohols (*d.r.* ≈ 5.5:1 for **60-H**). While no investigations in this direction were made, these findings indicate that the nature of C4 (ketone/*sec*-OH/*tert*-OH) may contribute to significant structural differences in the tricyclic core, which influence the behavior of substituents at C1.

2.2.2.2 MEINWALD Rearrangement

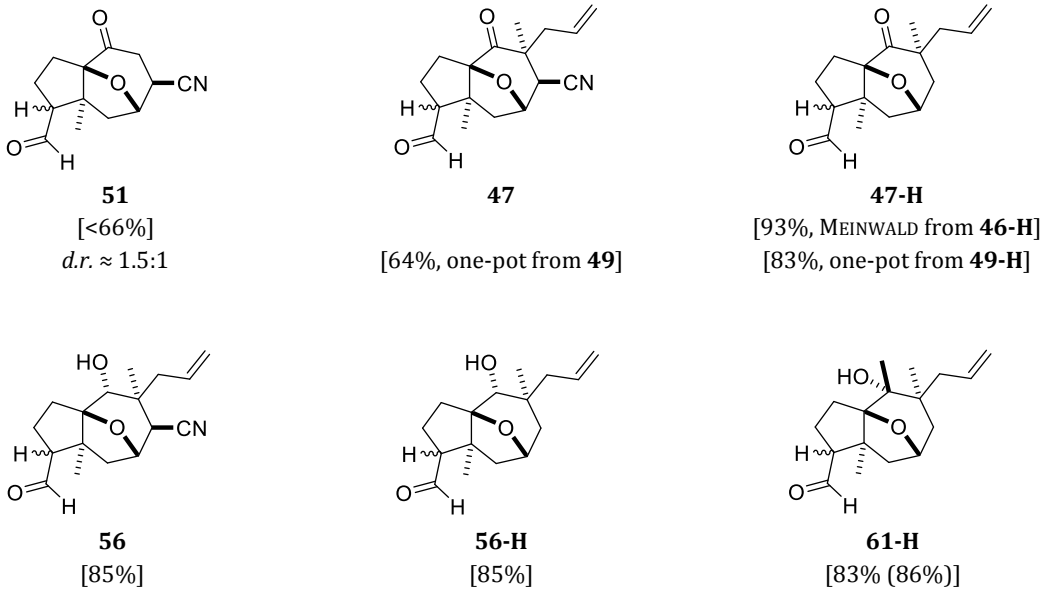

51
[<66%]
d.r. ≈ 1.5:1

47
[64%, one-pot from **49**]

47-H
[93%, MEINWALD from **46-H**]
[83%, one-pot from **49-H**]

56
[85%]

56-H
[85%]

61-H
[83% (86%)]

Figure 15. Prepared aldehydes with yields [(*b.r.s.m.*) in parentheses].

The MEINWALD rearrangement was readily conducted using catalytic amounts of $BF_3{\cdot}OEt_2$ (generally 10 mol%) in DCM at room temperature. Analysis of the reaction progress by TLC was often impeded by very similar R_f values of the epoxides and aldehydes even after eluting the TLC plate two or three times. Therefore, aliquots of the reaction mixture were analyzed by NMR, indicating a rapid full conversion (<2 h). In some cases, TLC analysis showed a clear separation (for **56-H** and **61-H**, respectively) and indicated full conversion in under 20 min with only 5 mol% $BF_3{\cdot}OEt_2$. Incidentally, aldehydes with secondary or tertiary alcohols on C4 (*contrary to ketone analogs*) appeared as *less polar spots* than the respective epoxide spots.

The MEINWALD rearrangement could be combined in a one-pot sequence with a previous TSUJI-TROST allylation in DCM, improving the yield of aldehyde **47-H**. The MEINWALD rearrangement step in the one-pot sequence was inhibited by THF, most likely due to insufficient LEWIS acidity of the LEWIS adduct $BF_3{\cdot}THF$. The yield of this one-pot TSUJI-TROST/MEINWALD sequence was determined to be 83% but was *not examined thoroughly*, since this method was only conducted once. The crude epoxide **46-H** obtained from the *unsuccessful* one-pot sequence (*in THF*) was converted to aldehyde **47-H** in a separate MEINWALD rearrangement. This crude product was then combined with that from the *successful* one-pot sequence (*in DCM*). The *combined crude products* were then purified, indicating the given yield for the one-pot sequence.

The one-pot sequence was also conducted on cyano analog **49**, with one slight difference in conditions: instead of the $(Pd_2(dba)_3$/dppp)-system, $Pd(PPh_3)_4$ was used for the initial TSUJI-TROST allylation, since the latter proved superior with nitrile substrates (*cf.* **Chapter 2.2.1.1**). However, the formation of significant amounts of side-products in the MEINWALD rearrangement

step was observed, resulting in a lower yield (64% of **47** vs. 83% of **47-H**). The main side-product was identified as allylic alcohol **47.a** (**Figure 16**). Similar isomerization reactions of epoxides to allylic alcohols with *either* LEWIS acids[261–263] *or* palladium catalysts[264] are known.

The *combination* of both these catalyst classes in the one-pot TSUJI-TROST/MEINWALD sequence may have facilitated the formation of allylic alcohol **47.a** (64% of **47** & 35% of impure **47.a**). Yet, the respective allylic alcohol was not observed in the one-pot TSUJI-TROST/MEINWALD sequence to decyano aldehyde **47-H**. The only other example, where this side-reaction was evident, was the MEINWALD rearrangement to aldehyde **56-H** (85% yield & 8% of **56-H.a**), where no palladium catalyst was present. A conclusive explanation for the formation of allylic alcohols cannot be deduced from these results.

While the allylic alcohols may also be transformed to the desired esters, such a 'detour' in the synthetic route is clearly not the approach of choice. Nevertheless, alternatives routes proceeding from allylic alcohol **47.a** were briefly examined in later pursuits (**Chapter 2.4.5.3**).

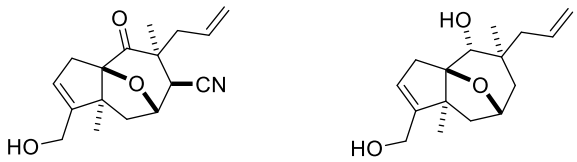

47.a **56-H.a**

Figure 16. Allylic alcohols as side-product of the MEINWALD rearrangement.

It was also observed that the diastereomeric ratios of the aldehydes did not always match that of the used epoxide substrates. While generally only small deviations were evident in NMR for ketone substrates (e.g., 1.5:1 to 1.2:1 from **46-H** to **47-H**), a very distinct change was evident for tertiary alcohol **60-H** (5.5:1 to 9:1). Secondary alcohols also led to a noticeable, but less pronounced change (~1.8:1 to ~2.3 from **55** to **56**; ~3:1 to 4.8:1 from **55-H** to **56-H**).

Furthermore, some aldehydes were prone to autoxidation to their respective carboxylic acids. Dissolving a sample of aldehyde **47-H** in ethyl acetate and letting the solution stand in a vial with some exposure to air (for about 2 weeks) led to a complete and clean conversion to the carboxylic acid, as indicated by NMR. For **47**, this autoxidation was noticeably faster but proceeded in a seemingly less clean conversion.

2.2.2.3 PINNICK Oxidation

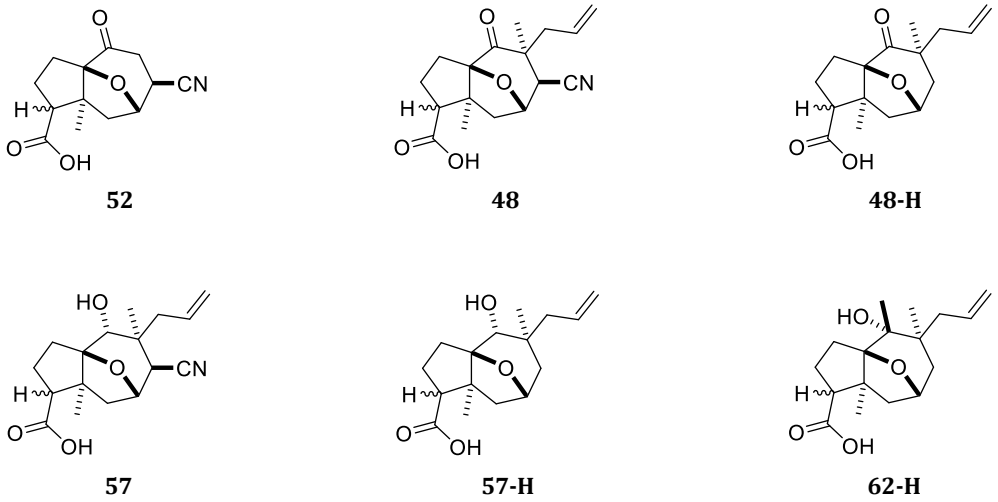

Figure 17. Prepared carboxylic acids.

The carboxylic acids obtained by PINNICK oxidation were generally used without further purification. Due to their polar nature, separation or purification by flash chromatography was not engaged. Incidentally, the carboxylic acid **48** exhibited higher R_f values than the substrate in TLC analysis, suggesting a lower polarity of the acid compared to aldehyde **47**.

The slightly acidic environment of the reaction mixture was found to be sufficient to facilitate complete extraction of the carboxylic acids into organic solvents (DE or EA). Adding hydrochloric acid in the extraction process in early attempts resulted in a discoloration of the organic phase. Even though the yellow color dissipated during evaporation, and the colored component condensed in the receiving flask of the rotary evaporator, the carboxylic acids extracted with additional HCl seemed to require more $TMSCHN_2$ in the following methylation reaction (~1.6–2 eq instead of 1.2–1.4 eq).

2.2.2.4 Esterification

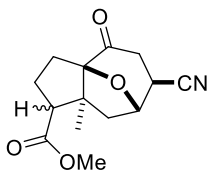

53
[<45%, 4 steps (Ø ≤ 82%)]

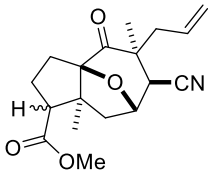

6
[33%, 5 steps (Ø = 80%) (**seq. B**)]

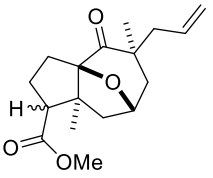

6-H
[43%, 5 steps (Ø = 85%) (**seq. A**)]
[66%, 5 steps (Ø = 92%) (**seq. B**)]

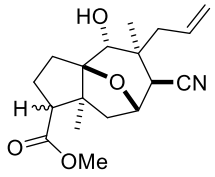

58
[59%, 4 steps (Ø = 88%)]

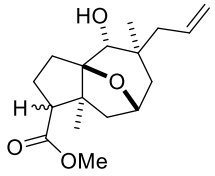

58-H
[68%, 4 steps (Ø = 91%)]

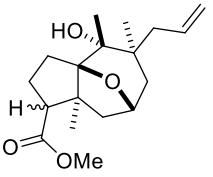

63-H
[62%, 4 steps (Ø = 88%)]

Figure 18. Prepared methyl esters with yields over 4 or 5 steps.
Details are discussed in the text and shown in **Table 3** on page **81**.

For a better comparison of the overall sequence from *exo*-methylidene group to the methyl ester, the yields over 4 or 5 steps are given in **Figure 18**. The 4-step 'methylidene-to-ester sequence' (epoxidation/MEINWALD/PINNICK/esterification) can be quantified as **59–68% over 4 steps**, corresponding to an average yield of **88–91% per step**. The yields for esters bearing 4-ketones (**6**, **6-H**, and **53**) warrant further discussion.

For esters **6** and **6-H**, the TSUJI-TROST allylation has to be included for an adequate discussion of yield. Incorporating the TSUJI-TROST allylation *in between* epoxidation and MEINWALD rearrangement proved superior to conducting the TSUJI-TROST allylation *before* the 4-step 'methylidene-to-ester sequence'. This circumvented a yield-limiting epoxidation of allyl-substituted ketones. From allyl β-ketoester **43-H**, ester **6-H** was obtained in 43% yield over 5 steps (Ø = 85%), when the TSUJI-TROST allylation was conducted *before* the 4-step sequence (*seq. A* in **Figure 18**. Incorporating the TSUJI-TROST allylation *within* the 4-step sequence (*seq. B*) improved this yield to **66% over 5 steps** (**Ø = 92%**). Moreover, the TSUJI-TROST allylation could be combined with the MEINWALD rearrangement in a one-pot sequence.

For the cyano analog **6**, this sequence gave a noticeably lower yield of **33% over 5 steps** (**Ø = 80%**). The lower yield resulted from side-reactions in the MEINWALD rearrangement step of the one-pot sequence, which also led to the formation of allylic alcohol **47.a**.

The esterification was typically conducted with crude carboxylic acids and $TMSCHN_2$, resulting in good yields (≥85% over 2 steps from the aldehydes). In earlier attempts, a combination of

DBU and MeI was used for the preparation of **53**. The overall yield of ester **53** could not be determined adequately due to significant amounts of residual solvents in the product. Incidentally, the co-evaporation procedure was not yet applied at that point. For ester **6-H**, this esterification method (DBU/MeI) proved vastly inferior to that with $TMSCHN_2$, resulting in merely 35% instead of 86% yield over 2 steps.

In the last attempts, other methods of esterification were evaluated on carboxylic acid **48** (with either TMSCl/MeOH, H_2SO_4/MeOH, or Cs_2CO_3/MeI). All of these methods gave ester **6** with the same yield as that with $TMSCHN_2$ (57% over 2 steps). This moderate yield is unrelated to the esterification step and was a consequence of the side-reactions in the prior MEINWALD step. Therefore, this comparison of esterification methods indicates that $TMSCHN_2$ can effectively be substituted with more commonly available and inexpensive reagents.

As noted earlier, the preparation of the methyl esters was initially carried out for one purpose: to evaluate whether ester groups would tolerate the LEWIS-acidic conditions of an epoxyazulene-to-decalone rearrangement. Thus, most sequences to the respective esters were only conducted once and not optimized. Consequently, some issues could not be resolved adequately. This especially includes the unexpected side-reactions in the MEINWALD rearrangement step towards ester **6**. On the collection of the prepared esters, different aspects could be elucidated.

Generally, the 4- or 5-step sequences were convenient and high-yielding. Some potential improvements may be implemented, such as omitting purification of the aldehyde and proceeding with the PINNICK reaction promptly to avoid partial decomposition. This practice was employed for some esters and was both efficient and more convenient.

Since the diastereomeric nature of the tricyclic esters was deemed inconsequential, a complete separation of the diastereomers by repeated flash chromatography was not pursued. The diastereomers were separated mainly for analytical purposes, where this was feasible without excessive effort. While the NMR signal set of at least one diastereomer of each ester was assigned to its structure, the configuration of the diastereomers was not determined. Ester **6-H** was only isolated as a diastereomeric mixture, which could be separated somewhat more readily after the next step, the oxidative cleavage of the allyl moiety.

2.2.3 Oxidative Cleavage of the C5-Allyl Group to an Aldehyde

Next, we investigated the oxidative cleavage of the allyl moiety to an aldehyde, which was to be used as an electrophile in the 3-furylation reaction. For this oxidative cleavage, the variant of the LEMIEUX-JOHNSON oxidation[265] introduced by JIN *et al.*, which uses catalytic OsO_4 in combination with $NaIO_4$ *and 2,6-lutidine,*[266] was found to be well-suited (**Scheme 54**).

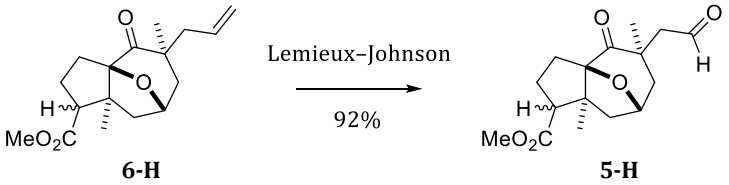

6-H **5-H**

Scheme 54. LEMIEUX-JOHNSON oxidation of **6-H** to aldehyde **5-H**.

Reagents and conditions: 1,4-dioxane/H_2O (3:1, 0.05 M), 2,6-lutidine (2 eq), OsO_4 (2 mol%), $NaIO_4$ (4 eq), 5.5 h; **92%**.

Aldehyde **5-H** was obtained from *isolated* methyl ester **6-H** in 92% yield. *Crude* methyl esters could also used in some cases without detriment to yield. Via *crude* **6-H**, aldehyde **5-H** was obtained in 74–79% yield over 3 steps (Ø ≈ 90–92%, from **47-H**). While the two diastereomers of **5-H** could be separated by flash chromatography more readily than those of the allyl substrate, a full separation was still not feasible in a single column.

Other aldehydes prepared by this method are depicted in **Figure 19**. Decyano aldehyde **64-H** was obtained in a good yield of 79%, but appeared to slowly autoxidize to the carboxylic acid, as indicated by a gradually increasing signal in ^{13}C NMR (δ = 177.7 ppm). The cyano aldehydes **39** and **5** were also prepared. Ester-substituted aldehyde **5**, prepared only once in the late phase of the project, was obtained in a moderate yield of 59% due to incomplete conversion.

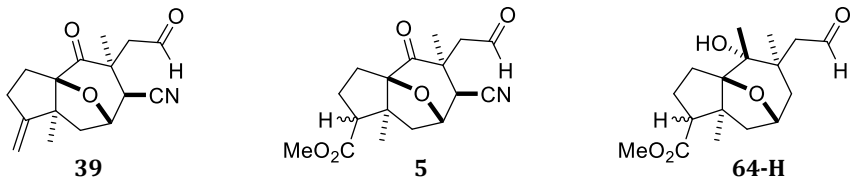

39 [70%] **5** [59%] **64-H** [79%]

Figure 19. Prepared aldehydes by oxidative cleavage of the allyl moiety.

Our focus was mainly laid on aldehyde **39**, which was prepared in 70% yield from *bis*-alkene **7** in multiple runs. The yield-limiting factors were identified as (i) the competing oxidative cleavage of the *exo*-methylidene group and (ii) the incomplete cleavage of the initially formed 1,2-diols. After isolating aldehyde **39** by flash chromatography, the remaining fractions of several runs were collected, stored, and combined later on. It has to be noted that this was a *very* complex

mixture, which is unsurprising considering that 4 diol diastereomers, 4 tetrol diastereomers, and two other products from oxidative cleavage are *conceivable*.

When this complex mixture was treated with 2,2-dimethoxypropane and *p*-TsOH·H_2O in acetone, the double oxidative cleavage of *bis*-alkene **7** became evident. Through acetalization of *tris*-carbonyl **39.a**, the diketo dimethylacetal **39.b** was isolated (**Figure 20**). The remaining, still very complex, fractions were hydrolyzed under acidic conditions. Resubjecting this crude product to the oxidative cleavage/acetalization sequence gave additional **39.b**. However, a decomposition of **39.a** during work-up of the oxidative cleavage was apparent in TLC. While the yield of **39.a** or **39.b** cannot be assessed, the degree of overoxidation seemed rather substantial.

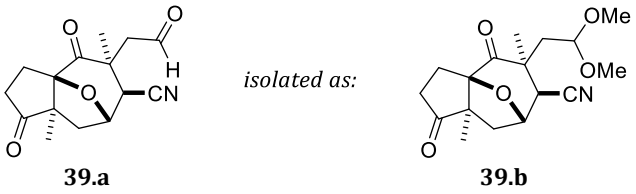

39.a **39.b**

Figure 20. *Tris*-carbonyl **39.a**, isolated as diketo dimethylacetal **39.b**.

Such a decomposition was also observed during the first attempts at preparing aldehyde **39** by the LEMIEUX-JOHNSON oxidation. Those early attempts were conducted *without the addition of 2,6-lutidine* or *with DABCO instead*, resulting in decomposition during work-up. These attempts did not allow for any isolation of aldehyde **39**. In general, a metallic-grey discoloration of the crude products was evident after LEMIEUX-JOHNSON oxidations. It is now *presumed* that this indicated osmium-based impurities, which somehow catalyze the occasionally observed decomposition and autoxidation. These impurities partially co-eluted with the aldehydes in chromatography, especially with nitrile compounds. In a couple of experiments which primarily aimed at finding conditions for a more regioselective oxidation of **7**, treating the reaction mixtures with $Na_2S_2O_3$ to quench OsO_4 and excess $NaIO_4$ was examined for an optimized work-up process.

Adding (half-)saturated aq. $Na_2S_2O_3$ to the reaction mixture resulted in poor phase separation with DCM and other solvents. Washing the organic extracts with saturated aq. $Na_2S_2O_3$ failed to effectively remove the discoloration. The best approach seemed to be adding *solid* $Na_2S_2O_3 \cdot 5H_2O$ (10–20 eq) to the reaction mixture and stirring for ~30 min, before diluting the mixture with water and extracting with DCM. With this procedure, the metallic-grey discoloration was retained in the aqueous phase. A quantitative evaluation of these work-up methods is not possible since these experiments were focused on optimizing regioselectivity, and thus, several factors were adjusted. More systematic investigations into different work-up methods might be worthwhile for future approaches.

The regioselectivity issue could not be resolved with the briefly investigated alternative reagents and conditions – e.g., by using less $NaIO_4$ (2–3 eq) but prolonging reaction time or cooling the reaction mixture to 0 °C for a more selective oxidative cleavage. All of these variations led to incomplete conversion of the allyl moiety of *bis*-alkene **7**. Similarly, the alternative approach via *sequential* dihydroxylation and subsequent oxidative cleavage, introduced by NICOLAOU *et al.*,[267] resulted in very low conversion in the dihydroxylation step.

In later pursuits, another case of decomposition was observed, which could be ascribed more clearly to osmium-based impurities. This is discussed in **Chapter 2.4.5.3**, which also includes a route utilizing diketo dimethylacetal **39.b** as a substrate for further functionalization. With that approach, a *complete* oxidative cleavage of *both* alkene moieties would be desired, rendering regioselectivity issues obsolete. For this double oxidative cleavage, an adaptation of the presented LEMIEUX-JOHNSON oxidation or, alternatively, an ozonolysis may be considered. Such a *deliberate* double oxidative cleavage, however, was not investigated within this work.

2.3 LEWIS ACID-INDUCED REARRANGEMENT TO THE DECALONE CORE

As outlined in our planned synthetic route towards salvinorin A (**Chapter 1.3**), the central epoxyazulene-to-decalone rearrangement hinged on the examples published by SAMMES *et al*. Within their work, LEWIS acid-induced rearrangements of similar 3a,7-epoxyazulenes were achieved. Most notably, treating secondary alcohol *exo*-**I-174** with $SnCl_4$ or $TiCl_4$ in DCM[151,154] led to a 1,2-rearrangement of the C3a–C8a bond, displacing the hydroxy function at C4.[<17>] Hydrolysis of the resulting oxonium intermediate **I-175.I** revealed *cis*-decalone **I-175**, which could subsequently be isomerized to *trans*-decalone **I-176** (**Scheme 55**).

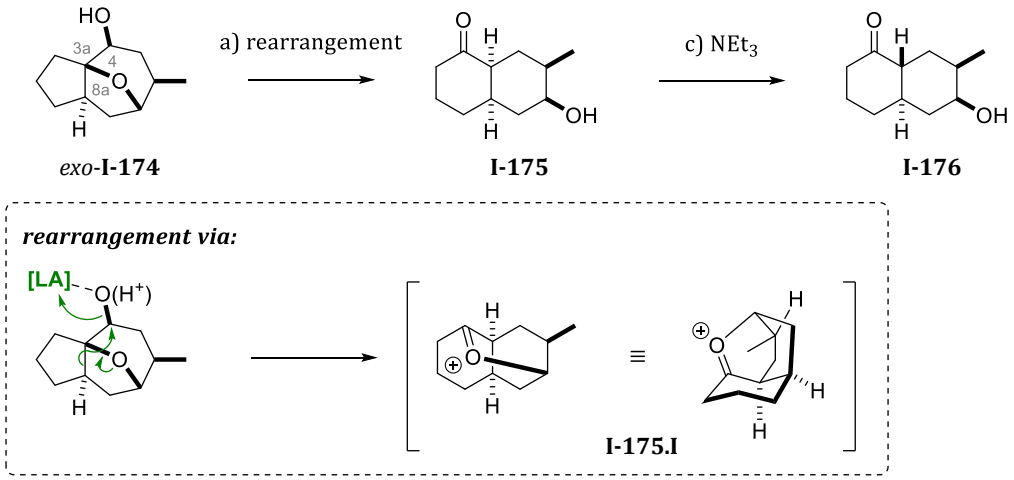

Scheme 55. LEWIS acid-induced rearrangement of *exo*-**I-174** to *cis*-decalone **I-175**.

Reagents and conditions: **a)** DCM (0.55 M), $SnCl_4$ (0.17 eq), rt, 16 h; **60%**. **b)** NEt_3 (1 eq); *no further details given*.

cis-Decalone **I-175** was also obtained in similar yields when *exo*-**I-174** was treated with $SOCl_2$. Interestingly, its epimer *endo*-**I-174** did not rearrange under either conditions, instead giving chloride **I-205** with *retention of configuration* at C4 (**Scheme 56** on the next page). A similar behavior was observed for its C8a-methylated analog **I-206**. This contrast in the behavior of *exo*- and *endo*-alcohols was explained by the formation of tricyclic oxonium intermediates **I-208.I**, which are subject to nucleophilic opening by chloride. This neighboring group participation of the ether bridge ultimately resulted in retention of configuration by double inversion.[154]

The main reason for this different behavior was rationalized to stem from the different arrangement of the migrating C3a–C8a bond relative to the *exo*- or *endo*-C–OH bond. The *exo*-alcohols presumably adopt an antiperiplanar orientation, which is a prerequisite for such rearrangements due to orbital overlap. In stark contrast to this, the epimeric *endo*-alcohols seem to not be "favourably orientated for rearrangement," leading to substitution instead.[154]

[<17>] Indicating *endo*/*exo*-substituents with α- (for *endo*-) or β- (for *exo*-), as occasionally done by SAMMES *et al.*,[149,154] is omitted to avoid ambiguity. For our epoxyazulenes, α- and β-prefixes are used as *locants* (e.g., α-methyl β-ketoesters).

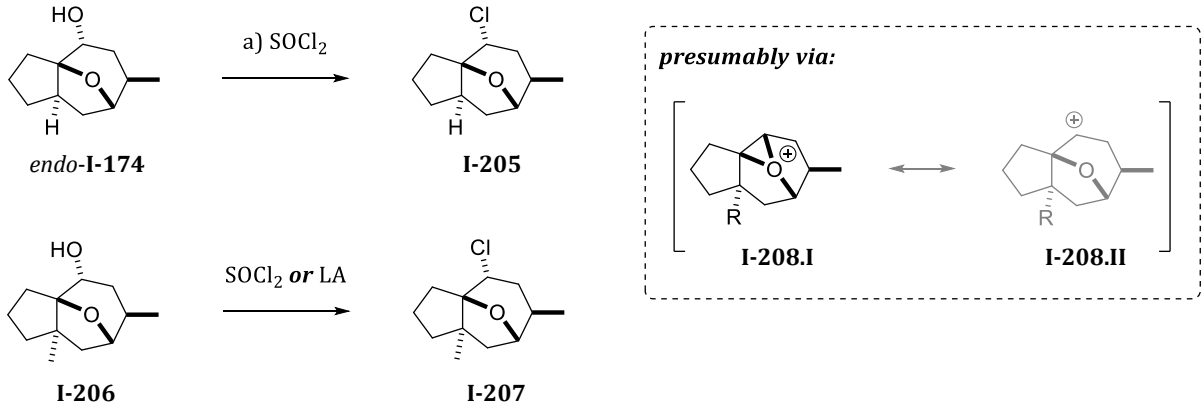

Scheme 56. Under rearrangement conditions, *endo*-alcohols give *endo*-chlorides instead.

Reagents and conditions: **a)** HMPA (0.44 M), $SOCl_2$ (2.27 eq), rt, 16 h; **68%**. *Conditions for* **I-206** *not reported.*

It is important to note that such a neighboring group participation could, in theory, also result when *exo*-alcohols would lead to a *prior abstraction of the hydroxy group* by LEWIS acids. However, for *exo*-alcohols, a *concerted rearrangement* via migration of the C–C bond and the displacement of the C–O bond seems to be highly favored (*cf.* **Scheme 55** on the last page).

Since this concerted process is not possible in *endo*-alcohols, an abstraction of the hydroxy group seems to take place instead, resulting in the formation of the tricyclic oxonium intermediates **I-208.I**. These can be considered as resonance structures of the secondary carbocations **I-208.II**, which should also be able to rearrange to decalones due to the planarity of the carbocation center. Yet, the 'presence' of such carbocations apparently is avoided, and a stabilization by the involvement of the ether bridge is preferred. Furthermore, other effects such as *complexation/chelation* of the LEWIS acid with the ether bridge or with solvents, as well as the influence of particular *types of ion pairs*, such as tight ion pairs, have to be considered. Therefore, a prediction whether a rearrangement 'should' occur seems to be rather difficult, which is also evident from the examples using *tertiary* alcohols (**Scheme 57**).[154]

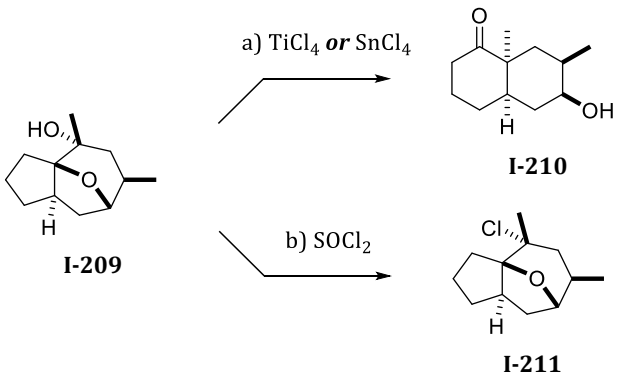

Scheme 57. Rearrangement ***or*** chloro substitution of tertiary *endo*-alcohols (*endo*-**I-209**).

Reagents and conditions: **a)** DCM (0.64 M), $SnCl_4$ (1.5 eq), rt, 16 h; **65%**. *Conditions with $TiCl_4$ not reported.* **b)** HMPA, $SOCl_2$; **76%**. *Conditions similar to those with* **I-205**.

Treating tertiary *endo*-alcohol **I-209** with LEWIS acids ($SnCl_4$ or $TiCl_4$ in DCM) gave *cis*-decalone **I-210**. This would 'generally be expected' by the *relative* ease of formation and stability of tertiary carbocations which do not seem to necessitate a stabilization via the respective tricyclic oxonium intermediate, therefore allowing for a rearrangement despite of the initial *endo*-configuration of the C–OH bond. However, using $SOCl_2$ in HMPA did not result in rearrangement, as was the case for secondary *exo*-alcohols, but instead gave *endo*-chloride **I-211**. While a S_Ni reaction might explain this chloride substitution, a neighboring group participation of the ether bridge, or other effects mentioned in the last paragraph, seem to explain this – and some of our own observations – in a more conclusive way.[152]

Other rearrangements of tertiary alcohols reported by SAMMES *et al.* are summarized in **Scheme 58**. Typically, this proceeded very quickly with either $TiCl_4$, $SnCl_4$ or $BF_3{\cdot}OEt_2$, requiring only 30 min to a couple of hours, even with cooling in an ice bath. From these examples, some information can be deduced for our substrates, which incorporate both an 8-methyl and a 1-methylidene group. The 8a-methylated substrate **I-214** gives cryptofauronol **I-215**,[154] which predominantly exists in the hemiacetal form imposed by the 5,10-dimethylated *cis*-decalone structure.[18] Moreover, the 1-methylidene of **I-216** was subject to a very fast alkene isomerization. The undesired alkene isomerization could be circumvented by masking the alkene as a sulfide before rearrangement. Afterwards, the rearranged sulfide was oxidized to the sulfoxides that, after elimination, revealed the *exo*-methylidene in decalone **I-218**.[155]

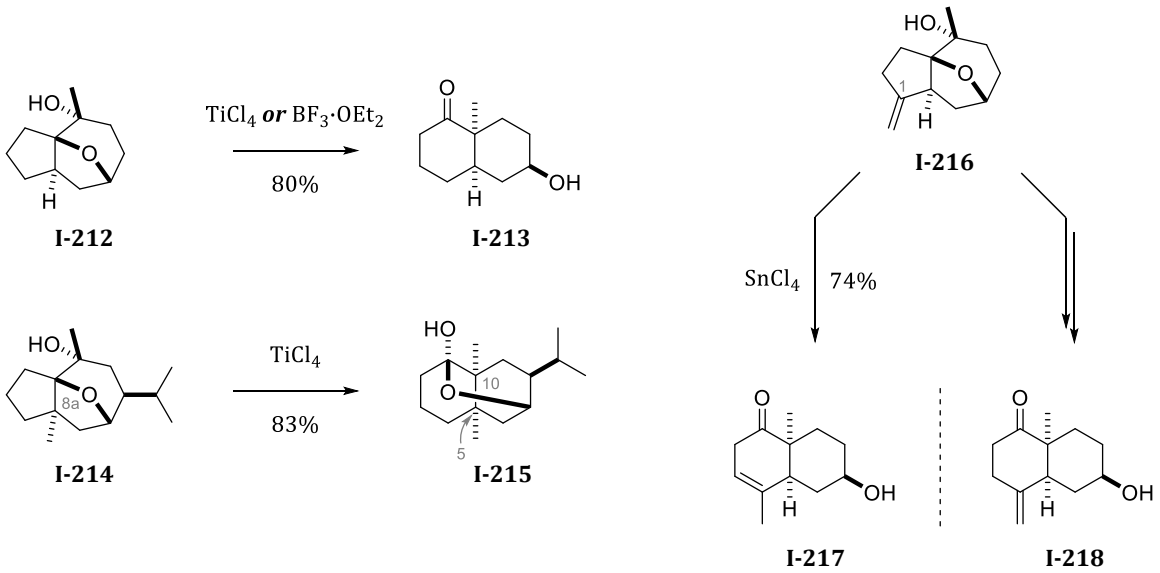

Scheme 58. Summary of tertiary alcohols and their rearrangement products.

[18] For [6,6]-fused compounds like decalones and their derivatives (e.g., **I-215**), the numbering system of the salvinorin framework is adopted for better comparability and consistency.

Notably, only the rearrangements of tertiary *endo*-alcohols were reported. These were obtained as the sole products from *exo*-selective methylation of the ketones (77–94% yield).

The only exception to this *exo*-selective approach of nucleophiles within the reports of SAMMES *et al.* was the formation of the *secondary exo*-alcohol **I-174** (*cf.* pages **91–92**). In this case, an *endo*-approach of the hydride ($LiAlH_4$ or $NaBH_4$) to the ketone was preferred (*exo*-/*endo*-**I-174** ≈ 1.8:1).[149,153] The only other secondary alcohol, *endo*-alcohol **I-206** was only mentioned incidentally in a *failed* rearrangement attempt.[152] The reduction of the respective ketone was neither elaborated on, nor was the *exo*-epimer *exo*-**I-206** or its rearrangement reported, indicating that *endo*-**I-206** might have been obtained as the sole product. This strongly suggest that the presence of the C8a-methyl group increases the preference for *exo*-face-selective addition by inducing additional steric hindrance on the *endo*-face of the substrates.

SAMMES *et al.* also extended their investigations to ketone substrates (**Scheme 59**).[154] Treating ketone **I-219** with $TiCl_4$ *in DCM* afforded hydroxy acyloin **I-220** in moderate yield. With ketone **I-221**, optimization of the conditions revealed the use of $TiCl_4$ *in MeCN* to be superior, resulting in an equilibrated mixture of **I-221** and hydroxy acyloin **I-222** in high yield.

Incidentally, the rearrangements of the *ethylene* or *dimethyl acetals* of **I-221** were also briefly mentioned but were less conclusive. Furthermore, treating ketone **I-221** with the LEWIS acid *aluminum triiodide* in MeCN led to an addition of acetonitrile to the α-C of the ketone, affording β-amino-enone **I-223**.[156]

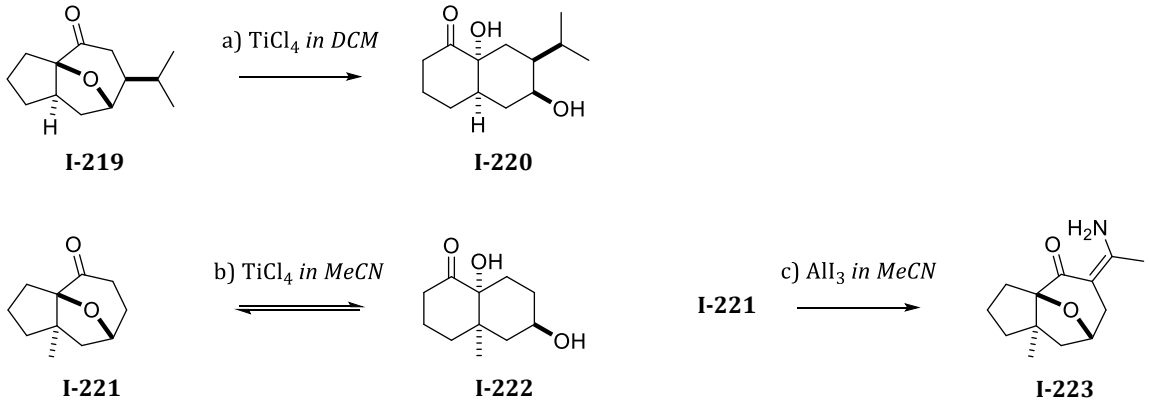

Scheme 59. Rearrangement of tricyclic ketone substrates **I-219** and **I-221**.

Reagents and conditions: **a)** DCM (0.19 M), $TiCl_4$ (2.4 eq), rt, 16 h; **48%**. *No substrate recovery reported.* **b)** MeCN (0.56 M), $TiCl_4$ (2.8 eq), rt, 2 h; **50%** (95% *b.r.s.m.*). **c)** MeCN (0.53 M), Al (1.75 eq), I_2 (1.42 eq), reflux, 8 h, *then* addition of **I-221** (1 eq), reflux, 21 h; **61%** (68% *b.r.s.m.*).

Integrating their work on both the *preparation* of the cycloadducts (*cf.* **Chapter 1.3.2**) and the *rearrangement* of these cycloadducts, SAMMES *et al.* demonstrated the versatility of tricyclic epoxyazulenes. With their findings, they opened up concise synthetic routes to several terpene classes and natural products, some of which are shown in **Figure 21**.

Epoxyazulene-to-decalone rearrangements gave different sesquiterpenes of the valerane class, such as cryptofauronol (**I-215**), fauronyl acetate (**I-224**), valeranone (**I-225**), and valerane (**I-226**).[154] On the other hand, 4-chloro epoxyazulenes like *endo*-chloride **I-207** (*cf.* page **92**) could be reductively cleaved to gain access to other sesquiterpenes, or key intermediates in the syntheses of those. These include β-bulnesene (**I-227**),[151,152] α-copaene (**I-228**) and α-ylangene (**I-229**), or the respective β-isomers of the latter two.[155]

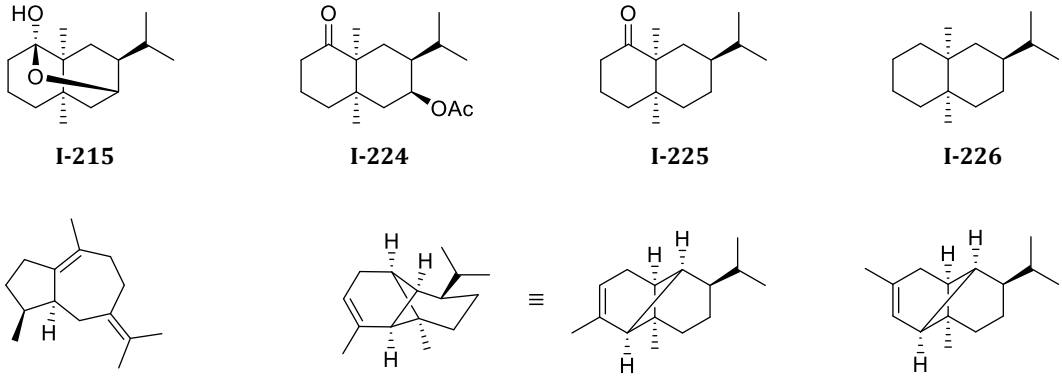

I-215 **I-224** **I-225** **I-226**

I-227 **I-228** **I-229**

Figure 21. Natural products and terpene classes accessed by SAMMES *et al*. Within their work, the respective racemates were prepared.

2.3.1 Planned Utilization of the LEWIS Acid-Induced Rearrangement

In this work, we planned to employ our tricyclic substrates in rearrangements with the goal of adding yet another terpene class to the those already accessed by SAMMES *et al*: the *class of neo-Clerodane diterpenoids* and its most prominent representative, salvinorin A (**I-11**). Central to this strategy was the rearrangement of secondary alcohols, as exemplified by that of *exo*-**I-174** in **Scheme 55** (page **91**). While the number of previously shown examples is rather limited, and similar rearrangements to decalones have, to the best of our knowledge, not been reported by other working groups, we opted to investigate this method in more detail.

Our main strategy was to utilize this rearrangement for secondary *exo*-alcohols or *exo*-hydroxynitriles such as *exo*-**65** or *exo*-**58** (**Scheme 60**).[19] Ultimately, these approaches aimed at obtaining **1**, the 7-hydroxylated analog of 2-deacetoxysalvinorin A (**I-52**), from which salvinorin A (**I-11**) is readily accessible (*cf.* **Chapter 1.2**). For this purpose, the removal of the 7-OH group from the precursor **1** may be approached via elimination to the respective α,β-unsaturated lactone and subsequent reduction.

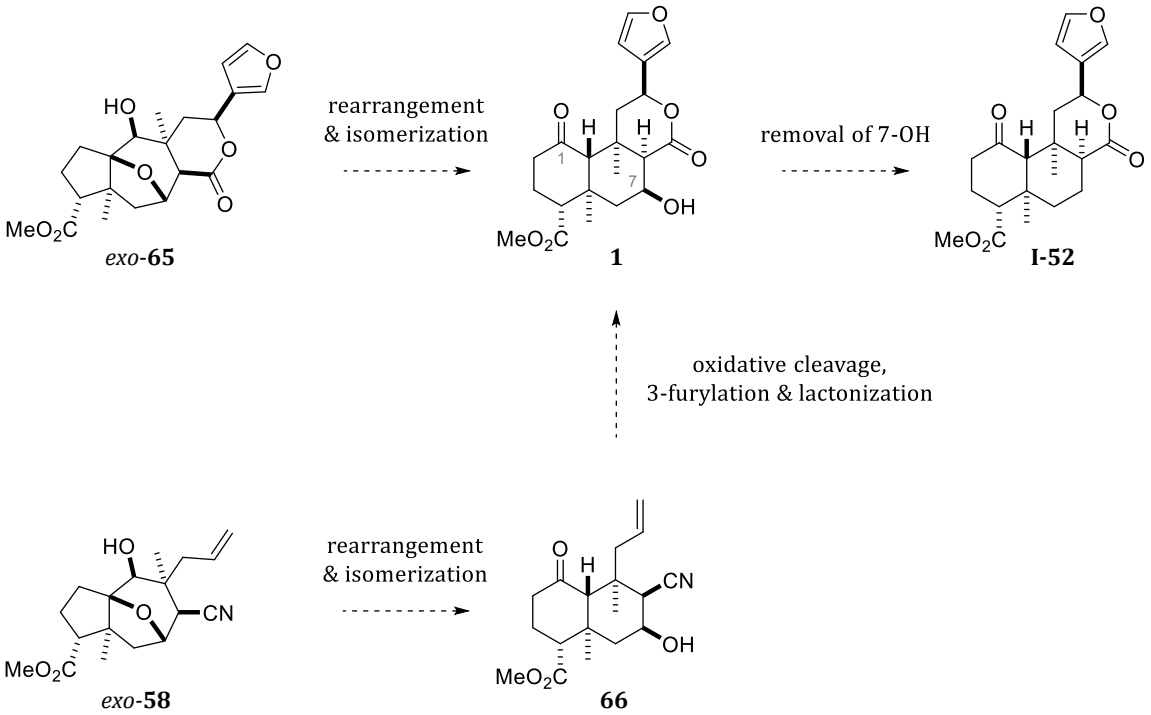

Scheme 60. Planned synthetic route utilizing the rearrangement of secondary hydroxynitriles.

[19] Some *endo*-OH analogs of our substrates were already covered and numbered starting from **Chapter 2.2.2**. To differentiate the *exo*- or *endo*-configuration of the hydroxy group, the prefix "*exo*-" is added henceforth.

To investigate on which 'level of functionalization' the rearrangement would be utilized best, several substrates were investigated. When the C1-*exo*-methylidene group was present, an alkene isomerization was observed, as expected from the reports of SAMMES *et al.* (*cf.* **Scheme 58** on page **93**). While this issue could be circumvented by the prior transformation of the *exo*-methylidene group to a methyl ester (**Chapter 2.2.2**), two other main issues with our substrates became progressively evident: the presence of the nitrile group, as well as the selective reduction of ketones to the undesired *endo*-alcohols. To circumvent the latter issues, we chose to also examine decyano substrates, as well as several reduction methods to obtain *exo*-alcohols or, alternatively, facilitate the rearrangement of *endo*-alcohols or their activated derivatives.

While the nitrile group was intended as a C_1 building block for the lactone group, this building block would be missing in decyano substrates. A possible alternative approach was 'relocating' this C_1 building block from the C8 carbon of the decalone to the 3-furyl alcohol moiety. After rearrangement, oxidation of the 7-OH to a ketone should provide a nucleophilic center at C8, which should allow C–C bond formation via enolate chemistry. Thus, an intramolecular CLAISEN condensation with the 3-furyl carbonate should open up an access to the lactone, as exemplified in **Scheme 61** by the sequence from **67** to 2-deacetoxysalvinorin A (**I-52**).

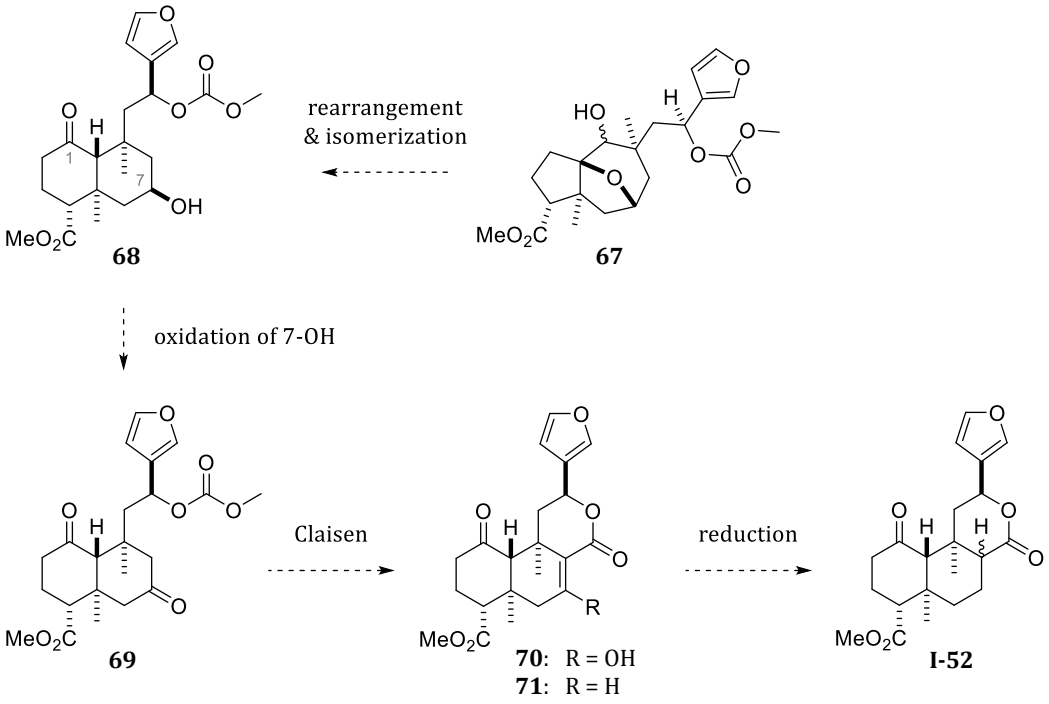

Scheme 61. Alternative approach using decyano substrates such as **67**.

After CLAISEN condensation, β-keto lactone **70** (*shown as its enol tautomer*) was to be transformed to α,β-unsaturated lactone **71**, which should give lactone **I-52** after conjugate reduction. Such a sequence was reported on the similar β-keto lactone **I-36** in the total synthesis

of EVANS *et al.* (**Chapter 1.2.2**), and lactone **I-52**, in turn, represents a central intermediate in the syntheses of HAGIWARA *et al*. (**Chapter 1.2.4**). Since regioselectivity problems may emerge in the CLAISEN condensation of diketone **69** due to the presence of the C1 ketone, a prior protection of this ketone group may be necessary.

While such a CLAISEN condensation may open up an access to δ-lactones, only a surprisingly low number of examples employing such a method could be found in the literature. Those examples predominantly cover the formation of the β-keto analogs of γ-lactones[248,268–270] or *aromatic* δ-lactones, i.e. benzopyranones.[271–273] Thus, investigating whether this sequence may be utilized for an efficient preparation of non-aromatic δ-lactones also seemed intriguing on a more fundamental level.

With these considerations, we approached the rearrangement of our cyano and decyano substrates. To gain further insights, such as regarding tolerances of different functional groups to the highly LEWIS acidic conditions, several differently functionalized substrates were evaluated. As a proof-of-concept, some tertiary alcohols and ketones were also used as substrates. These approaches ultimately cumulated in over 100 reactions with 22 different substrates, not counting in various derivatives used for the activation of *endo*-hydroxy groups.

Some substrates or rearrangement attempts will not be mentioned to avoid redundant or inconclusive information which were deemed to add little to no value overall. Generally, most reactions were not optimized or evaluated thoroughly, focusing on route scouting purposes instead to identify promising substrates and synthetic routes. For this purpose, we switched back and forth between cyano/decyano and secondary/tertiary alcohol or ketone substrates at different levels of functionalization.

With the intention to convey our findings and insights in the most concise and conclusive way, the following subchapters cover the preparation of tertiary and secondary alcohols, after which the rearrangement of the three substrate classes (tertiary alcohols, ketones, and secondary alcohols) will be treated separately and, ultimately, concluded collectively in **Chapter 2.3.6**.

2.3.2 Preparation of Substrates used in Rearrangement Attempts

2.3.2.1 Tertiary Alcohols

The tertiary alcohols used in proof-of-concept rearrangements were prepared by methylation of the respective ketones with MeMgBr (**Scheme 62**). The first attempts with decyano ketone **8-H** and ketonitrile **8** were presumably conducted with too much caution, resulting in only moderate conversions. However, sufficient amounts of both the tricyclic alcohols **72-H** and **72** were obtained for investigations into their respective behavior under rearrangement conditions. Therefore, these methylation reactions were not optimized or evaluated further. When ketone **7-H** was methylated under comparably more forcing conditions by using a higher excess of MeMgBr (4.5 eq) and heating the reaction mixture to reflux, the C5-substituted tertiary alcohol **59-H** was obtained in an excellent yield of 89% (98% *b.r.s.m.*).

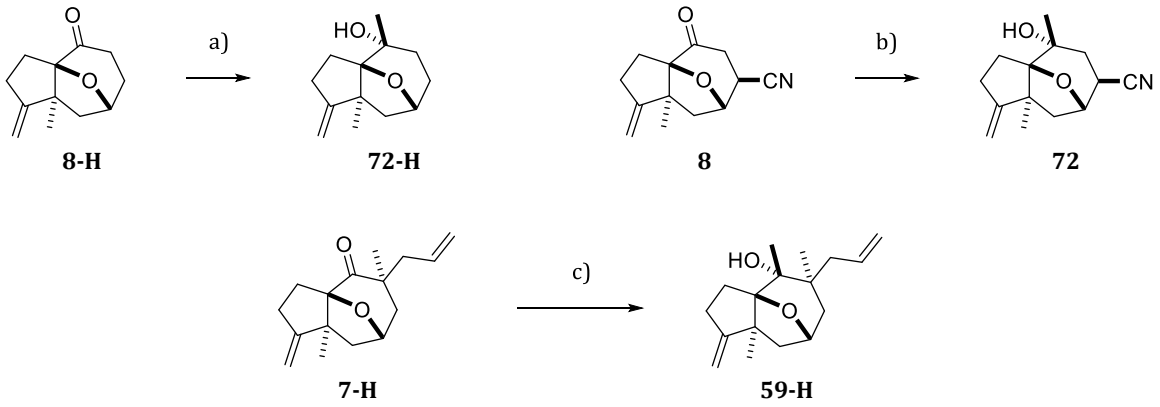

Scheme 62. Methylation of tricyclic ketones to tertiary alcohols.

Reagents and conditions: **a)** THF (0.11 M), MeMgBr (3 M in Et_2O, 1.2 eq), 0 °C to rt, 18 h, then additional MeMgBr (3 M in Et_2O, 1.2 eq), rt, 23 h; **56%** (81% *b.r.s.m.*). **b)** THF (0.12 M), MeMgBr (3 M in Et_2O, 1 eq), 0 °C to rt, 23 h; **not evaluated** thoroughly (see Experimental Section). **c)** THF (0.1 M), MeMgBr (3 M in Et_2O, 4.5 eq), reflux (80 °C), 15 h; **89%** (98% *b.r.s.m.*).

Since C4-methylated tertiary alcohols would introduce an undesired methyl group in the decalone core, an alternative for a potentially 'reversible tertiarization' was envisioned. By *C*-silylation of the ketone moiety, a *C*-silyl alcohol was to be prepared, which could be considered a tertiary alcohol and may enable a similar rearrangement reaction. Afterwards, the silyl group should be removable by desilylation.

Incidentally, silyl *nucleophiles* rarely find appliance in current natural product synthesis but have been used more frequently in the 1970s to 1990s. As carbon nucleophile analogs, they were used for reactions such as 1,2- or 1,4-additions to carbonyl compounds,[274–276] the silicon–lithium exchange of silyl enol ethers to lithium enolates,[277] or silylcuprations of alkynes.[278]

To test our hypothesis, ketone **8-H** was treated with DMPSLi to give α-hydroxysilane **73-H** (**Scheme 63**). Even though the yield of 38% (67% *b.r.s.m.*) leaves room for improvement, an optimization was not pursued due to unpromising results in the attempted rearrangement of **73-H**. Notable insights into the *C*-silylation are briefly summarized below.

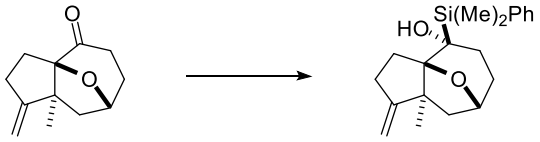

8-H **73-H**

Scheme 63. *C*-silylation of ketone **8-H** to α-hydroxysilane **73-H**.

Reagents and conditions: Et_2O (0.1 M), DMPSLi (0.3 M in Et_2O, 1.25 eq), –50 °C to 5 °C, 2.5 h, rt, 2.5 h; **38%** (67% *b.r.s.m.*).

Using THF as the solvent, only low conversion of **8-H** with DMPSLi was observed (NMR ratio of **8-H/73-H** ≤ 1:0.2), even when a stochiometric amount of $BF_3{\cdot}OEt_2$ was used to enhance electrophilicity of the ketone. As described in literature, using THF instead of Et_2O as solvent in the *C*-silylation of 4-*tert*-butylcyclohexanone resulted in "significant by-product formation".[274] Yet, using Et_2O instead of THF as the solvent was complicated due to the impeded *preparation* of the required silyl lithium reagents in Et_2O. For instance, TBDPSLi only began to form when some THF was added to the initial Et_2O solution. The formation of these silyl lithium reagents (DMPSLi or TBDPSLi), indicated by an intense red color, was determined by titration.

To ensure an efficient *C*-silylation, THF was removed in vacuo after preparation of the silyl lithium reagents. After co-evaporation of residual THF with Et_2O, the silyl lithium reagents were dissolved in Et_2O. While the addition of TBDPSLi to **8-H** (in either Et_2O/THF or Et_2O) resulted in no conversion, the addition of DMPSLi to **8-H** in only Et_2O (details listed in **Scheme 63**) led to the highest conversion within our attempts (NMR ratio of **8-H/73-H** ≈ 1:1).

2.3.2.2 Secondary Alcohols

As mentioned in the previous subchapter, the reduction of ketones was approached with the goal of preparing *exo*-alcohols. This endeavor proved fruitless, as only the *endo*-alcohols were obtained with our substrates. For our investigations into a potential rearrangement of *endo*-alcohols, both the 5-unsubstituted and 5-allyl-5-methyl-substituted alcohols, either with or without the nitrile group at C6, were prepared (**Scheme 64**).

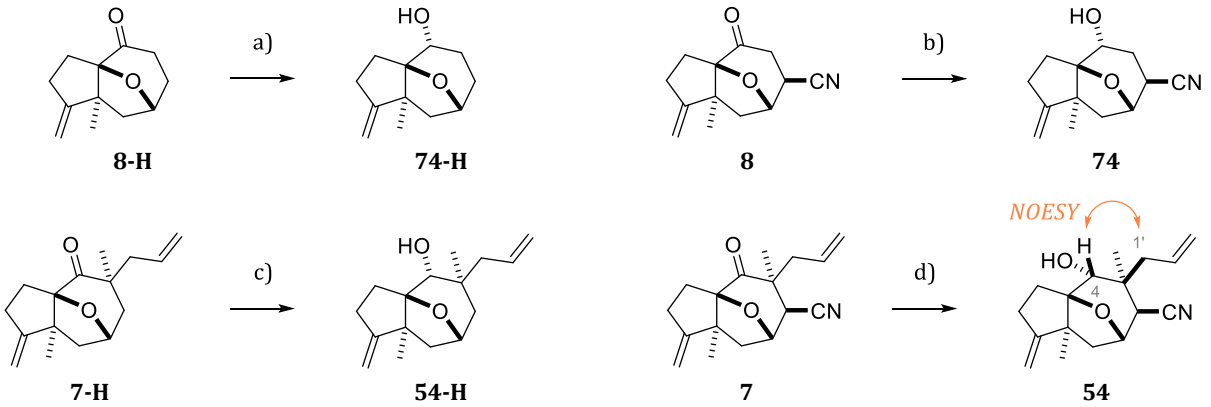

Scheme 64. Reduction of tricyclic ketones to secondary alcohols. For **54**, a NOE signal between 4-H and 1'-H_b affirms the *exo*-face selectivity of the hydride addition.

Reagents and conditions: **a)** MeOH (0.11 M), $NaBH_4$ (0.78 M in EtOH, 0.375 eq, equaling 1.5 hydride eq), 0 °C, 15 min; **82%**. **b)** MeOH (0.12 M), $NaBH_4$ (0.78 M in EtOH, 0.5 eq, equaling 2 hydride eq), 0 °C, 30 min; **97%**. **c)** THF (0.1 M), Red-Al (0.125 M in toluene/THF, 1.1 eq, over 5 min), –30 °C to 0 °C, 1.25 h; **quantitative yield**. **d)** MeOH (0.11 M), $NaBH_4$ (in total 12 eq, equaling 48 hydride eq; see Experimental Section), 0 °C to rt, 20 h, **74%**.

The 5-unsubstituted alcohols **74-H** and **74** were obtained efficiently by reduction with sodium borohydride (82% and 97%, respectively). Since a precise dosage of $NaBH_4$ in small-scale test experiments can be complicated, a solution of known molarity was prepared before reduction reactions. For this purpose, a $NaBH_4$ solution in EtOH was prepared. Compared to that in MeOH, the solvolysis of $NaBH_4$ in EtOH proceeds only very slowly, as reported by BROWN *et al.*[279]

While the reductions to **74-H** and **74** proceeded smoothly with only 1.5–2 hydride equivalents, the more sterically encumbered 5-substituted ketones required up to 48 hydride equivalents. Furthermore, the yields were considerably lower (74% of **54**; 45% (86% *b.r.s.m.*; not listed) of **54-H**). In latter case, the reduction of ketone **7-H** with Red-Al proved far superior, affording **54-H** in quantitative yield. The Red-Al reduction was, however, not evaluated for the other substrates.

In all reduction reactions, only the depicted *endo*-alcohols were obtained. While this C4-configuration could not be determined unambiguously for most compounds due to superimposed NMR signals, the NOESY spectrum of **54** allowed for a better determination. As indicated in **Scheme 64**, the protons 4-H and one allylic proton at C1' (denoted as 1'-H_b in the Experimental Section) are clearly separated from other proton signals and exhibit a NOE signal between them, affirming the depicted *endo*-configuration of the hydroxy function at C4.

An unambiguous confirmation of this *endo*-configuration was achieved by X-ray analysis of crystals obtained by slow evaporation of a C_6D_6 solution of **54** (**Figure 22**). The *exo*-face selective addition pattern of substituents introduced into the tricyclic core up to this point can be deducted from this crystal structure. Evidently, (i) the 1,4-hydrocyanation afforded the 6-*exo*-nitrile, (ii) the TSUJI-TROST allylation introduced the 5-*exo*-allyl, and lastly, (iii) a reduction of ketones proceeds with an *exo*-addition of the hydride, giving the undesired 4-*endo*-alcohols.

Furthermore, the torsion angle between the C8a–C3a bond – which is supposed to be the migrating group in the desired rearrangement – and the 4-OH bond equals to θ = 68.35 °. Consequently, these two bonds assume a *synclinal/gauche* (θ = 30–90 °) instead of the desired *antiperiplanar* relation (θ = 150–180 °).[280] The torsion angle between C8a–C3a and 4–H equals to θ = 177.06 ° (*not shown*), suggesting that an antiperiplanar relation of the migrating group and the leaving group would be assumed in the desired, but not obtained, *exo*-alcohols.

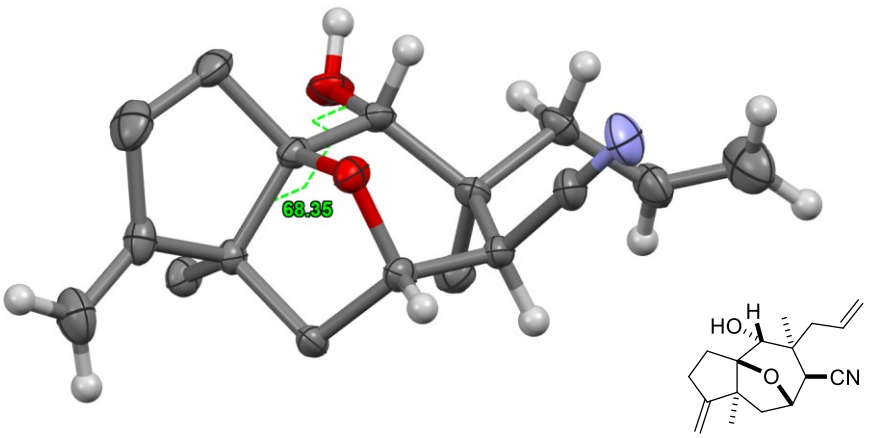

Figure 22. X-ray crystal structure of hydroxynitrile **54**. Disorders in the allyl moiety, as well as methylene and methyl protons are omitted for clarity (displayed in the **Appendix**).

Alternative reduction methods which may invert the *exo*-face selectivity and thus afford the desired *exo*-alcohols instead were also examined (**Scheme 65**). Reductions of ketone **8-H** with either L-Selectride or a combination of MAD (**75**) and *t*-BuMgCl gave the undesired *endo*-alcohol **74-H**. Especially the latter method, introduced by YAMAMOTO *et al.*,[281,282] seemed promising. With this method, a blocking of the sterically less hindered side due to complexation of the bulky aluminum reagent MAD with the carbonyl group was expected. The following GRIGNARD reduction with *t*-BuMgCl should then deliver the formal hydride from the other, originally sterically more encumbered side, resulting in an inversed (*anti*-Cram) selectivity by kinetic control.[283] While this method was successful on *tert*-butylcyclohexanone in our hands, giving the same isomer as reported in literature,[282] such an inversion of selectivity was not observed with our tricyclic ketone substrate **8-H**.

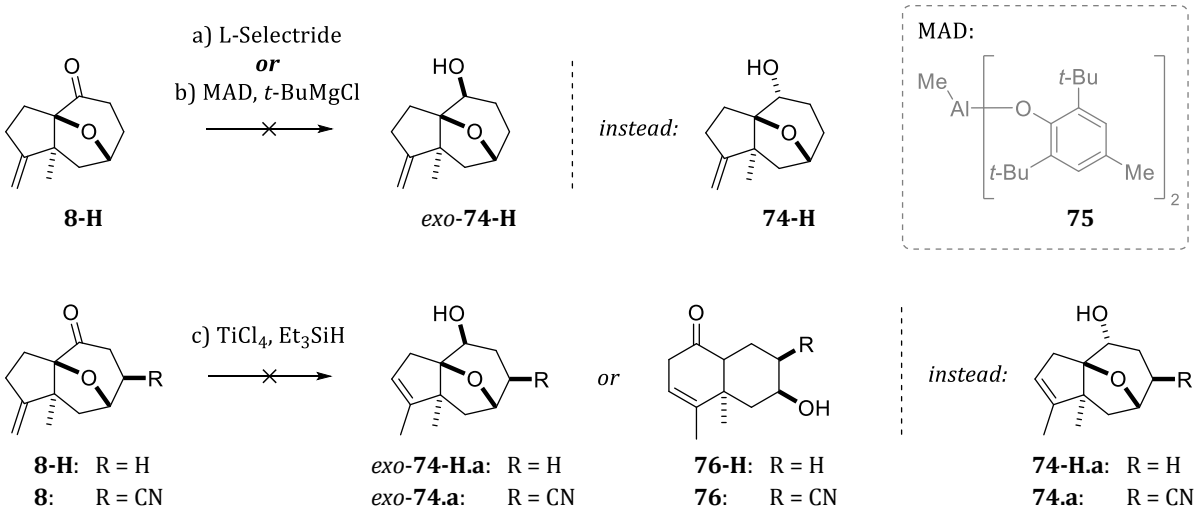

Scheme 65. Alternative reductions of ketone **8-H** and ketonitrile **8**.

Reagents and conditions: **a)** THF (0.1 M), L-Selectride (1 M in THF, 1.1 eq, over 5 min), 0 °C, 1.5 h; **reduction to *endo*-alcohol 74-H** (**70%**). **b)** Toluene (0.1 M), BHT (6 eq), $AlMe_3$ (2 M in toluene, 3 eq), rt, 1 h; *then* **8-H** (1 eq), 0 °C, 10 min, *t*-BuMgCl (1 M in THF, 3 eq, over 1 min), 0 °C to rt, 8 h; **reduction to *endo*-alcohol 74-H** (*not evaluated quantitatively*). **c)** DCM (0.1 M), Et_3SiH (4 eq), $TiCl_4$ (1 M in DCM, 1.2 eq, over 2 min), –78 °C to 0 °C, 2.5 h; **reduction to isomerized *endo*-alcohols 74-H.a** and **74.a**, respectively (*not evaluated quantitatively*).

In a former project within our group (USHAKOV & MAIER), an alternative reduction method with $TiCl_4$ and Et_3SiH proved successful for obtaining an otherwise inaccessible alcohol epimer.[284] It was anticipated that subjecting our tricyclic ketones **8-H** and **8** to these conditions may also result in a reduction to the *exo*-alcohols – perhaps followed by a rearrangement reaction to **76-H** or **76** due to the presence of $TiCl_4$. Unfortunately, merely the alkene-isomerized *endo*-alcohols **74-H.a** and **74.a** were obtained.

Another approach to the desired *exo*-configuration at C4 was the inversion of the obtained *endo*-alcohols, either to *exo*-alcohols, -esters or -halogenides, which should also allow for a rearrangement. All pursued variations of such an inversion, either via APPEL or MITSUNOBU reactions (**Scheme 66**) or a substitution of sulfonates were unsuccessful.

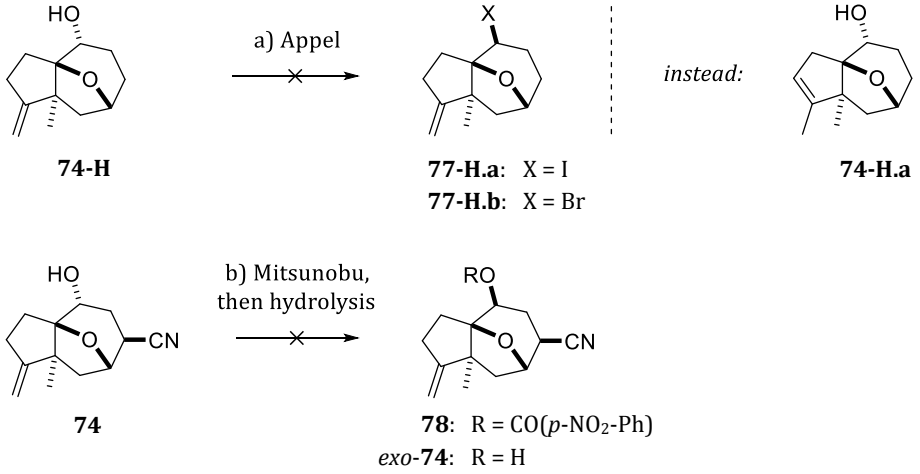

Scheme 66. Attempted C4-inversions to the *exo*-derivatives by APPEL or MITSUNOBU reactions.

Reagents and conditions: **a) (i)**: DCM (0.05 M), PPh_3 (1.5 eq), NEt_3 (1.375 eq), I_2 (1.25 eq), 0 °C to rt, 22 h; ***or* (ii)**: DCM (0.11 M), CBr_4 (1.2 eq), PPh_3 (1.3 eq), 0 °C to rt, 4 d; only **alkene isomerization** to **74-H.a** in both cases (*not evaluated quantitatively*). **b)** THF (0.09 M), PPh_3 (3.8 eq), *p*-NO_2-PhCOOH (4.1 eq), DEAD (~40% in toluene, 4.5 eq), 0°C to rt, 23 h, 40 °C, 4 h; separation by flash chromatography; then THF (0.06 M), aq. NaOH (10 w-%, ~44 eq), rt, 27 h; **recovery of substrate 74** (91%).

Both APPEL reactions on decyano alcohol **74-H** gave the alkene isomer **74-H.a** with no formation of the respective halide being evident. The MITSUNOBU reaction on hydroxynitrile **74** with *p*-nitrobenzoic acid[285] was not easily assessable due to the large amounts of excess reagents (700 mg crude product from 50 mg starting material). After flash chromatography, most of the reagents could be removed, indicating the presence of **74** and co-eluted *p*-nitrobenzoic acid. Treating this mixture with aqueous NaOH then led to the recovery of hydroxynitrile **74**.

To evaluate whether an activation of the *endo*-alcohols would make the rearrangement feasible, several ester-derivatives such as the acetates, trifluoroacetates, mesylates and triflates were investigated. It was rationalized that such a functionalization of the hydroxy group to a better leaving group may potentially enable a rearrangement reaction with LEWIS acids by enforcing the formation of a secondary cation at C4.

Mesylation of **74-H** gave mesylate **79-H** in a moderate yield of 65% (**Scheme 67**). With mesylate **79-H**, an alternative to the unsuccessful inversion by MITSUNOBU reaction was attempted. This alternative method uses sulfonate esters as substrates, which are heated at reflux with cesium acetate and 18-crown-6, allowing for an inversion to the respective acetates even with relatively hindered substrates.[286–289] However, *endo*-mesylate **79-H** remained unchanged under these conditions and showed no conversion to the desired *exo*-acetate **80-H**.

The mesylation of 5-substituted alcohol **54-H** was not successful, even with higher equivalents of reagents and prolonged reaction time, presumably due to steric hindrance induced by the 5-substitutents. Next to unreacted **54-H**, the formation of a distinctively non-polar compound was evident in TLC analysis. However, this new compound did not correspond to mesylate **81-H** in NMR, suggesting a conversion to the respective chloride instead. Due to the unpromising results, either from inversion or rearrangement attempts on mesylates, the preparation of mesylates was discontinued.

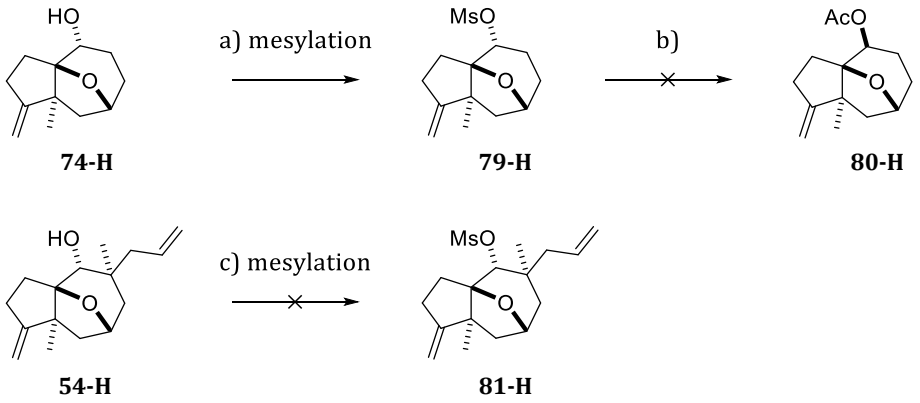

Scheme 67. Mesylation of alcohols **74-H** or **54-H** and attempted inversion of mesylate **79-H**.

Reagents and conditions: **a)** DCM (0.1 M), NEt_3 (2 eq), $MeSO_2Cl$ (1.5 eq), 0 °C, 1 h; **65%**. **b)** benzene (0.06 M), CsOAc (3 eq), 18-crown-6 (0.5 eq), reflux, 17 h, then additional CsOAc (3 eq) and 18-crown-6 (0.5 eq), reflux, 24 h; **no conversion**. **c)** DCM (0.1 M), NEt_3 (1.5 eq), $MeSO_2Cl$ (1.2 eq), 0 °C to rt, 1.5 h, then additional NEt_3 (2 eq) and $MeSO_2Cl$ (2 eq), rt, 17 h; **no formation of mesylate 81-H**.

The preparation of triflates analogs proved even more challenging than that of the mesylates. While TLC analysis indicated a possible formation of the triflates from the C5-unsubstituted alcohols **74-H** or **74**, the isolation of these triflates could not be achieved with different triflation conditions and either aqueous or non-aqueous work-up methods (**Scheme 68** on the next page).

When hydroxynitrile **74** was treated with Tf_2O and pyridine, the formation of the presumed triflate **82** (R_f = 0.65 in PE/EA, 1:1; R_f (**74**) = 0.44) and its subsequent decomposition during work-up was apparent on TLC. However, it was possible to isolate the other main component (R_f = 0.78), which was identified as *bis*-alkene **83**.

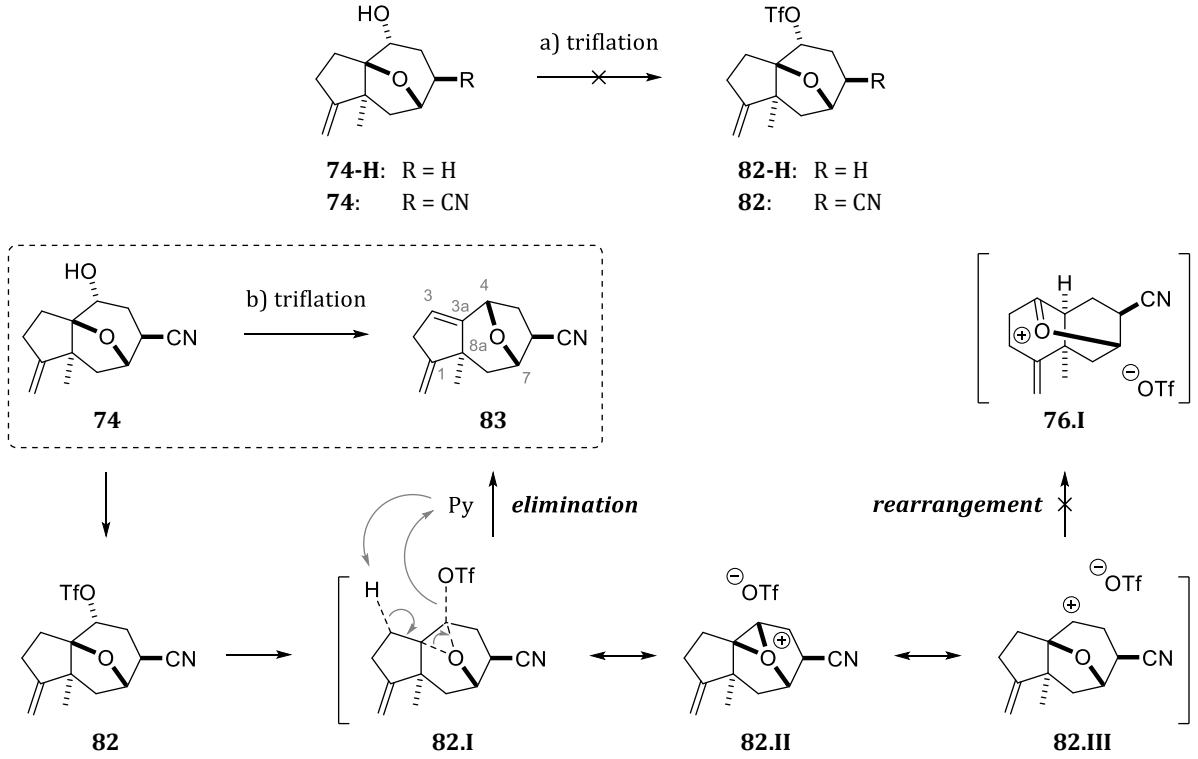

Scheme 68. Attempted triflation of **74-H** and **74** with formation of the elimination product **83** from hydroxynitrile **74** (dashed box).

Reagents and conditions: **a) (i)**: DCM (0.11 M), pyridine (1.5 eq), Tf_2O (1.1 eq), 0 °C to rt, 22 h; *filtration through silica gel*, **mostly decomposition**; ***or*** **(ii)**: DCM (0.075 M), Tf_2O (1.1 eq), 0 °C to rt, 24 h; *aqueous work-up*, **mostly decomposition**; ***or*** **(iii)** DCM (0.075 M), DMAP (1.3 eq), Tf_2NPh (1.2 eq), 0 °C to rt, 24 h; *aqueous work-up*, **low conversion** for **74-H**, **mostly decomposition** for **74**. **b)** DCM (0.11 M), pyridine (1.6 eq), Tf_2O (1.15 eq), 0 °C to rt, 16 h; *aqueous work-up*, **mostly decomposition & isolation of *bis*-alkene 83** (**30%**).

A plausible mechanism for this formal elimination would be a concerted displacement of the 4-triflate group with a concurrent abstraction of a 3-proton by pyridine. This elimination process with involvement of the ether bridge, inducing a shift from a [3a,7]- to a [4,7]-bridged epoxyazulene, is indicated on the intermediate **82.I**.

Alternatively, a stepwise elimination following the displacement of the triflate group to the oxonium species **82.III** or the secondary carbocation **82.II** would be conceivable. While the carbocation should allow for the desired rearrangement, this seems to be impeded by the more stable oxonium species, as also presumed by SAMMES *et al.* (**Chapter 2.3**). This neighboring group participation of the ether bridge also explains why attempted inversions of *endo*-alcohols result in substitution with retention of configuration – if a substitution occurs at all.

2.3.3 Rearrangement of Tertiary Alcohols

The rearrangement of tertiary alcohols was first attempted with our simplest tricyclic substrates. As anticipated, treating decyano alcohol **72-H** with $TiCl_4$ in DCM for two days afforded decalone **84-H** in a good yield of 82% (**Scheme 69**). The comparison to the reaction times reported for the substrates of SAMMES *et al.* (30 min to a few hours, cf. page **93**) seems to indicate a certain 'deactivation' of our substrates in the rearrangement. Later, $Sc(OTf)_3$ was identified as a very suitable alternative to $TiCl_4$ for **72-H**. Only catalytic amounts of $Sc(OTf)_3$ and a noticeably shorter reaction time were required for a complete rearrangement (10 mol%, <2.25 h). While TLC and NMR analysis of crude **84-H** from the rearrangement with $Sc(OTf)_3$ indicated less impurities than from that with $TiCl_4$, a quantitative evaluation was not pursued.

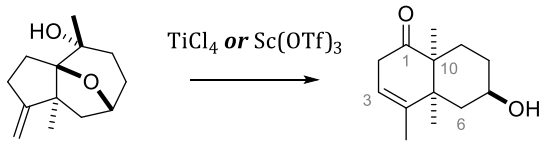

72-H **84-H**

Scheme 69. Rearrangement of decyano alcohol **72-H** to decalone **84-H**.

Reagents and conditions: **(i)**: DCM (0.1 M), $TiCl_4$ (1 M in DCM, 1 eq), 0 °C to rt, 45 h; **82%**. ***or*** **(ii)**: $MeNO_2$ (0.07 M), $Sc(OTf)_3$ (10 mol%), rt; **full conversion in <2.25 h**, *not evaluated quantitatively*.

In stark contrast to **72-H**, its 6-cyano analog **72** did not undergo rearrangement to nitrile-substituted decalone **84**. Instead, only alkene isomerization to **72.a** was observed with either $BF_3{\cdot}OEt_2$, $TiCl_4$ or $Sc(OTf)_3$ (**Scheme 70**). These findings clearly indicated that the presence of the 6-nitrile group completely obviated the desired rearrangement reaction.

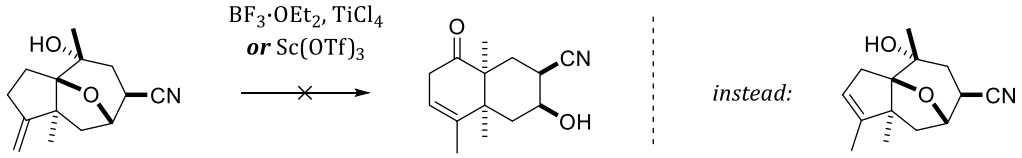

72 **84** **72.a**

Scheme 70. Attempted rearrangement of hydroxynitrile **72** to **84**.

Reagents and conditions: **(i)**: DCM (0.05 M), $BF_3{\cdot}OEt_2$ (1 M in DCM, 1.2 eq), 0 °C to rt, 19 h; ***or*** **(ii)**: DCM (0.05 M), $TiCl_4$ (1 M in DCM, 1.2 eq), rt, 2 d; ***or*** **(iii)**: $MeNO_2$ (0.05 M), $Sc(OTf)_3$ (10 mol%), rt, 8 h, 60 °C, 14 h; in all three cases, **only alkene isomerization to 72.a** was observed.

To further investigate the rearrangement reaction with more complex decyano substrates, 5-substituted tertiary alcohol **59-H** was treated with $TiCl_4$. While a rearrangement took place, an undesired concomitant halo-PRINS cyclization followed under these conditions, ultimately affording tetracyclic ether **86-H** as the sole product (**Scheme 71**). Notably, when acetonitrile was used as the solvent, only alkene isomerization was observed.

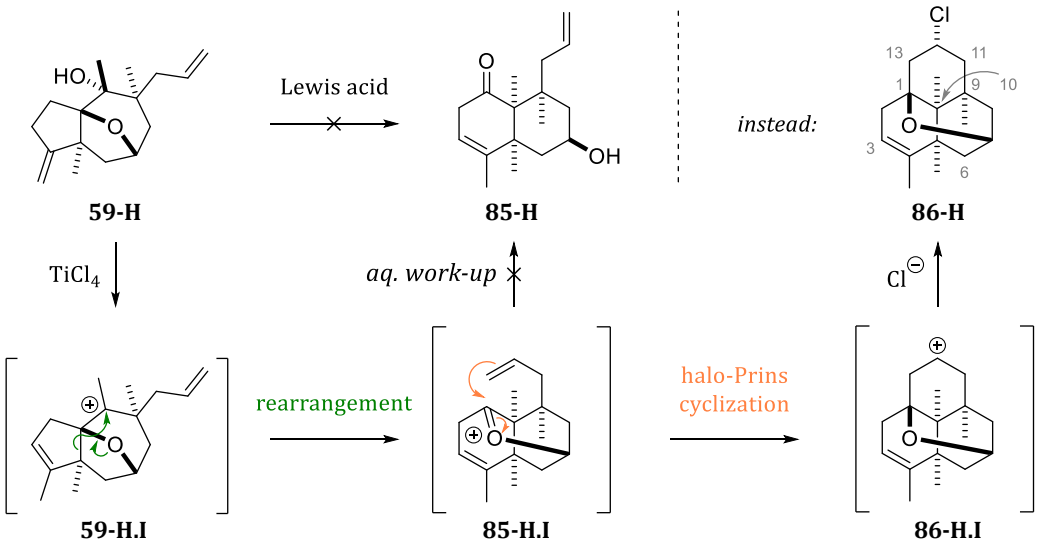

Scheme 71. Rearrangement of **59-H** with concomitant halo-PRINS cyclization to **86-H**.

Reagents and conditions: **(i)**: DCM (0.057 M), $TiCl_4$ (1 M in DCM, 0.92 eq), 0 °C to rt, 20 h; **65%**, *single diastereomer*. ***or*** **(iv)**: MeCN (0.053 M), $TiCl_4$ (1 M in MeCN, 1.25 eq), rt, 1 d; **only alkene isomerization** was observed.

Tetracyclic ether **86-H** possesses an intertwined 6/6/6/6-fused ring system with four quaternary bridgehead carbons (C1, C5, C9 and C10). This represents a hydrogenated and ether-bridged phenalene derivative and, to the best of our knowledge, an unprecedented core structure with no close match in literature (searched via SCIFINDER database in August 2024).

86-H was obtained as a single diastereomer exhibiting a strong NOESY correlation between 12-H and one of the protons at C8. Therefore, the depicted configuration was assumed. This correlation should only be possible when the *cis*-fused B and C rings are 'bent towards each other,' resulting in a relatively close arrangement of two *pseudo*-axial protons at C12 and C8. Interestingly, the NOESY correlation between 12-H and its *directly neighboring* vicinal protons at C11 or C13 appeared noticeably weaker.

The assigned configuration was confirmed by X-ray analysis of crystals obtained by slow evaporation of a $CDCl_3$/hexane solution of **86-H** (**Figure 23** on the next page). The spatial proximity of the *pseudo*-axially aligned 12-H and 8-H protons is evident from this crystal structure: with 2.026 Å, this distance is noticeably shorter than those of 12-H to the respective vicinal protons at C11 or C13 (2.345 Å and 2.321 Å, respectively).

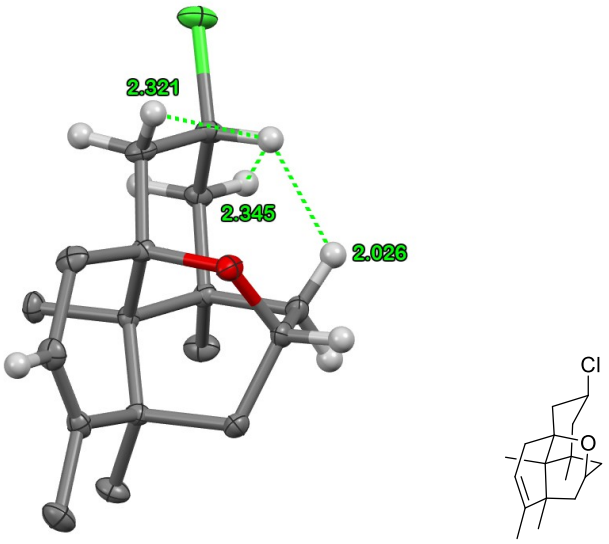

Figure 23. X-ray crystal structure of tetracyclic ether **86-H** with a structural formula representing the true structure more precisely.
Most methylene and methyl protons are omitted for clarity (displayed in the **Appendix**).

Due to the promising results in the $Sc(OTf)_3$-catalyzed rearrangement of **72-H**, some attempts were made to investigate whether $Sc(OTf)_3$ would also induce a rearrangement of tertiary alcohol **59-H**, ideally without a concomitant PRINS cyclization. Such attempts resulted only in alkene isomerization and, with prolonged reaction time or at elevated temperatures, significant decomposition. $Sc(OTf)_3$ was either used without prior treatment, as it had been used in the successful rearrangement of **72-H**, or after drying at elevated temperatures in vacuo. This drying led to a mass loss of 14%, indicating that the commercially obtained samples of $Sc(OTf)_3$ hold over 4 equivalents of water. It has to be noted that drying $Sc(OTf)_3$ increases its catalytic activity, but may also lead to side-reactions in some cases.[290]

The $Sc(OTf)_3$-catalyzed rearrangement was also attempted in Ac_2O/AcOH as solvent mixture to possibly (i) activate the catalyst by quenching residual water, (ii) facilitate rearrangement by prior acetate formation, and (iii) 'trap' the intermediary oxonium species **85-H.I** by nucleophilic addition of acetic acid at C7, which may obviate the intramolecular halo-PRINS cyclization.

This method was tried both with **59-H**, resulting in a complex mixture which was not further analyzed, and the 1,5-substituted tertiary alcohol **63-H** (**Scheme 72** on the next page). Unexpectedly, $Sc(OTf)_3$ failed to induce a rearrangement in all cases, giving only acetate **88-H** in a moderate yield of 55%. Interestingly, when acetonitrile was present, this acetylation was dramatically impeded, adding to the observations that nitrile groups seem to lower the activity of LEWIS acids in general. A rearrangement of **63-H** with $TiCl_4$ was not attempted due to the expected concomitant halo-PRINS cyclization.

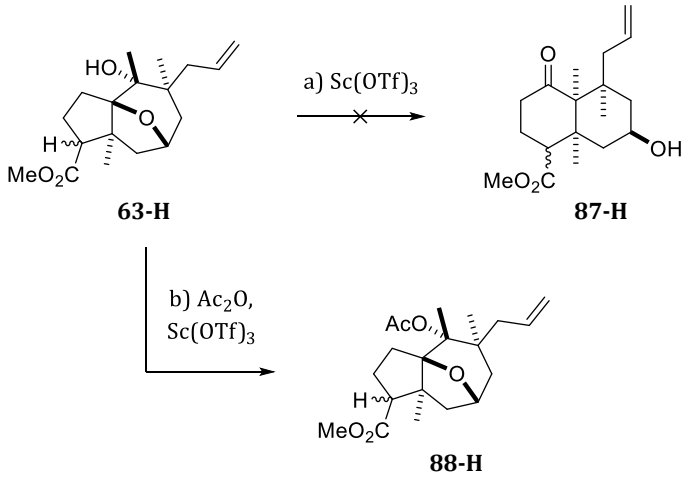

Scheme 72. Attempted rearrangement of 1,5-substituted tertiary alcohol **63-H**.

Reagents and conditions: **a)** $MeNO_2$ (0.04 M), $Sc(OTf)_3$ (10 mol%), rt, 30 h, 50 °C, 14 h; **no conversion**. **b)** Ac_2O (0.04 M), $Sc(OTf)_3$ (5 mol%), rt, 6 h; **full conversion** to acetate **88-H** (**55%**). ***or*** Ac_2O/MeCN (1:1, 0.04 M), $Sc(OTf)_3$ (5 mol%), rt, 2 d; **moderate conversion** to acetate **88-H**.

The method with $Sc(OTf)_3$ were also tested on a substrate, in which the allyl moiety was functionalized prior to the rearrangement (**Scheme 73**). From hydroxy aldehyde **64-H**, which seemed to partially autoxidize to its carboxylic acid (*cf.* page **88**), *bis*-alcohol **89-H** was obtained by reduction with borane. Subjecting **89-H** to the methods listed in **Scheme 72** did not indicate any rearrangement to **90-H**. Instead, the formation of *bis*-acetate **91-H**, accompanied by substantial decomposition, was evident. This acetylation was neither evaluated quantitatively, nor was a rearrangement with $TiCl_4$ attempted on *bis*-acetate **91-H**.

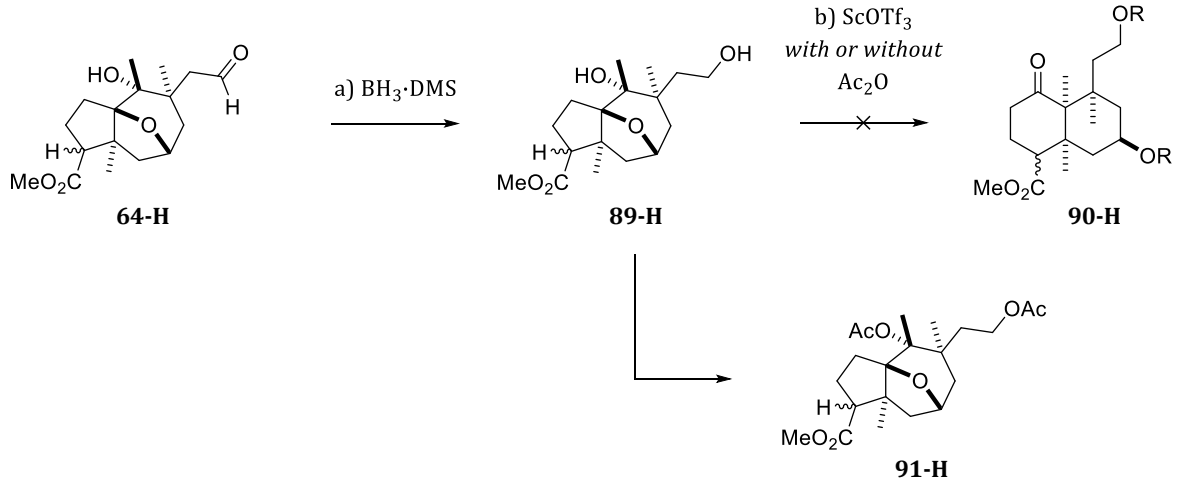

Scheme 73. Attempted rearrangement of 1,5-functionalized *bis*-alcohol **89-H**.

Reagents and conditions: **a)** THF (0.05 M), BH_3·DMS (0.5 M in THF, 0.75 eq), –40 °C to 0 °C, 45 min; **73%**. **b)** similar to the methods listed in **Scheme 72**. *This sequence is omitted in the Experimental Section*.

Rearrangements attempts of α-hydroxysilane **73-H** with $Sc(OTf)_3$ or $TiCl_4$ led to results ranging from no conversion to practically full decomposition, mainly depending on used solvents – in no case, however, a rearrangement to **92-H** was evident (**Scheme 74**). Next to alkene isomerization and decomposition, only one distinct compound was discernible and isolated. This compound, obtained by employing $TiCl_4$ in DCM, presumably corresponds to the dephenylated silyl species **73-H.a**, but was not analyzed in detail to confirm the chloro substitution at the silyl center.

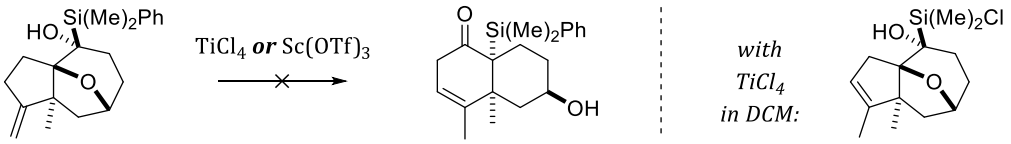

73-H **92-H** **73-H.a**

Scheme 74. Attempted rearrangement of α-hydroxysilane **73-H**.

Reagents and conditions: **(i)**: MeCN (0.05 M), $TiCl_4$ (1.25 eq), rt, 3 d; **partial alkene isomerization**. ***or*** **(ii)**: DCM (0.05 M), $TiCl_4$ (1 eq), rt, 3 d; **fast alkene isomerization & isolation of 73-H.a** (**38%**). ***or*** **(iii)**: MeCN (0.05 M), $Sc(OTf)_3$ (10 mol%), rt, occasionally warmed to 50 °C, in total 14 d; **no conversion**. ***or*** **(iv)**: DCM (0.05 M), $Sc(OTf)_3$ (10 mol%), rt, 3 d; **partial alkene isomerization**. ***or*** **(v)**: $MeNO_2$ (0.05 M), $Sc(OTf)_3$ (10 mol%), rt, 19 h; **decomposition**.

With these tertiary alcohols, important insights into the desired rearrangement could be gained. These include possible side reactions and, most notably, the observations that nitrile groups – either in the substrate or the solvent – completely hindered a potential rearrangement. Thus, the approaches on *tertiary* alcohols were concluded with some aspects remaining unresolved. Especially the behavior of $Sc(OTf)_3$ – which catalyzed the rearrangement of **72-H** efficiently but failed to do so with higher-functionalized substrates – lacks a conclusive explanation. While steric hindrance induced by the C5 substituents might be considered as a straightforward explanation, some aspects cannot be attributed to steric hindrance alone, especially when the observations with ketone substrates and $Sc(OTf)_3$ are considered, as discussed next.

2.3.4 Rearrangement of Ketones

Treating ketone **8-H** with $TiCl_4$ in DCM resulted in a 1:1 mixture of alkene isomer **8-H.a** (33% yield) and its rearrangement product, hydroxy acyloin **93-H** (32% yield) (**Scheme 75**). When MeCN was used as solvent, which proved superior for SAMMES *et al.* (*cf.* **Scheme 59** on page **94**), the rearrangement was obviated completely. This corroborated the inhibiting effect of MeCN which was already observed with tertiary alcohols, and thus expected.

Unexpectedly, $Sc(OTf)_3$ in $MeNO_2$ failed to induce a rearrangement, further indicating that a *general suitability* of $Sc(OTf)_3$ for this purpose cannot be assumed. In the case of tricyclic ketone substrates, the interaction of $Sc(OTf)_3$ with the carbonyl π-electrons may be insufficient for an adequate activation which would enable a rearrangement.

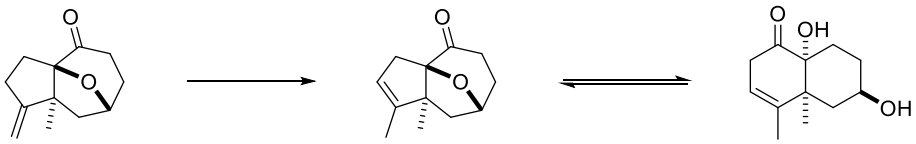

8-H **8-H.a** **93-H**

Scheme 75. Rearrangement of ketone **8-H** to acyloin **93-H**.

Reagents and conditions: **(i)**: DCM (0.14 M), $TiCl_4$ (1 eq), 0 °C to rt, 18 h; **33%** of **8-H.a** & **32%** of **93-H**.
or **(ii)**: MeCN (0.06 M), $TiCl_4$ (1.1 eq), rt, 7 d; **only slow alkene isomerization** to **8-H.a**.
or **(iii)**: $MeNO_2$ (0.09 M), $Sc(OTf)_3$ (10 mol%), rt, 2 d; **only alkene isomerization** to **8-H.a**.

With ketonitrile **8**, no rearrangement was evident with $TiCl_4$ in MeCN (**Scheme 76**). This attempt was made at a point in time when the inhibiting effect of MeCN was not yet realized. While a similar attempt using **8** with $TiCl_4$ *in DCM* would be interesting to further verify – or unexpectedly, falsify – the inhibiting effect of the nitrile group present in the substrate, such an experiment was not conducted.

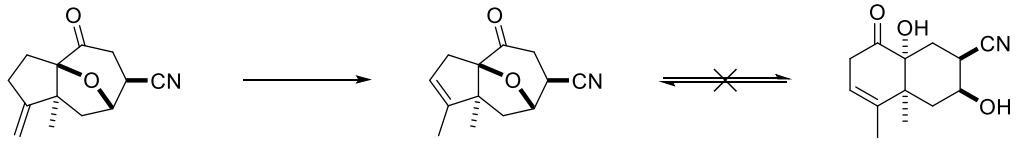

8 **8.a** **93**

Scheme 76. Attempted rearrangement of ketonitrile **8** to acyloin **93**.

Reagents and conditions: MeCN (0.14 M), $TiCl_4$ (2.5 eq), rt, 3 d; **only alkene isomerization** to **8.a**.

Treating 5-substituted ketone **7-H** with $TiCl_4$ in DCM resulted in a complex mixture in which four distinct TLC spots were discernible (**Scheme 77**). Next to the formation of alkene isomer **7-H.a** (24% yield), a concomitant halo-PRINS cyclization to **95-H** (13% yield) was evident, as expected from the formation of tetracyclic ether **86-H** (**Scheme 71** on page **108**). The other two compounds could not be isolated without impurities (in total 28 m-% of substrate weight) and did not exhibit allyl or carbonyl peaks in NMR spectra, which might suggest a formation of the halo-PRINS cyclization products **7-H.b**. No rearrangement to **94-H** without halo-PRINS cyclization was evident. Due to formation of the complex mixture within this attempt and the low yield with the 'successful' rearrangement of ketone **8-H**, this approach was not further investigated.

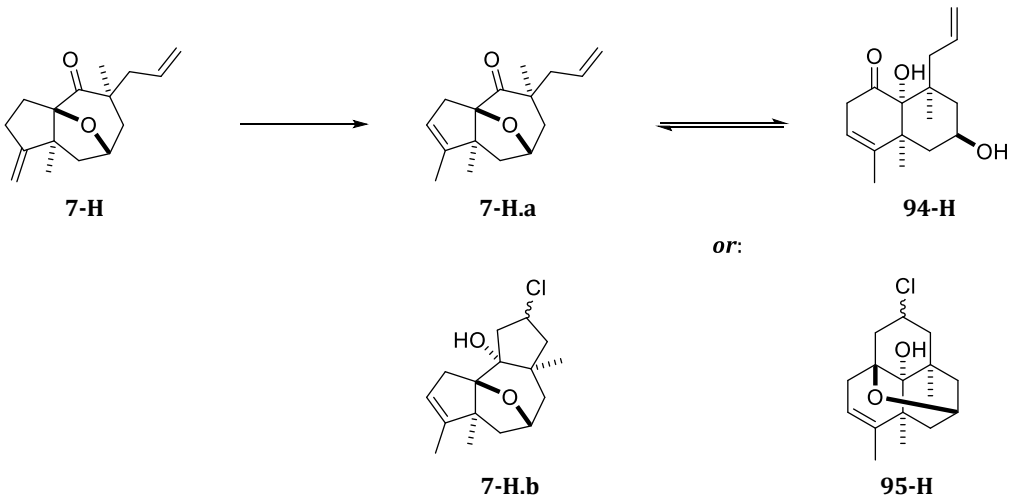

7-H **7-H.a** **94-H**

or:

7-H.b **95-H**

Scheme 77. Attempted rearrangement of 5-substituted ketone **7-H** to **94-H**.

Reagents and conditions: DCM (0.52 M), $TiCl_4$ (1 eq), 0 °C to rt, 4 d; **complex mixture** with **7-H.a** (**24%**) & **95-H** (13%), *not included in the Experimental Section*.

2.3.5 Rearrangement of Secondary Alcohols

Rearrangement attempts with our secondary alcohols resulted mostly in alkene isomerization (**Scheme 78**). With $TiCl_4$ in DCM, the formation of the chlorides **96-H** and **96** was indicated by an apolar spot in TLC, as was expected for secondary *endo*-alcohols due to the observations of SAMMES *et al.* (*cf.* page **92**). However, the amounts of chlorides or alkene isomers were not evaluated quantitatively. Subjection of the reaction mixtures to elevated temperatures or long reaction times generally was accompanied with significant decomposition, especially with $TiCl_4$.

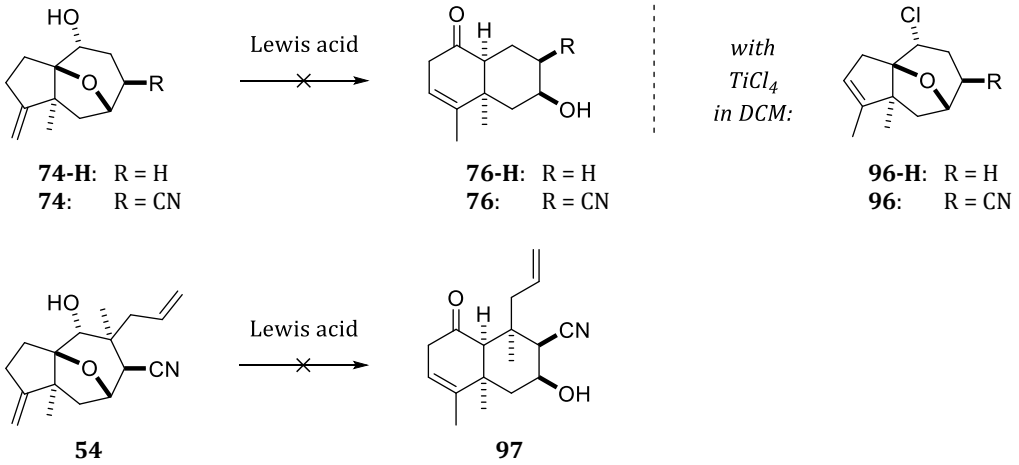

Scheme 78. Attempted rearrangement reactions with secondary alcohol substrates.

Used LEWIS acids: **BF_3·OEt_2** or **$TiCl_4$** in DCM (**74** or **74-H**), **$Sc(OTf)_3$** in $MeNO_2$ (**74-H**), or **$ZnCl_4$** in DCM (**54**).

The sulfonates of secondary alcohols were also used in rearrangement attempts. As discussed in **Chapter 2.3.2.2**, the isolation of the presumably formed triflates was not successful (**Scheme 68** on page **106**) and addition of LEWIS acids (BF_3·OEt_2 or $TiCl_4$) into triflation mixtures resulted in an high extent of decomposition with no rearrangement being evident. Similarly to alcohol **74-H**, isolated mesylate **79-H** (**Scheme 79**) only led to alkene isomerization, formation of chloride **96-H** with $TiCl_4$, and substantial decomposition. With $Sc(OTf)_3$, the mesylate was partially hydrolyzed due to the previously mentioned presence of water in undried $Sc(OTf)_3$.

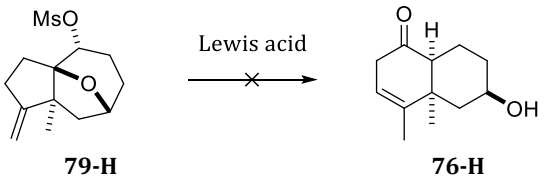

Scheme 79. Attempted rearrangement of mesylate **79-H**.

Used LEWIS acids: **BF_3·OEt_2** or **$TiCl_4$** in DCM, as well as **$Sc(OTf)_3$** in $MeNO_2$.

When decyano alcohol **74-H** was dissolved in trifluoroacetic anhydride (TFAA), trifluoroacetate **98-H** was obtained (**Scheme 80**). Notably, no alkene isomerization was evident in the presence of the formed trifluoroacetic acid, indicating that this isomerization is promoted by LEWIS acids, but not by BRØNSTED acids. Trifluoroacetate **98-H** showed similar behavior to alcohol **74-H** and mesylate **79-H** when treated with LEWIS acids: only alkene isomerization was observed with $Sc(OTf)_3$ in $MeNO_2$ or $BF_3{\cdot}OEt_2$ in DCM, while $TiCl_4$ in DCM additionally induced decomposition and some formation of chloride **96-H**. However, no polar spots in TLC or carbonyl signals in NMR were evident, which would be expected in cases of a successful rearrangement.

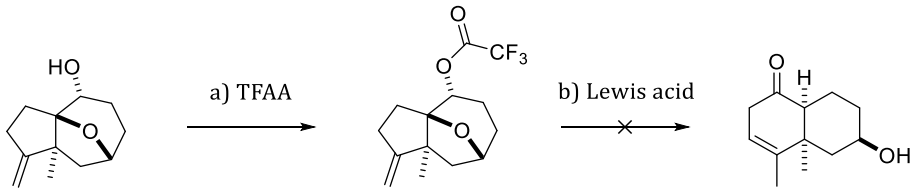

74-H **98-H** **76-H**

Scheme 80. Attempted rearrangement of trifluoroacetate **98-H**.

Reagents and conditions: **a)** TFAA (1 M), rt, 10 min; removal of TFAA in vacuo, addition of Na_2CO_3, filtration through silica gel; **88%**, *not included in the Experimental Section*. **b)** used LEWIS acids: **$BF_3{\cdot}OEt_2$** or **$TiCl_4$** in **DCM**, as well as **$Sc(OTf)_3$** in **$MeNO_2$**.

When decyano alcohol **74-H** was dissolved in Ac_2O instead of TFAA, no acetylation was evident. The presence of catalytic amounts of $Sc(OTf)_3$ promoted both acetylation and, finally, the formation of polar compounds exhibiting carbonyl signals in NMR. Different carbonyl compounds (δ = 208.7, 206.9 and 198.2 ppm in ^{13}C NMR) could be discerned with different conditions. Initially, these carbonyl compounds were presumed to correspond to the diastereomers of rearranged keto acetate **100-H** (**Scheme 81**). Due to the small scales of these test reactions, incomplete conversions – and thus the presence of multiple compounds in small quantities – these initial attempts were not yet conclusive, but nevertheless provided some hope that a rearrangement of secondary alcohols might be feasible after all. It was supposed that this may have also be effectuated by using acetic anhydride as solvent, quenching residual water, and consequently increasing the LEWIS acidity and catalytic activity of $Sc(OTf)_3$.

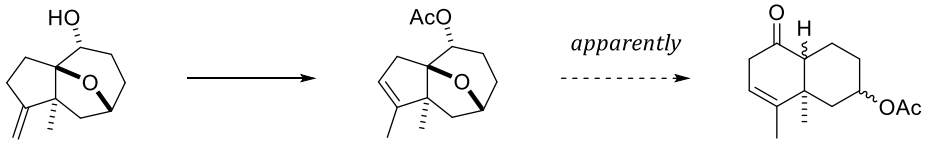

74-H **99-H** **100-H**

Scheme 81. *Apparent* rearrangement of acetate **99-H** with $Sc(OTf)_3$ in Ac_2O.

Reagents and conditions: Ac_2O (0.05–0.1 M), $Sc(OTf)_3$ (2.5–10 mol%), rt, 5–29 h; *formation of carbonyl compounds*.

Notably, when MeCN was used as a co-solvent (MeCN/Ac_2O, 1:1), the acetylation of **74-H** proceeded both without formation of carbonyl compounds and alkene isomerization. As with other secondary substrates, treating isolated acetate **99-H** with LEWIS acids resulted only in alkene isomerization ($Sc(OTf)_3$ in $MeNO_2$ or $BF_3{\cdot}OEt_2$ in DCM) or significant decomposition with some formation of chloride **96-H** ($TiCl_4$ in DCM).

To further investigate the possibly successful rearrangement with $Sc(OTf)_3$ in Ac_2O, several secondary alcohols, both as their decyano and cyano analogs, were employed (**Figure 24**). The formation of carbonyl compounds was evident even with hydroxynitriles **74** and **54**, though with noticeably slower conversion compared to decyano analogs **74-H** and **54-H**. To prevent a possible PRINS-cyclization of 5-allyl-5-methyl-substituted substrates **54** and **54-H**, a mixture of Ac_2O and AcOH (1:1) was used as solvent, so that acetic acid may act as a nucleophile, potentially trapping the rearranged oxonium intermediate (*cf.* **Scheme 71** on page **108**). While all of these attempts resulted in the formation of carbonyl compounds, methyl ester-substituted alcohols **58** and **58-H** only led to acetylation of the hydroxy group with no formation of carbonyl compounds. Incidentally, several other similar catalysts were also screened with **58-H** as substrate [$Zn(OTf)_2$, $Al(OTf)_3$, $La(OTf)_3$, $Er(OTf)_3$, $Hf(OTf)_4$].

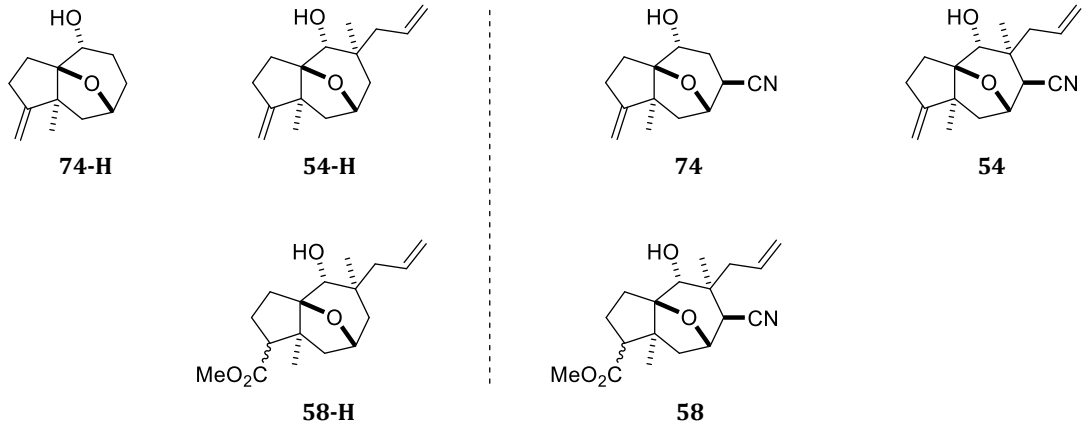

Figure 24. Secondary alcohols used in rearrangement attempts with $Sc(OTf)_3$ in Ac_2O.

These findings affirmed the growing suspicions that the new carbonyl compounds do not correspond to products from a rearrangement to decalones, but instead to those from a FRIEDEL-CRAFTS acylation. While a FRIEDEL-CRAFTS acylation is most often only considered for aromatic substrates, it is generally overlooked that such an acylation can also occur on simple aliphatic alkenes.[291,292] Moreover, lanthanide triflates like $Sc(OTf)_3$ are efficient catalysts for FRIEDEL-CRAFTS acylation on aromatic substrates.[293–295] Consequently, and in hindsight, it is not surprising that the chosen conditions effectuated this unexpected acylation on our substrates.

While this FRIEDEL-CRAFTS acylation was not evaluated thoroughly, some insights were gained from the reactions of the decyano substrates **74-H** and **54-H**. The presence of several carbonyl signals in the first attempts can be explained by the possible formation of several different α,β-unsaturated or β,γ-unsaturated ketones (upper dashed box in **Scheme 82**). These *formally* result from either 'ipso' or 'allylic' substitutions on the alkene. *Mechanistically*, several pathways are possible, including alkene isomerization before or after acylation, reversible acylation–deacylation sequences, or [1,5]-H shifts resulting in β,γ-unsaturated ketones.[291]

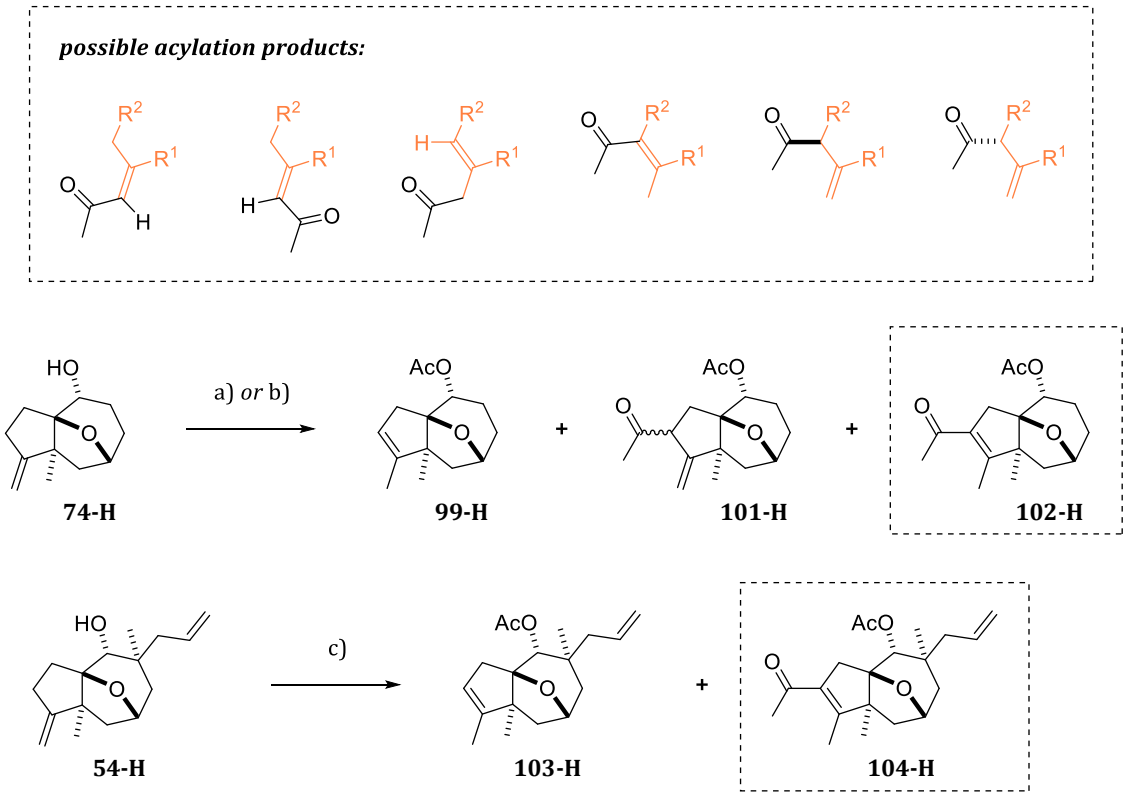

Scheme 82. Acetylation and FRIEDEL-CRAFTS acylation of **74-H** and **54-H**.

Reagents and conditions: **a)** Ac_2O (0.1 M), $Sc(OTf)_3$ (2.5 mol%), 0 °C, 1.5 h, rt, 2.5 h, then additional $Sc(OTf)_3$ (2.5 mol%), rt, 1 h; **99-H** (**41%**), **101-H** (**25%**) & **102-H** (**21%**). **b)** Ac_2O/AcOH (1:1, 0.12 M), $Sc(OTf)_3$ (5 mol%), 50 °C, 15 h, 80 °C, 4 h; *selective formation of* **102-H** (**48%**). **c)** Ac_2O/AcOH (1:1, 0.1 M), $Sc(OTf)_3$ (10 mol%), rt, 18.5 h, 50 °C, 5 h; **103-H** (**11%**) & **104-H** (**61%**).

When **74-H** was treated with $Sc(OTf)_3$ in Ac_2O, acetate **99-H** and both of its C2-acylation products – β,γ-unsaturated ketone **101-H** and α,β-unsaturated ketone **102** – were obtained (41%, 25% and 21% yield, respectively). While β,γ-unsaturated ketone **101-H** was obtained as a single diastereomer, its C2-configuration was not determined.

Subjecting **74-H** to more forcing conditions gave the presumably thermodynamically most stable α,β-unsaturated ketone **102-H** in a moderate yield of 48%. Further corroboration of the assumed structure of **102-H** resulted from saponification of **102-H** with sodium methoxide (to 2-acylated alcohol **102-H.a**, *not shown here but included in the Experimental Section*).

Similarly, 5-substituted alcohol **54-H** afforded α,β-unsaturated ketone **104-H** in a slightly higher yield of 61%. This indicates that this method might be optimized further and result in appreciable yields for a FRIEDEL-CRAFTS acylation of aliphatic alkenes. However, no such attempts were pursued, and the rearrangement of secondary alcohols, as well as the LEWIS acid-induced rearrangement in its entirety, was ultimately concluded with these results, since no approach gave promising results which seemed suitable for our goals.

2.3.6 Summary & Conclusion of the LEWIS Acid-Induced Rearrangement

While our initial goal was to realize the rearrangement to decalones from secondary *exo*-alcohols of our tricyclic epoxyazulenes, only *endo*-alcohols were obtained due to a pronouncedly *exo*-face-selective reduction of the ketones. These *secondary endo*-alcohols proved unsuitable, both for inversion to their *exo*-epimers and rearrangement reactions, even after activation as mesylates, triflates and (trifluoro)acetates. The most plausible reason for the peculiar behavior of these tricyclic epoxyazulenes is the involvement of the ether bridge. This *neighboring group participation* is evident both from (i) substitution reactions proceeding with retention of configuration and, in a more specific case, (ii) the formation of the 1,3-elimination product, *bis*-alkene **83** (see **Scheme 83** on the next page). Incidentally, the 4,7-epoxyazulene core of *bis*-alkene **83** is also present in guaiane class terpenes like englerin A (**I-113**). Therefore, this undesired side-reaction to **83** or similar analogs may be examined further for a utilization in respective synthetic routes to other terpene classes and natural products.

In contrast to *secondary endo*-alcohols, *tertiary endo*-alcohols and ketones underwent rearrangement, affording decaline-based hydroxy ketones and hydroxy acyloins, respectively (i.e., **84-H** and **93-H**). With higher-functionalized substrates, the presence of an allyl group at C5 led to a rearrangement/halo-PRINS cyclization sequence, giving rise to structurally intriguing and unprecedented tetracyclic ethers such as **86-H**. Another unexpected reaction was observed when $Sc(OTf)_3$ was used in a mixture of Ac_2O/AcOH as solvent. Under these conditions, the substrates underwent a FRIEDEL-CRAFTS acylation (i.e., to **102-H** or **104-H**).

Generally, the choice of solvent proved crucial for a potential rearrangement. Most notably, using LEWIS acids in *acetonitrile* obviated a rearrangement or even inhibited the isomerization of the *exo*-methylidene group, a usually very fast process with LEWIS acids. This isomerization was, as is also evident from other reactions covered in this work, not observed with BRØNSTED acids.

The incompatibility of the rearrangement of our substrates with acetonitrile proved to stem from a much more consequential issue: the incompatibility with *nitriles in general*. Consequently, the 6-cyano analogs of substrates which underwent rearrangement readily were found to be completely unsuitable.

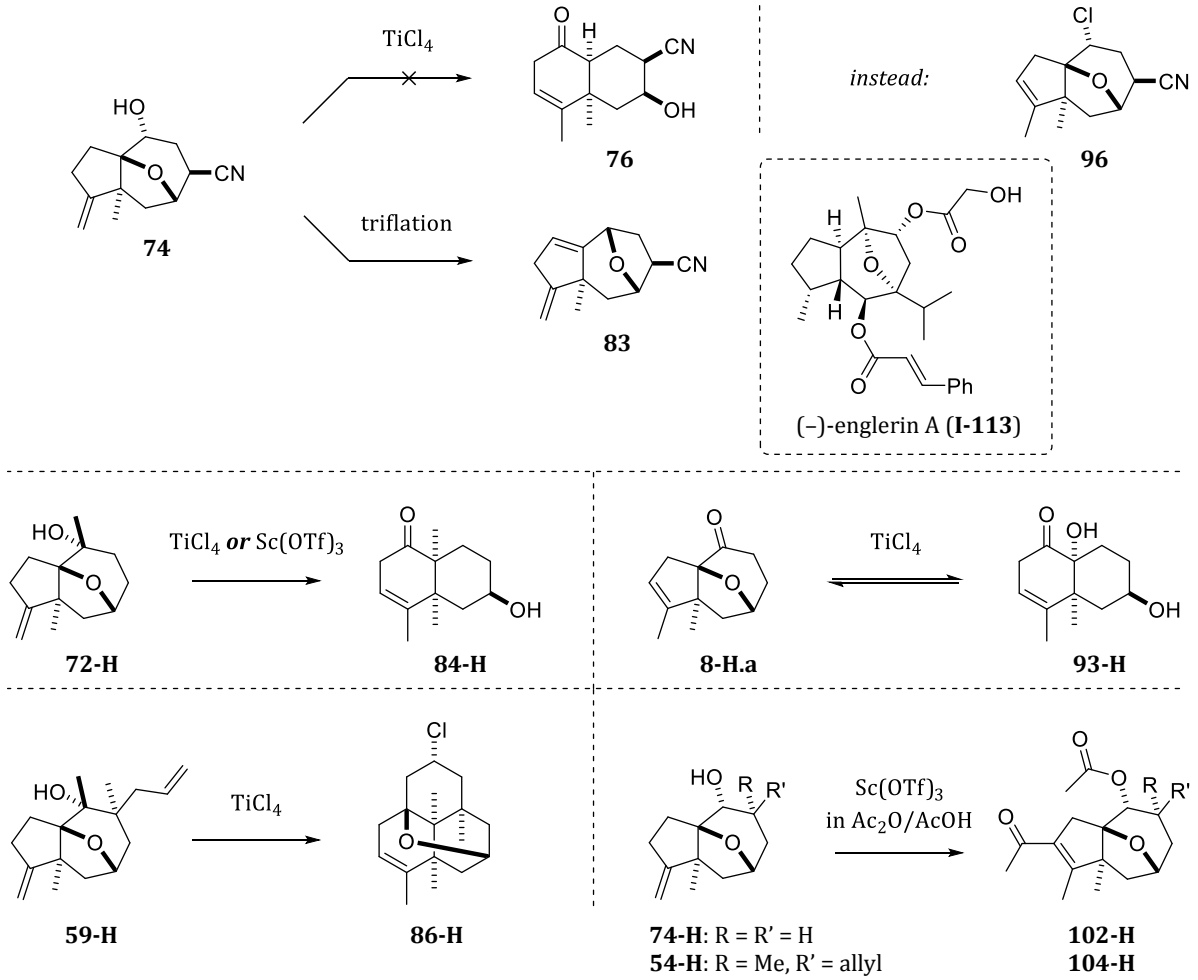

Scheme 83. Selection of rearrangement attempts. For further details, see previous subchapters.

The observations made within our attempts highlight the delicate '*internal and external aspects*' which have to be considered in LEWIS acid-induced reactions such as this rearrangement.

'*Internal aspects*' include substrate properties, such as stereoelectronic compatibility (*endo*/*exo*-configuration and thus, whether an antiperiplanar orientation is adopted) and more general effects of substrate structure. Notably, our substrates required considerably longer reaction times in successful rearrangements when compared to the substrates of SAMMES *et al.* (cf. **Scheme 58** on page **93**). While such a comparison admittedly is disputable, our failed rearrangement attempts with $TiCl_4$ in MeCN and $BF_3{\cdot}OEt_2$ in DCM clearly indicate a *certain deactivation of our substrates* which seems to be explicable only as a result of the additional substitution at *both* C8a and C1.

'External aspects' include choice of LEWIS acid and conditions, as well as often-overlooked complexation of LEWIS acids with solvents, which can lead to dramatic changes in LEWIS acidity. Thus, the combination of our 'deactivated' substrates and complexed LEWIS acids completely obviated a possible rearrangement. Especially the strong complexation of $TiCl_4$ with nitriles is also evident when *only* $TiCl_4$ is dissolved in MeCN, resulting in the highly exothermic formation of a yellow complex which precipitates in high concentrations.

It has to be noted that a complexation of LEWIS acids often is *desired*, since the decrease in LEWIS acidity can increase selectivity and allow for the employment of more sensitive substrates. This is also evident by the necessity of 'fine-tuning' LEWIS acid catalysts such as scandium triflate for different reactions. In general, $Sc(OTf)_3$ in DCM forms a heterogenous suspension but can be better suited than a homogenous solution of $Sc(OTf)_3$ in MeCN. In these cases, both the solubility and the complexation, and thus deactivation, of the LEWIS acid in the respective solvent have to be considered. In many other reactions, $Sc(OTf)_3$ in $MeNO_2$ seems to give the best combination of solubility and catalytic activity.[296–301] In our case, $Sc(OTf)_3$ proved an efficient catalyst for tertiary alcohol **72-H**, but failed to induce rearrangements of higher-substituted alcohol substrates or even 5-unsubstituted ketone substrates.

To conclude, we were able to gain crucial insights from our numerous attempts of the LEWIS acid-induced rearrangement. While the desired rearrangement of secondary *endo*-alcohols could not be achieved, some tertiary alcohols and ketone substrates could be successfully used in *proof-of-concept* attempts, which were not optimized or thoroughly evaluated. The rearrangement of ketone substrates gives access to *[6,6]-fused acyloins*, which open up alternate routes to the desired decalones and salvinorin A (**I-11**). However, such routes involving a LEWIS-acid induced rearrangement of ketones were not considered since some aspects of this reaction still eluded conclusive explanation, and a general applicability to higher-substituted substrates seemed hardly predictable.

Ultimately, such alternate routes via *[6,6]-fused acyloins* were investigated, as will be focused on in the following chapter. For this purpose, *another type of rearrangement* proved highly promising after implementing a '*change in paradigm*' – that is, by switching from LEWIS acids to strong bases.

2.4 BASE-INDUCED REARRANGEMENT TO THE DECALONE CORE

2.4.1 Ether Cleavage of β-Oxa-Bridged Nitriles

At the late stage of the research endeavor, alternative approaches for viable rearrangement reactions were pursued. These approaches resulted from observations suggesting a base-induced ether cleavage of nitrile substrates during early functionalization attempts of the tricyclic ketonitrile **8**. As briefly broached in **Chapter 2.2.1**, abstraction of the ketone α-H of 5-unsubstituted ketonitrile **8** with LDA, as well as a transmetalation of silyl enol ether **33** with MeLi, resulted in the formation of – *at that time* – undesired side products.

Among those, *O*-silylated acyloin **105** was isolated (25% yield) from the complex mixture of an attempted transmetalation of **33** with MeLi and subsequent epoxide opening to furfuryl alcohol **40** (**Scheme 84**). Treating silyl enol ether **33** with MeLi without addition of an electrophile led to formation of **105** with only little formation of ketonitrile **8** which would be the product of a successful transmetalation to lithium enolate **8.M** and subsequent hydrolysis.

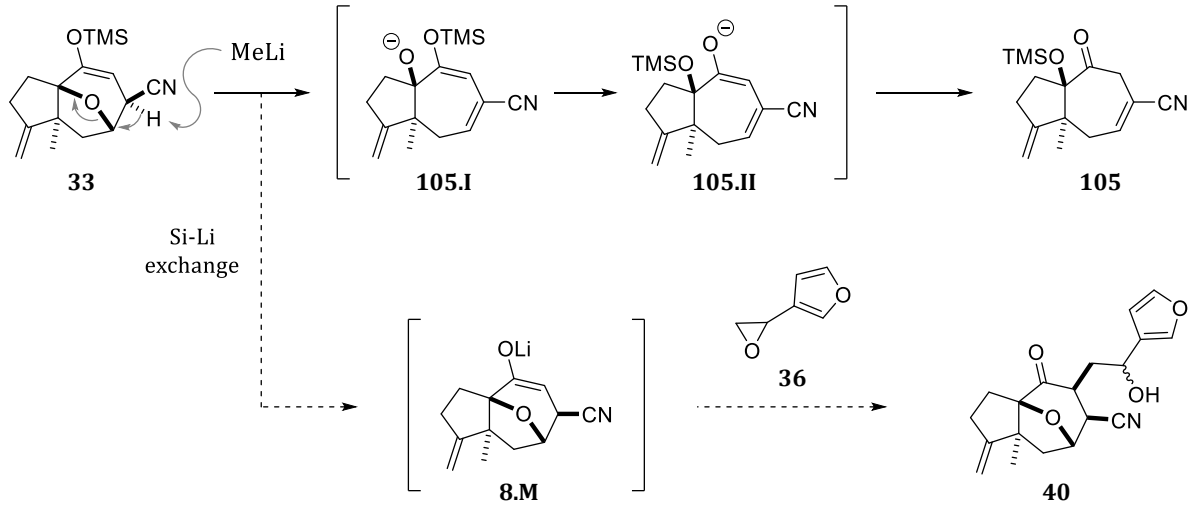

Scheme 84. Base-induced ether cleavage of silyl enol ether **33** by treatment with MeLi.

The isolation of **105** confirmed a *cleavage of the ether bridge*, as well as a silyl migration of the TMS group from the silyl enol ether to the revealed alkoxide moiety.

In the ^{1}H NMR spectrum of **105**, the most evident signal indicating an ether cleavage can be seen in the range of 6.62–6.66 ppm, which corresponds to the vinyl-H of the α,β-unsaturated nitrile (*henceforth also called vinyl nitrile*). Similar signals were observed in other complex reaction mixtures obtained from nitrile-substituted substrates, such as ketonitrile **8**, which had been treated with strong bases like LDA. Less strong bases like KHMDS or LHMDS did not lead to such an ether cleavage in a noticeable extent.

In the literature, only few examples of an ether cleavage of β-oxa-bridged nitriles are reported, induced most often *unintendedly* with strong bases. FLEMING *et al.* investigated this cleavage methodically in 2001 using rather simple β-epoxy nitriles such as **I-230** or **I-232** to synthesize hydroxylated α,β-unsaturated nitriles **I-231** and **I-233** (**Scheme 85**).[302] More elaborate substrates (**I-234** and **I-236**) were used by BALDWIN *et al.* and TROST *et al.*[303,304]

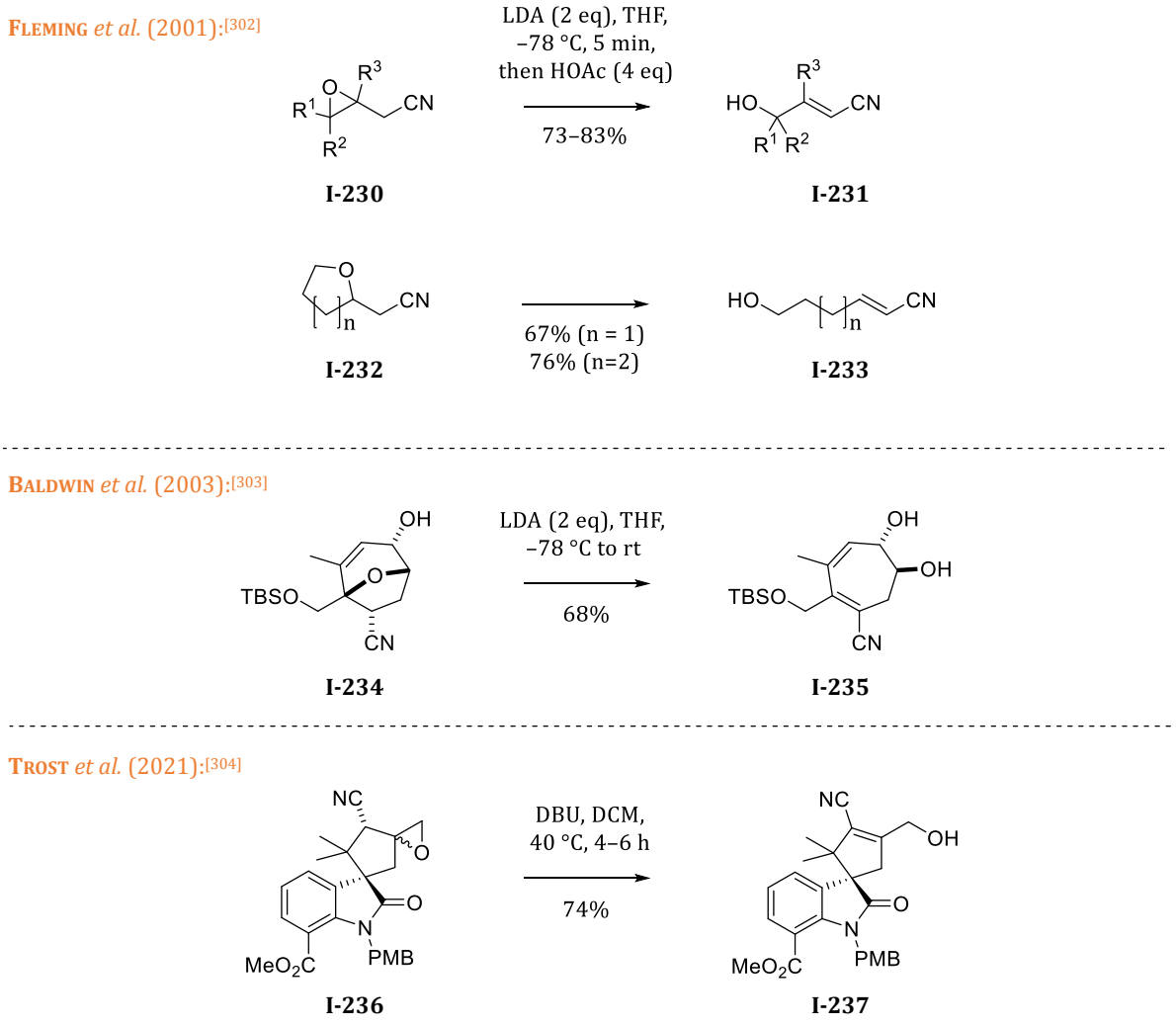

Scheme 85. Examples of ether cleavage reactions of β-oxa-bridged nitriles.

Most examples with *nitrile substrates* use LDA as base, while an ether cleavage with β-oxa-bridged *esters* also use milder bases like KHMDS, LHMDS, NaH or *t*-BuOK. Incidentally, *ester substrates* seem to be utilized more frequently and generally give the products in good yields.

An *intentional* ether cleavage was tested on two 'dummy' compounds to investigate this reaction on our epoxyazulenes (**Scheme 86**). First, hydroxynitrile **74** was treated with LDA at –78 °C and the intensely yellow-colored solution was allowed to warm to –55 °C. After addition of acetic acid and concentration of the solution, the formed ammonium salts were removed by filtration through silica gel with ethyl acetate. The crude product exhibited clean NMR spectra confirming an ether cleavage to *trans*-1,2-diol **106**.

Then, ketonitrile **8** was subjected to similar conditions in two different runs. Both led to full conversion within two minutes even at –95 °C, indicating a *practically instantaneous* ether cleavage. Compared to hydroxynitrile **74**, a *slightly less clean* conversion was evident. From these two runs, acyloin **107** was isolated in 80% yield. Interestingly, the only discernible 'impurity' was identified as 1,2-diol **106** (7% yield). This is explicable by an unusual, but occasionally occurring, reduction of the carbonyl moiety by a hydride transfer from LDA.[305] Such a reduction by LDA is generally observed on *non-enolizable or sterically hindered* ketones and can be deemed rather unexpected for the ketone moieties of **8** or **107**.

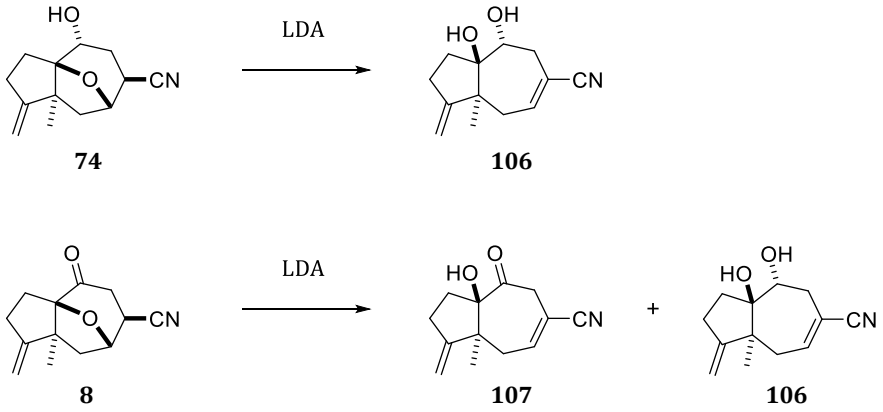

Scheme 86. Ether cleavage of hydroxynitrile **74** and ketonitrile **8** with LDA.

Reagents and conditions: **with 74**: THF (0.057 M), LDA (1 M in THF, 2.2 eq, rapid addition), –78 °C to –55 °C (45 min), HOAC (7 eq), filtration through silica gel with EtOAc; **107%** of *crude* **106**.
with 8: 2 runs (*run #1*: 0.156 mmol; run #2: 1.56 mmol); THF (0.03 M), LDA (1 M in THF, 2.2 eq), –88 °C (20 min, *run #1*) ***or*** –95 °C (10 min, *run #2*), HOAc (15 eq), filtration through silica gel with EtOAc, purification of *combined crude product* by flash chromatography; **80%** of **107** and **7%** of **106**.

2.4.2 Semipinacol and Acyloin Rearrangement

With the successful ether cleavage, alternative rearrangement reactions to the decalone core became conceivable. First considerations concentrated on 1,2-diols precursors like **108** or a derivative thereof (**Scheme 87**). Typically, free 1,2-diols can undergo a *pinacol rearrangement* via the formation of the more stable carbocation when subjected to highly acidic conditions. In the case of **108**, this would most likely result in undesired rearrangement products due to the formation of a tertiary carbocation at the bridge-head carbon C3a. On the other hand, *semi-pinacol rearrangements* make use of a reversed 1,2-migration *from the tertiary to the secondary center*. As outlined in **Scheme 87**, this would allow for a rearrangement with formation of a carbonyl on the previous tertiary center, as would be desired for the synthesis of **109.**

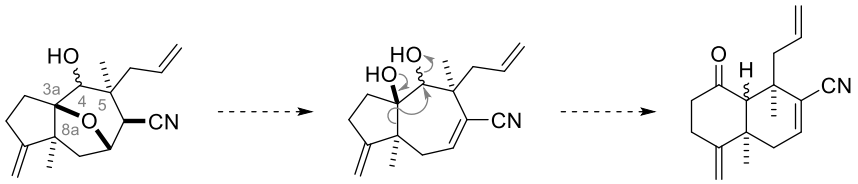

54 **108** **109**

Scheme 87. Considerations for a sequence involving a (semi)pinacol rearrangement to **109**.

In contrast to pinacol rearrangements, *semipinacol rearrangements* require derivatization of the secondary hydroxy group to a good leaving group such as a mesylate. This allows for a versatile rearrangement facilitated not only by acidic, but also basic or even neutral conditions.

Some potential issues were identified in the literature on (semi)pinacol rearrangements, with the most daunting being their occasionally 'unpredictable' outcome. As reported on other substrates, different rearrangement products can be obtained, since different groups may migrate depending on structural properties of the substrates. Which group is to migrate in a semipinacol rearrangement is mostly determined by *stereoelectronic effects* rather than by migratory aptitude of a potential migrating group or the formation of the most stable product. Consequently, the main product results from the migration of the *group antiperiplanar to the leaving group*, which is the most favorable or even required orbital alignment for rearrangement reactions, as demonstrated on our unsuccessful attempts in **Chapter 2.3**.[306,307]

A prominent example for the importance of this antiperiplanar orientation was reported by KINGSBURY & COREY in their total synthesis of the diterpenes isoedunol and β-araneosene.[308] The rearrangement products of *cis*- and *trans*-1,2-diol **I-238** (via the secondary mesylates) differed due to confirmational rigidity of the substrates. The migrating bond in each case was confirmed by crystallographic analysis to be the *C–C-bond antiperiplanar to the secondary C–O-bond*,

affording different $C_4 \rightarrow C_5$ ring expansion products (**Scheme 88**). Moreover, another product was obtained from an acyloin rearrangement by simply exposing acyloin **I-239** to silica gel.

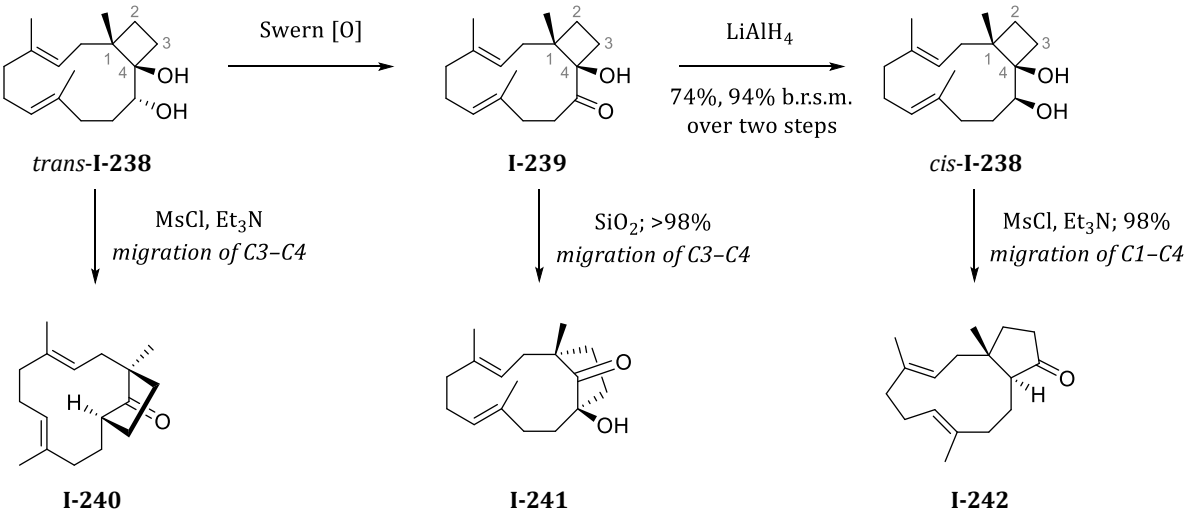

Scheme 88. Semipinacol rearrangement of *cis*- or *trans*-1,2-diols **I-238**, as well as acyloin rearrangement of acyloin **I-239**.[308]

An example, where different *conformers* of similar substrates changed the outcome of the semipinacol rearrangement was reported by HEATHCOCK *et al.*[309] In their work to pseudoguaiane sesquiterpenes, decaline-to-hydroazulene rearrangements were investigated – which essentially represents the 'opposite' of the rearrangement we aimed for. Treating *acetoxy-substituted* 1,2-diol monotosylate *OAc*-**I-243** with LiOH in *t*-BuOH gave the bridged keto acetate **I-244** (**Scheme 89** on the next page). With the *hydroxy* analog **I-243**, the same conditions resulted in another semipinacol rearrangement to the desired hydroazulene **I-245** (*trans*/*cis* = 4:1). Interestingly, the desired rearrangement to **I-245** was also achieved from *OAc*-**I-243**, when it was treated with *KOH instead of LiOH* in *t*-BuOH.

This dramatic change in outcome was explained by the conformation which the alkoxide **I-243.I** adopts to benefit from hydrogen bonding with the free hydroxy group. Consequently, the antiperiplanar migrating group in conformer *OAc*-**I-243.I** differs from that in conformer **I-243.I**, leading to different semipinacol rearrangement products even though both substrates share the same *cis*-1,2-diol monotosylate.

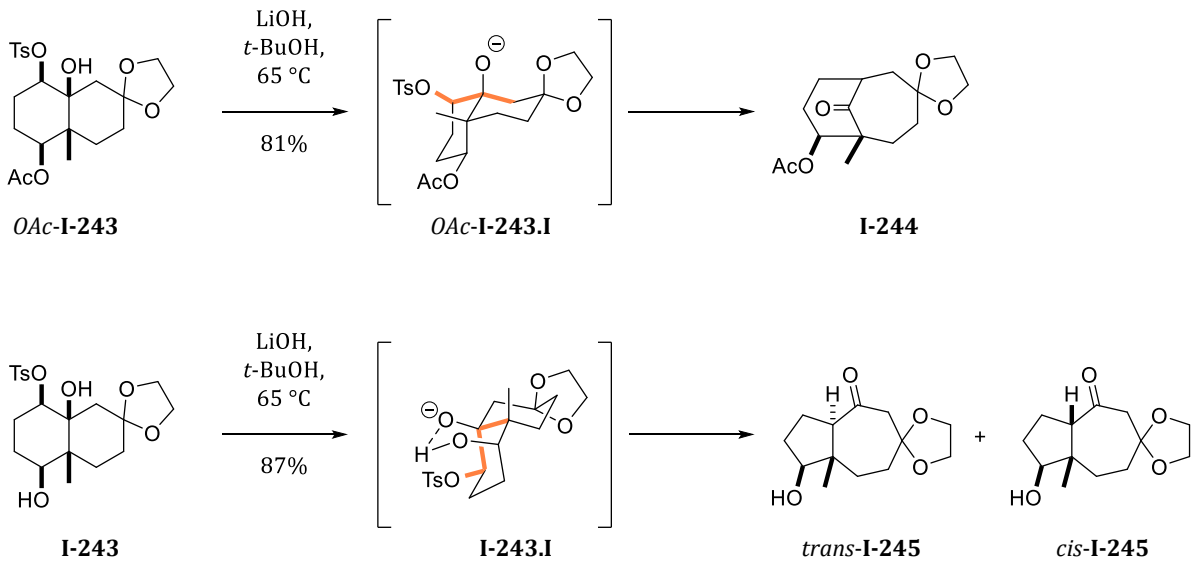

Scheme 89. Different semipinacol rearrangement products as a result of hydrogen bonding in conformer *OAc*-**I-243.a**.[309] The antiperiplanar aligned bonds are highlighted in orange.

The semipinacol rearrangement of sulfonates can also be further complicated by the required selective derivatization of the secondary, but not the tertiary alcohol. This proved challenging for GRAINGER *et al.* in their work on β-lactam diols such as **I-246** (**Scheme 90**).[310] To overcome selectivity issues in the mesylation or tosylation reaction, they resorted to a 'cyclic activation' of the 1,2-diols, either by derivatization to cyclic sulfite **I-247** or phosphorane **I-248**. Both of these cyclic derivatives led to a high-yielding rearrangement to bridged diketone **I-249**.

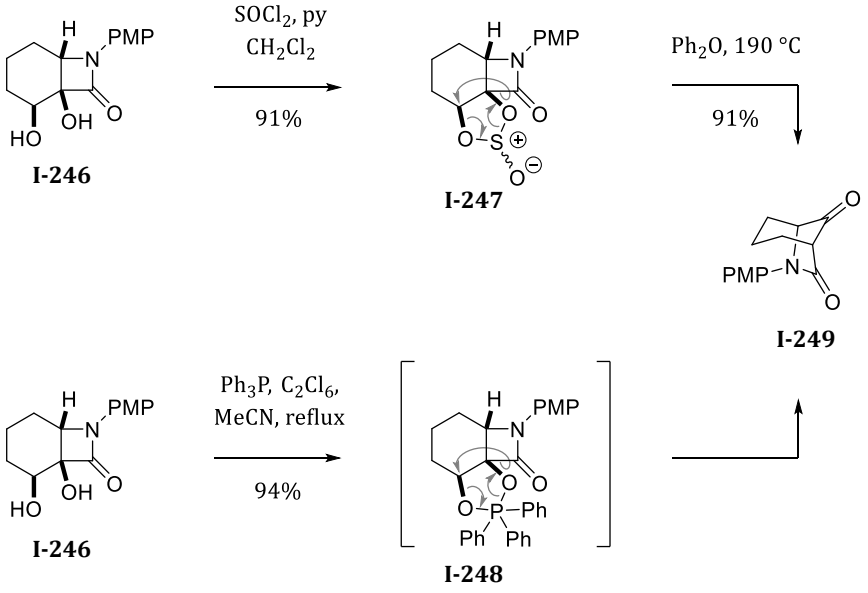

Scheme 90. Semipinacol rearrangement of cyclic derivatives to diketone **I-249**.[310]

While these semipinacol rearrangements of the *cis*-diol derivatives favored an acyl migration to diketone **I-249**, theoretical calculations by BAROUDI & KARTON suggest that the *trans*-isomers should result in a reversed selectivity with an alkyl migration to **I-251** instead (**Scheme 91**).[311] They also proposed that this alkyl migration of *trans*-**I-250** (X = Ph_3P or SO) should be "even faster and more exothermic" than the acyl migration of the *cis*-isomer.

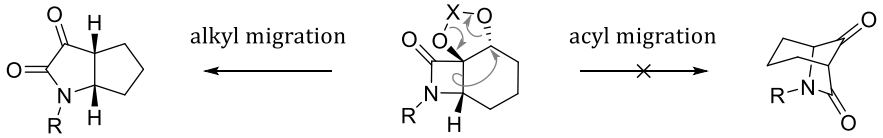

I-251 *trans*-**I-250** **I-248**

Scheme 91. Reversed selectivity of *trans*-**I-250**), as proposed by BAROUDI & KARTON.[311]

These examples demonstrate that the outcome of a semipinacol rearrangement is not always easily predictable due to potential structural subtleties of substrates or interactions within intermediates. A prediction that either the *trans*- or the *cis*-1,2-diol *should* result in the formation of a respective product seems premature and would probably have to be investigated experimentally on both isomers, while different activation methods may have to be examined to obtain the desired product.

For our purposes, an alternative reaction seemed more promising: the α-*ketol or acyloin rearrangement*, which can be considered a special type of semipinacol rearrangement.[307] The acyloin rearrangement was briefly mentioned as a undesired side reaction in the work of KINGSBURY & COREY (**Scheme 88** on page **125**). The versatility of acyloin rearrangements was illustrated in the 2003 review of PAQUETTE & HOFFERBERTH.[312] One feature of this acyloin rearrangement is the possibility of inducing the 1,2-migration under acidic, basic, or even neutral conditions – sometimes requiring only mild reagents like SiO_2 or Al_2O_3. In contrast to (semi)pinacol rearrangements, the substrate scope and functional group tolerance appear to be much broader while regioselectivity issues are limited.[307]

Due to the reversibility of the acyloin rearrangement, its principle driving force is the formation of the thermodynamically favored isomer, often dictated by relieve of ring strain. The stereoelectronical prerequisite of an antiperiplanar alignment is often less problematic due to the planarity of the carbonyl C=O-bond. In some cases, a coordination to metal atoms can induce co-planarity within the acyloin moiety, facilitating rearrangement via a more favorably aligned conformer. As reported by PAQUETTE *et al.*,[313] [6.2.1]-bicyclic acyloin **I-252**/**I-253** (shown as its two conformers in **Scheme 92**) gave cyclobutane-linked **I-254**, when treated with base (*t*-BuOK). However, coordination to aluminum enabled 'conformer-locking' of **I-253**, resulting in the desired acyloin rearrangement reaction to the isomeric [5.3.1]-bicyclic acyloin **I-255**.

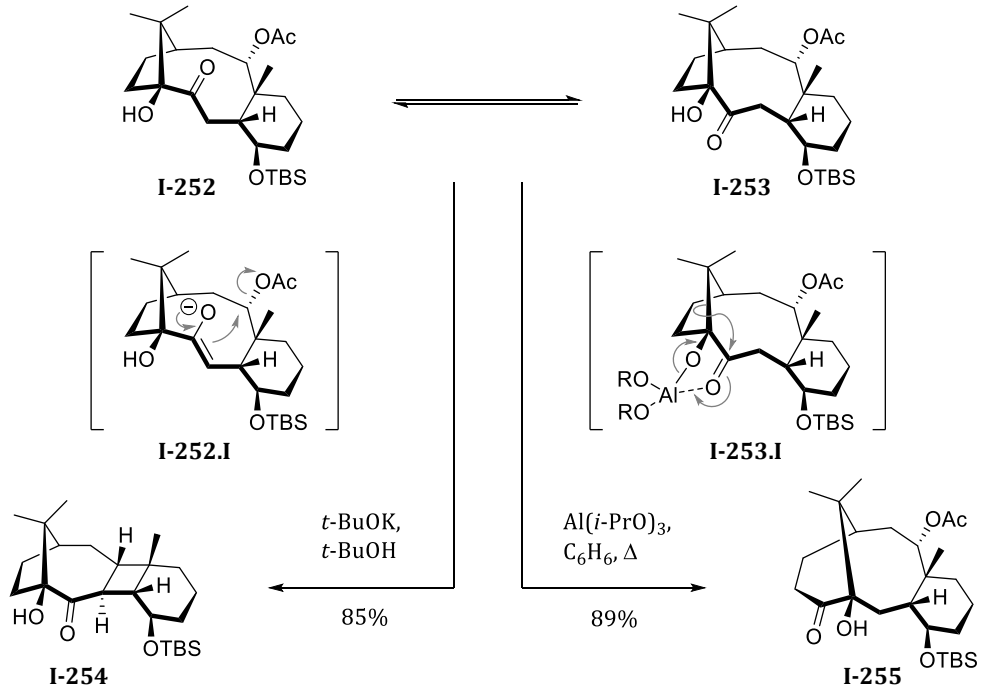

Scheme 92. Acyloin rearrangement of **I-253** to **I-255** via coordination to aluminum. Treatment of **I-252** with base results in cyclobutane formation and affords **I-254**.[313]

Two *very interesting* acyloin rearrangements were reported by WIJNBERG & GROOT *et al.* (**I-256** to **I-257**)[314] and XU *et al.* (**I-258** to **I-259**)[315] (**Scheme 93**). Several important aspects can be deduced from these two reports. First and foremost, the hydroazulene substrates bear a striking resemblance to our compounds, suggesting that an acyloin rearrangement may also be well-suited for our purposes.

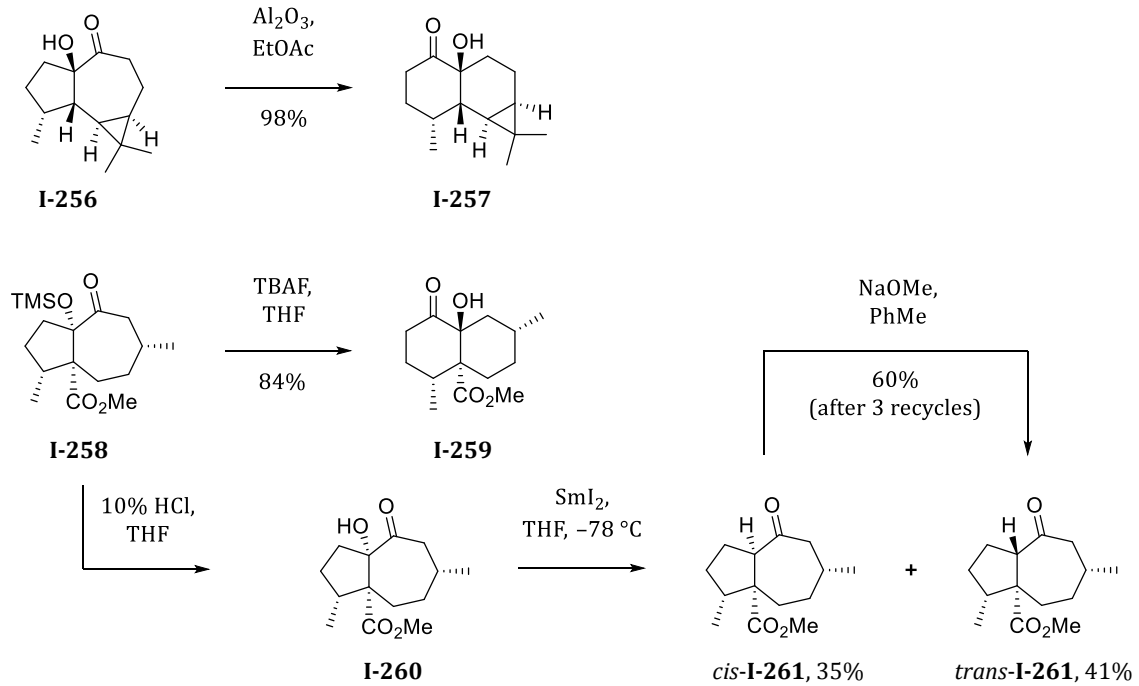

Scheme 93. Examples of acyloin rearrangements from hydroazulenes to decalones.[314,315]

Moreover, these two rearrangements to the decaline-based acyloins **I-257** and **I-259** proceeded readily – so readily, that both actually were unexpected and undesired. In the latter case, this resulted from desilylation of *O*-silylated acyloin **I-258** with TBAF and could be circumvented by acidic hydrolysis to acyloin **I-260**. A subsequent deoxygenation with SmI_2 gave a mixture of *cis*- and *trans*-**I-261**. The *cis*-fused isomer was then epimerized to the desired isomer, *trans*-**I-261**.

We then devised routes incorporating such semipinacol or acyloin rearrangements of our compounds (**Scheme 94**). As mentioned earlier, both *cis*- and *trans*-1,2-diols **108** – and their activated derivatives – might have to be examined for a potential semipinacol rearrangement to the desired decalone *trans*-**109**. While an β-ether cleavage of *endo*-hydroxynitrile **54** should afford *trans*-**108**, gaining access to *cis*-**108** may prove more complicated. A *selective reduction* of acyloin **110** to *cis*-**108** could be possible but potentially require elaborate reduction methods and/or a prior protection of the hydroxyl function with a bulky silyl protecting group.[316–318] However, the less-readily accessible 1,2-diol *cis*-**108** would, most likely, be the isomer which would facilitate the desired semipinacol rearrangement. Presumably, *trans*-**108** would share the non-antiperiplanar alignment which prevented the LEWIS acid-induced rearrangement of its precursor, *endo*-hydroxynitrile **54** (*cf.* X-ray structure of **54**, **Figure 22** on page **102**).

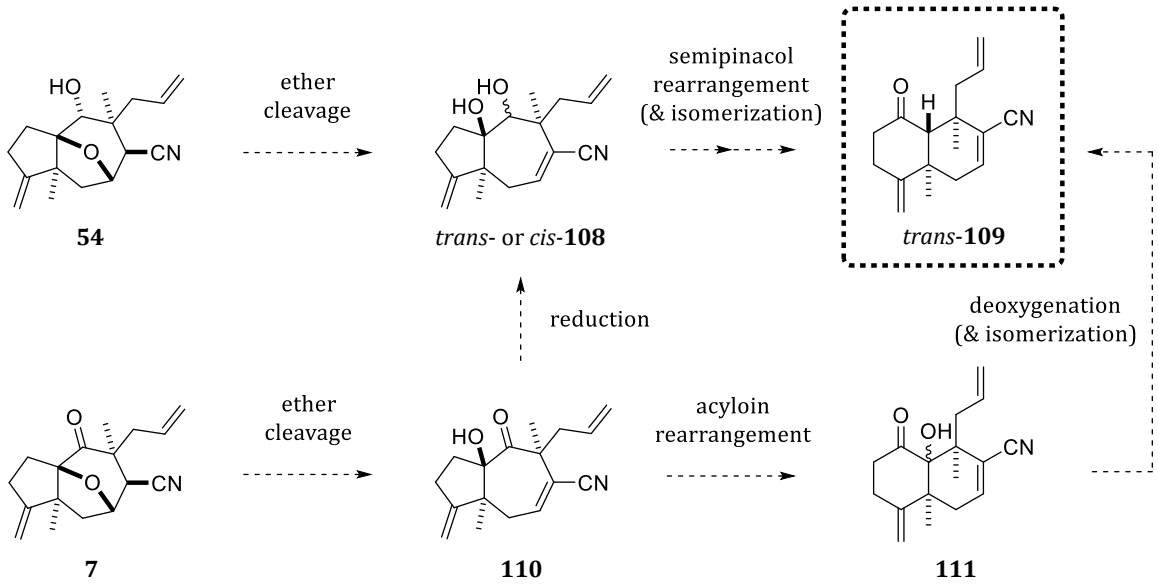

Scheme 94. Potential routes to decalone **109** involving semipinacol/acyloin rearrangements.

With these considerations, an *acyloin rearrangement* of [5,7]-fused acyloin **110** to [6,6]-fused acyloin **111** seemed more straightforward and promising. From **111**, a deoxygenation to the desired decalone **109** should be feasible with SmI_2. This reagent was also used in the deoxygenation of [5,7]-fused acyloin **I-260** (*cf.* **Scheme 93**) and in several conjugated reductions on decalone substrates in the previous total syntheses of salvinorin A, as shown in **Chapter 1.2**.

The [5,7]-fused acyloin **110** was to be obtained by β-ether cleavage of ketonitrile **7**. Next to being non-enolizable and thus averting potential side reactions, ketonitrile **7** represents the *minimally functionalized* substrate exhibiting a substitution pattern which should allow for a transformation to salvinorin A (**I-11**) after a potential rearrangement, as already outlined in **Chapter 1.3.2**. Furthermore, our investigations into the acyloin rearrangement were based on the assumption that β-ether cleavage of **7** may lead to a *concomitant* acyloin rearrangement from the alkoxide intermediate of **110**, rendering a stepwise sequence unnecessary.

2.4.3 Acyloin Rearrangement of Ketonitrile 7

Ketonitrile **7** was treated with LDA (1.1 eq) in two trial reactions at –95 °C. One reaction was quenched rapidly to intercept the β-ether cleavage product **110**, whereas the other run was allowed to warm to 0 °C. From the latter reaction, a new compound was isolated which, **very gratifyingly**, confirmed a *tandem ether cleavage/acyloin rearrangement sequence*. Depending on the conditions, ketonitrile **7** (mostly as its 6-epimer 6-*epi*-**7**), [5,7]-fused acyloin **110**, and its rearranged isomer, the desired [6,6]-fused acyloin **111** were obtained in varying ratios.

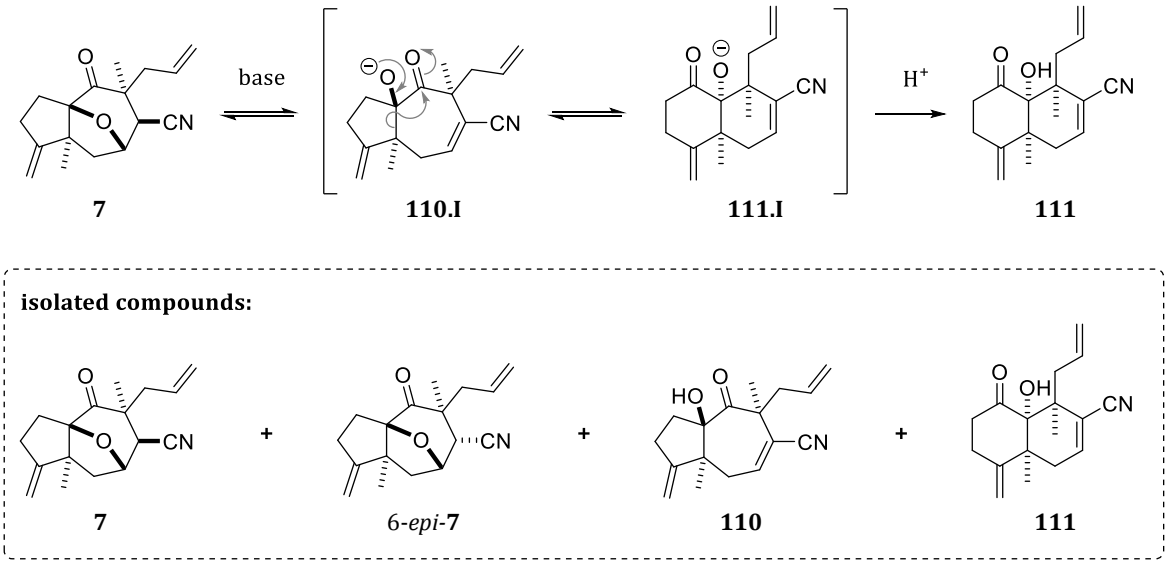

Scheme 95. Tandem ether cleavage/acyloin rearrangement of ketonitrile **7** to acyloin **111**. Reagents, conditions, and results in **Table 4** on the next page.

The yield of acyloin **111** was then improved through various optimization experiments, a selection of which is presented in **Table 4** on the next page. The main aspects of the optimization can be concisely summarized with following key factors:

- **choice and amount of base**: LDA was found to be well-suited. An excess of LDA (2 eq) facilitated high conversion to the desired acyloin **111**. A higher excess (3 eq) impeded the conversion of **110** to **111**. Using KHMDS (1–2 eq) led to a complex mixture.

- **choice of solvent**: THF was superior to toluene or MTBE. In those less polar solvents, the lithium intermediate **110.I**, or *possibly* the respective dilithium alkoxy enolate (*not shown*), precipitated. This impeded rearrangement to **111**.
- **reaction temperature and time**: allowing the reaction mixture to warm to room temperature for a short time (5–15 min) after stirring in the slowly warming cooling bath (–95 °C to 0 °C over the course of 2 h) was identified as the '*sweet spot*'. This resulted in a change of color from a *yellow to a cherry-red hue*, indicating maximum conversion. When quenched with acetic acid at this point, no [5,7]-fused acyloin **110** and only small amounts of (mostly epimerized) substrate (6-*epi*-)**7** were discernible. The desired rearranged acyloin **111** was obtained in 67% yield (74% *b.r.s.m.*). Stirring the reaction mixture for a prolonged time at room temperature slightly lowered both the yield of **111** and the amount of recoverable substrate (6-*epi*-)**7** (63% yield, 66% *b.r.s.m.* after stirring for 1 h at room temperature).

Table 4. Reagents and conditions for tandem ether cleavage/acyloin rearrangement to **111** (**Scheme 95**). The reactions were run in 0.05 molar solutions in a cooling bath with acetone cooled by liquid nitrogen, allowing the mostly solid acetone (–95 °C) to thaw after addition of the base. LDA was freshly prepared and added rapidly. The reactions were quenched with HOAc. The ratios (**111** in **bold**) were determined by *isolation* or *quantitative NMR*.

entry	reagents and conditions		**7** : 6-*epi*-**7** : **110** : **111** **results and remarks**
	scale, solvent & base, *time in slowly warming cooling bath*	*time after removal of cooling bath*	
1	0.245 mmol, THF, **LDA (1.1 eq)**, –95 °C to –75 °C (20 min);	–	18 : 35 : 36 : **0** (isolated) **no rearrangement at –75 °C**
2	0.241 mmol, THF, **LDA (1.1 eq)**, –95 °C to 0 °C (2.25 h)	–	18 : 25 : 0 : **48** (isolated) **rearrangement after slowly warming to 0 °C**
3	0.243 mmol, THF, **LDA (2.2 eq)**, –95 °C to –10 °C (2 h)	20 min	3 : 8 : 0 : **64** (isolated) **high conversion with 2.2 eq LDA after allowing to warm to rt**
4	**2.163 mmol**, THF, **LDA (2 eq)**, –95 °C to –15 °C (2 h)	1 h	0 : 5 : 0 : **63** (qNMR) **reproducible at ten-fold scale**
5	0.269 mmol, THF, **LDA (2 eq)**, –95 °C to 0 °C (2 h)	5 min	0 : 10 : 0 : **67** (qNMR) **allowing to warm to rt for *only a short time* improves yield slightly**
6	0.260 mmol, THF, **LDA (1 eq)**, –95 °C to 0 °C (2 h);	20 min	19 : 26 : 0 : **40** (qNMR) **low conversion with only 1 eq LDA**
7	0.265 mmol, THF, **LDA (1 eq)**, –95 °C to 0 °C (2 h);	1 h	27 : 25 : 0 : **34** (qNMR) **1 eq LDA with prolonged stirring at rt seems to favor reverse reaction**
8	0.077 mmol, THF, **KHMDS (1 eq)**, –95 °C to 9 °C (4 h)		**complex mixture with KHMDS** (TLC: >6 spots)
9	THF, **toluene** *or* **MTBE**, **LDA (3.3 eq)**, –95 °C to ambient temperatures		**low conversion with higher excess of LDA (3.3 eq)**, especially in **toluene** or **MTBE** due to **precipitation of intermediates.**

The most distinct signals in NMR spectra indicating a successful rearrangement were identified as those of (i) the tertiary hydroxy group in ^{1}H NMR, and especially (ii) the tertiary bridge-head carbon of the acyloin moiety in ^{13}C NMR. These signals shift noticeably going from [5,7]-fused acyloin **110** to [6,6]-fused acyloin **111** (δ = 1.88 to 3.97 ppm and 91.5 to 81.8 ppm, respectively). In contrast to the latter signals, the tertiary bridge-head carbon atoms (C3a) of the 3a,7-epoxyazulenes consistently exhibited a signal in the range of 95–100 ppm.

Particularly the ^{1}H-^{13}C HMBC correlations represent a good confirmation for the rearrangement, most evident by the cross-peaks of the carbonyl group (**Figure 26** on the next page). In [5,7]-fused **110**, the 5-substituents (5-CH_3 & 1'-H_2) exhibit a cross-peak to the C4 ketone. In [6,6]-fused **111,** no cross-peaks are seen between those substituents (9-CH_3 & 11-H_2) and the C1 ketone that '*moved one bond farther away*.'[<20>] Additionally, 5-CH_3 does not correlate to the bridge-head carbon C3a in **110**, whereas a correlation between 9-CH_3 and the new bridge-head carbon C10 is evident for **111**.

These conclusions from NMR were then confirmed by X-ray analysis of [6,6]-fused acyloin **111** (**Figure 25**), which provided crystals from slow evaporation of a $CDCl_3$/hexane solution. This also verified the relative stereochemistry of the *cis*-fused decalone core.

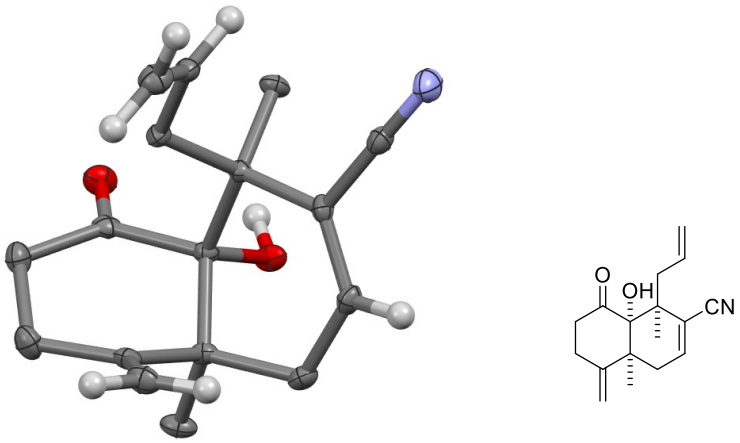

Figure 25. X-ray crystal structure of [6,6]-fused acyloin **111**.
Methylene and methyl protons are omitted for clarity (displayed in the **Appendix**).

[<20>] For [6,6]-fused compounds – that is, decaline-based systems – like **111**, the numbering system of the salvinorin framework is adopted for better comparability and consistency (*cf.* [<18>] on page **93**).

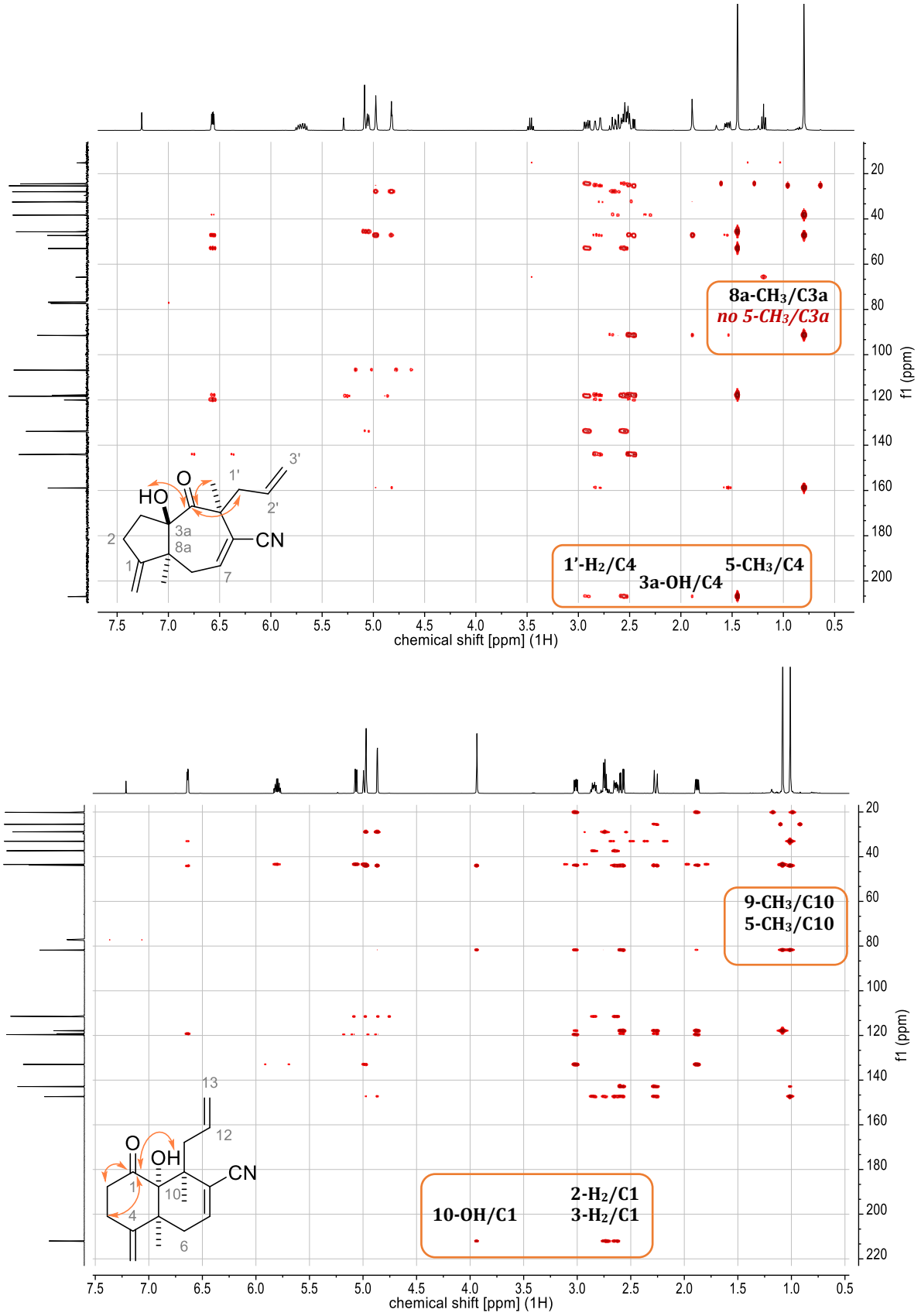

Figure 26. ^{1}H-^{13}C HMBC spectra of **110** ($CDCl_3$, 400 MHz) and **111** ($CDCl_3$, 700 MHz). The most revealing HMBC correlations are shown as orange double-headed arrows in the structures and marked in orange boxes in the spectra.

This rearrangement sequence was later revisited after attempts with other substrates suggested that LDA might enable undesired side-reactions, as will be discussed in the following chapters. For a more thorough examination of the acyloin rearrangement, three rationales were pursued:

- rearrangement of [5,7]-fused acyloin **110** by *coordination to metal complexes* similar to the rearrangement reported by PAQUETTE *et al.* (**Scheme 92** on page **128**),[313]
- treatment of ketonitrile **7** with a metal complex *and* LDA,
- treatment of ketonitrile **7** with *weaker bases* than LDA.

The results of these investigations are shown in **Table 5** and can be summarized as follows:

1) treatment with **Al(*i*-PrO)$_3$** (similarly to PAQUETTE *et al*)[313] had *no effect* on **110**.
2) treating **110** with **Ti(*i*-PrO)$_4$** also had no effect. Cooling this **toluene** solution and adding LDA surprisingly *reversed the ether-cleavage*, giving (6-*epi*-)**7**.
3) treating **7** with **(*i*-PrO)$_4$Ti** in **THF** and then adding LDA (2.2 eq in two portions) resulted in *low conversion, but good overall yield* (35% of **111**, 83% *b.r.s.m.*).
4) replacing LDA by **LHMDS** had no effect on the yield of **111** – however, a *very high overall yield* was achieved (67% of **111**, 92% *instead of* 72% *b.r.s.m.*).
5) replacing LDA by **[(thf)$_2$MgBr(HMDS)]** led to *no conversion* of **7**, presumably explicable by a reduced "kinetic basicity" due to complexation of the magnesium base (similar observations were reported on such Mg-(turbo-)HAUSER bases).[319,320]

Table 5. Summary of later investigations into the rearrangement of [5,7]-fused acyloin **110** and ketonitrile **7**. The ratios (**111** in **bold**) were determined by quantitative NMR.

entry	reagents and conditions	**7** : 6-*epi*-**7** : **110** : **111** **results and remarks**
1	0.079 mmol of **110**, **toluene** (0.05 M), **Al(*i*-PrO)$_3$** (3 eq), 70 °C, 20 h.	**no conversion** with [Al]
2	0.079 mmol of **110**, **toluene** (0.1 M), **Ti(*i*-PrO)$_4$**(1 eq), rt, 3 h; then 0 °C, **LDA** (2 eq), 1.5 h, rt, 30 min.	**no conversion** with [Ti]; **reversal of ether cleavage by addition of LDA**: 55 : 35 : 0 : **0** **no precipitation** – without (*i*-PrO)$_4$Ti, a precipitate is formed in toluene (*cf.* **Table 4**)
3	0.131 mmol of **7**, **THF** (0.05 M), **Ti(*i*-PrO)$_4$** (1 eq), **LDA (1.1 eq)**, –95 °C to 0 °C, 2 h, rt, 30 min; then additional **LDA (1.1 eq)**, –95 °C to –10 °C, 1.5 h, rt, 30 min.	33 : 25 : 0 : **35** **low conversion, good overall yield**
4	0.122 mmol of **7**, THF (0.05 M), **LHMDS (2 eq)**, –95 °C to 0 °C (2 h), rt, 5 min.	16 : 11 : 0 : **67** **good conversion, very high overall yield** compared to LDA (92% instead of 72% *b.r.s.m.*)
5	0.130 mmol, THF (0.05 M), **[(thf)$_2$MgBr(HMDS)] (2 eq)**, –95 °C to –20 °C (1.5 h), rt, 1.5 h.	**no conversion** [(thf)$_2$MgBr(HMDS)] was prepared according to WESTERHAUSEN *et al*[321] (*titration after 26 h indicated complete formation of the base*)

These findings again demonstrate the influence of factors such as the solvent and counter-cation on the reversible acyloin rearrangement. No rearrangement of [5,7]-fused acyloin **110** to [6,6]-fused acyloin **111** was observed by treatment with Al(III) or Ti(IV) isopropoxide. Interestingly, the latter titanium complex shifted the equilibrium towards the substrate-side, when LDA was added, even more so in toluene than in THF. This might be explained by the tendency of the nitrile moiety to form complexes with titanium ions (as demonstrated before in **Chapter 2.3**), presumably favoring the oxa-MICHAEL addition of the alkoxide of **110** to the activated vinyl nitrile which results in a ring closing to the epimeric ketonitriles 6-*epi*-**7**.

Replacing LDA with LHMDS did not change the yield of [6,6]-fused acyloin **111**, but markedly increased the amount of recoverable 6-*epi*-**7**. In stark contrast to that, KHMDS gave a complex mixture with no discernible **111** in previous attempts. While pronounced differences are observed by switching from KHMDS to LHMDS in some instances, or even depending on the *preparation method* of the bases,[322] the dramatic effect observed in our case is highly remarkable. Incidentally, LHMDS was *freshly prepared* from hexamethyldisilazane and n-BuLi, whereas KHMDS was *commercially obtained*.

With magnesium as counter-cation of the hexamethyldisilazide, no *rearrangement or epimerization* of **7** was observed. This may be helpful in optimizing reactions where (i) bases are needed for deprotonation and (ii) an epimerization at C6, or (iii) a rearrangement is not desired. For instance, the use of $[(thf)_2MgBr(HMDS)]$ could be investigated in the α-acylation of ketonitrile **8** with APF (*cf.* **Chapter 2.2.1.1**).

Overall, the desired [6,6]-fused acyloin **111** was conveniently obtained in a yield of 67% (72% *b.r.s.m.* with LDA, 92% *b.r.s.m.* with LHMDS). The recovered substrate and its 6-epimer could both be employed in another rearrangement cycle without detriment to yield. To fully appreciate these findings, it is essential to consider the numerous and ultimately unfruitful rearrangement attempts with LEWIS acids, as discussed in **Chapter 2.3**. With the paradigm shift to employing bases, the *tandem β-ether cleavage/acyloin rearrangement sequence* resulted in immediate success. After optimization, this sequence represents a highly satisfactory method for achieving the desired transformation to the [6,6]-fused core structure of salvinorin A.

The previously pursued LEWIS acid-induced rearrangement did not tolerate alkenes (i.e., the *exo*-methylidene and allyl groups) or the presence of nitriles, which pose no hindrance to this alternative rearrangement sequence. It does not lack a certain irony that the nitrile group *is not only tolerated but actually serves as a prerequisite* in this new sequence.

2.4.4 Acyloin Rearrangement of Allyl- and Acetal-Substituted Epoxyazulenes

With the established access to [6,6]-fused acyloin **111**, several potential routes towards salvinorin A opened up. Exemplified on the route depicted in **Scheme 96**, the transformation of **111** to SalA (**I-11**) would have to encompass:

- *deoxygenation of the acyloin moiety* to ketone **109**,
- a sequence affording **112** by (i) *oxidative cleavage of the allyl moiety* to the aldehyde, (ii) *3-furylation*, and (iii) *lactone formation*,
- *reduction of the 7,8-vinylic bond* either before (α,β-unsaturated nitrile) or after lactone formation (α,β-unsaturated lactone **112**),
- transformation of *the exo-methylidene group* to obtain 2-deacetoxysalvinorin A (**I-52**),
- the known α-*acetoxylation* of **I-52** to conclude the synthesis of salvinorin A (**I-11**).[105]

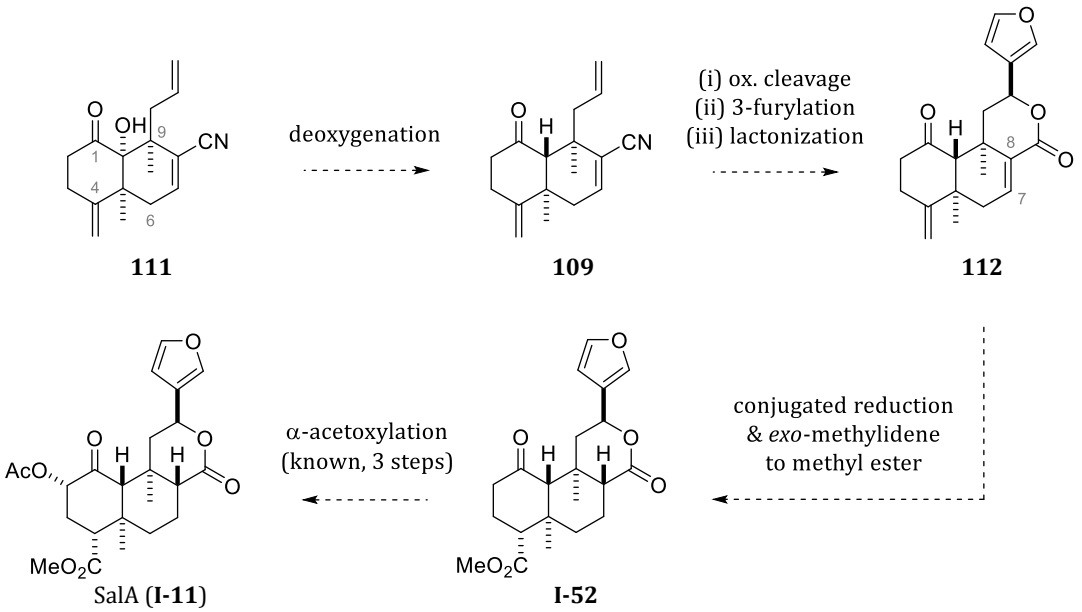

Scheme 96. An example of a potential synthetic route from acyloin **111** to SalA (**I-11**).

As broached in the discussed total syntheses of SalA (**Chapter 1.2**), several reactions within this or similar routes were previously reported on other decaline-based substrates. Compared to the rather unfamiliar tricyclic (3a,7)-epoxyazulenes, the functionalization of decaline substrates provide much more precedents in the literature. Of course, such pursuits may still include some, more or less, unforeseeable challenges with specific substrates. Towards the end of the doctoral research project, several routes towards a total synthesis of SalA were pursued to identify promising routes and resolve emerging issues within those routes.

To gain as many insights as possible, which may eventually allow for determining a potentially fruitful route, some of the reactions in the following chapters were only examined briefly. Consequently, several reactions from here forth were not analyzed or optimized to full extent. We opted to initially focus on qualitative assessments instead, since there would arguably be little use for an optimized reaction, if the following step(s) would then result in a dead end. Occasionally, not 'perfectly pure' substrates were used – or products were isolated after combining several runs in optimization processes, resorting to TLC analysis and/or (quantitative) NMR to determine suitable reagents and conditions for a reaction.

Notable unsuccessful reactions will be briefly mentioned to convey both the gained insights and the rationale to either discard or further pursue specific routes. To keep the length of this thesis within reasonable limits, reactions deemed "not worth pursuing further" are generally not listed in the Experimental Section. In those cases, the reagents, conditions, and noteworthy remarks are summarized in the captions of the respective schemes.

The first attempted steps proceeding from [6,6]-fused acyloin **111** are shown in **Scheme 97**. A transformation of the *exo*-methylidene to the methyl ester was briefly examined but not further pursued due to (i) a moderate yield of epoxide **113** (45%, 56% *b.r.s.m.*), and especially (ii) the formation of multiple compounds in the MEINWALD rearrangement to aldehyde **114**.

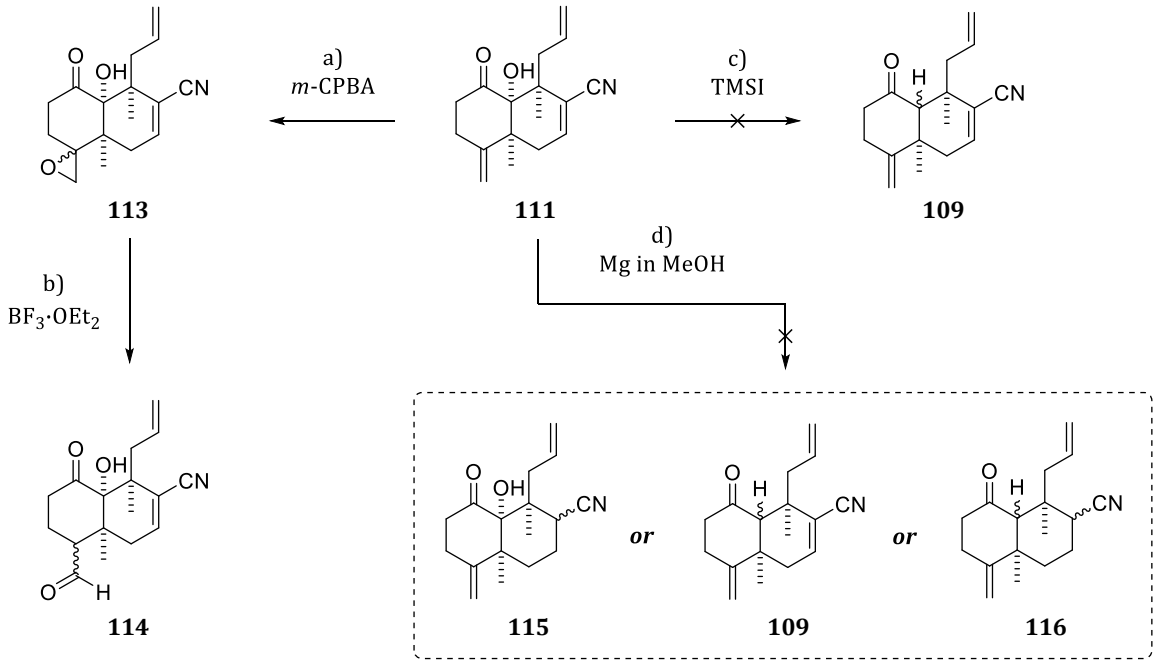

Scheme 97. First attempts at employing [6,6]-fused acyloin **111** in different reactions.

Reagents and conditions: **a)** run #1: DCM (0.1 M), *m*-CPBA (1.2 eq), 0 °C to rt, 38 h; run #2: DCM (0.05 M), $NaHCO_3$ (2 eq), *m*-CPBA (1.2 eq), 0 °C to rt, 22 h; combined runs: **45%** (56% *b.r.s.m.*); **b)** DCM (0.05 M), $BF_3{\cdot}OEt_2$ (5 mol%), 0 °C to rt, 20 h; **complex mixture**. **c)** DCM (0.075 M), TMSI (2 eq), 0 °C to rt, 17 h, then TMSI (2 eq), rt, 24 h; **complex NMR with no allyl signals**. **d)** MeOH (0.05 M), Mg (in portions, in total 5 eq), $HgCl_2$ (cat.), 0 °C to rt, 15 h; **complex NMR with no allyl or carbonyl signals**.

Before the *deoxygenation* with SmI_2 was investigated in more detail, an alternative method with TMSI[323] was tested. This resulted in a complex mixture with complete disappearance of the allyl signals in NMR. Acyloin **111** was also treated with Mg in MeOH – a known but infrequently used method for the *conjugate reduction* of α,β-unsaturated nitriles,[324] esters,[325] and lactones.[326] It was assumed that this radical reduction might also facilitate the *deoxygenation* of the acyloin moiety. However, the signals of the allyl and carbonyl groups disappeared in NMR spectra, while those of the vinyl nitrile remained.

These results indicated that the presence of the allyl group could pose an obstacle in further functionalization pursuits. A plausible reason for these unsuccessful reactions may be cyclization reactions between the allyl and the carbonyl group or its intermediates, similar to the halo-PRINS cyclization observed in the LEWIS-acid mediated rearrangement (*cf.* **Scheme 71** on page **108**). Further insights from reductions of other substrates also suggest that undesired reductions of the acyloin (to the 1,2-diol) and/or the allyl group (to a propyl group) may be involved, as discussed later.

To investigate the functional group tolerance of the rearrangement sequence, methyl ester **6** was treated with strong bases (**Scheme 98**). Treating the *less polar diastereomer* of **6** with KHMDS (1 eq or 2 eq) resulted in complex mixtures exhibiting no vinyl nitrile signals in NMR. This was attempted before KHMDS proved equally unsuitable for the rearrangement of **7**, as shown in the previous chapter. A diastereomeric mixture of **6** was then treated with LDA to examine whether a rearrangement and/or isomerization to a single diastereomer would ensue. In fact, only two compounds were discernible in TLC and NMR, which were then isolated and identified as [5,7]-fused acyloin **117** (20% yield, *impure*) and the desired [6,6]-fused acyloin **118** (30% yield), each as a single but undetermined diastereomer. While this first attempt with LDA led to a modest yield, it also suggested a certain tolerance of the ester group to the rearrangement conditions. Further investigations, such as using LHMDS instead of LDA, were not pursued due to the above-mentioned potential complications which might arise from the presence of the allyl moiety.

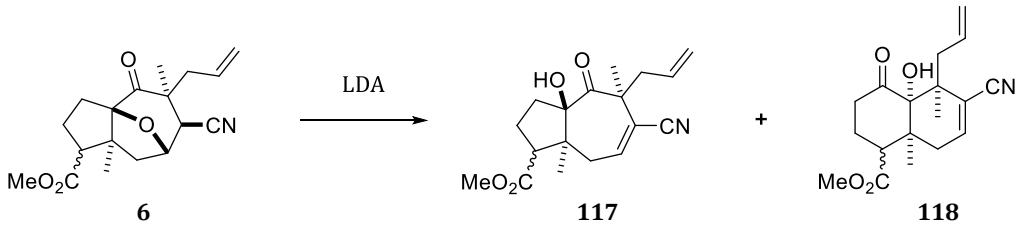

6 **117** **118**

Scheme 98. Rearrangement of methyl ester **6** to [6,6]-fused acyloin **118**.

Reagents and conditions: THF (0.05 M), LDA (2 eq), –95 °C to 3 °C, 2 h 30 min, rt, 20 min; **30%** of **118, 20%** of **117**.

To circumvent side reactions of the allyl group and investigate the acyloin rearrangement on other substrates, alternative routes were approached. In these pursuits, the allyl group was to be functionalized *on the epoxyazulene core*, either to acetal **119** or furyl lactone **38** (**Scheme 99**). The preparation of decalone aldehyde **121** was expected to entail potential complications due to a probable acetalization of the 1,5-linked keto aldehyde. This could necessitate protection of the ketone at C1 by, for instance, ketalization or reduction and silylation (*not shown in* **Scheme 99**).

Clearly, the 3-furylation of aldehyde **39** and lactonization to furyl lactone **38** represents the more straightforward approach, omitting the detour of acetalization and ketone protection. Consequently, this 3-furylation was examined first but led to rather inconclusive results initially. To gain further insights into the rearrangement and the subsequent deoxygenation to decalones, we concurrently examined these on allyl- and acetal-substituted substrates. These insights were then to be applied in routes proceeding from 3-furylated epoxyazulenes once a reliable access to those was achieved. The next subchapters will encompass our examinations with the 'dummy substrates' before routes proceeding from 3-furylated substrates are covered in **Chapter 2.4.5**.

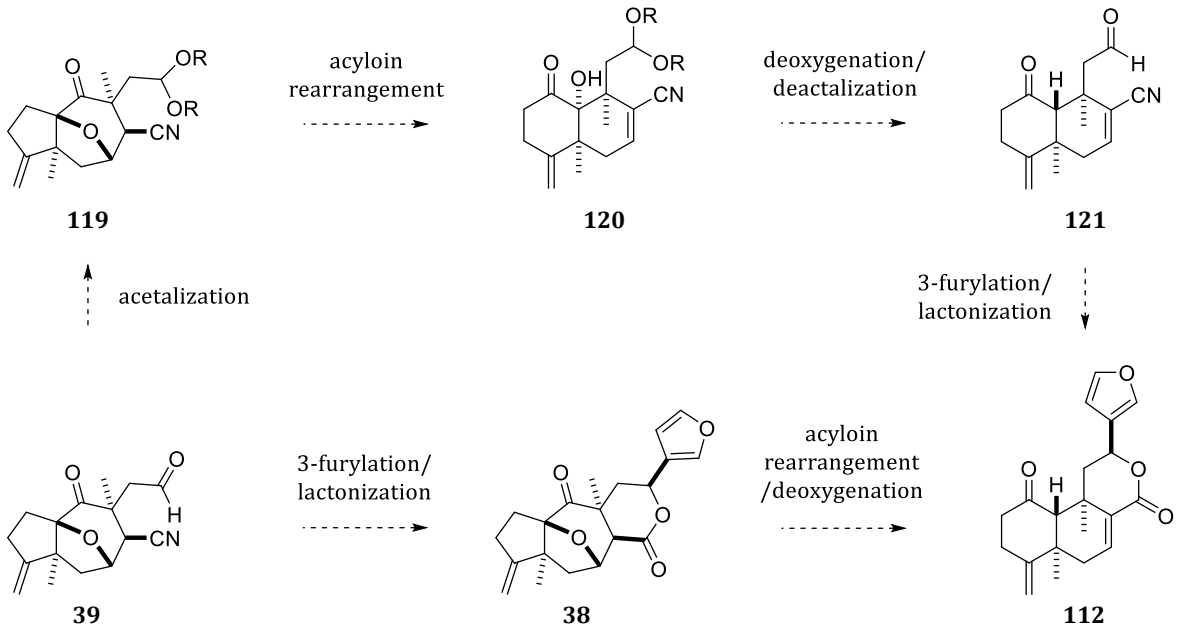

Scheme 99. Exemplified approaches to **112** from tricyclic acetal **119** or 3-furyl lactone **38**.

For first investigations, an impure batch of aldehyde **39** was protected as its dimethyl acetal **119.a**, which proved suitable for the rearrangement to **120.a** (**Scheme 100** on the next page). After chromatographic isolation and recording of the NMR spectra, dimethyl acetal **120.a** unexpectedly underwent spontaneous deterioration in the NMR tube within the same day. The resulting main compound was partially isolated via fractional crystallization from $CDCl_3$/hexane. While a definite confirmation was not pursued, NMR analysis suggested a transacetalization of **120.a** to a single but undetermined diastereomer of enol hemiacetal **122**.

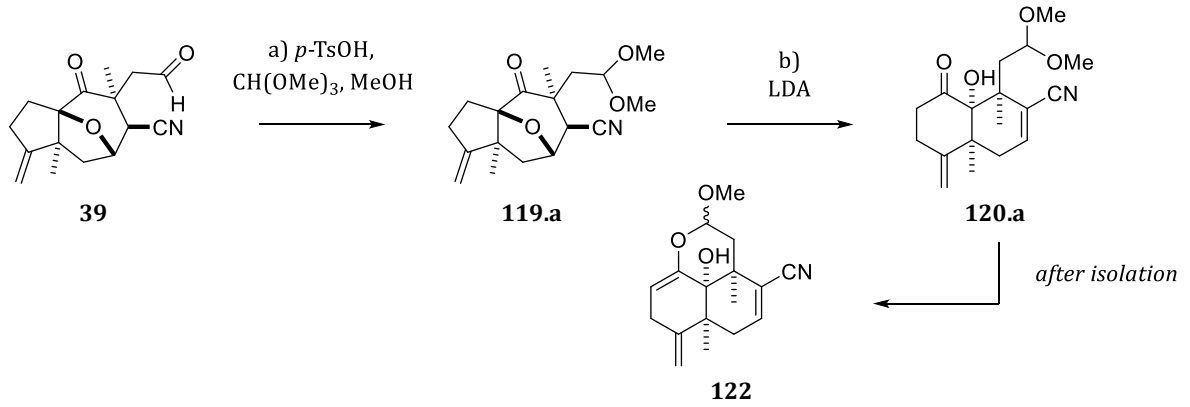

Scheme 100. Rearrangement to dimethyl acetal **120.a** with ensuing transacetalization to **122**.

Reagents and conditions: **a)** MeOH/$CH(OMe)_3$ (5:1, 0.05 M), *p*-TsOH·H_2O (5 mol%), rt, 15.5 h; "**72%**" (impure substrate). **b)** THF (0.05 M), LDA (2 eq), –95 °C to 0 °C, 2.75 h, rt, 35 min; **59%**.

To prevent this deterioration after rearrangement, the presumably more stable dioxolane analog **119.b** was prepared (**Scheme 101**). When trimethyl orthoformate was used as dehydrating agent, some dimethyl acetal **119.a** was obtained due to the liberation of methanol. Intriguingly, significant amounts of the two diastereomeric mixed acetals **119.c** were also isolated. It generally would be assumed that the 'closing' of the mixed acetals to dioxolane **119.b** should be highly favored and not allow for an isolation of such mixed acetals. In this case, strong interactions like hydrogen bonds between the free glycol hydroxy group and the nitrile or the ketone group may somehow impede the closing of the mixed acetals.

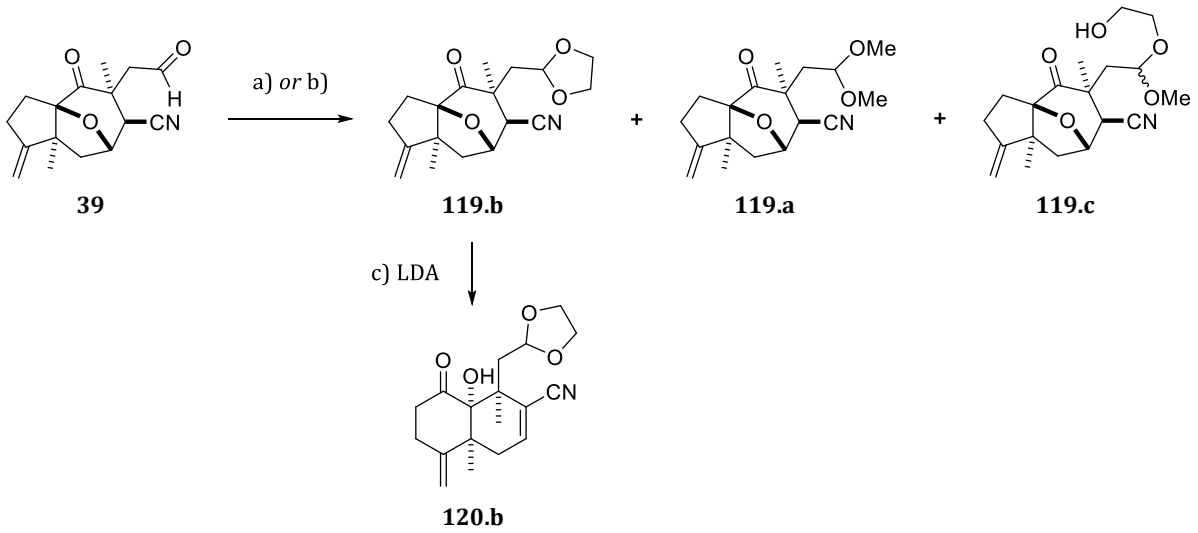

Scheme 101. Preparation and rearrangement of dioxolane **119.b**.

Reagents and conditions: **a)** toluene/ethylene glycol/$CH(OMe)_3$ (10:1:0.4, 0.06 M), *p*-TsOH·H_2O (5 mol%), 70 °C, 2.5 h; **~40%** of **119.b** & **~10%** of **119.a** & **~30%** of **119.c**. **b)** toluene/ethylene glycol (11:1, 0.1 M), *p*-TsOH·H_2O (5 mol%), reflux through an addition funnel packed with MS 4 Å, 2 h; **98%** of **119.b**. **c)** THF (0.05 M), LDA (2 eq), –95 °C to 0 °C, 2 h, rt, 1 h; **69%**.

A selective formation of dioxolane **119.b** was achieved with the method reported by STOLTZ *et al.,* making use of an azeotropic distillation of toluene and water, latter of which is trapped by molecular sieves in an addition funnel atop the reaction flask.[327] With this procedure, **119.b** was obtained in an excellent 98% yield with no discernible impurities in TLC and NMR. Slow evaporation of a Et_2O/hexane solution gave crystals suitable for X-ray analysis (**Figure 27**).

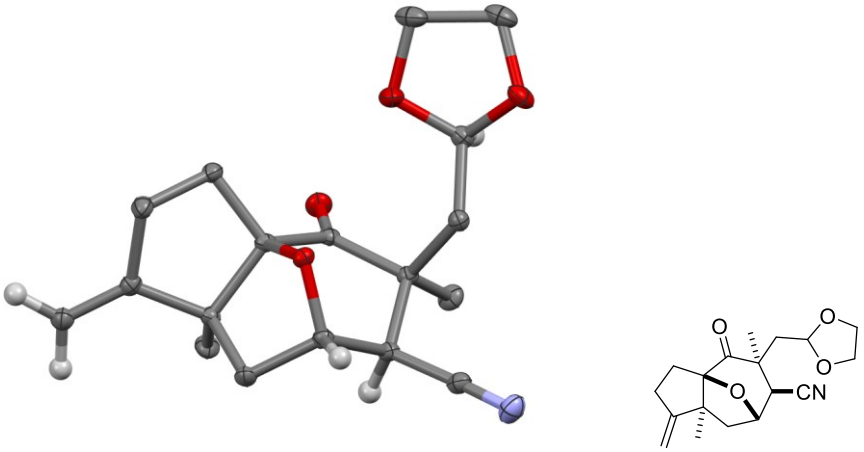

Figure 27. X-ray crystal structure of dioxolane **119.b**.
Methylene and methyl protons are omitted for clarity (displayed in the **Appendix**).

Rearrangement of **119.b** with LDA afforded [6,6]-fused dioxolane **120.b** in 69% yield. While replacing LDA with LHMDS might lead to higher yields, the procedure with LDA gave sufficient amounts of **120.b** for initial examinations of the following reactions. In stark contrast to dimethyl acetal **120.a**, dioxolane **120.b** did not show any signs of lability.

2.4.4.1 α-Deoxygenation of Allyl- and Acetal-Substituted Acyloins

Next, we pursued the deoxygenation of the rearranged [6,6]-fused acyloins substituted with either an allyl (**111**) or dioxolane moiety (**120.b**). As previously mentioned, using either TMSI or Mg/MeOH was not promising for allyl-substituted **111**. Consequently, the α-deoxygenation reaction with *samarium diiodide* was initially investigated on dioxolane **120.b**.

A similar deoxygenation of an acyloin with SmI_2 was shown in **Scheme 93** on page **128**. SmI_2 was also used for *conjugate reductions* in former syntheses of salvinorin A and F (**Chapter 1.2**). HAGIWARA *et al.* emphasized that determining suitable conditions for SmI_2 reductions can be complicated, as exemplified in more detail on the synthesis of SalF.[110]

Unfortunately, finding suitable conditions for the deoxygenation of acyloins can also prove very complicated. To contextualize our approaches and findings, a literature review is provided in the following subchapter, highlighting central aspects and issues observed in this reaction.

2.4.4.1.a Literature Review of SmI_2 Reductions of Acyloins and their Derivatives

The first report covering the preparation and first use-cases of SmI_2 was published by KAGAN *et al.* in 1980.[328] Since then, this versatile SET (single electron transfer) reagent has found application in a plethora of reaction types in synthesis. Many of those are treated in reviews such as those by NICOLAOU in 2009 and, more recently, by HERAVI in 2022.[329,330] A comprehensive book titled "*Organic Synthesis Using Samarium Diiodide: A Practical Guide*," which can be recognized as *the* book on SmI_2, was published by PROCTER, FLOWERS & SKRYDSTRUP in 2009.[331] With that and their later work, PROCTER and FLOWERS contributed greatly to unveiling "*many of the myths surrounding*" SmI_2, which was and still is considered a rather "*esoteric reagent*" at times.[332,333] The most crucial aspects will be summarized in this chapter – from the preparation of the reagent and the role of additives to examples of the desired α-deoxygenation of ketones.

Preparation of SmI_2 and Role of Additives:[331] Generally, THF solutions of SmI_2 (maximum concentration = 0.1 M) are employed. When the ability of THF to act as a hydrogen donor must be avoided, other solvents such as benzene and toluene are used. While KAGAN's original preparation method uses samarium metal and 1,2-diiodoethane in THF, MOLANDER and others have introduced alternative methods with diiodomethane.[328,334,335] PROCTER claimed that using diiodomethane leads to contamination with trivalent samarium impurities which can facilitate side-reactions.[332] A "foolproof" protocol to prepare SmI_2 with 1,2-diiodoethane or iodine was presented in the latter publication, stating that using iodine is convenient but fails with inactive samarium metal. This protocol also involved activating '*inactive*' samarium metal by dry-stirring, a procedure similar to that described for magnesium in this thesis (**Chapter 2.1.1**). Both PROCTER and FLOWERS emphasized that the color switch from green (initially formed SmI_3) to dark-blue (SmI_2) can be deceptive and full conversion to SmI_2 should be confirmed by titration.

The role of additives and (co)solvents is central in the chemistry of SmI_2. Many additives are used – often in combination – to fine-tune the reactivity of SmI_2, including (i) LEWIS bases like HMPA, the additive of choice for many reactions, (ii) a proton source like water, alcohols, or acids, (iii) a base like triethylamine, and (iv) inorganic additives or LEWIS acids like $NiCl_2$ or $AlCl_3$. The effects of additives are mostly attributed to the displacement of iodide and increased reduction potentials of the formed complexes. With higher concentration of additives, however, a saturation of the coordination sphere of the Sm(II) center and the steric encumbrance can inhibit substrate reduction.[331,336] In some cases, 'similar' additives (e.g., MeOH vs. *t*-BuOH) can lead to different products by favoring different reaction paths due to fast or slow protonation of intermediates.[337] Thus, a prediction about how different additives will influence the intended reaction is challenging, as demonstrated by the following examples from the literature.

Mechanism of the α-Deoxygenation of Ketones and Esters: Several synonyms are used for acyloins and their acetyl derivatives in the literature. For a better readability, the terminology of choice in this chapter will be ***α-ketols*** and ***α-ketol acetates***. The α-deoxygenation of ketones (in α-ketols) and their derivatives with SmI_2 was first examined by MOLANDER *et al.* in 1986.[338] While α-ketols resulted in low conversion, a prior activation (e.g., by acylation or silylation) facilitated the α-deoxygenation of these α-ketol derivatives (SmI_2 in THF/MeOH, –78 °C). Under these conditions, most functional groups are typically not reduced by SmI_2 (e.g., ketones, esters or nitriles *without* α-heteroatoms).[339] Moreover, α-acetoxy esters are not reduced as easily as α-acetoxy ketones and therefore require HMPA and an alcohol like MeOH in combination. In some cases, ethylene glycol (with or without HMPA) seems to be equally, if not better, suited. For α-hydroxy esters, the alcohol additive has to be replaced with an acid like pivalic acid.[340] Due to the impeded reduction of ester moieties, MOLANDER proposed differing mechanistic pathways for the reduction of α-heterosubstituted ketones (**Scheme 102**) and α-hetero-substituted esters (**Scheme 103** on the next page).

With α-heterosubstituted ketones, an initial SET generates a ketyl radical **I-263**, which is protonated by the (co)solvent or additives. After a second SET, the carbanion ejects the leaving group X to give enol **I-266**, which tautomerizes to ketone **I-267**. When no proton sources are available, or a *second SET is faster than protonation*, a carbanion is generated in which the Sm(III) is still "*bound*' to the oxygen (**I-265** with OSm(III) instead of OH).

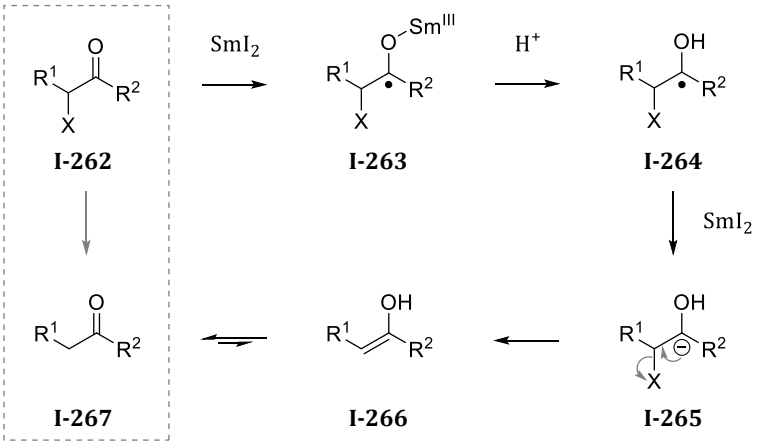

Scheme 102. Reduction of α-heterosubstituted ketones **I-262** to ketones **I-267**.[338]

With α-heterosubstituted esters, the reduction is believed to progress via an initial *SET onto the leaving group*, homolytic cleavage of the C-X bond, and a second SET to give a ***carbanion located at C2*** (**I-271** in **Scheme 103**, left-hand-side pathway). Alternatively, a coordination of Sm(II) between the ester moiety and the α-heteroatom can enable an initial *SET onto the carboxyl group* to give the hemiacetal radical **I-274** (right-hand-side pathway). A second SET then generates a ***carbanion located at C1*** which ejects the leaving group (**I-275**).

Both pathways give ester enolate **I-272**, which is then protonated and tautomerizes to ester **I-273**. Notably, it seems reasonable that a similar coordination of samarium may also occur with α-heterosubstituted ketones, but no such considerations were encountered in the literature.

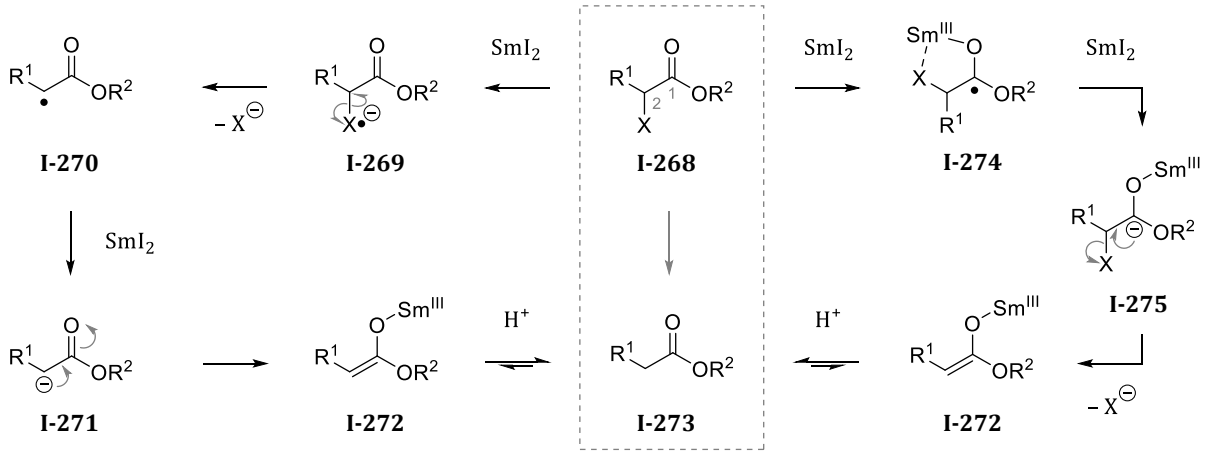

Scheme 103. Reduction of α-heterosubstituted esters **I-268** to esters **I-273**.[338] The right-hand side involves a complexation (**I-274**) postulated by PROCTER, FLOWERS & SKRYDSTRUP.[331]

Examples of the α-Deoxygenation of Ketones: As mentioned above, the α-deoxygenation of α-ketols proved complicated in many instances. While additives enabled this direct α-ketol reduction occasionally, the "best reaction protocol has perhaps not yet been developed," as MOLANDER put it in his 1994 review.[339] Since then, some examples of a direct reduction of α-ketols have been published but a much higher number of publications relied on using α-ketol acetates as substrates. In the following, two literature examples on the reductions of α-ketols and α-ketol acetates will be shown to showcase the rather elusive reaction pathways facilitated by SmI_2, before the effects of some additives are summarized.

The first example was reported by HOLTON *et al.* (**Scheme 104** on the next page).[341] Whereas α-ketol **I-276** was smoothly reduced to ketone **I-278**, its epimer **I-277** afforded the tertiary alcohol **I-279** by a cascade of (i) *acyloin rearrangement*, (ii) *α-ketol reduction*, and (iii) *reductive cyclization* (with 10 eq SmI_2, rt). With milder conditions (3 eq SmI_2, 0 °C), the rearranged α-ketol **I-280** could be isolated and then reduced to ketone **I-281** with only little reductive cyclization (10 eq SmI_2, 0 °C). The acyloin rearrangement was proven to be induced by Sm(III) acting as a LEWIS acid. The addition of NEt_3 prevented this undesired rearrangement but also inhibited the α-deoxygenation of **I-277**, giving only a mixture of the 1,2-diol isomers (not shown).

These findings also highlight stereoelectronical aspects of acyloin rearrangements, which have already been discussed in **Chapter 2.4.2**. Both α-ketols may be subject to rearrangement, yet the alignment of the migrating group in relation to the C=O-bond seems to be better suited in **I-277**, favoring the rearrangement over a reduction, while the opposite is the case for **I-276**.

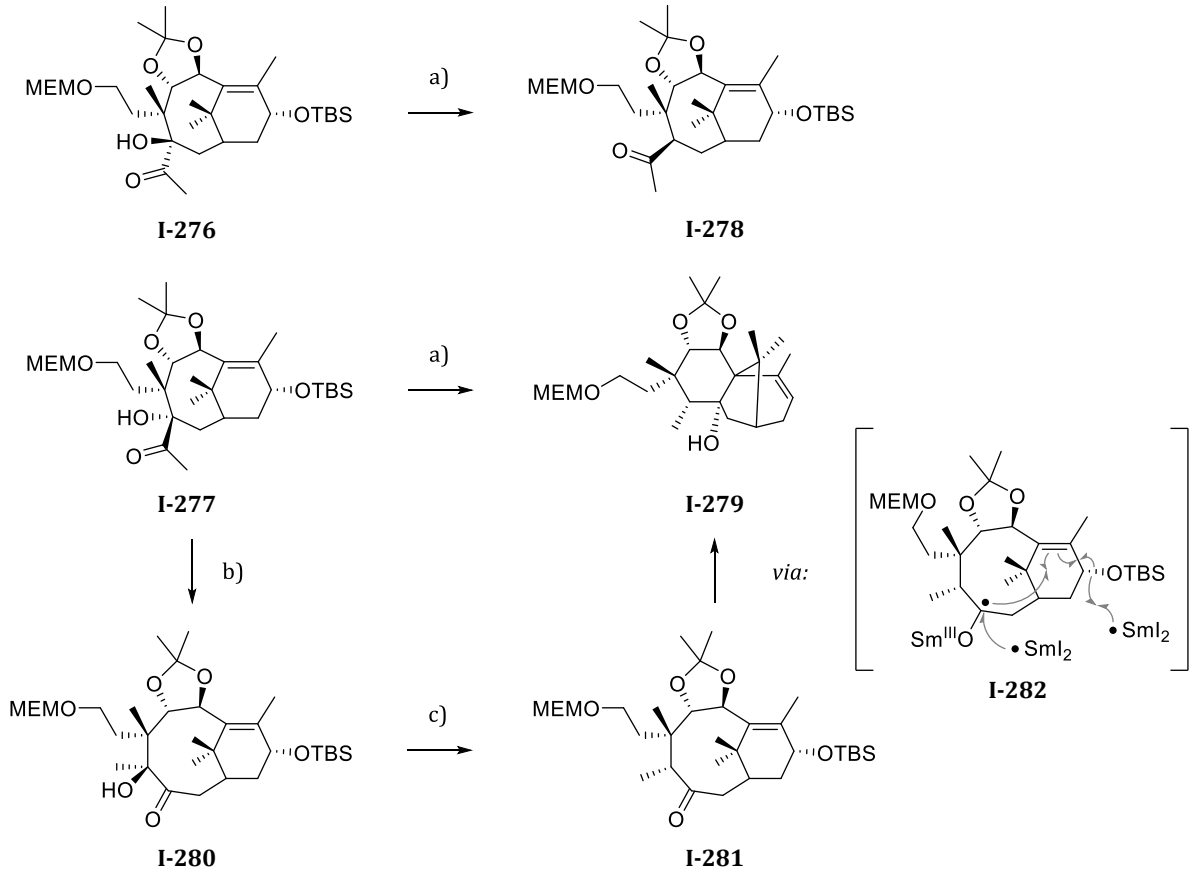

Scheme 104. SmI_2-mediated transformations of isomeric α-ketols **I-276** and **I-277**.[341]

Reagents and conditions: **a)** THF, SmI_2 (10 eq), rt, 2 h; for **I-278**: *no yield given*; for **I-279**: **92%**. **b)** THF, SmI_2 (3 eq), 0 °C, 1 h; **90%**. **c)** THF, SmI_2 (10 eq), 0 °C, 2 h; **70%** of **I-281**, *some* **I-280** and **I-279**.

In the second example, the role of additives in the α-deoxygenation of α-ketol acetates was examined. As reported by LINDERMAN *et al.,* α-ketol silyl ether **I-283** was reduced to ketone **I-284** with SmI_2 (3 eq) (**Scheme 105** on the next page).[342] However, the α,α'-dioxygenated analog **I-285** gave the hexanol derivative **I-286** by a concomitant reduction of the spirocyclic ketal. Thus, a protocol for the chemoselective reduction to the desired furanone **I-287** was sought.

On the dummy substrate **I-288**, several additives were examined to facilitate the reductive cleavage of the α-acetoxy group while obviating that of the α'-methoxy group. Without additives, only the simple furanone **I-289** was obtained. Addition of MeOH gave furanone **I-289** and enone **I-290** via an "unknown mechanism," which presumably involves the aromatic intermediate **I-291**. In the presence of NEt_3, the reduction was completely suppressed.

By replacing MeOH with ethylene glycol, the chemoselective reduction of the α-acetoxy group was achieved (from **I-288** to **I-292**). This protocol was then applied to the α-acetoxy analog of **I-285** (OAc instead of OTMS, *not shown*), affording the desired furanone **I-287** in 68% yield.

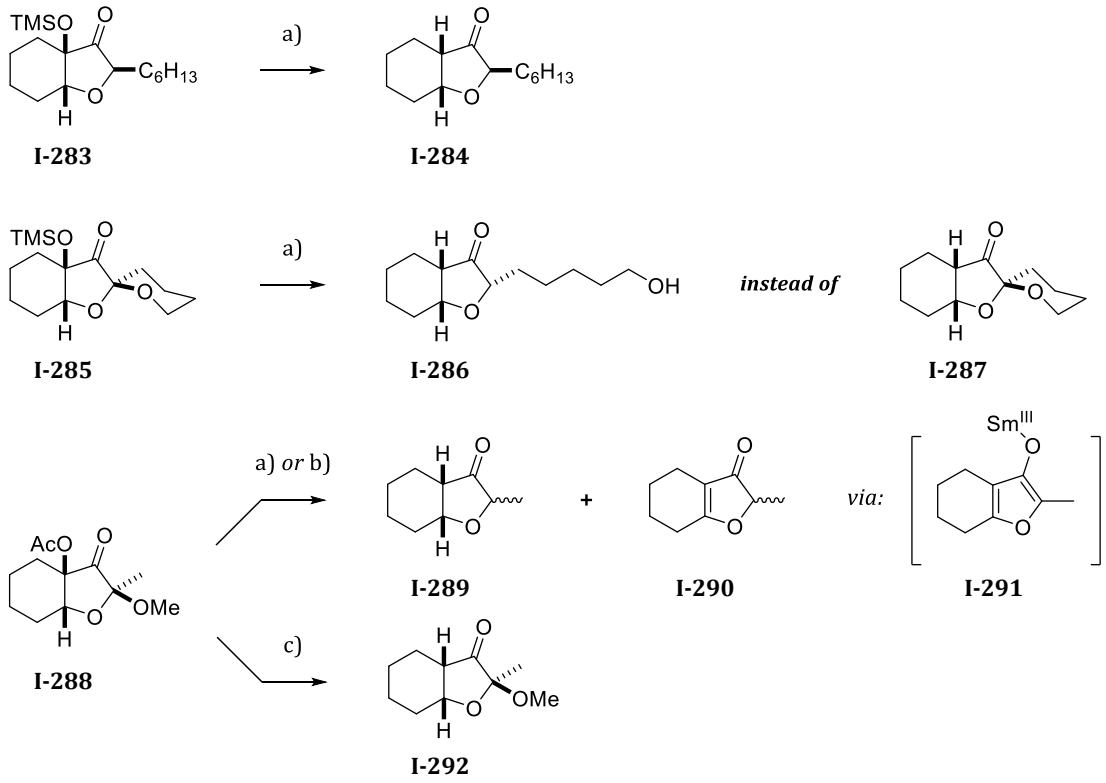

Scheme 105. SmI_2-mediated reductions of α,α'-dioxygenated 3-(2*H*)-furanones.[342]

Reagents and conditions: **a)** THF, SmI_2 (3 eq), –78 °C; for **I-283**: **73%** of **I-284**; for **I-285**: **74%** of **I-286**; for **I-288**: afforded only **I-289** (*no yield given*). **b)** THF *or* MeCN, MeOH (*no eq given*), –78 °C; afforded **I-289** (*no yield given*) and up to **35%** of **I-290**. **c)** THF, SmI_2 (3 eq), ethylene glycol (14 eq), –78 °C, 20 min; *no yield given*.

Integrating the observations in these and other examples, the *general* effects of some additives can be summarized as follows. It must however be considered that the effects of additives for one substrate are not necessarily applicable for other substrates, since the reductions are multifactorial and depend on specific substrate properties, reagents, and conditions.

Additives in the Reductions of α-Ketols:

- ***without additives***: Examples of α-ketol reductions without additives include those reported by HOLTON *et al.* in 1988 (towards the taxane taxusin, **Scheme 104**)[341] or in 1994 (with the taxane 10-deacetylbaccatin III).[343] As shown in **Scheme 93** on page **128**, XU *et al.* reported a reduction of a [5,7]-fused α-ketol in 2019.[315]
- ***HMPA***: While the reduction of 10-deacetylbaccatin III was possible without additives, the addition of HMPA increased yield and reduced the extent of undesired epimerization.[343]
- ***NEt_3***: Addition of NEt_3 prevented deoxygenation of α-ketol **I-277** (**Scheme 104**), giving the respective diols instead.[341]

- ***t-BuOH***: In 1987, WHITE *et al.* reported an α-ketol reduction with *t*-BuOH. This required stirring the reaction for 12 h at room temperature – a notable deviation from the usually very fast reductions with SmI_2 (several minutes to a couple of hours in the cold).[344]

- ***Ac_2O***: The addition of acetic anhydride eased the reduction of α-ketols.[338,345] This was attributed to the *in situ* generation of an α-ketol acetate by MOLANDER. However, insights into the reduction of α-ketol acetates suggest that the effect of Ac_2O may be both due to acetylation, as well as the effect of acetic acid complexing the samarium reagent.

Additives in the Reductions of α-Ketol Acetates:

- ***without additives***: Compared to the reduction of 10-deacetylbaccatin III (an α-ketol), those of baccatin III and taxol (both α-ketol acetates) proceeded more readily and in higher yields.[343] LINDERMAN *et al.* examined the reduction of α,α'-dioxygenated 3-(2*H*)-furanones with different additives. Without additives, this reduction suffered from chemoselectivity issues, as will be discussed in more detail below.[342] ARGADE *et al.* reported the reduction of an α-ketol acetate without additives in 2015.[345]

- ***HMPA***: HOLTON *et al.* showcased how the addition of HMPA can also facilitate unexpected side-reactions such as the reduction of "simple esters, e.g., methyl benzoate."[343]

- ***t-BuOH***: Similar to HOLTON *et al.*,[343] GEORG *et al.* examined the reduction of baccatin III and taxol.[346] Baccatin III was reduced slowly, incompletely, with partial epimerization, and in moderate yield using *t*-BuOH as additive. Intriguingly, a product of an *allylic oxidation*, presumed to be facilitated by *t*-$BuOSmI_2$, was also identified.

- ***HOAc***: GEORG *et al.* achieved the reduction of baccatin III and taxol when HOAc was added instead of *t*-BuOH,[346] leading to similarly effective reductions as those of HOLTON *et al.* (no additives).[343] To briefly condense the findings of both research groups, *using no additives or HOAc proved suitable, while t-BuOH either impeded the reduction or facilitated side-reactions*.

- ***NEt_3***: LINDERMAN *et al.* found that NEt_3 completely suppressed the desired reduction.[342]

- ***MeOH***: Addition of MeOH resulted in high yields of the desired ketone in several cases.[338,347,348] In some cases, a partial overreduction to the respective mono-alcohol (at the former carbonyl center) was observed.[349] For LINDERMAN, an overreduction, as well as a side-product from an "unknown mechanism" resulted when MeOH was used.[342]

- ***ethylene glycol***: Ethylene glycol was found to be effective in the reduction of α-acetoxy esters.[340] By replacing MeOH with ethylene glycol, LINDERMAN *et al.* achieved the desired reduction of α-acetoxy ketones in good chemoselectivity.[342]

With these observations, a general *'best practice'* for these reductions seems hardly predictable, since the effects of additives are rather inconclusive, and in parts contradictory, in the literature. Employing no additives can be better suited than using additives which might suppress the desired reduction or enable side-reactions. Moreover, an adequate preparation and amount of SmI_2, as well as other conditions like temperature and reaction time have to be considered.

Another crucial aspect is the general role of water in these reductions. As also demonstrated in **Chapter 2.1.1** for the carbocupration of alkynes, *'quenching'* a reaction with aqueous solutions is often more than simply terminating a reaction. In the case of SmI_2 reductions, water can play a central role, when no other additives are employed. A prominent example was reported by CURRAN *et al.* for the reduction of ketones: quenching a *dry reduction with dry air and subsequent aqueous work-up* resulted in the substrates being recovered. When water was present during the reduction (2.2 eq SmI_2, 33 eq water), the desired alcohols were obtained rapidly and cleanly with the same quench protocol.[350]

Other examples of single or combined additives include (i) water, (ii) water/NEt_3, or (iii) $AlCl_3$/MeCN, which enable the reduction of (i) vinyl nitriles to nitriles,[351] (ii) esters to alcohols[352] and nitriles to amines,[353] or (iii) acetals,[354] respectively. In many publications, including the total syntheses of salvinorin A (**Chapter 1.2**), a combination of MeOH/NEt_3 proved effective for the reduction of unsaturated esters and lactones. Since these functional groups would be present in some of our substrates, a careful consideration of reagents and conditions depending on the respective substrate seems crucial for a successful reduction with SmI_2.

Incidentally, other procedures for the deoxygenation of α-ketols may be considered. Several alternatives to SmI_2 have been established, including dissolving metal reductions (especially Zn/HOAc),[355–357] and low-valent metal ions [Cr(II) or V(II)].[358,359] Moreover, several metal-free alternatives were reviewed[360] and a new method was reported more recently,[361] underscoring the sustained general interest in such deoxygenations.

As discussed in the next chapter, we initially investigated the α-deoxygenation of dioxolane-substituted **α-ketol 120.b**. To quickly gain as much insight into this reduction as possible, several small-scale variations were first analyzed *qualitatively* by TLC and NMR while omitting the determination of yields. The resulting compounds were isolated from the combined crude products of these variations, allowing for a comparison of the general effect of additives. Some observations were better contextualized after additionally examining the reduction of α-ketol acetates. For conciseness and comprehensibility, key findings will be summarized to emphasize the rather cumbersome optimization process which allowed for an adequate deoxygenation of our allyl-substituted **α-ketol acetate**.

2.4.4.1.b α-Ketol Reductions

With the tested reaction variations, a *selective* reduction of α-ketol **120.b** to decalone **123** was not achieved (**Scheme 106**). Alongside decalone **123**, mainly diol **124** was isolated. Due to superimposition of most NMR signals and excessive decomposition under most conditions, methodical TLC analysis proved crucial. A schematic TLC plate indicating the observed compounds is depicted. The reactions conditions are summarized in **Table 6** on the next page.

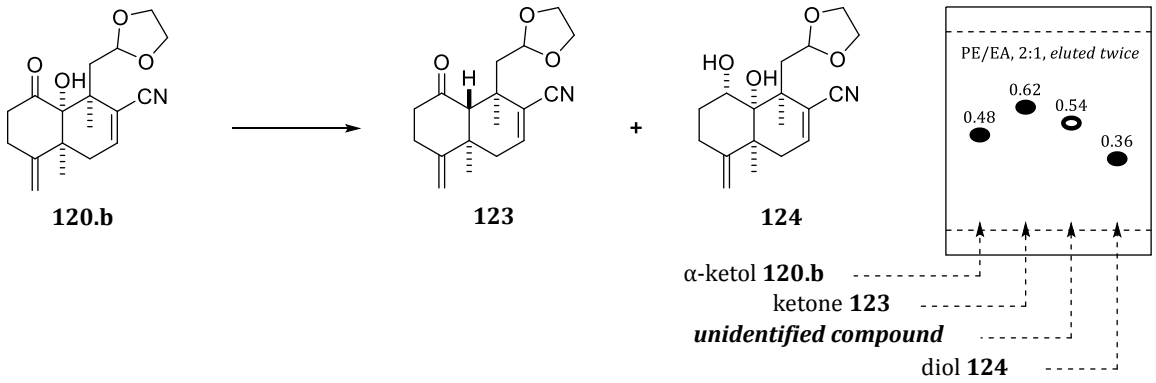

Scheme 106. Reduction of α-ketol **120.b** to ketone **123** and diol **124** with schematic TLC plate.

To summarize our findings, full conversion of α-ketol **120.b** was only observed with MeOH/NEt_3 and excess SmI_2 (4 eq, **entry 2**). This gave decalone **123** and, predominantly, diol **124**. Using less SmI_2 (2 eq, **entry 3**) led to incomplete conversion to **123** and **124**. The appearance of diols was also reported in some literature examples and can be explained by a 'premature' protonation of the intermediate(s) instead of a deoxygenation by ejection of the leaving-group oxygen (*cf.* **Scheme 102** on page **143**).

Replacing MeOH with ethylene glycol (**entry 4**) or *i*-PrOH (**entry 5**) impeded conversion. Notably, an *unidentified compound* was observed in TLC when no NEt_3 was present (**entries 1 and 4**), which then decomposed. A similar *unidentified compound* played a central role in the reductions of α-ketol acetates, as discussed below.

An alternative deoxygenation with Mg in MeOH (**entry 6**) was also briefly examined. This method was attempted with allyl-substituted α-ketol **111** before, resulting in complex mixtures (see page **137**). With the dioxolane analog **120.b**, a reduction pattern similar to that with SmI_2 was observed. Although reductions of the vinyl nitrile or the ketal group were anticipated,[324,362] no products from such reductions were evident. The initially sluggish conversion improved notably by adding catalytic amounts of $HgCl_2$ and lowering reaction temperature. This facilitated the reduction via SET by lowering the amount of magnesium metal that is unproductively solvolyzed by methanol.

Table 6. Reagents and conditions for the reduction of α-ketol **120.b** (**Scheme 106**). Procedural details can be seen in the Experimental Section. *The assessment of conversion is based on intensities of TLC spots & NMR signals and are qualitative approximations rather than precise evaluations.*

entry	reagents and conditions	results and remarks
1	with **MeOH**: **120.b** (0.139 mmol, 1 eq), THF, MeOH (10 eq); then SmI_2 (4 eq, over 1 min), –78 °C to –10 °C, 1 h, then rt, 45 min.	moderate conversion to diol and *unidentified compound*; then considerable decomposition.
2	with **MeOH/NEt_3 & 4 eq SmI_2**: **120.b** (0.098 mmol, 1 eq), THF, MeOH (40 eq), NEt_3 (16 eq); then SmI_2 (4 eq, over 4 min), –78 °C to –40 °C, 1 h.	**full and relatively clean conversion** to diol and ketone (NMR ratio of **124/123** ≈ 2:1).
3	with **MeOH/ NEt_3 & 2 eq SmI_2**: **120.b** (0.098 mmol, 1 eq), THF, MeOH (40 eq), NEt_3 (16 eq); then SmI_2 (2 eq, over 11 min), –95 °C to –50 °C, 30 min.	moderate conversion to diol and ketone.
4	with **no additives**: SmI_2 first (3 eq), THF; then **120.b** (0.107 mmol, 1 eq, over 1.5 min), –95 °C to 0 °C, 2 h. then with **ethylene glycol**: ethylene glycol (13 eq), 0 °C to 10 °C, 1 h.	with **no additives:** practically no conversion. with **ethylene glycol**: full conversion to *unidentified compound* & diol; then considerable decomposition.
5	with **NEt_3**: SmI_2 first (3 eq), THF, NEt_3 (12 eq); then **120.b** (0.032 mmol, 1 eq, over 1.5 min), –95 °C to –30 °C, 1 h. then with ***i*-PrOH/NEt_3**: *i*-PrOH (14 eq), –30 °C to –15 °C, 30 min; then –95 °C; SmI_2 (2 eq) & *i*-PrOH (14 eq), –95 °C to rt, overnight (~16 h).	with **NEt_3**: no conversion. with ***i*-PrOH/NEt_3**: low conversion. after additional **SmI_2 & *i*-PrOH** and **rt overnight**: moderate conversion to ketone
6	with **Mg in MeOH**: **120.b** (0.134 mmol, 1 eq), MeOH (0.05 M), Mg (2 × 5 eq), 0 °C, 6 h. then with **Mg in MeOH, cat. $HgCl_2$ & lower temperature**: $HgCl_2$ (~2.5 mol%), then Mg (3 × 10 eq), –18 °C to 0 °C, 6 h.	without **$HgCl_2$**: practically no conversion. with **$HgCl_2$ and lower temperature**: moderate conversion to ketone & diol.

As expected, deacetalization attempts with decalone **123** and enol hemiacetal **122** were unsuccessful and resulted in complex mixtures without distinct aldehyde peaks in NMR (**Scheme 107**). Since the preparation of keto aldehyde **121** or its protected analogs from dioxolane **123** would be complicated, our focus switched (back) to allyl-substituted analogs.

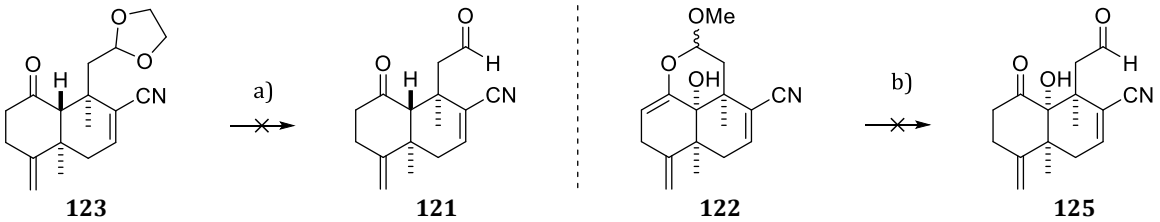

123 **121** **122** **125**

Scheme 107. Attempted acetal hydrolysis of decalone **123** and enol hemiacetal **122**.

Reagents and conditions: **a)** acetone (5 vol% water, 0.02 M), *p*-TsOH·H_2O (0.3 eq), 20 h; no conversion; then aq. HCl (2 M, 1 mL), rt, 10 h; full conversion to **complex mixture**. **b)** similar to a); slow conversion to **complex mixture**.

2.4.4.1.c α-Ketol Acetate Reductions

The investigations into the deoxygenation of α-ketol acetates were primarily conducted on the acetate of allyl-substituted acyloin **111**. For this purpose, **111** was acetylated with Ac_2O, NEt_3, and DMAP, which afforded α-ketol acetate **126** in an excellent yield of 95% (**Scheme 108**).

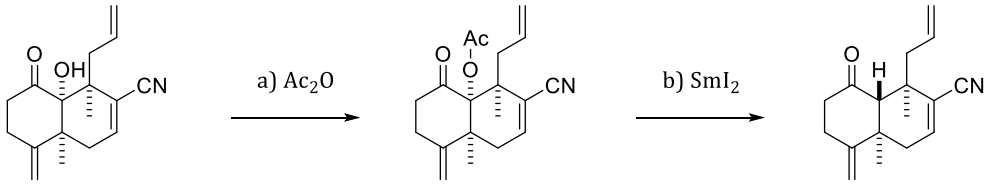

111 **126** **109**

Scheme 108. Acetylation of **111** and reduction of α-ketol acetate **126** to decalone **109**.

Reagents and conditions: **a)** THF (0.1 M), NEt_3 (5 eq), DMAP (10 mol%), Ac_2O (10 eq), 50 °C, 13 h; **95%** (*determined by qNMR*). **b)** discussed in the text & listed in **Table 7**.

Similar to some of the attempts with α-ketol **120.b**, deoxygenation of α-ketol acetate **126** with SmI_2 gave an ***unidentified compound***, followed by complete decomposition without formation of distinct compounds. This was also observed with the acetate of **120.b** (*not shown*), whereas no formation of decalone **123** and diol **124** was evident. While the nature of these elusive *unidentified compounds* still lacks a conclusive explanation, our observations suggest that these may correspond to unstable and reactive samarium complexes. Several variations were tested until this decomposition could be limited, and thus, a more adequate deoxygenation of **126** was achieved. The observations are briefly summarized in the following and the most 'insightful' reaction variations are listed in **Table 7** on the next page.

Formation of the *unidentified compound* occurred rapidly at –95 °C when no additives were used (**entry 1**), whereas addition of ethylene glycol or MeOH impeded this conversion. In the presence of **NEt_3**, the *unidentified compound* converted to decalone **109**. Several work-up methods were tested to maximize conversion to **109**. A basic environment during *and after* work-up had to be maintained: quenching with half-sat. NH_4Cl instead of half-sat. $NaHCO_3$ resulted in complete decomposition. Considerable decomposition was also observed, when the added NEt_3 evaporated too early, either by (i) exposing the organic extracts to air for an extended time or (ii) a 'premature' removal of volatiles. These insights were incorporated into a more adequate work-up procedure (**entry 2**). After quenching with half-sat. $NaHCO_3$ and extracting with diethyl ether containing 5 vol% NEt_3, the organic extracts were washed with saturated solutions of $NaHCO_3$, $Na_2S_2O_3$, and then NaCl. Additionally, the less volatile amine base 2,6-lutidine was added before removal of volatiles. With this work-up, the desired decalone **109** was obtained in a yield of **50%** (66% *b.r.s.m.*), as determined by qNMR.

In a later phase of our work, the reproducibility of this method was re-examined. The SmI_2 solution was now prepared using (i) *purified* 1,2-diiodoethane instead of *unpurified* diiodomethane and (ii) a higher excess of Sm (2 eq vs. 1.2 eq). Repeating the procedure of **entry 2** gave decalone **109** in yields of **45–55%**, but decomposition still could not be prevented completely.

Additionally, a non-aqueous work-up was designed to remove samarium complexes from the product solution (**entry 3**). After adding ethylene glycol and a mixture of PE/DE/NEt_3 to the reaction mixture, the gel-like ethylene glycol phase separated, from which samarium compounds precipitated (*insoluble in Et_2O, THF, DCM and EtOAc*). The biphasic mixture was then filtered through silica gel. As before, premature removal of volatiles had a negative impact on yield. Removing volatiles after letting the solution stand briefly (<10 min) gave **109** in a **~65%** yield. The conversion of the *unidentified compound* to **109** continued in the NMR solution (*see Experimental Section*). This was also seen in former attempts, albeit with much higher extent of decomposition. When the solution was let stand for a longer time before removal of volatiles (~2 h), decalone **109** was obtained in a – all things considered – *very satisfactory* yield of **~75%**.

With this α-deoxygenation of **126** to decalone **109**, the key transformation within our work was accomplished: the rearrangement of epoxyazulenes to decalones. While this deoxygenation proved exceptionally complicated, and decomposition posed a (in the end, much smaller) issue, our observations allowed us to develop a promising procedure employing a glycol-mediated precipitation of samarium complexes. Examining this method in more detail may be worthwhile, both for **109** and other equally challenging SmI_2 reductions.

Table 7. Reagents and conditions for the reduction of α-ketol acetate **126** (**Scheme 108**). Initial conversion resulted only in formation of the *unidentified compound* [R_f = 0.62 (UV active) in PE/EA, 2:1 (R_f (**126**) = 0.55 (not UV active)], which could then be converted to decalone **109** [R_f = 0.64 (not UV active)] in the presence of NEt_3.

entry	reagents and conditions	results and remarks
1	SmI_2 (3 eq), THF, –95 °C; then **126** in THF (0.6 M, 0.133 mmol, 1 eq), –95 °C to –10 °C, 1 h 15 min. Quenched with half-sat. $NaHCO_3$ and extracted with DE.	Very rapid (<7 min) and **full conversion** to *unidentified compound*. **Complete decomposition** after work-up.
2	SmI_2 (3 eq), THF, –95 °C; then **126** in THF (0.6 M, 0.160 mmol, 1 eq), –95 °C to –50 °C, 45 min; then NEt_3 (23 eq). Quenched with half-sat. $NaHCO_3$ and extracted with DE (5 vol% NEt_3). Organic extracts washed with sat. $NaHCO_3$, sat. $Na_2S_2O_3$, and then sat. NaCl. Addition of 2,6-lutidine (27 eq) before removal of solvents.	Incomplete conversion, presumably due to partially oxidized Sm metal. **50% yield** (66% *b.r.s.m.*) of **109** [*qNMR*]. *Details in Experimental Section.*
3	SmI_2 (2.2 eq), THF, –95 °C; then **126** in THF (0.5 M, 0.054 mmol, 1 eq), –95 °C to –65 °C, 15 min; then NEt_3 (13 eq), –65 °C to –20 °C, 45 min; then addition of ethylene glycol (66 eq) & dilution with a mixture of PE/DE (1:1) containing 5 vol% NEt_3; –20 °C to –5 °C, 45 min, rt, 30 min. Filtration through silica gel, eluting with PE/DE/NEt_3-mixture before removal of solvents.	SmI_2 prepared with purified 1,2-diiodoethane and checked by titration. **75% yield** of **109** [*qNMR*]. *Details in Experimental Section.*

As with tricyclic enone **9** before (*cf.* page **61**), the ^{1}H NMR signals of decalone **109** separated much better in C_6D_6 than in $CDCl_3$. NOESY affirmed the expected *trans*-fused decaline core of **109** (**Figure 28**). To facilitate interpretation, a more appropriate (*but simplified*) structural depiction of **109** is shown and key NOE correlations are labeled as **A1–A4** and **E1/E2**.

The bridge-head proton in question, **10-H**, correlates with both the (*pseudo*-)**axial** protons of the 'left-side ring' (2-H$_{ax}$; **A1**) and 'right-side ring' (6-H$_{ax}$; **A2**), as well as with the **allyl** moiety (11-H$_a$; **A3** & 12-H; **A4**). On the other hand, the (*pseudo*-)**equatorial** configuration of proton 6-H$_{eq}$ is indicated by its correlation with the bridge-head methyl group (5-CH$_3$; **E1**). Notably, no correlation between 6-H$_{eq}$ and the other methyl group (9-CH$_3$) is seen; both methyl groups, however, correlate with each other (5-CH$_3$/9-CH$_3$; **E2**).

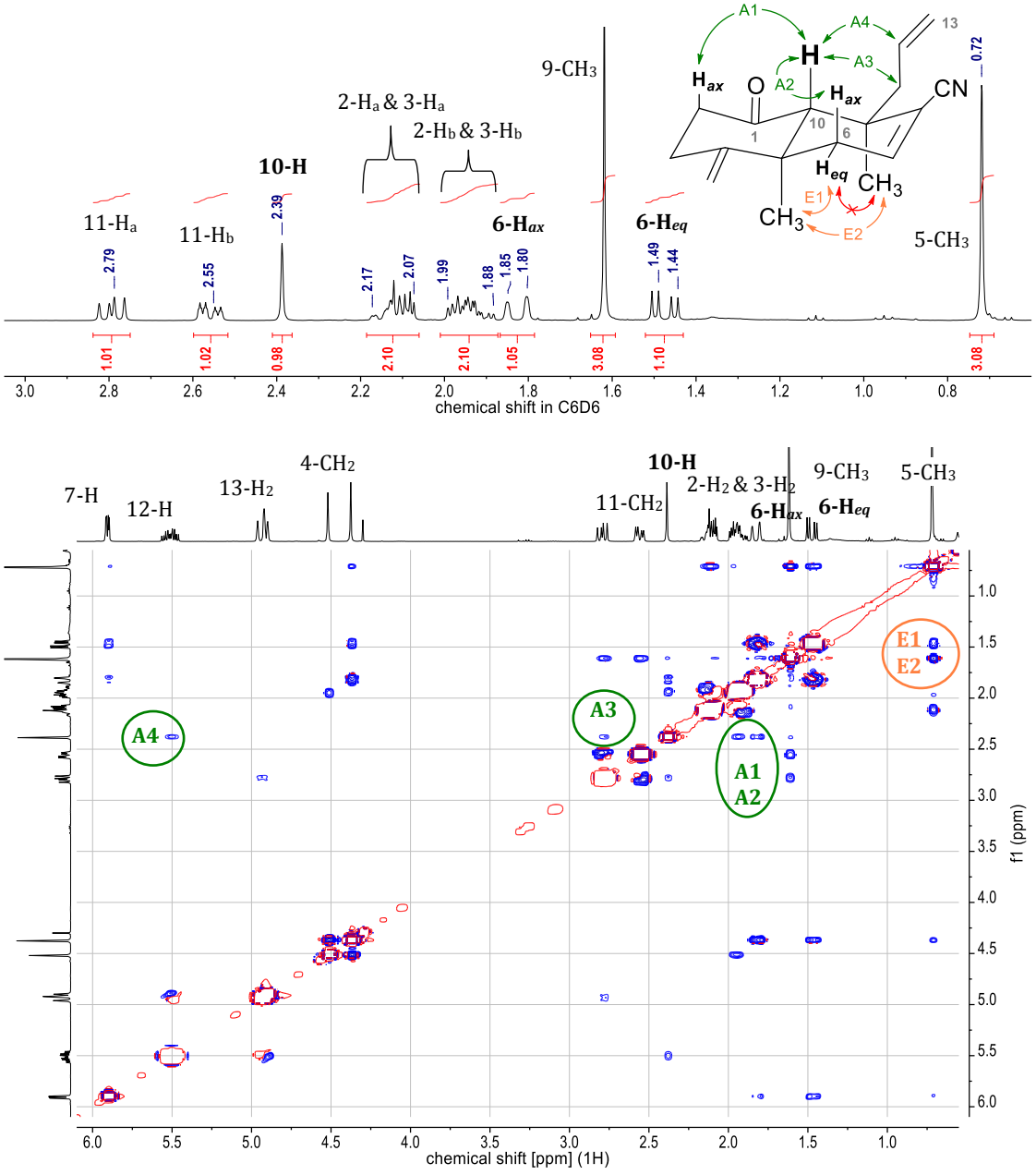

Figure 28. NMR spectra of decalone **109**: **^{1}H** (excerpt) and **NOESY** (both 400 MHz, C_6D_6).

Next, our developed rearrangement/deoxygenation sequence was to be applied to 3-furylated analogs. As broached before, those were expected to be less susceptible to undesired side-reactions promoted by radicals or LEWIS acidic samarium complexes than allyl-substituted compounds, and thus, may allow for a less complicated α-deoxygenation.

2.4.5 Acyloin Rearrangement of Furylated Epoxyazulenes

2.4.5.1 3-Furylation of Aldehyde 39

For the introduction of the 3-furyl moiety, the titanium complex (3-furyl)Ti(O*i*-Pr)$_3$ (**I-67**) was chosen as reagent. Titanium complex **I-67** was prepared according to the procedure reported by GAU *et al*.[114] Whereas they claim to have obtained "pale yellow crystals" without purification, we obtained a dark-brown oily solid. BARRIAULT *et al.* recently reported obtaining a "brown suspension," which they used without purification (*cf.* **Chapter 1.2**).[123] While this indicates that a purification may be omitted, we opted for recrystallization nonetheless. The resulting pale yellow crystals could be stored and employed as needed. With **I-67** in hands, the 3-furylation of aldehyde **39** with a potential *in situ* lactonization to lactone **38** was examined (**Scheme 109**).

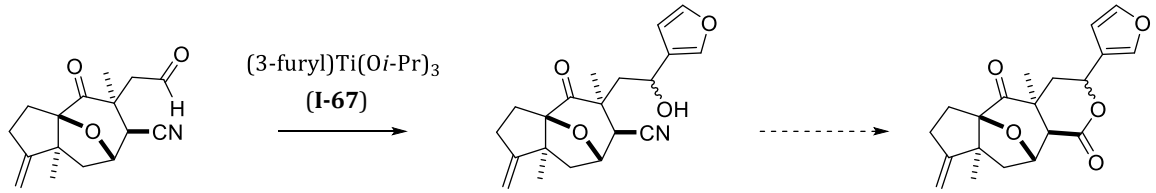

39 **37** **38**

Scheme 109. Preparation of 3-furyl δ-hydroxynitrile **37** and lactone **38**.

The first attempts *seemed* to give an inseparable diastereomeric mixture of 3-furyl δ-hydroxy-nitrile **37** in an unselective manner, complicating NMR analysis. After **37** was employed in various experiments such as silylation, this *apparent lack of diastereoselectivity* was refuted. Some important results are summarized in advance before details are discussed below.

To our surprise, the first silylation of crude **37** with TBSCl gave a total of ***six*** compounds (**Scheme 110** on the next page). Next to a diastereomeric mixture of TBS ether **127**, the 3-furyl hemiketal **37.a** and the desired furyl lactone **38** were obtained. Two of these four diastereomers of **127** resulted from suboptimal work-up, since exposure to alkaline quench media (1 M NaOH) led to an *epimerization of the nitrile group*. The mixture of diastereomers consisted mostly of those exhibiting the desired 2'-(*S**)-configuration (**127**/6-*epi*-**127**/2'-*epi*-**127**/6,2'-*epi*-**127** ≈ **77**:**14**:3:6). With these findings, the overall yield of this two-step sequence could be determined as **80%** (42% of **127** over two steps, 22% of **37.a**, and 16% of **38**), indicating an efficient and diastereoselective 3-furylation of **39** (*d.r.* ≈ 20:1).

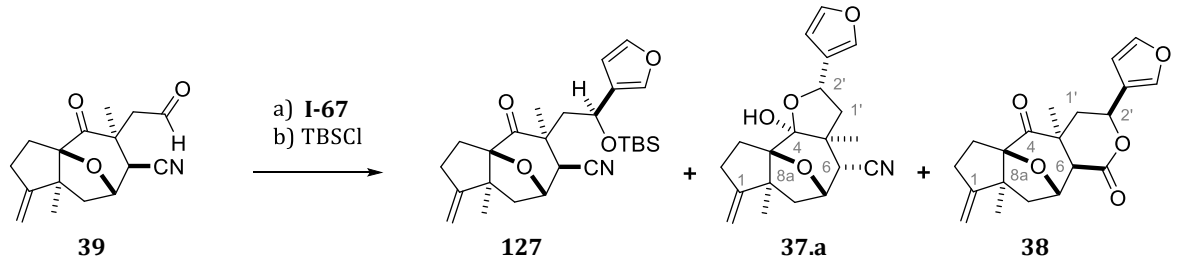

Scheme 110. 3-Furylation/silylation sequence from aldehyde **39** to TBS ether **127**.[21]

Reagents and conditions: **a)** **39** (0.732 mmol), THF (0.05 M), **I-67** (in THF, 1.4 eq, over 3 min), –70 °C, 6 h; ***quench with 1 M NaOH*** *& stirring for 1 h before extraction with* Et_2O; **b)** *crude* **37** ("0.732 mmol"), DMF (0.1 M), imidazole (6 eq), TBSCl (in PhMe, 2.5 eq), rt, 45 h; **42%** of **127** (over two steps, *'d.r.'* ≈ 77:14:3:6), **22%** of **37.a**, and 16% of **38** (total *d.r.* at C2' of **127**, **37.a** & **38** ≈ 20:1).

Subsequent furylation reactions showed that a rapid extraction after quenching the reaction mixture with 1 M NaOH afforded **37** with limited epimerization and without significant formation of **37.a** or **38**. One furylation reaction was exposed to the alkaline quench medium for a prolonged time before extraction (3.5 h), but surprisingly, no significant formation of lactone **38** and a strong preference for hemiketal **37.a** was evident. Using acidic quench media instead (half-sat. NH_4Cl *or* 1 M HCl) obviated epimerization altogether. In all of these furylation reactions, the undesired 2'-epimers were discernible only in traces (*d.r.* ≈ 15:1–30:1).

As expected at this point, the silylation of *non-epimerized* **37** afforded TBS ether **127** quite selectively. Since the previously conducted 3-furylation reactions of aldehyde **39** and subsequent silylation to TBS ether **127** could not be evaluated thoroughly due to incomplete conversion, epimerization, and/or concomitant side-reactions, a final experiment was to conclude this reaction sequence (**Scheme 111**). Due to a premature quench after inadequate reaction control by TLC, aldehyde **39** was not fully converted. Notably, NEt_3 in the eluent *alleviates* smearing of **37** but also *effects* smearing of **39**, complicating an assessment of reaction progress. After work-up with half-sat. NH_4Cl and separating the product by flash chromatography, the mixed fraction containing both **39** and **37** was resubjected to furylation, allowing the reaction solution to warm slightly more rapidly to ensure full conversion. The crude product was then combined with the previously isolated product and silylated with TBSCl. With this sequence, TBS ether **127** was obtained in an excellent yield of **87%** over two steps. Yet, the diastereoselectivity of the furylation was found to be lower than in previous runs (*d.r.* ≈ 10:1). Even though this still accounts for a high diastereoselectivity, it would likely have been better to apply the previous furylation conditions (–70 °C for 6 h), especially since **127** and 2'-*epi*-**127** were not separable by flash chromatography.

[21] The numbering of **37.a** and **38** was chosen to represent the previously used numbering of azulene derivatives. Numbering according to IUPAC or CAS (as generated by CHEMDRAW®) would be unsuitable for comparisons.

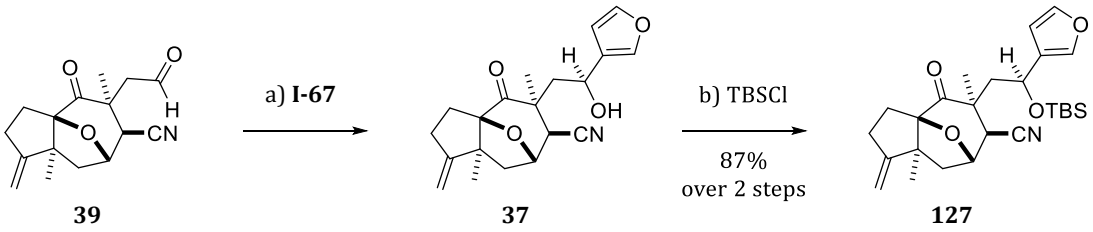

Scheme 111. Selective 3-furylation/silylation sequence from aldehyde **39** to TBS ether **127**.

Reagents and conditions: **a) (i)** **39** (0.681 mmol), THF (0.05 M), **I-67** (in hexane, 1.4 eq, over 10 min), –80 °C, 2 h, –80 °C to –50 °C, 1.25 h, –50 °C to –15 °C, 50 min; ***quench with half-sat. NH_4Cl***, separation of product and mixed fraction. **(ii)** mixed fraction of **39**/**37** (NMR ratio = 2.7:1; "0.300 mmol"), THF (0.05 M), **I-67** (in hexane, 1.4 eq, over 5 min), –80 °C, 1.5 h, –80 °C to –10 °C, 2 h; **b)** *partially crude* **37** ("0.732 mmol"), DMF (0.1 M), imidazole (5 eq), TBSCl (in PhMe, 1.5 eq), 50 °C, 21 h, then additional TBSCl (in PhMe, 0.5 eq), 50 °C, 2 h; **87%** (over 2 steps; *d.r.* ≈ 10:1).

Even with *non-epimerized* 3-furyl δ-hydroxynitrile **37**, a 1:1 ratio of two signal sets was seen in NMR. At elevated temperatures, however, the ratio of these signal sets dramatically changed from 1:1 to 5:1 (**Figure 29**). Upon cooling to room temperature, this ratio reverted to 1:1. These NMR experiments also refute a lack of diastereoselectivity and instead suggest molecular interactions that are disrupted or shifted towards the thermodynamically more stable interaction at elevated temperatures. Such interactions may involve hydrogen bonds between the hydroxy group and the C6 nitrile or the C4 ketone, resulting in conformers distinguishable by NMR and potentially causing the observed smearing on silica gel. While definitive evidence for these hypotheses cannot be provided, two plausible conformers – excluding the potential involvement of retained water traces – are schematically depicted.

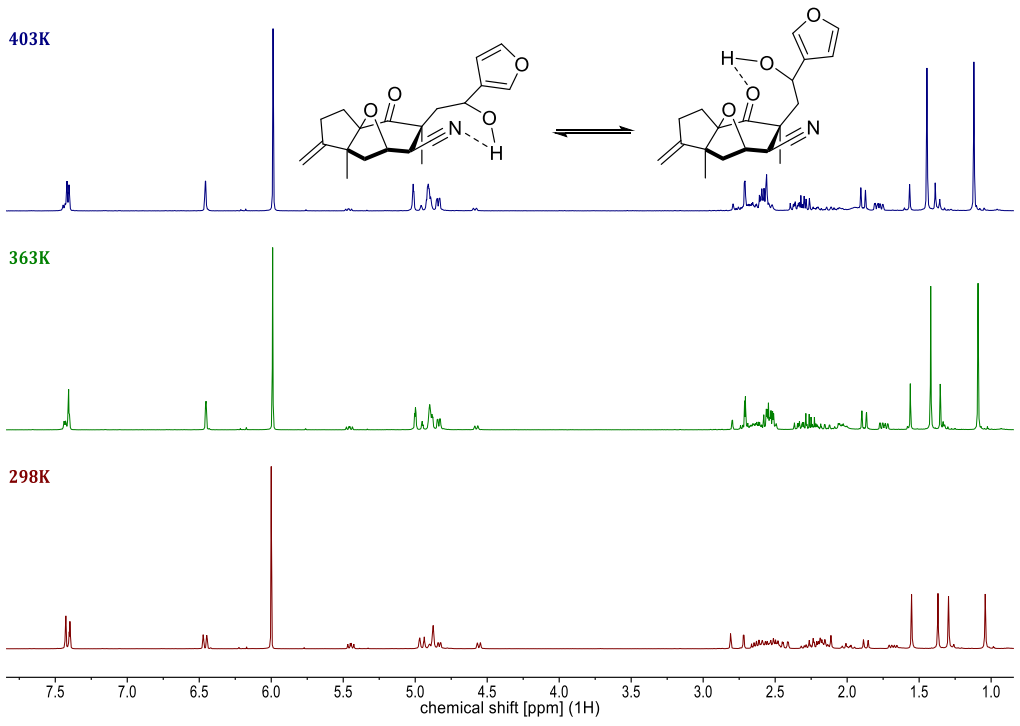

Figure 29. ^{1}H NMR spectra of 3-furyl δ-hydroxynitrile **37** at different temperatures [400 MHz, 1,1,2,2-tetrachloroethane-d_2, 4 Å MS in NMR tube; 298 K (red), 363 K (green), 403 K (blue)].

To corroborate that the furylation resulted in the desired relative stereochemistry, several experiments were pursued. When the main diastereomer of TBS ether **127** was desilylated with TBAF, hemiketal **37.a** was obtained (**Scheme 112**). No formation of lactone **38** was observed either with or without addition of a stochiometric amount of Ti(O*i*-Pr)$_4$, which was presumed to activate the nitrile and thus facilitate lactonization. In the NMR spectra of every probe of hemiketal **37.a** obtained by various reactions, another minor signal set (~5:1) was evident. Yet, 're-silylation' of hemiketal **37.a**, which required high temperatures and long reaction times, gave the epimerized TBS ether 6-*epi*-**127** exclusively and in good yield. While the minor signal set in **37.a** *may* indicate a minor diastereomer, the detection of an open-form isomer of the hemiketal seems more plausible, as also indicated by a small carbonyl peak in ^{13}C NMR.

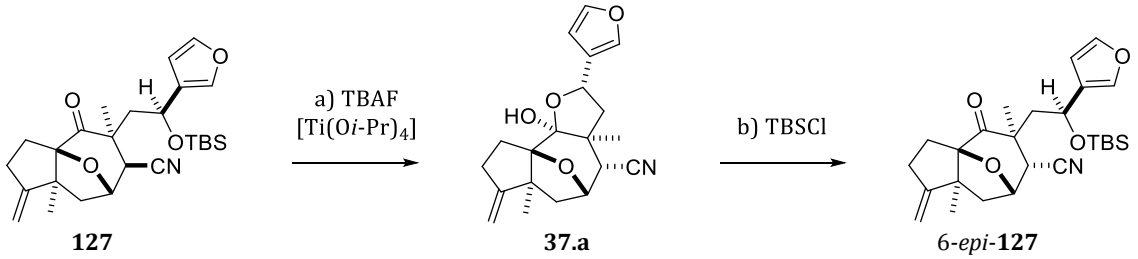

127 **37.a** 6-*epi*-**127**

Scheme 112. Desilylation of **127** to hemiketal **37.a** and re-silylation to 6-*epi*-**127**.

Reagents and conditions: **a) 127**, THF (0.04 M), TBAF (0.2 M in THF, 1 eq), [optionally: Ti(O*i*-Pr)$_4$, (0.2 M in THF, 1 eq)], –78 °C to rt, overnight; *yield not determined*. **b) 37.a** (0.117 mmol), DMF (0.1 M), imidazole (5 eq), TBSCl (in PhMe, 1.5 eq), 70 °C, 35 h, 100 °C, 20 h; **76%** (97% *b.r.s.m.*).

Since attempts at obtaining crystals of **37.a** suitable for X-ray analysis were to no avail, its relative stereochemistry was determined by NOESY (**Figure 30** on the next page). The 2'-(*S**)-configuration is indicated especially by the cross-peak of **2'-H** to the epimerized nitrile α-H (**6-H**). The latter shows a cross-peak to **7-H**. These cross-peaks indicate that those protons all occupy the *exo*-side of the epoxyazulene system. Furthermore, no cross-peaks of these protons to the *endo*-substituted methyl groups **5-CH$_3$** or **8a-CH$_3$** are discernible.

Similarly, the relative stereochemistry of lactone **38** was assigned by NOESY in which correlations between **6-H** and **both methyl groups** can be seen (**Figure 31** on the next page). Only weak cross-peaks between **6-H** and **2'-H** and **7-H** are evident, even though **6-H** and **7-H** 'should' be in spatial proximity. This low intensity results from their relative geometry (**6-H**: *pseudo*-axial; **7-H**: *pseudo*-equatorial). Most importantly, **5-CH$_3$** shows NOE signals with **2'-H** and **6-H**, indicating that these three substituents occupy the *endo*-site of the epoxyazulene system.

Lactone **38** was then crystallized by slow evaporation of a C_6D_6/hexane solution. X-ray analysis confirmed its structure and relative stereochemistry, further corroborating that the 3-furylation of aldehyde **39** furnished the desired 2'-(*S**) diastereomer (**Figure 32** on page **159**).

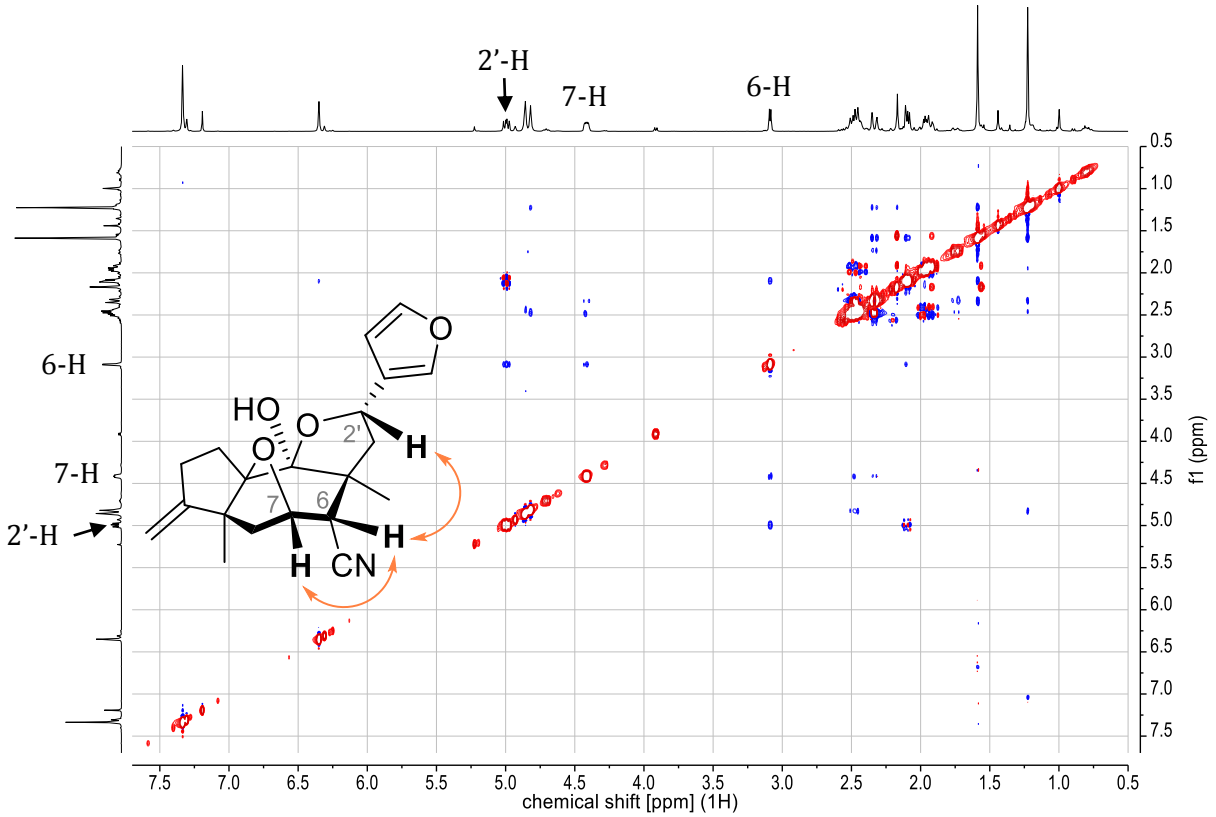

Figure 30. ^{1}H-^{1}H NOESY spectrum (400 MHz, C_6D_6) of hemiketal **37.a**.

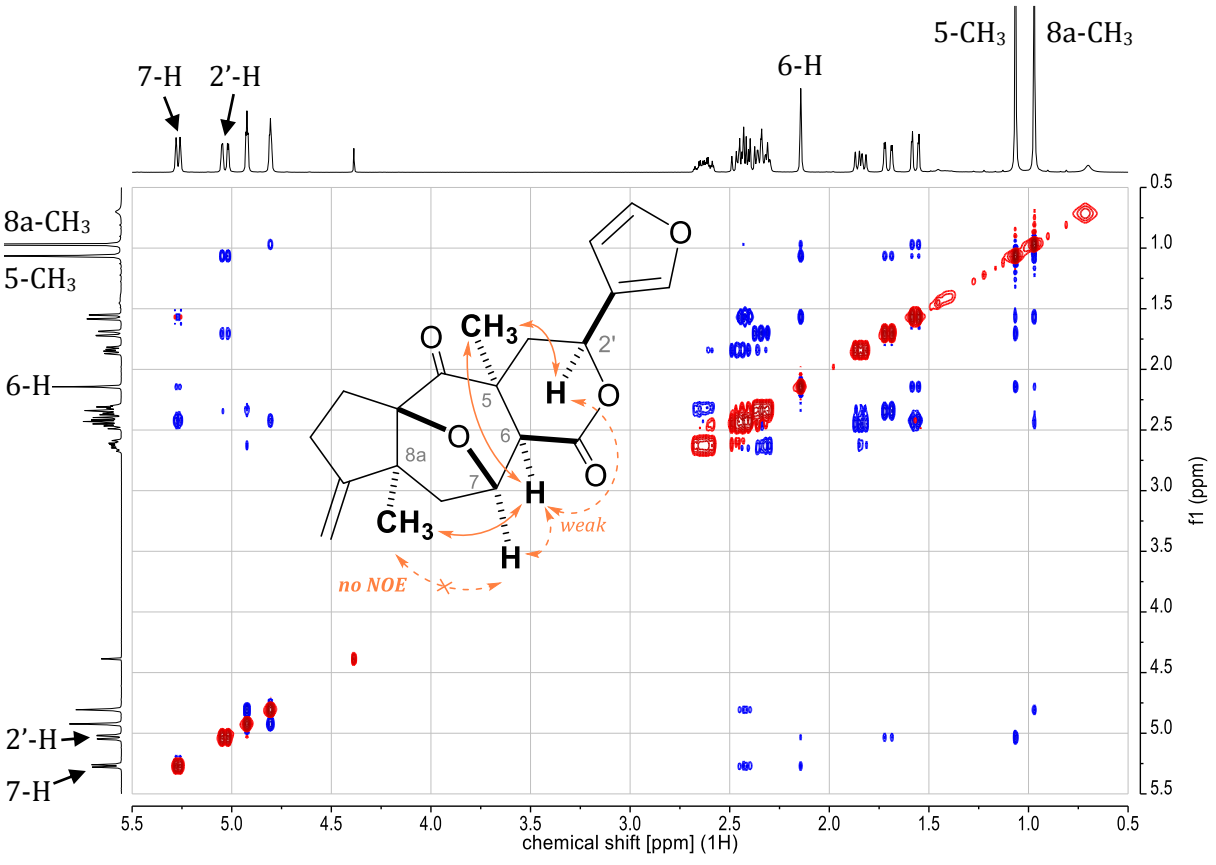

Figure 31. ^{1}H-^{1}H NOESY spectrum (400 MHz, C_6D_6) of lactone **38**.

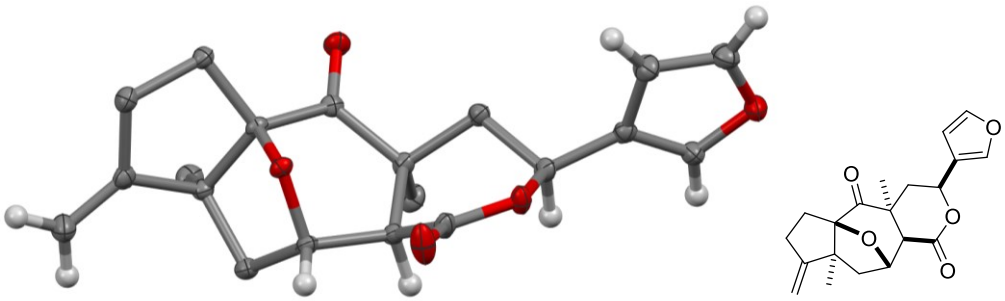

Figure 32. X-ray crystal structure of **38**. Methylene and methyl protons are omitted for clarity.

The influence of C6-epimerization on the structural features of the epoxyazulene core was further examined. Oxidation of *non-epimerized* **37** with DMP gave furyl ketone **128** as the sole product, while that of *partially epimerized* **37** and hemiketal **37.a** gave a mixture of (6-*epi*)-**128** (**Scheme 113**). X-ray analysis of 6-*epi*-**128** made evident the ***spatial proximity*** of 7-H and 6-H in the C6-epimerized epoxyazulene system (**Figure 33**).

In fact, 6-H and 7-H are 'closer to another' in 6-epimerized epoxyazulenes than in their *non*-epimerized analogs, even though the typical structural depiction suggests otherwise. This was, in general, also indicated by strong COSY and NOESY correlations in the 6-epimers, whereas those were weak or missing in *non*-epimerized analogs.

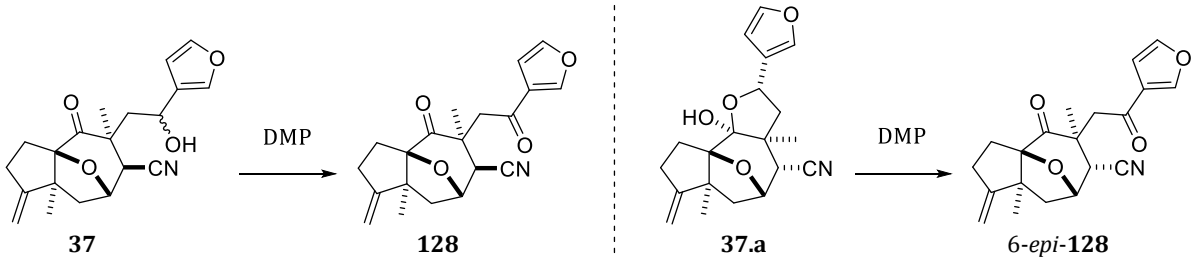

Scheme 113. Oxidation of a mixture of **37** and **37.a** to the ketones (6-*epi*-)**128**.

Reagents and conditions: DCM (0.05 M), DMP (1.2 eq), 0 °C to rt, 2.5 h; **55%** of 6-*epi*-**128** & **12%** of **128** over 2 steps from aldehyde **39** (via mostly epimerized crude **37**/**37.a**).

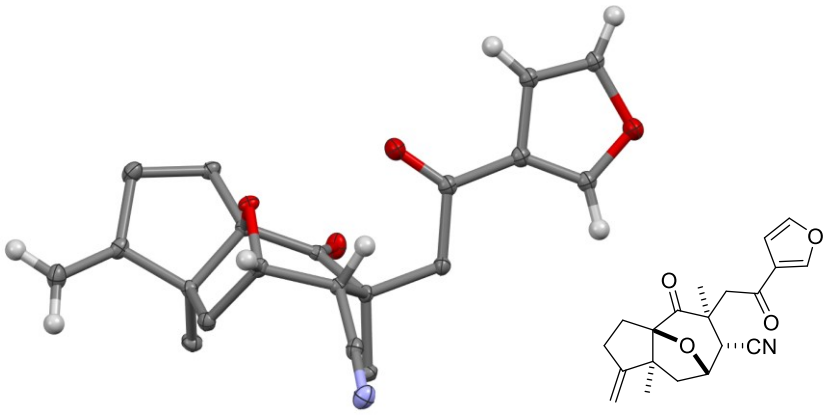

Figure 33. X-ray crystal structure of furyl ketone 6-*epi*-**128**. Disorders in the furyl moiety, as well as methylene and methyl protons are omitted for clarity.

The preparation of furyl lactone **38**, on which our initial plan hinged upon, was pursued by various lactonization attempts. *Luckily*, these attempts were not successful, since lactone **38** behaved undesirably in rearrangement attempts, as discussed in the next chapter. Consequently, these pursuits will only be briefly summarized and are not included in the Experimental Section.

As broached above, pursuits of *in situ* lactonization of 3-furyl δ-hydroxynitrile **37** during the furylation reaction were to no avail. The lactonization was only evident in one of eight runs. The 'most obvious' difference between these runs was using a less meticulously recrystallized batch of the 3-furyl titanium complex **I-67** in the run which afforded lactone **38**. Whereas **I-67** may activate the nitril group and facilitate lactonization via the titanium alkoxide of **37**, *other residual titanium impurities* were suspected to have caused lactonization. In hindsight, a slightly different addition of the NaOH solution to quench the reaction mixture (slightly slower addition at lower temperatures than in other runs) seems to be the more plausible explanation. This may have led to the appearance of some lactone **38** before hemiketalization and epimerization to **37.a**.

Lactonization attempts with 3-furyl δ-hydroxynitrile **37** led to (i) the formation of hemiketal **37.a** (THF or Et_2O solutions & aq. NaOH or LiOH), (ii) no conversion (CF_3COOH in DCE or TMSCl in DCE/MeOH[363]), or (iii) decomposition (MsOH in DCE[364] or $BF_3{\cdot}OEt_2$ in DCM[365]).

Reductions of the ketones (6-*epi*-)**128**, which could potentially yield lactone **38**, were also examined briefly, but resulted in unpromising results. Red-Al in THF led to epimerization to 6-*epi*-**128** with only little reduction. K-Selectride in THF led to a clean, yet rather unselective formation of hemiketal **37.a** and its C2'-epimer. An addition of Ti(*i*-OPr)$_4$ prior to the reduction with K-Selectride did not influence this outcome. Using $NaBH_4$ in MeOH gave a rather complex mixture, indicating unselective reduction of both ketones and C6 epimerization.

Full reduction and epimerization of the ketones and hemiketals gave diol **129** and some of its epimer 2'-*epi*-**129** (**Scheme 114**). An attempted lactonization to lactone **130** (THF/aq. NaOH) led to no conversion even after several days at 50 °C. Addition of a stochiometric amount of Ti(*i*-OPr)$_4$ also had no effect. This corroborated our growing suspicion that a lactonization is not feasible with the epimerized *endo*-nitrile since this would lead to a highly strained tetracyclic ring system. Concluding the lactonization attempts, **129** was silylated with TBSCl at 2'-OH and oxidized at C4 with DMP, which afforded TBS ether 6-*epi*-**127** (*cf.* **Scheme 112** on page **157**).

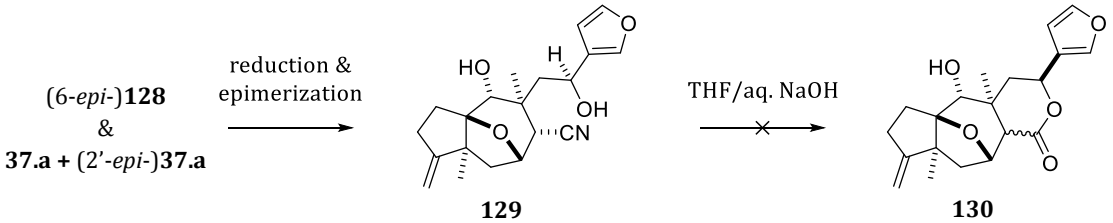

Scheme 114. Lactonization attempt of diol **129** to lactone **130**.

2.4.5.2 Rearrangement of 3-Furylated Substrates

To gain insights into the rearrangement of 3-furylated substrates, the prepared compounds were subjected to the previously established conditions – even if a (clean) rearrangement with these substrates was deemed unlikely (**Scheme 115**). Treating 3-furyl δ-hydroxynitrile **37** with LDA, in order to gauge if a lactonization and/or rearrangement would occur, gave a complex crude product which was not further analyzed. It was assumed that a rearrangement attempt of hemiketal **37.a** could also result in the formation of the rearranged lactone **131**. Yet, hemiketal **37.a** remained unchanged in the presence of LHMDS even after a prolonged time at room temperature. Although the presence of an enolizable ketone was expected to facilitate side-reactions, the sequence was also tried on furyl ketone 6-*epi*-**128**, which resulted in decomposition. While the protection of the ketone group was considered, an attempted ketalization of 6-*epi*-**128** to its dioxolane or dimethyl ketal indicated no conversion.

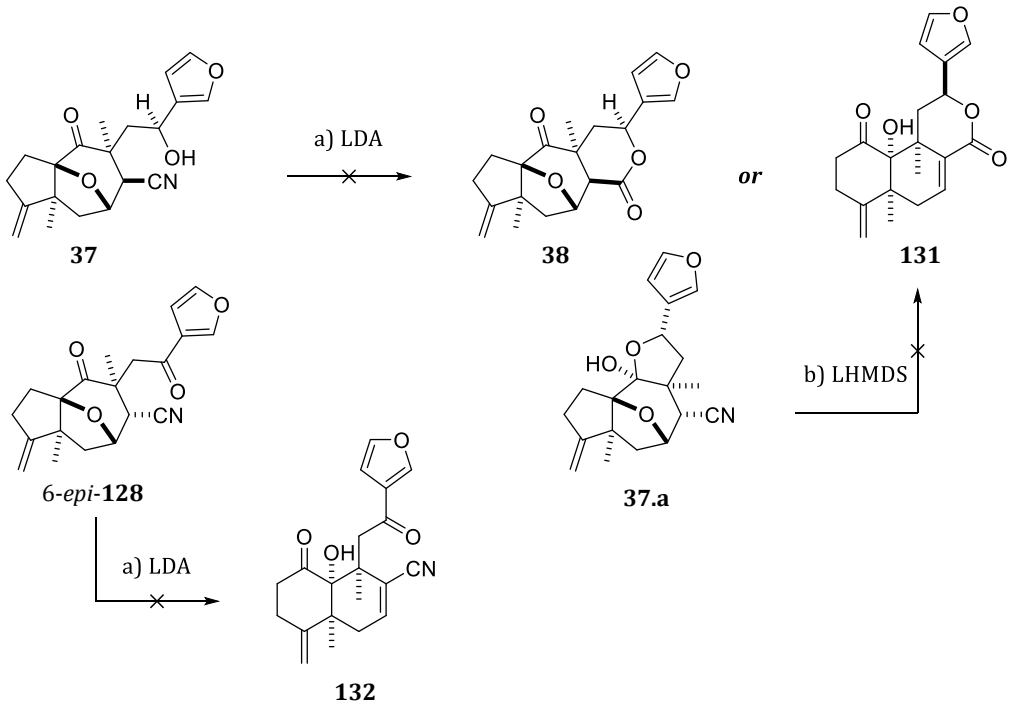

Scheme 115. First rearrangement attempts with 3-furylated substrates.

Reagents and conditions: **a)** with **37**: THF (0.05 M), LDA (2 eq), –95 °C to 0 °C, 2 h, rt, 20 min, then quench with 1 M HCl; **complex mixture**. With 6-*epi*-**128**: THF (0.05 M), LDA (2 eq), –95 °C to –5 °C, 1.5 h, rt, 35 min; **decomposition. b)** THF (0.05 M), LHMDS (2 eq), –95 °C to 0 °C, 2 h 15 min, rt, 3 h; **no conversion**.

As noted in **Chapter 2.4.1**, β-ether cleavage reactions of esters and lactones are more commonly encountered in the literature than those of nitriles. Thus, an ether cleavage/rearrangement sequence of lactone **38** seemed promising. Treating lactone **38** with LDA led to a clean, yet incomplete conversion. However, NMR analysis of the resulting compound indicated no rearrangement, but a *furyl addition to the C4 ketone*. While the formation of polycyclic lactone **133** (**Scheme 116**) seemed highly improbable at first, remaining doubts were dispelled by X-ray analysis (**Figure 34**). Considering its impressive structural complexity, **133** was obtained in a relatively good yield of 50% (73% *b.r.s.m.*). Neither the formation of the desired rearranged lactone **131**, nor C6-epimerization of the lactones **38** or **133** were discernible.

It was presumed that using LHMDS instead of LDA may prevent 2-lithiation of the furyl ring which gave rise to polycyclic lactone **133**. In fact, no formation of **133** was observed when lactone **38** was treated with LHMDS. However, lactone **38** simply remained unchanged in the presence of LHMDS even after a prolonged time at room temperature. These results indicate that achieving the desired rearrangement of lactone **38** to **131** may be rather futile.

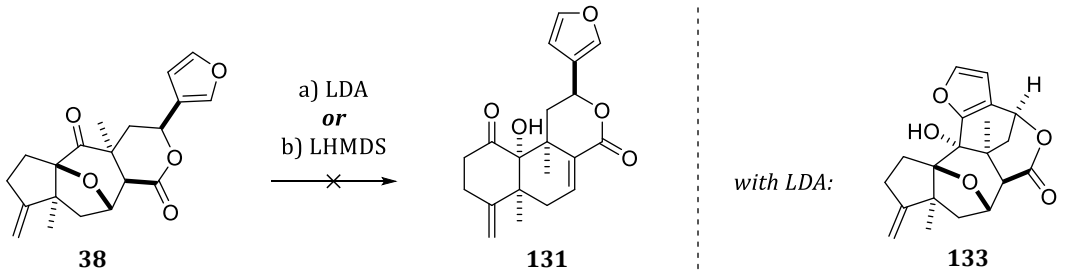

Scheme 116. Base-induced intramolecular 2-furyl addition of furyl lactone **38** to **133**.

Reagents and conditions: **a)** THF (0.05 M), LDA (2 eq), –95 °C to –4 °C, 2 h, rt, 45 min; **50%** of **133** (73% *b.r.s.m.*). **b)** THF (0.05 M), LHMDS (2 eq), –95 °C to –15 °C, 1 h, rt, 3.5 h; **no conversion**.

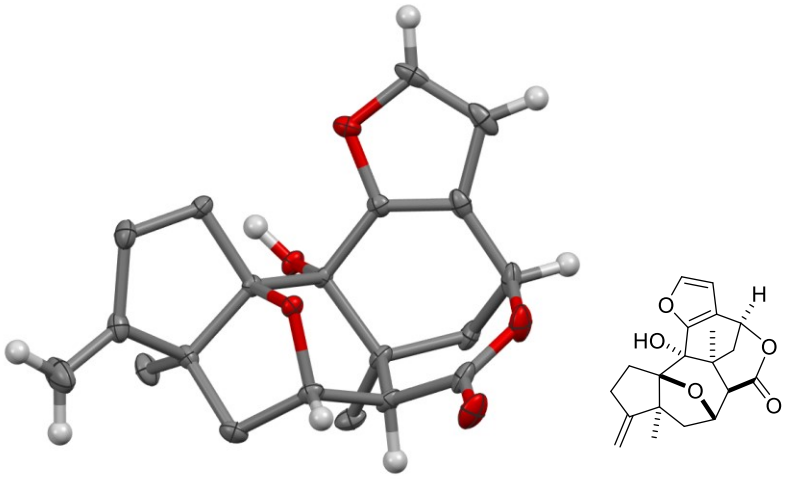

Figure 34. X-ray crystal structure of polycyclic lactone **133**. Methylene and methyl protons are omitted for clarity.

The rearrangement of TBS ether **127** showed more promise (**Scheme 117**). Using either LHMDS or LDA did not lead to 2-furyl addition to the ketone, likely also due to the bulky TBS-group. Initially, the yield and the amount of recoverable substrate seemed disappointing compared to those of the allyl analog **7** [**Chapter 2.4.3**; from **7** to **111**: 67% (92% *b.r.s.m.*)]. Several attempts with **127**, a selection of which is listed in **Table 8** on the next page, were conducted before realizing that the reason for this laid in the *unexpected volatility* of TBS ether **127**.

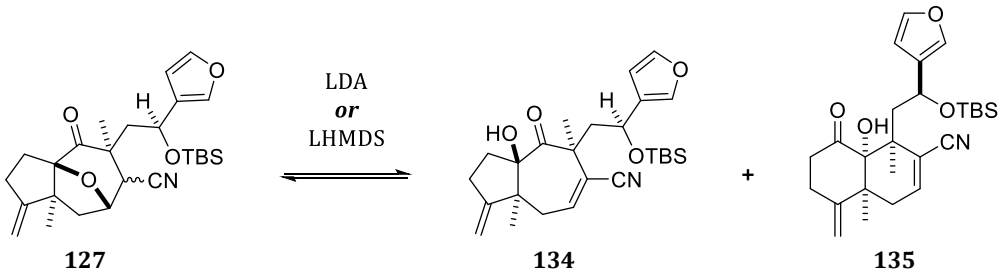

127 **134** **135**

Scheme 117. Rearrangement of TBS ether **127**. See **Table 8** on the next page for details.

Treating TBS ether **127** with LHMDS led to a clean conversion to [5,7]-fused acyloin **134** and [6,6]-fused acyloin **135**. Compared to the allyl analogs (**Table 8**, entry 0), the rearrangement of **134** to **135** was found to be slower (entries 1 & 2). Whereas the (partially 6-epimerized) substrate (6-*epi*-)**127** was still evident on TLC before adding acetic acid, the respective stains were barely visible in the crude product. The volatility of (6-*epi*-)**127** was not considered at that point and the work-up was adjusted to prevent an unlikely, but possible, incompatibility of the TBS group with acetic acid. Instead of adding acetic acid and removing volatiles before and after silica filtration with EtOAc, an aqueous work-up was implemented. Doing so led to a higher but still not satisfactory yield [52% (68% *b.r.s.m.*); entry 3].

An aqueous work-up, as also noted in early attempts with allyl analog **7**, gave rise to yet unidentified side-products which were not discernible with the standard procedure. In another variation, a stochiometric amount of lithium perchlorate was added to examine an influence of an additional LEWIS acid, similarly to the examined addition of aluminum and titanium LEWIS acids in the rearrangement of allyl analog **7**. While doing so seemed to reduce the amounts of side-products, the equilibrium shifted towards the substrates and the overall yield was practically unchanged [44% (68% *b.r.s.m.*); entry 4].

It has to be noted that the volatility of (6-*epi*-)**127** was still not considered, and a direct quantitative comparison between these entries is unviable. Yet, some qualitative insights could be gained from these and some other variations, which are not listed in **Table 8**. To summarize these unlisted variations, the presence of some 'inorganic' lithium compounds seemed beneficial in minimizing side-products formation. Addition of $LiClO_4$ (0.2–1 eq with 2 eq LHMDS) or water (1 eq with 3 eq LHMDS), however, reduced the amounts of side-products noticeably. Also,

complete rearrangement of **134** to **135** occurred faster with the addition of $LiClO_4$ (~10 min instead of ~25 min after removal of the cooling bath). Therefore, it is presumed that trace amounts of inorganic lithium compounds such as $LiClO_4$ or LiOH may play a beneficial role in this rearrangement, likely through influencing complexation at the acyloin group. This effect was not evaluated in more detail but might be interesting to consider in future approaches.

The volatility of TBS ether **127** was confirmed by the considerable weight losses of probes which were either let stand in an open flask or subjected to the 'rotovap protocol' used to remove acetic acid after rearrangement (50 °C, 5 mbar, 2 x 10 min). When an internal standard was present in NMR (TMOB), the ratio of **127**/TMOB decreased after this rotovap protocol. Incidentally, **127** exhibited a surprisingly apolar nature and was readily soluble even in hexane.

The last rearrangement run was conducted on 6-*epi*-**127**. The optimized procedure factored in the volatility – from the inerting of the reaction flask until isolation of the compounds (entry 5, details in Experimental Section). A catalytic amount of $LiClO_4$ (20 mol%) was added. Silica filtration with PE/DE (1:1) instead of EtOAc also removed acetic acid conveniently. The desired [6,6]-fused acyloin **135** was isolated in a *finally satisfactory* overall yield of **62%** (**94% *b.r.s.m.***). Next, the deoxygenation sequence on **135** and the preparation of higher-substituted analogs of TBS ether **127** were examined, the latter of which will be discussed first in the next chapter.

Table 8. Reagents and conditions for the rearrangement of TBS ether **127** (**Scheme 117**). The ratios (**135** in **bold**) were referenced to the internal standard used for qNMR (TMOB). In all but the last experiment (entry 5), a diastereomeric mixture of **127**/2'-*epi*-**127**, varying from ~20:1 to ~10:1, was used. The given yields were determined by qNMR, unless noted otherwise, and corrected to correspond to the amount of **127** in the diastereomeric mixtures.

entry	reagents and conditions	**127** : 6-epi-**127** : **134** : **135** **results and remarks**
0	0.122 mmol of **7**, THF (0.05 M), LHMDS (2 eq), –95 °C to 0 °C, 2 h, rt, 5 min; ***standard work-up***: quench with HOAc (6 eq), removal of volatiles, silica filtration with EtOAc, removal of volatiles	***standard procedure*** with allyl analog: **67% yield** (92% *b.r.s.m.*); removal of volatiles at 50 °C, 5 mbar.
1	0.094 mmol of **127**, THF (0.05 M), LHMDS (2 eq), –95 °C to –5 °C, 2 h, rt, 15 min; *standard work-up*	3 : 3 : 33 : **22** **22% yield** (36% *b.r.s.m.* including **134**)
2	0.092 mmol of **127**, THF (0.05 M), LHMDS (2 eq), –95 °C to –5 °C, 2 h, rt, 1 h; *standard work-up*	0 : 0 : 0 : **40** **40% yield** (no substrates recoverable)
3	0.103 mmol of **127**, THF (0.05 M), LHMDS (2 eq), –95 °C to 0 °C, 2 h, rt, 30 min; ***aqueous work-up***: quench with half-saturated $NaHCO_3$, extraction with diethyl ether	9 : 14 : 0 : **52** **52% yield** (68% *b.r.s.m.*) *small but significant amounts of side-products*
4	0.087 mmol of **127**, THF (0.05 M), **$LiClO_4$** (1 eq), LHMDS (2 eq), –95 °C to –5 °C, 2 h, rt, 30 min; ***aqueous work-up*** as in entry 3	7 : 28 : 0 : **44** **44% yield** (68% *b.r.s.m.*) *less side-products than in entry 3*
3	0.159 mmol of 6-*epi*-**127**, THF (0.05 M), $LiClO_4$ (20 mol%), LHMDS (2 eq), –95 °C to 0 °C, 2 h, rt, 30 min; ***adjusted work-up*** with HOAc (5 eq), silica filtration with PE/DE (1:1), and careful removal of volatiles	qNMR-ratio not determined **62% yield** (94% *b.r.s.m.*; 6-*epi*-**127**/**127** ≈ 4:1) *only traces of side-products*

2.4.5.3 Preparation & Rearrangement of Higher-Substituted 3-Furylated Substrates

Our observations so far indicated that the rearrangement sequence is compatible both with 3-furyl and ester moieties. Thus, the 3-furylation of tricyclic ester-substituted aldehydes was considered for an access to higher-functionalized decalone compounds. Next to the previously prepared ester-substituted aldehyde **5**, its enoate analog **137** was identified as a promising substrate for such routes (**Scheme 118**). Two *previously obtained side-products* were considered as precursors to obtain aldehyde **137**: allylic alcohol **47.a** and diketo dimethylacetal **39.b** (*cf.* **Figures 16** & **20** on page **84** & **89**, respectively).

These devised routes aimed at the synthesis of rearranged 3-furylated acyloins, functionalized at C1 with either an ester (**139**) or an α,β-unsaturated ester (**140**). From these, 2-deacetoxysalvinorin A (**I-52**) should be accessible by sequences involving α-deoxygenation, lactonization and reduction reactions, as outlined before on similar compounds.

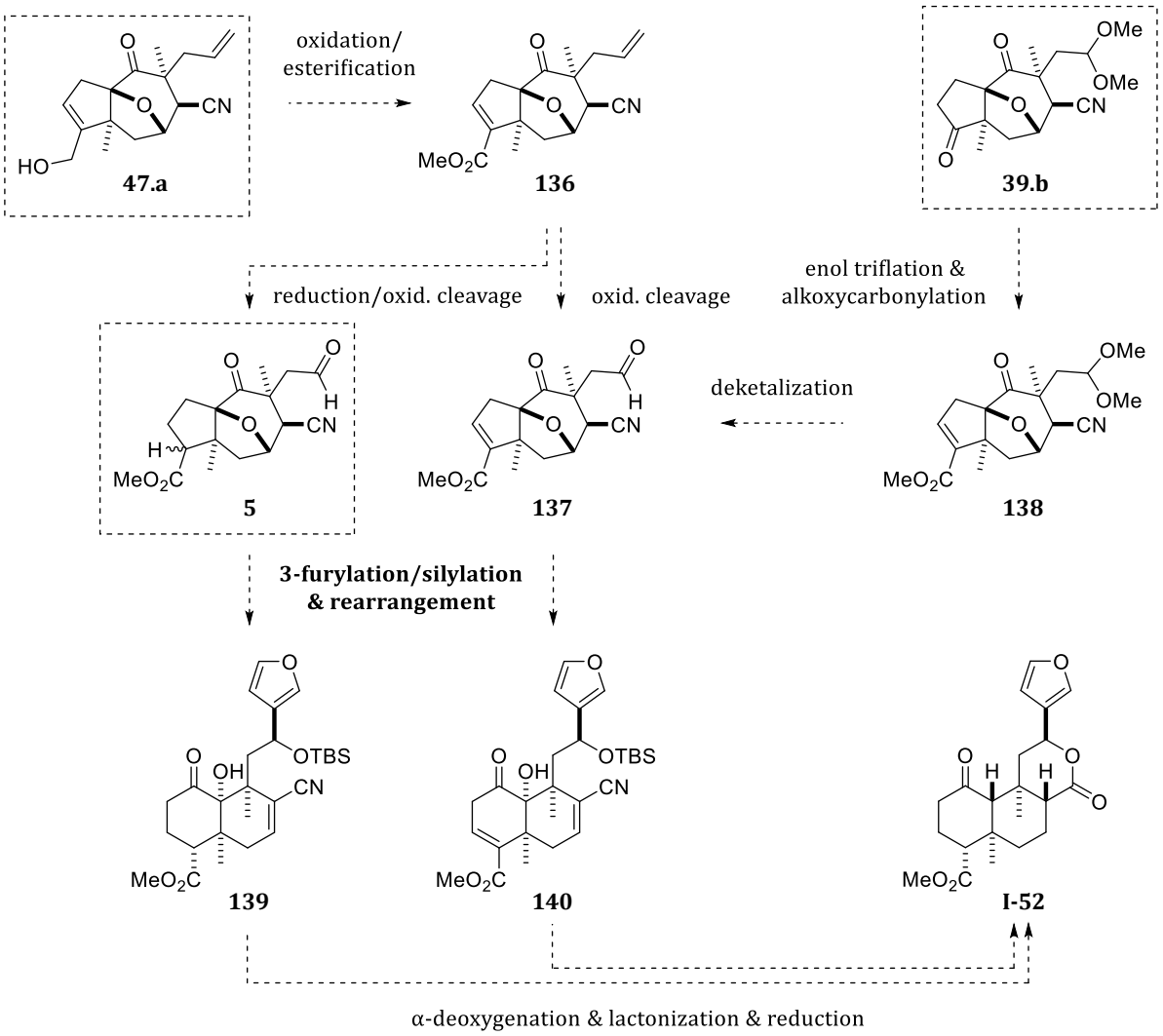

Scheme 118. Potential routes towards 2-deacetoxysalvinorin A (**I-52**). The compounds in dashed boxes were previously prepared (**5**) or obtained as side-products (**47.a** & **39.b**).

As mentioned, allylic alcohol **47.a** was obtained as a side-product within the route to ester **5**. To integrate this side-product into a 'convergent synthesis' of **5**, the allylic alcohol moiety was oxidized through a sequence of DMP and PINNICK oxidations with subsequent esterification, affording α,β-unsaturated ester **136** (**Scheme 119**). The purity of allylic alcohol **47.a** was determined by quantitative NMR beforehand (~55%), allowing for a calculation of an effective yield of 72% over 3 steps (Ø ≈ 90%).

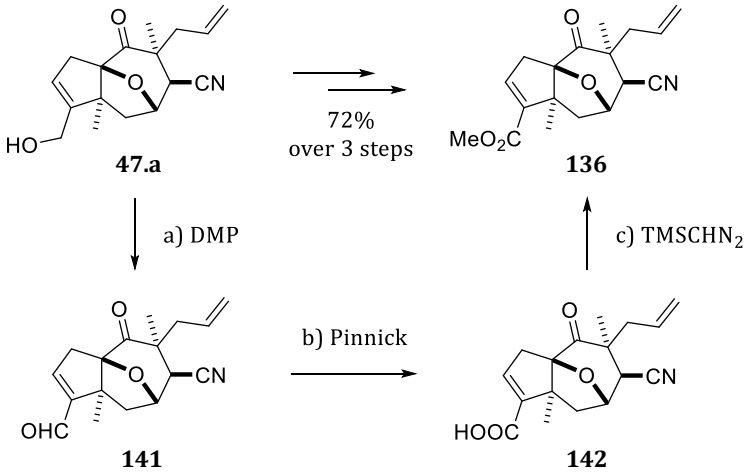

Scheme 119. Double oxidation/esterification sequence from **47.a** to **136**.

Reagents and conditions: **a) 47.a** (*impure*, "1.392 mmol", 1 eq), DCM (0.5 M), DMP (1 eq), 0 °C to rt, 6 h.
b) *crude* **141**, *t*-BuOH/H_2O (5:2, 0.05 M), 2-methyl-2-butene (15 eq), NaH_2PO_4 (1.2 eq), $NaClO_2$ (1.2 eq), rt, 4.5 h.
c) *crude* **142**, toluene/MeOH (3:2, 1 M), $TMSCHN_2$ (2.3 eq), rt, 2 h; **72% over 3 steps**.

To access ester-substituted aldehyde **5** from enoate **136**, the conjugate reduction to ester **6** was briefly examined. Ester **6** was then to be oxidatively cleaved to **5** (**Scheme 120**).

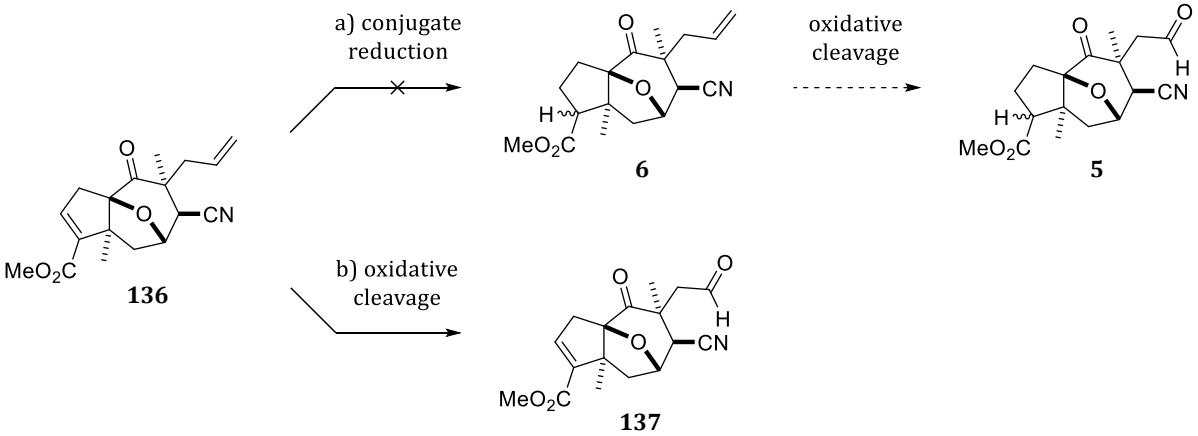

Scheme 120. Routes from enoate **136** to ester-substituted aldehyde **5** or enoate aldehyde **137**.

Reagents and conditions: **a) (i) 136** (0.181 mmol, 1 eq), MeOH (0.05 M), Mg (4 × 2 eq), rt; **complex mixture**. ***or*** **(ii) 136** (0.124 mmol, 1 eq), MeOH (0.05 M), $NiCl_2 \cdot 6H_2O$ (10 mol%), $NaBH_4$ (dissolved in ethanol, in total 2 eq), rt; **reduction of allyl group** (~75% conversion). **b) 136** (0.235 mmol, 1 eq), 1,4-dioxane/H_2O (3:1, 0.05 M), 2,6-lutidine (2 eq), OsO_4 (2 mol%), $NaIO_4$ (4 eq), rt, 21 h; **31%, gradual decomposition** before and after isolation.

An attempted conjugate reduction of enoate **136** with Mg in MeOH resulted in a complex mixture, similar to the attempted α-deoxygenation of allyl-substituted acyloin **111** (*cf.* page **137**). The complexity of the crude product was not significantly lessened when it was oxidized with DMP to reverse a potential concomitant reduction of the ketone moiety. Then, an alternative conjugate reduction with $NaBH_4$/Ni(II) was tested. This method generates nickel boride and can be used for the selective 1,4-reduction of enoates.[366–368] Although TLC analysis showed no apparent conversion, NMR spectra of the crude product revealed a relatively clean conversion (~75%) to a compound in which the enoate, ketone, and nitrile groups remained unchanged. Surprisingly, the allyl group was no longer discernible, despite being the group least expected to be affected by an undesired reduction. As these results indicate potentially challenging selectivity issues, the conjugate reduction of **136** was not pursued further.

Instead, the allyl group of enoate **136** was oxidatively cleaved in a LEMIEUX-JOHNSON oxidation, giving enoate aldehyde **137** in only 31% yield due to substantial decomposition during work-up and upon storage. The stability of aldehyde **137** was further examined when it was prepared by the alternative route proceeding from diketo dimethylacetal **39.b** (**Scheme 121**). After **39.b** was subjected to an enol triflation/carbonylation sequence, a subsequent deacetalization of **138** afforded keto aldehyde **137**. While this route resulted in appreciable yields (Ø = 72–80% per step), some insights were gained which could further improve the yield of **138** and prevent a low yield in the deacetalization to **137**.

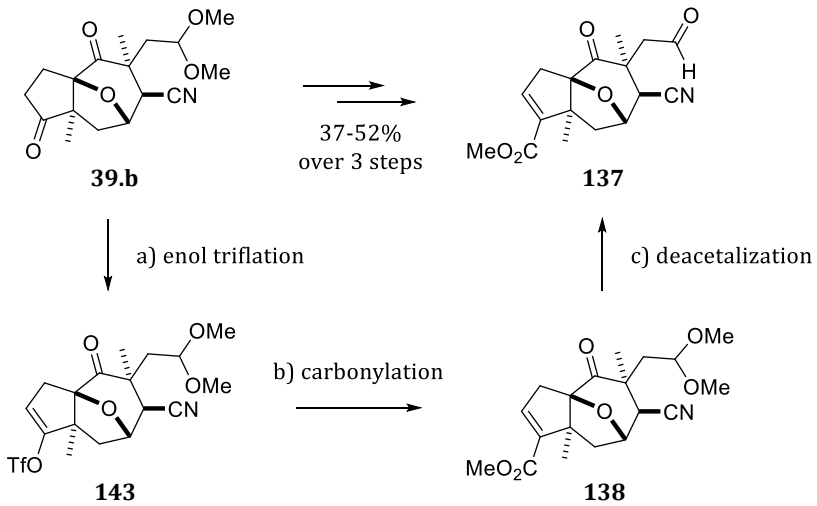

Scheme 121. Preparation of aldehyde **137** via enol triflation/carbonylation sequence.

Reagents and conditions: **a)** THF (0.05 M), KHMDS (1 M in THF, 1.1 eq), –78 °C, 35 min; then Tf_2NPh (1.3 eq), –78 °C to rt, 1 h. **b)** *crude* **143**, DMF/MeOH (1:1, 1 M), CO (balloon, 1 atm), NEt_3 (4 eq), $Pd(PPh_3)_4$ (5 mol%), rt, 17 h; **55%** of **138** & **20%** of unreacted **143**. **c) (i) 138** (0.083 mmol (*run #1*), 0.512 mmol (*run #2*), THF/2 M HCl (1:1, 0.025 M), rt, 2 d; **67%** (*determined by qNMR for run #1* **and** as *isolated yield for run #2*); ***or*** **(ii) 138** (0.028 mmol), wet acetone (~10 vol% water), *p*-TsOH·H_2O (20 mol%), rt, 3 d, 50 °C, 16 h, 70 °C, 11 h; **95%** (*determined by qNMR*).

Methyl enoate **138** was obtained in 55% yield over two steps, along with 20% of unreacted **143**, when *crude* enol triflate **143** was subjected to (alkoxy)carbonylation at room temperature. When *isolated* enol triflate **143** was used in a second carbonylation, the reaction mixture was warmed to 50 °C for a higher conversion. Notably, this led to palladium precipitation (*vide infra*). No enol triflate **143** was recovered – but the yield of methyl enoate **138** remained practically unchanged (58%), strongly suggesting that elevated temperatures were unfavorable in this case.

This valuable method for synthesizing α,β-unsaturated esters was introduced by ORTAR *et al.* in 1985.[369] Later publications by ORTAR *et al.* highlighted that the choice of phosphine ligand can significantly impact yields. Using $Pd(OAc)_2$, the addition of dppf "proved to be essential" in some cases, preventing *palladium precipitation* observed with PPh_3.[370,371] As shown in **Chapter 1.2**, this method was also applied in the total syntheses of salvinorin A by the groups of HAGIWARA, FORSYTH, and BARRIAULT. There, yields of 66–73% were achieved even in double carbonylations to *bis*-methyl enoates. These examples also employed dppf (using $Pd(PPh_3)_4$ at 60 °C for 18–20 h), with HAGIWARA noting that adding dppf "was crucial for the efficient double carbonylation."[106] Unfortunately, these notes were not noticed before our two carbonylation runs. Adhering to these recommendations of adding dppf as an additional phosphine ligand may have resulted in a significantly higher yield of methyl enoate **138**.

The dimethylacetal group of methyl enoate **138** was then hydrolyzed, yielding aldehyde **137**. The aldehyde's *intrinsic* stability was confirmed when prepared via hydrolysis rather than LEMIEUX-JOHNSON oxidation. This supported our assumptions that osmium-based impurities from the latter reaction may catalyze decomposition, even in trace amounts, as discussed in **Chapter 2.2.3**. Similar observations were made with other aldehydes prepared by LEMIEUX-JOHNSON oxidation. Addition of $Na_2S_2O_3$ in the work-up procedure may alleviate decomposition but was not conducted in this experiment. Aldehyde **137**, prepared by LEMIEUX-JOHNSON oxidation *and purified by flash chromatography*, exhibited the distinctive metallic-gray discoloration. The NMR sample was autoxidized to the carboxylic acid, as indicated by the appearance of a new signal in ^{13}C NMR (δ = 175.6 ppm). After three weeks in a sealed NMR tube (C_6D_6), no remaining aldehyde signal was evident in the now complex NMR spectra. In stark contrast, an NMR sample of aldehyde **137** prepared by hydrolysis with *p*-TsOH in wet acetone and *not even purified by flash chromatography* remained completely unchanged.

The intrinsic stability of aldehyde **137** was corroborated by its compatibility with the 'harsh' conditions required for hydrolysis with *p*-TsOH in wet acetone (over 4 days at up to 70 °C). An alternative hydrolysis with 2 M HCl in THF reduced the required temperature and reaction time (2 days at room temperature) and *seemed* better suited. Although no significant differences were visible in TLC or NMR analyses of the crude products from these two methods, qNMR revealed a markedly lower yield for that using HCl (95% with *p*-TsOH vs. 67% with HCl).

Regrettably, this discrepancy was noticed *after* the remainder of **138** had been subjected to a larger-scale hydrolysis with HCl. The isolation of aldehyde **137** from this larger-scale hydrolysis confirmed the moderate yield of 67%. Therefore, hydrolysis with *p*-TsOH in wet acetone, heating to 70 °C to shorten reaction time, seems highly preferable over the hydrolysis with HCl.

For the furylation of aldehyde **137**, reaction conditions similar to those with its simpler analog **39** (*cf.* **Scheme 111** on page **156**) were applied. The conditions were slightly adjusted to ensure full conversion in the furylation of aldehyde **137** and the subsequent silylation of *crude* 3-furyl δ-hydroxynitrile **144** (**Scheme 122**). TBS ether **145** was obtained in an excellent yield of **88**% over two steps, but the furylation proceeded with lower diastereoselectivity (*d.r.* ≈ 5.2:1). Since this sequence was only conducted once, reaction conditions better suited for a higher diastereoselectivity (e.g., prolonged reaction time at –80 or –70 °C) could not be examined. The relative stereochemistry of TBS ether **145** was not determined, but presuming the desired (*S**)-configuration in analogy to its simpler analog **127** seems very reasonable. As with **127**, TBS ether **145** was inseparable from its epimer 2'-*epi*-**145** by flash chromatography.

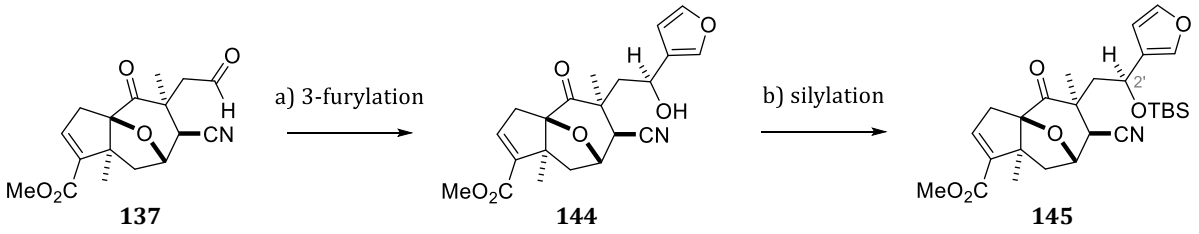

Scheme 122. Preparation of 3-furyl δ-hydroxynitrile **144** and its silylation to **145**.

Reagents and conditions: **a)** THF (0.05 M), **I-67** (in hexane, 1.4 eq), –80 °C, 5 h, –80 to –10 °C, 2 h, –10 °C to rt, 10 min. **b)** DMF (0.1 M), imidazole (5 eq), TBSCl (in PhMe, 2 eq), 50 °C, 20 h; **88% over 2 steps** (*d.r.* ≈ 5.2:1).

When TBS ether **145** was treated with LHMDS, reaction control by TLC showed a similar pattern to the rearrangements of other substrates. However, the TLC spot presumed to correspond to the desired [6,6]-fused acyloin dramatically decreased in intensity with reaction progress. In its place, *two new compounds* emerged. NMR analysis of the rather complex crude product indicated only traces of the desired rearrangement product and was overall not particularly promising. Analytical samples of the two new compounds were isolated by flash chromatography. Instead of affording the desired [6,6]-fused acyloin **140**, treating **145** with LHMDS gave catechol **146** and diene **147** (**Scheme 123** on the next page). This indicates a formation of the rearranged intermediate **140.I**, which then fragmented in a *retro-DIELS–ALDER reaction*, most likely driven by the formation of the aromatic catechol **146** by concomitant keto-enol-tautomerism of the C1 ketone. With **146** and **147** as the 'main products,' the attempted rearrangement to **140** was neither evaluated quantitatively nor pursued further.

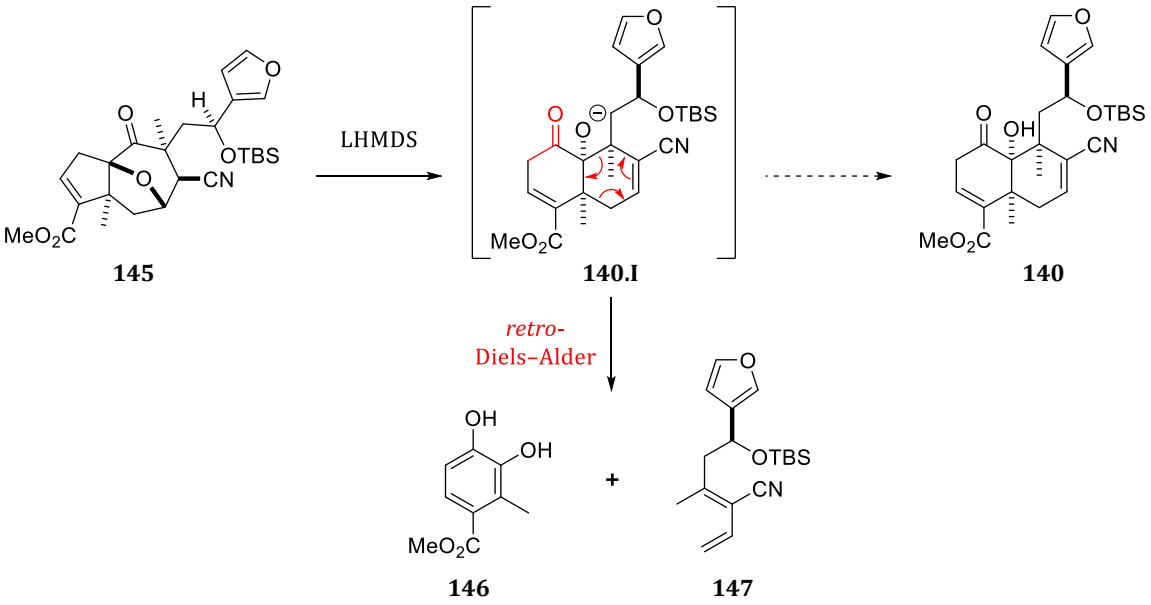

Scheme 123. Attempted rearrangement of **145** with retro-DIELS–ALDER reaction to **146** & **147**.

Reagents and conditions: THF (0.025 M), LHMDS (2 eq), –95 °C to 0 °C, 2 h, rt, 30 min; *not evaluated quantitatively*.

To prevent this retro-DIELS-ALDER reaction, the enoate group of TBS ether **145** was reduced to the methyl ester. Next to a Pd-catalyzed hydrogenation, the use of $NaBH_4/NiCl_2$ and Mg/MeOH was examined (**Scheme 124**). Notably, the latter two methods had failed on enoate **136** due to the presence of the allyl group (*cf.* page **166**). Now, the compatability of the 3-furyl group, *especially* with Mg/MeOH, was to be evaluated for a 'higher purpose,' as elaborated upon below.

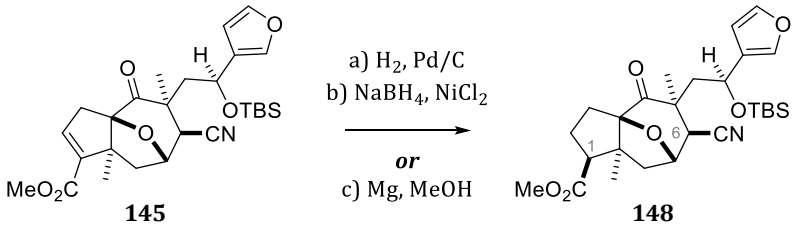

Scheme 124. Conjugate reduction of enoate **145** to methyl ester **148**.

Reagents and conditions: **a) 145** (0.040 mmol, 1 eq), THF/MeOH (3:1, 0.02 M), Pd/C (5 mol% Pd), H_2 (balloon, 1 atm), rt, 24 h; **very low conversion** (<5%). **b) 145** (0.036 mmol, 1 eq), MeOH/THF (2:1, 0.03 M), $NiCl_2 \cdot 6H_2O$ (20 mol%), $NaBH_4$ (dissolved in ethanol, in total 2 eq), rt; **very low conversion** (<5%). **c) 145** (0.126 mmol, 1 eq), MeOH (0.02 M), $HgCl_2$ (20 mol%), Mg (2 × 5 eq, second portion after 2.5 h), –18 °C to –5 °C, 4.5 h, rt, 45 min; **89%**.

Whereas the former two methods led to very low conversion, using magnesium in methanol furnished methyl ester **148**. Although the reaction mixture gave a single spot in TLC, NMR analysis indicated the presence of small amounts of compounds, which are believed to be diastereomers of **148**. The two most prominent diastereomers were present in a ratio of ~7.5:1. This ratio does not have to correspond to **148**/2'-*epi*-**148**, as is also evident from the different ratio of the used substrate (**145**/2'-*epi*-**145** ≈ 10:1). Both a 'not perfectly selective' 1,4-reduction and/or partial epimerization at C1 or C6 might have occurred under these basic conditions. With

the three stereocenters in question (C1, C6, C2'), a sum of $2^3 = 8$ diastereomers could be present. The potential occurrence of C1 (ester) and C6 (nitrile) diastereomers was deemed rather inconsequential. A following rearrangement would remove the nitrile stereocenter and, most likely, lead to an epimerization to the desired ester on the decalone core. Overall, this procedurally convenient conjugate reduction with magnesium in methanol gave **148** in a satisfactory yield of **89%**, while a 1,2-reduction of the C1-ketone was not evident.

The main diastereomer of **148** was partially separated from the other diastereomers (see Experimental Section), facilitating NMR interpretation. The relative stereochemistry of the main diastereomer was assigned by ^{1}H-^{1}H NOESY (**Figure 35**). Apparently, the C1 diastereomer with the 'undesired' relative (*R**)-configuration of the methyl ester was obtained, as indicated by the NOE signal between 1-H and 8a-CH_3. As mentioned above, the formation of this 'wrong' C1 diastereomer should be inconsequential due to epimerization during or after the rearrangement.

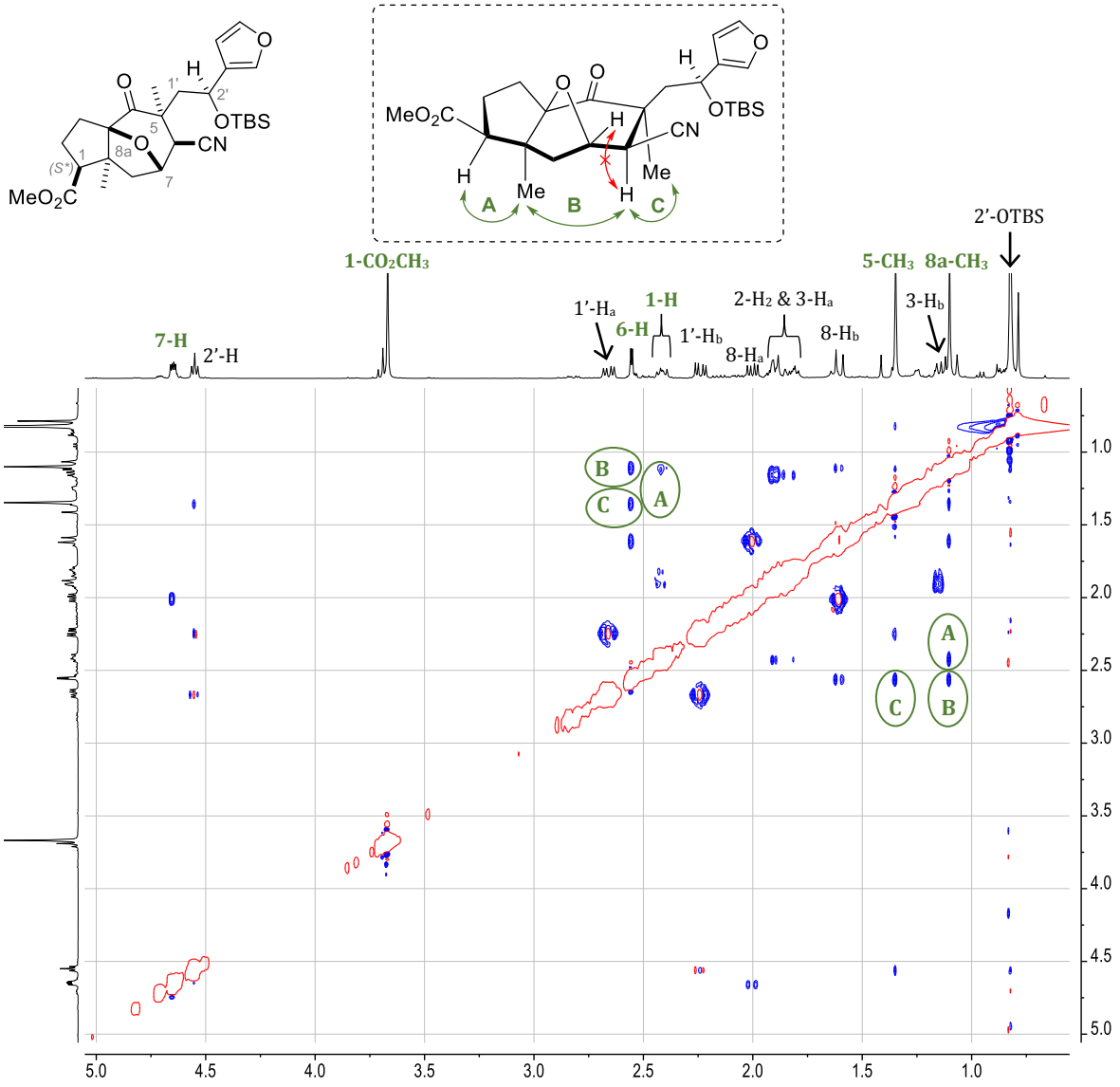

Figure 35. NOESY spectrum (400 MHz, $CDCl_3$; *excerpt*) of **148**. An alternative structural depiction, which represents the 'true structure' more adequately, is shown in the dashed box.

This conjugate reduction was one of the last reactions carried out in our work. Unfortunately, the rearrangement of **148** to acyloin **139** (*cf.* **Scheme 118** on page **165**) could therefore not be examined. In this final phase of the doctoral research project, we also focused on the α-deoxygenation of 3-furylated acyloins, for which the *exo*-methylene analog **135** was employed. The results of these investigations are discussed in the next chapter, before this thesis will be concluded with a summary and an outlook for future directions.

2.4.5.4 α-Deoxygenation of 3-Furylated Acyloins

Subjecting 3-furylated acyloin **135** to the acetylation conditions established on its allyl-substituted analog **111** gave α-ketol acetate **149** in an appreciable yield of **78%** (87% *b.r.s.m.*; **Scheme 125**). Next to some unreacted substrate (7%), enol diacetate **150** (10%) was isolated. Incidentally, such a significant extent of diacetylation was not evident with the allyl analog **111**. Both enol diacetate **150** and α-ketol acetate **149** were very readily and cleanly saponified to **135** when their THF solutions were treated with a 1 M NaOH solution.

A desilylation of the TBS group of enol diacetate **150** with TBAF was attempted to gauge a potential formation of unsaturated lactone **151**. The basic nature of the TBAF desilylation also led to partial saponification, resulting in a complex mixture that apparently included hemiketalization and lactonization products with varying extent of saponification. Thus, we refrained from further investigations into this desilylation (or attempts with less basic desilylation methods) in order to focus on the deoxygenation of α-ketol acetate **149** instead.

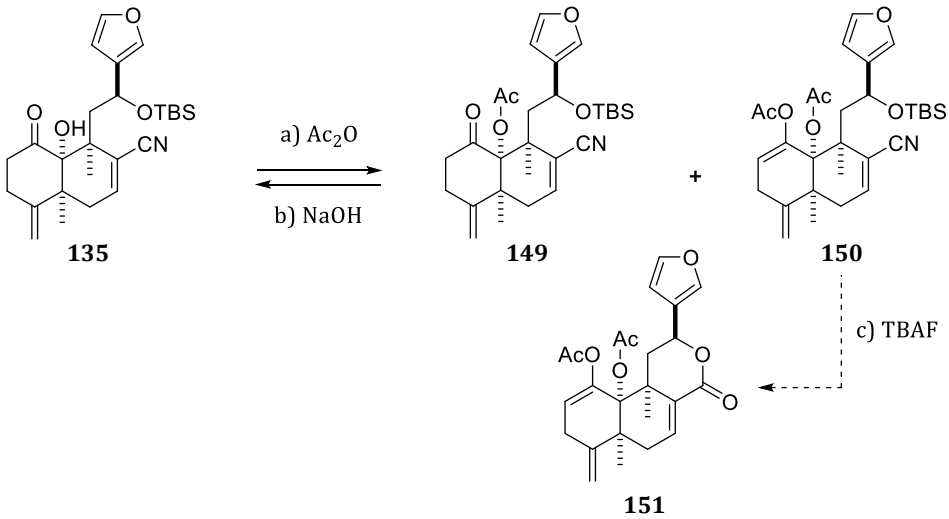

Scheme 125. Acetylation of **135** to α-ketol acetate **149** and enol diacetate **150** with attempted desilylation of **150** to unsaturated lactone **151**.

Reagents and conditions: **a)** THF (0.05 M), NEt_3 (5 eq), DMAP (20 mol%), Ac_2O (10 eq), 50 °C, 13.5 h; **7%** of unreacted **135**, **10%** of enol diacetate **150**, and **78%** of α-ketol acetate **149** (87% *b.r.s.m.*). **b)** THF/1 M NaOH (1:1, 0.014 M), rt, 1.5 h; clean conversion to **135**, *not evaluated quantitatively*. **c)** THF (0.02 M), TBAF (up to 4 eq), rt, 3 d; *mixture of desilylation and saponification products*.

Deoxygenation of α-ketol acetate **149** to the 3-furylated decalone **152** was first attempted with SmI_2 (**Scheme 126**). For this purpose, we resorted to the procedure which proved most promising for the preparation of its allyl analog **109** (from α-ketol acetate **126**; **Chapter 2.4.4**). This SmI_2-induced deoxygenation of α-ketol acetate **149** followed the same pattern as that of its allyl analog **126**, indicating a rapid spot-to-spot reaction of **149** to an *unidentified compound*. After addition of ethylene glycol and a mixture of PE/DE/NEt_3, and filtering the biphasic mixture through silica gel, this *unidentified compound* converted to decalone **152**. Similar to earlier attempts with the allyl analog, however, extensive decomposition followed. NMR analysis of the complex mixture indicated a lack of the typical furan signals and a low yield of decalone **152** (qNMR: ~30%). After isolating an analytical sample of the second most prominent compound (qNMR: ~12%), we were faced with quite the 'brain teaser' due to (i) missing furan signals and the appearance of ^{13}C signals at δ = 171.6 and 168.8 ppm in NMR, and (ii) HRMS indicating a loss of two hydrogen atoms and the presence of an additional oxygen atom relative to decalone **152**.

Eventually, this compound was identified as tetracyclic butenolide **153** in which the furan ring was both oxidized and attacked by the α-C of the C1 ketone (see Experimental Section for further details such as HMBC/NOESY spectra). While we refrain from postulating a definite mechanistical pathway to this intriguing butenolide, its formation supports our previous presumptions of the '*unidentified compounds*' being *samarium-containing intermediates*, which persist through work-up and are prone to decomposition. This decomposition seems to have been partially 'intercepted' by the formation of butenolide **153** in the present case, whereas no distinct compounds from the decomposition of the allyl and dioxolane analogs could be isolated.

Even though this adds some insight into the examined SmI_2-induced α-deoxygenation, it also challenged the expectation that 3-furylated acyloins may be more suited substrates than the allyl and dioxolane analogs. While 'similar' 3-furylated substrates were successfully used in SmI_2-mediated reactions in former syntheses of salvinorin A, those reactions aimed at conjugate reductions of enoates which did not contain a C1 ketone on the decalin core (see **Chapter 1.2**).

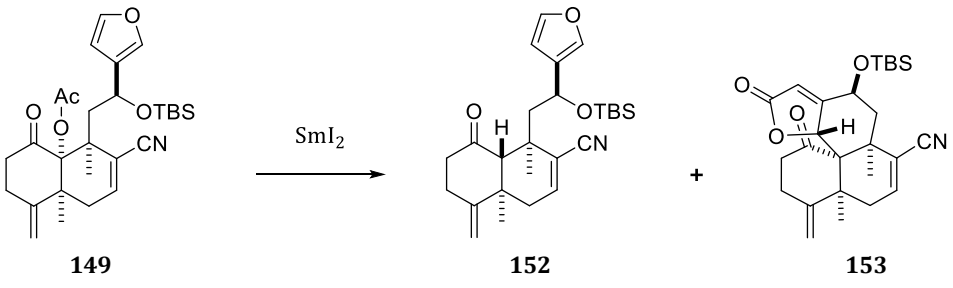

149 **152** **153**

Scheme 126. SmI_2-induced deoxygenation of α-ketol acetate **149** to decalone **152**. Tetracyclic butenolide **153** was isolated as a side product. Details in Experimental Section.

It is possible that a (re-)examination *may* reveal work-up conditions which limit decomposition. The addition of *more* ethylene glycol (or another complexing agent), or reverting to an aqueous work-up, for instance, could facilitate more effective removal of complexed samarium from the presumed intermediate. Yet, deoxygenation of **149** with SmI_2 was not pursued further, since doing so would have required time and substrate – both of which were very limited at this point.

Instead, an alternative method was (re-)investigated in hopes of concluding the deoxygenation with more insight in general and a higher yield of decalone **152** in particular. To this end, α-ketol acetate **149** was treated with **magnesium in methanol**. This *dissolving metal reduction* had been briefly examined on its simpler analogs. Similar to SmI_2, Mg/MeOH enabled a deoxygenation of the dioxolane-substituted acyloin **120.b**, affording some of the respective decalone and diol (*cf.* page **149**). The presence of the allyl group in acyloin **111**, however, led to a complex mixture (*cf.* page **137**). While a complex mixture also resulted from the conjugate reduction of allyl-substituted enoate **136** with Mg/MeOH (*cf.* page **166**), this method proved suitable for substrates not bearing the allyl group – i.e., 3-furylated enoate **145** (*cf.* page **170**).

With these observations, a Mg/MeOH-induced deoxygenation of α-ketol acetate **149** seemed worth investigating – even though, *or rather because*, no precedent for such a reaction was found in the literature. While it was expected that the acetate group might be saponified by the forming magnesium methoxide, it was hoped that the deoxygenation pathway would compete, or better yet, also proceed efficiently from the resulting acyloin **135**, potentially rendering the previous acetylation step redundant. Since deoxygenation had occurred only moderately with dioxolane analog **120.b** (~2.5 mol% $HgCl_2$), a higher amount of mercuric chloride (20 mol%, as with enoate **145**) was employed to achieve more efficient amalgamation, anticipating that this would favor reduction over saponification.

In a first attempt, a methanolic solution of α-ketol acetate **149** and $HgCl_2$ (20 mol%) was treated with Mg (2 × 5 eq). While a saponification of **149** to acyloin **135** was evident, decalone **152** was formed as the main product (**Scheme 127** on the next page). Another prominent compound was identified as diol **154**, as before in the SmI_2-induced deoxygenation of the dioxolane analog . TLC and NMR analysis also indicated the presence of several yet unidentified side-products in 'trace amounts,' which may correspond to compounds formed from *over-reduction* by (i) reduction of the resulting C1 ketone, (ii) conjugate reduction of the vinyl nitrile, or (iii) both, e.g., 1-hydroxy-8-nitrile **155**. Some conditions were screened for a rough qualitative assessment. These conditions, as well as some remarks and results, are listed in **Table 9** on the page after the next. For instance, the first attempt resulted in the formation of decalone **152**, acyloin **135**, and diol **154** in yields of approximately 37%, 25%, and 12%, respectively (*determined by qNMR*, **entry 1.1**). To fully convert the remaining acyloin **135** and gauge, if this would afford more of the

decalone or the diol, the crude product was resubjected to similar conditions (**entry 1.2**), which indicated that the formation of diol **154** was slightly favored. Decalone **152** and diol **154** were isolated in **47%** and **23%** yield, respectively. Practically the same yields resulted from repeating the reduction under slightly different conditions (**152**: 48%, **154**: 20%; **entries 2.1–2.3**). Keeping the reaction below –10 °C led to incomplete conversion even when run overnight.

Using acyloin **135** as the substrate – increasing the amount of magnesium (20 eq instead of 10 eq) and allowing the reaction mixture to warm to ambient temperatures – also furnished decalone **152** and diol **154**, whereas the diol was favored (**152**/**154** ≈ 1:1.65, **entry 3**).

It was investigated whether using a *stochiometric amount of $HgCl_2$ and reducing MeOH content* by using a THF/MeOH-mixture would limit the formation of diol **154** via protonation of (or hydrogen atom transfer to) the intermediates **154.I** and **154.II**. Diol **154** was subjected to such conditions (**entry 4**) to investigate if distinct compounds such as those from a conjugate reduction of the vinyl nitrile would emerge. However, diol **154** remained unchanged and the magnesium, unexpectedly, was not fully consumed overnight. Presumably, the diol (di)anion 'trapped' the mercury in a rather stable complex, also indicated by precipitation, which inhibited both a reduction and the solvolysis of magnesium. Under similar conditions, acyloin **135** showed only little conversion, too (**entry 5.1**). Next to **135**, a formerly unobserved compound was discernible in NMR. With TLC indicating only one spot, isolation of this compound seemed unfeasible and was therefore not attempted. Lowering $HgCl_2$ load and increasing MeOH content again, the crude product was treated with Mg (in part, without cooling) until full conversion of **135** (**entry 5.2**). These forcing conditions gave a rather complex mixture, which was not separated into its components yet.

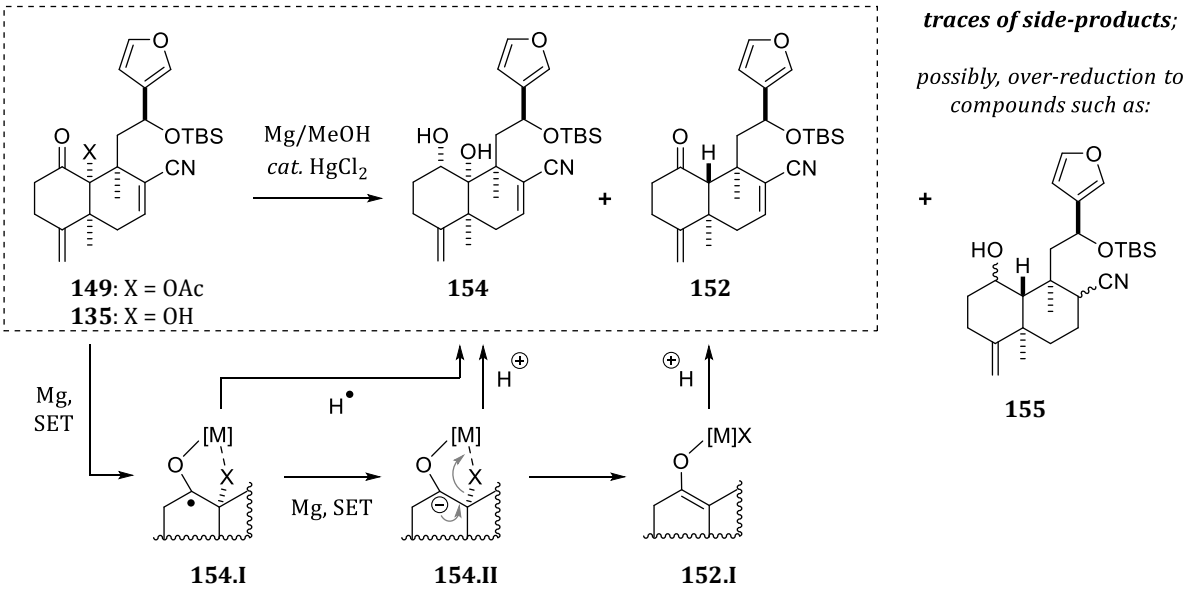

Scheme 127. Mg/MeOH-induced deoxygenation of α-ketol acetate **149** and acyloin **135** with simplified mechanistic considerations. Reagents, conditions, and results in **Table 9**.

Table 9. Attempts at α-deoxygenation of α-ketol acetate **149**, acyloin **135**, and diol **154** with Mg/MeOH. The rather simple procedure is presented in the Experimental Section on the example of **entry 1.1/1.2**. Small amounts of several side-products were observed in all reactions, but no distinct side-product could be identified or isolated.

entry	substrates, reagents, and conditions	results and remarks
1.1	α-ketol acetate **149** (0.060 mmol), MeOH (0.02 M), $HgCl_2$ (20 mol%), –18 °C; Mg (5 eq), –18 °C to –5 °C, 2.5 h, Mg (5 eq), –5 °C to 15 °C, 2.5 h, rt, 20 min.	*crude product analyzed by qNMR*: decalone **152** (37%), diol **154** (12%), acyloin **135** (25%); NMR ratio of **152/154/135** ≈ 1 : 0.35 : 0.69.
1.2	resubjection of crude product from **entry 1.1** ("0.060 mmol"), MeOH (0.02 M), $HgCl_2$ (20 mol%), –18 °C; Mg (5 eq), –18 °C to –5 °C, 2.5 h, Mg (5 eq), –5 °C to 10 °C, 1 h 45 min, rt, 20 min.	NMR ratio of **152/154/135** ≈ 1 : 0.50 : <0.10. ***isolated yields***: **152** (47%) & **154** (23%).
2.1	α-ketol acetate **149** (0.123 mmol), MeOH (0.02 M), $HgCl_2$ (20 mol%), –15 °C; Mg (5 eq), between –18 °C and –10 °C, 2.5 h, Mg (5 eq), between –18 ° and –10 °C, 3 h, rt, 45 min.	temperature maintained with ice/salt cooling bath, slow consumption of Mg at temperatures below –10 °C, some remaining Mg before removal of cooling bath. NMR ratio of **152/154/135** ≈ 1 : 0.45 : 0.45.
2.2	resubjection of crude product from **entry 2.1** ("0.123 mmol"), MeOH (0.02 M), $HgCl_2$ (**30 mol%**), –15 °C; Mg (**10 eq**), between –25 °C and –15 °C, 12.5 h, rt, 20 min.	temperature maintained with cryostat overnight; Mg fully consumed, but acyloin not fully converted. NMR ratio of **152/154/135** ≈ 1 : 0.45 : 0.30.
2.3	resubjection of crude product from **entry 2.2** ("0.123 mmol"), MeOH (0.02 M), $HgCl_2$ (30 mol%), –10 °C; Mg (10 eq), –10 °C to 10 °C, 4 h, rt, 15 min.	practically no remaining Mg or acyloin, when cooled to –10 °C and allowed to warm to rt. NMR ratio of **152/154/135** ≈ 1 : 0.45 : <0.10. ***isolated yields***: **152** (48%) & **154** (20%).
3	acyloin **135** (0.097 mmol), MeOH (0.02 M), $HgCl_2$ (**20 mol%**), –8 °C; Mg (10 eq), –8 °C to 12 °C, 4 h; Mg (10 eq), –1 °C to 10 °C, 3.5 h, rt, 30 min.	incomplete conversion after 1st addition (Mg fully consumed); full conversion after 2nd addition. NMR ratio of **152/154/135** ≈ 1 : 1.65 : <0.10. diol **154** favored over decalone **152**, *not isolated*.
4	diol **154** (0.031 mmol), **THF/MeOH** (10:1, 0.01 M), $HgCl_2$ (**1 eq**), –12 °C; Mg (5 eq), –12 °C to 13 °C, 5 h; Mg (10 eq), 0 °C to rt, 13 h, rt, 30 min.	no conversion of diol **154** in THF/MeOH with **1 eq $HgCl_2$**; *low consumption of Mg despite excess MeOH* (~240 eq).
5.1	acyloin **135** (0.042 mmol), **THF/MeOH** (10:1, MeOH (0.01 M), $HgCl_2$ (**1 eq**), –10 °C; Mg (10 eq), –10 °C to rt, 17 h;	TLC: apparently, no conversion of acyloin **135** in THF/MeOH with **1 eq $HgCl_2$**; Mg fully consumed overnight. NMR: acyloin **135** & a *formerly unobserved compound*.
5.2	resubjection of crude product from **entry 5.1** ("0.042 mmol"), **THF/MeOH** (**5:1**, 0.014 M), $HgCl_2$ (**50 mol%**), –13 °C; Mg (10 eq), –13 °C to rt, 15.5 h; **Mg (10 eq), rt**, 7 h.	*complex mixture* after rather forcing conditions (in total 20 eq Mg, 10 eq added at rt); only small amounts of **152** and **154**; *not isolated*.

The isolation and classification of side-products in the remaining mixtures could not yet be pursued. To facilitate their identification, reducing the complexity of these mixtures by *oxidizing* potentially diastereomeric alcohols (with or without 1,4-reduction of the vinyl nitrile) back to the respective acyloins and ketones could be considered. This may provide critical insights into the examined conditions and their effects on (i) solvolysis of magnesium, (ii) undesired protonation and saponification, and (iii) the desired reduction, potentially allowing for an expedient optimization of this method.

Although conditions for a *selective* deoxygenation of α-ketol acetate **149** or acyloin **135** have not yet been fully established, these 'preliminary' results are promising. With approximately **50% yield** of decalone **152** and **20% yield** of diol **154** from the reduction of α-ketol acetate **149**, using Mg/MeOH proved far superior to – and much more convenient than – using SmI_2.

At this point, our synthetic endeavors in this doctoral research project had to be ceased. Before this work is concluded with a summary and a 'general' outlook in the next chapters, considerations regarding potential synthetic approaches from decalone **152** and possible side-products of this deoxygenation will be provided.

These side-products are of interest not only for a more detailed examination of this promising reduction method but also for potential use in synthetic approaches. While the main 'side-product,' diol **154**, may be oxidized back to acyloin **135** for another reduction, compounds such as the over-reduced 1-hydroxy-8-nitrile **155** could be *equally desirable to* decalone **152**.

Proceeding from **152** or **155**, two converging routes for establishing the salvinorin framework are conceivable (**Scheme 128**). To prevent hemiketalization instead of lactonization, decalone **152** could be reduced to alcohol **156**, which should yield unsaturated lactone **157** after desilylation. While similar unsaturated lactones were subjected to conjugate reduction by SmI_2 in previous syntheses of salvinorin A, Mg/MeOH should also enable a more convenient reduction to lactone **158**. Oxidation of the alcohol with DMP would then furnish lactone **159**, representing deacetoxysalvinorin A with a methylene instead of an ester group at C4. Desilylation of 1-hydroxy-8-nitrile **155** to **158**, however, could open up a 'more direct' route to lactone **159**.

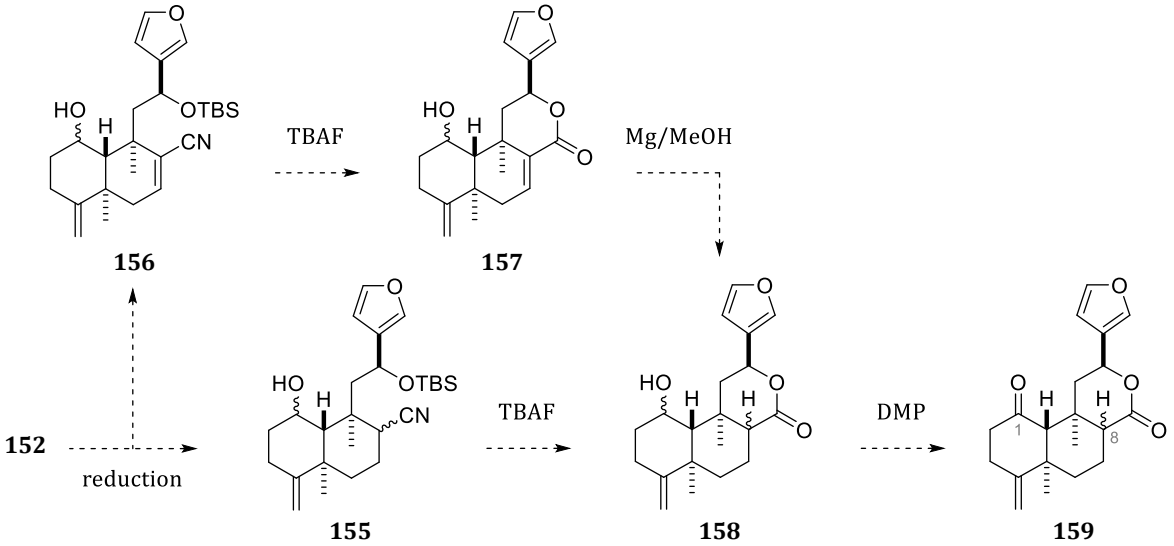

Scheme 128. Considerations for converging routes from **152** or **155** to lactone **159**.

While a selective deoxygenation/reduction cascade to **155** with Mg/MeOH seems *possible* in theory, it would have to be examined whether this is *feasible* in practice. If a *chemoselective* reduction to **155** ensues, *diastereoselectivity* may still pose a caveat, since a total of four (C1,C8)-diastereomers may result.

Ultimately, the presence of 'undesired' diastereomers would be inconsequential, since (i) the stereocenter at C1 would be removed by oxidation to the ketone and (ii) the C8 stereocenter of the salvinorin framework is prone to epimerization, as discussed in **Chapter 1**. However, the presence of diastereomers would certainly complicate an adequate analysis of the desilylation and lactonization to **158**. A selective 1,2-reduction of decalone **152** to, in the best case, one diastereomer of **156** seems more desirable – at least, to establish effective conditions for the desilylation and lactonization. Whereas a lactonization on the tricyclic epoxyazulene core (i.e., of 3-furyl δ-hydroxynitrile **37**) proved difficult, the decalin core is expected to facilitate the desired lactonization. With both the unsaturated and saturated nitriles (**156** and **155**, respectively), the ease of lactonization in relation to the configuration at C8 [sp^2- versus sp^3-hybridized with (*pseudo*-)equatorial or (*pseudo*-)axial nitrile] could be examined.

With our rather limited results from the deoxygenation of α-ketol acetate **149** and acyloin **135**, the *selective* preparation of decalone **152** seems more feasible than that of **155**. In addition to optimizing the conditions for **149** or **135**, employing other 'activated' acyloin derivatives, such as silyl ether analogs of **149** (e.g., OTMS instead of OAc), may be worth examining.

CHAPTER 3: SUMMARY AND OUTLOOK

3.1 SYNTHETIC ROUTE TO TRICYCLIC ENONE 9

The first key intermediate in our work, tricyclic enone **9**, was prepared by a six-step sequence in a good overall yield of 35% (**Scheme 129**). Starting with a carbocupration of alkenyne **21**, dienyl alcohol **19** was obtained in an exceptionally high yield of 95%, for which the grain size of CuBr·DMS and the hydrolysis method proved crucial. SWERN oxidation of **19** gave aldehyde **17**, which was then furylated to furfuryl alcohol **14**. By a subsequent one-pot ACHMATOWICZ reaction/acetylation sequence, pyranulose acetate **12** was obtained in much higher yield than from separately conducted reactions (78% vs. 22–49% over 2 steps). The tricyclic epoxyazulene core was then installed by subjecting **12** to an intramolecular (5+2) cycloaddition, which afforded tricyclic enone **9** in an appreciable yield of 74%.

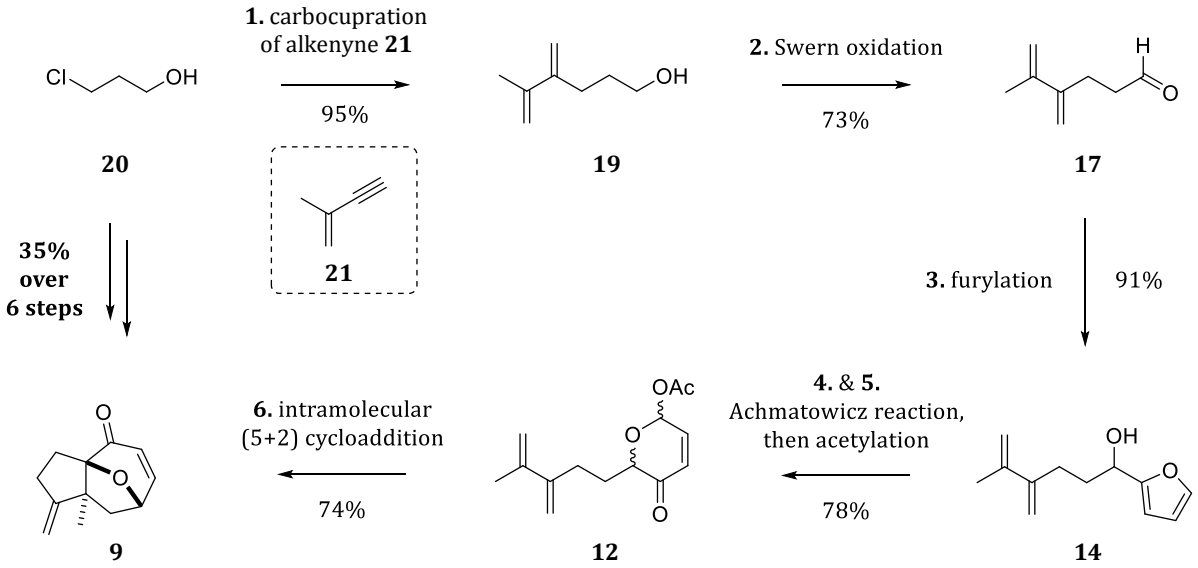

Scheme 129. Synthesis of tricyclic enone **9** starting with the carbocupration of alkenyne **21**.

3.2 FUNCTIONALIZATION OF THE EPOXYAZULENE CORE

Proceeding from tricyclic enone **9**, several higher-functionalized epoxyazulenes were prepared, both with and without a nitrile group on C6. First, tricyclic enone **9** was converted to either ketonitrile **8** or its decyano analog, ketone **8-H**, in high to quantitative yields (**Scheme 130** on the next page). Ketonitrile **8** was obtained by a two-step sequence (via 1,4-cyanosilylation to silyl enol ether **33** and desilylation) or by a direct 1,4-hydrocyanation using KCN/NH_4Cl.

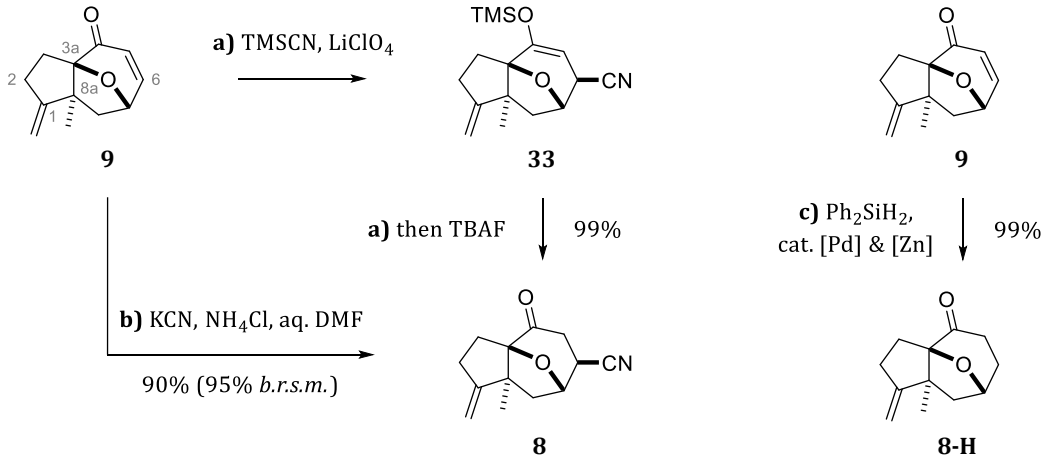

Scheme 130. 1,4-Hydrocyanation and 1,4-reduction of tricyclic enone **9**.

While initial C5-functionalization attempts with ketonitrile **8** or silyl enol ether **33** revealed a preference for undesired double alkylations and *O*-selective acylations, a sequence commencing with a *C*-selective acylation using APF (**41.a**) proved suitable for our purposes (**Scheme 131**). Subsequent methylation and TSUJI-TROST allylation afforded the desired 5-allyl-5-methyl-substituted ketonitrile **7** and ketone **7-H** in yields of 59% and 67% over 3 steps, respectively. For a high yield in the initial acylation of ketonitrile **8**, an adequate formation of the enolate and a proper work-up method had to be ensured. Notably, phosphorus-based impurities *extracted by ethyl acetate* promoted decomposition of allyl β-ketoester **42**. Such a decomposition was observed neither after extractions with other solvents, nor with its decyano analog **42-H**. Similarly, methylation of **42** led to some *O*-methylation, which was also not observed for **42-H**.

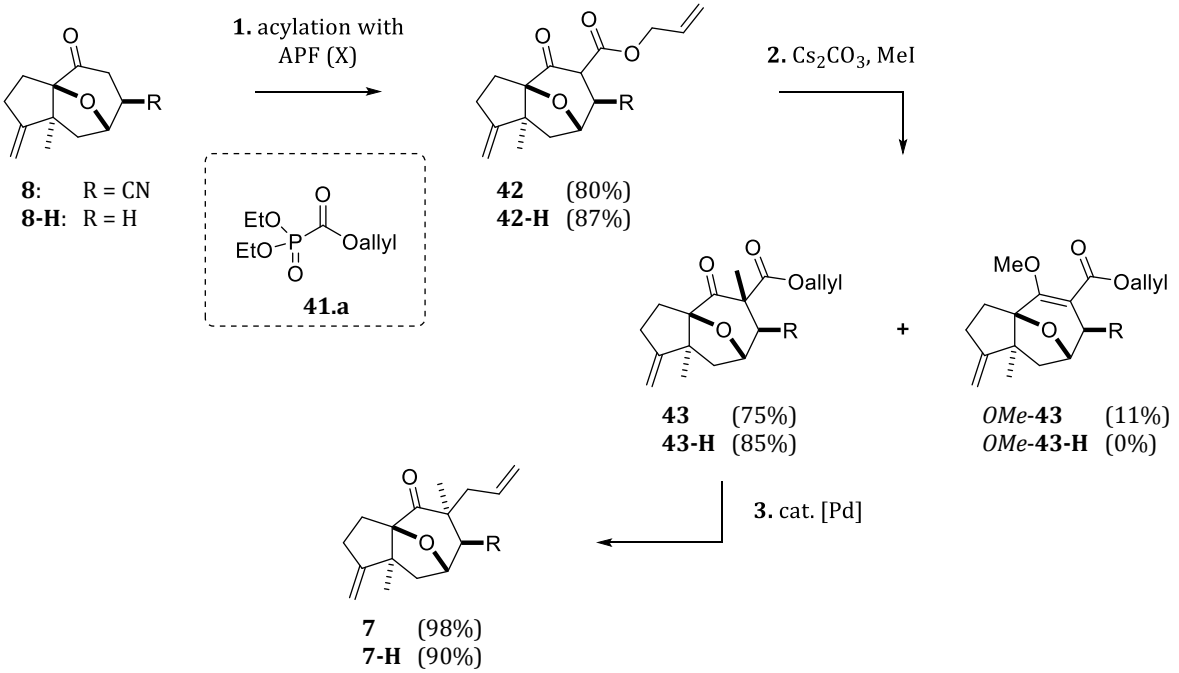

Scheme 131. Preparation of 5-allyl-5-methyl-substituted ketonitrile **7** and ketone **7-H**.

To examine the functional group tolerance of the pending rearrangement, the *exo*-methylidene at C1 was transformed to a methyl ester. Several methyl esters were obtained through a sequence of epoxidation, MEINWALD rearrangement, PINNICK oxidation, and esterification. Next to the 4-ketones **7** and **7**-H, secondary and tertiary 4-alcohol analogs were used as substrates in this sequence. The preparation of these alcohol substrates is summarized in the next chapter. Some methyl esters were then oxidatively cleaved at the allyl moiety by LEMIEUX-JOHNSON oxidation, giving aldehydes which were to be 3-furylated. The preparation of the methyl esters and the LEMIEUX-JOHNSON oxidation are summarized in **Scheme 132**.

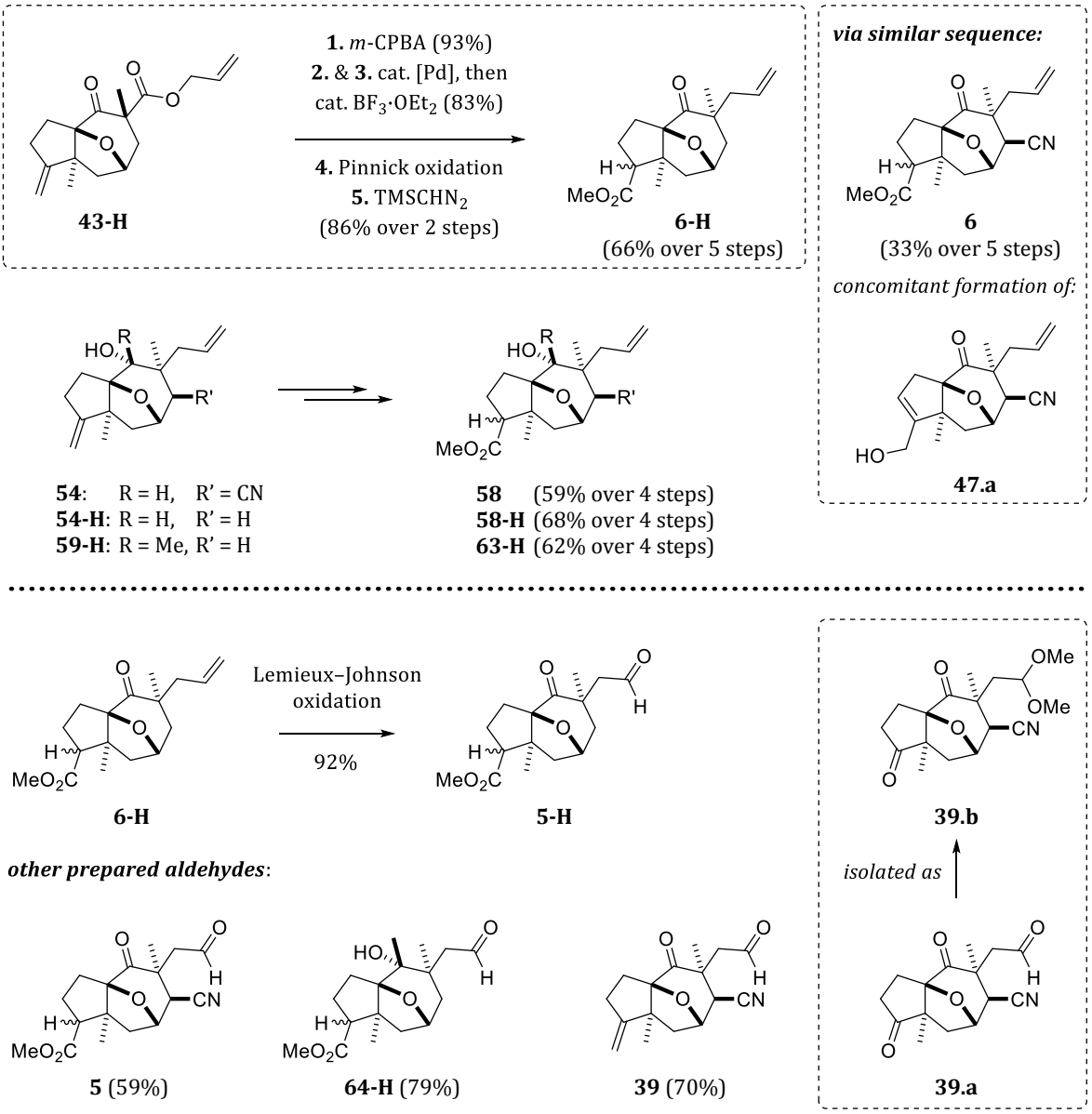

Scheme 132. Methyl ester preparation and LEMIEUX-JOHNSON oxidation.

The preparation of the methyl esters typically resulted in high yields, as exemplified by the synthesis of methyl ester **6-H**. While epoxidation of 5-allyl-5-methyl-substituted 4-ketone **7-H** led to only moderate yields, that of allyl β-ketoester **43-H** proceeded smoothly. After a one-pot TSUJI-TROST allylation/MEINWALD rearrangement sequence with subsequent PINNICK oxidation and esterification, methyl ester **6-H** was obtained in 66% over 5 steps. A similar preparation of the cyano analog **6** from **43**, however, proceeded with a lower yield of 33% over 5 steps. In this case, the MEINWALD rearrangement was accompanied by the formation of allylic alcohol **47.a**. Unfortunately, the preparation of **6** was only conducted once, and thus, this issue could not be addressed. In contrast to these 4-keto substrates, the initial epoxidation of the *secondary* and *tertiary* 4-hydroxyl substrates **54/54-H** and **59-H** posed no problem, and the respective methyl esters (**58/58-H** and **63-H**) were obtained in yields of 59–68% over 4 steps.

Overall, the methyl esters were prepared in a high average yield of ~90% per step. Even in the less efficient example of **6**, the average yield still amounts to 80% per step. The initial epoxidation gave diastereomeric mixtures and represents an exception from the *exo*-selective functionalizations at C6, C5, and C4. Yet, the lack in diastereoselectivity was deemed inconsequential since the undesired isomers should be epimerizable before, during, or after the rearrangement to decalones. It was observed that secondary and especially tertiary 4-alcohols led to a stronger preference for one diastereomer over the other when compared to 4-ketones (up to ~9:1 instead of ~1:1). Presumably, this is a result from 'long-range' structural changes across the fused ring system of the epoxyazulene core induced by the different nature of C4.

LEMIEUX-JOHNSON oxidation of **6-H** gave aldehyde **5-H** in an excellent yield of 92%. For other substrates, this oxidative cleavage resulted in incomplete reactions, which were only conducted once (for **5**) or twice (for **64-H**), and thus not optimized. With *bis*-alkene **7**, the desired aldehyde **39** was obtained in 70% yield in several runs. Next to incomplete cleavage of the hydroxylated intermediates, the concomitant oxidation of the *exo*-methylidene moiety was evident. This overoxidation gave *tris*-carbonyl **39.a**, which was isolated as its diketo dimethylacetal **39.b**. Notably, first attempts at obtaining **39** without addition of 2,6-lutidine led to decomposition. In general, aldehydes prepared by LEMIEUX-JOHNSON oxidation were also more or less prone to partial decomposition when suboptimal work-up methods were employed. Such decompositions are presumed to be promoted by residual osmium-based impurities, as was also indicated by later observations on aldehyde **137** (*cf.* **Chapter 2.4.5.3**).

3.3 LEWIS ACID-INDUCED REARRANGEMENT TO THE DECALONE CORE

While the LEWIS acid-induced rearrangement of epoxyazulenes is summarized in more detail in **Chapter 2.3.6**, some crucial aspects will be condensed in the following. This rearrangement type was examined in numerous variations with different substrates bearing secondary or tertiary alcohol and ketone moieties at C4. As observed at C6 and C5 before, functionalizations at C4 proceeded *exo*-selectively. Consequently, only the undesired secondary *endo*-alcohols were obtained, which – even as their activated ester derivatives – did not undergo inversion to their *exo*-epimers or rearrangement. In contrast to *secondary endo*-alcohols, *tertiary endo*-alcohols and ketones could be rearranged to decaline-based products in *proof-of-principle* attempts. In successful rearrangements, 5-allylated substrates led to an undesired concomitant halo-PRINS cyclization. Most importantly, the presence of a nitrile in either the substrate or solvent completely obviated a potential rearrangement of otherwise suitable substrates. Notable findings from our investigations are briefly summarized in **Scheme 133** on the next page. In this overview, higher-functionalized compounds such as those bearing methyl esters at C1 are omitted, since their compatibility with this rearrangement could not be conclusively assessed due to the aforementioned issues or unsuitable reaction conditions. Generally, the preparation and the rearrangement of the substrates were not optimized or evaluated thoroughly. Instead, the focus was laid on gaining qualitative insights to identify suitable substrates.

The alcohol substrates were prepared by either reduction or methylation at C4. Reductions afforded the secondary *endo*-alcohols **74/74-H** and **54/54-H** in good to quantitative yields with no formation of the *exo*-isomers being evident. Methylations at C4 gave, for instance, tertiary *endo*-alcohol **59-H** in an excellent yield of 89% (98% *b.r.s.m.*).

Attempted rearrangements of various ***secondary*** *endo*-alcohols and their activated derivatives resulted mostly in *exo*-methylidene isomerization and decomposition. Treating **74** with Tf_2O and pyridine induced a shift to the [4,7]-bridged epoxyazulene **83** via elimination with involvement of the ether bridge. Rearrangement attempts with $Sc(OTf)_3$ in Ac_2O/AcOH resulted in an FRIEDEL-CRAFTS acylation, as exemplified by the C2-acylation products **102-H** and **104-H**.

Tertiary *endo*-alcohol **72-H** could be rearranged to hydroxy decalone **84-H** in a good yield of 82% with $TiCl_4$. While $Sc(OTf)_3$ catalyzed this rearrangement efficiently, it proved unsuitable for higher-functionalized analogs. Treating 5-allylated analogs like **59-H** with $TiCl_4$ gave rise to concomitant halo-PRINS cyclization, affording structurally intriguing tetracyclic ethers such as **86-H**. The simple decyano ketone **8-H**, via its alkene isomer **8-H.a**, was rearranged to the decalone-based hydroxy acyloin **93-H** in a rather low-yielding equilibrium reaction. All of these rearrangements were unsuccessful with the respective 6-cyano analogs or when acetonitrile was used as solvent.

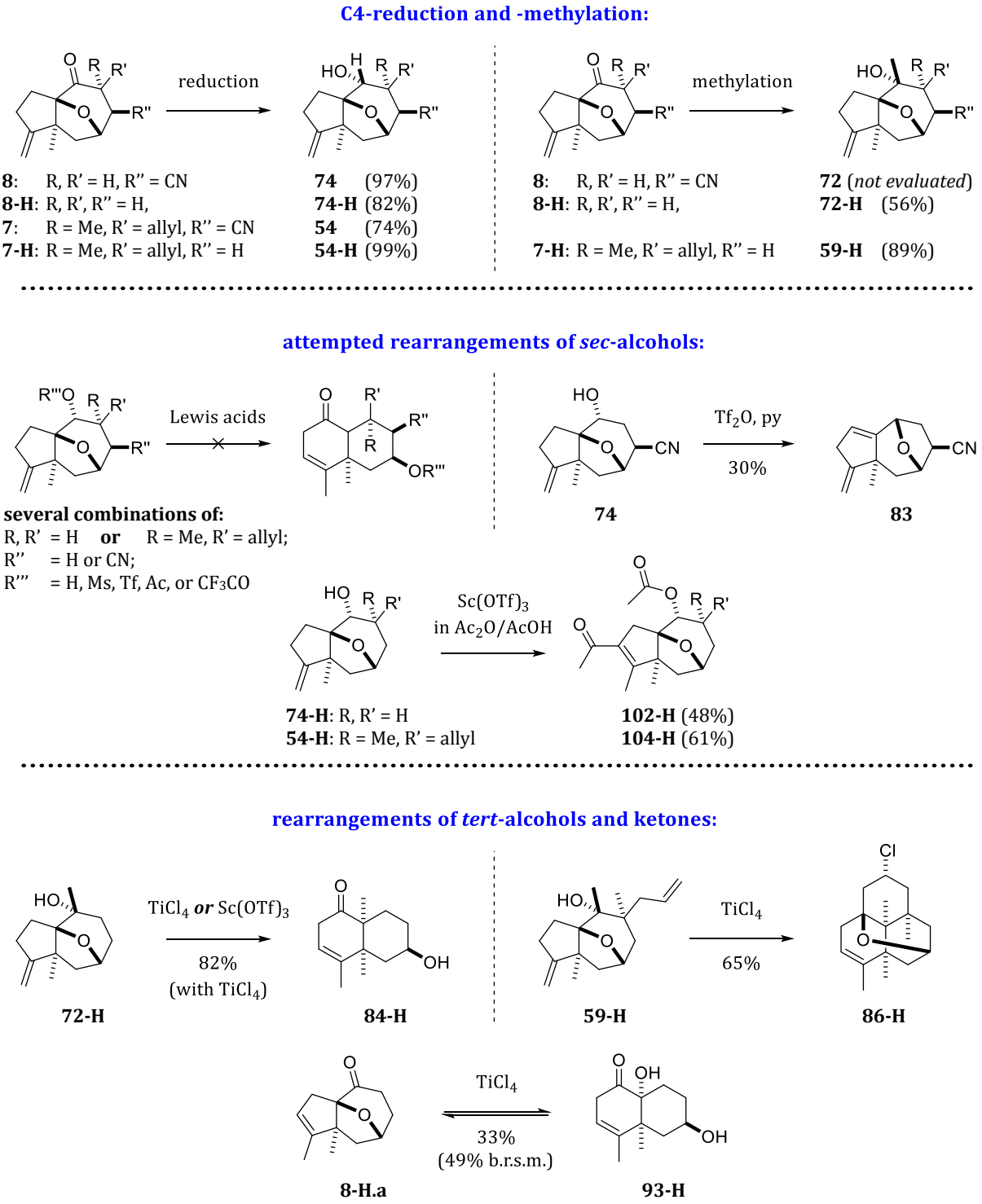

Scheme 133. Overview of the investigations into the LEWIS acid-induced rearrangement.

While rearrangements of ketones to higher-functionalized analogs of acyloin **93-H** may afford the desired decalones en route to salvinorin A, the LEWIS acid-induced rearrangement was deemed unpromising due to the mentioned issues. Much to our delight, the synthesis of such acyloins was achieved by a sequence involving an acyloin rearrangement, which proved promising right from the start. Consequently, the **LEWIS acid**-induced rearrangement was discontinued in order to investigate the somewhat 'opposite' **base**-induced rearrangement.

3.4 BASE-INDUCED REARRANGEMENT TO THE DECALONE CORE

In early C5 functionalization attempts with ketonitrile **8** and silyl enol ether **33**, a base-induced β-ether cleavage was observed. In later stages of our work, this rather serendipitous finding was leveraged to establish a β-ether cleavage/acyloin rearrangement sequence. This sequence was then applied to several differently functionalized 6-cyano epoxyazulenes, finally allowing for an expedient access to the desired decalones.

After LEMIEUX-JOHNSON oxidation of ketonitrile **7**, aldehyde **39** was either acetalized to dioxolane **119.b** or subjected to 3-furylation (**Scheme 134**). First attempts at 3-furylation were inconclusive since 3-furyl δ-hydroxynitrile **37** exhibited two signal sets in NMR, which falsely suggested a lack of diastereoselectivity. Further investigations indicated that this double NMR signal set stemmed from the differentiation of **37** into two conformers. It was discovered that alkaline work-up led to epimerization of the 6-nitrile and formation of hemiketal **37.a**. In one furylation run, the initially desired lactone **38** was obtained. Since lactone **38** did not rearrange as intended (*see below*), attempts at lactonization were ceased. The 3-furylation, implementing an acidic work-up to prevent C6-epimerization, was evaluated after subsequent silylation. TBS ether **127** was obtained in high yield and diastereoselectivity (87% over 2 steps, *d.r.* ≈ 10:1). Incidentally, former attempts indicated an even higher *d.r.* of ~15:1–30:1 when the reaction was kept at low temperatures for a longer reaction time. The desired (*S**)-configuration at C2' was confirmed via X-ray and NOESY analysis of lactone **38** and hemiketal **37.a**.

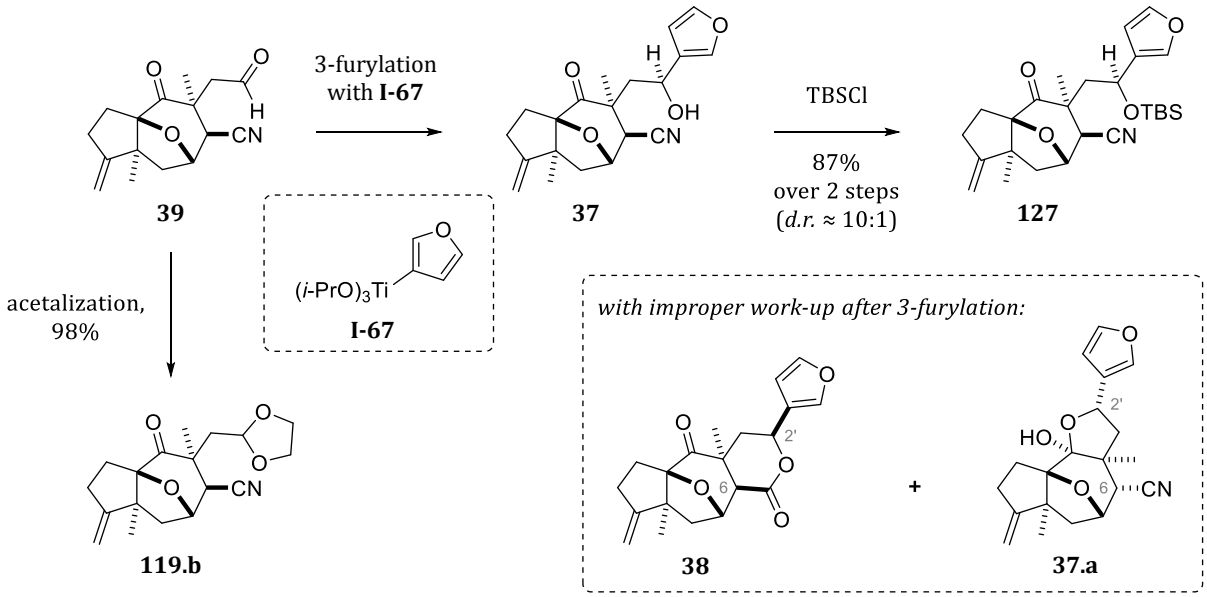

Scheme 134. Acetalization or 3-furylation/silylation sequence proceeding from aldehyde **39**.

Our devised rearrangement sequence was initially investigated on ketonitrile **7**. Gratifyingly, treating **7** with LDA resulted in β-ether cleavage to [5,7]-fused acyloin **110** with concomitant acyloin rearrangement to [6,6]-fused acyloin **111** (**Scheme 135**). Using LHMDS instead of LDA significantly increased the amount of recoverable substrate (6-*epi*-)**7**. This afforded acyloin **111** in an excellent overall yield of 67% (92% *b.r.s.m*), whereas the conversion was limited almost exclusively by the equilibrium of the acyloin rearrangement.

Treating dimethylacetal **119.a** or dioxolane **119.b** with LDA gave the [6,6]-fused acyloins **120.a** and **120.b**, respectively. Whereas **120.a** deteriorated with apparent formation of enol hemiketal **122**, its dioxolane analog **120.b** proved stable. An attempt with methyl ester **6** suggested a certain tolerance of the ester group to the rearrangement conditions. These rearrangements were not optimized or examined with the use of LHMDS instead of LDA, which might have improved overall yields. Notably, using KHMDS was found to be unsuitable and led to very complex mixtures with both **6** and **7**, indicating that the nature of the counter-ion has an unexpectedly decisive influence on this acyloin rearrangement.

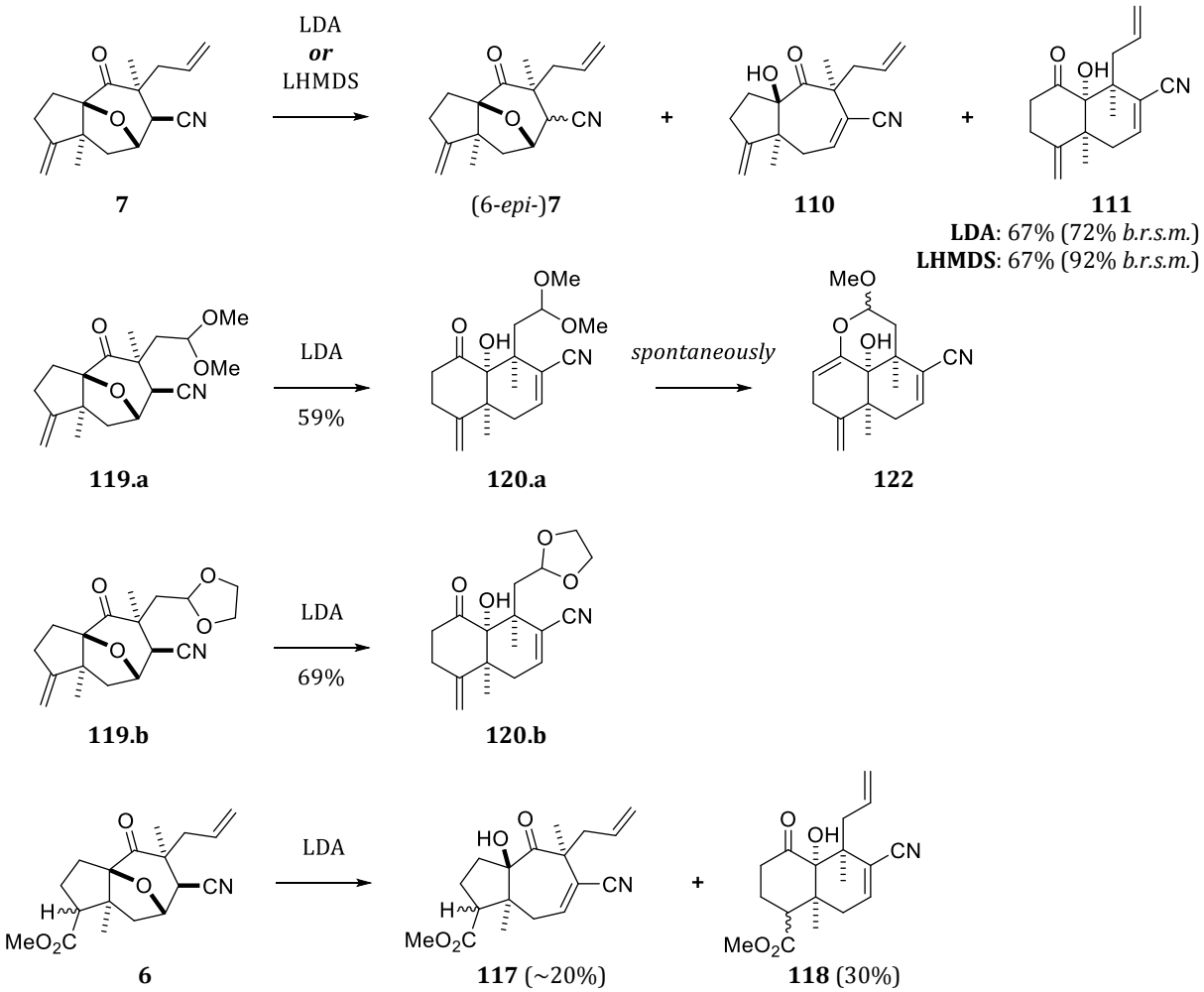

Scheme 135. Acyloin rearrangement sequence of 5-allyl- or acetal-substituted substrates.

This rearrangement was then applied to 3-furylated substrates. As mentioned above, furyl lactone **38** did not rearrange as intended. Instead, LDA induced an intramolecular furyl addition to the intricate polycyclic lactone **133** (**Scheme 136**). When treated with LHMDS instead, furyl lactone **38** remained unchanged. Gratifyingly, TBS ether **127** rearranged to [6,6]-fused acyloin **135** with no indication of an intramolecular furyl addition. Initial attempts however gave only modest overall yields with no substrate being recoverable. The reason for this was identified as the unexpected volatility of TBS ether **127**. Taking that into consideration, the rearrangement of (6-*epi*-)**127** was optimized by using LHMDS and a catalytic amount of $LiClO_4$ which appeared to accelerate the rearrangement step and suppress side-product formation. Thus, the synthesis of the 3-furylated acyloin **135** was achieved in a very satisfactory yield of 62% (94% *b.r.s.m.*).

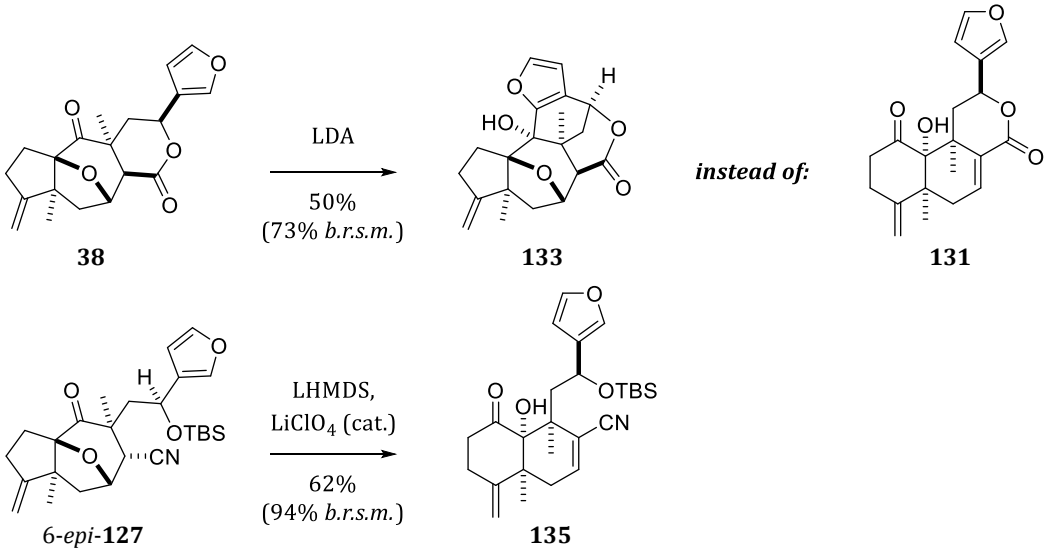

Scheme 136. Application of the rearrangement sequence on lactone **38** and TBS ether **127**.

Final pursuits aimed at the rearrangement of higher-substituted 3-furylated substrates. For this purpose, enoate aldehyde **137** was 3-furylated after its preparation from previously obtained side-products, i.e., diketo dimethylacetal **39.b** and allylic alcohol **47.a** (**Scheme 137** on the next page). Enol triflation of **39.b** and alkoxycarbonylation gave enoate dimethylacetal **138** in 55% yield over 2 steps with a significant amount of unreacted enol triflate. Notably, addition of dppf might have improved this conversion and yield, as described in the literature for similar substrates. Deacetalization of **138** then afforded enoate aldehyde **137**, whereas *p*-TsOH in wet acetone proved superior to aq. HCl in THF (95% vs. 67% yield). Additionally, **137** was prepared from allylic alcohol **47.a**. Double oxidation and esterification afforded 5-allyl enoate **136** in a high yield of 72% over 3 steps. LEMIEUX-JOHNSON oxidation of **136** gave enoate aldehyde **137** in only 31% yield, most likely due to osmium-based impurities promoting decomposition of **137**. Similar decompositions were also observed with other aldehydes and could be prevented by a slightly adjusted work-up, as elaborated upon in more detail in **Chapter 2.2.3** and **2.4.5.3**.

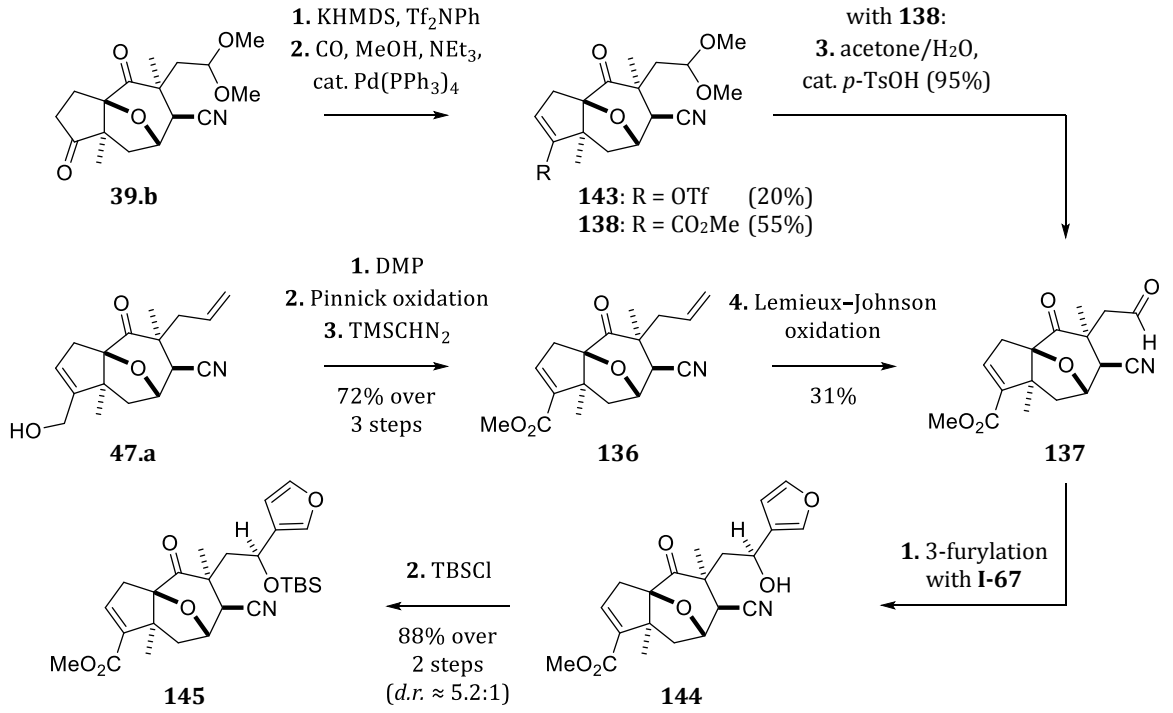

Scheme 137. Preparation of enoate aldehyde **137** and its furylation/silylation to TBS ether **145**.

Applying the 3-furylation/silylation sequence on aldehyde **137** gave TBS ether **145** in an excellent yield of 88% over 2 steps, but with a lower *d.r.* than that obtained with aldehyde **39** (*d.r.* ≈ 5.2:1 vs. >10:1). Since this sequence was carried out only once, potential effects of different conditions on the diastereoselectivity could not be examined. The main diastereomer of **145** is, by analogy to **127**, presumed to be the depicted and desired 2'-(*S**)-isomer. Unfortunately, the rearrangement of **145** was followed by a *retro*-DIELS–ALDER reaction to diene **147** and catechol **146**, most likely driven by the aromatic character of the latter (**Scheme 138**).

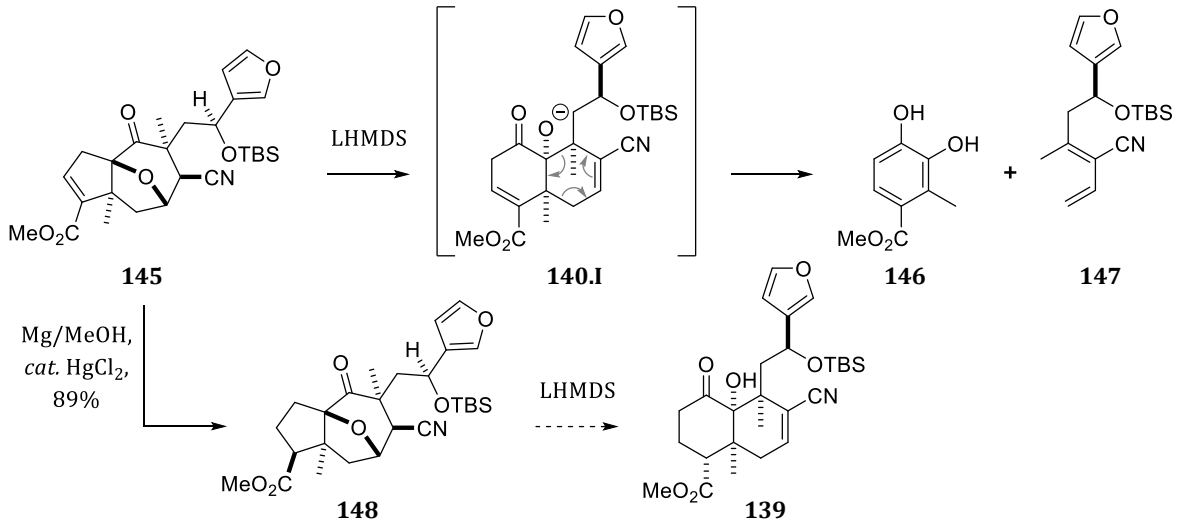

Scheme 138. Unsuccessful rearrangement of **145** and planned rearrangement of **148**.

To circumvent this *retro*-DIELS-ALDER reaction, the enoate group of **145** was subjected to a conjugate reduction with Mg/MeOH, affording **148** and some of its diastereomers in an 89% yield. The rearrangement of **148** to acyloin **139**, however, could not yet be examined due to time constraints. Instead, our final experiments focused on assessing the compatibility of the previously prepared 3-furylated acyloin **135** with another key step – the α-deoxygenation of acyloins (or 'α-ketols'), which had been examined before on non-furylated analogs.

Deoxygenation of the dioxolane-substituted α-ketol **120.b** with SmI_2 gave – at best – mostly diol **124** and some of the desired decalone **123** (**124/123** ≈ 2:1, **Scheme 139**). This deoxygenation also proved exceptionally delicate with α-ketol acetate **126**, prepared by near-quantitative acetylation of **111**. As with α-ketol **120.b** and its acetate, there was a strong tendency towards complete decomposition after improper use of additives and inadequate work-up. After tedious optimization, conditions were established that gave decalone **109** in yields of ~50–75%, with best results obtained using a non-aqueous work-up with NEt_3 and ethylene glycol. Although irreproducibility remained an issue (albeit a much smaller one), this marked a satisfying improvement over initial attempts that had resulted in complete decomposition.

Acetylation of 3-furylated acyloin **135** gave unreacted **135** (7%), enol diacetate **150** (10%), and α-ketol acetate **149** [**78%** (87% *b.r.s.m.*); **Scheme 140** on the next page]. Although the optimized conditions for **126** were applied, the SmI_2-mediated deoxygenation of **149** led to substantial decomposition. In addition to the desired decalone **152** (~30%), butenolide **153** (~12%) was obtained. This seems to support our (*admittedly, debatable*) earlier presumption that *samarium-containing intermediates* not only form during the deoxygenation, but can also *persist through work-up* – and subsequently either convert to the decalone or decompose. In this case, decomposition of the intermediate appears to have been partially intercepted by the formation of butenolide **153** via oxidation of, and enol(ate) addition to, the furan ring.

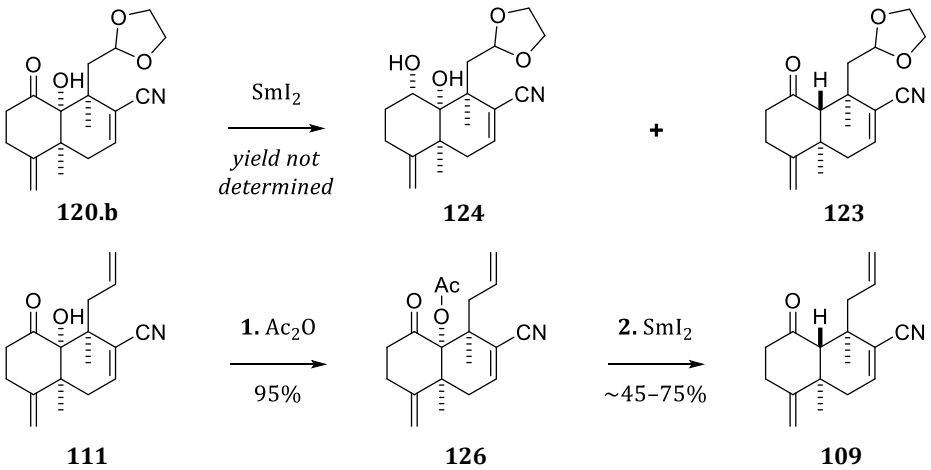

Scheme 139. Deoxygenation of α-ketol **120.b** and α-ketol acetate **126** with SmI_2.

Gratifyingly, a highly promising alternative for the SmI_2-mediated deoxygenation was found: when α-ketol acetate **149** was treated with magnesium in methanol, decalone **152** (47%) and diol **154** (23%) were obtained. The appearance of diol **154** is thought to follow from partial saponification of **149** to acyloin **135**. Similarly to its dioxolane analog **120.b**, acyloin **135** gave mostly diol **154** in a separately conducted deoxygenation (**154**/**152** ≈ 1.65:1). Most notably, no decomposition and good reproducibility was indicated by the preliminary results using this method. Small amounts of side-products, likely arising from concomitant reductions of the ketone and the vinyl nitrile, were discernible. As discussed in **Chapter 2.4.5.4**, such 'side-products' may also prove valuable for synthetic approaches towards the salvinorin framework.

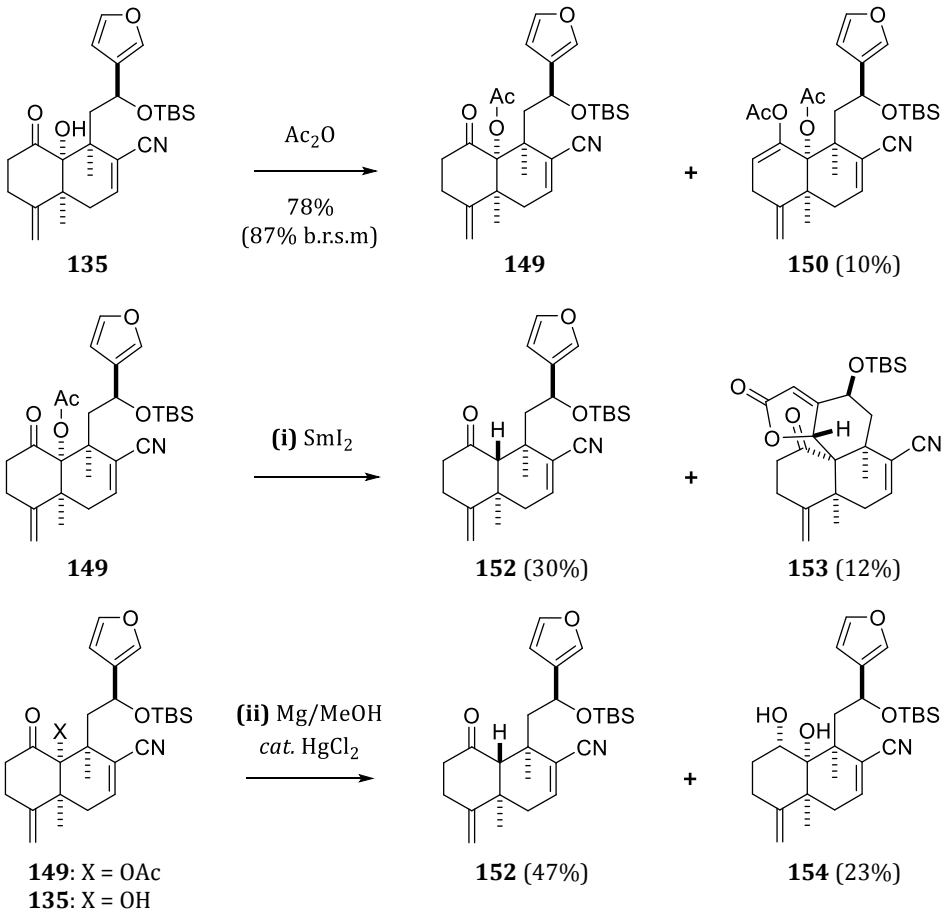

Scheme 140. Deoxygenation of α-ketol acetate **149** to **(i)** decalone **152** and butenolide **153** (with SmI_2) or **(ii)** decalone **152** and diol **154** (with Mg/MeOH).

Although conditions for a *selective* deoxygenation of α-ketol acetate **149** or acyloin **135** with Mg/MeOH have not yet been fully established, this convenient method stands as an strong contender for the commonly encountered α-deoxygenation with SmI_2. This *and* other methods developed or optimized in this work, such as the key acyloin rearrangement, can hopefully contribute to identifying new approaches and expedient solutions to other synthetically challenging endeavors.

3.5 OUTLOOK FOR FUTURE DIRECTIONS

During this doctoral research project, several compounds have been prepared and identified as promising candidates for the transformation to the salvinorin framework. While certain steps remain to be explored in detail, route-scouting efforts have provided valuable insights that allowed us to adapt general strategies and develop suitable methods for challenging reactions. Some promising approaches towards the salvinorin framework are *briefly* outlined below.

bis-Alkenyl decalone **109** was prepared mostly as a result of examining the devised acyloin rearrangement and α-deoxygenation on 'dummy substrates.' Nevertheless, the alkene groups of **109** represent viable precursors for the functional groups of the salvinorin framework (**Route A**, **Scheme 141**). After reduction of the C1 ketone, its protected alcohol **160** could be subjected to double oxidative cleavage of the alkene groups (e.g., by ozonolysis). 3-Furylation of the C12 aldehyde with concomitant lactonization, and then, alkoxycarbonylation of the C4 enol triflate would give *bis*-unsaturated ester **161**. With TES as the protecting group, this corresponds to **I-54**, a late-stage intermediate in HAGIWARA's total synthesis of salvinorin A (*cf.* page **20**). HAGIWARA *et al.* emphasized the difficulty of the double conjugate reduction with SmI_2 – and implied that employing Mg/MeOH was unsuccessful. Applying our conditions of the Mg/MeOH-mediated reduction of enoate **145** to **I-54** would therefore be interesting. An alternative approach could also make use of an acetyl protecting group (**161**, R = Ac) which may combine the desired reduction by Mg/MeOH with a deprotection by saponification to **I-55**/**I-56**.

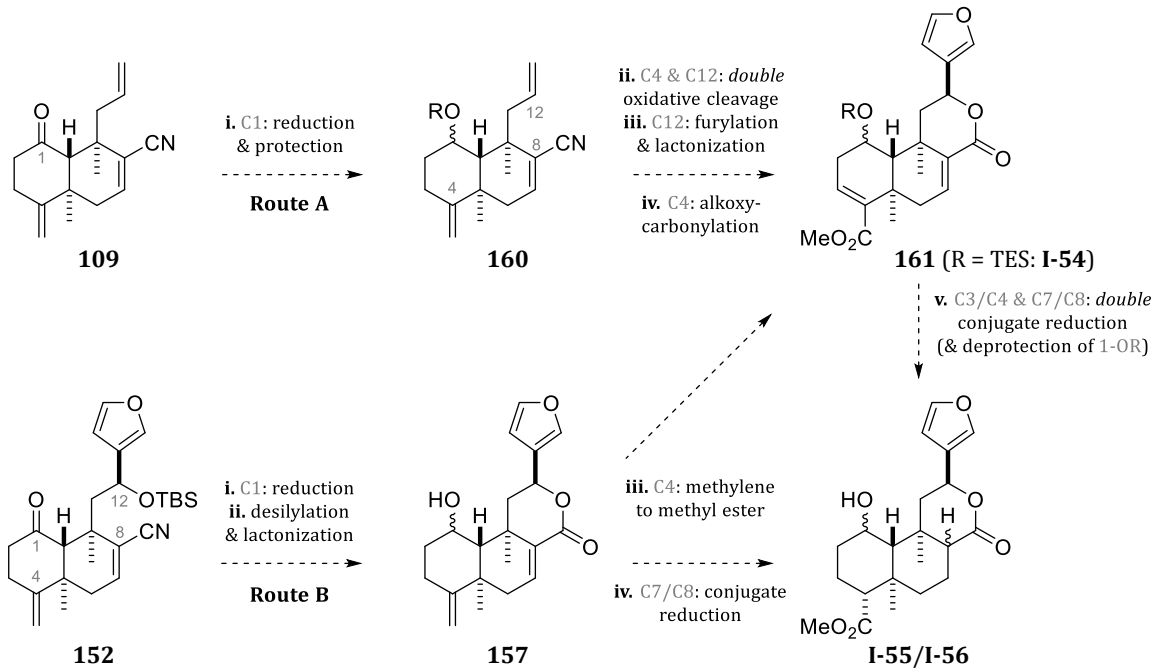

Scheme 141. Potential routes proceeding from the decalones **109** and **152**.

When the 3-furylated epoxyazulene **127** was rearranged and subsequently α-deoxygenated, the 3-furylated decalone **152** was obtained. Proceeding with decalone **152**, a reduction of the C1 ketone to prevent hemiketalization may suffice for the next steps, with no protecting group being necessary (**Route B**). Some considerations regarding this and alternative routes from **152** were also given in **Chapter 2.4.5.4**. With lactone **157**, the transformation of the methylene group to the ester could be approached via the epoxidation-initiated sequence described in **Chapter 2.2.2** or by oxidative cleavage/enol triflation/alkoxycarbonylation. Subsequent (*single or double*) conjugate reduction of the respective products would, again, furnish **I-55/I-56**.

The final approach sets the rearrangement after 'full functionalization' on the epoxyazulene core, aiming at a decaline system with both the 3-furyl and ester moieties already in place. To this end, methyl ester **148** was prepared by using side-products of different routes as substrates, which gave **148** with moderate success. The preparation of **148** and its precursors should be examined in more detail, including insights we gained from the route-scouting process, to prepare aldehyde **5** more efficiently before furylation and silylation to **148** (**Route C**, **Scheme 142**). Methyl ester **148** may also be accessed by a *deliberate* double oxidative cleavage to tricarbonyl **39.a** and installing the 3-furyl before the ester moiety (**Route D**).

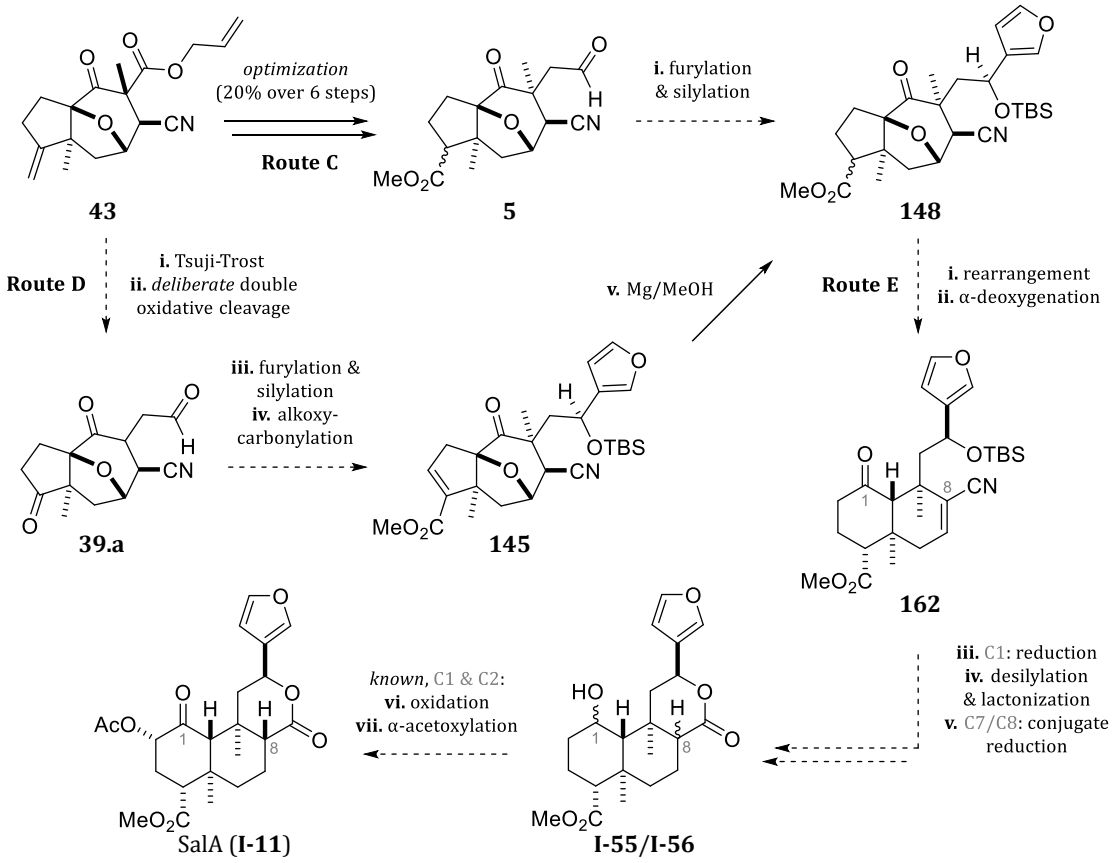

Scheme 142. Route optimization of the *fully functionalized* ketonitrile **148** and its envisioned late-stage transformation to salvinorin A (**I-11**).

With **148** in hands, our novel total synthesis of salvinorin A seems within reach. Applying our developed rearrangement and α-deoxygenation methods to **148** is expected to give decalone **162** (**Route E**). The devised lactonization sequence should then furnish the diastereomeric lactones **I-55**/**I-56**. Salvinorin A (**I-11**) is known to be easily accessible from the desired C8 diastereomer **I-56** through oxidation to deacetoxysalvinorin A (**I-52**) and its subsequent α-acetoxylation (see **Scheme 7** on page **20** for details).

These outlined approaches include a yet unexamined lactonization of the (unsaturated) nitrile on the decaline core. While this transformation is expected to be feasible, its exploration remains a compelling direction for future investigation. This lactonization – as well as the rearrangement of **148** and a more detailed study of the α-deoxygenation with Mg/MeOH – could not be pursued due to time constraints and the necessity of bringing this already extensive thesis to completion. However, *should time permit a brief examination* of these final steps before the thesis defense, any results will be included in our forthcoming journal publication.

CHAPTER 4: EXPERIMENTAL SECTION

4.0 GENERAL REMARKS

The experimental procedures are organized to align with the synthetic sequences outlined in **Chapter 2**. The given procedures represent an example of the conducted reactions. In most cases, these were repeated several times to ensure reproducibility, paying careful attention to maintaining consistency with the given procedure. Deviations from the usual conditions, changes in results, and noteworthy aspects of the reactions are summarized in *notes below the procedure* occasionally. Such findings are typically discussed in greater detail in **Chapter 2**; however, the notes serve to offer crucial information at a glance.

The procedures omit or only briefly mention some conventional aspects for brevity. These include conducting reactions in an inert atmosphere, stirring reaction mixtures, removing solvents/volatiles in vacuo ('concentration' of solutions), monitoring reaction progress, and purification methods. Details on these aspects are described in the following subchapters.

4.0.1 General Working Techniques

The reactions were typically conducted in an inert atmosphere using nitrogen or argon gas, if not explicitly stated otherwise. For this purpose, common Schlenk techniques were employed. A VACUUBRAND RZ 6 rotary vane pump was connected to the dual manifold ('Schlenk line') via a cold trap (cylindrical DEWAR flask filled with liquid nitrogen), resulting in a working vacuum of approx. $1 \cdot 10^{-1}$ mbar. Flasks and apparatuses were connected to the dual manifold via vacuum tubing attached to either glass joint adapters or syringes with cannulas. The cannulas were pierced through rubber septa fitted on the ground joints of the flasks and apparatuses. Glass joints were greased with mineral oil-based vacuum grease.

Flasks and apparatuses were evacuated and flushed with nitrogen or argon gas three times. Solid and non-volatile compounds present from the beginning of a reaction were placed in the flasks beforehand. For addition of small volumes of liquids, syringes were used which were previously flushed with inert gas three times. Solids, or large volumes of liquids, were added into reaction flasks by maintaining an outflow of inert gas through the opened joint.

Reactions, as well as distillations, drying suspensions of organic extracts *et cetera* were stirred with magnetic stirring bars. Unless noted otherwise, reactions were conducted at room temperature (~22–26 °C). For low-temperature reactions, cooling baths were prepared by cooling acetone with liquid nitrogen in a hemispherical DEWAR flask. Often, such cooling baths were allowed to warm to the indicated temperature over a specified time (e.g., "the reaction mixture was allowed to warm to −40 °C over the course of 1 h"). When cooling baths were used overnight, the residual cooling medium (*wet acetone*) typically indicated a temperature of 12 °C (e.g., "the reaction mixture was allowed to warm to 12 °C over the course of 11 h"). When low temperatures were to be maintained over a prolonged period of time, cryostats from HAAKE were utilized. The use of cryostats is noted in the respective procedures.

After extraction, drying, and filtration of the combined organic extract, solvents and volatiles were removed on BÜCHI rotary evaporators connected to VACUUBRAND vacuum pumps (e.g., BÜCHI Rotavapor R-210® and VACUUBRAND PC 3001 Vario^{pro}®). The heating bath of the rotary evaporator was set at 50 °C for non- and low-volatile or 40 °C for more volatile compounds. Non-volatile compounds were concentrated to a vacuum of up to 5 mbar, flushed with air, and concentrated again (repeated twice, ~5 min each) to remove residual solvents more efficiently. For compounds prone to retain solvents, a later-established method proved very useful for the removal of residual solvents – occasionally affording solids instead of viscous oils. For this purpose, the compounds were dissolved in some DCM or Et_2O and concentrated as described above after adding some hexane. The synthesized compounds were generally stored (in closed flasks or screw-top vials) in a laboratory freezer (–28 °C).

4.0.2 Reagents and Solvents

The used reagents and solvents were obtained from common chemical suppliers such as ABCR, ACROS, ALFA AESAR, CARBOLUTION, FLUKA, FLUROCHEM, MERCK, SIGMA-ALDRICH, STREM CHEMICALS, TCI or THERMO FISHER SCIENTIFIC. Most of the reagents were used without further purification. Some reagents were purified by drying in vacuo at elevated temperatures [e.g., $Sc(OTf)_3$], crystallization [e.g., $VO(acac)_2$ and CuBr], or by common distillation methods [e.g., amine bases (DBU, NEt_3, pyridine, *i*-$PrNH_2$ *et cetera*) distilled from CaH_2 and stored over KOH or 4 Å MS].

Solvents used for 'general purposes' (e.g., for extractions or chromatography) were purified by distillation in a rotary evaporator. Petroleum ether (PE) with a boiling range of 40–60 °C was used unless noted otherwise. Solvents used in (inert atmosphere) reactions were further purified and dried according to common techniques, such as (i) Et_2O, THF, and toluene from sodium/benzophenone, (ii) DCM, amine bases, hexane, DMSO, MeCN from CaH_2, (iii) DMF from P_2O_5, or (iv) MeOH from magnesium turnings with iodine. These solvents were stored in Schlenk flasks over dried molecular sieves (3–5 Å depending on solvent, most often 4 Å).[210,372]

4.0.3 Chromatography (TLC & flash chromatography)

Reaction progress was assessed by thin-layer chromatography (TLC) using precoated TLC plates with a fluorescence indicator (MACHERY-NAGEL Polygram® SIL G/UV_{254}). Notably, in several cases, a repeated elution of the same TLC plate facilitated a better assessment, as indicated in the procedures. Substance spots were visualized by irradiation with UV light (λ = 254 nm), dipping the TLC plates in an adequate staining solution, and subsequent development of the stains (also called spots) with a heat gun. Most of our compounds could not be detected by UV irradiation. The best and most-used staining solution proved to be $KMnO_4$, followed by CAM (cerium ammonium molybdate) and Vanillin. These staining solutions were prepared as follows:

- **$KMnO_4$**: water (150 mL), NaOH (0.25 g), K_2CO_3 (10 g), $KMnO_4$ (1.5 g).
- **CAM**: water (180 mL), conc. H_2SO_4 (98%, 20 mL), $MoO_4(NH_4)_2$ (5 g), $Ce(SO_4)_2$ (2 g).
- **Vanillin**: ethanol (200 mL), conc. H_2SO_4 (98%, 1 mL), Vanillin (4 g).

The products were purified by flash chromatography using silica gel from THERMO FISHER SCIENTIFIC (ultra-pure, 35–70 µm, 60 Å). The size/diameter of the column, as well as the fraction tube size, was chosen according to the amount of substance and the required resolution. When only moderate resolution was required, the recommendations of STILL *et al.* were well-suited for a first orientation.[373] Small amounts of substances (<10 mg) were purified in a microscale column using a disposable PASTEUR pipette.

With our substances, *gradient elution* proved superior to isocratic eluents in many cases and was therefore established as a general practice. The used gradients are indicated in the respective procedures (starting and end points; *without gradual increases*). The elution was conducted with pressurized air and an excess pressure of ~0.2–0.8 bar, depending on column size.

4.0.4 Nuclear Magnetic Resonance (NMR) Spectroscopy

NMR spectra were recorded on either a BRUKER (i) **Avance III HD 300** (^{1}H: 300 MHz, ^{13}C: 75 MHz), (ii) **Avance III HD 400** or **HDX 400** (^{1}H: 400 MHz, ^{13}C: 101 MHz), (iii) **Avance III HDX 600** (^{1}H: 600 MHz, ^{13}C: 151 MHz), or (iv) **Avance III HDX 700** (^{1}H: 700 MHz, ^{13}C: 176 MHz). Chemical shifts **δ** are given in [ppm] relative to tetramethylsilane, while coupling constants ***J*** are given in [Hz]. The residual ^{1}H signals, as well as the ^{13}C signals, of the solvents were used as references values [**$CDCl_3$**: δ = 7.26 (^{1}H) & 77.0 ppm (^{13}C); **C_6D_6** δ = 7.16 (^{1}H) & 128.0 ppm (^{13}C)]. The reference values of less-frequently used solvents can be seen in the respective NMR spectra attached in the **Appendix** (**Chapter 6.2**).

Combinations of the following NMR experiments were used for structure elucidation: (i) **^{1}H**, (ii) **^{13}C** (proton decoupled), typically with an **UDEFT** sequence, (iii) **DEPT-135 ^{13}C**, (iv) **^{1}H-^{1}H COSY**, (v) **^{1}H-^{13}C HSQC**, (vi) **^{1}H-^{13}C HMBC**, and (vii) **^{1}H-^{1}H NOESY**. Notably, NOESY spectra of our compounds occasionally exhibited significant *t_1 noise*, especially seen as vertical smudging of the most intense signals and burying weak cross-peaks underneath, when the spectra were not processed adequately (phasing & baseline correction in both dimensions). The spectra were processed and interpretated using NMR software from ACD, BRUKER, and MESTRELAB RESEARCH (ACD/Labs® 12.0, TopSpin® 3.6.3, and MestReNova® 8.0). MestReNova was used for the depiction of the NMR Spectra.

To describe the multiplicity of signals, common abbreviations are used: **s** = singlet; **d** = doublet; **t** = triplet; **q** = quartet; **quin** = quintet; **sext** = sextet; **sept** = septet; **m** = multiplet. Additionally, some signals are further described by a combination of these multiplicities, as well as '**br** or **v br**' for 'broad' and 'very broad', respectively. For example, a '**v br ddd**' would indicate a *very broad doublet of doublet of doublet*. Generally, *true* triplets or higher multiplicities were scarce within our tricyclic compounds due to the diastereotopic nature of magnetically inequivalent protons. For example, some doublets of doublets ***appeared*** *as* triplets (or broad doublets appeared as broad singlets), which is occasionally indicated by '***app.***' In some cases, an approximate range of the coupling constant is given (e.g., br dd, $J \approx 1$–1.4 Hz), when a more certain determination was not possible due to superimposition. Most signals were further complicated by higher-order spin systems, which were not determined.

As demonstrated in several examples, **quantitative NMR** (qNMR) proved an exceptionally convenient tool for quick yet highly accurate assessments of purities and yields.[374,375] This was particularly valuable for comparing different variations of a given reaction during optimization processes. This method was implemented in a rather late stage of the doctoral research project but would been equally beneficial in earlier pursuits. Given that its utility is, arguably, not emphasized enough in the synthetic chemistry literature, we would like to take this opportunity to emphasize that the *implementation of qNMR as a common practice is highly recommended*.

Quantitative NMR was typically conducted using a one-ninth molar equivalent of TMOB (1,3,5-trimethoxybenzene) relative to the compound being analyzed (analyte). By comparing the ^{1}H NMR signal integrals of the compound and TMOB, the purity or yield of the compound was determined. An example is provided for a hypothetic compound (**X1**) with a molar mass of $\mathbf{M_{X1}}$ = 234.56 g/mol, which exhibits a distinct, isolated NMR signal for one of its protons at δ = 2.34 ppm. **TMOB**, with a molar mass of $\mathbf{M_{TMOB}}$ = 168.19 g/mol, exhibits two NMR signals at δ = 6.07 (s, 3H, 3 × aryl-H) and 3.75 ppm (s, 9H, 3 × OCH_3) [in $CDCl_3$]. The purity and yield of **X1** would be determined as follows:

- 42 mg of *crude* **X1** → $\mathbf{n_{X1}}$ = 0.1791 mmol (*crude*)
- $\mathbf{n_{TMOB}} = \mathbf{n_{X1}/9}$ = 0.0199 mmol → 3.346 mg of TMOB is added to **X1**
- ^{1}H NMR reveals an integral value of **0.87** for the proton of **X1**, when the integral value of the methoxy signal of TMOB is normalized to 1.00 (integral value of 3 × aryl-H = 0.33)
- the ratio of 0.87/1.00 indicates **87% purity** of *crude* **X1**
- effectively, *crude* **X1** contains 0.1791 mmol × 0.87 × 234.56 mg/mmol = 36.54 mg of **X1**
- assuming a '*crude yield*' of 111%, the true **yield** of **X1** is 97%.

A more direct determination of yield is shown in the following example, where **X1** was prepared in a hypothetical 0.037 mmol test reaction from its precursor **X2**:

- $\mathbf{n_{TMOB}} = \mathbf{n_{X2}/9}$ = 0.0041 mmol → 0.691 mg of TMOB is added to the crude product
- ^{1}H NMR reveals an integral ratio of **0.79**/1.00/0.33, indicating a yield of **79%**.

In the latter case, weighing exactly 0.691 mg TMOB would be difficult. Therefore, for small-scale experiments, a solution of TMOB in hexane or pentane was prepared, and an aliquot was added to the crude product. For instance, 6.91 mg of TMOB were dissolved in 10 mL of hexane or pentane, and a 1 mL aliquot of this solution was added to the crude product. After removing the solvents, the TMOB-containing crude product was analyzed.

TMOB proved to be a suitable internal standard for several reasons. Its sharp methoxy signals (corresponding to 9 protons) allowed for similar peak heights for the signals of TMOB and the analyte, despite using only a one-ninth molar equivalent of TMOB. This low level of 'contamination' with TMOB could easily be removed chromatographically – or, in most subsequent reactions, simply ignored. As expected, no undesired reactions between TMOB and our compounds were observed. Additionally, TMOB exhibited no noticeable volatility.

4.0.5 (High-Resolution) Mass Spectrometry

Mass spectrometry (MS) analysis was generally conducted by the MS department of the Institute of Organic Chemistry, University of Tübingen (Dr. DOROTHEE WISTUBA, Dr. NOBERT GRZEGORZEK, Dr. PETER HAISS, and CLAUDIA KRAUSE). High-resolution mass spectrometry (**HRMS**) analysis was performed on a BRUKER maXis 4G [electrospray ionization & time-of-flight analyzer (ESI-TOF)]. While this system could also be equipped with an atmospheric-pressure chemical ionization (APCI) source, our compounds generally were measured using **ESI-TOF**.

On some occasions, low-resolution MS (LRMS) analysis, such as GC-MS and HPLC-MS, was performed on an AGILENT GC-MS 5977B MSD [electron ionization & quadrupole mass analyzer (EI-QMS)] and a BRUKER amaZon SL [ESI or APCI & ion trap (ESI or APCI-ion trap)], respectively. For nonpolar substances, a direct inlet probe (DIP) was used.

4.0.6 Melting Point Measurements

The melting points were measured on a BÜCHI melting point apparatus B-540. For better comparability and to avoid influence of residual polar solvents like EA, the measured solids were prepared by evaporation from a DCM/hexane solution, unless explicitly stated otherwise.

4.0.7 X-ray Crystallography

Preparation of the measured crystals:

Generally, the crystals were obtained by slow evaporation of a solution of the respective compound. The solvent(s) for each case are noted within the discussion of the compounds. For the purpose of slow evaporation, the compound solutions were placed in a 3.5 mL screw-top vial fitted with a solid polypropylene screw cap previously punctured by a syringe or needle. The vial was placed in a small cork ring, angled at about 45 °, and left standing until crystals formed. For our compounds, this crystallization method proved far superior to other attempted methods, such as (liquid or vapor) diffusion methods. Incidentally, some crystals (i.e., those of **54** and **86-H**) formed only when the solutions slowly evaporated to *apparent dryness*.

Data collection:

The measurement and processing of crystal structures was carried out by Dr. HARTMUT SCHUBERT from the working group of Prof. Dr. LARS WESEMANN (Institute of Inorganic Chemistry, University of Tübingen). X-ray data were collected on a BRUKER Smart APEX II diffractometer with graphite-monochromated Mo Kα radiation. The programs used were BRUKER APEX2v2011.8-0, including SADABS for absorption correction, SAINT for data reduction and SHELXS for structure solution, as well as the WinGX suite of programs version 1.70.01 or the GUI ShelXle, including SHELXL for structure refinement.[376–379] All details of the structure refinement and solution can be found in the **Appendix** (**Table 10** on page **303**).

Generation of graphics:

The X-ray structure graphics depicted in **Chapter 2** were generated with CDCC Mercury 3.0. Within these processed crystal structures, disorders, as well as methylene and methyl protons were omitted for clarity. The crystal structures obtained from the *.cif files without further processing* are shown in the **Appendix** (**Figure 36** & **Figure 37** on pages **305** & **306**).

Notably, in the case of lactone **38**, the *.cif* file provided the mirror image representation, which was inverted using ORTEP-3[380] to maintain consistency with the depicted structural formulas. This does, however, not imply the synthesis of the 'other' enantiomer, as all our research was conducted with racemic compounds.

4.1 SYNTHETIC ROUTE TO TRICYCLIC ENONE 9

4.1.1 Carbocupration and Synthesis of Dienyl Furfuryl Alcohol 14

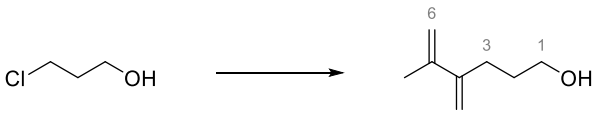

20 **19**

19: **5-Methyl-4-methylenhex-5-en-1-ol**

In a 1 L Schlenk flask equipped with an addition funnel, 3-chloro-1-propanol (**20**, 20.0 mL, 241 mmol, 1 eq) was dissolved in THF (450 mL) and cooled in an ice bath, before *i*-PrMgCl[b] (1.35 M in THF; 178 mL, 240 mmol, 1 eq) was added dropwise (25 min). After stirring in the ice bath (30 min) and at room temperature (30 min), magnesium turnings[a] (6.28 g, 258 mmol, 1.07 eq) and 1,2-dibromoethane (1.1 mL, 12.7 mmol, 5 mol%) were added. The progress of NORMANT GRIGNARD reagent formation was analyzed after 20 h, indicating complete conversion (*titration of a 0.1 mL aliquot with 0.1 M $HCl_{(aq)}$ against phenolphthalein: 0.74 N resp. 0.37 M; theoretically possible: 0.37 M*). After cooling to –55 °C, CuBr·DMS[c] (24.60 g, 120 mmol, 0.5 eq) was added. The mixture was stirred for 2 h at temperatures between –55 and –40 °C, before alkenyne **21**[d] (8.03 g, 121 mmol, 0.5 eq) was added at –55 °C.

The greenish-black mixture was stirred in the cooling bath, which was allowed to warm to room temperature, and hydrolyzed after 17 h by slow addition of saturated NH_4Cl solution (400 mL, 1.5 h) at room temperature with continuous stirring, diluting with small amounts of water and cooling in an ice bath as needed. After addition of water (100 mL) and diethyl ether (300 mL), the phases were filtered through a plug of sand and then separated. The aqueous phase was extracted with diethyl ether (2 × 300 mL) and the combined organic phases were washed with saturated NaCl solution (150 mL), dried over $MgSO_4$, and concentrated (40 °C, 50 mbar). The crude orange oil was fractionally distilled (10 mbar, b.p. 75 °C) to give dienyl alcohol **19** (13.43 g, 0.106 mol, **89%**) as a colorless oil.

R_f = 0.54 (PE/DE, 2:3).
^{1}H NMR (400 MHz, $CDCl_3$): δ = 5.08 & 4.96 (2 × br s, 4H, 4-CH_2 & 6-H_2), 3.62 (t, ^3J = 6.5 Hz, 2H, 1-H_2), 2.33 (t, ^3J = 7.6 Hz, 2H, 3-H_2), 2.32 (br s, 1H, 1-OH), 1.88 (s, 3H, 5-CH_3), 1.76–1.66 (m, 2H, 2-H_2). **^{13}C NMR** (101 MHz, $CDCl_3$): δ = 147.3 (C4), 142.4 (C5), 112.6 (4-CH_2), 112.2 (C6), 62.4 (C1), 31.6 (C3), 29.8 (C2), 21.0 (5-CH_3). (**Figure 38**)
HRMS: calcd. for $C_8H_{14}NaO$ 149.09369 $[M+Na]^+$, found 149.09351 (Δ = 1.15 ppm).

Notes: Analogously conducted syntheses of **19** were also purified by flash chromatography (PE/DE, gradient from 2:1 to 1:2), resulting in similar yields (usually **89-98%**). The reproducibility of high yields was strongly dependent of the utilized reagents but could be ensured very well by complying with the following recommendations:

[a]: *Activated magnesium turnings*: Magnesium turnings (42.0 g, 1.73 mol; *freshly ground in a mortar*) were placed in a 250 mL Schlenk flask and suspended in THF (150 mL), before Iodine (1.0 g, 3.94 mmol, 0.23 mol%) was added in portions and the resulting brownish turbid suspension stirred for 1 h. Maintaining an inert atmosphere in the flask, the supernatant was decanted off and the magnesium turnings were washed in the same way with THF (3 × 50 mL) and diethyl ether (3 × 50 mL). Residual solvents were removed in vacuo using the vacuum pump connected to the Schlenk line. The magnesium turnings were further activated by vigorous dry-stirring[188] in an inert atmosphere until they adopted a metallic-blackish appearance (2-3 d).

With proper inert storage, the activated magnesium turnings showed no loss of activity even after several months. The turnings were transferred from the Schlenk flask to a new vessel as needed by placing both vessels in close proximity and maintaining a stream of inert gas in which the turnings were transferred by spatula. Generally, a screw-top vial was purged with inert gas and used to weigh out the turnings, before adding those to the according flask.

[b]: *Preparation of i-PrMgCl solution*: Activated magnesium turnings[a] (14.81 g, 609 mmol, 1.34 eq) were placed into a 250 mL two-neck flask equipped with a septum and a reflux condenser fitted with a gas inlet adapter. After addition of THF (300 mL) and a portion (ca. 25%) of isopropyl chloride (in total 41.5 mL, 455 mmol, 1 eq) the suspension *was let sit* for 10 min and the remaining isopropyl chloride then added dropwise (1 h, syringe pump) into the now stirring suspension while gradually raising the temperature of the reaction mixture to a gentle reflux. After complete addition, the reaction mixture was refluxed for additional 2 h. Formation of the GRIGNARD reagent was analyzed by titration, indicating a complete conversion (*1.34 M, titration of a 0.1 mL aliquot with 0.1 M $HCl_{(aq)}$ against phenolphthalein; theoretically possible: 1.33 M*).

[c]: *Purification of CuBr and preparation of CuBr·DMS*: CuBr was purified by stirring in glacial acetic acid and decanting the supernatant off before repeating this process with methanol. The respective washings were adjusted regarding amounts of solvent, duration, and number of repetitions according to the impurity of employed CuBr. Each washing process was generally repeated once or twice with a stirring duration of 1–2 d until a discoloration of the respective solvent (AcOH: green, MeOH: yellow) was no longer visible. Afterwards, the purified CuBr was washed with diethyl ether and residual solvents were removed in vacuo.
Dimethyl sulfide (200 mL) was placed in a 1 L Schlenk flask and cooled in an ice bath before purified CuBr (*before purification*: 78.00 g, 544 mmol) was added in portions (*highly exothermic reaction*). The resulting yellowish turbid solution was filtered through a cotton plug into a 1 L Schlenk flask and the portion of CuBr·DMS which precipitated during filtration was dissolved with approximately 100 mL of DMS. The solution was layered with hexane (500 mL) and let sit for 3 d, before the formed crystals were filtered, washed with hexane, and dried in vacuo. The exceptionally large crystals were finely ground with a glass rod to yield colorless powdered CuBr·DMS (99.75 g, 485 mmol, **89%**).

d: *Preparation of 2-methylbut-1-en-3-yne* (21):[193]

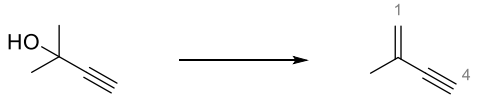

31 **21**

21: **2-Methylbut-1-en-3-yne**

2-Methylbut-3-yn-2-ol (**31**; 43.0 mL, 440 mmol, 1 eq) was placed into a 100 mL two-neck flask equipped with a short-head distillation head and an addition funnel *without* pressure equalization arm. A mixture of acetic anhydride (52 mL, 550 mmol, 1.25 eq) and conc. sulfuric acid (96%, 1.22 mL, 22 mmol, 5 mol%) was added dropwise (1.5 h) while heating the reaction mixture to 80 °C. The distillate was collected by submerging the receiving flask in a cooling bath (below –50 °C) and occasionally adding small portions of liquid nitrogen into the cooling bath or cautiously applying vacuum very briefly, both leading to a 'pull' of condensate from the black reaction mixture into the receiving flask. The condensate was purified by distillation, providing the highly volatile alkenyne **21** (17.48 g, 0.264 mol, **60%**) as a colorless liquid (b.p.: 31 °C).

Due to its highly volatile nature, alkenyne **21** was stored, tightly closed, at –28 °C. It is advised to handle and weigh out still cooled alkenyne **21** in a *precooled syringe* as needed.

^{1}H NMR (400 MHz, $CDCl_3$): δ = 5.38 & 5.28 (2 × s, 2H, 1-H_2), 2.86 (s, 1H, 4-H), 1.89 (br t, 3H, 2-CH_3). **^{13}C NMR** (101 MHz, $CDCl_3$): δ = 125.9 (C2), 123.4 (C2), 84.9 (C3), 76.1 (C4), 23.2 (2-CH_3). (**Figure 39**)

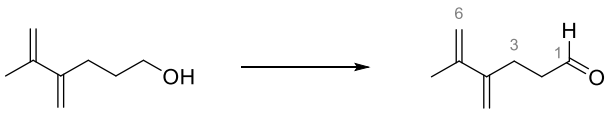

19 **17**

17: **5-Methyl-4-methylenhex-5-enal**

In a 100 mL flask, oxalyl chloride (0.75 mL, 8.71 mmol, 1.1 eq) was dissolved in DCM (22 mL) and cooled to –60 °C. After addition of dimethyl sulfoxide (1.24 mL, 17.42 mmol, 2.2 eq; over 5 min) and (12 min later) dienol **19** (1.00 g in 8 mL DCM; 7.92 mmol, 1 eq; over 9 min), the resulting suspension was stirred for 15 min at temperatures between –75 and –60 °C. Then, triethylamine (5.5 mL, 39.60 mmol, 5 eq) was added (over 6 min) at –75 °C and the thick suspension vigorously stirred in the cooling bath (20 min) and at room temperature (30 min). After quenching with water (36 mL), the phases were separated, and the aqueous phase extracted with DCM (3 × 36 mL). The combined organic phases were dried over $MgSO_4$, filtered, and concentrated in vacuo (40 °C, 50 mbar). Purification by flash chromatography (PE/DE, 15:1) afforded dienyl aldehyde **17** (720 mg, 5.80 mmol, **73%**) as a colorless oil.

R_f = 0.61 (PE/DE, 2:1).

^{1}H NMR (400 MHz, $CDCl_3$): δ = 9.78 (s, 1H, 1-H), 5.13–4.97 (m ("4 × s"), 4H, 4-CH_2 & 6-H_2), 2.62 (s, 4H, 2-H_2 & 3-H_2), 1.90 (s, 3H, 5-CH_3). **^{13}C NMR** (101 MHz, $CDCl_3$): δ = 202.1 (C1), 145.9 (C4), 142.1 (C5), 112.9 (2 ×, 4-CH_2 & C6), 42.9 (C2), 25.8 (C3), 21.1 (5-CH_3). (**Figure 40**)
HRMS: *not ionizable with ESI or APCI*.

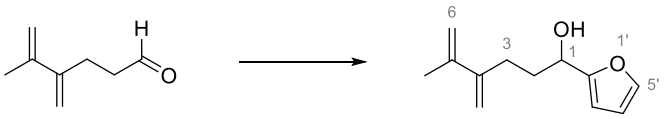

17 **14**

14: **1-(Furan-2-yl)-5-methyl-4-methylenehex-5-en-1-ol**

In a 250 mL Schlenk flask equipped with an addition funnel, dienyl aldehyde **17** (1.90 g, 15.31 mmol, 1 eq) was dissolved in THF (80 mL) and cooled to –78 °C. A freshly prepared solution of 2-lithiofuran[a] (0.84 M in THF; 18.2 mL, 15.29 mmol, 1 eq) was added dropwise (over 18 min). After 30 min, the cooling bath was removed (at –40 °C) and the reaction was quenched with saturated NH_4Cl solution (80 mL). The precipitate was dissolved with water and the mixture extracted with diethyl ether (3 × 100 mL), before the combined organic phases were washed with saturated NaCl solution (100 mL), dried over $MgSO_4$, and concentrated in vacuo (40 °C, 25 mbar). The resulting yellow oil was purified by flash chromatography (PE/DE, 6:1) to give furfuryl alcohol **14** (2.682 g, 13.95 mmol, **91%**) as a slightly yellow oil.

R_f = 0.44 (PE/DE, 2:1).
^{1}H NMR (400 MHz, $CDCl_3$): δ = 7.37 (dd, *J* = 1.8 Hz, 0.8 Hz, 1H, 5'-H), 6.33 (dd, *J* = 3.2 Hz, 1.8 Hz, 1H, 4'-H), 6.25 (br d, *J* = 3.2 Hz, 3'-H), 5.12–4.99 (m, 4H, 4-CH_2 & 6-H_2), 4.70 (t, *J* = 6.7 Hz, 1H, 1-H), 2.50–2.28 (m, 2H, 3-H_2), 2.08–1.99 (m, 2H, 2-H_2), 1.94 (br s, 1H, 1-OH), 1.91 (s, 3H, 5-CH_3).
^{13}C NMR (101 MHz, $CDCl_3$): δ = 156.6 (C2'), 147.1 (C4), 142.3 (C5'), 141.9 (C5), 112.9 (4-CH_2), 112.6 (C6), 110.1 (C4'), 105.9 (C3'), 67.5 (C1), 34.7 (C2), 29.6 (C3), 21.1 (5-CH_3). (**Figure 41**)
HRMS: calcd. for $C_{12}H_{16}NaO_2$ 215.10441 $[M+Na]^+$, found 215.10425 (Δ = 0.74 ppm).

[a]: *Preparation of 2-lithiofuran solution*: In a 25 mL flask, distilled furan[b] (1.34 mL, 18.37 mmol, 1.2 eq) was dissolved in THF (11 mL) and cooled to –78 °C. Then, *n*-BuLi (2.5 M in hexane; 6.12 mL, 15.30 mmol, 1 eq) was added dropwise (over 13 min). After 30 min, the cooling bath was replaced by an ice bath. The suspension was stirred in the ice bath (30 min) and at room temperature (30 min) to give a slightly yellow solution (max. solubility: ~0.88 M). The solution was used promptly.

[b]: *Purification of furan*: Furan was shaken with 5% aq. KOH, dried with Na_2SO_4 and distilled under nitrogen from KOH.[210] The purified furan can be stored at –28 °C for several months.

4.1.2 ACHMATOWICZ Reaction and Cycloaddition to Tricyclic Enone 9

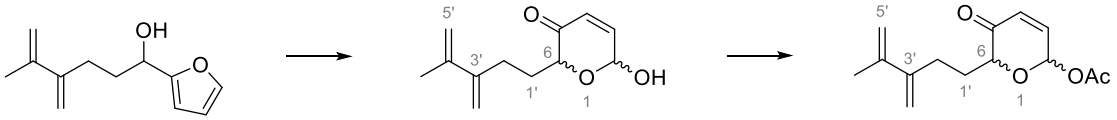

14 **13** **12**

13: **6-Hydroxy-2-(4-methyl-3-methylenepent-4-en-1-yl)-2*H*-pyran-3(6*H*)-one**

12: **6-(4-Methyl-3-methylenepent-4-en-1-yl)-5-oxo-5,6-dihydro-2*H*-pyran-2-yl acetate**

In a 250 mL flask, furfuryl alcohol **14** (1.50 g, 7.80 mmol, 1 eq) was dissolved in DCM (89 mL) and cooled in an ice bath. After addition of $VO(acac)_2$ (91 mg, 0.34 mmol, 4.4 mol%) and stirring for 10 min, *t*-BuOOH (~5.5 M in nonane; 1.84 mL, 10.14 mmol, 1.3 eq) was added dropwise (5 min). The reaction mixture was stirred in the ice bath (1.5 h) and at room temperature (4 h), before cooling in an ice bath again and adding trimethyl phosphite (0.37 mL, 3.12 mmol, 0.4 eq). After 1 h, DMAP (50 mg, 0.39 mmol, 5 mol%), pyridine (0.82 mL, 10.14 mmol, 1.3 eq) and acetic anhydride (0.89 mL, 9.36 mmol, 1.2 eq) were added sequentially. After 30 min, the reaction was quenched with a mixture of 50 mL saturated NH_4Cl solution and 10 mL water. The resulting mixture was concentrated in vacuo moderately to remove most of the DCM and subsequently extracted with ethyl acetate (3 × 60 mL). The combined organic phases were washed with saturated NaCl solution (2 × 50 mL), dried over $MgSO_4$, and concentrated in vacuo (40 °C, 25 mbar). The slightly turbid brownish oil was purified by flash chromatography (PE/DE, gradient from 10:1 to 3:1) to yield pyranulose acetate **12** (1.525 g, 6.09 mmol, **78%** (*effectively over 2 steps*); *d.r.* ≈ 1.86:1) as a slightly yellow oil.

Notes: Pyranulose acetate **12** was isolated and used as a mixture of both diastereomers in the next step. The diastereomers of **12** could be separated to an extent for analytical purposes. The NMR signals were assigned for the *major, less polar DS*. In early attempts, pyranulose **13** was isolated before acetylation to **12**, resulting in lower overall yield due to polymerization. The NMR signals of the inseparable diastereomeric mixture of **13** could not be fully assigned.

12: $\mathbf{R_f}$ = 0.65 & 0.59 (PE/DE, 1:2).
^{1}H NMR (400 MHz, $CDCl_3$, ***major, less polar DS***): δ = 6.86 (dd, *J* = 10.2 Hz, 3.7 Hz, 1H, 3-H), 6.50 (d, *J* = 3.7 Hz, 1H, 2-H), 6.18 (d, *J* = 10.2 Hz, 1H, 4-H), 5.09 (br d, *J* ≈ 7.0 Hz, 2H, 5-H_a & 3-CH_{2a}), 4.97 (br d, *J* ≈ 11 Hz, 2H, 5-H_b & 3-CH_{2b}), 4.47 (dd, *J* = 8.1 Hz, 3.6 Hz, 1H, 6-H), 2.47–2.32 (m, 2H, 2'-H_2), 2.17–2.06 (m, 1H, 1'-H_b), 2.11 (s, 3H, 2-OC(O)CH_3), 1.91–1.83 (m, 1H, 1'-H_b), 1.87 (s, 3H, 4'-CH_3). **^{13}C NMR** (101 MHz, $CDCl_3$, ***major, less polar DS***): δ = 195.6 (C5), 169.5 (2-O<u>*C*</u>(O)CH_3), 146.8 (C3'), 142.0 (C4'), 141.4 (C3), 128.7 (C4), 113.2 & 112.9 (C5' & 3'-CH_2), 87.0 (C2), 75.1 (C6), 28.8 (C1'), 28.5 (C2'), 21.0 (5-CH_3), 20.9 (2-OC(O)<u>*C*</u>H_3). (**Figure 43** & **Figure 44**)
HRMS: calcd. for $C_{14}H_{18}NaO_4$ 273.10973 $[M+Na]^+$, found 273.10994 (Δ = 0.79 ppm).

13: $\mathbf{R_f}$ = 0.46 (PE/DE, 1:2).
^{1}H NMR (400 MHz, $CDCl_3$, ***diastereomeric mixture***): δ = 6.93 (dd, *J* = 10.3 Hz, 1.5 Hz, 0.3H, 3-H) & 6.89 (d, *J* = 10.3 Hz, 3.4 Hz, 0.7H, 3-H), 6.15 (dd, *J* = 10.3 Hz, 1.6 Hz, 0.3H, 4-H) & 6.11 (br d, *J* = 10.3 Hz, 0.7H, 4-H), 5.69–5.65 (m, 1H, 2-H), 5.13 & 5.00 (2 × br s, 4H, 5'-H_2 & 3'-CH_2), 4.58 (dd,

J = 8.7 Hz, 3.6 Hz, 0.7H, 6-H) & 4.10 (ddd, *J* = 8.4 Hz, 3.8 Hz, 1.1 Hz, 6-H), 3.18 & 2.93 (2 × br s, 0.29H & 0.72H, 2-OH), 2.55–2.34 (m, 2H, 2 × 1'-H_2 *or* 2'-H_2), 2.19–2.08 (m, 1H, 1 × 1'-H_2 *or* 2'-H_2), 2.00–1.84 (m, 1H, 1 × 1'-H_2/2'-H_2), 1.90 (s, 3H, 4'-CH_3);
^{13}C NMR (101 MHz, $CDCl_3$, ***diastereomeric mixture***): δ = 196.3 & 196.0 (C5), 147.5 & 144.1 (C3), 147.1 (C3'), 142.2 (C4'), 128.9 & 127.7 (C4), 113.0 & 113.0 & 112.8 & 112.8 (4 ×, C5'/3'-CH_2), 91.0 & 87.7 (C2), 78.3 & 73.6 (C6), 29.9 & 29.1 & 28.9 & 28.9 (4 ×, C1'/C2'), 21.1 (4'-CH_3); *three 'missing' signals, most likely due to superimposition*. (**Figure 42**)

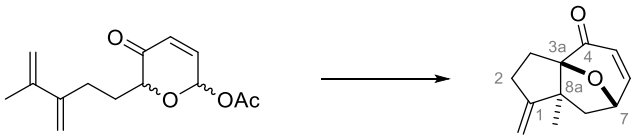

12 **9**

9: **(3a*R**,7*S**,8a*S**)-8a-Methyl-1-methylene-1,2,3,7,8,8a-hexahydro-4*H*-3a,7-epoxyazulen-4-one**[22]

Pyranulose acetate **12** (1.0 g, 3.99 mmol, 1 eq) was dissolved in acetonitrile (43 mL) in a 100 mL Schlenk flask equipped with a reflux condenser fitted with a gas inlet adapter. After addition of triethylamine (2.22 mL, 15.98 mmol, 4 eq), the mixture was heated to 90 °C for 17 h, and then concentrated in vacuo (40 °C, 25 mbar). The brown oil was purified by flash chromatography (PE/DE, gradient from 15:1 to 2:1), affording tricyclic enone **9** (564 mg, 2.97 mmol, **74%**) as a viscous oil which solidified slowly to an off-white solid (m.p. 48–51 °C).

R_f = 0.44 (PE/DE, 1:1 – *barely distinguishable from* **12** *by eluting 2–3 times*).
^{1}H NMR (400 MHz, C_6D_6): δ = 6.29 (dd, *J* = 9.7 Hz, 4.5 Hz, 1H, 6-H), 5.79 (d, *J* = 9.7 Hz, 1H, 5-H), 4.87 & 4.67 (2 × dd, *J* ≈ 2.6 Hz, 1.6 Hz, 2H, 1-CH_2), 4.18 (dd, *J* = 7.3 Hz, 4.5 Hz, 1H, 7-H), 2.68–2.50 (m, 2H, 2-H_a & 3-H_a), 2.30–2.24 (m, 1H, 2-H_b), 2.09 (dd, *J* = 12 Hz, 7.3 Hz, 1H, 8-H_a), 1.95–1.90 (m, 1H, 3-H_b), 1.38 (d, *J* = 12 Hz, 1H, 8-H_b), 0.98 (s, 3H, 8a-CH_3). **^{13}C NMR** (101 MHz, C_6D_6): δ = 195.5 (C4), 162.1 (C1), 152.1 (C6), 126.4 (C5), 107.1 (1-CH_2), 100.6 (C3a), 74.5 (C7), 53.6 (C8a), 45.1 (C8), 30.9 (C2), 26.8 (C3), 25.4 (8a-CH_3). (**Figure 45** & **Figure 46**)
HRMS: calcd. for $C_{12}H_{14}NaO_2$ 213.08860 $[M+Na]^+$, found 213.08890 (Δ = 1.40 ppm).

---

[22] The relative stereochemistry of the racemic compounds treated in this work is indicated by the addition of asterisks to stereodescriptors (*e.g.*, 3a*R**).

4.2 FUNCTIONALIZATION OF THE TRICYCLIC CORE STRUCTURE

4.2.1 Functionalization Reactions at C5 and C6

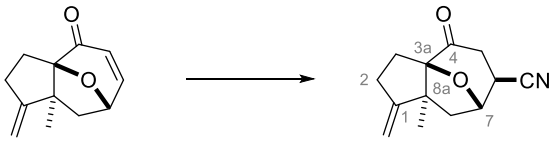

9 **8**

8: **(3a*R**,6*S**,7*S**,8a*S**)-8a-Methyl-1-methylene-4-oxooctahydro-1*H*-3a,7-epoxyazulene-6-carbonitrile**

Method A (TMSCN, then TBAF): Enone **9** (1.60 g, 8.41 mmol, 1 eq) and $LiClO_4$ (44.7 mg, 0.42 mmol, 5 mol%) were placed in a 10 mL flask. After addition of TMSCN (4.2 mL, 33.64 mmol, 4 eq), the reaction mixture was stirred at 80 °C for 4 h, and then concentrated using the vacuum pump connected to the Schlenk line, co-evaporating residual TMSCN with THF until an oily solid was obtained. Crude silyl enol ether **33** was dissolved in THF (40 mL) and transferred into a 100 mL flask. The solution was cooled to −78 °C and TBAF (1 M in THF; 2.8 mL, 2.80 mmol, 0.33 eq) was added (over 3 min). After 45 min, the reaction mixture was quenched with water (30 mL, at −30 °C) and extracted with diethyl ether (3 × 50 mL). The combined organic phases were washed with saturated NaCl solution (50 mL), dried over $MgSO_4$, and concentrated. Purification by flash chromatography (PE/EA, gradient from 10:1 to 5:1) gave ketonitrile **8** (1.80 g, 8.29 mmol, **99%**) as an off-white solid (m.p. 137 °C).

Method B (KCN/NH_4Cl): Enone **9** (951 mg, 5.00 mmol, 1 eq) was dissolved in DMF (45 mL) and water (5 mL) in a 100 mL flask (*under air*). After addition of NH_4Cl (321 mg, 6.00 mmol, 1.2 eq) and KCN (521 mg, 8.00 mmol, 1.6 eq), the mixture was stirred at room temperature for 25 h. Another portion of NH_4Cl (107 mg, 2.00 mmol, 0.4 eq) was added, the mixture was stirred in the open flask for 2 h, and then concentrated. The residue was diluted with water (50 mL) and extracted with ethyl acetate (3 × 50 mL). The combined organic phases were washed with saturated NaCl solution (25 mL), dried over $MgSO_4$, and concentrated to give a colorless solid (1.048 g, 96%) consisting of ketonitrile **8** and enone **9** (qNMR: **90%** of **8** & **5%** of unreacted **9**).

R_f = 0.56 (PE/DE, 1:1).
^{1}H NMR (400 MHz, $CDCl_3$): δ = 5.01 & 4.92 (2 × br dd, *J* ≈ 2.3–2.7 Hz, 2H, 1-CH_2), 4.74 (br dd, *J* ≈ 8.0 Hz, 1H, 7-H), 3.08 (ddd, *J* ≈ 8.6 Hz, 2.6 Hz, 1.5 Hz, 1H, 6-H), 2.86–2.81 (ddd, *J* ≈ 18.2 Hz, 2.6 Hz, 1.5 Hz, 1H, 5-H_a), 2.72–2.48 (m, 4H, 2-H_2, 5-H_b, 8-H_a), 2.32–2.23 (m, 1H, 3-H_a), 1.93–1.86 (m, 2H, 3-H_b, 8-H_b), 1.04 (s, 3H, 8a-CH_3). **^{13}C NMR** (101 MHz, $CDCl_3$): δ = 201.3 (C4), 160.0 (C1), 120.4 (4-CN), 107.6 (1-CH_2), 100.4 (C3a), 75.7 (C7), 56.4 (C8a), 45.2 (C8), 36.0 (C5), 33.8 (C6), 29.0 (C2), 25.5 (C3), 22.8 (8a-CH_3). (**Figure 49**)
HRMS: calcd. for $C_{13}H_{15}NNaO_2$ 240.09950 $[M+Na]^+$, found 240.09968 (Δ = 0.74 ppm).

Notes: In early attempts, both *O*-TMS cyanohydrin **32** and cyano silyl enol ether **33** were also isolated by flash chromatography before desilylation with TBAF.

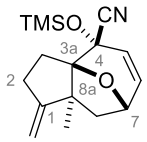

32

32: **(3a*R**,4*S**,7*S**,8a*S**)-8a-Methyl-1-methylene-4-((trimethylsilyl)oxy)-2,3,4,7,8,8a-hexahydro-1*H*-3a,7-epoxyazulene-4-carbonitrile**

R_f = 0.74 (PE/DE, 1:1).

^{1}H NMR (400 MHz, $CDCl_3$): δ = 6.06 (dd, *J* = 9.5 Hz, 3.9 Hz, 1H, 6-H), 5.65 (d, *J* = 9.5 Hz, 1H, 5-H), 4.86 & 4.79 (d × br dd, *J* ≈ 2.3–2.7 Hz, 2H, 1-CH_2), 4.55 (dd, *J* = 6.6 Hz, 3.9 Hz, 1H, 7-H), 2.74–2.63 (m, 1H, 2-H_a), 2.43–2.37 (m, 1H, 2-H_b), 2.29 (dd, *J* = 11.8 Hz, 6.7 Hz, 1H, 8-H_a), 2.11–2.02 (m, 2H, 3-H_2), 1.96 (d, *J* = 11.8 Hz, 1H, 8-H_b), 1.32 (s, 3H, 8a-CH_3), 0.27 (s, 9H, 4-OSi$(CH_3)_3$).

^{13}C NMR (101 MHz, $CDCl_3$): δ = 163.1 (C1), 135.4 (C6), 125.2 (C5), 119.8 (4-CN), 104.8 (1-CH_2), 95.0 (C3a), 75.0 (C7), 72.3 (C4), 54.8 (C8a), 51.3 (C8), 30.1 (C2), 29.0 (C3), 26.4 (8a-CH_3), 1.1 (4-OSi$(CH_3)_3$). (**Figure 47**)

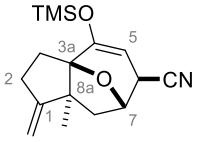

33

33: **(3a*R**,6*S**,7*S**,8a*S**)-8a-Methyl-1-methylene-4-((trimethylsilyl)oxy)-2,3,6,7,8,8a-hexahydro-1*H*-3a,7-epoxyazulene-6-carbonitrile**

R_f = 0.62 (PE/DE, 1:1).

^{1}H NMR (400 MHz, $CDCl_3$): δ = 4.94 & 4.84 (2 × dd, *J* ≈ 2.3–2.7 Hz, 2H, 1-CH_2), 4.60 (m, 2H, 5-H & 7-H), 2.92 (d, *J* ≈ 4.3 Hz, 1H, 6-H), 2.69–2.47 (m, 3H, 2-H_2 & 8-H_a), 2.18–2.10 (m, 1H, 3-H_a), 1.91–1.85 (m, 1H, 3-H_b), 1.68 (dd, *J* ≈ 12.8 Hz, 1.8 Hz, 1H, 8-H_b), 1.08 (s, 3H, 8a-CH_3), 0.25 (s, 9H, 4-OSi$(CH_3)_3$). **^{13}C NMR** (101 MHz, $CDCl_3$): δ = 160.3 (C1), 155.9 (C4), 120.2 (6-CN), 106.5 (1-CH_2), 93.3 (C3a), 91.6 (C5), 75.7 (C7), 61.8 (C8a), 46.4 (C8), 34.6 (C6), 29.4 (C2), 25.0 (C3), 23.4 (8a-CH_3), 0.1 (4-OSi$(CH_3)_3$). (**Figure 48**)

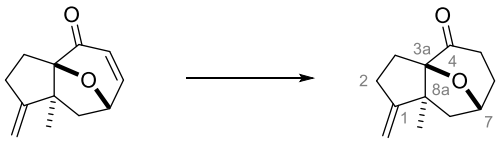

9 **8-H**

8-H: **(3a*R**,7*S**,8a*S**)-8a-Methyl-1-methyleneoctahydro-4*H*-3a,7-epoxyazulen-4-one**

Zinc chloride[a] (0.209 g, 1.53 mmol, 25 mol%) was placed in a 100 mL flask and enone **9** (1.166 g in 36 mL chloroform; 6.13 mmol, 1 eq) was added. Then, Ph_2SiH_2 (1.35 mL, 7.36 mmol, 1.2 eq) and $Pd(PPh_3)_4$ (141 mg, 0.123 mmol, 2 mol%) were added. After complete conversion, also indicated by a change of color from yellow to orange (<15 min), the solution was concentrated. The orange oil was purified by flash chromatography (PE/DE, gradient from 10:1 to 5:1), affording ketone **8-H** (1.163 g, 6.05 mmol, **99%**) as a colorless waxy solid (m.p. 42–45 °C).

R_f = 0.58 (PE/DE, 2:1 – *barely distinguishable from* **9** *by eluting 2–3 times*).
^{1}H NMR (400 MHz, $CDCl_3$): δ = 4.97 & 4.91 (2 × br dd, *J* ≈ 2.3 Hz, 2H, 1-CH_2), 4.59–4.53 (m, 1H, 7-H), 2.65–2.45 (m, 4H, 2-H_2 & 5-H_a & 8-H_a), 2.39–2.21 (m, 3H, 3-H_a & 5-H_b & 6-H_a), 1.90 (dd, *J* = 12.7 Hz, 1.7 Hz, 1H, 8-H_b), 1.86–1.74 (m, 2H, 3-H_b & 6-H_b), 1.07 (s, 3H, 8a-CH_3).
^{13}C NMR (101 MHz, $CDCl_3$): δ = 206.9 (C4), 161.6 (C1), 106.8 (1-CH_2), 99.5 (C3a), 74.7 (C7), 56.7 (C8a), 45.9 (C8), 33.5 (C5), 31.2 (C6), 29.3 (C2), 25.6 (C3), 22.7 (8a-CH_3). (**Figure 50**)
HRMS: calcd. for $C_{12}H_{16}NaO_2$ 215.10425 $[M+Na]^+$, found 215.10436 (Δ = 0.50 ppm).

Notes: [a]$ZnCl_2$ was previously fused by heating in vacuo *(150 °C, 1 mbar, several hours)* and stored under inert atmosphere. The handling was conducted in air, *allowing* the very hygroscopic $ZnCl_2$ to become slightly wet, as indicated by deliquescence.

A reduction of enone **9** using L-Selectride [THF (0.06 M), L-Selectride (1 M in THF, 1.05 eq), –78 °C to –65 °C, 15 min] resulted in the concomitant formation of dimer **34-H** (**33%**) along with the desired ketone **8-H** (**49%**). While the configuration was not determined, the depicted configuration seems the most plausible due to the *exo*-selectivity of functionalizations at C5, as became evident throughout this work.

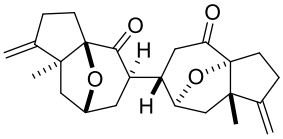

Dimer **34-H**

^{1}H NMR (400 MHz, $CDCl_3$): δ = 4.97–4.88 (m, 4H), 4.59–4.53 (m, 1H), 4.37 (d, *J* = 7.6 Hz, 1H), 2.70–1.94 (m, 17H), 1.80–1.71 (m, 2H), 1.07 (s, 6H). **^{13}C NMR**: *not recorded*. (**Figure 51**)
HRMS: calcd. for $C_{24}H_{31}O_4$ 383.22169 $[M+H]^+$, found 383.22161 (Δ = 0.21 ppm).

4.2.1.1 *C*-Acylation & Methylation at C5 and subsequent TSUJI-TROST Allylation

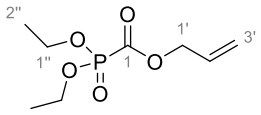

41.a

41.a: **Allyl diethylphosphonoformate (APF)**

Triethyl phosphite (8.65 mL, 50.45 mmol, 1 eq) was placed in a 50 mL flask. Allyl chloroformate (5.3 mL, 50.45 mmol, 1 eq) was added dropwise (15 min; *exothermic reaction, evolution of chloroethane gas*). After 1.5 h, residual chloroethane was removed in vacuo using the vacuum pump connected to the Schlenk line.

The prepared APF (**41.a**) (**purity: 99%**; determined by qNMR) can be stored under inert gas without loss of quality for several months.

^{1}H NMR (400 MHz, $CDCl_3$): δ = 5.94–5.84 (m, 1H, 2'-H), 5.37–5.22 (m, 2H, 3'-H_2), 4.71–4.67 (m, 2H, 1'-H_2), 4.28–4.20 (2 × br dq (*superimposed*), J ≈ 7.1 Hz, <1.0 Hz, 4H, 2 × 1''-H_2), 1.34 (br t, J ≈ 7.1 Hz, 0.6 Hz, 6H, 2 × 2''-CH_3). **^{13}C NMR** (101 MHz, $CDCl_3$): δ = 166.5 (d, $J_{C,P}$ = 269 Hz, C1), 130.6 (C2'), 119.7 (C3'), 66.1 (d, $J_{C,P}$ = 5.1 Hz, C1'), 64.4 (d, $J_{C,P}$ = 6.5 Hz, C1''), 16.2 (d, $J_{C,P}$ = 5.9 Hz, C2''). **^{31}P NMR** (162 MHz, $CDCl_3$): δ = –4.88. (**Figure 52**)

As discussed in **Chapter 2.2.1.1**, chromatographic purification of **42-H** and **42** was impeded by keto-enol tautomerism and could be omitted by implementing a *Kugelrohr* distillation instead. Doing so removed the phosphorus-based impurities, and thus, allowed for the following methylation in equal yields as with chromatographically *isolated* substrates. The procedures represent this two-step sequence and were chosen for a suitable comparison of this sequence proceeding from ketone **8-H** and ketonitrile **8**, respectively.

The yields of the ***C*-acylation** were determined to be **87%** (**8-H** to **42-H**) and **80%** (**8** to **42**). For the latter, an *adequate enolate formation* and, less obviously, *refraining from extractions with ethyl acetate* were crucial to ensure good yields. Next to the procedure for the two-step sequence, that of a more adequate acylation to **42** (with partial chromatographic separation) is given. In this case, the smaller reaction scale allowed for a more adequate enolate formation as a result of the mixture (of ketonitrile **8** and KHMDS) being able to warm to room temperature more rapidly than a similarly prepared mixture from an almost ten-fold reaction scale.

The subsequent **methylation** of *isolated* **42-H** gave **43-H** (**86%** yield) without *O*-methylation, whereas *isolated* **42** gave **43** (**75%** yield) and *OMe*-**43** (**11%** yield).

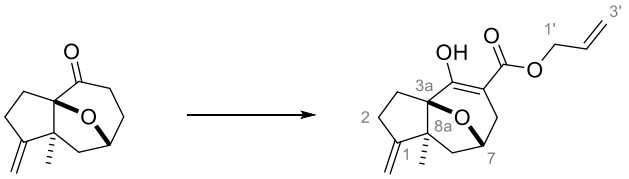

8-H **42-H**

42-H: **Allyl (3a*R**,7*S**,8a*S**)-4-hydroxy-8a-methyl-1-methylene-2,3,6,7,8,8a-hexahydro-1*H*-3a,7-epoxyazulene-5-carboxylate**

In a 50 mL Schlenk flask, a solution of ketone **8-H** (500 mg, 2.60 mmol, 1 eq) in MTBE (26 mL) was cooled to –78 °C, before KHMDS (1 M in THF; 2.86 mL, 2.86 mmol, 1.1 eq) was added dropwise (5 min). The reaction mixture was allowed to warm to –40 °C over the course of 1 h. After stirring at room temperature for 30 min, the reaction mixture was cooled to –78 °C and a solution of APF (**41.a**) in MTBE [699 mg, 3.12 mmol, 1.2 eq; *2.5 mL aliquot of a freshly prepared solution of* **41.a** *(1 mL, 1.119 g) in 3 mL MTBE*] was added dropwise (2 min 45 s). The reaction mixture was allowed to warm to –10 °C over the course of 3 h, then stirred at room temperature for 19 h. The resulting yellow solution was quenched with half-saturated NH_4Cl solution (50 mL) and extracted with ethyl acetate (3 × 50 mL). The combined organic phases were dried over $MgSO_4$, filtered, and concentrated [*rotary evaporator*, then *Kugelrohr* (120 °C, 5 mbar, 1 h)]. The slightly yellow oil (745 mg) was used for the preparation of **43-H** without further purification.

R_f = 0.84 (PE/DE, 1:1).
^{1}H NMR (400 MHz, $CDCl_3$): δ = 12.03 (br s, 1H, 4-OH), 5.98–5.89 (m, 1H, 2'-H), 5.31 (ddd, *J* = 17.2 Hz, 3.0 Hz, 1.5 Hz, 1H, 3'-H_a), 5.23 (ddd, *J* = 10.4 Hz, 2.6 Hz, 1.3 Hz, 1H, 3'-H_b), 4.93 & 4.85 (2 × br dd, *J* ≈ 2.0–2.5 Hz, 2H, 1-CH_2), 4.71–4.60 (m, 2H, 1'-H_2), 4.58–4.55 (m, 1H, 7-H), 2.80 (ddd, *J* = 15.5 Hz, 5.4 Hz, 1.0 Hz, 1H, 6-H_a), 2.72–2.50 (m, 3H, 2-H_2 & 8-H_a), 2.35–2.25 (m, 1H, 3-H_a), 2.01 (d, *J* = 15.5 Hz, 1H, 6-H_b), 1.91 (ddd, *J* = 14.0 Hz, 8.5 Hz, 1.8 Hz, 1H, 3-H_b), 1.71 (dd, *J* = 12.5 Hz, 1.7 Hz, 1H, 8-H_b), 1.13 (s, 3H, 8a-CH_3).
^{13}C NMR (101 MHz, $CDCl_3$): δ = 172.3 (C4 *or 5-<u>C</u>OOallyl*), 172.1 (5-<u>C</u>OOallyl *or C4*), 160.8 (C1), 132.0 (C2'), 118.0 (C3'), 106.3 (1-CH_2), 93.1 (C4), 91.9 (C3a), 74.2 (C7), 64.8 (C1'), 62.7 (C8a), 47.6 (C8), 31.5 (C6), 29.6 (C2), 24.9 (C3), 23.5 (8a-CH_3). (**Figure 53**)
HRMS: calcd. for $C_{16}H_{21}O_4$ 277.14344 $[M+H]^+$, found 277.14367 (Δ = 0.83 ppm).

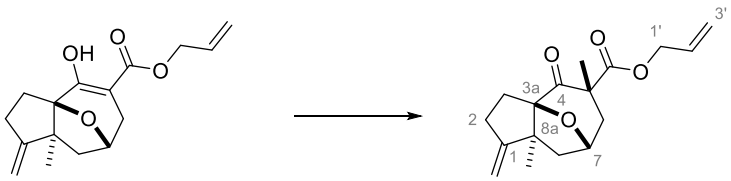

42-H **43-H**

43-H: **Allyl (3a*R**,5*S**,7*S**,8a*S**)-5,8a-dimethyl-1-methylene-4-oxooctahydro-1*H*-3a,7-epoxyazulene-5-carboxylate**

Enol **42-H** (572 of 745 mg *crude substrate*, "2.07 mmol," 1 eq) and Cs_2CO_3 (1.349 g, 4.14 mmol, 2 eq) were placed in a 25 mL flask. Acetone (6.9 mL) was added, and the suspension stirred for 30 min. Then, iodomethane (0.26 mL, 4.14 mmol, 2 eq) was added and the syringe connected to the Schlenk line removed from the flask's septum to prevent evaporation of iodomethane. The

reaction mixture was stirred for 3 h and filtered through a pad of Celite, eluting with ethyl acetate (125 mL). The filtrate was concentrated and the slightly yellow oil purified by flash chromatography (PE/DE, gradient from 20:1 to 2.5:1) to give ketone **8-H** (29 mg, 0.15 mmol, 8% recovered) and α-methyl β-ketoester **43-H** [439 mg, 1.51 mmol, **76%** over 2 steps (80% *b.r.s.m.*)] as a colorless oil.

R_f = 0.55 [**R_f** (**42-H**) = 0.74] (PE/DE, 3:1).
^{1}H NMR (400 MHz, $CDCl_3$): δ = 5.92–5.83 (m, 1H, 2'-H), 5.31 (ddd, *J* = 17.2 Hz, 2.9 Hz, 1.5 Hz, 1H, 3'-H_a), 5.22 (ddd, *J* = 10.4 Hz, 2.5 Hz, 1.2 Hz, 1H, 3'-H_b), 4.92 & 4.86 (2 × br dd, *J* ≈ 2.0–2.3 Hz, 2H, 1-CH_2), 4.66–4.58 (m, 3H, 1'-H_2 & 7-H), 2.67–2.45 (m, 3H, 2-H_2 & 8-H_a), 2.35–2.18 (m, 3H, 6-H_2 & 3-H_a), 1.92 (dd, 1H, *J* = 12.6 Hz, 1.5 Hz, 1H, 8-H_b), 1.79 (ddd, 1H, *J* = 13.8 Hz, 8.1 Hz, 1.8 Hz, 1H, 3-H_b), 1.55 (s, 3H, 5-CH_3), 1.11 (s, 3H, 8a-CH_3).
^{13}C NMR (101 MHz, $CDCl_3$): δ = 208.1 (C4), 172.4 (5-*C*OOallyl), 161.2 (C1), 131.6 (C2'), 118.5 (C3'), 106.3 (1-CH_2), 99.5 (C3a), 73.0 (C7), 66.1 (C1'), 57.4 (C8a), 53.5 (C5), 48.7 (C8), 39.0 (C6), 30.0 (C2), 27.8 (C3), 26.6 (5-CH_3), 23.6 (8a-CH_3). (**Figure 55**)
HRMS: calcd. for $C_{17}H_{23}O_4$ 291.15909 $[M+H]^+$, found 294.15912 (Δ = 0.13 ppm).

8 **42**

42: **Allyl (3a*R**,6*S**,7*S**,8a*S**)-6-cyano-4-hydroxy-8a-methyl-1-methylene-2,3,6,7,8,8a-hexahydro-1*H*-3a,7-epoxyazulene-5-carboxylate**

In a 250 mL Schlenk flask, a solution of ketonitrile **8** (2.003 g, 9.22 mmol, 1 eq) in MTBE (103 mL) was cooled to –78 °C, before KHMDS (1 M in THF; 9.7 mL, 9.70 mmol, 1.05 eq) was added dropwise (5 min). The reaction mixture was allowed to warm to –20 °C over the course of 1.5 h. After stirring at room temperature for 20 min, the reaction mixture was cooled to –78 °C again and a solution of APF (**41.a**) in MTBE [2.46 g, 1.2 eq; *8.8 mL aliquot of a freshly prepared solution of* **41.a** *(5 mL, 5.587 g) in 15 mL MTBE*] was added dropwise (2 min 45 s). The reaction mixture was allowed to warm to 12 °C over the course of 10 h, then stirred at room temperature for another hour. The orange suspension was quenched with half-saturated NH_4Cl solution (150 mL) and extracted with petroleum ether (2 × 100 mL). Notably, an undetermined amount of unreacted ketonitrile remained in the aqueous phase. The combined organic phases were dried over $MgSO_4$, filtered, and concentrated [*rotary evaporator*, then *Kugelrohr* (120 °C, 5 mbar, 1 h)]. The residue was filtered through a pad of silica gel, eluting with diethyl ether (150 mL), to give a very viscous orange oil (2.131 g) which was used for the preparation of **43**.

Alternative procedure with adequate enolate formation and partial chromatographic separation: In a 25 mL flask, a solution of ketonitrile **8** (207 mg, 0.953 mmol, 1 eq) in MTBE (10 mL) was cooled to –78 °C, before KHMDS (1 M in THF; 1.0 mL, 1.0 mmol, 1.05 eq) was added dropwise (5 min). The reaction mixture was allowed to warm to 0 °C over the course of 1.25 h. After stirring at room temperature for 20 min, the reaction mixture was cooled to –78 °C again

and a solution of APF (**41.a**) in MTBE [254 mg, 1.2 eq; *0.88 mL aliquot of a freshly prepared solution of* **41.a** *(0.5 mL, 561 mg) in 1.5 mL MTBE*] was added dropwise (2 min 30 s). The reaction mixture was allowed to warm to 12 °C over the course of 11 h, then stirred at room temperature for 2 h. The orange suspension was quenched with half-saturated NH_4Cl solution (20 mL) and extracted with diethyl ether (3 × 20 mL). The combined organic phases were dried over $MgSO_4$, filtered, and concentrated in vacuo. The residual orange oil was purified by flash chromatography (PE/DCM/MeOH, gradient from 10:1:0.01 to 1:1:0.01), affording cyano enol **42** (169 mg, 0.561 mmol, **59%**) as a slightly yellow viscous oil. Additionally, a mixed fraction of **42** and **8** was obtained, also as a slightly yellow viscous oil (64 mg, NMR-ratio of **42**/**8** = 1:0.17). With this mixed fraction, the yield of cyano enol **42** can be quantified as **80%**.

$\mathbf{R_f}$ = 0.84 (PE/DE, 1:1).
^{1}H NMR (400 MHz, $CDCl_3$): δ = 12.40 (br s, 1H, 4-OH), 6.02–5.92 (m, 1H, 2'-H), 5.42 (ddd, *J* = 17.2 Hz, 2.9 Hz, 1.5 Hz, 1H, 3'-H_a), 5.30 (ddd, *J* = 10.5 Hz, 2.5 Hz, 1.2 Hz, 1H, 3'-H_b), 4.98 & 4.88 (2 × br dd, *J* ≈ 2.0–2.5 Hz, 2H, 1-CH_2), 4.84–4.67 (m, 2H, 1'-H_2) *superimposed with* 4.74 (br dd, *J* ≈ 8.2 Hz, 1.4 Hz, 1H, 7-H), 3.20 (d, *J* ≈ 0.7 Hz, 1H, 6-H), 2.73–2.54 (m, 3H, 2-H_2 & 8-H_a), 2.37–2.28 (m, 1H, 3-H_a), 2.02 (ddd, *J* ≈ 14.1 Hz, 8.3 Hz, 2.0 Hz, 1H, 3-H_b), 1.70 (dd, *J* = 13.1 Hz, 2.0 Hz, 1H, 8-H_b), 1.10 (s, 3H, 8a-CH_3). **^{13}C NMR** (101 MHz, $CDCl_3$): δ = 174.9 (C4), 170.4 (5-*C*OOallyl), 159.1 (C1), 131.1 (C2'), 119.5 (6-CN), 119.0 (C3'), 107.2 (1-CH_2), 92.5 (C5), 90.2 (C3a), 76.4 (C7), 65.8 (C1'), 62.4 (C8a), 45.4 (C8), 33.5 (C6), 29.2 (C2), 24.5 (C3), 23.2 (8a-CH_3). (**Figure 54**)
HRMS: calcd. for $C_{17}H_{19}NNaO_4$ 324.12063 $[M+Na]^+$, found 324.12074 (Δ = 0.35 ppm).

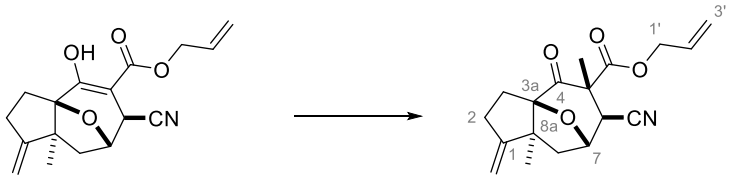

42 **43**

43: **Allyl (3a*R**,5*S**,6*S**,7*S**,8a*S**)-6-cyano-5,8a-dimethyl-1-methylene-4-oxooctahydro-1*H*-3a,7-epoxyazulene-5-carboxylate**

Cyano enol **42** (2.078 of 2.131 g *crude substrate*, "6.90 mmol," 1 eq) and Cs_2CO_3 (3.372 g, 10.34 mmol, 1.5 eq) were placed in a 100 mL flask. Acetone (35 mL) was added, and the suspension stirred for 10 min. Then, iodomethane (1.27 mL, 31.02 mmol, 3 eq) was added and the syringe connected to the Schlenk line removed from the septum to prevent iodomethane from evaporating. The reaction mixture was stirred for 15.5 h, quenched with half-saturated NH_4Cl solution (35 mL), and extracted with diethyl ether (3 × 100 mL). The combined organic phases were washed with saturated NaCl solution (50 mL), dried over $MgSO_4$, and concentrated in vacuo to give an orange oil (2.096 g). The yield was determined by quantitative NMR:

- α-methyl β-ketoester **43**: **46%** over 2 steps;
- *O*-methyl enol *OMe*-**43**: 8% over 2 steps; unreacted ketonitrile **8**: 7%.

Chromatographic separation of these compounds was typically conducted with eluent mixtures of PE/DE (gradients from 10:1 to 1.5:1).

R_f = 0.70 [**R_f** (**42**) = 0.63] [**R_f** (*OMe*-**43**) = 0.40] (PE/EA, 4:1; *eluted twice*).
^{1}H NMR (700 MHz, $CDCl_3$): δ = 5.92–5.87 (m, 1H, 2'-H), 5.36 (br ddd, *J* ≈ 17.2 Hz, 2.8 Hz, 1.4 Hz, 1H, 3'-H_a), 5.27 (br ddd, *J* ≈ 10.4 Hz, 2.4 Hz, 1.2 Hz, 1H, 3'-H_b), 4.95 & 4.87 (2 × br dd, *J* ≈ 1.7–2.5 Hz, 2H, 1-CH_2), 4.81 (br dd, *J* ≈ 7.3 Hz, 1.8 Hz, 1H, 7-H), 4.68 (br ddd, *J* ≈ 5.6 Hz, 2.9 Hz, 1.5 Hz, 2H, 1'-H_2), 3.66 (d, *J* = 1.8 Hz, 1H, 6-H), 2.64–2.58 (m, 1H, 2-H_a), 2.55 (dd, *J* = 13.1 Hz, 7.3 Hz, 1H, 8-H_a), 2.50 (br ddd, *J* ≈ 16.4 Hz, 8.8 Hz, 1.5 Hz, 1H, 2-H_b), 2.29–2.24 (m, 1H, 3-H_a), 2.00 (dd, *J* = 13.1 Hz, 0.9 Hz, 1H, 8-H_b), 1.85 (ddd, *J* = 13.8 Hz, 8.0 Hz, 1.4 Hz, 1H, 3-H_b), 1.81 (s, 3H, 5-CH_3), 1.08 (s, 3H, 8a-CH_3).
^{13}C NMR (176 MHz, $CDCl_3$): δ = 204.2 (C4), 169.5 (5-*C*OOallyl), 159.7 (C1), 131.0 (C2'), 119.2 (C3'), 117.9 (6-CN), 106.9 (1-CH_2), 100.4 (C3a), 76.8 (C7), 67.1 (C1'), 56.5 (C8a), 55.2 (C5), 49.6 (C8), 39.0 (C6), 30.3 (C2), 28.4 (C3), 23.8 (8a-CH_3), 22.0 (5-CH_3). (**Figure 56**)
HRMS: calcd. for $C_{18}H_{21}NNaO_4$ 338.13628 $[M+Na]^+$, found 338.13629 (Δ = 0.02 ppm).

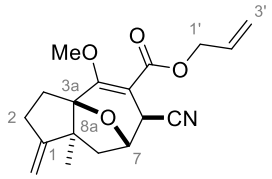

OMe-**43**

OMe-**43**: **Allyl (3a*R**,6*S**,7*S**,8a*S**)-6-cyano-4-methoxy-8a-methyl-1-methylene-2,3,6,7,8,8a-hexahydro-1*H*-3a,7-epoxyazulene-5-carboxylate**

^{1}H NMR (700 MHz, $CDCl_3$): δ = 6.00–5.94 (m, 1H, 2'-H), 5.38 (ddd, *J* = 17.2 Hz, 2.8 Hz, 1.3 Hz, 1H, 3'-H_a), 5.27 (ddd, *J* = 10.3 Hz, 2.5 Hz, 1.1 Hz, 1H, 3'-H_b), 4.94 & 4.85 (2 × br dd, *J* ≈ 2.1–2.4 Hz, 2H, 1-CH_2), 4.73–4.67 (m, 3H, 1'-H_2 & 7-H), 3.85 (s, 3H, 4-OCH_3), 3.20 (s, 1H, 6-H), 2.69–2.63 (m, 1H, 2-H_a), 2.57–2.52 (m, 2H, 2-H_b & 8-H_a), 2.34–2.29 (m, 1H, 3-H_a), 1.97 (ddd, *J* ≈ 13.8 Hz, 8.6 Hz, 1.5 Hz, 1H, 3-H_b), 1.68 (dd, *J* = 13.1 Hz, 2.0 Hz, 1H, 8-H_b), 1.06 (s, 3H, 8a-CH_3).
^{13}C NMR (176 MHz, $CDCl_3$): δ = 169.9 (C4), 163.9 (5-*C*OOallyl), 159.5 (C1), 131.6 (C2'), 119.5 (6-CN), 119.0 (C3'), 106.9 (1-CH_2), 99.4 (C5), 93.5 (C3a), 75.5 (C7), 65.8 (C1'), 62.9 (C8a), 45.7 (C8), 36.6 (C6), 29.5 (C2), 25.1 (C3), 23.4 (8a-CH_3). (**Figure 57**)
HRMS: calcd. for $C_{18}H_{21}NNaO_4$ 338.13628 $[M+Na]^+$, found 338.13631 (Δ = 0.08 ppm).

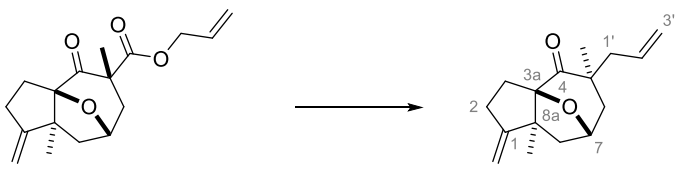

43-H **7-H**

7-H: **(3a*R**,5*S**,7*S**,8a*S**)-5-Allyl-5,8a-dimethyl-1-methylene-octahydro-4*H*-3a,7-epoxyazulene-4-one**

A solution of palladium catalyst was prepared by dissolving $Pd_2(dba)_3{\cdot}CHCl_3$ (89.1 mg, 0.097 mmol) and dppf (119.4 mg; 0.215 mmol) in DCM (19 mL) and stirring the resulting solution for 1.5 h. In a separate 100 mL flask, **43-H** (1.00 g, 3.44 mmol, 1 eq) was dissolved in

DCM (55 mL). An aliquot of the palladium catalyst solution (~1 mol% [Pd_2], *7.6 mL aliquot of 19 mL catalyst solution*) was added and the reaction mixture stirred for 2 h, before being concentrated in vacuo. The residual red oil was purified by flash chromatography (PE/DE, gradient from 20:1 to 1:1) to give ketone **7-H** (765 mg, 3.11 mmol, **90%**) as a colorless oil.

R_f = 0.73 [**R_f** (**43-H**) = 0.60] (PE/DE, 3:1; *eluted twice*).
^{1}H NMR (400 MHz, $CDCl_3$): δ = 5.73–5.61 (m, 1H, 2'-H), 5.05–5.01 (m, 2H, 3'-H_2), 4.92 & 4.86 (2 × br dd, *J* ≈ 2.5 Hz, 1.7 Hz, 2H, 1-CH_2), 4.55 (br dd, *J* ≈ 8.7 Hz, 7.4 Hz ,1H, 7-H), 2.64–2.51 (m, 1H, 2-H_a), 2.48–2.33 (m, 5H, 1'-H_2 & 2-H_b & 6-H_a & 8-H_a), 2.31–2.20 (m, 1H, 3-H_a), 1.75–1.67 (m, 2H, 3-H_b & 8-H_b), 1.27 (dd, *J* = 14.3 Hz, 1.7 Hz, 1H, 6-H_b), 1.06 (s, 3H, 5-CH_3), 1.00 (s, 3H, 8a-CH_3).
^{13}C NMR (101 MHz, $CDCl_3$): δ = 214.0 (C4), 161.4 (C1), 133.6 (C2'), 118.3 (C3'), 105.8 (1-CH_2), 99.6 (C3a), 73.3 (C7), 56.7 (C8a), 50.1 (C8), 46.7 (C1'), 44.5 (C5), 38.9 (C6), 30.4 (C2), 27.7 (C3), 24.6 (8a-CH_3), 24.1 (5-CH_3). (**Figure 58**)
HRMS: calcd. for $C_{16}H_{22}NaO_2$ 269.15120 $[M+Na]^+$, found 269.15121 (Δ = 0.04 ppm).

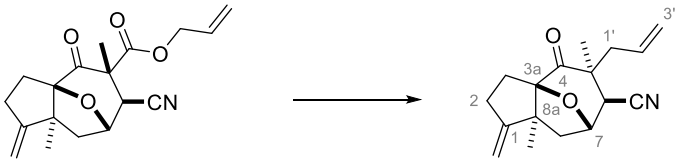

43 **7**

7: **(3a*R**,5*S**,6*S**,7*S**,8a*S**)-5-Allyl-5,8a-dimethyl-1-methylene-4-oxooctahydro-1*H*-3a,7-epoxyazulene-6-carbonitrile**

Cyano allyl ester **43** (927 mg, 2.94 mmol, 1 eq) was dissolved in DCM (65 mL) in a 100 mL flask. The solution was degassed by briefly applying vacuum using the vacuum pump connected to the Schlenk line and purging with argon (*repeated 3 times*). After addition of $Pd(PPh_3)_4$ (34.0 mg, 0.029 mmol, 1 mol%) the reaction mixture was stirred for 2.5 h and then concentrated in vacuo. The residual orange turbid oil was purified by flash chromatography (PE/DE, gradient from 3:1 to 1:1) to give ketonitrile **7** (784 mg, 2.89 mmol, **98%**) as a colorless oil.

R_f = 0.35 (PE/EA, 5:1 – *barely distinguishable from* **43** *by eluting 2–3 times*).
^{1}H NMR (400 MHz, $CDCl_3$): δ = 5.64–5.54 (m, 1H, 2'-H_2), 5.07–5.04 (m, 2H, 3'-H_2), 4.93 & 4.83 (2 × br dd, *J* ≈ 2.6 Hz, 1.5 Hz, 2H, 1-CH_2), 4.78 (br dd, *J* ≈ 6.8 Hz, 2.3 Hz, 1H, 7-H), 3.05 (br dd, *J* ≈ 13.7 Hz, 7.7 Hz, 1H, 1'-H_a), 2.64–2.54 (m, 1H, 2-H_a) *superimposed with* 2.63 (d, *J* = 2.3 Hz, 1H, 6-H), 2.52–2.41 (m, 3H, 2-H_b & 8-H_a & 1'-H_b), 2.24–2.14 (m, 1H, 3-H_a), 1.83–1.74 (m, 1H, 3-H_b) *superimposed with* 1.83 (d, *J* = 12.7 Hz, 1H, 8-H_b), 1.18 (s, 3H, 5-CH_3), 1.00 (s, 3H, 8a-CH_3).
^{13}C NMR (101 MHz, $CDCl_3$): δ = 209.1 (C4), 160.0 (C1), 132.4 (C2'), 118.8 (C3'), 118.7 (6-CN), 106.5 (1-CH_2), 100.8 (C3a), 76.7 (C7), 56.1 (C8a), 51.1 (C8), 47.1 (C5), 42.9 (C1'), 42.7 (C6), 30.7 (C2), 28.3 (C3), 24.9 (8a-CH_3), 21.4 (5-CH_3). (**Figure 59**)
HRMS: calcd. for $C_{17}H_{21}NNaO_2$ 294.14645 $[M+Na]^+$, found 294.14670 (Δ = 0.86 ppm).

4.2.2 Transformation of the *exo*-Methylidene to a Methyl Ester

The reaction sequence is listed as a series of general procedures, exemplified on the sequence proceeding from allyl α-methyl β-ketoester **43-H**. Significant deviations from these general procedures are remarked in the notes for the respective products.

4.2.2.1 Epoxidation of the *exo*-Methylidene

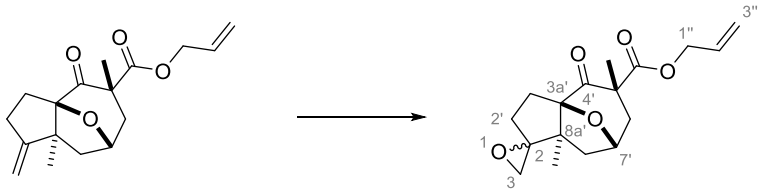

43-H **49-H**

49-H: **Allyl (3a'*R**,5'*S**,7'*S**,8a'*S**)-5'8a'-dimethyl-4'-oxooctahydrospiro[oxirane-2,1'-[3a,7]epoxyazulene]-5'-carboxylate**

❖ **General procedure for the epoxidation of the *exo*-methylidene group:**

β-Ketoester **43-H** (1.078 g, 3.713 mmol, 1 eq) was dissolved in DCM (19 mL) in a 25 mL flask. After cooling the solution in an ice bath, *m*-CPBA (≤77%, 998 mg, 3.428 mmol, ~1.2 eq) was added in portions (10 portions over the course of 10 min). The reaction mixture was allowed to warm to room temperature and stirred for 19 h, before the resulting suspension was added to a stirring mixture of saturated solutions of $Na_2S_2O_3$ (25 mL) and $NaHCO_3$ (25 mL). The emulsified phases were diluted with water (20 mL) and extracted with DCM (3 × 50 mL). The combined organic phases were dried over $MgSO_4$, filtered, and concentrated in vacuo. Purification by flash chromatography (PE/DE, gradient from 10:1 to 1:3) afforded epoxide **49-H** as two separately isolated colorless oils. The two fractions amounted to 921 mg of a *diastereomeric mixture* (*d.r.* = 1.21:1) and 134 mg of the *major, less polar DS* (*in total* 1.055 g, 3.444 mmol, **93%**; *d.r.* ≈ 1.65:1).

R_f = 0.16 [**R_f** (**43-H**) = 0.44] (PE/DE, 3:1).
^{1}H NMR (400 MHz, $CDCl_3$; ***major, less polar DS***): δ = 5.90–5.80 (m, 1H, 2''-H), 5.29 (br d, *J* ≈ 17.3 Hz, 1H, 3''-H_a) & 5.20 (br d, *J* ≈ 10.4 Hz, 1H, 3''-H_b), 4.63–4.57 (m, 3H, 7'-H & 1''-CH_2), 2.71 & 2.55 (2 × d, *J* = 4.4 Hz, 2H, 3-H_2), 2.46–2.14 (m, 5H, 2'-H_a & 3'-H_2 & 6'-H_2 & 8'-H_a), 1.86–1.95 (m, 2H, 2'-H_b & 3-H_b), 1.52 (s, 3H, 5'-CH_3), 1.39 (dd, *J* = 12.6 Hz, 1.7 Hz, 1H, 8'-H_b), 1.00 (s, 3H, 8a'-CH_3).
^{13}C NMR (101 MHz, $CDCl_3$; ***major, less polar DS***): δ = 207.8 (C4'), 172.5 (5'-*C*OOallyl), 131.5 (C2''), 118.6 (C3''), 98.8 (C3a'), 73.7 (C7'), 69.0 (C2), 66.0 (C1''), 55.3 (C8a'), 53.2 (C5'), 47.3 (C3), 40.1 (C6'), 39.1 (C8'), 29.7 (C2'), 26.8 (5'-CH_3), 26.3 (C3'), 19.0 (8a'-CH_3). (**Figure 60**)

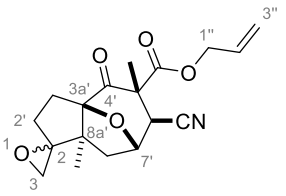

49

49: **Allyl (3a'*R**,5'*R**,6'*S**,7'*S**,8a'*S**)-6'-cyano-5',8a'-dimethyl-4'-oxooctahydrospiro[oxirane-2,1'-[3a,7]epoxyazulene]-5'-carboxylate**

Prepared from **43**: **91%** yield (96% *b.r.s.m.*; *d.r.* ≈ 1:1).

R_f = 0.41 [**R_f** (**43**) = 0.67] (PE/EA, 2:1).
^{1}H NMR (400 MHz, $CDCl_3$; ***more polar DS***): δ = 5.95–5.86 (m, 1H, 2''-H), 5.37 (dd, *J* = 17.2 Hz, 1.4 Hz, 1H, 3''-H_a) & 5.28 (dd, *J* = 10.5 Hz, 1.2 Hz, 1H, 3''-H_b), 4.84 (dd, *J* = 6.5 Hz, 2.4 Hz, 1H, 7'-H), 4.70 (dd, *J* = 5.8 Hz, 1.2 Hz, 2H, 1''-CH_2), 3.69 (d, *J* = 2.4 Hz, 1H, 6'-H), 2.84 & 2.62 (2 × d, *J* = 4.3 Hz, 2H, 3-H_2), 2.51–2.34 (m, 3H, 2'-H_a & 3'-H_a & 8'-H_a), 1.89–1.80 (m, 2H, 2'-H_b & 8'-H_b) *superimposed with* 1.85 (s, 3H, 5'-CH_3), 1.63–1.58 (m, 1H, 3'-H_b), 0.83 (s, 3H, 8a'-CH_3).
^{13}C NMR (101 MHz, $CDCl_3$; ***more polar DS***): δ = 203.1 (C4'), 169.2 (5'-*C*OOallyl), 131.0 (C2''), 119.2 (C3''), 117.7 (6'-CN), 99.6 (C3a'), 76.9 (C7'), 69.7 (C2), 67.2 (C1''), 55.9 (C8a'), 53.5 (C5'), 48.2 (C3), 47.9 (C8'), 37.6 (C6'), 30.4 (C3'), 28.5 (C2'), 21.6 (5'-CH_3), 18.3 (8a'-CH_3). (**Figure 61**)

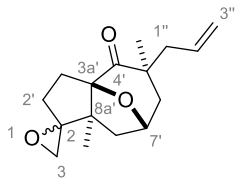

46-H

46-H: **(3a'*R**,5'*S**,7'*S**,8a'*S**)-5'-Allyl-5',8a'-dimethylhexahydrospiro[oxirane-2,1'-[3a,7]-epoxyazulen]-4'(5'*H*)-one**

Prepared from **7-H**: **64%** yield (*d.r.* ≈ 1.5:1).
Prepared from **49-H**: **82%** yield [by TSUJI-TROST allylation (0.05 M THF, $Pd_2(dba)_3{\cdot}CHCl_3$ (2 mol%), dppp (5 mol%), 0 °C to rt, 3.5 h)].

R_f = 0.40 [**R_f** (**7-H**) = 0.78] [**R_f** (**49-H**) = 0.22] (PE/DE, 2:1).
^{1}H NMR (400 MHz, $CDCl_3$; ***diastereomeric mixture***): δ = 5.74–5.62 (m, 1H, 2''-H), 5.08–4.99 (m, 2H, 3''-H_2), 4.63–4.55 (m, 1H, 7'-H), 2.79 & 2.70 & 2.59 (3 x d, *J* = 4.4 Hz, 2H, 3-H_2), 2.50–2.15 (m, alkyl-H), 1.98–1.69 (m, alkyl-H), 1.56–1.48 (m, alkyl-H), 1.33–1.14 (m, alkyl-H), 1.09 & 1.03 (2 × s, 3H, 5'-CH_3), 0.92 & 0.73 (2 × s, 3H, 8a'-CH_3).
^{13}C NMR (101 MHz, $CDCl_3$; ***diastereomeric mixture***): δ = 214.0, 212.9, 133.5, 133.4, 118.4, 99.2, 98.7, 74.0, 73.3, 70.1, 69.2, 54.4, 53.5, 48.5, 48.4, 48.3, 47.1, 46.1, 44.9, 44.6, 41.0, 39.9, 37.3, 30.6, 29.9, 27.8, 26.0, 25.0, 22.7, 20.4, 19.2. (**Figure 62**)

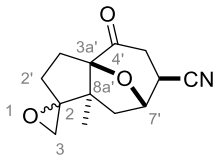

50

50: **(3a'*R**,6'*S**,7'*S**,8a'*S**)-8a'-Methyl-4'-oxooctahydrospiro[oxirane-2,1'-[3a,7]epoxyazulene]-6'-carbonitrile**

Prepared from **8**: **87%** yield (*d.r.* ≈ 1.5:1).

R_f = 0.30 [**R_f** (**8**) = 0.53] (PE/EA, 1:1).
^{1}H NMR (400 MHz, $CDCl_3$; ***minor, less polar DS***): δ = 4.82 (d, *J* = 7.3 Hz, 1H), 3.03–2.99 (m, 1H), 2.93–2.85 (m, 2H), 2.74–2.68 (m, 2H), 2.50–2.34 (m, 3H), 1.91–1.86 (m, 1H), 1.75–1.70 (m, 1H), 1.66 (dd, *J* = 13.7 Hz, 1.4 Hz, 1H), 0.86 (s, 3H).
^{13}C NMR (101 MHz, $CDCl_3$; ***minor, less polar DS***): δ = 201.5, 120.3, 100.0, 76.2, 70.2, 53.0, 50.2, 44.5, 36.2, 31.9, 30.0, 25.8, 17.7. (**Figure 63**)

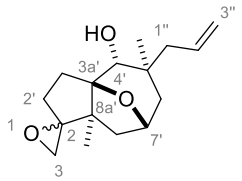

55-H

55-H: **(3a'*R**,4'*R**,5'*S**,7'*R**,8a'*S**)-5'-Allyl-5',8a'-dimethyloctahydrospiro[oxirane-2,1'-[3a,7]-epoxyazulen]-4'-ol**

Prepared from **54-H**: **79%** yield (82% *b.r.s.m.*; *d.r.* ≈ 3.6:1).

R_f = 0.27 & 0.21 [**R_f** (**54-H**) = 0.66] (PE/DE, 1:1).
^{1}H NMR (400 MHz, $CDCl_3$; ***major, more polar DS***): δ = 5.99–5.88 (m, 1H, 2''-H), 5.13–5.06 (m, 2H, 3''-H_2), 4.25–4.20 (m, 1H, 7'-H), 3.81 (d, *J* = 3.5 Hz, 1H, 4'-H), 2.66 & 2.46 (2 × d, *J* = 4.4 Hz, 2H, 3-H_2), 2.38–2.23 (m, 2H, 2'-H_a & 3'-H_a), 2.15–2.03 (m, 2H, 1''-H_2), 1.96–1.87 (m, 2H, 6'-H_a & 8'-H_a), 1.83–1.75 (m, 3H, 2'-H_a & 3'-H_a & OH), 1.62–1.52 (m, 2H, 6'-H_b & 8'-H_b), 1.27 (s, 3H, 5'-CH_3), 1.25 (s, 3H, 8a'-CH_3).
^{13}C NMR (101 MHz, $CDCl_3$; ***major, more polar DS***): δ = 135.7 (C2''), 117.9 (C3''), 92.6 (C3a'), 78.4 (C4'), 75.1 (C7'), 70.6 (C2), 52.5 (C1''), 51.5 (C8a'), 46.4 (C3), 44.4 (C6'), 37.2 (C5'), 34.8 (C8'), 28.0 (C2' or C3'), 27.9 (C2' or C3'), 23.5 (5'-CH_3), 17.8 (8a'-CH_3). (**Figure 64**)

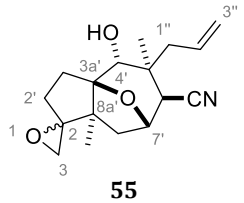

55

55: **(3a'*R**,4'*R**,5'*S**,6'*S**,7'*S**,8a'*S**)-5'-Allyl-4'-hydroxy-5',8a'-dimethyloctahydrospiro[oxirane-2,1'-[3a,7]epoxyazulene]-6'-carbonitrile**

Prepared from **54**: **77%** yield (87% *b.r.s.m.*; *d.r.* ≈ 2.9:1).

Adjusted procedure: DCM (0.05 M), *m*-CPBA (1.2 eq), $NaHCO_3$ (2 eq), 0 °C to 10 °C (3 h), rt (2 h)

$\mathbf{R_f}$ = 0.28 [$\mathbf{R_f}$ (**54**) = 0.65] (PE/EA, 2:1).
^{1}H NMR (400 MHz, $CDCl_3$; ***major, more polar DS***): δ = 6.03–5.92 (m, 1H, 2''-H), 5.32–5.19 (m, 2H, 3''-H_2), 4.49 (d, *J* = 8.4 Hz, 1H, 7'-H), 3.91 (s, 1H, 4'-H), 2.71 (m, 2H), 2.57–2.28 (m, 5H), 2.08–2.03 (m, 2H), 1.95–1.82 (m, 2H), 1.72–1.68 (dd, *J* = 13.4 Hz, 1.8 Hz, 1H), 1.38 (s, 3H), 1.26 (s, 3H). **^{13}C NMR** (101 MHz, $CDCl_3$; ***major, more polar DS***): δ = 133.9, 120.2, 119.9, 93.5, 76.8, 76.8, 70.3, 51.6, 49.7, 46.4, 44.7, 38.6, 34.4, 27.7, 23.1, 17.4. (**Figure 65**)

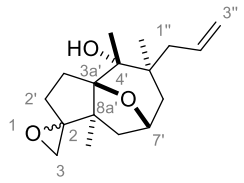

60-H

60-H: **(3a'*R**,4'*R**,5'*S**,7'*R**,8a'*S**)-5'-Allyl-4',5',8a'-trimethyloctahydrospiro[oxirane-2,1'-[3a,7]epoxyazulen]-4'-ol**

Prepared from **59-H**: **83%** yield (*d.r.* ≈ 5.6:1).

$\mathbf{R_f}$ = 0.10–0.24 [$\mathbf{R_f}$ (**59-H**) = 0.60] (PE/DE, 2:1).
^{1}H NMR (400 MHz, $CDCl_3$; ***diastereomeric mixture***): δ = 5.95–5.85 (m, 1H, 2''-H), 5.08–5.04 (m, 2H, 3''-H_2), 4.23–4.20 (m, 1H, 7'-H), 2.86 & 2.71 (2 × d, *J* = 4.3 Hz, 0.3H (*minor DS*), 3-H_2), 2.64 & 2.42 (2 × d, *J* = 4.2 Hz, 1.7H (*major DS*), 3-H_2), 2.39–2.16 (m, 3H), 2.09–1.93 (m, 2H), 1.86–1.64 (m, 4H), 1.52–1.48 (m, 1H), 1.41–1.34 (m, 9H).
^{13}C NMR (101 MHz, $CDCl_3$; ***diastereomeric mixture***): δ = 135.4, 117.7, 117.7, 96.1, 95.0, 78.4, 78.2, 75.5, 74.8, 71.9, 71.0, 55.2, 53.3, 52.4, 48.1, 47.7, 4.3, 44.3, 43.6, 40.0, 39.9, 37.8, 27.5, 27.4, 26.7, 26.4, 25.3, 25.0, 24.3, 23.5, 18.2, 16.7. (**Figure 66**)

4.2.2.2 MEINWALD Rearrangement

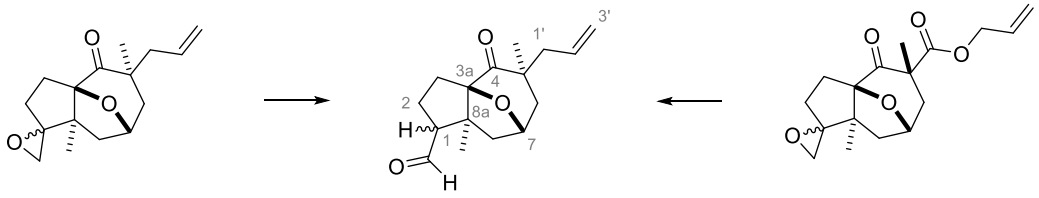

46-H **47-H** **49-H**

47-H: **(3a*R**,5*S**,7*S**,8a*S**)-5-Allyl-5,8a-dimethyl-4-oxooctahydro-1H-3a,7-epoxyazulene-1-carbaldehyde**

❖ **General procedure for the MEINWALD rearrangement:**

Epoxide **46-H** (174 mg, 0.663 mmol, 1 eq; *d.r.* ≈ 1:1) was dissolved in DCM (12.6 mL) in a 25 mL flask. After cooling the solution in an ice bath (*cf*. **Notes**), a freshly prepared solution of $BF_3{\cdot}OEt_2$ (0.5 M in DCM; 0.13 mL, 0.066 mmol, 10 mol%) was added dropwise (1 min). The reaction mixture was allowed to warm to room temperature (17.5 h, *cf*. **Notes**), quenched with half-saturated $NaHCO_3$ solution (13 mL), and extracted with DCM (3 × 30 mL). The combined organic phases were dried over $MgSO_4$, filtered, and concentrated in vacuo. Purification by flash chromatography (PE/DE, gradient from 10:1 to 1:2) afforded the aldehyde **47-H** (149 mg, 0.568 mmol, **90%**; *d.r.* ≈ 1.57:1) as a barely yellow oil.

❖ **One-pot TSUJI-TROST/MEINWALD sequence:**

A solution of palladium catalyst was prepared by stirring $Pd_2(dba)_3{\cdot}CHCl_3$ (22.8 mg, 0.025 mmol) and dppf (30.5 mg; 0.055 mmol) in degassed DCM (5 mL) for 1.5 h.

In a separate 25 mL flask, epoxy β-ketoester **49-H** (221 mg, 0.720 mmol, 1 eq; *d.r.* ≈ 1.2:1) was dissolved in degassed DCM (14.4 mL). An aliquot of the freshly prepared palladium catalyst solution (~1 mol% [Pd_2]; 2 of 5 mL catalyst solution) was added and the mixture stirred for 2 h, before a freshly prepared solution of $BF_3{\cdot}OEt_2$ (0.5 M in DCM; 0.15 mL, 0.075 mmol, 10 mol%) was added dropwise (1 min). The reaction mixture was stirred overnight (15 h, *cf*. **Notes**) and quenched with half-saturated $NaHCO_3$ solution (15 mL).

The quenched mixture was combined with that of a second run of the MEINWALD rearrangement. In that second run, 267 mg of epoxy β-ketoester **49-H** was employed in an analogously conducted one-pot TSUJI-TROST/MEINWALD sequence ***in THF***, which resulted in *no conversion in the MEINWALD rearrangement*. The crude product was then subjected to MEINWALD rearrangement ***in DCM*** according to the procedure described above.

After extracting the *combined quenched mixtures* with DCM (3 × 75 mL), the combined phases were dried over $MgSO_4$, filtered, and concentrated. The residual brownish oil was purified by flash chromatography (PE/DE, gradient from 10:1 to 1:1) to give aldehyde **47-H** (348 mg, 1.326 mmol, **83%** (effectively over 2 steps); *d.r.* ≈ 1:1) as a slightly yellow oil.

$\mathbf{R_f}$ = 0.53–0.67 [$\mathbf{R_f}$ (**46-H**) = 0.68–0.75] (PE/DE, 2:1, *eluted twice*).
^{1}H NMR (300 MHz, $CDCl_3$; ***less polar DS***): δ = 9.68 (d, *J* = 1.7 Hz, 1H), 5.74–5.60 (m, 1H), 5.09–4.98 (m, 2H), 4.55–4.50 (m, 1H), 2.46–2.31 (m, 4H), 2.28–2.10 (m, 2H), 2.07–1.92 (m, 2H),

1.82–1.75 (m, 1H), 1.54 (dd, *J* = 12.5 Hz, 0.7 Hz, 1H), 1.26 (dd, *J* = 14.5 Hz, 2.0 Hz, 1H), 1.16 (s, 3H), 1.04 (s, 3H). **^{13}C NMR** (75 MHz, $CDCl_3$; ***less polar DS***): δ = 213.2, 202.5, 133.3, 118.5, 99.0, 72.9, 62.9, 55.3, 46.3, 44.9, 44.1, 37.5, 29.4, 26.8, 24.0, 23.0. (**Figure 67**)

Notes: The MEINWALD rearrangement generally was found to be much more rapid than suggested by these two procedures. In cases of a clearly ascertainable reaction progress control by TLC (especially for **56-H** or **61-H**), a full conversion was determined within 20 min. In other cases, NMR analysis of an aliquot of the reaction mixture verified full conversion in <2 h.

Cooling the epoxide solution before the addition of $BF_3{\cdot}OEt_2$ occasionally impeded a full conversion even after the reaction mixture was allowed to warm to room temperature, thus necessitating further addition of $BF_3{\cdot}OEt_2$. Therefore, the addition to a non-cooled solution is advised and was carried out accordingly in later runs of the MEINWALD rearrangement.

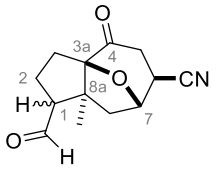

51

51: **(3a*R**,6*S**,7*S**,8a*S**)-1-Formyl-8a-methyl-4-oxooctahydro-1*H*-3a,7-epoxyazulene-6-carbonitrile**

Prepared from **50**: **66%** yield.

R_f = 0.38 & 0.45 (PE/EA, 1:2, *not distinguishable from* **50**).
^{1}H NMR (400 MHz, $CDCl_3$; ***less polar DS***): δ = 9.63 (d, *J* = 2.6 Hz, 1H), 4.68 (d, *J* = 7.6 Hz, 1H), 3.03–2.99 (m, 1H), 2.91–2.85 (m, 1H), 2.71–2.57 (m, 2H), 2.47–2.39 (m, 2H), 2.19–2.09 (m, 2H), 2.02–1.95 (m, 1H), 1.16 (s, 3H). **^{13}C NMR** (101 MHz, $CDCl_3$; ***less polar DS***): δ = 202.6, 201.6, 120.1, 100.2, 75.8, 61.7, 56.4, 40.2, 36.1, 32.0, 27.7, 24.0, 24.0. (**Figure 68**)

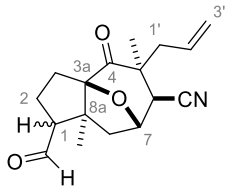

47

47: **(3a*R**,5*S**,6*S**,7*S**,8a*S**)-5-Allyl-1-formyl-5,8a-dimethyl-4-oxooctahydro-1*H*-3a,7-epoxyazulene-6-carbonitrile**

Prepared from **49**: ~**64% yield** of aldehyde **47**,
~**35% yield** of impure allylic alcohol **47.a**.

Via one-pot TSUJI-TROST/MEINWALD sequence (4 mmol scale, DCM (0.05 M), $Pd(PPh_3)_4$ (1 mol%), 1.5 h, then $BF_3{\cdot}OEt_2$ (0.1 M in DCM, 10 mol%), 1 h).

$\mathbf{R_f}$ = 0.35 & 0.41 [$\mathbf{R_f}$ (**47.a**) = 0.17] [$\mathbf{R_f}$ (**46**) = 0.50 & 0.56] [$\mathbf{R_f}$ (**49**) = 0.58 & 0.65] (PE/DE, 1:2, *eluted twice*).

Notes: Possible reasons for the relatively complex mixture and moderate yield of aldehyde **47** are discussed in **Chapter 2.2.2**. The aldehyde diastereomers could neither be fully separated by flash chromatography nor assigned due to fast autoxidation to carboxylic acid **48**. The complex NMR spectra of the fractions containing mostly the ***more polar DS*** are attached in **Figure 69**.

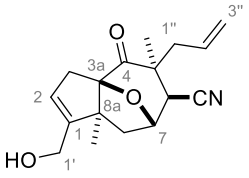

47.a

47.a: **(3a*R**,5*S**,6*S**,7*S**,8a*S**)-5-Allyl-1-(hydroxymethyl)-5,8a-dimethyl-4-oxo-4,5,6,7,8,8a-hexahydro-3*H*-3a,7-epoxyazulene-6-carbonitrile**

^{1}H NMR (400 MHz, $CDCl_3$): δ = 5.64–5.53 (m, 1H, 2''-H), 5.49 (br s, 1H, 2-H), 5.08–5.03 (m, 2H, 3''-H_2), 4.79 (br d, $J \approx 6.5$ Hz, 2.7 Hz, 1H, 7-H), 4.17 (m, 2H, 1'-H_2), 3.11–2.99 (m, 2H, 3-H_a & 1''-H_a), 2.65 (d, J = 2.7 Hz, 1H, 6-H), 2.42–2.37 (m, 2H, 8-H_a & 1''-H_b), 2.36–2.32 (m, 1H, 3-H_b), 1.84–1.73 (v br s, 1H, 1'-OH), 1.67 (d, J = 12.6 Hz, 1H, 8-H_b), 1.20 (s, 3H, 5-CH_3), 1.00 (s, 3H, 8a-CH_3). **^{13}C NMR** (101 MHz, $CDCl_3$): δ = 208.9 (C4), 146.2 (C1), 132.4 (C2''), 122.3 (C2), 118.9 (C3''), 118.6 (6-CN), 99.8 (C3a), 76.3 (C7), 60.3 (C8a), 59.4 (C1'), 47.1 (C5), 45.2 (C8), 42.7 (C1'), 42.2 (C6), 36.2 (C3), 23.3 (8a-CH_3), 21.1 (5-CH_3). (**Figure 70**)
HRMS: calcd. for $C_{17}H_{21}NNaO_3$ 310.14136 $[M+Na]^+$, found 310.14160 (Δ = 0.77 ppm).

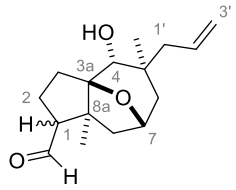

56-H

56-H: **(3a*R**,4*R**,5*S**,7*R**,8a*S**)-5-Allyl-4-hydroxyl-5,8a-dimethyloctahydro-1*H*-3a,7-epoxyazulene-1-carbaldehyde**

Prepared from **55-H**: **85% yield** of aldehyde **56-H**,
8% yield of allylic alcohol **56-H.a**.

R_f = 0.47 [**R_f** (**56-H.a**) = 0.04] [**R_f** (**55-H**) = 0.32] (PE/DE, 1:2).
^{1}H NMR (400 MHz, $CDCl_3$; ***major, more polar DS***): δ = 9.77 (d, *J* = 1.6 Hz, 1H), 5.95–5.84 (m, 1H), 5.10–5.04 (m, 2H), 4.40–4.37 (m, 1H), 3.74 (s, 1H), 2.98–2.94 (m, 1H), 2.49–2.30 (m, 2H), 2.14–1.64 (m, 8H), 1.55–1.49 (br d, *J* ≈ 14 Hz, 1H), 1.24 & 1.22 (2 × s, 6H).
^{13}C NMR (101 MHz, $CDCl_3$; ***major, more polar DS***): δ = 205.1, 135.5, 117.9, 94.1, 77.9, 75.2, 64.5, 53.6, 52.4, 44.3, 41.2, 37.1, 29.6, 23.7, 21.0, 15.2. (**Figure 71**)

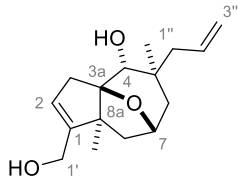

56-H.a

56-H.a: **(3a*R**,4*R**,5*S**,6*S**,7*R**,8a*S**)-5-Allyl-1-(hydroxymethyl)-5,8a-dimethyl-4,5,6,7,8,8a-hexahydro-3*H*-3a,7-epoxyazulen-4-ol**

^{1}H NMR (400 MHz, $CDCl_3$): δ = 6.01–5.90 (m, 1H), 5.50 (br s, 1H), 5.16–5.08 (m, 2H), 4.27–4.14 (m, 2H), 3.91 (s, 1H), 2.90 (br d, *J* = 17 Hz, 1H), 2.39 (dd, *J* = 13.2, 8.4 Hz, 1H), 2.22–2.07 (m, 3H), 1.96 (br dd, *J* ≈ 14.1 Hz, 5.3 Hz, 1H), 1.85 (d, *J* = 13.1 Hz, 1H), 1.77–1.66 (v br s, 2H, 2 × OH), 1.56 (d, *J* = 14.1 Hz, 1H), 1.39 (s, 3H), 1.29 (s, 3H).
^{13}C NMR (101 MHz, $CDCl_3$;): δ = 151.8, 135.9, 120.4, 117.9, 92.5, 78.1, 74.4, 59.5, 56.6, 52.9, 44.5, 37.9, 37.3, 23.7, 20.4. (**Figure 72**)

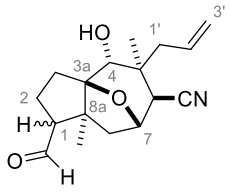

56

56: **(3a*R**,4*R**,5*S**,6*S**,7*S**,8a*S**)-5-Allyl-1-formyl-4-hydroxy-5,8a-dimethyloctahydro-1*H*-3a,7-epoxyazulene-6-carbonitrile**

Prepared from **55**: *yield not determined*; *used without further purification*.

$\mathbf{R_f}$ = 0.56 & 0.63 [$\mathbf{R_f}$ (**55**) = 0.50 & 0.58] (PE/EA, 2:1, *eluted three times*).
^{1}H NMR (400 MHz, $CDCl_3$; ***major, more polar DS***): δ = 9.77 (d, *J* = 1.6 Hz, 1H), 5.99–5.87 (m, 1H), 5.29–5.18 (m, 2H), 4.66–4.64 (m, 1H), 3.85 (s, 1H), 2.99–2.94 (m, 1H), 2.73 (br s, 1H), 2.61–2.47 (m, 2H), 2.41–1-81 (m, 8H), 1.36 & 1.24 (2 × s, 6H).
^{13}C NMR (101 MHz, $CDCl_3$; ***major, more polar DS***): δ = 204.4, 133.6, 120.0, 95.0, 93.6, 76.8, 76.5, 64.3, 53.6, 49.7, 44.6, 40.6, 38.5, 29.4, 23.1, 21.1, 14.8. (**Figure 73**)

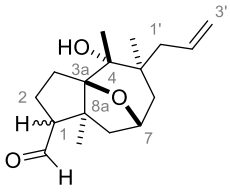

61-H

61-H: **(3a*R**,4*R**,5*S**,7*R**,8a*S**)-5-Allyl-4-hydroxy-4,5,8a-trimethyloctahydro-1*H*-3a,7-epoxyazulene-1-carbaldehyde**

Prepared from **60-H**: **~85% yield** (*excluding* ~19 wt.% DCM, as determined by NMR).

$\mathbf{R_f}$ = 0.51 [$\mathbf{R_f}$ (**60-H**) = 0.37] (PE/DE, 1:2).
^{1}H NMR (400 MHz, $CDCl_3$; ***major, more polar DS***): δ = 9.81 (d, *J* = 1.3 Hz, 1H), 5.95–5.85 (m, 1H), 5.09–5.04 (m, 2H), 4.44–4.41 (m, 1H), 3.01 (br dd, *J* ≈ 11.2 Hz, 7.8 Hz, 1H), 2.47 (dd, *J* = 13.1 Hz, 8.2 Hz, 1H), 2.30–2.18 (m, 3H), 2.08–1.75 (m, 5H), 1.52 (dd, *J* = 14.0 Hz, 1.5 Hz, 1H), 1.38 (s, 3H), 1.37 (s, 3H), 1.36 (s, 3H).
^{13}C NMR (101 MHz, $CDCl_3$; ***major, more polar DS***): δ = 205.2, 135.3, 117.9, 97.2, 78.6, 75.7, 65.7, 54.8, 48.1, 44.3, 40.8, 40.0, 28.9, 25.3, 25.0, 20.5, 15.6. (**Figure 74**)

4.2.2.3 PINNICK Oxidation

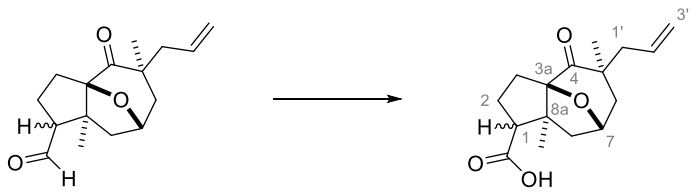

47-H **48-H**

48-H: **(3a*R**,5*S**,7*S**,8a*S**)-5-Allyl-5,8a-dimethyl-4-oxooctahydro-1*H*-3a,7-epoxyazulene-1-carboxylic acid**

❖ **General procedure for the PINNICK oxidation:**

Aldehyde **47-H** (214 mg, 0.816 mmol, 1 eq) was dissolved in *t*-BuOH/H_2O (5:2, 16.3 mL) in a 25 mL flask (*under air*). 2-Methyl-2-butene (1.3 mL, 4.08 mmol, 15 eq), NaH_2PO_4 (117.4 mg, 0.979 mmol, 1.2 eq) and $NaClO_2$ (80%; 110.7 mg, 0.979 mmol, 1.2 eq) were added sequentially, and the flask closed to prevent 2-methyl-2-butene from evaporating. After stirring for 2.5 h, the reaction mixture was diluted with water (10 mL) and EA (30 mL). The phases were separated, the slightly turbid organic phase washed with saturated NaCl solution (5 mL), and the aqueous phase extracted with ethyl acetate (2 × 30 mL). The combined organic phases were dried over $MgSO_4$, filtered, and concentrated, affording carboxylic acid **48-H** (225 mg) as a slightly yellow oil, which solidified in the freezer and was used without further purification.

R_f = 0.52–0.60 [**R_f** (**47-H**) = 0.65–0.78] (PE/EA, 1:1).
^{1}H NMR (400 MHz, $CDCl_3$; ***diastereomeric crude product***): δ = 5.74–5.61 (m, 1H), 5.09–5.00 (m, 2H), 4.71–4.55 (m, 1H), 3.03 & 2.74 (2 × dd, *J* = 11.4 Hz, 7.7 Hz and 13.2 Hz, 7.8 Hz, 1H), 2.52–1.83 (m, alkyl-H), 1.76–1.23 (m, alkyl-H), 1.19 & 1.11 & 1.02 & 0.93 (4 × s, 6H).
^{13}C NMR (101 MHz, $CDCl_3$; ***diastereomeric crude product***): δ = 213.9, 213.5, 179.6, 179.1, 133.6, 133.4, 118.6 (2 ×), 100.0, 98.7, 74.7, 72.6, 57.2, 56.4, 55.2, 55.0, 47.4, 46.0 (2 ×), 45.2, 44.6, 40.2, 36.5, 29.3, 28.3, 27.1, 26.2, 25.4 (2 ×), 22.2, 17.5. (**Figure 75**)

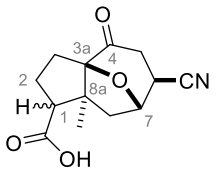

52

52: **(3a*R**,6*S**,7*S**,8a*S**)-6-Cyano-8a-methyl-4-oxooctahydro-1*H*-3a,7-epoxyazulene-1-carboxylic acid**

Prepared from **51**: *yield not determined*; *used without further purification*.

R_f = 0.38 & 0.45 (PE/EA, 1:2, *not distinguishable from* **51**).
^{1}H NMR (400 MHz, CD_3OD; ***diastereomeric crude product***): δ = 4.80 (dd, *J* = 8.1 Hz, 1.5 Hz, 0.6H – *superimposed with* CD_3OH) & 4.69 (br d, *J* = 7.3 Hz, 1.5 Hz, 0.4H), 3.36 (dd, *J* = 8.7 Hz, 1.3 Hz, 0.6H) & 3.29 (m, 0.4H – *superimposed with* CD_3OH), 3.02 (dd, *J* = 11.7 Hz, 8.0 Hz, 0.6H), 2.96–2.50 (m, 4H), 2.30 (dd, *J* = 13.7 Hz, 7.3 Hz, 0.4H), 2.15–1.65 (m, 5H), 1.20 & 0.92 (2 × s, 3H). **^{13}C NMR** (101 MHz, CD_3OD; ***diastereomeric crude product***): δ = 204.5, 202.5, 176.1 (2 ×), 122.5, 122.2, 102.3, 100.6, 78.1, 77.7, 57.5, 56.7, 55.8, 55.2, 44.0, 41.8, 37.6, 37.1, 35.7, 31.9, 29.1, 26.3 (2 ×), 26.1, 25.8, 15.0 (**Figure 76**)

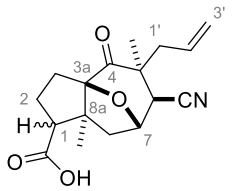

48

48: **(3a*R**,5*S**,6*S**,7*S**,8a*S**)-5-Allyl-6-cyano-5,8a-dimethyl-4-oxooctahydro-1H-3a,7-epoxyazulene-1-carboxylic acid**

Prepared from **47**: *yield not determined*; *used without further purification*.

R_f = 0.54 & 0.59 [**R_f** (**47**) = 0.35 & 0.41] (PE/DE, 1:2, *eluted twice*).
^{1}H NMR (400 MHz, $CDCl_3$; ***diastereomeric crude product***): δ = 5.62–5.51 (m, 1H), 5.07–4.76 (m, 3H), 3.04–2.79 (m, 2H), 2.66 & 2.60 (2 × d, *J* = 2.8 Hz and 1.8 Hz, 1H), 2.55–1.73 (m, alkyl-H), 1.18 & 1.14 & 0.91 (4 × s, 6H).
^{13}C NMR (101 MHz, $CDCl_3$; ***diastereomeric crude product***): δ = 209.4, 207.9, 178.4, 178.1, 132.3 (2 ×), 119.1, 118.9, 118.5 (2 ×), 100.7, 99.5, 77.8, 76.3, 56.8, 56.3, 55.3, 54.6, 47.9, 47.6, 47.1, 45.6, 43.8, 43.2, 42.8, 41.1, 29.6, 29.3, 27.2, 27.1, 25.3, 21.9, 20.9, 18.2. (**Figure 77**)
HRMS: calcd. for $C_{17}H_{21}NO_4$ 302.13978 $[M-H]^-$, found 302.14030 (Δ = 1.71 ppm).

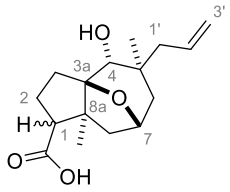

57-H

57-H: **(3a*R**,4*R**,5*S**,7*R**,8a*S**)-5-Allyl-4-hydroxy-5,8a-dimethyloctahydro-1H-3a,7-epoxyazulene-1-carboxylic acid**

Prepared from **56-H**: *yield not determined*; *used without further purification*.

R_f = 0.68 [**R_f** (**56-H**) = 0.75] (PE/EA, 1.5:1).
^{1}H NMR (400 MHz, $CDCl_3$; ***diastereomeric crude product***): δ = 5.98–5.86 (m, 1H), 5.13–5.07 (m, 2H), 4.39 & 4.24 (2 × m, 0.7H & 0.3H), 3.89 & 3.77 (2 × s, 0.3H & 0.7H), 3.09 (dd, *J* = 11.2 Hz, 8.2 Hz, 0.7H), 2.74–2.68 (m, 0.3 H), 2.62 (dd, *J* = 13.5 Hz, 8.4 Hz, 0.7 H), 2.37–2.03 (m, 5H), 1.96–1.63 (m, 5H), 1.55 (br d, *J* ≈ 14 Hz, 1H), 1.48 (s, 1H), 1.27 & 1.26, 1.24 (4 × s, 6H).
^{13}C NMR (101 MHz, $CDCl_3$; ***diastereomeric crude product***): δ = 179.8, 178.8, 135.7, 135.5, 118.2, 118.0, 93.8, 93.1, 78.2, 78.0, 75.3, 74.2, 59.6, 56.7, 54.2, 53.8, 52.6, 44.4, 43.4, 41.0, 40.5, 37.1, 37.0, 32.3, 31.1, 29.4, 25.1, 24.2, 23.7, 23.6, 23.2, 14.6. (**Figure 78**)

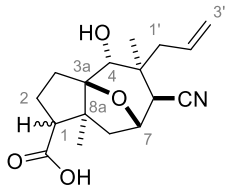

57

57: **(3a*R**,4*R**,5*S**,6*S**,7*S**,8a*S**)-5-Allyl-6-cyano-4-hydroxy-5,8a-dimethyloctahydro-1*H*-3a,7-epoxyazulene-1-carboxylic acid**

Prepared from **56**: *yield not determined*; *used without further purification*.

R_f = 0.21–0.31 [**R_f** (**56**) = 0.46 & 0.52] (PE/EA, 2:1, *eluted twice*).

Notes: The NMR spectra of the crude *diastereomeric mixture* are attached in **Figure 79**. A significant amount of residual ethyl acetate is discernible.

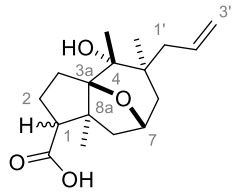

62-H

62-H: **(3a*R**,4*R**,5*S**,7*R**,8a*S**)-5-Allyl-4-hydroxy-4,5,8a-trimethyloctahydro-1H-3a,7-epoxyazulene-1-carboxylic acid**

Prepared from **61-H**: *yield not determined*; *used without further purification*.

$\mathbf{R_f}$ = 0.65 [$\mathbf{R_f}$ (**61-H**) = 0.73] (PE/DE, 1:2, *eluted twice*).

^{1}H NMR (400 MHz, $CDCl_3$; ***major, more polar DS***): δ = 5.95–5.85 (m, 1H), 5.09–5.04 (m, 2H), 4.40–4.36 (m, 1H), 3.14–3.09 (m, 1H), 2.62 (dd, *J* = 13.6 Hz, 8.3 Hz, 1H), 2.27–2.22 (m, 2H), 2.08–1.79 (m, 7H), 1.52–1.49 (m, 2H), 1.38 (s, 3H), 1.37 (2 × s, 2 × 3H).

^{13}C NMR (101 MHz, $CDCl_3$; ***major, more polar DS***): δ = 180.0, 135.4, 117.8, 96.9, 78.6, 75.7, 57.7, 55.1, 48.2, 44.2, 40.0, 39.9, 28.6, 25.3, 24.8, 22.6, 14.9. (**Figure 80**)

4.2.2.4 Esterification

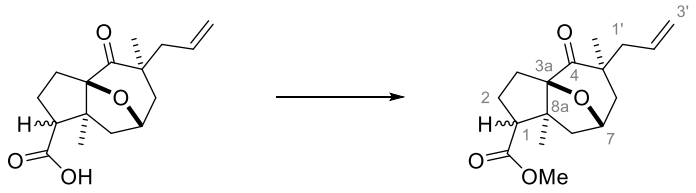

48-H **6-H**

6-H: **Methyl (3a*R**,5*S**,7*S**,8a*S**)-5-allyl-5,8a-dimethyl-4-oxooctahydro-1*H*-3a,7-epoxyazulene-1-carboxylate**

❖ **General procedure for the esterification with $TMSCHN_2$:**

Carboxylic acid **48-H** (*crude*, 225 mg, "0.816 mmol," 1 eq) was dissolved in toluene/MeOH (3:2, 8.2 mL) in a 10 mL flask. $TMSCHN_2$ (2 M in Et_2O) was added dropwise until no further evolution of gas was observable and the yellow color of the $TMSCHN_2$ solution persisted (0.57 mL, 1.14 mmol, ~1.4 eq) over the course of 13 min). Excess $TMSCHN_2$ was quenched with acetic acid (6 drops, ~0.01 mL) and the almost colorless solution concentrated, affording methyl ester **6-H** (234 mg, 0.800 mmol, **98% crude**) as a barely yellow oil which solidified in the freezer.

The methyl ester obtained in this run showed only small amounts of impurities in NMR spectra and was used without further purification in the oxidative cleavage of the allyl moiety (**79%** yield). When isolated methyl ester **6-H** was employed, the oxidative cleavage afforded aldehyde **5-H** with a yield of **92%**. Thus, the PINNICK oxidation and subsequent esterification conducted in this run can be quantified as **85%** over 2 steps.

$\mathbf{R_f}$ = 0.76 [$\mathbf{R_f}$ (**48-H**) = 0.69] (PE/EA, 1:1).
^{1}H NMR (400 MHz, $CDCl_3$; ***diastereomeric mixture***): δ = 5.72–5.62 (m, 1H), 5.10–4.99 (m, 2H), 4.68–4.53 (m, 1H), 3.68 (2 × s, 3H), 2.98 & 2.72 (2 × dd, *J* = 11.4 Hz, 7.7 Hz & 13.2 Hz, 7.8 Hz, 1H), 2.51–1.68 (m, 8H), 1.50–1.45 (m, 1H), 1.30 & 1.24 (2 × dd, *J* = 14.1 Hz, 1.0 Hz & 14.5 Hz, 2.2 Hz, 1H), 1.17 & 1.11 & 1.02 & 0.86 (4 × s, 6H).
^{13}C NMR (101 MHz, $CDCl_3$; ***diastereomeric mixture***): δ = 213.9, 213.5, 173.7, 173.4, 133.6, 133.4, 118.5 (2 ×), 100.0, 98.7, 74.6, 72.5, 57.1, 56.4, 55.4, 54.9, 51.6, 51.5, 47.3, 46.2, 45.9, 45.8, 45.1, 44.5, 40.2, 36.6, 29.3, 28.4, 27.2, 26.5, 25.7, 25.3, 22.2, 17.7. (**Figure 81**)
HRMS: calcd. for $C_{17}H_{24}NaO_4$ 315.15668 $[M+Na]^+$, found 315.15685 (Δ = 0.54 ppm).

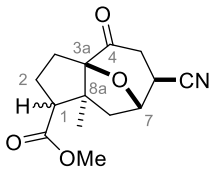

53

53: **Methyl (3a*R**,6*S**,7*S**,8a*S**)-6-cyano-8a-methyl-4-oxooctahydro-1H-3a,7-epoxyazulene-1-carboxylate**

Prepared from **52**: **<45%** over four steps from **8**.

Via alternative esterification [MeCN (0.075 M), DBU (1.1 eq), MeI (1.2 eq), 1 h]. Substantial amounts of residual solvents are discernible in the NMR spectra (EA, DCM).

$\mathbf{R_f}$ = 0.48 & 0.59 [$\mathbf{R_f}$ (**52**) = 0.39 & 0.48] (PE/EA, 1:2).
^{1}H NMR (400 MHz, $CDCl_3$; ***less polar DS***): δ = 4.74 (d, *J* = 7.0 Hz, 1H, 7-H), 3.69 (s, 3H, 1-$COOCH_3$), 2.93–2.83 (m, 2H, 5-H_a & 6-H), 2.66 (dd, *J* = 16.3 Hz, 6.4 Hz, 1H, 5-H_b), 2.52 (dd, *J* = 11.8 Hz, 6.5 Hz, 1H, 1-H), 2.18 (dd, *J* = 13.5 Hz, 7.0 Hz, 1H, 8-H_a), 2.10–2.05 (m, 2H, 2-H_a & 3-H_a), 1.94–1.81 (m, 2H, 2-H_b & 3-H_b), 1.66 (d, *J* = 13.5 Hz, 1H, 8-H_b), 1.17 (s, 3H, 8a-CH_3).
^{1}H NMR (400 MHz, $CDCl_3$; ***more polar DS***): δ = 4.83 (br d, *J* ≈ 7.8 Hz, 1H, 7-H), 3.69 (s, 3H, 1-$COOCH_3$), 3.09–3.04 (m, 2H, 1-H & 6-H), 2.93 (dd, *J* = 14.2 Hz, 8.1 Hz, 1H, 8-H_a), 2.84–2.80 (m, 1H, 5-H_a), 2.67–2.53 (m, 2H, 5-H_b & 1 × 2-/3-H*), 2.21–1.98 (m, 2H, 2 × 2-/3-H*) *superimposed with residual EtOAc*, 1.82–1.74 (m, 1H, 1 × 2-/3-H*), 1.60 (dd, *J* = 14.2 Hz, 1.8 Hz, 1H, 8-H_b), 0.86 (s, 3H, 8a-CH_3). **Protons on C2 and C3 not clearly distinguishable.*
^{13}C NMR (101 MHz, $CDCl_3$; ***less polar DS***): δ = 203.0 (C4), 172.7 (1-<u>*C*</u>$OOCH_3$), 120.4 (6-CN), 99.4 (C3a), 76.0 (C7), 56.3 (C1), 54.3 (C8a), 51.8 (1-COO<u>*C*</u>H_3), 43.9 (C8), 36.5 (C5), 30.0 (C6), 28.4 (C3), 26.3 (8a-CH_3), 25.4 (C2).
^{13}C NMR (101 MHz, $CDCl_3$; ***more polar DS***): δ = 200.2 (C4), 172.8 (1-<u>*C*</u>$OOCH_3$), 120.2 (6-CN), 101.1 (C3a), 76.2 (C7), 56.0 (C8a), 54.5 (C1), 51.7 (1-COO<u>*C*</u>H_3), 41.4 (C8), 35.8 (C5), 34.2 (C6), 25.2 (C2 *or* C3), 25.1 (C2 *or* C3), 15.1 (8a-CH_3). (**Figure 82** & **Figure 83**)
HRMS: calcd. for $C_{14}H_{17}NNaO_4$ 286.10498 $[M+Na]^+$, found 286.10508 (Δ = 0.34 ppm).

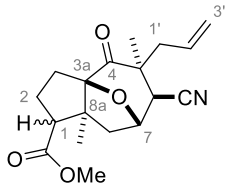

6

6: **Methyl (3a*R**,4*R**,5*S**,6*S**,7*S**,8a*S**)-5- allyl-6-cyano-5,8a-dimethyl-4-oxooctahydro-1*H*-3a,7-epoxyazulene-1-carboxylate**

Prepared from **48**: **66%** over 2 steps from aldehyde **47**.

R_f = 0.57–0.67 [**R_f** (**48**) = 0.43–0.51] (PE/DE, 1:2, *eluted twice*).
^{1}H NMR (400 MHz, $CDCl_3$; ***less polar DS***): δ = 5.62–5.52 (m, 1H, 2'-H), 5.06–5.02 (m, 2H, 3'-H_2), 4.73 (dd, *J* = 6.1 Hz, 2.8 Hz, 1H, 7-H), 3.86 (s, 3H, 1-$COOCH_3$), 3.00 (dd, *J* = 13.6 Hz, 7.6 Hz, 1H, 1'-H_a), 2.65 (d, *J* = 2.8 Hz, 1H, 6-H), 2.49–2.44 (m, 2H, 1'-H_b & 1-H), 2.10–1.88 (m, 4H, 8-H_a & 3 × 2-/3-H*), 1.76–1.72 (m, 1H, 1 × 2-/3-H*), 1.65 (d, *J* = 12.8 Hz, 1H, 8-H_b), 1.17 (s, 3H, 5-CH_3), 1.12 (s, 3H, 8a-CH_3). **Protons on C2 and C3 not clearly distinguishable.*
^{13}C NMR (101 MHz, $CDCl_3$; ***less polar DS***): δ = 207.9 (C4), 172.7 (1-$\underline{C}OOCH_3$), 132.3 (C2'), 118.8 (C3'), 118.5 (6-CN), 99.5 (C3a), 76.3 (C7), 56.4 (C1), 54.6 (C8a), 51.7 (1-COO$\underline{C}H_3$), 47.6 (C5), 45.4 (C8), 42.8 (C1'), 41.2 (C6), 29.3 (C2 *or* C3), 27.3 (8a-CH_3), 25.6 (C2 *or* C3), 20.9 (5-CH_3). (**Figure 84** & **Figure 85**).
HRMS: calcd. for $C_{18}H_{23}NNaO_4$ 340.15193 $[M+Na]^+$, found 340.15196 (Δ = 0.08 ppm).

Notes: The esterification of **47** was also conducted with three alternative methods resulting in the **same yield** as the method using $TMSCHN_2$ as reagent (determined by qNMR):

- MeOH (0.07 M), TMSCl (5 eq), 17 h;
- MeOH (0.1 M), H_2SO_4 (1.2 eq), 17 h;
- MeCN (0.1 M), Cs_2CO_3 (1.5 eq), MeI (2 eq), 17 h;

Presumably, full conversion occurred well before the 17 h mark but *each reaction was tried only once by running the experiment overnight*. The reaction mixtures were quenched with saturated $NaHCO_3$ solution, diluted with water, and extracted with EA.

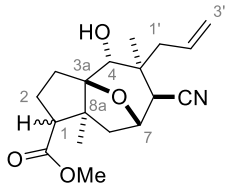

58

58: **Methyl (3a*R**,4*R**,5*S**,6*S**,7*S**,8a*S**)-5-allyl-6-cyano-4-hydroxy-5,8a-dimethyloctahydro-1*H*-3a,7-epoxyazulene-1-carboxylate**

Prepared from **57**: **88%** over three steps from epoxide **55**.

R_f = 0.61 [**R_f** (**57**) = 0.41] (PE/EA, 1:1).
^{1}H NMR (300 MHz, $CDCl_3$; ***less polar DS***): δ = 6.02–5.88 (m, 1H), 5.30–5.17 (m, 2H), 4.42 (br dd, *J* ≈ 6.3 Hz, 2.7 Hz, 1H), 4.08 (s, 1H), 3.69 (s, 3H), 2.78 (d, *J* = 2.8 Hz, 1H), 2.63–2.40 (m, 3H), 2.21–1.99 (m, 3H), 1.85–1.74 (m, 4H), 1.53 (s, 3H), 1.27 (s, 3H).
^{1}H NMR (300 MHz, $CDCl_3$; ***more polar DS***): δ = 6.02–5.88 (m, 1H), 5.30–5.17 (m, 2H), 4.60 (br d, *J* = 8.5 Hz, 1H), 3.83 (s, 1H), 3.66 (s, 3H), 3.04 (dd, *J* = 11 Hz, 8.3 Hz, 1H), 2.75–2.68 (m, 2H), 2.55–1.70 (m, 9H), 1.35 (s, 3H), 1.16 (s, 3H).
^{13}C NMR (75 MHz, $CDCl_3$; ***more polar DS***): δ = 174.1, 133.8, 120.2, 119.9, 94.6, 76.8, 76.7, 56.8, 53.6, 51.4, 49.8, 44.6, 40.1, 38.4, 29.2, 23.3, 23.1, 14.4. (**Figure 86** & **Figure 87**). *The ^{13}C spectrum of the **less polar DS** was not recorded and that of the crude product attached instead.*
HRMS: calcd. for $C_{18}H_{25}NNaO_4$ 342.16758 $[M+Na]^+$, found 342.16808 (Δ = 1.46 ppm).

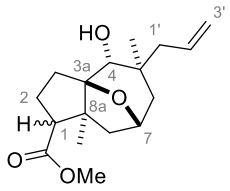

58-H

58-H: **Methyl (3a*R**,4*R**,5*S**,7*R**,8a*S**)-5-allyl-4-hydroxy-5,8a-dimethyloctahydro-1H-3a,7-epoxyazulene-1-carboxylate**

Prepared from **57-H**: **97%** over 2 steps from aldehyde **56-H**.

R_f = 0.42 [**R_f** (**57-H**) = 0.14] (PE/DE, 1:1).
^{1}H NMR (400 MHz, $CDCl_3$; ***less polar DS***): δ = 5.96–5.86 (m, 1H, 2'-H), 5.12–5.05 (m, 2H, 3'-H_2), 4.36–4.33 (m, 1H, 7-H), 3.73 (s, 1H, 4-H), 3.65 (s, 3H, 1-$COOCH_3$), 3.04 (dd, *J* = 11.3 Hz, 8.3 Hz, 1H, 1-H), 2.59 (dd, *J* = 13.5 Hz, 8.4 Hz, 1H, 8-H_a), 2.36–2.28 (m, 1H, 3-H_a), 2.19–2.01 (m, 3H, 2-H_a & 1'-H_2), 1.93–1.80 (m with br s, 4H, 2-H_b & 4-OH & 6-H_a & 8-H_b), 1.67–1.60 (m, 1H, 3-H_b), 1.52 (dd, *J* = 14 Hz, 0.9 Hz, 1H, 6-H_b), 1.25 (s, 3H, 5-CH_3), 1.15 (s, 3H, 8a-CH_3).
^{13}C NMR (101 MHz, $CDCl_3$; ***less polar DS***): δ = 174.7 (1-$\underline{C}OOCH_3$), 135.7 (C2'), 118.0 (C3'), 93.8 (C3a), 78.2 (C4), 75.2 (C7), 57.0 (C1), 53.8 (C8a), 52.7 (C1'), 51.3 (1-COO$\underline{C}H_3$), 44.4 (C6), 40.7 (C8), 37.2 (C5), 29.5 (C3), 23.7 (5-CH_3), 23.5 (C2), 14.9 (8a-CH_3). (**Figure 88** & **Figure 89**)
HRMS: calcd. for $C_{17}H_{27}O_4$ 295.19039 $[M+H]^+$, found 295.19072 (Δ = 1.12 ppm).

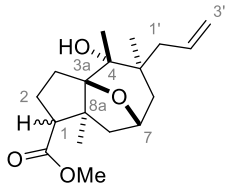

63-H

63-H: **Methyl (3a*R***,4*R***,5*S***,7*R***,8a*S***)-5-allyl-4-hydroxy-4,5,8a-trimethyloctahydro-1H-3a,7-epoxyazulene-1-carboxylate**

Prepared from **62-H**: **88%** over 2 steps from aldehyde **61-H**.

R_f = 0.78 [**R_f** (**62-H**) = 0.57] (PE/DE, 1:2, *eluted twice*).

^{1}H NMR (400 MHz, $CDCl_3$; ***major, more polar DS***): δ = 5.97–5.83 (m, 1H, 2'-H), 5.09–5.03 (m, 2H, 3'-H_2), 4.38–4.34 (m, 1H, 7-H), 3.67 (s, 3H, 1-$COOCH_3$), 3.10–3.04 (m, 1H, 1-H), , 2.60 (dd, *J* = 13.5 Hz, 8.4 Hz, 1H, 8-H_a), 2.28–2.20 (m, 2H, 3-H_a & 1'-H_a), 2.14–2.01 (m, 2H, 2-H_a & 8-H_b), 1.95–1.78 (m, 4H, 2-H_b & 3-H_b & 1-H_b & 6-H_a), 1.49 (dd, *J* = 14.0 Hz, 1.6 Hz, 1H, 6-H_b), 1.38 & 1.36 (2 × s, 2 × 3H, 4-CH_3 & 5-CH_3, *not clearly distinguishable*), 1.28 (s, 3H, 8a-CH_3).

^{13}C NMR (101 MHz, $CDCl_3$; ***major, more polar DS***): δ = 174.6 (1-$\underline{C}OOCH_3$), 135.4 (C2'), 117.7 (C3'), 96.9 (C3a), 78.5 (C4), 75.6 (C7), 57.9 (C1), 55.0 (C8a), 51.3 (1-COO$\underline{C}H_3$), 48.2 (C1'), 44.3 (C6), 40.0 & 40.0 (C5 & C8, *not clearly distinguishable*), 28.7 (C3), 25.3 & 24.8 (4-CH_3 & 5-CH_3, *not clearly distinguishable*), 22.9 (C2), 15.0 (8a-CH_3). (**Figure 90**)

HRMS: calcd. for $C_{18}H_{28}NaO_4$ 331.18798 $[M+Na]^+$, found 331.18805 (Δ = 0.20 ppm).

4.2.3 Oxidative Cleavage of the C5-Allyl Group to an Aldehyde

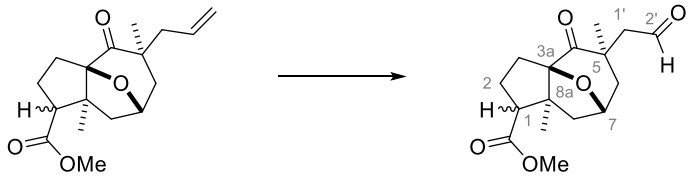

6-H **5-H**

5-H: **Methyl (3a*R**,5*S**,7*S**,8a*S**)-5,8a-dimethyl-4-oxo-5-(2'-oxoethyl)octahydro-1*H*-3a,7-epoxyazulene-1-carboxylate**

❖ **General Procedure for the modified**[266] **LEMIEUX-JOHNSON oxidation:**

Methyl ester **6-H** (*crude*, 234 mg, "0.800 mmol," 1 eq) was dissolved in 1,4-dioxane/H_2O (3:1, 16.3 mL) in a 25 mL flask (*under air*). After addition of 2,6-lutidine (0.19 mL, 1.60 mmol, 2 eq), OsO_4 (4 wt.% in H_2O; 0.10 mL, 0.016 mmol, 2 mol%), and $NaIO_4$ (698 mg, 3.20 mmol, 4 eq), the resulting suspension was stirred for 5.5 h. The reaction mixture was diluted with water (30 mL) and extracted with DCM (3 × 30 mL). The combined organic phases were dried with $MgSO_4$, filtered, and concentrated in vacuo. Purification by flash chromatography (PE/DE, gradient from 20:1 to 1:2) gave the diastereomers of aldehyde **5-H** (*in total* 189.8 mg, 0.645 mmol, **79% over 3 steps** from aldehyde **47-H**) as colorless, very viscous oils which solidified in the freezer. The diastereomers of **5-H** (epimers at C1) could be separated to an extent:

- 48.8 mg of *minor, less polar DS*
- 48.8 mg of a mixture of diastereomers (*less polar DS/more polar DS* ≈ 1:2)
- 92.2 mg of predominantly *major, more polar diastereomer*

$\mathbf{R_f}$ = 0.33 & 0.36 [$\mathbf{R_f}$ (**6-H**) = 0.63] (PE/EA, 2:1).
^{1}H NMR (400 MHz, $CDCl_3$, ***minor, less polar DS***): δ = 9.64 (br dd, *J* ≈ 2.4–2.8 Hz, 1H), 4.56 (ddd, *J* = 9.2 Hz, 6.3 Hz, 2.3 Hz, 1H), 3.68 (s, 3H), 2.67 (d, *J* = 2.8 Hz, 2H), 2.55–2.44 (m, 2H), 2.19–1.84 (m, 4H), 1.73 (dd, *J* = 12.8 Hz, 4.9 Hz, 1H), 1.52 (d, *J* = 12.3 Hz, 1H), 1.45 (dd, *J* = 14.9 Hz, 2.3 Hz, 1H), 1.20 (s, 3H), 1.19 (s, 3H).
^{1}H NMR (400 MHz, $CDCl_3$, ***major, more polar DS***): δ = 9.61 (br dd, *J* ≈ 2.3–2.7 Hz, 1H), 4.67 (br dd, *J* ≈ 7.7 Hz, 2.4 Hz, 1H), 3.66 (s, 3H), 2.99 (dd, *J* = 11.3 Hz, 7.7 Hz, 1H), 2.74–2.42 (m, 6H), 2.25–2.14 (m, 1H), 2.04–1.94 (m, 1H), 1.80–1.72 (m, 1H), 1.55 (dd, *J* ≈ 14.3 Hz, 0.9 Hz, 1H), 1.53 (dd, *J* ≈ 13.3 Hz, 1.4 Hz, 1H), 1.26 (s, 3H), 0.86 (s, 3H).
^{13}C NMR (101 MHz, $CDCl_3$, ***minor, less polar DS***): δ = 212.3, 200.3, 173.1, 98.8, 72.3, 56.5, 55.0, 54.6, 51.6, 45.5, 43.3, 37.5, 29.5, 27.0, 25.6, 23.3.
^{13}C NMR (101 MHz, $CDCl_3$, ***major, more polar DS***): δ = 212.6, 200.2, 173.4, 100.2, 74.5, 57.1, 56.0, 55.4, 51.5, 45.4, 42.5, 41.5, 28.4, 26.3, 17.4. (**Figure 91** & **Figure 92**)

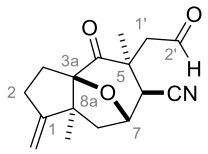

39

39: **(3a*R**,5*S**,6*S**,7*S**,8a*S**)-5,8a-dimethyl-1-methylene-4-oxo-5-(2'-oxoethyl)-1*H*-3a,7-epoxyazulene-6-carbonitrile**

Prepared from **7**: **70%** yield.

R_f = 0.37 [**R_f** (**7**) = 0.68] (PE/EA, 3:1).
^{1}H NMR (700 MHz, $CDCl_3$): δ = 9.66 (br dd, *J* ≈ 2.4 Hz, 1H), 4.96 & 4.86 (2 × br dd, *J* ≤ 2.0 Hz, 2H), 4.78 (br dd, *J* ≈ 7.1 Hz, 1.6 Hz, 1H), 3.19 (dd, *J* = 15.7 Hz, 1.9 Hz, 1H), 2.84 (dd, *J* = 15.5 Hz, 2.6 Hz, 1H), 2.73 (d, *J* = 2.2 Hz, 1H), 2.64–2.58 (m, 1H), 2.52 (dd, *J* = 13.1 Hz, 7.2 Hz, 1H) 2.51–2.48 (m, 1H), 2.30–2.25 (m, 1H), 1.91–1.88 (m, 2H), 1.38 (s, 3H), 1.04 (s, 3H).
^{13}C NMR (176 MHz, $CDCl_3$): δ = 208.3, 198.2, 159.8, 118.6, 106.9, 100.9, 76.5, 56.4, 51.9, 49.7, 45.0, 42.9, 30.3, 28.4, 24.5, 23.8. (**Figure 93**)
HRMS: calcd. for $C_{16}H_{19}NNaO_3$ 296.12571 $[M+Na]^+$, found 296.12579 (Δ = 0.27 ppm).

Notes: The oxidative cleavage of **7** was conducted multiple times over a substrate scale ranging from 45 mg to 1.184 g (1.184 g scale with *impure substrate*: **65%** of **39** as slightly beige solid). After separating the product by flash chromatography, the remaining fractions from several reactions were combined and subjected to acetalization conditions (1.034 g in acetone; 2,2-dimethoxypropane, cat. *p*-TsOH·H_2O), affording diketo dimethylacetal **39.b** (304 mg, colorless solid) after flash chromatography. The remaining fractions from the acetalization reaction were hydrolyzed and resubjected to another oxidative cleavage/acetalization process, yielding additional **39.b** (146 mg). During this process, substantial decomposition after work-up of the oxidative cleavage was apparent.

Generally, the addition of solid $Na_2S_2O_3$ (10 eq) to the reaction suspension before extraction seemed to alleviate the extent of decomposition for some aldehydes. This alternative work-up method was however not examined thoroughly.

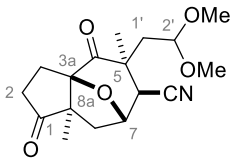

39.b

39.b: **(3a*R**,5*S**,6*S**,7*S**,8a*R**)-5-(2',2'-dimethoxyethyl)-5,8a-dimethyl-1,4-dioxooctahydro-1*H*-3a,7-epoxyazulene-6-carbonitrile**

R_f = 0.54 (PE/EA, 1:1).
^{1}H NMR (400 MHz, $CDCl_3$): δ = 4.74 (br dd, *J* ≈ 7.0 Hz, 1.5 Hz, 1H), 4.34 (dd, *J* = 8.2 Hz, 2.2 Hz, 1H), 3.28 (s, 3H), 3.20 (s, 3H), 2.82 (dd, *J* = 13.5 Hz, 8.2 Hz, 1H), 2.65 (dd, *J* = 13.5 Hz, 7.2 Hz, 1H), 2.54–2.45 (m, 4H), 2.31–2.25 (m, 1H), 1.97 (dd, *J* = 13.5 Hz, 2.2 Hz, 1H), 1.61 (d, *J* = 13.5 Hz, 1H),

1.27 (s, 3H), 0.99 (s, 3H). **^{13}C NMR** (101 MHz, $CDCl_3$): δ = 218.6, 208.5, 118.1, 101.1, 97.6, 76.2, 59.1, 54.6, 51.2, 46.6, 44.6, 43.9, 43.4, 33.8, 24.0, 22.7, 18.4. (**Figure 94**)
HRMS: calcd. for $C_{17}H_{23}NNaO_5$ 344.14684 $[M+Na]^+$, found 344.14686 (Δ = 0.06 ppm).

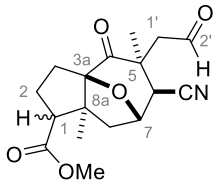

5

5: **Methyl (3a*R**,5*S**,6*S**,7*S**,8a*S**)-6-cyano-5,8a-dimethyl-4-oxo-5-(2'-oxoethyl)octahydro-1*H*-3a,7-epoxyazulene-1-carboxylate**

Prepared from **6**: **59%** yield (68% *b.r.s.m.*).

Notes: This oxidative cleavage was only conducted once (132.4 mg of **6** as a mixture of diastereomers in a ratio of ~1.5:1). Some substrate and intermediary diols could be discerned, suggesting an incomplete conversion (after 6 h). The diastereomers of **5** were separated readily by flash chromatography (PE/DE, gradient from 20:1 to 1:2).

$\mathbf{R_f}$ = 0.46 & 0.57 [$\mathbf{R_f}$ (**6**) = 0.67] (PE/DE, 1:2, *eluted twice*).
^{1}H NMR (400 MHz, $CDCl_3$, ***minor, less polar DS***): δ = 9.63 (br dd, *J* = 2.6–3 Hz, 1H), 4.74 (dd, *J* = 6.1 Hz, 2.9 Hz, 1H), 3.69 (s, 3H), 3.12 (dd, *J* = 14.8 Hz, 2.3 Hz, 1H), 2.76 (dd, *J* = 14.8 Hz, 3.2 Hz, 1H), 2.71 (d, *J* = 2.9 Hz, 1H), 2.50 (dd, *J* = 12.0 Hz, 6.6 Hz, 1H), 2.16–1.88 (m, 4H), 1.81 (br dd, *J* ≈ 13 Hz, 4.8 Hz, 1H), 1.70 (d, *J* = 13.1 Hz, 1H), 1.35 (s, 3H), 1.16 (s, 3H).
^{1}H NMR (400 MHz, $CDCl_3$, ***major, more polar DS***): δ = 9.64 (*app.* br s, 1H), 4.86 (br d, *J* ≈ 7.7 Hz, 1H), 3.67 (s, 3H), 3.16 (br d, *J* ≈ 16.4 Hz, 1H), 2.97 (dd, *J* = 11.4 Hz, 7.6 Hz, 1H), 2.89–2.81 (m, 2H), 2.47 (ddd, *J* = 14.1 Hz, 10.8 Hz, 3.0 Hz, 1H), 2.27–2.16 (m, 1H), 2.08–2.00 (m, 1H), 1.95–1.87 (m, 1H), 1.62 (dd, *J* = 14 Hz, 1.0 Hz, 1H), 1.36 (s, 3H), 0.86 (s, 3H).
^{13}C NMR (101 MHz, $CDCl_3$, ***minor, less polar DS***): δ = 207.4, 198.1, 172.5, 118.0, 99.8, 76.1, 56.4, 54.6, 51.8, 51.0, 45.7, 45.2, 41.2, 29.8, 27.1, 25.6, 22.3.
^{13}C NMR (101 MHz, $CDCl_3$, ***major, more polar DS***): δ = 208.1, 197.9, 172.7, 118.9, 101.1, 77.1, 56.7, 55.4, 52.9, 51.6, 45.5, 44.6, 43.8, 29.1, 26.5, 25.2, 17.5. (**Figure 95** & **Figure 96**)

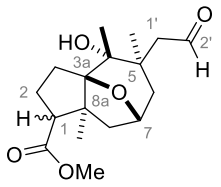

64-H

64-H: **Methyl (3a*R**,4*R**,5*R**,7*R**,8a*S**)-4-hydroxy-4,5,8a-trimethyl-5-(2'-oxoethyl)octahydro-1*H*-3a,7-epoxyazulene-1-carboxylate**

Prepared from **63-H**: **79%** yield from major diastereomer.

R_f = 0.47 [**R_f** (**63-H**) = 0.72] (PE/EA, 1:1).
^{1}H NMR (400 MHz, $CDCl_3$): δ = 9.69 (*app*. br s, 1H), 4.36–4.30 (m, 1H), 3.70 (s, 1H), 3.65 (s, 3H), 3.06–3.00 (m, 1H), 2.72–2.50 (m, 3H), 2.40–2.32 (m, 1H), 2.14–2.04 (m, 1H), 2.00 (br dd, *J* ≈ 13.5 Hz, 1.0 Hz, 1H), 1.84–1.72 (m, 3H), 1.52 (br dd, *J* ≈ 13.9 Hz, 1.2 Hz, 1H), 1.42 (s, 3H), 1.29 (s, 3H), 1.17 (s, 3H). **^{13}C NMR** (101 MHz, $CDCl_3$): δ = 203.7, 174.5, 96.5, 76.2, 75.2, 59.2, 57.8, 55.0, 51.2, 44.7, 40.5, 40.0, 28.9, 25.8, 25.5, 22.9, 14.9. (**Figure 97**)

4.3 LEWIS ACID-INDUCED REARRANGEMENT TO THE DECALONE CORE

4.3.2 Preparation of Substrates used in Rearrangement Attempts

4.3.2.1 Tertiary Alcohols

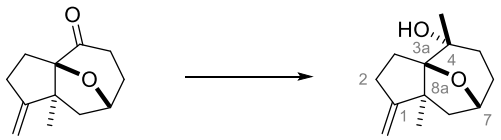

8-H **72-H**

72-H: **(3a*R**,4*R**,7*R**,8a*S**)-4,8a-Dimethyl-1-methyleneoctahydro-1*H*-3a,7-epoxyazulen-4-ol**

In a 10 mL flask, ketone **8-H** (109 mg, 0.557 mmol, 1 eq) was dissolved in THF (5 mL). Cooling the solution in an ice bath, MeMgBr (3 M in Et_2O; 0.23 mL, 0.690 mmol, 1.2 eq) was added, and the reaction mixture was allowed to warm to room temperature. After 18 h, another portion of MeMgBr (3 M in Et_2O; 0.23 mL, 0.690 mmol, 1.2 eq) was added, before the reaction mixture was stirred for another 21 h and quenched with saturated NH_4Cl solution (5 mL) and water (1 mL). The biphasic mixture was extracted with ethyl acetate (3 × 15 mL). The combined organic phases were dried over $MgSO_4$, filtered, and concentrated in vacuo. Purification by flash chromatography (PE/EA, gradient from 10:1 to 2.5:1) gave ketone **8-H** (34 mg, 31% recovered) and tertiary alcohol **72-H** [66 mg, 0.317 mmol, **56%** (81% *b.r.s.m.*)] as a colorless solid (m.p. 99 °C).

R_f = 0.24 [**R_f** (**8-H**) = 0.47] (PE/DE, 2:1).
^{1}H NMR (400 MHz, $CDCl_3$): δ = 4.89 & 4.86 (2 × br dd, *J* ≈ 2.2–2.5 Hz, 2H, 1-CH_2), 4.34–4.29 (m, 1H, 7-H), 2.59–2.42 (m, 3H, 2-H_2 & 8-H_a), 2.08–1.75 (m, 5H, 3-H_2 & 5-H_a & 6-H_a & 8-H_b), 1.69–1.63 (m (br dddd, *J* ≈ 13 Hz, 5.1 Hz, 1.3–1.5 Hz), 1H, 5-H_b), 1.45 (br dddd, *J* ≈ 13.3 Hz, 5.6 Hz, 1.3–1.7 Hz, 1H, 6-H_b), 1.38 (s, 3H, 8a-CH_3), 1.36 (d, *J* = 0.9 Hz, 3H, 4-CH_3), 1.32 (br s, 1H, 4-OH).
^{13}C NMR (101 MHz, $CDCl_3$): δ = 165.1 (C1), 105.4 (1-CH_2), 95.6 (C3a), 75.4 (C7), 72.6 (C4), 56.1 (C8a), 46.2 (C8), 33.1 (C5), 31.2 (C6), 28.5 (C2), 25.9 (4-CH_3), 25.5 (C3), 23.9 (8a-CH_3). (**Figure 98**)
HRMS: calcd. for $C_{13}H_{20}NaO_2$ 231.13555 $[M+Na]^+$, found 231.13600 (Δ = 1.94 ppm).

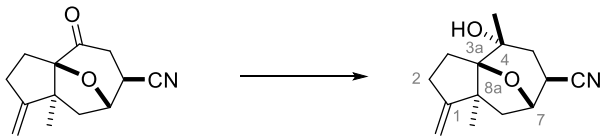

8 **72**

72: **(3a*R**,4*R**,6*S**,7*S**,8a*S**)-4-Hydroxy-4,8a-dimethyl-1-methyleneoctahydro-1*H*-3a,7-epoxyazulen-6-carbonitrile**

In a 10 mL flask, ketonitrile **8** (100 mg, 0.460 mmol, 1 eq) was dissolved in THF (4.6 mL). Cooling the solution in an ice bath, MeMgBr (1 M in Et_2O; 0.46 mL, 0.460 mmol, 1 eq) was added, and the reaction mixture was allowed to warm to room temperature. After 23 h, the reaction mixture was quenched with saturated NH_4Cl solution (5 mL) and water (1 mL). The biphasic mixture was extracted with ethyl acetate (3 × 15 mL). The combined organic phases were dried over $MgSO_4$, filtered, and concentrated in vacuo. The crude product exhibited an NMR ratio of 1:0.5 (tertiary alcohol **72**/ketonitrile **8**). Purification by flash chromatography (PE/EA, gradient from 10:1 to 5:1) failed to separate the remaining substrate from the product adequately. Next to a mixed fraction (68 mg), an analytical sample of tertiary alcohol **72** (13 mg) was isolated as a colorless solid.

The mixed fraction was resubjected to methylation by dissolving it in THF (6 mL, ~0.05 M) in a 10 mL flask. After addition of MeMgBr (3 M in Et_2O, 0.13 mL, "1.2 eq"), the reaction mixture was stirred at 60 °C for 4.5 h and subsequently quenched with saturated NH_4Cl solution (5 mL) and water (1 mL). The biphasic mixture was extracted with ethyl acetate (3 × 15 mL). The combined organic phases were dried over $MgSO_4$, filtered, and concentrated in vacuo, affording **72** (65 mg) as a colorless solid.

Notes: No adequate evaluation was pursued for this methylation. Since no significant impurities were discernible in NMR and TLC analysis, the product from the second methylation was used in rearrangement attempts without further purification. Assuming a pure product from the second methylation, a yield of **~73%** could be given. The *true yield* may however differ significantly in either direction. The second sample could have contained impurities which were not evident in NMR or TLC analysis, implying a higher yield than the true yield. On the other hand, other similarly polar nitrile-substituted compounds were partially retained in chromatography columns when relatively apolar eluents such as that in the first experiment (PE/EA, 5:1) were used, which may have led to a lower yield due to loss of product in the column.

$\mathbf{R_f}$ = 0.24 [$\mathbf{R_f}$ (**8**) = 0.45] (PE/DCM/MeOH, 1:1:0.1).
^{1}H NMR (400 MHz, $CDCl_3$): δ = 4.92 & 4.86 (2 × br dd, *J* ≈ 2.1–2.5 Hz, 2H), 4.49 (br d, *J* ≈ 8.1 Hz, 1H), 2.70 (br dd, *J* ≈ 6.8 Hz, 1.2 Hz, 1H), 2.62–2.45 (m, 3H), 2.31 (br dd, *J* ≈ 14.2 Hz, 7.0 Hz, 1H), 2.02–1.85 (m, 3H), 1.78 (dd, *J* = 13.1 Hz, 1.7 Hz, 1H), 1.61 (d, *J* = 0.5 Hz, 3H), 1.58–1.49 (v br s, 1H), 1.35 (s, 3H). **^{13}C NMR** (101 MHz, $CDCl_3$): δ = 163.8, 121.3, 106.0, 96.5, 75.6, 71.3, 55.8, 46.2, 34.6, 32.9, 28.3, 27.3, 25.5, 24.3. (**Figure 99**)
HRMS: calcd. for $C_{14}H_{29}NNaO_2$ 256.13080 $[M+Na]^+$, found 256.13087 (Δ = 0.27 ppm).

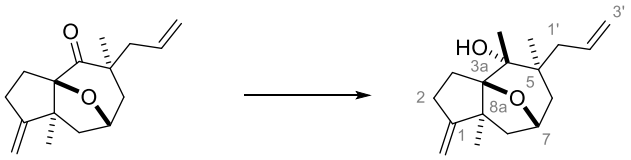

7-H **59-H**

59-H: **(3a*R**,4*R**,5*S**,7*R**,8a*S**)-5-allyl-4,5,8a-trimethyl-1-methyleneoctahydro-1*H*-3a,7-epoxyazulen-4-ol**

In a 100 mL flask, ketone **7-H** (765 mg, 3.105 mmol, 1 eq) was dissolved in THF (30 mL). MeMgBr (3 M in Et_2O; 4.4 mL, 4.5 eq) was added over the course of 3.5 min. The flask's septum was replaced with a reflux condenser and the reaction mixture was heated to reflux (oil bath temperature: 80 °C). After 15 h, the reaction mixture was quenched with saturated NH_4Cl solution (30 mL) and water (15 mL). The biphasic mixture was extracted with ethyl acetate (3 × 100 mL). The combined organic phases were dried over $MgSO_4$, filtered, and concentrated in vacuo. Purification by flash chromatography (PE/DE, gradient from 20:1 to 1:1) afforded unreacted substrate **7-H** (63 mg, 9% recovered) as well as tertiary alcohol **59-H** [722 mg, 2.752 mmol, **89%** (98% *b.r.s.m.*)] as a colorless solid (m.p. 88 °C).

$\mathbf{R_f}$ = 0.40 [$\mathbf{R_f}$ (**7-H**) = 0.70] (PE/DE, 3:1).
^{1}H NMR (400 MHz, $CDCl_3$): δ = 5.96–5.85 (m, 1H, 2'-H), 5.07–5.03 (m, 2H, 3'-H_2), 4.81 & 4.77 (2 × br dd, J ≈ 2.1–2.3 Hz, 2H, 1-CH_2), 4.27–4.21 (m, 1H, 7-H), 2.50–2.34 (m, 3H, 2-H_2 & 8-H_a), 2.28–2.16 (m, 2H, 8-H_b & 1'-H_a), 2.16–2.08 (m, 1H, 3-H_a), 1.99–1.91 (m, 2H, 3-H_b & 1'-H_b), 1.78 (dd, J = 14.1 Hz, 4.5 Hz, 1H, 6-H_a), 1.50 (dd, J = 14.1 Hz, 1.4 Hz, 1H, 6-H_b), 1.41 (s, 3H, 8a-CH_3), 1.40 (s, 3H, 4-CH_3), 1.38 (s, 3H, 5-CH_3), 1.25 (s, 1H, 4-OH).
^{13}C NMR (101 MHz, $CDCl_3$): δ = 166.6 (C1), 135.5 (C2'), 117.5 (C3'), 104.5 (1-CH_2), 96.1 (C3a), 78.0 (C4), 74.9 (C7), 56.3 (C8a), 48.2 (C1'), 44.2 (C6), 42.4 (C8), 39.9 (C5), 27.3 (C3), 27.1 (C2), 25.2 (5-CH_3), 24.6 (4-CH_3), 22.9 (8a-CH_3). (**Figure 100**)
HRMS: calcd. for $C_{17}H_{26}NaO_2$ 285.18250 $[M+Na]^+$, found 285.18241 (Δ = 0.32 ppm).

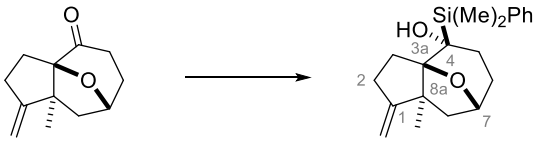

8-H **73-H**

73-H: **(3a*R**,4*S**,7*R**,8a*S**)-4-(Dimethyl(phenyl)silyl)-8a-methyl-1-methyleneoctahydro-1*H*-3a,7-epoxyazulen-4-ol**

Preparation of DMPSLi: Lithium (228 mg, 32.85 mmol, 3 eq) was suspended in THF (25 mL) in a 50 mL flask. After cooling the suspension to −10 °C using a cryostat, $Ph(Me)_2SiCl$ (1.84 mL, 10.96 mmol, 1 eq) was added. The reaction mixture was stirred at −10 °C for 2 d. The flask containing a dark-red solution of DMPSLi and some unreacted lithium metal was sealed thoroughly with parafilm and sticky tape, before being stored at −28 °C.

In later silylation reactions, the THF was removed in vacuo using the vacuum pump connected to the Schlenk line, removing residual THF by co-evaporation with Et_2O. The DMPSLi was then dissolved in Et_2O. The concentration of DMPSLi was determined by titration of an aliquot with 0.1 M $HCl_{(aq)}$ against phenolphthalein before use.

***C*-Silylation of ketone 8-H**: Ketone **8-H** (221 mg, 1.15 mmol, 1 eq) was dissolved in Et_2O (7 mL) in a 25 mL flask. The solution was cooled to −50 °C, before DMPSLi (0.3 M in Et_2O; 4.8 mL, 1.44 mmol, 1.25 eq) was added over 7 min. The orange reaction mixture was allowed to warm to 5 °C over the course of 2.5 h, and then stirred at room temperature for 2.5 h. After quenching with saturated NH_4Cl solution (12 mL) and water (3 mL), the biphasic mixture was extracted with Et_2O (3 × 25 mL). The combined organic phases were dried over $MgSO_4$, filtered, and concentrated to give a yellow viscous oil which was purified by flash chromatography (PE/DE, gradient from 20:1 to 2.5:1). Next to unreacted ketone **8-H** (94 mg, 0.489 mmol, 43% recovered), α-hydroxysilane **73-H** [145 mg, 0.441 mmol, **38%** (67% *b.r.s.m.*)] was obtained as a colorless solid (m.p. 97 °C).

Notes: While an optimization of this *C*-silylation was not pursued further, a higher conversion to **73-H** was observed when Et_2O was used as solvent instead of THF. On the other hand, the prior preparation of the silyl lithium reagent seems to be impeded in Et_2O. This was noted in a similar attempt at preparing TBDPSLi which was formed only after some THF was added.

$\mathbf{R_f}$ = 0.68 [$\mathbf{R_f}$ (**8-H**) = 0.40] (PE/DE, 2:1).
^{1}H NMR (400 MHz, $CDCl_3$): δ = 7.65–7.63 (m, 2H, Si-Ph), 7.39–7.36 (m, 3H, Si-Ph), 4.86 & 4.84 (2 × br dd, $J \approx 1.9$–2.2 Hz, 2H, 1-CH_2), 4.35 (br d, $J \approx 7.7$ Hz, 1H, 7-H), 2.62–2.42 (m, 3H, 2 × 2-H/3-H & 8-H_a), 1.95–1.77 (m, 6H, 2 × 2-H/3-H & 5-H_2 & 6-H_a & 8-H_b), 1.44–1.41 (m, 1H, 6-H_b), 1.37 (s, 3H, 8a-CH_3), 1.22 (s, 1H, 4-OH), 0.54 & 0.50 (2 × s, 2 × 3H, Si-CH_3).
^{13}C NMR (101 MHz, $CDCl_3$): δ = 164.8 (C1), 138.2 (Si-Ph, *ipso-C*), 134.8 (2 × Si-Ph, *ortho- or meta-C*), 129.1 (Si-Ph, *para-C*), 127.7 (2 × Si-Ph, *ortho- or meta-C*), 105.1 (1-CH_2), 96.0 (C3a), 75.3 (C7), 71.0 (C4), 58.0 (C8a), 46.7 (C8), 31.7 (C6), 29.6 (C5), 29.1 (C2 *or* C3), 29.0 (C2 *or* C3), 23.5 (8a-CH_3), −1.3 & −1.6 (2 × Si-CH_3). (**Figure 101**)
HRMS: calcd. for $C_{20}H_{28}NaO_2Si$ 351.17508 $[M+Na]^+$, found 351.17465 (Δ = 1.21 ppm).

4.3.2.2 Secondary Alcohols

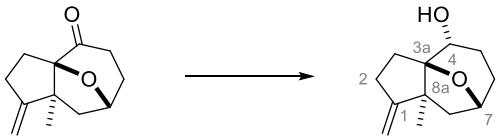

8-H **74-H**

74-H: **(3a*R**,4*R**,7*R**,8a*S**)-8a-Methyl-1-methyleneoctahydro-1*H*-3a,7-epoxyazulen-4-ol**

Preparation of $NaBH_4$ solution: $NaBH_4$ (113 mg) was placed in a 10 mL flask. After addition of EtOH (3.8 mL), the suspension was stirred until a clear solution was obtained (~45 min).

Reduction of ketone 8-H: In a 25 mL flask, a solution of ketone **8-H** (300 mg, 1.56 mmol, 1 eq) in MeOH (13.7 mL) was cooled in an ice bath. An aliquot of the prepared $NaBH_4$ solution (0.78 M in EtOH; 0.75 mL, 0.585 mmol, 0.375 eq of $NaBH_4$, equaling 1.5 hydride eq) was added, and the reaction mixture was stirred for 15 min. The reaction mixture was quenched with water (10 mL) and extracted with ethyl acetate (3 × 25 mL), before the combined organic phases were dried over $MgSO_4$, filtered, and concentrated in vacuo. Purification by flash chromatography (PE/DE, gradient from 10:1 to 1:1) gave alcohol **74-H** (249 mg, 1.28 mmol, **82%**) as a colorless solid.

$\mathbf{R_f}$ = 0.39 [$\mathbf{R_f}$ (**8-H**) = 0.72] (PE/EA, 1:1).
^{1}H NMR (400 MHz, $CDCl_3$): δ = 4.87 & 4.84 (2 × br dd, *J* ≈ 2.2–2.4 Hz, 2H, 1-CH_2), 4.27 (v br d, *J* ≈ 7.9 Hz, 1H, 7-H), 3.83 (br dd, *J* ≈ 10.5 Hz, 5.7 Hz, 1H, 4-H), 2.62–2.52 (m, 1H, 2-H_a), 2.48–2.40 (m, 2H, 2-H_b & 8-H_a), 2.14 (ddd, *J* = 13.5 Hz, 10.3 Hz, 10.2 Hz, 1H, 3-H_a), 2.04 (v br s, 1H, 4-OH), 1.96–1.79 (m, 4H, 5-H_a & 6-H_2 & 8-H_b), 1.62 (ddd, 1H, *J* = 13.5 Hz, 8.6 Hz, 2.0 Hz, 1H, 3-H_b), 1.52–1.48 (m, 1H, 5-H_b), 1.29 (s, 3H, 8a-CH_3).
^{13}C NMR (101 MHz, $CDCl_3$): δ = 165.0 (C1), 105.6 (1-CH_2), 93.8 (C3a), 74.9 (C7), 71.4 (C4), 55.2 (C8a), 46.3 (C8), 31.8 (C5), 28.7 (C2), 27.9 (C3), 26.8 (C6), 22.5 (8a-CH_3). (**Figure 102**)
HRMS: calcd. for $C_{12}H_{18}NaO_2$ 217.11990 $[M+Na]^+$, found 217.12032 (Δ = 1.92 ppm).

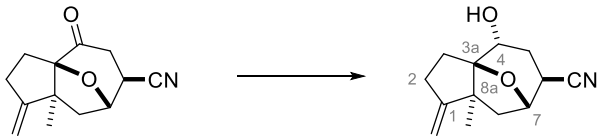

8 **74**

74: **(3a*R**,4*R**,6*S**,7*S**,8a*S**)-4-Hydroxy-8a-methyl-1-methyleneoctahydro-1*H*-3a,7-epoxyazulen-6-carbonitrile**

Preparation of $NaBH_4$ solution: $NaBH_4$ (126 mg) was placed in a 5 mL flask. After addition of EtOH (4.3 mL), the suspension was stirred until a clear solution was obtained (~45 min).

Reduction of ketone 8: In a 25 mL flask, a solution of ketone **8** (200 mg, 0.921 mmol, 1 eq) in MeOH (8 mL) was cooled in an ice bath. An aliquot of the prepared $NaBH_4$ solution (0.78 M in EtOH; 0.58 mL, 0.452 mmol, 0.5 eq of $NaBH_4$, equaling 2 hydride eq) was added, and the reaction mixture was stirred for 30 min. The reaction mixture was quenched with saturated NH_4Cl solution (10 mL), diluted with water (2 mL), and extracted with ethyl acetate (3 × 25 mL). The combined organic phases were dried over $MgSO_4$, filtered, and concentrated in vacuo, before the yellowish viscous oil was purified by flash chromatography (PE/EA, from 10:1 to 1:1). Hydroxynitrile **74** (195 mg, 0.889 mmol, **97%**) was obtained as a colorless solid (m.p. 155 °C).

$\mathbf{R_f}$ = 0.47 [$\mathbf{R_f}$ (**8**) = 0.53] (PE/EA, 1:1) *or*, for a more adequate reaction control:
$\mathbf{R_f}$ = 0.19 [$\mathbf{R_f}$ (**8**) = 0.47] (PE/DCM/MeOH, 1:1:0.1)
^{1}H NMR (400 MHz, $CDCl_3$): δ = 4.89 & 4.86 (2 × br dd, *J* ≈ 2.1 Hz, 2H, 1-CH_2), 4.44 (br d, *J* ≈ 2.1 Hz, 1H, 7-H), 4.16 (dd, *J* = 11.5 Hz, 5.9 Hz, 1H, 4-H), 2.75 (br d, *J* ≈ 6.1 Hz, 1H, 6-H), 2.65–2.44 (m, 3H, 3-H_2 & 8-H_a), 2.27–2.10 (m, 4H, 2-H_a & 4-OH & 5-H_2), 1.82–1.75 (m, 2H, 2-H_b & 8-H_b), 1.30 (s, 3H, 8a-CH_3). **^{13}C NMR** (101 MHz, $CDCl_3$): δ = 163.7 (C1), 121.0 (6-CN), 106.2 (1-CH_2), 94.8 (C3a), 74.9 (C7), 68.2 (C4), 54.6 (C8a), 45.8 (C8), 33.8 (C6), 28.9 (C5), 28.4 (C2), 27.6 (C3), 22.5 (8a-CH_3). (**Figure 103**)
HRMS: calcd. for $C_{13}H_{17}NNaO_2$ 242.11515 $[M+Na]^+$, found 242.11545 (Δ = 1.22 ppm).

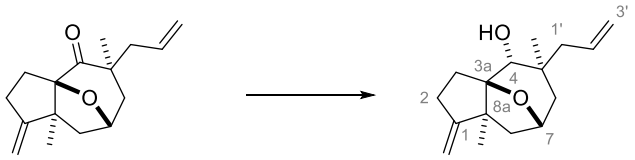

7-H **54-H**

54-H: **(3a*R**,4*R**,5*S**,7*R**,8a*S**)-5-Allyl-5,8a-dimethyl-1-methyleneoctahydro-1*H*-3a,7-epoxyazulen-4-ol**

Red-Al (~60 w-% in toluene) was diluted in THF (2 mL of THF for every milliliter of Red-Al solution), resulting in a ~1.03 M solution in THF/toluene.

In a 50 mL flask, ketone **7-H** (504 mg, 2.05 mmol, 1 eq) was dissolved in THF (20 mL) and cooled to –30 °C. The diluted Red-Al solution (~1.03 M; 2.2 mL, 2.26 mmol, 1.1 eq) was added over 5 min. After 1.25 h, half-saturated NH_4Cl solution (30 mL) was added at 0 °C and the biphasic mixture was extracted with Et_2O (3 × 50 mL). The combined organic phases were dried over $MgSO_4$, filtered, and concentrated in vacuo. Purification by flash chromatography (PE/DE, gradient from 10:1 to 2.5:1) afforded alcohol **54-H** (512 mg, 2.05 mmol, **quantitative yield**) as a colorless, very viscous oil.

$\mathbf{R_f}$ = 0.43 [$\mathbf{R_f}$ (**7-H**) = 0.79] (PE/DE, 2:1).
^{1}H NMR (400 MHz, $CDCl_3$): δ = 5.99–5.88 (m, 1H), 5.13 (br d, *J* ≈ 16.0 Hz, 1H), 5.07 (br d, *J* ≈ 10.0 Hz, 1H), 4.86 & 4.81 (2 × br dd, *J* ≈ 1.9–2.3 Hz, 2H), 4.25 (br dd, *J* ≈ 8.2 Hz, 5.1 Hz, 1H), 3.83 (d, *J* = 6.0 Hz, 1H), 2.59–2.44 (m, 2H), 2.40 (br dd, *J* ≈ 12.9 Hz, 8.5 Hz, 1H), 2.33–2.24 (m, 1H), 2.19–2.04 (m, 3H), 1.89 (dd, *J* = 14.1 Hz, 4.9 Hz, 1H), 1.69–1.63 (m, 2H), 1.55 (d, *J* = 14.1 Hz, 1H), 1.31 (s, 3H), 1.28 (s, 3H). **^{13}C NMR** (101 MHz, $CDCl_3$): δ = 165.8, 135.7, 117.9, 117.9, 105.3, 92.7, 78.5, 74.5, 54.4, 52.6, 44.2, 43.5, 37.0, 29.4, 27.5, 23.5, 22.5. (**Figure 104**)
HRMS: calcd. for $C_{16}H_{24}NNaO_2$ 271.16685 $[M+Na]^+$, found 271.16659 (Δ = 0.94 ppm).

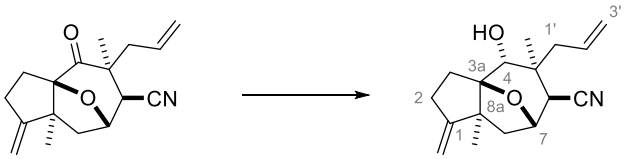

7 **54**

54: **(3a*R**,4*R**,5*S**,6*S**,7*S**,8a*S**)-5-Allyl-4-hydroxy-5,8a-dimethyl-1-methyleneoctahydro-1*H*-3a,7-epoxyazulen-6-carbonitrile**

Preparation of $NaBH_4$ solution: $NaBH_4$ (252 mg) was placed in a 25 mL flask. After addition of EtOH (8.4 mL), the suspension was stirred until a clear solution was obtained (~45 min).

Reduction of ketone 7: In a 25 mL flask, a solution of ketone **7** (268 mg, 0.988 mmol, 1 eq) in MeOH (8.6 mL) was cooled in an ice bath. An aliquot of the prepared $NaBH_4$ solution (0.78 M in EtOH; 0.47 mL, 0.367 mmol, 0.37 eq of $NaBH_4$, equaling 1.5 hydride equivalents) was added, and the reaction mixture was stirred for 45 min. Due to low conversion, several additional portions of $NaBH_4$ were added – initially, in the form of the prepared solution and later, as solid $NaBH_4$. In total, ~12 eq $NaBH_4$ (equaling ~48 hydride equivalents) were added over the course of 20 h, cooling the reaction mixture in an ice bath before each addition to minimize methanolysis of the borohydride. The reaction mixture was quenched with saturated NH_4Cl solution (20 mL), diluted with water (5 mL), and extracted with ethyl acetate (3 × 30 mL). The combined organic phases were dried over $MgSO_4$, filtered, and concentrated in vacuo. Purification by flash chromatography (PE/EA, from 10:1 to 1:1) afforded alcohol **54** (199 mg, 0.729 mmol, **74%**) as a colorless solid (m.p. 152 °C from DCM/hexane; 135–140 °C from C_6D_6).

$\mathbf{R_f}$ = 0.53 [$\mathbf{R_f}$ (**7**) = 0.64] (PE/EA, 2:1).
^{1}H NMR (400 MHz, $CDCl_3$): δ = 6.04–5.94 (m, 1H, 2'-H), 5.28 (br d, *J* ≈ 17.0 Hz, 1H, 3'-H_a), 5.20 (br d, *J* ≈ 10.0 Hz, 1H, 3'-H_b), 4.89 & 4.82 (2 × br dd, *J* ≈ 2.1–2.4 Hz, 2H, 1-CH_2), 4.50 (br d, *J* ≈ 8.4 Hz, 1H, 7-H), 3.94 (d, *J* = 5.8 Hz, 1H, 4-H), 2.73 (*app*. s, 1H, 6-H), 2.64–2.46 (m, 4H, 2-H_2 & 8-H_a & 1'-H_a), 2.39 (br dd, *J* ≈ 13.3 Hz, 5.8 Hz, 1H, 1'-H_b), 2.31–2.22 (m, 2H, 3-H_a & 8-H_b), 1.82–1.76 (m, 2H, 3-H_b & 4-OH), 1.39 (s, 3H, 5-CH_3), 1.31 (s, 3H, 8a-CH_3).
^{13}C NMR (101 MHz, $CDCl_3$): δ = 164.7 (C1), 134.0 (C2'), 120.3 (6-CN), 119.9 (C3'), 105.8 (1-CH_2), 93.6 (C3a), 77.0 (C4), 76.4 (C7), 54.3 (C8a), 49.9 (C1'), 44.7 (C6), 43.1 (C8), 38.5 (C5), 29.3 (C3), 27.4 (C2), 23.0 (5-CH_3), 22.2 (8a-CH_3). (**Figure 105**)
HRMS: calcd. for $C_{17}H_{23}NNaO_2$ 296.16210 $[M+Na]^+$, found 296.16216 (Δ = 0.20 ppm).
X-ray structure analysis: **Figure 22** on page **102.**

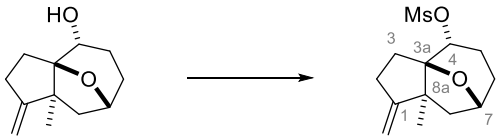

74-H **79-H**

79-H: **(3a*R**,4*R**,7*R**,8a*S**)-8a-Methyl-1- methyleneoctahydro-1*H*-3a,7-epoxyazulen-4-yl methanesulfonate**

In a 5 mL flask, a solution of alcohol **74-H** (50.5 mg, 0.26 mmol, 1 eq) in DCM (2.7 mL) was cooled in an ice bath. After addition of NEt_3 (0.072 mL, 0.52 mmol, 2 eq) and $MeSO_2Cl$ (0.03 mL, 0.39 mmol, 1.5 eq), the reaction mixture was stirred for 1 h and quenched with half-saturated $NaHCO_3$ solution (5 mL). The biphasic mixture was extracted with DCM (3 × 15 mL) before the combined organic phases were dried over $MgSO_4$, filtered, and concentrated in vacuo. Purification by flash chromatography (PE/DE, gradient from 10:1 to 2.5:1) afforded mesylate **79-H** (46 mg, 0.17 mmol, **65%**) as a colorless, very viscous oil.

R_f = 0.58 [**R_f** (**74-H**) = 0.39] (PE/EA, 1:1).
^{1}H NMR (400 MHz, $CDCl_3$): δ = 4.91 & 4.89 (2 × br dd, *J* ≈ 2.1–2.5 Hz, 2H), 4.80 (dd, *J* = 11.1 Hz, 6.3 Hz, 1H), 4.36–4.32 (m, 1H), 3.01 (s, 3H), 2.64–2.42 (m, 3H), 2.26–1.92 (m, 4H), 1.86 (dd, *J* = 12.6 Hz, 1.5 Hz, 1H), 1.74 (ddd, *J* = 13.7 Hz, 8.4 Hz, 1.8 Hz, 1H), 1.61–1.57 (m, 1H), 1.29 (s, 3H).
^{13}C NMR (101 MHz, $CDCl_3$): δ = 163.5, 106.2, 92.1, 79.6, 75.1, 55.5, 46.1, 38.6, 31.6, 28.5, 28.3, 24.9, 22.4. (**Figure 106**)

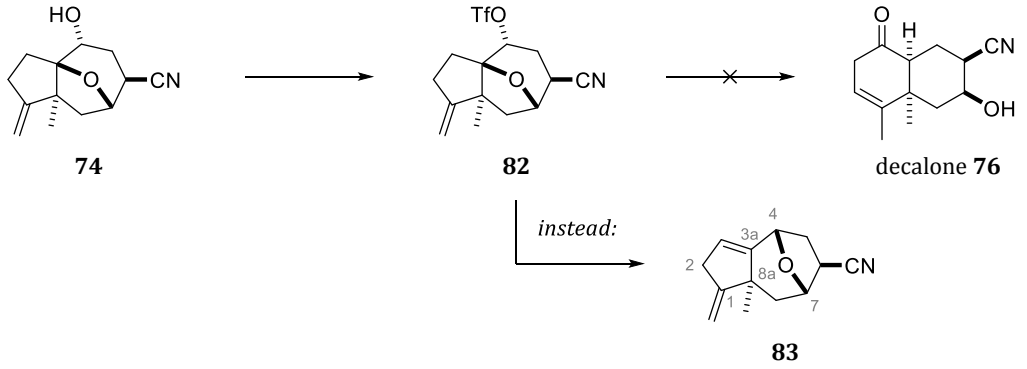

83: **(4*S**,6*S**,7*S**,8a*S**)-8a-Methyl-1-methylene-1,2,4,5,6,7,8,8a-octahydro-4,7-epoxyazulene-6-carbonitrile**

In a 10 mL flask, hydroxynitrile **74** (50 mg, 0.228 mmol, 1 eq) was dissolved in DCM (2 mL). In a separate flask, Tf_2O (0.21 mL) was diluted in DCM (0.79 mL). The solution of **74** was cooled in an ice bath, before pyridine (0.03 mL, 0.365 mmol, 1.6 eq) and an aliquot of the Tf_2O solution (1.25 M in DCM; 0.21 mL, 0.263 mmol, 1.15 eq) was added dropwise. The reaction mixture was allowed to warm to room temperature in the thawing ice bath. After 16 h, saturated $NaHCO_3$ solution (5 mL) was added. The biphasic mixture was extracted with DCM (3 × 10 mL). The combined organic phases were dried over $MgSO_4$, filtered, and concentrated in vacuo. Purification by flash chromatography (PE/DE, gradient from 10:1 to 2.5:1) afforded the elimination product **83** (13 mg, 0.069 mmol, **30%**) as a colorless oil.

Note: Before quenching the reaction mixture, another compound was observed in TLC analysis (R_f = 0.65, eluting with PE/EA, 1:1). This compound presumably corresponds to the triflate **82**. However, it was not possible to isolate this compound either with aqueous work-up or non-aqueous work-up (filtration through silica gel). A triflation procedure with Tf_2NPh (1.2 eq) and DMAP (3 eq) in DCM (0.1 M) proceeded similarly.

R_f = 0.78 [**R_f** (**74**) = 0.44] (PE/EA, 1:1).
^{1}H NMR (400 MHz, $CDCl_3$): δ = 5.59 (br dd, *app*. br s, *J* ≈ 2.3–2.4 Hz, 1H, 3-H), 4.92 (d, *J* = 7.2 Hz, 1H, 7-H), 4.77 (dd, *J* = 2.2 Hz, 1.3 Hz, 1H, 1-CH_a), 4.73 (br d, *J* ≈ 4.6 Hz, 1H, 4-H), 4.67–4.65 (m, 1H, 1-CH_b), 3.32 (dd, *J* = 9.2 Hz, 5.3 Hz, 1H, 6-H), 3.21–2.82 (m, 2H, 2-H_2), 2.52–2.38 (m, 2H, 8-H_2), 2.10 (dd, *J* ≈ 14.0 Hz, 4.7 Hz, 1H, 6-H_a), 1.90 (br d, *J* ≈ 14.1 Hz, 1H, 6-H_b), 1.24 (s, 3H, 8a-CH_3).
^{13}C NMR (101 MHz, $CDCl_3$): δ = 161.5 (C1), 146.2 (C3a), 122.6 (6-CN), 122.1 (C3), 104.0 (1-CH_2), 78.9 (C7), 76.2 (C4), 44.6 (C8a), 41.9 (C6), 36.3 (C2), 35.2 (C8), 32.4 (C6), 29.3 (8a-CH_3). (**Figure 107**)
HRMS: calcd. for $C_{13}H_{15}NNaO$ 224.10458 $[M+Na]^+$, found 224.10466 (Δ = 0.33 ppm).

4.3.3 Rearrangement of Tertiary Alcohols

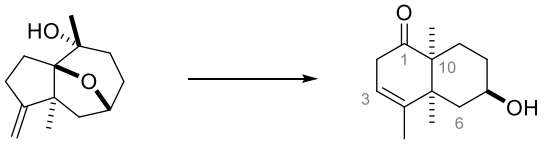

72-H **84-H**

Decalone 84-H: In a 5 mL flask, tertiary alcohol **72-H** (51.3 mg, 0.246 mmol, 1 eq) was dissolved in DCM (2.4 mL). The solution was cooled in an ice bath, before a $TiCl_4$ solution (1 M in DCM; 0.25 mL, 0.25 mmol, 1 eq) was added dropwise. After 1 h, the ice bath was removed, and the yellow suspension was stirred at room temperature for 45 h before being quenched with water (5 mL). After hydrolysis of the alcoholate, a clear solution was obtained for a short period of time before titanium oxide precipitated. DCM was removed in vacuo and the suspension was extracted with ethyl acetate (3 × 10 mL). Purification by flash chromatography (PE/EA, from 10:1 to 2.5:1) afforded decalone **84-H** (42 mg, 0.202 mmol, **82%**) as a slightly yellowish solid.

Notes: The rearrangement proceeded much quicker and, judging from TLC and NMR, with less impurities when **72-H** was treated a catalytic amount of $Sc(OTf)_3$ (10 mol%) in $MeNO_2$ (0.07 M). A complete conversion was noted after 2.25 h. This alternative was not evaluated quantitatively.

$\mathbf{R_f}$ = 0.40 [$\mathbf{R_f}$ (**72-H**) = 0.63] (PE/EA, 1:1).
^{1}H NMR (400 MHz, $CDCl_3$): δ = 5.36–5.32 (m, 1H, 3-H), 5.28 (br dddd, *J* ≈ 10.8 Hz, 4.3 Hz, 1H, 7-H), 2.98–2.70 (m, 2H, 2-H_2), 2.19 (br ddd, *J* ≈ 13.5 Hz, 3.9 Hz, 3.2 Hz, 1H, 9-H_a), 4.50 (br ddd, *J* ≈ 12.8 Hz, 3.9 Hz, 2.3 Hz, 1H, 6-H_a), 1.83–1.80 (m, 1H, 8-Ha), 1.71 (br dd, *J* ≈ 3.6 Hz, 2.0 Hz, 3H, 4-CH_3), 1.08 (s, 3H, 5-CH_3), 0.98 (br dd, *J* ≈ 12.1 Hz, 1H, 6-H_b), 0.98 (s, 3H, 10-CH_3).
^{13}C NMR (101 MHz, $CDCl_3$): δ = 213.5 (C1), 140.3 (C4), 116.7 (C3), 66.8 (C7), 50.3 (C10), 45.5 (C6), 44.6 (C5), 37.7 (C2), 32.3 (C8), 28.1 (C9), 21.4 (10-CH_3), 19.4 (4-CH_3), 19.1 (5-CH_3). (**Figure 108**)
HRMS: calcd. for $C_{13}H_{20}NaO_2$ 231.13555 $[M+Na]^+$, found 231.13556 (Δ = 0.03 ppm).

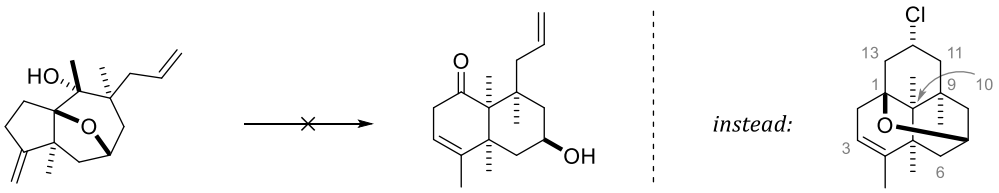

59-H **85-H** **86-H**

Tetracyclic Ether 86-H: In a 5 mL flask, tertiary alcohol **59-H** (43 mg, 0.164 mmol, 1 eq) was dissolved in DCM (2.9 mL). The solution was cooled in an ice bath, before a $TiCl_4$ solution [1 M in DCM; 0.15 mL, 0.150 mmol, 0.92 eq (*instead of intended 1 eq due to miscalculation*)] was added dropwise. The reaction mixture was allowed to warm to room temperature in the thawing ice bath. After stirring for 20 h, the blue suspension was quenched with sat. $NaHCO_3$ solution (2.5 mL). The resulting yellow emulsion was diluted with water (10 mL) and extracted with DCM (3 × 15 mL). The combined organic phases were dried over $MgSO_4$, filtered, and concentrated in vacuo. Purification by flash chromatography (PE/DE, gradient from 20:1 to 2.5:1) afforded tetracyclic ether **86-H** (30 mg, 0.107 mmol, **65%**) as a colorless solid (m.p. 69 °C).

$\mathbf{R_f}$ = 0.59 [$\mathbf{R_f}$ (**59-H**) = 0.37] (PE/DE, 3:1).
^{1}H NMR (400 MHz, $CDCl_3$): δ = 5.15–5.13 (m, 1H, 3-H), 4.46–4.38 (br dddd, *J* ≈ 12.1 Hz, 5.3 Hz, 1H, 12-H), 3.86 (br dd, *J* ≈ 5.1 Hz, 1H, 7-H), 2.12 (br ddd, *J* ≈ 14.1 Hz, 4.8 Hz, 2.9 Hz, 1H, 8-H_a), 2.07–1.79 (m, 6H, 2-H_2 & 6-H_a & 11-H_a & 13-H_2), 1.69–1.66 (m, 3H, 4-CH_3), 1.60 (br ddd, *J* ≈ 13.1 Hz, 5.1 Hz, 2.4 Hz, 1H, 11-H_b), 1.36 (d, *J* = 14.2 Hz, 1H, 8-H_b), 1.33 (d, *J* = 13.2 Hz, 1H, 6-H_b), 1.25 (s, 3H, 9-CH_3), 1.24 (s, 3H, 5-CH_3), 0.92 (s, 3H, 10-CH_3).
^{13}C NMR (101 MHz, $CDCl_3$): δ = 142.8 (C4), 116.4 (C3), 77.9 (C1), 63.7 (C7), 54.8 (C12), 50.0 (C11), 45.1 (C13), 44.4 (C6), 42.8 (C8), 39.4 (C5), 38.6 (C10), 38.3 (C2), 37.8 (C9), 30.8 (9-CH_3), 23.4 (5-CH_3), 20.6 (4-CH_3), 11.0 (10-CH_3). (**Figure 109**)
HRMS: calcd. for $C_{17}H_{25}ClNaO$ 303.14861 $[M+Na]^+$, found 303.14876 (Δ = 0.48 ppm).
Isotope pattern confirming chlorine substitution: 303.14876, 304.15207, 305.14607, 306.14892.
X-ray structure analysis: **Figure 23** on page **109.**

4.3.4 Rearrangement of Ketones

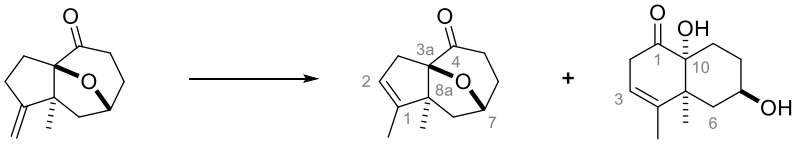

8-H **8-H.a** **93-H**

8-H.a: **(3a*R**,7*R**,8a*S**)-1,8a-Dimethyl-3,5,6,7,8,8a-hexahydro-4*H*-3a,7-epoxyazulen-4-one**

Hydroxy Acyloin 93-H: In a 3.5 mL screw-top vial, ketone **8-H** (26.2 mg, 0.136 mmol, 1 eq) was dissolved in DCM (1 mL). The solution was cooled in an ice bath, before a $TiCl_4$ solution (1 M in DCM; 0.14 mL, 0.140 mmol, 1 eq) was added dropwise. The reaction mixture was allowed to warm to room temperature in the thawing ice bath. After stirring for 18 h, the reddish-brown suspension was quenched with water (5 mL) and extracted with DCM (4 × 5 mL). The combined organic phases were dried over $MgSO_4$, filtered, and concentrated in vacuo. Purification by flash chromatography (PE/DE, gradient from 15:1 to 1:1) afforded both alkene isomer **8-H.a** (8.7 mg, 0.045 mmol, **33%**) and hydroxy acyloin **93-H** (8.5 mg, 0.044 mmol, **32%**) as colorless solids.

8-H.a: $\mathbf{R_f}$ = 0.62 [$\mathbf{R_f}$ (**8-H**) = 0.68] (PE/EA, 2:1).
^{1}H NMR (400 MHz, $CDCl_3$): δ = 5.20–5.16 (m, 1H, 2-H), 4.58 (br dd, *J* ≈ 6.5 Hz, 4.7 Hz, 1H, 7-H), 3.00 (br dddd, *J* ≈ 17.5 Hz, 4.5 Hz, 2.5 Hz, 2.2 Hz, 1H, 3-H_a), 2.63–2.54 (m, 1H, 5-H_a), 2.44–2.33 (m, 3H, 5-H_b & 6-H_a & 8-H_a), 2.18 (br dddd, *J* ≈ 17.5 Hz, 4.1 Hz, 1.9–2.1 Hz, 1H, 5-H_b), 1.82–1.74 (m, 1H, 6-H_b), 1.66 (s, 3H, 1-CH_3), 1.54 (dd, *J* ≈ 12.6 Hz, 0.9 Hz, 1H, 8-H_b), 1.04 (s, 3H, 8a-CH_3).
^{13}C NMR (101 MHz, $CDCl_3$): δ = 207.4 (C4), 143.2 (C1), 120.3 (C2), 98.8 (C3a), 74.2 (C7), 60.6 (C8a), 40.6 (C8), 33.9 (C3), 33.4 (C5), 29.9 (C6), 20.1 (8a-CH_3), 12.3 (1-CH_3). (**Figure 110**)

93-H: $\mathbf{R_f}$ = 0.47 (PE/EA, 2:1).
^{1}H NMR (300 MHz, $CDCl_3$): δ = 5.30–5.33 (m, 1H, 3-H), 4.18–4.12 (m, 1H, 7-H), 3.86 (s, 1H, 10-OH), 3.25–2.86 (m, 2H, 2-H_2), 2.47 (br ddd, *J* ≈ 13.5 Hz, 13.3 Hz, 4.0 Hz, 1H, 9-H_a), 2.11–1.98 (m, 2H, 6-H_a & 8-H_a), 1.90 (br dd, *J* ≈ 3.3 Hz, 1.8 Hz, 3H, 4-CH_3), 1.62 (m, 2H, 6-H_b & 8-H_b), 1.28 (br ddd, *J* ≈ 13.3 Hz, 3.3 Hz, 9-H_b), 0.85 (s, 3H, 5-CH_3).
^{13}C NMR (76 MHz, $CDCl_3$): δ = 212.3 (C1), 143.3 (C4), 115.4 (C3), 79.0 (C10), 66.8 (C7), 45.1 (C5), 37.6 (C2), 36.7 (C6), 27.8 (C8), 26.9 (C9), 24.2 (5-CH_3), 20.0 (4-CH_3). (**Figure 111**)

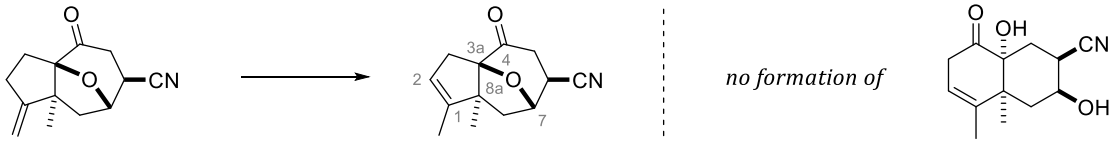

8 **8.a** **93**

8.a: **(3a*R**,6*S**,7*S**,8a*S**)-1,8a-Dimethyl-4-oxo-4,5,6,7,8,8a-hexahydro-3*H*-3a,7-epoxyazulen-6-carbonitrile**

In a 3.5 mL screw-top vial, ketonitrile **8** (29.6 mg, 0.136 mmol, 1 eq) was dissolved in MeCN (1 mL). The solution was cooled in an ice bath, before a $TiCl_4$ solution (1 M in DCM; 0.34 mL, 0.340 mmol, 2.5 eq) was added dropwise. The reaction mixture was allowed to warm to room temperature in the thawing ice bath. After stirring for 3 d, the reddish-brown suspension was quenched with water (5 mL) and extracted with ethyl acetate (3 × 5 mL). The combined organic phases were dried over $MgSO_4$, filtered, and concentrated in vacuo, affording crude alkene isomer **8.a**.

Notes: No rearrangement was observed. The crude product was not purified but exhibited exceptionally clean NMR spectra with the only discernible impurity being residual DCM.

$\mathbf{R_f}$ = 0.44, *not distinguishable from substrate* **8** *by eluting only once* (PE/EA, 1:1).
^{1}H NMR (400 MHz, $CDCl_3$): δ = 5.21–5.18 (m, 1H, 2-H), 4.74 (dd, *J* = 7.6 Hz, 0.8 Hz, 1H, 7-H), 3.06–2.96 (m, 2H, 3-H_a & 6-H), 2.85 (ddd, *J* = 18.1 Hz, 4.6 Hz, 0.9 Hz, 1H, 5-H_a), 2.70 (dd, *J* = 18.1 Hz, 8.4 Hz, 1H, 5-H_b), 2.46 (dd, *J* = 13.4 Hz, 7.6 Hz, 1H, 8-H_a), 2.30 (br ddd, *J* ≈ 2.5 Hz, 3H, 1-CH_3), 1.58 (br dd, *J* ≈ 13.3 Hz, 1.0 Hz, 1H, 8-H_b), 1.00 (s, 3H, 8a-CH_3).
^{13}C NMR (101 MHz, $CDCl_3$): δ = 202.0 (C4), 142.2 (C1), 120.63 (C2), 120.57 (6-CN), 99.5 (C3a), 75.9 (C7), 60.4 (C8a), 40.2 (C8), 36.3 (C5), 33.9 (C3), 32.9 (C6), 20.3 (8a-CH_3), 12.1 (1-CH_3). (**Figure 112**)

4.3.5 Rearrangement of Secondary Alcohols

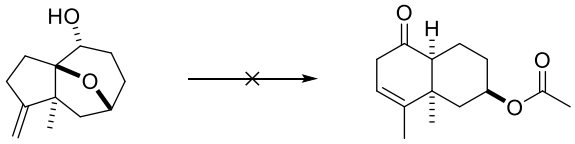

74-H **100-H**

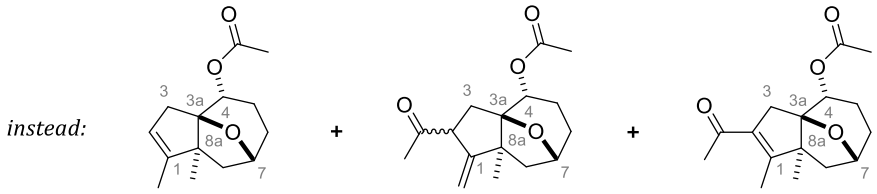

instead: **99-H** **101-H** **102-H**

99-H: **(3a*R**,4*R**,7*R**,8a*S**)-1,8a-Dimethyl-4,5,6,7,8,8a-hexahydro-3*H*-3a,7-epoxyazulen-4-yl acetate**

101-H: **(3a*R**,4*R**,7*R**,8a*S**)-2-Acetyl-8a-methyl-1-methyleneoctahydro-1*H*-3a,7-epoxyazulen-4-yl acetate**

102-H: **(3a*R**,4*R**,7*R**,8a*S**)-2-Acetyl-1,8a-dimethyl-4,5,6,7,8,8a-hexahydro-3*H*-3a,7-epoxyazulen-4-yl acetate**

Formation of 99-H, 101-H and 102-H: In a 10 mL flask, alcohol **74-H** (50 mg, 0.257 mmol, 1 eq) was dissolved in Ac_2O (2.5 mL) (*under air*). The solution was cooled in an ice bath, $Sc(OTf)_3$ (3.2 mg, 6.43 µmol, 2.5 mol%) was added, and the reaction mixture was stirred at 0 °C for 1.5 h and then at room temperature for 2.5 h. Another portion of $Sc(OTf)_3$ (3.2 mg, 6.43 µmol, 2.5 mol%) was added, before the reaction mixture was quenched with saturated $NaHCO_3$ solution (10 mL) after stirring for another hour. The combined organic phases from extraction with DCM (3 × 10 mL) were washed with saturated $NaHCO_3$ solution (10 mL), dried over $MgSO_4$, and concentrated in vacuo. Purification by flash chromatography (PE/DE, gradient from 20:1 to 1:1.5) afforded acetate **99-H** (24.9 mg, 0.105 mmol, **41%**) and the 2-acylated acetates **101-H** (17.9 mg, 0.064 mmol, **25%**) and **102-H** (15.1 mg, 0.054 mmol, **21%**), respectively.

Notes: All compounds were obtained as slightly yellow, very viscous oils. Some impurities were discernible in TLC and NMR. While two diastereomers of **101-H** are conceivable, only one of those was obtained. The C2-configuration of the obtained diastereomer was not determined.

A third carbonyl compound co-eluted with **102-H** (δ = 206.9 ppm in ^{13}C NMR). This compound could not be isolated due to the very close R_f values. With the following procedure, a selective formation of **102-H** was achieved, albeit in moderate yield.

Selective formation of 102-H: In a 25 mL flask, alcohol **74-H** (182 mg, 0.937 mmol, 1 eq) was dissolved in Ac_2O/AcOH (1:1, 8 mL) (*under air*). After addition of $Sc(OTf)_3$ (23 mg, 0.047 mmol, 5 mol%), the solution was stirred at 50 °C for 15 h and then at 80 °C for 4 h. The volatiles were removed in vacuo, before the residue was quenched with saturated $NaHCO_3$ solution (3 mL) and water (6 mL). The combined organic phases from the extraction with DCM (3 × 10 mL) were dried over $MgSO_4$, filtered, and concentrated. Purification by flash chromatography (PE/DE, gradient from 10:1 to 1:1.5) afforded **102-H** (126 mg, 0.453 mmol, **48%**) as a colorless oil.

99-H: $\mathbf{R_f}$ = 0.76 [$\mathbf{R_f}$ (**74-H**) = 0.42] (PE/EA, 1:1).
^{1}H NMR (400 MHz, $CDCl_3$): δ = 5.15 (v br s, 1H), 5.07 (br dd, *J* ≈ 10.6 Hz, 5.8 Hz, 1H), 4.35–4.29 (m, 1H), 2.46–2.38 (m, 1H), 2.32 (dd, *J* = 12.8 Hz, 7.9 Hz, 1H), 2.15–1.89 (m, 4H) *superimposed with* 2.04 (s, 3H), 1.66 (br ddd, *J* ≈ 2.5 Hz, 1.5 Hz, 1.3 Hz, 3H), 1.58–1.53 (m, 1H), 1.46 (dd, *J* = 12.7 Hz, 1.0 Hz, 1H), 1.30 (s, 3H). **^{13}C NMR** (101 MHz, $CDCl_3$): δ = 170.2, 146.5, 119.3, 91.6, 75.0, 72.0, 58.7, 39.0, 35.9, 31.4, 23.7, 21.2, 19.1, 12.0. (**Figure 113**)
HRMS: calcd. for $C_{14}H_{20}NaO_3$ 259.13047 $[M+Na]^+$, found 259.13032 (Δ = 0.56 ppm).

101-H: $\mathbf{R_f}$ = 0.58 [$\mathbf{R_f}$ (**74-H**) = 0.42] (PE/EA, 1:1).
^{1}H NMR (400 MHz, $CDCl_3$): δ = 5.17 & 5.06 (2 × br d, *J* ≈ 1.9–2.1 Hz, 1H, 1-CH_2), 5.01 (br dd, *J* ≈ 10.9–11.1 Hz, 5.9–6.1 Hz, 1H, 4-H), 4.34–4.28 (m, 1H, 7-H), 3.36 (dddd, *J* ≈ 8.9 Hz, 3.8 Hz, 2.0 Hz, 1.9 Hz, 1H, 2-H), 2.50 (dd, *J* = 12.7 Hz, 7.9 Hz, 1H, 8-H_a), 2.20–2.00 [m, 9H, 2-C(O)CH_3 (s, 3H) & 4-OC(O)CH_3 (s, 3H) & 3-H_2 & 5-H_a], 1.96–1.75 (m, 3H, 5-H_b & 6-H_a & 8-H_b), 1.56–1.48 (m, 1H, 6-H_b), 1.34 (s, 3H, 8a-CH_3).
^{13}C NMR (101 MHz, $CDCl_3$): δ = 208.7 (2-<u>*C*</u>(O)CH_3), 170.0 (4-O<u>*C*</u>(O)CH_3), 161.7 (C1), 110.2 (1-CH_2), 91.7 (C3a), 75.0 (C7), 71.8 (C4), 56.4 (C8a), 55.4 (C2), 46.0 (C8), 32.1 (C3), 31.1 (C6), 26.9 (2-C(O)<u>*C*</u>H_3), 23.2 (C5), 22.7 (8a-CH_3), 21.2 (4-OC(O)<u>*C*</u>H_3). (**Figure 114**)
HRMS: calcd. for $C_{16}H_{22}NaO_4$ 301.14103 $[M+Na]^+$, found 301.14121 (Δ = 0.61 ppm).

102-H: $\mathbf{R_f}$ = 0.50 [$\mathbf{R_f}$ (**74-H**) = 0.42] (PE/EA, 1:1).
^{1}H NMR (400 MHz, $CDCl_3$): δ = 5.01 (br dd, *J* ≈ 10.9 Hz, 6.0 Hz, 1H, 4-H), 4.24 (v br d, *J* ≈ 5.2 Hz, 1H, 7-H), 2.72–2.45 (m, 2H, 3-H_2), 2.35 (br dd, *J* ≈ 12.9 Hz, 7.9 Hz, 1H, 8-H_a), 2.16 (s, 3H, 2-C(O)CH_3), 2.08–1.90 [m, 8H, 1-CH_3 (1.97, br s, 3H) & 4-OC(O)CH_3 (2.00, s, 3H) & 5-H_a & 6-H_a], 1.86–1.75 (m, 1H, 5-H_b), 1.56–1.48 (m, 2H, 6-H_b & 8-H_b), 1.27 (s, 3H, 8a-CH_3).
^{13}C NMR (101 MHz, $CDCl_3$): δ = 197.9 (2-<u>*C*</u>(O)CH_3), 169.8 (4-O<u>*C*</u>(O)CH_3), 158.5 (C1), 130.4 (C2), 88.9 (C3a), 74.5 (C7), 71.2 (C4), 61.9 (C8a), 39.4 (C8), 37.2 (C3), 30.9 (C6), 30.3 (2-C(O)<u>*C*</u>H_3), 23.5 (C5), 21.0 (4-OC(O)<u>*C*</u>H_3), 18.4 (8a-CH_3), 12.9 (1-CH_3). (**Figure 115**)
HRMS: calcd. for $C_{16}H_{22}NaO_4$ 301.14103 $[M+Na]^+$, found 301.14109 (Δ = 0.21 ppm).

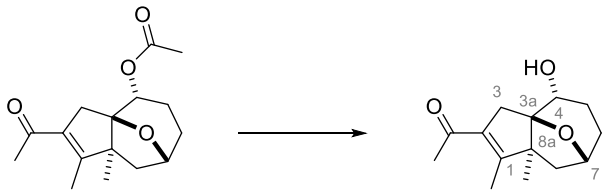

102-H **102-H.a**

102-H.a: **1-((3a*R**,4*R**,7*R**,8a*S**)-4-Hydroxy-1,8a-dimethyl-4,5,6,7,8,8a-hexahydro-3*H*-3a,7-epoxyazulen-2-yl)ethan-1-one**

In a 10 mL flask, 2-acetylated acetate **102-H** (48.5 mg, 0.174 mmol, 1 eq) was dissolved in DCM (3.4 mL) (*under air*). After addition of a NaOMe solution (~5.4 M in MeOH; 0.1 mL, 0.54 mmol 3.1 eq), the reaction mixture was stirred for 1 h before saturated NH_4Cl solution (3 mL) and water (6 mL) were added. The combined organic phases from the extraction with DCM (3 × 15 mL) were dried over $MgSO_4$, filtered, and concentrated in vacuo, affording 2-acylated alcohol **102-H.a** (43.8 mg, 0.185 mmol, 107% crude yield) as a yellow viscous oil.

Notes: This methanolysis was conducted for structural elucidation of **102-H** before confirmation of its structure by NMR and HRMS analysis. The crude product exhibited clean NMR spectra which allowed for an assignment of the NMR signals without purification. In a second experiment, the obtained crude product was resubjected to methanolysis with prolonged exposure (~4 d) to a greater excess of NaOMe (12.4 eq). As expected, the starting material remained unchanged, reaffirming a *C*-acylation at C2.

R_f = 0.19 [**R_f** (**102-H**) = 0.51] (PE/EA, 1:1).
^{1}H NMR (400 MHz, $CDCl_3$): δ = 4.23 (br dd, *J* ≈ 7.6 Hz, 1H, 7-H), 3.95–3.89 (m, 1H, 4-H), 3.12–2.44 (m, 2H, 3-H_2), 2.35 (dd, *J* = 13.0 Hz, 8.0 Hz, 1H, 8-H_a) *superimposed with* 2.40–2.25 (v br s, 1H, 4-OH), 2.21 (s, 3H, 2-C(O)CH_3), 2.02–1.82 [m, 6H, 1-CH_3 (2.00, br dd, 3H) & 5-H_2 & 6-H_a], 1.57–1.50 (m, 2H, 6-H_b & 8-H_b), 1.31 (s, 3H, 8a-CH_3).
^{13}C NMR (101 MHz, $CDCl_3$): δ = 198.6 (2-*C*(O)CH_3), 159.5 (C1), 130.9 (C2), 90.3 (C3a), 74.5 (C7), 70.4 (C4), 61.9 (C8a), 39.8 (C8), 37.1 (C3), 31.5 (C6), 30.5 (2-C(O)*C*H_3), 27.0 (C5), 18.5 (8a-CH_3), 13.2 (1-CH_3). (**Figure 116**)
HRMS: calcd. for $C_{14}H_{20}NaO_3$ 259.13047 $[M+Na]^+$, found 259.13051 (Δ = 0.17 ppm).

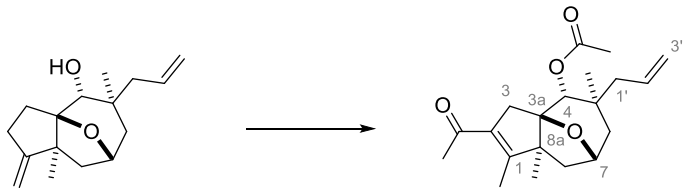

54-H **104-H**

104-H: **(3a*R**,4*R**,5*S**,7*R**,8a*S**)-2-Acetyl-5-allyl-1,5,8a-trimethyl-4,5,6,7,8,8a-hexahydro-3*H*-3a,7-epoxyazulen-4-yl acetate**

In a 3.5 mL screw-top vial, alcohol **54-H** (20.5 mg, 0.083 mmol, 1 eq) was dissolved in Ac_2O/AcOH (1:1, 0.84 mL) (*under air*). After addition of $Sc(OTf)_3$ (4.06 mg, 8.3 µmol, 10 mol%), the reaction mixture was stirred for 18.5 h and then at 50 °C for 5 h. The purple solution was filtered through silica gel, eluting with ethyl acetate. After removal of volatiles in vacuo, the residue was purified by flash chromatography (PE/DE, gradient from 20:1 to 1:1), affording α,β-unsaturated ketone **104-H** (16.7 mg, 0.050 mmol, **61%**) as a slightly yellow, very viscous oil.

$\mathbf{R_f}$ = 0.36 [$\mathbf{R_f}$ (**54-H**) = 0.64] (PE/EA, 3:1).

^{1}H NMR (400 MHz, $CDCl_3$): δ = 5.84–5.74 (m, 1H, 2'-H), 5.26 (s, 1H, 4-H), 5.09–5.03 (m, 2H, 3'-H_2), 4.29–4.24 (m, 1H, 7-H), 2.65–2.55 (m, 2H, 3-H_2), 2.33 (dd, *J* = 13.3 Hz, 8.3 Hz, 1H, 8-H_a), 2.19 (s, 3H, 2-C(O)CH_3), 2.11–2.04 [m, 6H, 4-OC(O)CH_3 (2.08, s, 3H) & 6-H_a & 1'-H_2], 2.01 (br dd, *J* ≈ 1.7–1.9 Hz, 3H, 1-CH_3), 1.90 (dd, *J* = 13.3 Hz, 1.3 Hz, 1H, 6-H_b), 1.50 (br d, *J* = 14.3 Hz, 1H, 8-H_b), 1.34 (s, 3H, 5-CH_3), 1.24 (s, 3H, 8a-CH_3).

^{13}C NMR (101 MHz, $CDCl_3$): δ = 198.3 (2-*C*(O)CH_3), 170.3 (4-O*C*(O)CH_3), 159.9 (C1), 133.8 (C2'), 129.5 (C2), 118.5 (C3'), 88.9 (C3a), 76.5 (C4), 73.8 (C7), 61.0 (C8a), 50.9 (C1'), 43.1 (C6), 39.0 (C3), 38.5 (C8), 36.4 (C5), 30.5 (2-*C*(O)CH_3), 24.6 (5-CH_3), 21.0 (4-OC(O)*C*H_3), 18.9 (8a-CH_3), 13.2 (1-CH_3). (**Figure 117**)

4.4 BASE-INDUCED REARRANGEMENT TO THE DECALONE CORE

4.4.1 Ether Cleavage of β-Oxa-Bridged Nitriles

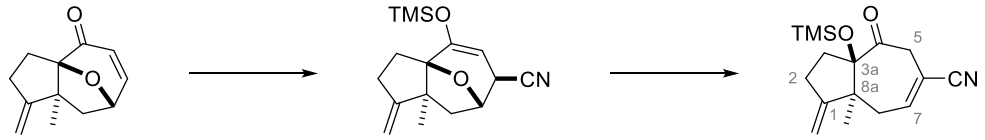

9 **33** **105**

105: **(3a*R**,8a*S**)-8a-Methyl-1-methylene-4-oxo-3a-((trimethylsilyl)oxy)-1,2,3,3a,4,5,8,8a-octahydroazulene-6-carbonitrile**

Silyl enol ether **33** was prepared from enone **9** (50 mg, 0.263 mmol, 1 eq) according to the previously described procedure (**Chapter 4.2.1**). This crude silyl enol ether was dissolved in THF (0.5 mL) in a 3.5 mL screw-top vial fitted with a septum. The solution was cooled to –78 °C before MeLi (1.6 M in hexane; 0.16 mL, 0.256 mmol, 0.97 eq) was added (5 min). The reaction mixture was allowed to warm to room temperature (20 h) and quenched with water (5 mL). After extraction with ethyl acetate (3 × 10 mL), the combined organic phases were dried over $MgSO_4$, filtered, and concentrated in vacuo. A yellow oil was obtained which consisted mainly of *O*-silylated acyloin **105** (62.3 mg, "0.215 mmol," 81% crude yield).

Notes: An analytical sample of **105** was isolated as a colorless oil from a previous epoxide opening attempt, in which **33** was treated with MeLi and then (3-furyl)-oxirane, as briefly described in **Chapters 2.2.1** and **2.4.1**.

$\mathbf{R_f}$ = 0.84 [$\mathbf{R_f}$ (**33**) = 0.77] [$\mathbf{R_f}$ (**9**) = 0.47] (PE/EA, 1:1).
^{1}H NMR (400 MHz, $CDCl_3$): δ = 6.65–6.63 (m, 1H), 4.92 & 4.78 (2 × br dd, *J* ≈ 1.7–2.6 Hz, 2H), 3.85–3.78 (m, 1H), 3.12–3.07 (m, 1H), 2.83–2.75 (m, 1H), 2.61–2.33 (m, 4H), 1.74–1.67 (m, 1H), 0.77 (s, 3H), 0.10 (s, 9H). **^{13}C NMR** (101 MHz, $CDCl_3$): δ = 204.3, 157.7, 146.0, 119.9, 106.7, 105.8, 92.8, 50.3, 42.0, 34.9, 29.5, 27.7, 23.4, 1.2. (**Figure 118**)
HRMS: calcd. for $C_{16}H_{23}NNaO_2Si$ 312.13903 $[M+Na]^+$, found 312.13912 (Δ = 0.30 ppm).

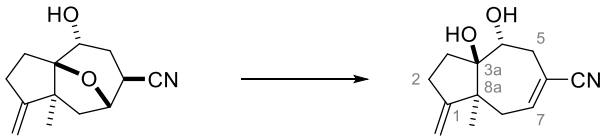

74 **106**

106: **(3a*R**,4*R**,8a*S**)-3a,4-Dihydroxy-8a-methyl-1-methylene-1,2,3,3a,4,5,8,8a-octahydroazulene-6-carbonitrile**

Preparation of LDA solutions: Diisopropylamine (0.39 mL, 2.78 mmol, 1.1 eq; *distilled from NaOH and stored over NaOH under argon*) was dissolved in THF (1.1 mL) in a 5 mL flask. The solution was cooled to –78 °C before *n*-BuLi (2.5 M in hexane; 1.0 mL, 2.50 mmol, 1 eq) was added dropwise (1 min). The reaction mixture was allowed to warm to –10 °C over the course of 1 h. After stirring at room temperature for 1 h, the LDA solution (1 M) was used promptly.

Hydroxynitrile **74** (50 mg, 0.228 mmol, 1 eq) was dissolved in THF (4 mL) in a 10 mL flask. The solution was cooled to –78 °C before a freshly prepared LDA solution (1 M in THF/hexane; 0.25 mL, 0.250 mmol, 1.1 eq) was added rapidly. The same volume of LDA solution was added again after 20 min and the yellow reaction mixture quenched with acetic acid (0.2 mL, 3.50 mmol, ~15 eq) after another 30 min (at –55 °C). After removal of volatiles in vacuo, the residue was filtered through a plug of silica gel, eluting with ethyl acetate (total volume ~25 mL). The filtrate was concentrated, affording *trans*-diol **106** (53.3 mg, "0.243 mmol," 107% crude yield) as a very viscous oil.

Notes: The LDA solution prepared in this specific experiment contained a slight excess of *n*-BuLi as a result of miscalculation: 0.31 mL instead of 0.39 mL diisopropylamine were employed, resulting in a ratio of 1.0:1.1 instead of 1.1:1.0 (DIPA/*n*-BuLi). The second portion of LDA solution was added after no conversion was clearly determinable after 10 min (TLC control) due to very similar R_f values of hydroxynitrile **74** and *trans*-diol **106**. Crude *trans*-diol **106** exhibited exceptionally clean NMR spectra.

R_f = 0.64 [**R_f** (**74**) = 0.70] (PE/EA, 1:1; *eluted twice*).
^{1}H NMR (400 MHz, $CDCl_3$): δ = 6.84–6.79 (m, 1H), 4.88 & 4.78 (2 × br dd, *J* ≈ 1.4–2.4 Hz, 2H), 3.98 (br d, *J* ≈ 4.3 Hz, 1H), 3.17 (br ddd, *J* ≈ 15.5 Hz, 4.5 Hz, 2.2 Hz, 1H), 2.65–2.34 (m, 5H), 2.23 (dd, *J* = 14.7 Hz, 9.2 Hz, 1H), 2.19 (v br s, 1H), 1.50 (v br s, 1H), 1.46–1.41 (m, 1H), 1.10 (s, 3H).
^{13}C NMR (101 MHz, $CDCl_3$): δ = 157.7, 149.1, 121.3, 113.8, 104.8, 83.9, 72.8, 49.5, 32.5, 32.2, 30.7, 25.3, 23.1. (**Figure 119**)

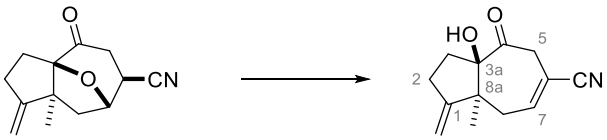

8 **107**

107: **(3a*R**,8a*S**)-3a-Hydroxy-8a-methyl-1-methylene-4-oxo-1,2,3,3a,4,5,8,8a-octahydroazulene-6-carbonitrile**

Ketonitrile **8** (372.9 mg, 1.716 mmol, 1 eq) was dissolved in THF (55 mL) in a 100 mL flask.[a] The solution was cooled to –95 °C before a freshly prepared LDA solution (1 M in THF/hexane; 3.74 mL, 3.740 mmol, 2.2 eq) was added rapidly. The yellow reaction mixture was quenched with acetic acid (1.65 mL, 28.9 mmol, ~17 eq) after 10 min (at –95 °C). After removal of volatiles in vacuo, the residue was filtered through a plug of silica gel, eluting with ethyl acetate (total volume ~120 mL). The concentrated filtrate was purified by flash chromatography (PE/DE, gradient from 10:1 to 1:2), affording both acyloin **107** (296.8 mg, 1.366 mmol, **80%**) and *trans*-diol **106** (28 mg, 0.128 mmol, **7%**) as very viscous oils which solidified in the freezer.

Notes: Two separate runs were conducted with 33.9 mg and 339 mg of **8**, respectively. The crude products were combined before purification by flash chromatography. The unexpected appearance of *trans*-diol is explicable by a reduction of **107** by LDA.

$\mathbf{R_f}$ = 0.74 [$\mathbf{R_f}$ (**8**) = 0.48] (PE/EA, 1:1).
^{1}H NMR (400 MHz, $CDCl_3$): δ = 6.66–6.64 (m, 1H), 4.97 & 4.84 (2 × br s, 2H), 4.07–4.03 (m, 1H), 3.01 (d, *J* = 16.5 Hz, 1H), 2.80 (br d, *J* ≈ 17.8 Hz, 1H), 2.66–2.50 (m, 4H), 2.41 (dd, *J* = 17.8 Hz, 8.2 Hz, 1H), 1.60–1.55 (m, 1H), 0.79 (s, 3H). **^{13}C NMR** (101 MHz, $CDCl_3$): δ = 204.4, 157.1, 145.9, 119.9, 107.0, 106.7, 90.1, 49.3, 41.7, 34.3, 30.6, 27.2, 23.6. (**Figure 120**)

4.4.3 Acyloin Rearrangement of Ketonitrile 7

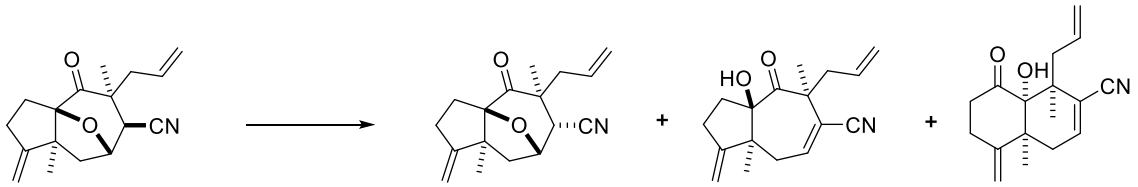

7 6-*epi*-**7** **110** **111**

Depending on conditions, either [5,7]-fused acyloin **110** or the desired [6,6]-fused acyloin **111** could be isolated. The substrate **7** and its epimer 6-*epi*-**7** were also recovered.

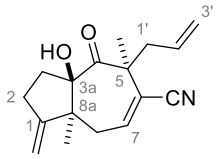

110

110: **(3a*R**,5*S**,8a*S**)-5-Allyl-3a-hydroxy-5,8a-dimethyl-1-methylene-4-oxo-1,2,3,3a,4,5,8,8a-octahydroazulene-6-carbonitrile**

Ketonitrile **7** (66.6 mg, 0.245 mmol, 1 eq) was dissolved in THF (4.9 mL) in a 10 mL flask. The solution was cooled to –95 °C before a freshly prepared LDA solution (1 M in THF/hexane; 0.27 mL, 0.270 mmol, 1.1 eq) was added rapidly. The yellow solution was quenched with acetic acid (0.2 mL, 3.50 mmol, ~14 eq) after 20 min (at –80 °C). After removal of volatiles in vacuo, the residue was filtered through a plug of silica gel, eluting with ethyl acetate (total volume ~25 mL). The concentrated filtrate was purified by flash chromatography (PE/DE, gradient from 20:1 to 1:1), affording substrate **7** (11.9 mg, 0.044 mmol, **18%**), its epimer 6-*epi*-**7** (23 mg, 0.085 mmol, **35%**), as well as [5,7]-fused acyloin **110** [24.3 mg, 0.090 mmol, **37%** (77% *b.r.s.m.*)] as colorless, very viscous oils.

$\mathbf{R_f}$ = 0.56 [$\mathbf{R_f}$ (**7**) = 0.65] [$\mathbf{R_f}$ (6-*epi*-**7**) = 0.70] (PE/EA, 3:1).
^{1}H NMR (400 MHz, $CDCl_3$): δ = 6.56 (dd, *J* = 6.1 Hz, 3.2 Hz, 1H, 7-H), 5.75–5.65 (m, 1H, 2'-H), 5.10–5.03 (m, 2H, 3'-H_2), 4.98 & 4.82 (2 × br dd, *J* ≈ 1.8–2.2 Hz, 2H, 1-CH_2), 2.91 (dd, *J* = 14 Hz, 6.9 Hz, 1H, 1'-H_a), 2.81 (dd, *J* = 20 Hz, 2.9 Hz, 1H, 1'-H_b), 2.70–2.45 (m, 5H, 2-H_2 & 3-H_a & 8-H_2), 1.89 (s, 1H, 3a-OH), 1.57–1.52 (m, 1H, 3-H_b), 1.45 (s, 3H, 8a-CH_3), 0.80 (s, 3H, 5-CH_3).
^{13}C NMR (101 MHz, $CDCl_3$): δ = 206.9 (C4), 158.9 (C1), 144.1 (C7), 133.9 (C2'), 120.0 (6-CN), 118.3 (C3'), 118.0 (C6), 106.8 (1-CH_2), 91.5 (C3a), 53.1 (C5), 47.3 (C8a), 45.7 (C1'), 38.3 (C8), 32.5 (C3), 28.0 (C2), 25.4 (8a-CH_3), 24.5 (5-CH_3). (**Figure 121**)
HRMS: calcd. for $C_{17}H_{21}NNaO_2$ 294.14645 $[M+Na]^+$, found 294.14646 (Δ = 0.04 ppm).

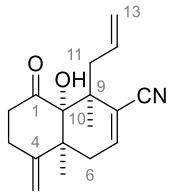

111

Preparation of LHMDS solutions: Hexamethyldisilazane (1.2 mL, 5.76 mmol, 1.15 eq) was dissolved in THF (1.8 mL) in a 5 mL flask. The solution was cooled to –78 °C before *n*-BuLi (2.5 M in hexane; 2.0 mL, 5.00 mmol, 1 eq) was added dropwise (1.5 min). The reaction mixture was allowed to warm to –10 °C over the course of 1 h. After stirring at room temperature for 1 h, the LHMDS solution (1 M) was used promptly.

[6,6]-Fused Acyloin 111: Ketonitrile **7** (33.1 mg, 0.122 mmol, 1 eq) was dissolved in THF (2.4 mL) in a 5 mL flask. The solution was cooled to –95 °C before a freshly prepared LHMDS solution (1 M in THF/hexane; 0.24 mL, 0.240 mmol, 2 eq) was added rapidly. The yellow reaction mixture was allowed to warm to 0 °C over the course of 2 h, after which the cooling bath was removed. After 5 min, the reaction mixture was quenched with acetic acid (0.04 mL, 0.70 mmol, ~6 eq) and volatiles removed in vacuo. The residue was filtered through a plug of silica gel, eluting with ethyl acetate (total volume ~25 mL). Concentration of the filtrate yielded a slightly yellow oily solid which consisted of ketonitrile **7** (**16%**), its epimer 6-*epi*-**7** (**10%**), and [6,6]-fused acyloin **111** [**67% (92% *b.r.s.m.*)**], as determined by qNMR.

Notes: Using LDA instead of LHMDS gave similar yields of 64–68% (*qNMR* and *isolated yield*) over a substrate scale ranging from 48 to 587 mg. With LHMDS, the *overall yield* was significantly improved (from 72% to 92% *b.r.s.m.*). Purification by flash chromatography (PE/EA, gradient from 20:1 to 2:1) gave **111** as a colorless crystalline solid (m.p. 122 °C).

$\mathbf{R_f}$ = 0.44 [$\mathbf{R_f}$ (**7**) = 0.60] [$\mathbf{R_f}$ (6-*epi*-**7**) = 0.68] (PE/EA, 3:1).
^{1}H NMR (700 MHz, $CDCl_3$): δ = 6.68 (dd, *J* = 5.3 Hz, 2.8 Hz, 1H, 7-H), 5.88–5.82 (m, 1H, 12-H), 5.12–4.91 (m, 4H, 4-CH_2 & 13-H_2), 3.98 (s, 1H, 10-OH), 3.06 (dd, *J* = 13.0 Hz, 7.6 Hz, 1H, 11-H_a), 2.93–2.66 (m, 4H, 2-H_2 & 3-H_2), 2.63 (dd, *J* = 20.0 Hz, 5.4 Hz, 1H, 6-H_a), 2.31 (dd, *J* = 20.0 Hz, 2.8 Hz, 1H, 6-H_b), 1.93 (dd, *J* = 13.0 Hz, 6.7 Hz, 1H, 11-H_b), 1.13 (s, 3H, 9-CH_3), 1.06 (s, 3H, 5-CH_3).
^{13}C NMR (176 MHz, $CDCl_3$): δ = 211.9 (C1), 147.3 (C4), 142.8 (C7), 132.9 (C12), 119.5 (C13), 119.2 (8-CN), 117.8 (C8), 111.3 (4-CH_2), 81.7 (C10), 43.9 (C5), 43.7 (C9), 43.4 (C11), 37.3 (C2), 33.0 (C6), 28.8 (C3), 25.4 (5-CH_3), 20.0 (9-CH_3). (**Figure 122**)
HRMS: calcd. for $C_{17}H_{21}NNaO_2$ 294.14645 $[M+Na]^+$, found 294.14630 (Δ = 0.50 ppm).
X-ray structure analysis: **Figure 25** on page **132.**

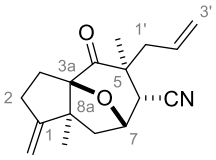

6-*epi*-**7**

6-*epi*-**7**: **(3a*R**,5*S**,6*R**,7*S**,8a*S**)-5-Allyl-5,8a-dimethyl-1-methylene-4-oxooctahydro-1*H*-3a,7-epoxyazulene-6-carbonitrile**

R_f = 0.70 (PE/EA, 3:1).
^{1}H NMR (400 MHz, $CDCl_3$): δ = 5.68–5.57 (m, 1H, 2'-H_2), 5.24–5.13 (m, 2H, 3'-H_2), 4.99 & 4.93 (2 × br dd, *J* ≈ 1.8–2.1 Hz, 2H, 1-CH_2), 4.74–4.70 (m, 1H, 7-H), 3.61 (d, *J* = 6.5 Hz, 1H, 6-H), 2.63–2.52 (m, 4H, 2-H_2 & 8-H_a, 1'-H_a), 2.40–2.22 (m, 3H, 3-H_a & 8-H_b & 1'-H_b), 1.82–1.76 (m, 1H, 3-H_b), 1.41 (s, 3H, 5-CH_3), 1.04 (s, 3H, 8a-CH_3).
^{13}C NMR (101 MHz, $CDCl_3$): δ = 208.7 (C4), 160.3 (C1), 132.1 (C2'), 120.8 (C3'), 117.6 (6-CN), 107.4 (1-CH_2), 100.1 (C3a), 74.8 (C7), 57.3 (C8a), 47.4 (C1'), 45.9 (C5), 42.8 (C8), 38.9 (C6), 29.1 (C2), 26.8 (C3), 24.9 (5-CH_3), 23.4 (8a-CH_3). (**Figure 123**)

4.4.4 Acyloin Rearrangement of Allyl- and Acetal-Substituted Epoxyazulenes

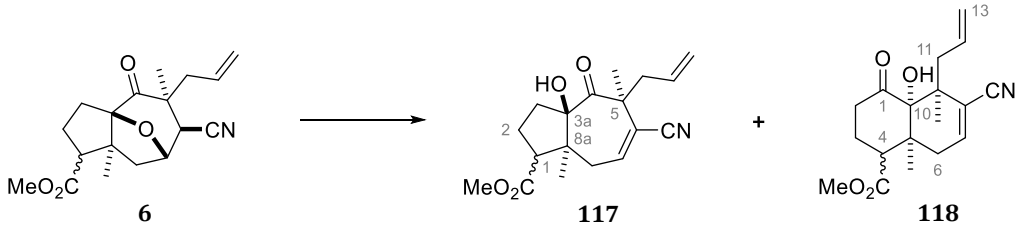

[6,6]-Fused Acyloin 118: Methyl ester **6** (56.9 mg, 0.179 mmol, 1 eq) was dissolved in THF (3.6 mL) in a 10 mL flask. The solution was cooled to –95 °C before a freshly prepared LDA solution (1 M in THF/hexane; 0.36 mL, 0.360 mmol, 2 eq) was added rapidly. The yellow reaction mixture was allowed to warm to 3 °C over the course of 2.5 h, after which the cooling bath was removed. After 20 min, the reaction mixture was quenched with acetic acid (0.1 mL, 1.75 mmol, ~10 eq) and volatiles removed in vacuo. The residue was filtered through a plug of silica gel, eluting with ethyl acetate (total volume ~30 mL). The filtrate was concentrated to a slightly yellow oil and purified by flash chromatography (PE/EA, gradient from 20:1 to 1:1), affording the [6,6]-fused acyloin **118** (16.8 mg, 0.053 mmol, **30%**) and impure [5,7]-fused acyloin **117** (11.1 mg, 0.035 mmol, **20%**), as very viscous colorless oils.

R_f (**118**) = 0.53 [**R_f** (**117**) = 0.54] [**R_f** (**6**) = 0.60] (PE/EA, 1.5:1).
118: **^{1}H NMR** (400 MHz, $CDCl_3$): δ = 6.60 (dd, *J* ≈ 4.2–4.4 Hz, 1H), 5.80–5.70 (m, 1H), 5.15–5.09 (m, 2H), 4.45 (s, 1H), 3.72 (s, 3H), 3.20 (dd, *J* = 11 Hz, 5.6 Hz, 1H), 2.93–2.83 (ddd, *J* = 17.2 Hz, 7.7 Hz, 3.5 Hz, 1H), 2.70–2.53 (m, 3H), 2.34–2.25 (m, 1H), 2.22 (d, *J* = 4.4 Hz, 2H), 2.15–2.06 (m, 1H), 1.19 (s, 3H), 1.05 (s, 3H). **^{13}C NMR** (101 MHz, $CDCl_3$): δ = 212.1, 173.7,

142.0, 132.6, 120.0, 119.5, 118.5, 81.2, 52.1, 44.5, 43.6, 43.5, 42.8, 36.4, 34.2, 23.4, 22.3, 19.8. (**Figure 124**)
HRMS: calcd. for $C_{18}H_{23}NNaO_4$ 340.15193 $[M+Na]^+$, found 340.15245 (Δ = 1.52 ppm).

117: **^{1}H NMR** (400 MHz, $CDCl_3$): δ = 6.89 (dd, *J* = 8.6 Hz, 7.4 Hz, 1H), 5.64–5.53 (m, 1H), 5.16–5.08 (m, 2H), 3.94 (s, 1H), 3.73 (s, 3H), 2.89 (dd, *J* = 11.8 Hz, 8.0 Hz, 1H), 2.67 (dd, *J* = 7.6 Hz, 2H), 2.63–2.45 (m), 2.15–1.83 (m), 1.35 (s, 3H), 1.04 (s, 3H).
^{13}C NMR (101 MHz, $CDCl_3$): δ = 212.4, 173.3, 145.3, 131.0, 121.5, 120.3, 118.9, 89.0, 62.0, 52.8, 51.8, 51.5, 44.2, 35.1, 33.6, 27.0, 22.13, 22.08. (**Figure 125**)

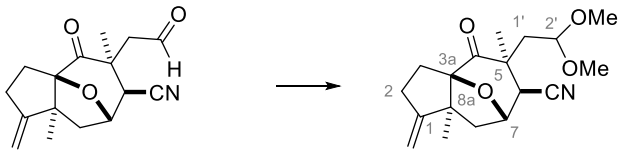

39 **119.a**

119.a: **(3a*R**,5*S**,6*S**,7*S**,8a*S**)-5-(2',2'-dimethoxyethyl)-5,8a-dimethyl-1-methylene-4-oxooctahydro-1*H*-3a,7-epoxyazulene-6-carbonitrile**

For route scouting purposes, dimethyl acetal **119.a** was prepared by two separate runs:

a) **39** (54 mg, 0.198 mmol), MeOH/$CH(OMe)_3$ (7:1, 0.05 M), *p*-TsOH·H_2O (5 mol%), rt, 14 h.
b) **39** (229 mg, 0.838 mmol; ***impure***), MeOH/$CH(OMe)_3$ (5:1, 0.05 M), *p*-TsOH·H_2O (5 mol%), rt, 15.5 h.

The combined crude product was purified by flash chromatography (PE/EA, gradient from 40:1 to 4:1), affording **119.a** as a slightly yellow solid (240 mg, 0.751 mmol, **72%** *from mostly impure substrate*). The discoloration was removed by partial crystallization from DCM/hexane.

$\mathbf{R_f}$ = 0.63 [$\mathbf{R_f}$ (**39**) = 0.47] (PE/EA, 2:1).
^{1}H NMR (700 MHz, $CDCl_3$): δ = 4.91 & 4.81 (2 × br dd, *J* ≤ 2.0 Hz, 2H, 1-CH_2), 4.74 (dd, *J* = 6.7 Hz, 2.6 Hz, 1H, 7-H), 4.31 (dd, *J* = 8.1 Hz, 2.3 Hz, 1H, 2'-H), 3.25 & 3.16 (2 × s, 2 × 3H, 2 × 2'-OCH_3), 2.74 (dd, *J* = 13.6 Hz, 8.0 Hz, 1H, 1-H_a), 2.63–2.57 (m, 1H, 2-H_a), 2.53 (d, *J* = 2.8 Hz, 1H, 6-H), 2.45–2.39 (m, 2H, 2-H_b & 8-H_a), 2.21–2.16 (m, 1H, 3-H_a), 1.93–1.91 (m, 2H, 3-H_b & 1'-H_b), 1.80 (d, *J* = 12.7 Hz, 1H, 8-H_b), 1.24 (s, 3H, 5-CH_3), 1.00 (s, 3H, 8a-CH_3).
^{13}C NMR (176 MHz, $CDCl_3$): δ = 209.3 (C4), 160.5 (C1), 118.5 (6-CN), 106.2 (1-CH_2), 101.3 (C3a), 101.1 (C2'), 76.5 (C7), 55.9 (C8a), 54.2 (2'-OCH_3), 51.4 (C8), 51.1 (2'-OCH_3), 44.5 (C5), 43.3 (C1'), 42.7 (C6), 30.8 (C2), 29.1 (C3), 25.0 (8a-CH_3), 22.5 (5-CH_3). (**Figure 126**)
HRMS: calcd. for $C_{18}H_{25}NNaO_4$ 342.16758 $[M+Na]^+$, found 342.16782 (Δ = 0.71 ppm).

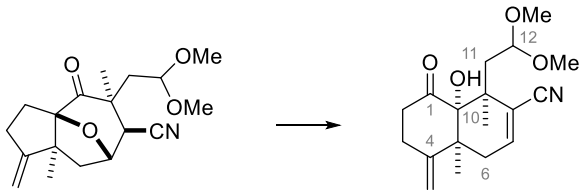

119.a dimethyl acetal **120.a**

[6,6]-Fused Acyloin 120.a: Dimethyl acetal **119.a** (82.9 mg, 0.260 mmol, 1 eq) was dissolved in THF (5 mL) in a 10 mL flask. The solution was cooled to –95 °C before a freshly prepared LDA solution (1 M in THF/hexane; 0.52 mL, 0.520 mmol, 2 eq) was added rapidly. The yellow solution was allowed to warm to 5 °C over the course of 2 h 45 min, after which the cooling bath was removed. After 15 min, the reaction mixture was quenched with acetic acid (0.1 mL, 1.75 mmol, ~7 eq) and volatiles removed in vacuo. The residue was filtered through a plug of silica gel, eluting with ethyl acetate (~30 mL). Concentration of the filtrate yielded a slightly yellow oil, which was purified by flash chromatography (PE/EA, gradient from 40:1 to 2:1). Dimethyl acetal **120.a** (49.1 mg, 0.154 mmol, **59%**) was obtained as a colorless, very viscous oil.

$\mathbf{R_f}$ = 0.38 [$\mathbf{R_f}$ (**119.a**) = 0.60] (PE/EA, 2:1).
^{1}H NMR (400 MHz, $CDCl_3$): δ = 6.64 (dd, *J* = 4.8 Hz, 3.3 Hz, 1H), 5.03 & 4.93 (2 × dd, *J* ≤ 2.0 Hz, 2H), 4.53 (dd, *J* = 5.3 Hz, 4.7 Hz, 1H), 4.07 (s, 1H), 3.28 & 3.27 (2 × s, 2 × 3H), 2.90–2.52 (m, 6H), 2.24 (dd, *J* = 20.2 Hz, 3.2 Hz, 1H), 1.51 (dd, *J* = 13.6 Hz, 4.1 Hz, 1H), 1.21 (s, 3H), 1.07 (s, 3H).
^{13}C NMR (101 MHz, $CDCl_3$): δ = 211.9, 147.3, 142.4, 118.9, 117.9, 111.6, 102.2, 81.9, 53.3, 53.1, 44.3, 42.0, 41.7, 37.4, 33.4, 29.4, 25.4, 20.5. (**Figure 127**)

Notes: Dimethyl acetal **120.a** underwent spontaneous deterioration in the NMR tube ($CDCl_3$). The resulting main compound was isolated via fractional crystallization from $CDCl_3$/hexane. Based on the disappearance of the carbonyl signal and the loss of one methoxy group, the NMR spectra suggest a transacetalization to enol hemiacetal **122**. However, a definite confirmation of the presumed structure by 2D-NMR and HRMS was not pursued.

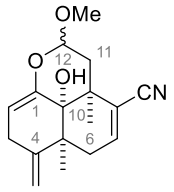

122

$\mathbf{R_f}$ = 0.47 [Rf (**120.a**) = 0.38] (PE/EA, 2:1).
^{1}H NMR (400 MHz, $CDCl_3$): δ = 6.42 (br dd, *J* ≈ 5.6 Hz, 2.0 Hz, 1H), 5.23 (br dd, *J* ≈ 4.4 Hz, 2.4 Hz, 1H), 5.17 & 5.07 (2 × br s, 2H), 4.71 (br s, 1H), 3.30 (s, 3H), 3.10 (br dd, *J* ≈ 19.5 Hz, 2.0 Hz, 1H), 2.78 (br dd, *J* ≈ 19.5 Hz, 4.6 Hz, 1H), 2.21–1.96 (m, 3H), 1.73 (s, 1H), 1.36 (s, 3H), 1.27 (s, 3H).
^{13}C NMR (101 MHz, $CDCl_3$): δ = 150.4, 147.2, 139.5, 121.6, 118.4, 113.8, 108.6, 97.7, 71.8, 55.2, 44.7, 38.9, 38.0, 35.6, 31.5, 24.2, 20.9. (**Figure 128**)

39 **119.b**

119.b: **(3a*R**,5*S**,6*S**,7*S**,8a*S**)-5-((1'',3''-dioxolan-2''-yl)methyl)-5,8a-dimethyl-1-methylene-4-oxooctahydro-1*H*-3a,7-epoxyazulene-6-carbonitrile**

In a 5 mL flask, aldehyde **39** (100 mg, 0.366 mmol, 1 eq) was dissolved in toluene (3.3 mL). After addition of ethylene glycol (0.3 mL, 5.365 mmol, ~15 eq) and *p*-TsOH·H_2O (3.5 mg, 18.4 µmol, 5 mol%), the flask was connected to an addition funnel, which was packed with 4 Å molecular sieves and fitted with a reflux condenser. The reaction mixture was heated to reflux for 2 h and then quenched with half-saturated $NaHCO_3$ solution (10 mL). After extraction with diethyl ether (3 × 15 mL), the combined organic phases were dried over $MgSO_4$, filtered, and concentrated to yield **119.b** (114 mg, 0.359 mmol, **98%**) as a colorless solid.

$\mathbf{R_f}$ = 0.54 [Rf (**39**) = 0.46] (PE/EA, 2:1).
^{1}H NMR (400 MHz, C_6D_6): δ = 4.93 (dd, *J* = 5.0 Hz, 3.6 Hz, 1H, 2''-H), 4.77 & 4.65 (2 × br dd, *J* < 2.0 Hz, 2H, 1-CH_2), 4.36 (br dd, *J* ≈ 6.5 Hz, 2.7 Hz, 1H, 7-H), 3.49–3.35 (m, 2H, 4''-H_2 *or* 5''-H_2), 3.26–3.20 (m, 2H, 4''-H_2 *or* 5''-H_2), 2.93 (dd, *J* ≈ 14.1 Hz, 5.1 Hz, 1H, 1'-H_a), 2.56–2.47 (m, 1H, 2-H_a), 2.32 (dd, *J* = 14.1 Hz, 3.5 Hz, 1H, 1'-H_b), 2.27–2.15 (m, 2H, 2-H_b & 3-H_a), 2.01–1.91 (m, 3H, 3-H_b & 6-H & 8-H_a), 1.19 (s, 3H, 5-CH_3), 1.12 (d, *J* = 12.7 Hz, 1H, 8-H_b), 0.78 (s, 3H, 8a-CH_3).
^{13}C NMR (101 MHz, C_6D_6): δ = 208.8 (C4), 161.3 (C1), 118.7 (6-CN), 106.0 (1-CH_2), 101.9 (C-2''), 101.3 (C3a), 76.7 (C7), 64.65 (C4'' *or* C5''), 64.58 (C4'' *or* C5''), 56.0 (C8a), 51.0 (C8), 45.1 (C5), 43.4 (C1'), 43.0 (C6), 31.1 (C2), 29.7 (C3), 25.1 (8a-CH_3), 22.7 (5-CH_3). (**Figure 129**)
X-ray structure analysis: **Figure 27** on page **141.**

Notes: Dioxolane **119.b** was obtained without impurities in TLC and NMR when prepared by this procedure. When trimethyl orthoformate was used as drying agent, significant amounts of dimethyl acetal **119.a** and the diastereomeric mixed acetals **119.c** were also obtained.

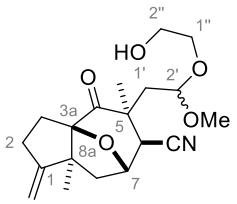

119.c

119.c: **(3a*R**,5*S**,6*S**,7*S**,8a*S**)-5-(2'-(2''-hydroxyethoxy)-2''-methyoxyethyl)-5,8a-dimethyl-1-methylene-4-oxooctahydro-1*H*-3a,7-epoxyazulene-6-carbonitrile**

$\mathbf{R_f}$ = 0.14 & 0.10 (PE/EA, 2:1).
^{1}H NMR (400 MHz, $CDCl_3$): δ = 4.91–4.82 (m, 2H), 4.74 (br dd, *J* ≈ 5.6 Hz, 2.4 Hz, 1H), 4.52 (dd, *J* = 8.2 Hz, 2.5 Hz, 1H; *less polar DS*) or 4.39 (dd, *J* = 7.7 Hz, 2.8 Hz, 1H; *more polar DS*), 3.70–3.27 (m, 4H), 3.27 (s, 3H; *less polar DS*) or 3.19 (s, 3H; *more polar DS*), 2.81–2.64 (dd, *J* = 13.8 Hz, 8.2 Hz (*less polar DS*) or *J* = 13.5 Hz, 7.7 Hz (*more polar DS*), 1H), 2.64–2.52 (m, 2H), 2.46–2.38

(m, 2H), 2.22–2.13 (m, 1H), 2.04–1.89 (m, 2H), 1.81 (d, *J* = 12.8 Hz, 1H), 1.25 (s, 3H), 0.99 (s, 3H). **^{13}C NMR** (101 MHz, $CDCl_3$, *less polar DS/more polar DS*): δ = 211.2/209.7, 160.2/160.3, 118.4/118.5, 106.4/106.3, 101.2/101.3, 100.5/100.9, 76.5/76.5, 69.9/65.8, 61.5/61.9, 56.3/56.0, 51.5/54.2, 51.4/51.3, 45.0/44.7, 42.9/43.5, 42.7/42.7, 30.7/30.8, 29.1/29.2, 24.9/25.0, 21.8/22.4. (**Figure 130** & **Figure 131**)

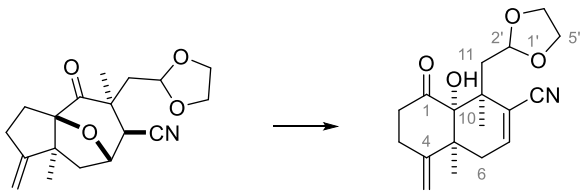

119.b **120.b**

[6,6]-Fused acyloin 120.b: Dioxolane **119.b** (300 mg, 0.945 mmol, 1 eq) was dissolved in THF (38 mL) in a 50 mL flask. The solution was cooled to –95 °C before a freshly prepared LDA solution (1 M in THF/hexane; 1.9 mL, 1.90 mmol, 2 eq) was added rapidly. The yellow reaction mixture was allowed to warm to 0 °C over the course of 2 h, after which the cooling bath was removed. After 1 h, the reaction mixture was quenched with acetic acid (0.28 mL, 4.90 mmol, ~5 eq) and volatiles removed in vacuo. The residue was filtered through a plug of silica gel, eluting with ethyl acetate (total volume ~160 mL). Concentration of the filtrate yielded a slightly yellow oil, which was purified by flash chromatography (PE/EA, gradient from 20:1 to 1:1). Dioxolane **120.b** (208 mg, 0.655 mmol, **69%**) was obtained as a colorless, very viscous oil, which solidified in the freezer.

R_f = 0.44 [**R_f** (**119.b**) = 0.54] (PE/EA, 2:1).
^{1}H NMR (400 MHz, $CDCl_3$): δ = 6.65 (dd, *J* = 4.6 Hz, 3.5 Hz, 1H, 7-H), 5.03 & 4.93 (2 × br s, 2H, 4-CH_2), 4.98 (dd, *J* ≈ 4.6 Hz, 2.3 Hz, 1H, 2'-H), 4.12 (s, 1H, 10-OH), 3.92–3.75 (m, 4H, 4'-H_2 & 5'-H_2), 2.88–2.65 (m, 4H, 2-H_2 & 3-H_2), 2.60 (dd, *J* = 20.0 Hz, 4.8 Hz, 1H, 6-H_a), 2.52 (dd, *J* = 14.0 Hz, 4.6 Hz, 1H, 11-H_a), 2.24 (dd, *J* = 20.0 Hz, 3.3 Hz, 1H, 6-H_b), 1.80 (dd, *J* = 14.6 Hz, 4.4 Hz, 1H, 11-H_b) 1.25 (s, 3H, 9-CH_3), 1.08 (s, 3H, 5-CH_3).
^{13}C NMR (101 MHz, $CDCl_3$): δ = 212.0 (C1), 147.2 (C4), 142.6 (C7), 118.7 (8-CN), 118.2 (C8), 111.9 (4-CH_2), 101.4 (C2'), 81.7 (C10), 64.53 & 64.46 (C4' & C5'), 44.6 (C5), 42.2 (C11), 41.9 (C9), 37.3 (C2), 33.5 (C6), 29.6 (C3), 25.1 (5-CH_3), 20.5 (9-CH_3). (**Figure 132**)
HRMS: calcd. for $C_{18}H_{23}NNaO_4$ 340.15193 $[M+Na]^+$, found 340.15182 (Δ = 0.31 ppm).

4.4.4.1 α-Deoxygenation of Allyl- and Acetal-Substituted Acyloins

4.4.4.1.b α-Ketol Reductions

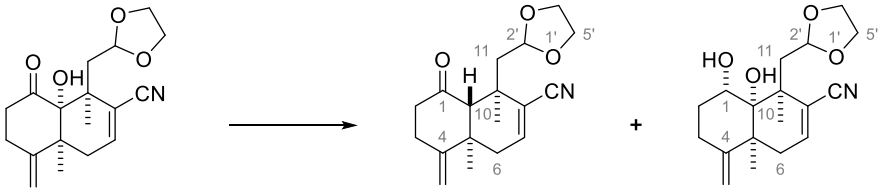

120.b **123** **124**

Decalone 123 and **Diol 124**: In a 25 mL flask, samarium (222 mg, 1.467 mmol, 1.2 eq) was suspended in THF (12 mL). After addition of diiodomethane (0.1 mL, 1.240 mmol, 1 eq), the mixture was stirred for 4 h. The suspension was allowed to settle for 1 h before the required volume of the supernatant (*presumably 0.1 M solution, not titrated*) was taken out by syringe.

[6,6]-Fused acyloin **120.b** (31 mg, 0.098 mmol, 1 eq) was dissolved in THF (1.5 mL) in a 25 mL flask. After addition of MeOH (0.16 mL, 3.96 mmol, ~40 eq) and NEt_3 (0.22 mL, 1.59 mmol, ~16 eq), the solution was cooled to −78 °C. The previously prepared SmI_2 solution (0.1 M in THF; 3.9 mL, 0.39 mmol, 4 eq) was added over the course of 4 min. The blue reaction mixture was allowed to warm to −40 °C over the course of 1 h, quenched with half-saturated $NaHCO_3$ solution (10 mL), and extracted with diethyl ether (3 × 15 mL). The combined organic phases were dried over $MgSO_4$, filtered, and concentrated in vacuo to give a yellow oil (30 mg).

Notes: This deoxygenation was not evaluated thoroughly. The crude products of several attempts (*cf.* **Table 6** on page **68**) were combined and purified by flash chromatography (PE/EA, gradient from 20:1 to 1:1), affording mainly *cis*-diol **124** as a colorless solid and decalone **123** as a colorless oil. Since isolated *cis*-diol **124** was barely soluble in $CDCl_3$, its NMR spectra were recorded in DMSO-d_6. NOESY indicated the *cis*-configuration of the diol moiety.

Notably, decalone **123** could not be isolated with satisfactory purity. HRMS indicated the presence of [M + 2], which likely correspond to the respective mono-alcohol(s). Despite rather unclean NMR spectra, **123** could be identified as the depicted *trans*-decalone, as indicated by NOESY and comparison of the spectra with those of decalone **109**.

Decalone 123: $\mathbf{R_f}$ = 0.60 [$\mathbf{R_f}$ (**120.b**) = 0.48] (PE/EA, 1:1).
^{1}H NMR (400 MHz, $CDCl_3$): δ = 6.60 (dd, *J* = 6.4 Hz, 2.3 Hz, 1H, 7-H), 4.93 & 4.86 (2 × br s, 2H, 4-CH_2), 4.70 (dd, *J* = 7.0 Hz, 2.8 Hz, 1H, 2'-H), 3.88–3.71 (m, 4H, 4'-H_2 & 5'-H_2), 3.17 (s, 1H, 10-H), 2.70–2.28 (m, 7H, 2-H_2 & 3-H_2 & 6-H_2 & 11-H_a), 1.98 (dd, *J* = 15.0 Hz, 2.8 Hz, 1H, 11-H_b), 1.58 (s, 3H, 9-CH_3), 1.17 (s, 3H, 5-CH_3).
^{13}C NMR (101 MHz, $CDCl_3$): δ = 208.7 (C1), 153.2 (C4), 141.3 (C7), 122.1 (C8), 117.8 (8-CN), 108.1 (4-CH_2), 102.3 (C2'), 64.9 & 64.2 (C4' & C5'), 55.0 (C10), 43.6 (C11), 42.6 (C2), 40.8 (C5), 38.9 (C6), 37.7 (C9), 31.7 (C3), 25.1 (5-CH_3), 23.0 (9-CH_3). (**Figure 133**)
HRMS: calcd. for $C_{18}H_{23}NNaO_3$ 324.15701 $[M+Na]^+$, found 324.15708 (Δ = 0.19 ppm).

Diol 124: $\mathbf{R_f}$ = 0.42 [$\mathbf{R_f}$ (**120.b**) = 0.48] (PE/EA, 1:1).
^{1}H NMR (700 MHz, DMSO-d_6): δ = 6.60 (dd, *J* = 5.8 Hz, 1.9 Hz, 1H, 7-H), 5.18 (br d, *J* ≈ 5.9 Hz, 1H, 2'-H), 4.87 & 4.74 (2 × br s, 2H, 4-CH_2), 4.67 (d, *J* = 3.2 Hz, 1H, 1-OH), 3.93 & 3.84 & 3.75 & 3.69 (4 × br ddd, *J* ≈ 13.1–13.5 Hz, 6.5–7.1 Hz, 4H, 4'-H_2 & 5'-H_2), 3.88 (s, 1H, 10-OH), 3.82 (br d, *J* ≈ 2.4 Hz, 1H, 1-H), 3.25 (d, *J* = 18.5 Hz, 1H, 6-H_a), 2.76 (d, *J* = 14.8 Hz, 1H, 11-H_a), 2.62–2.57 (m, 1H, 3-H_a), 1.98–1.93 (m, 2H, 2-H_a & 3-H_b), 1.78 (dd, *J* = 15.1 Hz, 5.8 Hz, 1H, 11-H_b), 1.62 (dd, *J* = 18.9 Hz, 6.0 Hz, 1H, 11-H_b), 1.60–1.55 (m, 1H, 2-H_b), 1.27 (s, 3H, 9-CH_3), 1.12 (s, 3H, 5-CH_3). **^{13}C NMR** (176 MHz, DMSO-d_6): δ = 152.4 (C4), 145.1 (C7), 120.6 (C8), 119.3 (8-CN), 110.6 (4-CH_2), 102.4 (C2'), 77.0 (C10), 70.7 (C1), 64.5 & 63.4 (C4' & C5'), 44.4 (C5), 42.5 (C9), 41.7 (C11), 37.7 (C6), 31.3 (C2), 27.3 (C3), 22.8 (5-CH_3), 22.1 (9-CH_3). (**Figure 134**)
HRMS: calcd. for $C_{18}H_{25}NNaO_4$ 342.16758 [M+Na]$^+$, found 342.16779 (Δ = 0.60 ppm).

4.4.4.1.c α-Ketol Acetate Reductions

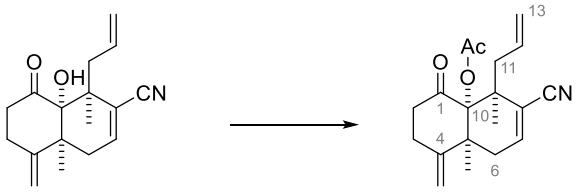

111 **126**

α-Ketol Acetate 126: [6,6]-Fused acyloin **111** (185 mg, 0.682 mmol, 1 eq) was dissolved in THF (6.8 mL) in a 25 mL flask. Then, NEt_3 (0.47 mL, 3.410 mmol, 5 eq), DMAP (8.33 mg, 68.2 µmol, 10 mol%), and Ac_2O (0.64 mL, 6.820 mmol, 10 eq) were added. The solution was stirred at 50 °C for 15 h. After addition of saturated $NaHCO_3$ solution (15 mL), the biphasic mixture was extracted with DCM (3 × 30 mL). The combined organic phases were dried over $MgSO_4$, filtered, and concentrated. The crude product was analyzed by qNMR, indicating a yield of **95%**. α-Ketol acetate **126** was purified by flash chromatography (PE/EA, gradient from 20:1 to 3:1) and obtained as a colorless solid (m.p. 134 °C).

$\mathbf{R_f}$ = 0.44 [$\mathbf{R_f}$ (**111**) = 0.53] (PE/EA, 2:1).
^{1}H NMR (400 MHz, $CDCl_3$): δ = 6.66 (br dd, *J* ≈ 4.2–4.4 Hz, 1H, 7-H), 5.95–5.85 (m, 1H, 12-H), 5.10–5.00 (m, 2H, 13-H_2), 5.05 & 4.95 (2 × br s, 2H, 4-CH_2), 2.95–2.83 & 2.71–2.55 & 2.23–2.10 (3 × m, 3H & 3H & 2H, 2-H_2 & 3-H_2 & 6-H_2 & 11-H_2; *not clearly distinguishable*), 2.09 (s, 3H, 10-OC(O)CH_3), 1.37 (s, 3H, 9-CH_3), 1.29 (s, 3H, 5-CH_3). **^{13}C NMR** (101 MHz, $CDCl_3$): δ = 203.9 (C1), 169.3 (10-O*C*(O)CH_3), 147.3 (C4), 141.8 (C7), 133.1 (C12), 119.5 (8-CN), 119.3 (C13), 118.9 (C8), 111.5 (4-CH_2), 86.6 (C10), 46.0 (C5), 44.9 (C9), 41.3 (C11), 38.4 (C2), 34.7 (C6), 28.5 (C3), 27.5 (10-OC(O)*C*H_3), 21.0 (5-CH_3), 20.1 (9-CH_3). (**Figure 135**)
HRMS: calcd. for $C_{19}H_{23}NNaO_3$ 336.15701 [M+Na]$^+$, found 336.15729 (Δ = 0.83 ppm).

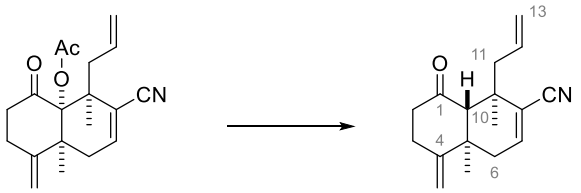

126 **109**

Decalone 109: In a 25 mL flask, samarium (222 mg, 1.467 mmol, 1.2 eq) was suspended in THF (12 mL). After addition of diiodomethane (0.1 mL, 1.240 mmol, 1 eq), the mixture was stirred for 21 h. The suspension was allowed to settle for 1 h before the required volume of the supernatant (*presumably 0.1 M solution, not titrated*) was taken out by syringe.

The above SmI_2 solution (0.1 M in THF; 4.8 mL, 0.480 mmol, 3 eq) was placed in a 25 mL flask containing some samarium metal (2.4 mg). The suspension was cooled to –95 °C, before α-ketol acetate **126** (50 mg, 0.160 mmol, 1 eq), dissolved in 2.7 mL THF, was added rapidly (~15 s). After 30 min (*full conversion to unidentified compound*), NEt_3 (0.5 mL, 3.587 mmol, ~23 eq) was added at –50 °C. The cooling bath was removed after 15 min, and the reaction mixture stirred at room temperature for 10 min. After addition of half-saturated $NaHCO_3$ solution (12 mL) and diethyl ether (containing 5 vol% NEt_3, 12 mL), the biphasic mixture was stirred rigorously for 5 min. The aqueous phase was separated, and the organic phase was washed with saturated $NaHCO_3$ solution (6 mL). The combined aqueous phases were extracted with diethyl ether twice (containing 5 vol% NEt_3, 12 mL). The combined organic phases were washed with saturated $Na_2S_2O_3$ solution (12 mL) and saturated NaCl solution (6 mL). After addition of 2,6-lutidine (0.5 mL, 4.316 mmol, 27 eq), the combined organic phases were dried over $MgSO_4$, filtered, and concentrated in vacuo. The crude product was analyzed by qNMR, indicating the presence of unreacted **126** (24%) and decalone **109** (**50%,** 66% *b.r.s.m.*). Decalone **109** was purified by flash chromatography (PE/DE, gradient from 20:1 to 5:1) and obtained as a colorless oil which solidified in the freezer.

Notes: While this deoxygenation experiment resulted in relatively good overall yield with the given work-up method, an incomplete conversion was observed. Similarly carried out attempts (*with unoptimized work-up*) led to full conversion, but lower yields due to decomposition. The incomplete conversion most likely resulted from *partially oxidized samarium metal*, apparent from the presence of a grey powder among the metal, which was used for the preparation of the SmI_2 solution. A full conversion might have been ensured by using a greater excess of the samarium metal to compensate for its degradation. The used samarium metal was stored in a Schlenk flask under argon and weighed in air.

Alternative procedure:[332] In a 25 mL flask, samarium (1 g, 6.651 mmol, 2 eq) was placed and stirred under argon atmosphere for 1.5 h. After addition of purified[332] 1,2-diiodoethane (937 mg, 3.324 mmol, 1 eq), dissolved in THF (30 mL), the suspension was stirred for 5 h. Vacuum was applied to the reaction mixture briefly (5 times) to remove ethene. The suspension was stirred for another 13.5 h, before it was allowed to settle for 1 h. The required volume of the supernatant was taken out by syringe. The concentration of SmI_2 (0.1 M) was determined by titration using the procedure reported by HILMERSSON *et al.*, for which 2-hexanone instead of 2-heptanone was used.[332,381]

The above SmI_2 solution (0.11 M in THF; 1.4 mL, 0.154 mmol, 2.2 eq) was placed in a 10 mL flask containing some samarium metal (1.2 mg). The suspension was cooled to –95 °C, before α-ketol acetate **126** (17.2 mg, 0.054 mmol, 1 eq), dissolved in 1 mL THF, was added rapidly (~15 s). After 15 min (*full conversion to unidentified compound*), NEt_3 (0.1 mL, 0.721 mmol, ~13 eq) was added at –65 °C. After another 45 min, ethylene glycol (0.2 mL, 3.577 mmol, ~66 eq) was added at –20 °C, before the reaction mixture was diluted with 3 mL of a mixture of PE/DE (1:1) containing 5 vol% NEt_3. The cooling bath was removed 45 min later at –5 °C. After stirring vigorously for 30 min at room temperature, the biphasic mixture was filtered through a plug of silica gel, eluting with 30 mL of the above PE/DE/NEt_3-mixture. The colorless solution was let stand for 2 h before it was concentrated in vacuo. The crude product was analyzed by qNMR, indicating the formation of decalone **109** (**75%** yield) with very little decomposition.

Notes: As with aqueous work-up methods, this work-up method also indicated conversion of the *unidentified compound* to decalone **109** in TLC and NMR. However, this conversion was much cleaner with the presented work-up. In one attempt, in which the solution was only let stand for less than 10 min before it was concentrated in vacuo, this conversion was observable in the NMR tube (**Figure 138**). This conversion in the NMR tube was also observed in earlier attempts – but with much more decomposition, and thus, complex spectra.

$\mathbf{R_f}$ = 0.73 [$\mathbf{R_f}$ (**126**) = 0.55] (PE/EA, 1.5:1).
^{1}H NMR (400 MHz, C_6D_6): δ = 5.90 (dd, *J* = 6.4 Hz, 2.3 Hz, 1H, 7-H), 5.56–5.46 (m, 1H, 12-H), 4.96–4.90 (m, 2H, 13-H), 4.52 & 4.38 (2 × br s, 2H, 4-CH_2), 2.80 (dd, *J* = 14.4 Hz, 9.7 Hz, 1H, 11-H_a), 2.53 (dddd, *J* = 14.4 Hz, 5.4 Hz, 1.5 Hz, 1.4 Hz, 1H, 11-H_b), 2.39 (s, 1H, 10-H), 2.17–2.07 (m, 2H, 2-H_a & 3-H_a), 1.99–1.88 (m, 2H, 2-H_b & 3-H_b), 1.83 (br dd, *J* ≈ 18.5 Hz, 2.0 Hz, 1H, 6-H_a), 1.62 (s, 3H, 9-CH_3), 1.47 (dd, *J* = 18.5 Hz, 6.4 Hz, 1H, 6-H_b), 0.72 (s, 3H, 5-CH_3).
^{13}C NMR (101 MHz, C_6D_6): δ = 206.6 (C1), 153.3 (C4), 140.8 (C7), 134.4 (C12), 122.3 (C8), 119.0 (C13), 117.9 (8-CN), 107.7 (4-CH_2), 55.0 (C10), 44.7 (C11), 42.5 (C2), 40.4 (C5), 39.8 (C9), 38.4 (C6), 31.4 (C3), 24.7 (5-CH_3), 22.5 (9-CH_3). (**Figure 136**, spectra in $CDCl_3$ in **Figure 137**)
HRMS: calcd. for $C_{17}H_{21}NNaO$ 278.15153 $[M+Na]^+$, found 278.15156 (Δ = 0.08 ppm).

4.4.5 Acyloin Rearrangement of Furylated Epoxyazulenes

4.4.5.1 3-Furylation of Aldehyde 39

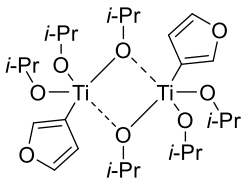

I-67

I-67: **Furan-3-yltriisopropoxytitanium**

3-Bromofuran was either purchased or prepared according to literature.[382–384] It was noticed that samples of 3-bromofuran not stored over $CaCO_3$ deteriorated significantly, resulting in a brown liquid with crystalline precipitate. This was especially pronounced for the commercially purchased sample (FLUOROCHEM). After distillation, 3-bromofuran was therefore stabilized with $CaCO_3$ (~0.5 w-%) and stored in a screw-top vial at –28 °C. The colorless liquid could be stored for several months without deterioration, as indicated by colorlessness and NMR.

Preparation of (3-furyl)Ti(O*i*-Pr)$_3$ (I-67):[114] 3-Bromofuran (2.0 mL, 22.25 mmol, 1.1 eq) was dissolved in THF (24 mL) in a 100 mL flask. The solution was cooled to –70 °C using a cryostat, before *n*-BuLi (2.5 M in hexane; 8 mL, 20.0 mmol, 1 eq) was added over 5 min.

In a separate 10 mL flask, Ti(O*i*-Pr)$_3$Cl was prepared by dropwise addition of $TiCl_4$ (0.55 mL, 5 mmol, 0.25 eq; over 10 min) to *neat* Ti(O*i*-Pr)$_4$ (97%; 4.6 mL, 0.155 mmol, 0.78 eq), cooling the flask slightly with an water bath (~15 °C).[385] The mixture was stirred until the initially formed waxy solids were dissolved (~30 min).

The freshly prepared Ti(Oi-Pr)$_3$Cl (20.0 mmol, 1 eq) was transferred into a 100 mL flask and dissolved in THF (20 mL). The solution was cooled to –80 °C using a cryostat, before the 3-lithiofuran solution (20.0 mmol, 1 eq), which was stirred at –70 °C for 2 h in total, was added via transfer canula (over 13 min), rinsing residual 3-lithiofuran solution with THF (2 × 2 mL). The resulting yellow solution was kept at –80 °C for 1.5 h, before the cooling bath was allowed to warm to –10 °C over the course of 1.5 h. The cooling bath was removed, and the brown solution was stirred at room temperature for 1 h. The solvents were removed in vacuo using the vacuum pump connected to the Schlenk line. Residual THF was co-evaporated with hexane (2 × 10 mL), before the residue was extracted into a separate 100 mL flask. To this means, the residue was stirred in hexane and filtered through a modified transfer cannula with a glass microfiber filter attached on a flat end.<23> After extraction with hexane (4 × 12 mL), the hexane was removed (using the vacuum pump connected to the Schlenk line) to give crude **I-67** as a brown oily solid. After recrystallization from hexane (3 times, *see below*), **I-67** (3.564 g, 12.197 mmol, **61%**) was obtained as a yellowish crystalline solid.

<23> The modified transfer cannula was provided by the group of Prof. Lars WESEMANN, University of Tübingen.

Notes: Titanium complex **I-67** was prepared three times. It could be recrystallized and stored (both at –28 °C and under argon) for several months without loss of quality (as indicated by its color and NMR) when the flask's septum was sealed with sticky tape and parafilm. Recrystallization was generally carried out 3 times for 1–2 d per crystallization step. For this purpose, **I-67** was dissolved in hexane (approx. 2 mL hexane per gram) at room temperature before the solution was cooled in the freezer. The mother-liquor (*brown in first recrystallization, then orange/yellow*) was removed by syringe promptly after taking the flask out of the freezer, preventing the content from thawing.

Moderate yields after three recrystallization cycles were accepted, preferring quality over quantity. In one case, additional **I-67** was also readily obtained from recrystallization of the remaining mother liquors. The color of the complex is highly dependent of its crystallinity. When noticeably yellow crystals of **I-67** were dissolved and the solvent (hexane or THF) removed in vacuo rapidly, an only slightly beige powder was obtained.

To employ **I-67** in the 3-furylation, it was dissolved in hexane and a portion of the solution was transferred into a separate flask. After removing hexane, the weight of the transferred complex was determined. Dissolving and transferring in THF did complicate an accurate determination of weight, since THF was retained in significant amounts even after prolonged removal in vacuo. Residual THF could, however, be co-evaporated with hexane. The transferred **I-67** was then dissolved in THF and the required aliquot of this solution was added to the aldehyde.

The NMR data were in accordance with those reported by GAU *et al*.[114] Similarly to the reported spectra, the ^{1}H integral ratio does not completely match the 'expected ratio' of 1:1:1:3:18.

^{1}H NMR (400 MHz, $CDCl_3$): δ = 7.35 [br s, 1H (*0.78H*)], 7.29 [br dd, *J* = 1.4 Hz, 1H (*0.80H*)], 6.39 [br dd, *J* ≈ 1.5 Hz, 0.9 Hz, 1H (*1H*)], 4.59 [sept, *J* = 6.1 Hz, 3H (*3.48H*)], 1.30 [d, *J* = 6.2 Hz, 18H (*26.12H*)]. **^{13}C NMR** (101 MHz, $CDCl_3$): δ = 147.6, 138.9, 115.4, 77.9, 26.6. (**Figure 139**)

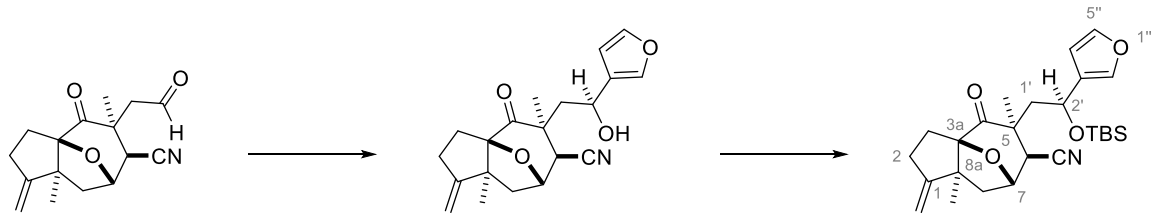

39 **37** **127**

37: **(3a*R**,5*S**,6*S**,7*S**,8a*S**)-5-((*S**)-2'-(furan-3''-yl)-2'-hydroxyethyl)-5,8a-dimethyl-1-methylene-4-oxooctahydro-1*H*-3a,7-epoxyazulene-6-carbonitrile**

127: **(3a*R**,5*S**,6*S**,7*S**,8a*S**)-5-((*S**)-2'-((*tert*-butyldimethylsilyl)oxy)-2'-(furan-3''-yl)ethyl)-5,8a-dimethyl-1-methylene-4-oxooctahydro-1*H*-3a,7-epoxyazulene-6-carbonitrile**

Aldehyde **39** (186 mg, 0.681 mmol, 1 eq) was dissolved in THF (13.6 mL) in a 25 mL flask, before being cooled to −78 °C using a cryostat. (3-Furyl)Ti(O*i*-Pr)$_3$ (**I-67**) was dissolved in THF (496.5 mg in 4 mL THF) and an aliquot (2.54 mL of 4.55 mL; 278.4 mg, 0.953 mmol, 1.4 eq) was added to the aldehyde solution over the course of 10 min. After 2 h, the cryostat was set to −50 °C, and the reaction mixture stirred for 1.25 h at this temperature, before allowing the reaction mixture to warm to −15 °C over the course of 50 min. The yellow solution was quenched with half-saturated NH_4Cl solution (40 mL in total) and extracted with ethyl acetate (3 × 30 mL). The combined organic phases were dried over $MgSO_4$, filtered, and concentrated in vacuo. The crude product was purified by flash chromatography (PE/DE with 0.2 vol% NEt_3, gradient from 10:1 to 1:2), separating 3-furyl δ-hydroxy nitrile **37** (151 mg) from a mixed fraction of unreacted substrate **39** and some **37** (82 mg, NMR-ratio of **39**/**37** = 2.71:1).

The mixed fraction was resubjected to 3-furylation by dissolving it in THF (6 mL) in a 25 mL flask, before being cooled to −78 °C using a cryostat. An aliquot of the previously prepared solution of **I-67** (1.1 mL solution; corresponding to 122.7 mg, 0.420 mmol, "1.4 eq") was added over 5 min. After 1.5 h, the cryostat was switched off, allowing the reaction mixture to warm to −10 °C over the course of 2 h. The yellow solution was quenched with half-saturated NH_4Cl solution (20 mL in total) and extracted with ethyl acetate (3 × 30 mL). The combined organic phases were dried over $MgSO_4$, filtered, and concentrated in vacuo. The crude yellowish oily solid (97.1 mg) was combined with the mixed fraction from the first reaction.

The combined 3-furyl δ-hydroxy nitrile **37** (248.1 mg, ~0.732 mmol, 1 eq) was dissolved in DMF (7.3 mL) in a 25 mL flask. After addition of imidazole (249 mg, 3.657 mmol, ~5 eq) and TBSCl (50 w-% in toluene; 0.38 mL, 1.098 mmol, ~1.5 eq), the reaction mixture was stirred at 50 °C for 21 h. At this point, reaction control by TLC suggested minute amounts of unreacted **37**. Therefore, another portion of TBSCl (50 w-% in toluene; 0.13 mL, 0.376 mmol, ~0.5 eq) was added and the reaction mixture stirred at 50 °C for 2 h. The solution was added to half-saturated $NHCO_3$ solution (26 mL) and extracted once with diethyl ether (70 mL). The slightly turbid extract was washed with saturated NaCl solution (10 mL), before the combined aqueous phases were extracted with diethyl ether (2 × 70 mL). The combined organic phases were dried over $MgSO_4$, filtered, and concentrated in vacuo. The crude product was purified by flash chromatography (PE/DE, gradient from 20:1 to 2:1), affording TBS ether **127** as a colorless oil [268.5 mg, 0.589 mmol, **87%** over 2 steps; *d.r.* (**127**/2'-*epi*-**127**) ≈ 10:1].

Notes: Isolated 3-furyl δ-hydroxynitrile **37** exhibits *two signal sets* (1:1 ratio) in NMR spectra which is explained by a differentiation into two stable conformers. The signals were assigned with NMR spectra recorded at 403 K which favored one of the two conformers (~5:1 ratio).

The depicted diastereomer of **127** was obtained when *non-epimerized* **37** was silylated. This main diastereomer of **127** was not separable from the minor diastereomer 2'-epi-**127**. One particular silylation with *partially epimerized* **37** afforded – next to **127** – some 6-*epi*-**127**, hemiketal **37.a**, and lactone **38**.

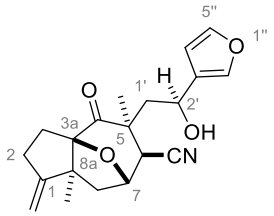

37

Appearance: colorless waxy solid.
$\mathbf{R_f}$ = 0.52–0.64 [$\mathbf{R_f}$ (**39**) = 0.38] (PE/DE, 1:2; with 3 drops of NEt_3).
^{1}H NMR (400 MHz, 1,1,2,2-tetrachloroethane-d_2, **403 K**): δ = 7.43 (br dd, *J* < 2.0 Hz, 1H, 4''-H), 7.43 (br dd, *J* < 2.0 Hz, 1H, 5''-H), 6.47 (br dd, *J* < 2.0 Hz, 1H, 2''-H), 5.03 (br dd, *J* < 2.0 Hz, 1H, 1-CH_a), 4.92–4.84 (m, 2H, 1-CH_b & 2'-H), 4.85 (br dd, *J* ≈ 6.8 Hz, 1.8 Hz, 1H, 7-H), 2.81–2.53 (4H, 2-H_2 & 1'-H_a & 8-H_a), 2.71 (d, *J* = 2.2 Hz, 1H, 6-H), 2.41–2.28 (m, 2H, 3-H_a, 1'-H_b), 1.96 (v br s, 1H, 2'-OH), 1.91 (d, *J* = 12.8 Hz, 8-H_b), 1.46 (s, 3H, 5-CH_3), 1.13 (s, 3H, 8a-CH_3).
^{13}C NMR (101 MHz, 1,1,2,2-tetrachloroethane-d_2, **403 K**): δ = 209.1 (C4), 160.3 (C1), 143.0 (C5''), 138.8 (C4''), 129.2 (C3''), 118.4 (6-CN), 108.4 (C2''), 106.1 (1-CH_2), 101.0 (C3a), 77.1 (C7), 64.2 (C2'), 56.3 (C8a), 50.7 (C8), 48.9 (C1'), 46.1 (C5), 44.0 (C6), 30.5 (C2), 28.8 (C3), 24.7 (5-CH_3), 24.3 (8a-CH_3). (**Figure 140** & **Figure 141**)
HRMS: calcd. for $C_{20}H_{23}NNaO_4$ 364.15193 $[M+Na]^+$, found 364.15195 (Δ = 0.05 ppm).

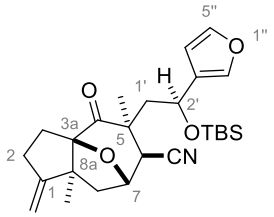

127

Appearance: colorless oil. $\mathbf{R_f}$ = 0.69 (PE/EA, 3:1).
^{1}H NMR (700 MHz, C_6D_6): δ = 7.07 (*app.* s, 1H, 2''-H), 6.96 (br dd, *J* ≈ 1.0–1.4 Hz, 1H, 5''-H), 6.24 (br dd, *J* ≈ 1.0–1.4 Hz, 1H, 4''-H), 4.74 & 4.59 (2 × br dd, *J* ≈ 1.0–2.4 Hz, 2H, 1-CH_2), 4.69 (dd, *J* = 6.6 Hz, 4.7 Hz, 1H, 2'-H), 4.25 (dd, *J* = 6.5 Hz, 2.8 Hz, 1H, 7-H), 2.85 (dd, *J* = 14.1 Hz, 4.7 Hz, 1H, 1'-H_a), 2.55 (dd, *J* = 14.1 Hz, 6.7 Hz, 1H, 1'-H_b), 2.46–2.37 (m, 1H, 2-H_a), 2.14–2.00 (m, 2H, 2-H_b & 3-H_a), 1.89 (d, *J* = 2.8 Hz, 1H, 6-H), 1.81 (dd, *J* = 12.7 Hz, 6.6 Hz, 1H, 8-H_a), 1.36 (s, 3H, 5-CH_3), 1.31 (dd, *J* ≈ 13.5 Hz, 7.5 Hz, 1H, 3'-H_b), 1.05 (d, *J* = 12.6 Hz, 1H, 8-H_b), 0.97 (s, 9H, $SiC(CH_3)_3$), 0.72 (s, 3H, 8a-CH_3), 0.18 & –0.12 (2 × s, 6H, $Si(CH_3)_2$).

^{13}C NMR (101 MHz, C_6D_6): δ = 209.4 (C4), 160.7 (C1), 143.3 (C5''), 139.4 (C2''), 129.8 (C3''), 118.6 (6-CN), 109.4 (C4''), 106.1 (1-CH_2), 101.0 (C3a), 76.8 (C7), 64.7 (C2'), 56.0 (C8a), 50.8 (C8), 48.2 (C1'), 46.9 (C5), 43.2 (C6), 31.2 (C2), 28.6 (C3), 26.1 (3C, SiC($\underline{C}H_3)_3$), 24.9 (8a-CH_3), 22.5 (5-CH_3), 18.3 (Si$\underline{C}(CH_3)_3$), –4.2 & –4.7 (Si$(CH_3)_2$). (**Figure 142**)
HRMS: calcd. for $C_{26}H_{37}NNaO_4Si$ 478.23841 $[M+Na]^+$, found 478.23851 (Δ = 0.22 ppm).

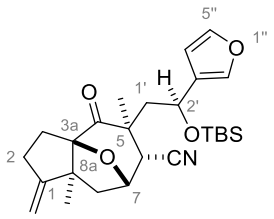

6-*epi*-**127**

Appearance: colorless oil. **R_f** = 0.72 (PE/EA, 3:1).
^{1}H NMR (400 MHz, C_6D_6): δ = 7.01 (*app.* s, 1H, 2''-H), 6.97 (br dd, *J* ≈ 1.0–1.6 Hz, 1H, 5''-H), 6.11 (br dd, *J* ≈ 1.0–1.6 Hz, 1H, 4''-H), 4.79 & 4.68 (2 × br dd, *J* ≈ 1.7–2.0 Hz, 2H, 1-CH_2), 4.76 (dd, *J* = 7.8 Hz, 4.0 Hz, 1H, 2'-H), 4.29 (ddd, *J* = 7.8 Hz, 7.6 Hz, 2.8 Hz, 1H, 7-H), 4.18 (d, *J* = 7.6 Hz, 1H, 6-H), 2.50–2.42 (m, 1H, 2-H_a), 2.38 (dd, *J* = 14.4 Hz, 7.8 Hz, 1H, 1'-H_a), 2.30–2.23 (m, 2H, 2-H_b & 3-H_a), 2.20 (dd, *J* = 13.6 Hz, 1.7 Hz, 1H, 8-H_a), 2.11 (dd, *J* = 13.6 Hz, 7.5 Hz, 1H, 8-H_b), 1.80 (d, *J* = 14.4 Hz, 4.0 Hz, 1H, 1'-H_b), 1.62–1.55 (m, 1H, 3-H_b), 1.52 (s, 3H, 5-CH_3), 0.96 (s, 3H, 8a-CH_3), 0.95 (s, 9H, SiC$(CH_3)_3$), 0.15 & –0.16 (2 × s, 6H, Si$(CH_3)_2$).
^{13}C NMR (101 MHz, C_6D_6): δ = 209.2 (C4), 160.9 (C1), 143.5 (C5''), 139.4 (C2''), 129.5 (C3''), 118.4 (6-CN), 109.0 (C4''), 106.8 (1-CH_2), 100.5 (C3a), 74.6 (C7), 65.2 (C2'), 56.9 (C8a), 50.9 (C1'), 45.6 (C5), 44.3 (C8), 38.8 (C6), 30.0 (C2), 28.0 (C3), 26.1 (3C, SiC($\underline{C}H_3)_3$), 23.9 (8a-CH_3), 23.4 (5-CH_3), 18.2 (Si$\underline{C}(CH_3)_3$), –4.3 & –4.6 (Si$(CH_3)_2$). (**Figure 143**)

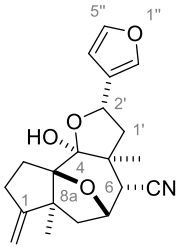

37.a

Appearance: colorless foamy solid (m.p. 107–111 °C). **R_f** = 0.58 (PE/EA, 2:1).
^{1}H NMR (400 MHz, $CDCl_3$): δ = 7.40 (*app.* s, 2H, 4''-H & 5''-H), 6.42 (*app.* s, 1H, 2''-H), 5.06 (dd, *J* = 9.8 Hz, 6.9 Hz, 1H, 2'-H), 4.93 & 4.89 (2 × br dd, *J* ≈ 2.0 Hz, 2H, 1-CH_2), 4.48 (ddd, *J* = 8.1 Hz, 4.2 Hz, 1.6 Hz, 1H, 7-H), 3.15 (d, *J* = 6.5 Hz, 1H, 6-H), 2.58–2.50 (m, 3H, 2-H_2 & 8-H_a), 2.39 (dd, *J* ≈ 13.6 Hz, 1.4 Hz, 1H, 8-H_b), 2.37 (br s, 1H, 4-OH), 2.18–2.15 (m, 2H, 1'-H_2), 2.05–1.98 (m, 2H, 3-H_2), 1.66 (s, 3H, 5-CH_3), 1.29 (s, 3H, 8a-CH_3).
^{13}C NMR (101 MHz, $CDCl_3$): δ = 163.7 (C1), 143.7 (C5''), 139.9 (C4''), 125.8 (C3''), 117.5 (6-CN), 108.7 (C2''), 106.2 (1-CH_2), 103.7 (C4), 95.4 (C3a), 74.7 (C7), 71.1 (C2'), 55.5 (C8a), 48.0 (C1'), 46.2 (C5), 41.5 (C8), 40.3 (C6), 27.7 (C2), 25.5 (C3), 23.4 (8a-CH_3), 22.2 (5-CH_3). (**Figure 144**)
HRMS: calcd. for $C_{20}H_{23}NNaO_4$ 364.15193 $[M+Na]^+$, found 364.15229 (Δ = 0.98 ppm).

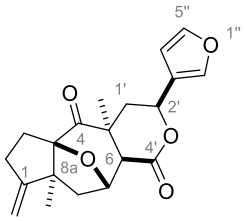

38

Appearance: colorless crystalline solid (m.p. 133 °C). $\mathbf{R_f}$ = 0.30 (PE/EA, 1:1).
^{1}H NMR (400 MHz, C_6D_6): δ = 7.02 (*app.* s, 1H, 2''-H), 6.96 (br dd, *J* ≈ 1.6 Hz, 1H, 5''-H), 6.03 (br d, *J* = 1.0 Hz, 4''-H), 5.18 (br d, *J* = 7.9 Hz, 1H, 7H), 4.94 (dd, *J* = 11.7 Hz, 2.2 Hz, 1H, 2'-H), 4.83 & 4.71 (2 × br dd, *J* ≈ 2.0 Hz, 2H, 1-CH_2), 2.59–2.49 (m, 1H, 2-H_a), 2.40–2.20 (m, 4H, 2-H_b & 3-H_a & 8-H_a & 1'-H_a), 2.05 (br s, 1H, 6-H), 1.75 (br dd, *J* ≈ 13.8 Hz, 8.2 Hz, 1H, 3-H_b), 1.61 (dd, *J* = 14 Hz, 2.1 Hz, 1H, 1'-H_b), 1.47 (dd, *J* = 13.1 Hz, 1.6 Hz, 1H, 8-H_b), 0.97 (s, 3H, 5-CH_3), 0.88 (s, 3H, 8a-CH_3).
^{13}C NMR (101 MHz, C_6D_6): δ = 209.5 (C4), 170.6 (C4'), 160.8 (C1), 143.7 (C5''), 139.9 (C4''), 124.8 (C3''), 108.6 (C2''), 106.7 (1-CH_2), 99.9 (C3a), 78.2 (C7), 70.3 (C2'), 57.0 (C8a), 51.8 (C6), 48.0 (C8), 43.2 (C5), 40.1 (C1'), 30.2 (C2), 27.8 (C3), 24.3 (5-CH_3), 24.3 (8a-CH_3). (**Figure 145**)
HRMS: calcd. for $C_{20}H_{22}NaO_5$ 365.13594 $[M+Na]^+$, found 365.13605 (Δ = 0.28 ppm).
X-ray structure analysis: **Figure 32** on page **159.**

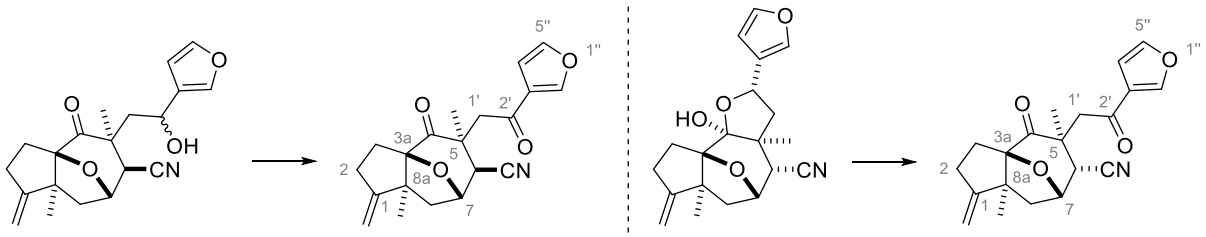

37 **128** **37.a** 6-*epi*-**128**

128: **(3a*R**,5*S**,6*S**,7*S**,8a*S**)-5-(2'-(furan-3''-yl)-2'-oxyethyl)-5,8a-dimethyl-1-methylene-4-oxooctahydro-1*H*-3a,7-epoxyazulene-6-carbonitrile**

6-*epi*-**128**: **(3a*R**,5*S**,6*R**,7*S**,8a*S**)-5-(2'-(furan-3''-yl)-2'-oxyethyl)-5,8a-dimethyl-1-methylene-4-oxooctahydro-1*H*-3a,7-epoxyazulene-6-carbonitrile**

Aldehyde **39** (130 mg, 0.476 mmol, 1 eq) was dissolved in THF (8.2 mL) in a 25 mL flask and cooled to –85 °C using a cryostat. (3-Furyl)Ti(O*i*-Pr)$_3$ (**I-67**) was dissolved in THF (716 mg in 9.8 mL THF) and an aliquot (2.7 mL of 10.5 mL; corresponding to 194 mg, 0.664 mmol, 1.4 eq) was added over 30 min to the aldehyde solution. After 4.5 h, the cryostat was set to –50 °C, and the reaction mixture stirred for 1 h, before an aqueous sodium hydroxide solution (15 mL; 1 M, 32 eq) was added over 11 min (at –50 °C). The cooling bath was removed, and the biphasic mixture was stirred at room temperature for 3.5 h. The mixture was diluted with water (20 mL) and extracted with diethyl ether (3 × 50 mL). The combined organic phases were dried over $MgSO_4$, filtered, and concentrated in vacuo.

The crude product (135 mg) – consisting mainly of **37.a** and some (6-*epi*-)**37** – was dissolved in DCM (8 mL) in a 25 mL flask. The solution was cooled in an ice bath and DMP (202 mg, 0.467 mmol, ~1.2 eq) was added, before the reaction mixture was allowed to

warm to room temperature over the course of 2.5 h. After quenching with 15 mL of a 1:1–mixture of saturated solutions of $Na_2S_2O_3$ and $NaHCO_3$, the biphasic mixture was diluted with water (15 mL) and extracted with DCM (3 × 45 mL). The combined organic phases were dried over $MgSO_4$, filtered, and concentrated in vacuo. The crude product was analyzed by qNMR, indicating the formation of 6-*epi*-**128** (**55%** over 2 steps) and **128** (**12%** over 2 steps).

Notes: The ketones (6-*epi*-)**128** were prepared for analytical and route-scouting purposes. When isolated hemiketal **37.a** was used as substrate, 6-*epi*-**128** was obtained as sole product. In contrast, only **128** was obtained, when *non-epimerized* δ-hydroxynitrile **37** was oxidized. The ketones from these three experiments were combined and purified by flash chromatography (PE/DE, gradient from 20:1 to 1:1). The ketones were isolated as colorless solids. Moreover, 6-*epi*-**128** crystallized readily in the NMR tube (C_6D_6).

128: $\mathbf{R_f}$ = 0.33 [$\mathbf{R_f}$ (**37**) = 0.40] (PE/EA, 2:1, with 3 drops of NEt_3).
^{1}H NMR (400 MHz, C_6D_6): δ = 7.40 (dd, *J* = 1.4 Hz, 0.9 Hz, 1H), 6.74 (dd, *J* = 1.8 Hz, 1.4 Hz, 1H), 6.55 (dd, *J* = 1.9 Hz, 0.8 Hz, 1H), 4.77 & 4.65 (2 × br dd, *J* ≈ 2.5 Hz, 1.6 Hz, 2H), 4.31 (br dd, *J* ≈ 7.0 Hz, 1.6 Hz, 1H), 3.45 & 3.02 (2 × d, *J* = 14.7 Hz, 2H), 2.54–2.44 (m, 1H), 2.40–2.30 (m, 1H), 2.21–2.14 (m, 1H), 2.11–2.05 (br ddd, *J* ≈ 13.7 Hz, 8.0 Hz, 1.4 Hz, 1H), 2.02–1.97 (m, 2H), 1.16 (dd, *J* = 13.0 Hz, 1.0 Hz, 1H), 1.12 (s, 3H), 0.80 (s, 3H). **^{13}C NMR** (101 MHz, C_6D_6): δ = 207.5, 190.3, 161.3, 147.9, 144.3, 128.6, 119.1, 109.0, 106.3, 101.2, 76.6, 56.6, 49.8, 48.9, 45.6, 42.8, 30.5, 29.2, 24.5, 24.3. (**Figure 146**)
HRMS: calcd. for $C_{20}H_{21}NNaO_4$ 362.13628 $[M+Na]^+$, found 362.13646 (Δ = 0.51 ppm).

6-*epi*-**128**: $\mathbf{R_f}$ = 0.44 [$\mathbf{R_f}$ (**37.a**) = 0.47] (PE/EA, 2:1, with 3 drops of NEt_3).
^{1}H NMR (400 MHz, C_6D_6): δ = 7.18 (dd, *J* = 1.2 Hz, 0.9 Hz, 1H), 6.77 (dd, *J* = 1.8 Hz, 1.2 Hz, 1H), 6.47 (dd, *J* = 1.8 Hz, 0.9 Hz, 1H), 4.82 & 4.71 (2 × br dd, *J* ≤ 2.5 Hz, 2H), 4.28 (ddd, *J* = 7.8 Hz, 5.5 Hz, 2.0 Hz, 1H), 3.40 (d, *J* = 5.6 Hz, 1H), 2.98 & 2.51 (2 × d, *J* = 17 Hz, 2H), 2.54–2.41 (m, 1H), 2.31–2.24 (m, 1H), 2.22 (dd, *J* = 13.8 Hz, 8.2 Hz, 1H), 2.07–2.02 (m, 2H), 1.37 (s, 3H), 0.89 (s, 3H).
^{13}C NMR (101 MHz, C_6D_6): δ = 207.2, 190.1, 161.7, 147.9, 144.2, 127.5, 117.4, 108.7, 107.0, 100.3, 100.2, 75.2, 57.7, 52.4, 43.6, 42.0, 40.5, 29.0, 27.2, 26.1, 22.9. (**Figure 147**)
HRMS: calcd. for $C_{20}H_{22}NO_4$ 340.15433 $[M+H]^+$, found 340.15435 (Δ = 0.04 ppm).
X-ray structure analysis: **Figure 33** on page **159.**

4.4.5.2 Rearrangement of 3-Furylated Substrates

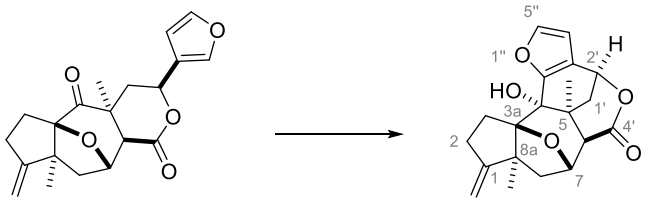

38 **133**

Polycyclic Lactone 133: Lactone **38** (26.3 mg, 0.077 mmol, 1 eq) was dissolved in THF (1.5 mL) in a 5 mL flask. The solution was cooled to –95 °C before a freshly prepared LDA solution (1 M in THF/hexane; 0.16 mL, 0.160 mmol, 2 eq) was added. The reaction mixture was allowed to warm to –5 °C over the course of 2 h, after which the cooling bath was removed. After 45 min, the reaction mixture was quenched with acetic acid (0.04 mL, 0.70 mmol, 9 eq) and volatiles removed in vacuo. The residue was filtered through a plug of silica gel, eluting with ethyl acetate (~25 mL). The concentrated filtrate was purified by flash chromatography (PE/EA, gradient from 20:1 to 1.5:1). Along with substrate **38** (8.6 mg, 0.025 mmol, **33%** recovered), polycyclic lactone **133** [13 mg, 0.038 mmol, **50%** (73% *b.r.s.m.*)] was isolated as a colorless crystalline solid (m.p. 227–234 °C, decomposition into a brown oil).

Notes: When LHMDS was used instead of LDA, lactone **38** remained unchanged.

$\mathbf{R_f}$ = 0.30 [$\mathbf{R_f}$ (**38**) = 0.68] (PE/EA, 1:1).
^{1}H NMR (400 MHz, $CDCl_3$): δ = 7.33 (d, *J* = 1.8 Hz, 1H, 5''-H), 6.37 (d, *J* = 1.8 Hz, 1H, 4''-H), 5.18 (dd, *J* = 3.1 Hz, 2.6 Hz, 1H, 2'-H), 4.98 (br d, *J* = 8.7 Hz, 1H, 7-H), 4.85 (br dd, *J* ≤ 1.8 Hz, 1H, 1-CH_a), 4.83 (br dd, *J* ≤ 2.1 Hz, 1H, 1-CH_b), 2.66 (d, *J* = 1.0 Hz, 1H, 6-H), 2.59 (dd, *J* = 13.4 Hz, 8.8 Hz, 1H, 8-H_a), 2.58–2.44 (m, 3H, 2-H_2 & 3-H_a), 2.40 (dd, *J* = 13.3 Hz, 1.9 Hz, 1H, 8-H_b), 2.29–2.22 (m, 1H, 3-H_b), 2.21 (s, 1H, 4-OH), 2.09 (dd, *J* = 14.2 Hz, 2.2 Hz, 1H, 1'-H_a), 1.91 (dd, *J* = 14.2 Hz, 3.4 Hz, 1H, 1'-H_b), 1.66 (s, 3H, 8a-CH_3), 1.50 (s, 3H, 5-CH_3). **^{13}C NMR** (101 MHz, $CDCl_3$): δ = 171.5 (C4'), 165.1 (C1), 154.0 (C2''), 142.2 (C5''), 122.3 (C3''), 109.2 (C4''), 105.1 (1-CH_2), 96.1 (C3a), 77.9 (C7), 74.6 (C4), 68.6 (C2'), 57.0 (C8a), 56.1 (C6), 42.6 (C8), 40.3 (C1'), 38.4 (C5), 28.7 (5-CH_3), 28.5 (C3), 27.4 (C2), 23.1 (8a-CH_3). (**Figure 148**)
HRMS: calcd. for $C_{20}H_{22}NaO_5$ 365.13594 $[M+Na]^+$, found 365.13646 (Δ = 1.52 ppm).
X-ray structure analysis: **Figure 34** on page **162**.

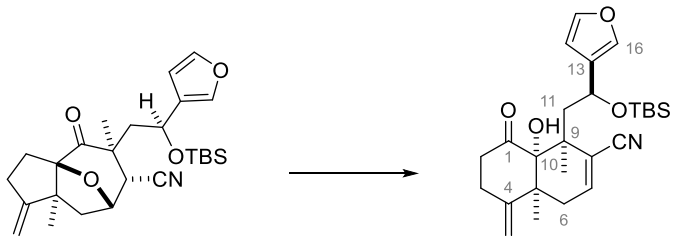

127 **135**

[6,6]-Fused Acyloin 135: TBS ether 6-*epi*-**127** (72.6 mg, 0.159 mmol, 1 eq; *single diastereomer*) was placed in a 10 mL flask. The flask, *submerged in liquid nitrogen*, was evacuated briefly and filled with argon (repeated five times). After dissolving the substrate in THF (3.2 mL), a THF solution of $LiClO_4$ (0.5 mL containing 3.33 mg $LiClO_4$, 3.13 µmol, 20 mol%) was added. The solution was cooled to –95 °C before a freshly prepared LHMDS solution (1 M in THF/hexane; 0.32 mL, 0.320 mmol, 2 eq) was added rapidly. The yellow reaction mixture was allowed to warm to 0 °C over the course of 2 h, after which the cooling bath was removed. After 30 min, the reaction mixture was quenched with a hexane solution of acetic acid (1 mL containing 0.045 mL acetic acid, 0.786 mmol, 5 eq). After removing most of the volatiles in vacuo (150 mbar, 40 °C), the residue was diluted with PE/DE (1:1; 4 mL) and stirred for 30 min. The resulting suspension was filtered through a plug of silica gel, eluting with PE/DE (1:1; 50 mL). The filtrate was concentrated and purified by flash chromatography (PE/DE, gradient from 20:1 to 1:1). Next to TBS ether (6-*epi*-)**127** [24.6 mg, 0.054 mmol, **34%**; 6-*epi*-**127**/**127** ≈ 4:1], the desired [6,6]-fused acyloin **135** [45.3 mg, 0.099 mmol, **62%** (**94%** ***b.r.s.m.***)] was obtained as a colorless oil.

Notes: Initial attempts (with either **127** or 6-*epi*-**127**) resulted in lower overall yields with almost no substrates being recoverable – until it was discovered that the TBS ethers (6-*epi*-)**127** are unexpectedly volatile. Therefore, the procedure was adjusted by (i) cooling the reaction flask before the inerting procedure, and (ii) adjusting the work-up procedure (silica filtration with PE/DE = 1:1 instead of EA, concentration in vacuo at 40 °C instead of 50 °C). Residual solvents were removed by successively concentrating solutions of diethyl ether, then hexane, then pentane (40 °C, 25 mbar for 5 min after removal of pentane).

$\mathbf{R_f}$ = 0.52 [$\mathbf{R_f}$ (6-*epi*-**127**) = 0.72] [$\mathbf{R_f}$ (**127**) = 0.63] (PE/EA, 3:1).
^{1}H NMR (400 MHz, $CDCl_3$): δ = 7.37 (br dd, *J* ≤ 1.5 Hz, 1H, 16-H), 7.32 (br dd, *J* ≤ 1.5 Hz, 1H, 15-H), 6.70 (dd, *J* = 5.0 Hz, 3.1 Hz, 7-H), 6.31 (br d, *J* ≤ 1.0 Hz, 1H, 14-H), 5.04 (br t, *J* ≈ 5.5 Hz, 1H, 12-H), 5.02 & 4.95 (2 × br d, *J* ≈ 1.7–2.1 Hz, 2H, 4-CH_2), 3.95 (s, 1H, 10-OH), 2.94 (dd, *J* = 13.5 Hz, 5.4 Hz, 1H, 11-H_a), 2.92–2.65 (m, 5H, 2-H_2, 3-H_2, 6-H_a), 2.30 (dd, *J* = 20.1 Hz, 3.1 Hz, 6-H_b), 1.61 (dd, *J* = 13.5 Hz, 5.5 Hz, 1H, 11-H_b), 1.07 (s, 3H, 5-CH_3), 1.03 (s, 3H, 9-CH_3), 0.81 [s, 9H, $SiC(CH_3)_3$)], 0.04 (s, 3H, $Si(CH_3)_a$), –0.25 (s, 3H, $Si(CH_3)_b$).
^{13}C NMR (101 MHz, $CDCl_3$): δ = 212.1 (C1), 147.2 (C4), 143.3 (C15), 143.1 (C7), 139.5 (C16), 129.7 (C13), 119.7 (8-CN), 117.9 (C8), 111.5 (4-CH_2), 108.5 (C14), 82.0 (C10), 63.5 (C12), 48.6 (C11), 44.1 (C5), 43.6 (C9), 37.5 (C2), 33.3 (C6), 29.1 (C3), 25.8 (4C, 5-CH_3 & $SiC(\underline{C}H_3)_3$), 20.3 (9-CH_3), 18.1 ($Si\underline{C}(CH_3)_3$), –4.3 ($Si(CH_3)_a$), –5.1 ($Si(CH_3)_b$). (**Figure 149**)
HRMS: calcd. for $C_{26}H_{37}NNaO_4Si$ 478.23841 $[M+Na]^+$, found 478.23824 (Δ = 0.35 ppm).

4.4.5.3 Preparation & Rearrangement of Higher-Substituted 3-Furylated Substrates

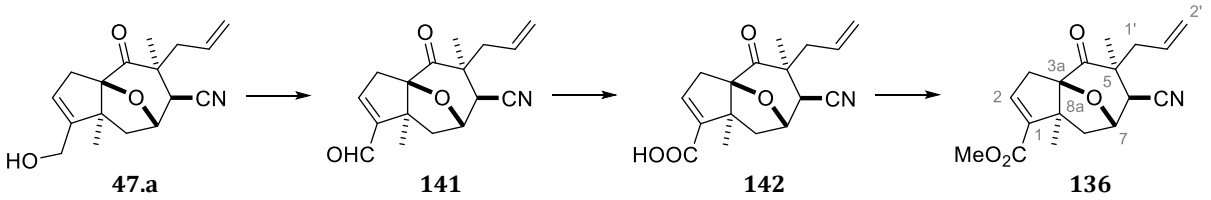

47.a **141** **142** **136**

136: **Methyl (3a*R**,5*S**,6*S**,7*S**,8a*S**)-5-allyl-6-cyano-5,8a-dimethyl-4-oxo-4,5,6,7,8,8a-hexahydro-3*H*-3a,7-epoxyazulene-1-carboxylate**

Impure allylic alcohol **47.a** [400 mg, "1.392 mmol, 1 eq" – analysis by qNMR: *55% purity*, *effectively* 0.766 mmol] was dissolved in DCM (28 mL) in a 50 mL flask. The solution was cooled in an ice bath and DMP (590 mg, 1.392 mmol, "1 eq") was added. The reaction mixture was allowed to warm to room temperature in the thawing ice bath. After 6 h, a mixture of saturated solutions of $Na_2S_2O_3$ (2 mL) and $NaHCO_3$ (10 mL) was added. The biphasic mixture was diluted with water (10 mL) and extracted with DCM (3 × 50 mL). The combined organic phases were washed with water (25 mL) and the washing solution extracted with DCM (50 mL). The combined organic phases were dried over $MgSO_4$, filtered, and concentrated in vacuo, before the crude product (380 mg) was used in the next step without purification.

The crude α,β-unsaturated aldehyde **141** was dissolved in *t*-BuOH/H_2O (5:2, 27.8 mL) in a 50 mL flask (*under air*). 2-Methyl-2-butene (2.22 mL, 20.89 mmol, "15 eq"), NaH_2PO_4 (200 mg, 1.667 mmol, "1.2 eq") and $NaClO_2$ (80%; 189 mg, 1.667 mmol, "1.2 eq") were added sequentially, and the flask closed to prevent 2-methyl-2-butene from evaporating. After stirring for 4.5 h, the reaction mixture was diluted with water (17 mL) and extracted with ethyl acetate (3 × 50 mL). The combined organic phases were dried over $MgSO_4$, filtered, and concentrated in vacuo, before the crude product (411 mg) was used in the next step without purification.

The crude α,β-unsaturated carboxylic acid **142** was dissolved in toluene/MeOH (3:2, 14 mL) in a 25 mL flask. $TMSCHN_2$ (2 M in Et_2O) was added dropwise until no further evolution of gas was observable and the yellow color of the $TMSCHN_2$ solution persisted [addition of 1.0 mL (2.00 mmol, "1.4 eq") over the course of 15 min]. Excess $TMSCHN_2$ was quenched with acetic acid (10 drops, ~0.02 mL) and the solution concentrated in vacuo. The crude product was filtered through a pad of silica gel, eluting with ethyl acetate (~150 mL), before the filtrate was purified by flash chromatography (PE/EA, gradient from 20:1 to 1:2), affording α,β-unsaturated methyl ester **136** (174 mg, 0.552 mmol, *effectively* **~72%** over three steps) as a colorless viscous oil which solidified in the freezer.

R_f = 0.61 (PE/EA, 1.5:1).
^{1}H NMR (400 MHz, $CDCl_3$): δ = 6.59 (br dd, *J* ≈ 2.2 Hz, 1H), 5.64–5.53 (m, 1H), 5.08–5.02 (m, 2H), 4.78 (dd, *J* = 6.6 Hz, 2.7 Hz, 1H), 3.73 (s, 3H), 3.17 (dd, *J* = 19.5 Hz, 2.1 Hz, 1H), 3.05 (dd, *J* = 13.7 Hz, 7.7 Hz, 1H), 2.67 (d, *J* = 2.8 Hz, 1H), 2.53–2.45 (m, 3H), 1.89 (d, *J* = 13.3 Hz, 1H), 1.21 (s, 3H), 1.10 (s, 3H). **^{13}C NMR** (101 MHz, $CDCl_3$): δ = 208.1, 163.8, 139.3, 139.2, 132.3, 118.9, 118.5, 98.8, 76.4, 59.5, 51.5, 47.1, 46.2, 42.8, 42.1, 36.7, 23.0, 21.1. (**Figure 150**)
HRMS: calcd. for $C_{18}H_{21}NNaO_4$ 338.13628 $[M+Na]^+$, found 338.13620 (Δ = 0.24 ppm).

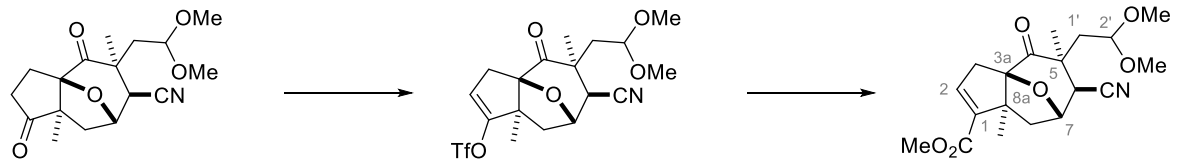

39.b **143** **138**

138: **Methyl (3a*R**,5*S**,6*S**,7*S**,8a*S**)-6-cyano-5-(2',2'-dimethoxyethyl)-5,8a-dimethyl-4-oxo-4,5,6,7,8,8a-hexahydro-3*H*-3a,7-epoxyazulene-1-carboxylate**

Diketo dimethylacetal **39.b** (150 mg, 0.467 mmol, 1 eq) was dissolved in THF (9.4 mL) in a 25 mL flask. The solution was cooled to −78 °C and KHMDS (1 M in THF; 0.51 mL, 0.51 mmol, 1.1 eq) was added over 2 min. After 35 min, Tf_2NPh (217 mg, 0.553 mmol, 1.3 eq) was added and the reaction mixture was stirred at −78 °C for 1 h, before saturated NH_4Cl solution (10 mL) was added. The biphasic mixture was diluted with water (2 mL) and extracted with diethyl ether (3 × 30 mL). The combined organic phases were dried over $MgSO_4$, filtered, and concentrated.

The crude yellow oil (376 mg) was dissolved in MeOH/DMF (1:1, 4.7 mL) in a 25 mL flask. The flask was connected to a balloon filled with carbon monoxide. After purging the solution with carbon monoxide, NEt_3 (0.26 mL, 1.865 mmol, 4 eq) and $Pd(PPh_3)_4$ (27 mg, 23.4 µmol, 5 mol%) was added. Maintaining the carbon monoxide atmosphere, the reaction mixture was stirred for 17 h, before adding saturated NH_4Cl solution (10 mL) and extracting the biphasic mixture with diethyl ether (3 × 30 mL). The combined organic phases were dried over $MgSO_4$, filtered, and concentrated in vacuo. After purification by flash chromatography (PE/DE, gradient from 20:1 to 1:2), methyl enoate **138** (93 mg, 0.256 mmol, **55%** over 2 steps) and unreacted enol triflate (43 mg, 0.095 mmol, **20%**) were obtained as colorless solids.

143: $\mathbf{R_f}$ = 0.58 [$\mathbf{R_f}$ (**39.b**) = 0.33] (PE/EA, 2:1).
^{1}H NMR (400 MHz, $CDCl_3$): δ = 5.53 (br dd, *J* ≈ 2.4 Hz, 1H), 4.83 (dd, *J* = 6.5 Hz, 2.8 Hz, 1H), 4.29 (dd, *J* = 8.6 Hz, 2.0 Hz, 1H), 3.27 (s, 3H), 3.16 (s, 3H), 3.02 (dd, *J* = 17.5 Hz, 2.0 Hz, 1H), 2.80 (dd, *J* = 13.3 Hz, 8.6 Hz, 1H), 2.53–2.43 (m, 3H), 1.93 (dd, *J* = 13.3 Hz, 2.0 Hz, 1H), 1.62 (d, *J* = 12.8 Hz, 1H), 1.27 (s, 3H), 1.07 (s, 3H). **^{13}C NMR** (101 MHz, $CDCl_3$): δ = 207.7, 149.8, 118.4 (q, $J_{C,F}$ = 320 Hz, CF_3), 117.9, 110.6, 101.0, 96.2, 76.1, 57.6, 54.4, 51.3, 44.6, 44.1, 43.3, 42.1, 33.1, 22.2, 21.6. (**Figure 151**)

138: $\mathbf{R_f}$ = 0.45 (PE/EA, 2:1).
^{1}H NMR (400 MHz, $CDCl_3$): δ = 6.60 (br dd, *J* ≈ 2.4 Hz, 1H, 2-H), 4.74 (dd, *J* = 6.5 Hz, 2.8 Hz, 1H, 7-H), 4.30 (dd, *J* = 8.3 Hz, 2.0 Hz, 1H, 2'-H), 3.72 (s, 3H, 1-$COOCH_3$), 3.26 (s, 3H, 2'-OCH_3), 3.16 (s, 3H, 2'-OCH_3), 3.13 (dd, *J* = 19.7 Hz, 2.1 Hz, 1H, 3-H_a), 2.78 (br dd, *J* ≈ 13.3 Hz, 8.3 Hz, 1H, 1-H_a), 2.59 (dd, *J* = 19.7 Hz, 2.8 Hz, 2H, 3-H_b & 6-H), 2.45 (dd, *J* = 13.2 Hz, 6.6 Hz, 1H, 8-H_a), 1.91 (dd, *J* = 13.3 Hz, 2.1 Hz, 1H, 1-H_b), 1.85 (d, *J* = 13.2 Hz, 1H, 8-H_b), 1.26 (s, 3H, 5-CH_3), 1.10 (s, 3H, 8a-CH_3). **^{13}C NMR** (101 MHz, $CDCl_3$): δ = 208.6 (C4), 163.9 (1'-$\underline{C}OOCH_3$), 139.5 (C2), 139.4 (C1), 118.3 (6-CN), 101.1 (C1'), 99.1 (C3a), 76.1 (C7), 59.4 (C8a), 54.2 (2'-OCH_3), 51.5 (1-$COO\underline{C}H_3$), 51.2 (2'-OCH_3), 46.4 (C8), 44.4 (C5), 43.3 (C1'), 42.1 (C6), 37.7 (C3), 23.1 (8a-CH_3), 22.3 (5-CH_3). (**Figure 152**)
HRMS: calcd. for $C_{19}H_{25}NNaO_6$ 386.15741 $[M+Na]^+$, found 386.15800 (Δ = 1.54 ppm).

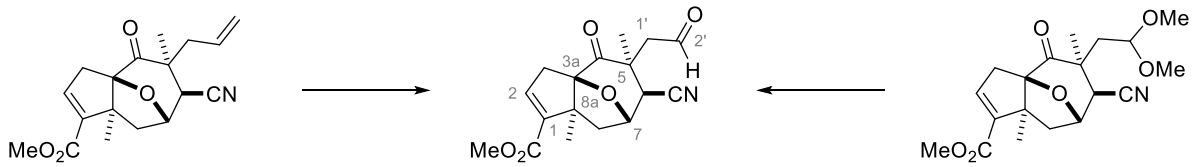

137: **Methyl (3a*R**,5*S**,6*S**,7*S**,8a*S**)-6-cyano-5,8a-dimethyl-4-oxo-5-(2'-oxoethyl)-4,5,6,7,8,8a-hexahydro-3*H*-3a,7-epoxyazulene-1-carboxylate**

Aldehyde **137** was prepared by either (i) LEMIEUX-JOHNSON oxidation of allyl substrate **136** or (ii) acidic hydrolysis of dimethyl ketal **138**. For the acidic hydrolysis, two methods were examined.

LEMIEUX-JOHNSON oxidation of **136**: Methyl enoate **136** (74 mg, 0.235 mmol, 1 eq) was dissolved in 1,4-dioxane/H_2O (3:1, 4.7 mL) in a 25 mL flask (*under air*). After addition of 2,6-lutidine (0.06 mL, 0.517 mmol, 2.2 eq), OsO_4 (4 wt.% in H_2O; 0.03 mL, 4.7 µmol, 2 mol%), and $NaIO_4$ (201 mg, 0.940 mmol, 4 eq), the resulting suspension was stirred for 21 h. The reaction mixture was diluted with water (20 mL) and extracted with DCM (3 × 25 mL). The combined organic phases were dried with $MgSO_4$, filtered, and concentrated in vacuo. Purification by flash chromatography (PE/EA, gradient from 10:1 to 1:1) gave aldehyde **137** (23 mg, 0.072 mmol, **31%**) as a slightly metallic-gray oil which solidified in the freezer.

Notes: To ensure full oxidative cleavage of the allyl group, the reaction mixture was stirred for a prolonged time compared to other LEMIEUX-JOHNSON oxidation experiments (*cf.* **Chapter 4.2.3**). TLC analysis indicated a significant decomposition after work-up, with aldehyde **137** exhibiting a notably decreased TLC spot intensity while various low-intensity spots became evident, which were previously not observed. As discussed in **Chapters 2.4.5.3** and **2.2.3**, this decomposition most likely resulted from osmium-based impurities catalyzing decomposition and autoxidation. This may have been prevented by addition of $Na_2S_2O_3$ in the work-up process.

Hydrolysis of **138** with *p*-TsOH: A solution of *p*-TsOH·H_2O (10.5 mg, 55.2 µmol) in acetone (5.5 mL) was prepared. An aliquot of 0.55 mL (containing 1.05 mg of *p*-TsOH·H_2O, 5.5 µmol, 20 mol%) was used to dissolve dimethyl ketal **138** (10 mg, 0.028 mmol, 1 eq) in a 3.5 mL screw-top vial (*under air*). Water (5 drops, ~0.05 mL) was added, and the solution was first stirred at room temperature for 3 d, then at 50 °C for 16 h, and lastly at 70 °C for 11 h. Some solid $NaHCO_3$ (~10–20 mg) was added to quench the acid. The resulting orange suspension was filtered through a pad of silica, eluting with ethyl acetate. After the filtrate was concentrated, aldehyde **137** (**95%** yield, determined by qNMR) was obtained as a colorless solid.

Hydrolysis of **138** with 2 M HCl: Dimethyl ketal **138** (30 mg, 0.083 mmol, 1 eq) was dissolved in THF (1.7 mL) in a 5 mL flask (*under air*). Aqueous HCl (2 M, 1.7 mL) was added, and the solution was stirred for 2 d before quenching the acid with half-saturated $NaHCO_3$ solution (10 mL). After extraction with ethyl acetate (3 × 15 mL), the combined organic phases were dried over $MgSO_4$, filtered, and concentrated in vacuo, affording aldehyde **137** (**67%** yield, determined by qNMR) as a slightly beige solid.

Notes: The hydrolysis with 2 M HCl was repeated on a larger scale using the remainder of dimethyl ketal **138** (187 mg, 0.512 mmol). Purification by flash chromatography (PE/EA, gradient from 10:1 to 1.5:1) afforded aldehyde **137** as a colorless solid and confirmed the yield of **67%**. Consequently, hydrolysis with *p*-TsOH in wet acetone (at 70 °C) is strongly advised.

$\mathbf{R_f}$ = 0.43 [$\mathbf{R_f}$ (**138**) = 0.53] (PE/EA, 1.5:1).
^{1}H NMR (400 MHz, $CDCl_3$): δ = 9.67 (br dd, *J* ≈ 2.5 Hz, 1H), 6.62 (br dd, *J* ≈ 2.4 Hz, 1H), 4.77 (dd, *J* = 6.6 Hz, 2.7 Hz, 1H), 3.74 (s, 3H), 3.23 (dd, *J* = 19.7 Hz, 2.1 Hz, 1H), 3.20 (dd, *J* = 15.2 Hz, 2.2 Hz, 1H), 2.83 (dd, *J* = 15.2 Hz, 2.9 Hz, 1H), 2.71 (d, *J* = 2.7 Hz, 1H), 2.56 (dd, *J* = 19.7 Hz, 2.9 Hz, 1H), 2.52 (dd, *J* = 13.5 Hz, 6.7 Hz, 1H), 1.92 (d, *J* = 13.5 Hz, 1H), 1.39 (s, 3H), 1.14 (s, 3H).
^{13}C NMR (101 MHz, $CDCl_3$): δ = 207.5, 198.0, 163.7, 139.24, 139.19, 118.1, 99.1, 76.2, 59.6, 51.6, 51.5, 45.8, 45.1, 42.3, 37.2, 22.88, 22.85. (**Figure 153**)

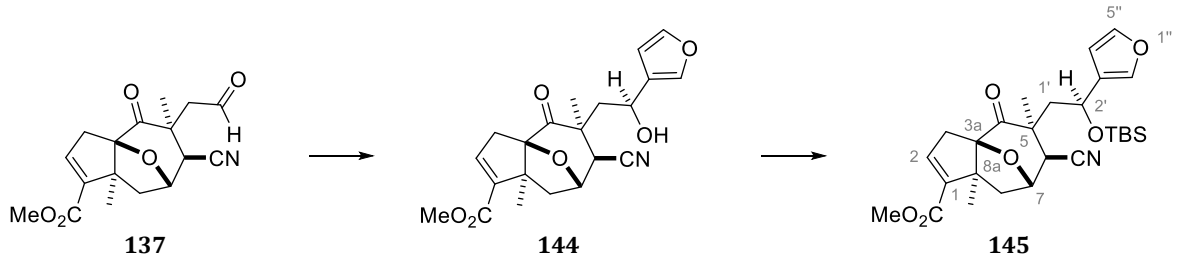

145: **Methyl (3a*R**,5*S**,6*S**,7*S**,8a*S**)-5-((*S**)-2'-((*tert*-butyldimethylsilyl)oxy)-2'-(furan-3''-yl)-ethyl)-6-cyano-5,8a-dimethyl-4-oxo-4,5,6,7,8,8a-hexahydro-3*H*-3a,7-epoxyazulene-1-carboxylate**

Aldehyde **137** (165 mg, 0.520 mmol, 1 eq) was dissolved in THF (10.4 mL) in a 25 mL flask and cooled to −78 °C using a cryostat. (3-Furyl)Ti(O*i*-Pr)$_3$ (**I-67**) was dissolved in THF (549 mg in 4.4 mL THF) and an aliquot (1.8 mL of 4.6 mL; corresponding to 212.7 mg, 0.728 mmol, 1.4 eq) was added to the aldehyde solution over the course of 25 min. After 2.5 h, the cryostat was switched off, allowing the reaction mixture to warm to −10 °C over the course of 2 h. The cooling bath was removed, and the yellow solution stirred at room temperature for 10 min. After quenching with half-saturated NH_4Cl solution (30 mL in total), the biphasic mixture was extracted with ethyl acetate (3 × 50 mL). The combined organic phases were dried over $MgSO_4$, filtered, and concentrated in vacuo, giving a slightly yellow solid (207 mg, 0.534 mmol, 103% crude) which was used in the next step without purification.

Crude 3-furyl δ-hydroxy nitrile **144** was dissolved in DMF (5.4 mL) in a 25 mL flask. After addition of imidazole (183 mg, 2.688 mmol, ~5 eq) and TBSCl (50 w-% in toluene; 0.37 mL, 1.068 mmol, ~2 eq), the reaction mixture was stirred at 50 °C for 20 h. The solution was added to half-saturated $NHCO_3$ solution (26 mL), diluted with water (20 mL), and the mixture extracted with diethyl ether (3 × 50 mL). The combined organic phases were dried over $MgSO_4$, filtered, and concentrated in vacuo. Purification by flash chromatography (PE/DE, gradient from 20:1 to 1:1) gave TBS ether **145** as a colorless solid (228.6 mg, 0.458 mmol, **88%** over 2 steps, d.r. ≈ 5.2:1). For analytical purposes, **145** was fractionally crystallized from DE/hexane, affording **145** in a higher diastereomeric ratio of 10:1 (m.p. 128 °C).

$\mathbf{R_f}$ = 0.66 [$\mathbf{R_f}$ (**144**) = 0.40] (PE/EA, 1.5:1; with 3 drops of NEt_3).
^{1}H NMR (400 MHz, $CDCl_3$): δ = 7.32 (br dd, *J* ≈ 1.4–1.6 Hz, 1H, 5''-H), 7.14 (v br dd, *J* ≈ 1.4 Hz, 1H, 2''-H), 6.49 (br dd, *J* ≈ 2.3–2.7 Hz, 1H, 2-H), 6.40 (br d, *J* ≈ 1.2 Hz, 1H, 4''-H), 4.70 (dd, *J* = 6.4 Hz, 3.0 Hz, 1H, 7-H), 4.56 (dd, *J* = 6.9 Hz, 4.6 Hz, 1H, 2'-H), 3.71 (s, 3H, 1-$COOCH_3$), 2.86 (dd, *J* = 19.6 Hz, 2.1 Hz, 1H, 3-H_a), 2.77 (dd, *J* = 13.8 Hz, 6.9 Hz, 1H, 1'-H_a), 2.57 (d, *J* = 3.1 Hz, 1H, 6-H), 2.36 (dd, *J* = 13.2 Hz, 6.5 Hz, 1H, 8-H_a), 2.24 (dd, *J* = 13.8 Hz, 4.6 Hz, 1H, 1'-H_b), 1.85 (dd, *J* = 19.8 Hz, 3.1 Hz, 1H, 3-H_b), 1.84 (d, *J* = 13.3 Hz, 1H, 8-H_b), 1.37 (s, 3H, 5-CH_3), 1.07 (s, 3H, 8a-CH_3), 0.82 (s, 9H, $SiC(CH_3)_3$), 0.05 & –0.18 (2 × s, 2 × 3H, $Si(CH_3)_2$).
^{13}C NMR (101 MHz, $CDCl_3$): δ = 208.7 (C4), 163.8 (1-$\underline{C}OOCH_3$), 142.8 (C5''), 139.7 (C2''), 139.3 (C1), 139.2 (C2), 128.8 (C3''), 118.3 (6-CN), 109.5 (C4''), 99.0 (C3a), 76.3 (C7), 63.6 (C2'), 59.7 (C8a), 51.5 (1-COO$\underline{C}H_3$), 47.8 (C1'), 46.3 (C8), 46.2 (C5), 42.6 (C6), 36.0 (C3), 25.7 (3C, $SiC(\underline{C}H_3)_3$), 23.1 (8a-CH_3), 22.0 (5-CH_3), 18.0 ($Si\underline{C}(CH_3)_3$), –4.6 & –4.9 ($Si(CH_3)_2$). (**Figure 154**)
HRMS: calcd. for $C_{27}H_{37}NNaO_6Si$ 522.22824 $[M+Na]^+$, found 522.22806 (Δ = 0.34 ppm).

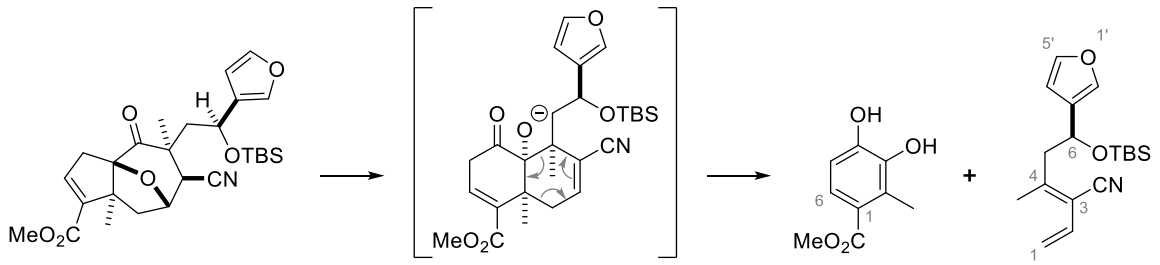

145 **140.I** **146** **147**

Catechol 146 and **Diene 147**: TBS ether **145** (23.9 mg, 0.048 mmol, 1 eq) was dissolved in THF (1.9 mL) in a 5 mL flask. The solution was cooled to –95 °C before a freshly prepared LHMDS solution (0.5 M in THF/hexane; 0.2 mL, 0.10 mmol, 2.09 eq) was added. The reaction mixture was allowed to warm to 0 °C over the course of 2 h, after which the cooling bath was removed. After 30 min, the reaction mixture was quenched with acetic acid (0.027 mL, 0.478 mmol, 10 eq) and volatiles removed in vacuo. The residue was filtered through a plug of silica gel, eluting with diethyl ether (~20 mL). The filtrate was concentrated, and the crude product was combined with those of other attempts.

Notes: This procedure was repeated thrice with slightly different conditions (with 14.3 mg, 18.6 mg, and 18.9 mg of **145**, respectively). These attempts included addition of $LiClO_4$ and/or an aqueous work-up, as described in the rearrangement of TBS ether **127**. Since no successful rearrangement was indicated, a quantitative evaluation was not pursued. The crude products were combined in order to recover (partially epimerized) substrate and isolate analytical samples of the undesired side-products. Flash chromatography (PE/DE, gradient from 10:1 to 1:1) gave – next to the TBS ethers (6-*epi*-)**145** – some catechol **146** and diene **147**. Catechol **146** exhibited low solubility in DE, DCM and $CDCl_3$, while diene **147** seemed to be rather volatile.

The melting point of catechol **146** was in accordance with that reported in the literature.[386] Its NMR spectra can only be compared to an extent, since the authors of the cited paper used $CDCl_3$ + DMSO-d_6, while we chose CD_3CN as solvent.

Catechol 146: slightly yellow solid (m.p. 159 °C). $\mathbf{R_f}$ = 0.46 (PE/EA, 1.5:1).
^{1}H NMR (400 MHz, CD_3CN): δ = 7.32 (d, *J* = 8.4 Hz, 1H), 6.96 (v br s, 2H), 6.72 (d, *J* = 8.4 Hz, 1H), 3.78 (s, 3H), 2.41 (s, 3H). **^{13}C NMR** (101 MHz, CD_3CN): δ = 168.7, 148.3, 144.0, 127.9, 124.0, 112.5, 52.1, 13.2. (**Figure 155**)
HRMS: calcd. for $C_9H_9O_4$ 181.05063 $[M-H]^+$, found 181.05089 (Δ = 1.41 ppm).

Diene 147: colorless oil. $\mathbf{R_f}$ = 0.93 (PE/EA, 1.5:1).
^{1}H NMR (400 MHz, $CDCl_3$): δ = 7.36 (br dd, *J* ≈ 1.6 Hz, 1H, 5'-H), 7.33–7.31 (m, 1H, 2'-H), 6.50 (dd, *J* = 17.0 Hz, 10.6 Hz, 1H, 2-H), 6.42 (br dd, *J* ≈ 0.6–1.5 Hz, 1H, 4'-H), 5.64 (d, *J* = 17.0 Hz, 1H, 1-H_a), 5.34 (d, *J* = 10.6 Hz, 1H, 1-H_b), 4.94 (dd, *J* = 8.5 Hz, 4.6 Hz, 1H, 6-H), 2.92 (dd, *J* = 13.1 Hz, 8.6 Hz, 1H, 5-H_a), 2.68 (dd, *J* = 13.1 Hz, 4.7 Hz, 1H, 5-H_a), 1.98 (s, 3H, 4-CH_3), 0.85 (s, 9H, $SiC(CH_3)_3$), –0.01 & –0.10 (2 × s, 2 × 3H, $Si(CH_3)_2$).
^{13}C NMR (101 MHz, $CDCl_3$): δ = 153.2 (C4), 143.1 (C5'), 138.7 (C2'), 128.9 (C3'), 128.5 (C2), 118.3 (C1), 116.3 (3-CN), 113.1 (C3), 108.6 (C4'), 66.7 (C6), 48.8 (C5), 25.7 (3C, $SiC(\underline{C}H_3)_3$), 20.0 (4-CH_3), 18.0 ($Si\underline{C}(CH_3)_3$), –4.8 & –5.2 ($Si(CH_3)_2$). (**Figure 156**)
HRMS: calcd. for $C_{18}H_{27}NNaO_2Si$ 340.17033 $[M+Na]^+$, found 340.17047 (Δ = 0.43 ppm).

145 **148**

148: **Methyl (1*S**,3a*R**,5*S**,6*S**,7*S**,8a*S**)-5-((*S**)-2'-((*tert*-butyldimethylsilyl)oxy)-2'-(furan-3''-yl)-ethyl)-6-cyano-5,8a-dimethyl-4-oxooctahydro-1*H*-3a,7-epoxyazulene-1-carboxylate**

Enoate **145** (63.2 mg, 0.126 mmol, 1 eq) was dissolved in MeOH (6.4 mL) in a 25 mL flask (*under air*). The flask was connected to the Schlenk line for pressure equalization (*argon atmosphere*). The solution was cooled to –18 °C using an ice/sodium chloride mixture and kept between –18 to –5 °C throughout the reaction course. Mercury(II) chloride (6.9 mg, 25.4 µmol, 20 mol%) and magnesium turnings (15.4 mg, 0.634 mmol, 5 eq) were added. After 2.5 h, another portion of magnesium turnings (15.4 mg, 0.634 mmol, 5 eq) was added. The grey suspension was stirred for another 2 h, before the cooling bath was removed and the reaction mixture stirred at room temperature for 45 min. Half-saturated NH_4Cl solution (13 mL) and some diethyl ether were added. After stirring the biphasic mixture for 30 min, it was diluted with half-saturated NH_4Cl solution (7 mL) and extracted with diethyl ether (3 × 30 mL). The combined organic phases were dried over $MgSO_4$, filtered, and concentrated in vacuo. Purification by flash chromatography (PE/DE, gradient from 10:1 to 1:2) afforded a diastereomeric mixture of methyl ester **148** (56.6 mg, 0.118 mmol, **89%**) as a colorless oil.

Notes: The used enoate **145** exhibited a diastereomeric ratio of ~10:1 (**145**/2'-*epi*-**145**). The NMR spectra of the obtained methyl ester **148** indicated the presence of the two most dominant diastereomers in a ~7.5:1 ratio, while small amounts of other diastereomers were also apparent. For a better NMR interpretation, the main diastereomer was partially separated from the others by flash chromatography. While the collective of diastereomers gave a single TLC spot, the fraction tubes 'in the middle' contained primarily the main diastereomer. ^{1}H-^{1}H NOESY of the main diastereomer of **148** indicated the depicted relative stereochemistry. The NMR spectra of the two product samples (i.e., that from the middle fraction tubes, as well as that from the remaining fraction tubes) are attached.

$\mathbf{R_f}$ = 0.70 [$\mathbf{R_f}$ (**145**) = 0.75] (PE/EA, 1.5:1).
^{1}H NMR (400 MHz, $CDCl_3$): δ = 7.30 (br dd, *J* ≈ 1.1–1.5 Hz, 1H, 5''-H), 7.14 (*app.* br s, 1H, 2''-H), 6.40 (br d, *J* ≈ 1.1 Hz, 1H, 4''-H), 4.65 (dd, *J* = 5.9 Hz, 3.1 Hz, 1H, 7-H), 4.55 (br dd, *J* ≈ 5.5–5.7 Hz, 1H, 2'-H), 3.67 (s, 3H, 1-$COOCH_3$), 2.66 (dd, *J* = 13.8 Hz, 5.7 Hz, 1H, 1-H_a), 2.55 (d, *J* = 3.1 Hz, 1H, 6-H), 2.44–2.39 (m, 1H, 1-H), 2.23 (dd, *J* = 13.8 Hz, 5.5 Hz, 1H, 1'-H_b), 2.00 (dd, *J* = 12.8 Hz, 6.1 Hz, 1H, 8-H_a), 1.79-1.94 (m, 3H, 2-H_2 & 3-H_a), 1.60 (d, *J* = 12.8 Hz, 1H, 8-H_b), 1.35 (s, 3H, 5-CH_3), 1.13 (dd, *J* ≈ 15.8 Hz, 8.0 Hz, 1H, 3-H_b), 1.10 (s, 3H, 8a-CH_3), 0.82 (s, 9H, $SiC(CH_3)_3$), 0.05 & –0.20 (2 × s, 2 × 3H, $Si(CH_3)_2$). (**Figure 157**)
^{13}C NMR (101 MHz, $CDCl_3$): δ = 208.6 (C4), 172.6 (1-$\underline{C}OOCH_3$), 142.8 (C5''), 139.4 (C2''), 129.1 (C3''), 118.4 (6-CN), 109.3 (C4''), 99.7 (C3a), 76.1 (C7), 63.8 (C2'), 56.5 (C1), 54.8 (C8a), 51.8 (1-COO$\underline{C}H_3$), 47.9 (C1'), 46.9 (C5), 45.2 (C8), 41.9 (C6), 29.0 (C3), 27.3 (8a-CH_3), 25.8 (3C, $SiC(\underline{C}H_3)_3$), 25.6 (C2), 22.0 (5-CH_3), 18.0 ($Si\underline{C}(CH_3)_3$), –4.5 & –5.0 ($Si(CH_3)_2$). (**Figure 158**)
HRMS: calcd. for $C_{27}H_{39}NNaO_6Si$ 524.24389 $[M+Na]^+$, found 524.24417 (Δ = 0.55 ppm).

4.4.5.4 α-Deoxygenation of 3-Furylated Acyloins

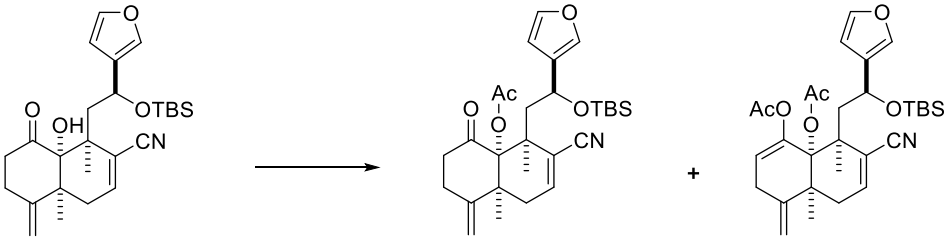

135 **149** **150**

α-Ketol acetate 149 and **Enol diacetate 150**: [6,6]-Fused acyloin **135** (77.8 mg, 0.171 mmol, 1 eq) was dissolved in THF (3.4 mL) in a 10 mL flask. Then, NEt_3 (0.12 mL, 0.874 mmol, 5 eq), DMAP (4.2 mg, 34.4 µmol, 20 mol%), and Ac_2O (0.16 mL, 1.733 mmol, 10 eq) were added. The solution was stirred at 50 °C for 13.5 h. Half-saturated $NaHCO_3$ solution (6 mL) and DCM (2 mL) were added, and the biphasic mixture was stirred until gas evolution ceased (20 min). After addition of another portion of half-saturated $NaHCO_3$ solution (4 mL), the mixture was extracted with DCM (3 × 20 mL). The combined organic phases were dried over $MgSO_4$, filtered, and concentrated. The crude product was purified by flash chromatography (PE/DE, gradient from 20:1 to 1:1), affording some unreacted **135** (7.6 mg, 0.017 mmol, **10%**), enol diacetate (6.6 mg, 0.012 mmol, **7%**), and the desired α-ketol acetate **149** [66 mg, 0.133 mmol, **78%** (87% *b.r.s.m.*)].

α-Ketol acetate 149: colorless solid (m.p. 117 °C). $\mathbf{R_f}$ = 0.56 [$\mathbf{R_f}$ (**135**) = 0.68] (PE/EA, 2:1).
^{1}H NMR (400 MHz, $CDCl_3$): δ = 7.31 (*app.* br s, 2H), 6.75 (br dd, *J* ≈ 4.5–4.7 Hz, 1H), 6.30 (*app.* br s, 1H), 4.96–4.91 (br s, 3H), 2.98–2.82 (m, 2H), 2.68 (dd, *J* = 18.8 Hz, 4.6 Hz, 1H), 2.60–2.50 (m, 3H), 2.25 (dd, *J* = 18.8 Hz, 4.7 Hz, 1H), 2.03 (s, 3H), 1.75 (dd, *J* = 14.3 Hz, 5.6 Hz, 1H), 1.32 (s, 3H), 1.24 (s, 3H), 0.80 (s, 9H), 0.04 (s, 3H), –0.25 (s, 3H). **^{13}C NMR** (101 MHz, $CDCl_3$): δ = 203.8, 169.4, 148.0, 143.1, 142.7, 139.1, 129.8, 119.8, 119.1, 110.7, 108.7, 86.5, 63.6, 46.1, 45.0, 44.8, 38.9, 35.4, 28.6, 28.0, 25.7 (3C), 20.9, 20.1, 18.0, –4.4, –5.0. (**Figure 159**)
HRMS: calcd. for $C_{28}H_{39}NNaO_5Si$ 520.24897 $[M+Na]^+$, found 520.24942 (Δ = 0.86 ppm).

Enol diacetate 150: colorless, very viscous oil. $\mathbf{R_f}$ = 0.47 (PE/EA, 2:1).
^{1}H NMR (400 MHz, $CDCl_3$): δ = 7.31 (br dd, *J* ≈ 1.0–1.5 Hz, 1H), 7.27 (*app.* br s, 1H), 6.59 (dd, *J* = 5.6 Hz, 2.6 Hz, 1H), 6.32 (br d, *J* ≈ 1.0 Hz, 1H), 6.01 (br dd, *J* ≈ 3.5–4.0 Hz, 1H), 4.97 (br dd, *J* = 4.2 Hz, 6.1 Hz, 1H), 4.74 (br dd, *J* ≈ 10.5 Hz, 2.0 Hz, 1H), 3.27–3.22 (m, 1H), 2.68–2.58 (m, 2H), 2.31–2.19 (m, 2H), 2.09 (s, 3H), 2.06 (s, 3H), 2.02 (dd, *J* = 15.2 Hz, 4.0 Hz, 1H), 1.42 (s, 3H), 1.24 (s, 3H), 0.81 (s, 9H), 0.02 (s, 3H), –0.28 (s, 3H). **^{13}C NMR** (101 MHz, $CDCl_3$): δ = 168.4, 167.2, 145.7, 143.0, 142.5, 140.5, 138.8, 130.2, 120.1, 119.3, 114.9, 109.3, 108.8, 85.5, 63.4, 47.0, 45.9, 45.1, 33.2, 30.9, 28.8, 25.8 (3C), 22.1, 21.6, 20.6, 18.0, –4.3, –5.0. (**Figure 160**)
HRMS: calcd. for $C_{30}H_{41}NNaO_6Si$ 562.25954 $[M+Na]^+$, found 562.25903 (Δ = 0.89 ppm).

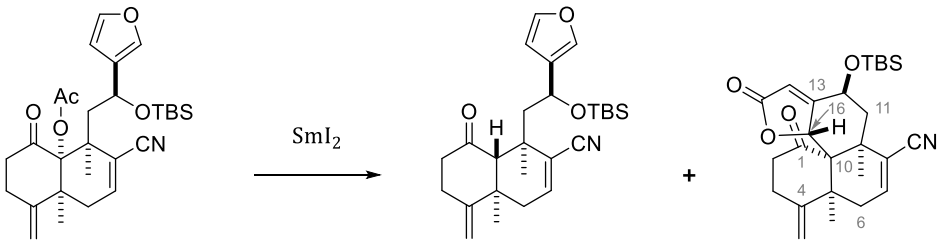

149 **152** **153**

Decalone 152 and **Tetracyclic Butenolide 153**: A SmI_2 solution was prepared from samarium and 1,2-diiodoethane (see procedure for decalone **109**). The SmI_2 solution (0.11 M in THF; 1.2 mL, 0.132 mmol, 2.2 eq) was placed in a 10 mL flask, which was previously charged with some samarium metal (2.8 mg). The suspension was cooled to –95 °C, before α-ketol acetate **149** (30.0 mg, 0.060 mmol, 1 eq), dissolved in 0.95 mL THF, was added (1 min). After 15 min (full conversion of **149** to *unidentified compound*; R_f = 0.56 to R_f = 0.73), NEt_3 (0.1 mL, 0.721 mmol, 12 eq) was added at –68 °C. After another 40 min, ethylene glycol (0.15 mL, 2.682 mmol, ~45 eq) was added at –20 °C, and the reaction mixture was diluted with 3 mL of a mixture of PE/DE (1:1) containing 5 vol% NEt_3. The cooling bath was removed 10 min later at –13 °C. After stirring vigorously for 20 min at room temperature, the biphasic mixture was filtered through a plug of silica gel, eluting with 30 mL of the above PE/DE/NEt_3-mixture. After letting it stand overnight, the filtrate was concentrated in vacuo to give a colorless, very viscous oil which darkened to a brownish-orange hue and formed an insoluble precipitate with time under air in the flask and in the NMR tube (C_6D_6).

Notes: As in the deoxygenation of **111**, the crude product indicated a complex and 'dynamic' mixture in NMR and TLC. An ongoing reaction with extensive decomposition was observed. The two most prominent compounds were identified as decalone **152** (qNMR: ~30%; analytical data below procedure with Mg/MeOH) and tetracyclic butenolide **153** (qNMR: ~12%). By chromatographic purification (PE/DE, gradient from 20:1 to 1:1), analytical samples of **152** (5.2 mg, colorless oil, slightly impure) and **153** (2.6 mg, colorless solid) were isolated.

The structural elucidation of **153** was achieved by HRMS and 2D NMR. HRMS revealed a molecular formula of $C_{26}H_{\underline{35}}NO_{\underline{4}}Si$, indicating a loss of two hydrogen atoms and the presence of an additional oxygen atom relative to decalone **152** ($C_{26}H_{\underline{37}}NO_{\underline{3}}Si$). In NMR, the typical 3-furan signals were missing and, instead, the distinct ^{13}C signals of the butenolide moiety (171.6 and 168.8 ppm) stood out. Next to the ^1H and ^{13}C NMR spectra, the HMBC spectrum and NOESY spectra are attached. The 'most revealing' signals are highlighted. In NOESY, those include those of 16-H to the *(pseudo-)axial* 6-H_{ax} and that of the *(pseudo-)equatorial* 6-H_{eq} to 5-CH_3. The signals of the TBS group were cut off in the HMBC and NOESY spectra for a higher resolution of the other signals, since the TBS group did not correlate to other atoms beyond the TBS ether oxygen.

Butenolide 153: R_f = 0.52 [Rf (**152**) = 0.76; R_f (**149**) = 0.56] (PE/EA, 2:1).
^{1}H NMR (600 MHz, $CDCl_3$): δ = 6.49 (dd, *J* = 6.2 Hz, 2.2 Hz, 1H, 7-H), 5.77 (d, *J* = 1.7 Hz, 1H, 14-H), 5.09 (d, *J* = 1.5 Hz, 1H, 16-H), 4.96 & 4.91 (2 × br s, 2 × 1H, 4-CH_2), 4.78 (br dd, *J* ≈ 2.5–2.8 Hz, 1H, 12-H), 2.91 (br d, *J* = 19.6 Hz, 1H, 6-H_a), 2.88–2.81 (m, 2H, 3-H_2), 2.63 (dd, *J* = 15.2 Hz, 2.9 Hz, 1H, 11-H_a), 2.60–2.50 (m, 2H, 2-H_2), 2.44 (dd, *J* = 15.2 Hz, 2.8 Hz, 1H, 11-H_b), 2.38 (dd, *J* = 19.7 Hz, 6.2 Hz, 1H, 6-H_b), 1.43 (s, 3H, 5-CH_3), 1.33 (s, 3H, 9-CH_3), 0.86 (s, 9H, $SiC(CH_3)_3$), 0.13 & 0.01

(2 × s, 2 × 3H, $Si(CH_3)_2$). **^{13}C NMR** (151 MHz, $CDCl_3$): δ = 207.9 (C1), 171.6 (C15), 168.8 (C13), 149.3 (C4), 137.5 (C7), 124.5 (C8), 118.2 (8-CN), 113.6 (C14), 107.7 (4-CH_2), 79.8 (C16), 64.9 (C12), 63.3 (C10), 46.1 (C11), 42.1 (C5), 40.3 (C9), 38.8 (C2), 34.4 (C6), 29.3 (5-CH_3), 26.6 (C3), 25.7 (3C, $SiC(\underline{C}H_3)_3$), 25.3 (9-CH_3), 18.1 ($Si\underline{C}(CH_3)_3$), –5.1 & –5.3 ($Si(CH_3)_2$). (**Figure 161**)
HRMS: calcd. for $C_{26}H_{35}NNaO_4Si$ 476.22276 $[M+Na]^+$, found 476.22316 (Δ = 0.41 ppm).

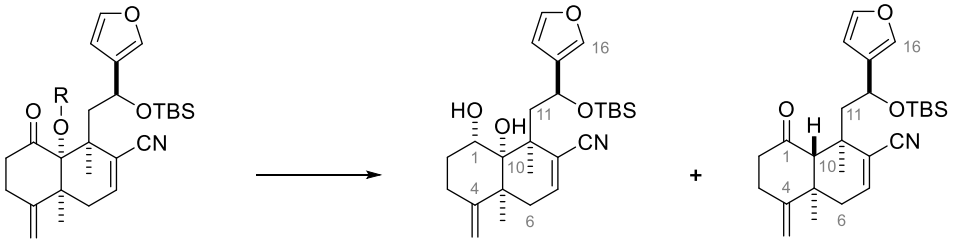

149: R = Ac
135: R = H

154 **152**

Decalone 152 and **Diol 154**: α-Ketol acetate **149** (30.0 mg, 0.060 mmol, 1 eq) was dissolved in MeOH (3 mL) in a 10 mL flask (*under air*). The flask was connected to the Schlenk line for pressure equalization (*argon atmosphere*). The solution was cooled to –18 °C using an ice/sodium chloride mixture, before mercury(II) chloride (3.3 mg, 12.2 µmol, 20 mol%) and magnesium turnings (7.3 mg, 0.300 mmol, 5 eq) were added. The cooling bath was allowed to warm slowly. After 2.5 h, the cooling bath reached –5 °C, and another portion of magnesium turnings (15.4 mg, 0.634 mmol, 5 eq) was added. The grey suspension was stirred for another 2.5 h, before the cooling bath was removed at 15 °C. After stirring the reaction mixture at room temperature for 20 min, half-saturated NH_4Cl solution (5 mL) and diethyl ether (2 mL) were added. After stirring the biphasic mixture for 30 min, it was diluted with half-saturated NH_4Cl solution (5 mL) and extracted with diethyl ether (3 × 15 mL). The combined organic phases were dried over $MgSO_4$, filtered, and concentrated in vacuo. Next to decalone **152** and diol **154**, acyloin **135** was seen in the crude product (NMR ratio of **152**/**154**/**135** ≈ 1 : 0.35 : 0.69).

To fully convert remaining **135**, the crude product was resubjected to the same procedure – with the exception of a shorter stirring time after the second addition of magnesium turnings (stirred for another 1 h 45 min, before the cooling bath was removed at 10 °C). Then, the crude product was purified by flash chromatography (PE/DE, gradient from 10:1 to 1:1), affording decalone **152** as a colorless oil (12.5 mg, 0.027 mmol, **47%**) and diol **154** as a colorless solid (6.4 mg, 0.014 mmol, **23%**).

Notes: This method was repeated with 60.0 mg instead of 30.0 mg of α-ketol acetate **149**. Although the conditions were slightly adapted, necessitating a total of 3 reduction runs, the yields of decalone **152** and **154** were reproducible (**48%** and **20%**, respectively).

Similar to its allyl analog **109**, decalone **152** exhibited highly superimposed ^{1}H NMR signals in $CDCl_3$. Therefore, both the NMR spectra of **152** and **154** were recorded in C_6D_6.

The hydroxyl protons of diol **154** were identified as the signals at 0.32 ppm (1-OH) and 1.50 ppm (10-OH). The signal at 3.57 ppm was identified to be that of 1-H, which correlated with C1 in HSQC. Weak cross-peak of 1-H to 2-H_2 and 1-OH were seen in COSY. Due to its chemical

shift, the signal of 1-H could easily be misinterpreted for either an acyloin 10-OH (e.g., 3.95 ppm for acyloin **135**; in $CDCl_3$) or a decalone 10-H (e.g., 3.35 ppm for decalone **152**; in C_6D_6). The configuration at C1 was not determined by NOESY, but assumed to be *cis*, since a similar *cis*-diol was obtained from the SmI_2-mediated deoxygenation of the dioxolane analog (*cf.* **Chapter 4.4.4.1.b**). In any case, determining the configuration of the diol does not seem crucial.

The NOESY spectrum of decalone **152** can be seen in **Figure 166**. Unfortunately, some of the most revealing signals are superimposed even in C_6D_6. With the allyl-substituted decalone **109**, the configuration of C10 was determined especially with NOE correlations of 10-H to (i) 2-H, (ii) the (*pseudo*-)axial 6-H_{ax}, (iii) and the protons of the allyl group (see **Figure 28** on page **153**).

In the spectra of decalone **152**, however, the signals of 2-H_2, 3-H_a and 6-H_{ax} are superimposed – as well as 6-H_{eq} and 9-CH_3. While this complicates an unambiguous analysis, 10-H is strongly believed to be (*pseudo*-)axial, corresponding to a *trans*-fused decalone core. This is corroborated especially by (i) the presence of the NOE signals 10-H/11-H_a, 10-H/12-H, and 10-H/ $SiC(CH_3)_3$, and also by (ii) the *absence* of 10-H/5-CH_3 and 10-H/9-CH_3. Particularly 10-H/9-CH_3 would be expected in a putative *cis*-fused decalone.

Diol 154: R_f = 0.63 [Rf (**149**) = 0.56; R_f (**135**) = 0.66] (PE/EA, 2:1).
^{1}H NMR (400 MHz, C_6D_6): δ = 7.11 (br s, 1H, 16-H), 7.02 (br s, 1H, 15-H), 6.32 (br s, 1H, 14-H), 6.02 (dd, *J* = 5.9 Hz, 2.2 Hz, 1H, 7-H), 5.33 (br d, *J* ≈ 7.1 Hz, 1H, 12-H), 4.79 & 4.62 (2 × br s, 2 × 1H, 4-CH_2), 3.58 (br s, 1-H), 2.94 (br d, *J* = 18.8 Hz, 1H, 6-H_a), 2.75 (dd, *J* = 15.3 Hz, 6.6 Hz, 1H, 11-H_a), 2.50 (br d, *J* = 15.3 Hz, 1H, 11-H_b), 2.30 (br ddd, *J* ≈ 13.5 Hz, 13.3 Hz, 4.4 Hz, 1H, 3-H_a), 1.71 (s, 3H, 9-CH_3), 1.71–1.65 (m, 1H, 3-H_b), 1.61–1.52 (m, 1H, 2-H_a), 1.50 (s, 1H, 10-OH), 1.19 (dd, *J* = 18.8 Hz, 5.9 Hz, 1H, 6-H_b), 1.03–1.00 (m, 1H, 2-H_b), 1.00 (s, 9H, $SiC(CH_3)_3$), 0.87 (s, 3H, 5-CH_3), 0.19 & –0.10 (2 × s, 2 × 3H, $Si(CH_3)_2$).
^{13}C NMR (101 MHz, C_6D_6): δ = 152.3 (C4), 143.7 (C15), 143.0 (C7), 138.0 (C16), 131.5 (C13), 122.3 (C8), 119.1 (8-CN), 113.0 (4-CH_2), 109.4 (C14), 77.6 (C10), 72.6 (C1), 65.1 (C12), 48.3 (C11), 45.4 (C5), 45.0 (C9), 36.9 (C6), 32.9 (C2), 27.6 (C3), 26.2 (3C, $SiC(\underline{C}H_3)_3$), 23.6 (5-CH_3), 22.7 (9-CH_3), 18.3 ($Si\underline{C}(CH_3)_3$), –3.9 & –4.6 ($Si(CH_3)_2$). (**Figure 164**)
HRMS: calcd. for $C_{26}H_{39}NNaO_4Si$ 480.25406 $[M+Na]^+$, found 480.25455 (Δ = 0.50 ppm).

Decalone 152: R_f = 0.76 [Rf (**149**) = 0.56; R_f (**135**) = 0.66] (PE/EA, 2:1).
^{1}H NMR (400 MHz, C_6D_6): δ = 7.19 (br s, 1H, 16-H), 6.97 (br dd, *J* ≈ 1.0–1.6 Hz, 1H, 15-H), 6.28 (br d, *J* ≈ 1.0 Hz, 1H, 14-H), 6.03 (dd, *J* = 6.4 Hz, 2.3 Hz, 1H, 7-H), 4.81 (dd, *J* = 9.2 Hz, 2.3 Hz, 1H, 12-H), 4.59 & 4.48 (2 × br s, 2 × 1H, 4-CH_2), 3.35 (s, 1H, 10-H), 2.91 (dd, *J* = 15.5 Hz, 9.2 Hz, 1H, 11-H_a), 2.26–2.21 (m, 4H, 2-H_2 & 3-H_a & 6-H_a), 2.08–2.03 (m, 1H, 3-H_b), 1.98 (dd, *J* = 15.5 Hz, 2.4 Hz, 1H, 11-H_b), 1.59 (dd, 1H, *J* = 18.5 Hz, 9.2 Hz, 1H, 6-H_b) *superimposed with* 1.58 (s, 3H, 9-CH_3), 0.83 (s, 9H, $SiC(CH_3)_3$), 0.75 (s, 3H, 5-CH_3), 0.06 & –0.22 (2 × s, 2 × 3H, $Si(CH_3)_2$).
^{13}C NMR (101 MHz, C_6D_6): δ = 207.6 (C1), 153.4 (C4), 143.3 (C15), 140.8 (C7), 138.7 (C16), 130.7 (C13), 122.8 (C8), 118.2 (8-CN), 109.2 (C14), 107.2 (4-CH_2), 65.5 (C12), 55.0 (C10), 49.4 (C11), 42.8 (C2), 40.8 (C5), 40.0 (C9), 38.0 (C6), 31.4 (C3), 26.3 (3C, $SiC(\underline{C}H_3)_3$), 25.3 (5-CH_3), 23.9 (9-CH_3), 18.2 ($Si\underline{C}(CH_3)_3$), –4.0 & –4.2 ($Si(CH_3)_2$). (**Figure 165**)
HRMS: calcd. for $C_{26}H_{37}NNaO_3Si$ 462.24349 $[M+Na]^+$, found 462.24404 (Δ = 1.19 ppm).

CHAPTER 5: BIBLIOGRAPHY

[1] K. Brook, J. Bennett, S. P. Desai, *J. Anesth. Hist.* **2017**, *3*, 50–55.

[2] M. J. Brownstein, *Proc. Natl. Acad. Sci. U. S. A.* **1993**, *90*, 5391–5393.

[3] M. F. Balandrin, A. D. Kinghorn, N. R. Farnsworth, Plant-Derived Natural Products in Drug Discovery and Development, in *Human Medicinal Agents from Plants, Vol. 534* (Eds.: A. D. Kinghorn, M. F. Baladrin), American Chemical Society, Washington, **1993**, pp. 2–12.

[4] J. Achan, A. O. Talisuna, A. Erhart, A. Yeka, J. K. Tibenderana, F. N. Baliraine, P. J. Rosenthal, U. D'Alessandro, *Malar. J.* **2011**, *10*, 144.

[5] D. F. Musto, *Sci. Am.* **1991**, *265*, 40–47.

[6] J. C. Ballantyne, *Anesth. Analg.* **2017**, *125*, 1769–1778.

[7] M. J. Ignaszewski, *J. Clin. Pharmacol.* **2021**, *61*, S10–S17.

[8] S. P. Hermans, J. Samiec, A. Golec, C. Trimble, J. Teater, O. T. Hall, *J. Adolesc. Heal.* **2023**, *72*, 397–403.

[9] A. S. Yekkirala, D. P. Roberson, B. P. Bean, C. J. Woolf, *Nat. Rev. Drug Discov.* **2017**, *16*, 545–564.

[10] R. C. Heel, R. N. Brogden, T. M. Speight, G. S. Avery, *Drugs* **1978**, *15*, 33–52.

[11] C. N. Stanciu, S. A. Gnanasegaram, *J. Psychoactive Drugs* **2017**, *49*, 18–21.

[12] V. Spahn, G. Del Vecchio, D. Labuz, A. Rodriguez-Gaztelumendi, N. Massaly, J. Temp, V. Durmaz, P. Sabri, M. Reidelbach, …, C. Stein, *Science* **2017**, *355*, 966–969.

[13] S. R. Edwards, B. E. Blough, K. Cowart, G. H. Howell, A. A. Araujo, J. P. Haskell, S. L. Huskinson, J. K. Rowlett, M. F. Brackeen, K. B. Freeman, *Neuropharmacology* **2024**, *255*, 110002.

[14] A. Hofmann, *LSD – Mein Sorgenkind*, Klett-Cotta, Stuttgart, **1979**.

[15] A. Shulgin, A. Shulgin, *PiHKAL: A Chemical Love Story*, Transform Press, Berkeley, **1995**.

[16] J. Fadiman, *The Psychedelic Explorer's Guide: Safe, Therapeutic, and Sacred Journeys*, Park Street Press, **2011**.

[17] B. Sessa, *Lancet* **2012**, *380*, 200–201.

[18] D. E. Nichols, *Pharmacol. Rev.* **2016**, *68*, 264–356.

[19] T. Noorani, *J. Psychedelic Stud.* **2019**, *4*, 34–39.

[20] T. S. Krebs, P.-Ø. Johansen, *J. Psychopharmacol.* **2012**, *26*, 994–1002.

[21] J. Calleja-Conde, J. A. Morales-García, V. Echeverry-Alzate, K. M. Bühler, E. Giné, J. A. López-Moreno, *Addict. Biol.* **2022**, *27*, 1–13.

[22] E. Krediet, T. Bostoen, J. Breeksema, A. van Schagen, T. Passie, E. Vermetten, *Int. J. Neuropsychopharmacol.* **2020**, *23*, 385–400.

[23] C. M. Reiff, E. E. Richman, C. B. Nemeroff, L. L. Carpenter, A. S. Widge, C. I. Rodriguez, N. H. Kalin, W. M. McDonald, *Am. J. Psychiatry* **2020**, *177*, 391–410.

[24] J. J. Breeksema, A. Niemeijer, E. Krediet, T. Karsten, J. Kamphuis, E. Vermetten, W. van den Brink, R. Schoevers, *Sci. Rep.* **2024**, *14*, 1–12.

[25] M. Karst, J. H. Halpern, M. Bernateck, T. Passie, *Cephalalgia* **2010**, *30*, 1140–1144.

[26] E. A. D. Schindler, *Neuropharmacology* **2022**, *215*, 109166.

[27] V. Lewis, E. M. Bonniwell, J. K. Lanham, A. Ghaffari, H. Sheshbaradaran, A. B. Cao, M. M. Calkins, M. A. Bautista-Carro, E. Arsenault, …, J. D. McCorvy, *Cell Rep.* **2023**, *42*, 112203.

[28] R. Haridy, *Nature* **2023**, *619*, 227–228.

[29] A. Gomez-Escolar, D. Folch-Sanchez, J. Stefaniuk, Z. Swithenbank, A. Nisa, F. Braddick, N. I. Chaudhary, P. B. van der Meer, A. Batalla, *CNS Drugs* **2024**, *38*, 771–789.

[30] R. B. Hernández-Alvarado, A. Madariaga-Mazón, A. Ortega, K. Martinez-Mayorga, *ACS Chem. Neurosci.* **2020**, *11*, 3979–3992.

[31] S. Chakraborty, S. Majumdar, *Biochemistry* **2021**, *60*, 1381–1400.

[32] D. B. Yaden, M. E. Yaden, R. R. Griffiths, *JAMA Psychiatry* **2021**, *78*, 469.

[33] L. J. Valdés, J. Díaz, A. G. Paul, *J. Ethnopharmacol.* **1983**, *7*, 287–312.

[34] A. E. Maqueda, *Plant Med. Heal. Psychedelic Sci. Cult. Perspect.* **2018**, 55–70.

[35] A. Hofmann, A. Frey, H. Ott, T. Petrzilka, F. Troxler, *Experientia* **1958**, *14*, 397–399.

[36] A. Hofmann, *LSD: My Problem Child*, MAPS (Multidisciplinary Association For Psychedelic Studies), Santa Cruz, **2009**.

[37] A. Ortega, J. F. Blount, P. S. Manchand, *J. Chem. Soc. Perkin Trans. 1* **1982**, 2505.

[38] L. J. Valdes, W. M. Butler, G. M. Hatfield, A. G. Paul, M. Koreeda, *J. Org. Chem.* **1984**, *49*, 4716–4720.

[39] L. J. Valdés, H. M. Chang, D. C. Visger, M. Koreeda, *Org. Lett.* **2001**, *3*, 3935–3937.

[40] W. W. Harding, K. Tidgewell, M. Schmidt, K. Shah, C. M. Dersch, J. Snyder, D. Parrish, J. R. Deschamps, R. B. Rothman, T. E. Prisinzano, *Org. Lett.* **2005**, *7*, 3017–3020.

[41] J. R. Hanson, *Sci. Prog.* **2010**, *93*, 171–180.

[42] L. J. Valdés, G. M. Hatheld, M. Koreeda, A. G. Paul, *Econ. Bot.* **1987**, *41*, 283–291.

[43] J. B. Zawilska, J. Wojcieszak, *Hum. Psychopharmacol. Clin. Exp.* **2013**, *28*, 403–412.

[44] L. J. Valdés, *J. Psychoactive Drugs* **1994**, *26*, 277–283.

[45] J. E. Mendelson, J. R. Coyle, J. C. Lopez, M. J. Baggott, K. Flower, E. T. Everhart, T. A. Munro, G. P. Galloway, B. M. Cohen, *Psychopharmacology (Berl).* **2011**, *214*, 933–939.

[46] D. N. Albertson, L. E. Grubbs, *J. Psychoactive Drugs* **2009**, *41*, 213–217.

[47] K. A. MacLean, M. W. Johnson, C. J. Reissig, T. E. Prisinzano, R. R. Griffiths, *Psychopharmacology* **2013**, *226*, 381–392.

[48] S. H. Snyder, *Drugs and the Brain (Scientific American Library Series #18)*, Scientific American, New York City, **1996**.

[49] D. M. Ciucă Anghel, G. V. Nițescu, A. T. Tiron, C. M. Guțu, D. L. Baconi, *Molecules* **2023**, *28*, 1–27.

[50] J. E. Leysen, *Curr. Drug Targets CNS Neurol. Disord.* **2004**, *3*, 11–26.

[51] J. F. López-Giménez, J. González-Maeso, *Curr. Top. Behav. Neurosci.* **2018**, *36*, 45–73.

[52] B. L. Roth, K. Baner, R. Westkaemper, D. Siebert, K. C. Rice, S. A. Steinberg, P. Ernsberger, R. B. Rothman, *Proc. Natl. Acad. Sci. USA* **2002**, *99*, 11934–11939.

[53] P. Seeman, H. C. Guan, H. Hirbec, *Synapse* **2009**, *63*, 698–704.

[54] W. A. Carlezon, C. Béguin, A. T. Knoll, B. M. Cohen, *Pharmacol. Ther.* **2009**, *123*, 334–343.

[55] J. Listos, A. Merska, S. Fidecka, *Pharmacol. Reports* **2011**, *63*, 1305–1309.

[56] A. M. Brito-da-Costa, D. Dias-da-Silva, N. G. M. Gomes, R. J. Dinis-Oliveira, Á. Madureira-Carvalho, *Pharmaceuticals* **2021**, *14*, 1–36.

[57] T. S. Shippenberg, A. Zapata, V. I. Chefer, *Pharmacol. Ther.* **2007**, *116*, 306–321.

[58] Z. Zheng, X. P. Huang, T. J. Mangano, R. Zou, X. Chen, S. A. Zaidi, B. L. Roth, R. C. Stevens, V. Katritch, *J. Med. Chem.* **2017**, *60*, 3070–3081.

[59] M. L. Dalefield, B. Scouller, R. Bibi, B. M. Kivell, *Front. Pharmacol.* **2022**, *13*, 1–26.

[60] M. Imanshahidi, H. Hosseinzadeh, *Phyther. Res.* **2006**, *20*, 427–437.

[61] T. E. Prisinzano, *J. Med. Chem.* **2013**, *56*, 3435–3443.

[62] J. J. Roach, R. A. Shenvi, *Bioorganic Med. Chem. Lett.* **2018**, *28*, 1436–1445.

[63] D. Tholl, Biosynthesis and Biological Functions of Terpenoids in Plants, in *Advances in Biochemical Engineering/Biotechnology*, Springer International Publishing, Basel, **2015**, pp. 63–106.

[64] L. Kutrzeba, F. E. Dayan, J. Howell, J. Feng, J. L. Giner, J. K. Zjawiony, *Phytochemistry* **2007**, *68*, 1872–1881.

[65] X. Chen, A. Berim, F. E. Dayan, D. R. Gang, *J. Exp. Bot.* **2017**, *68*, 1109–1122.

[66] J. J. Roach, R. A. Shenvi, *Bioorganic Med. Chem. Lett.* **2018**, *28*, 1436–1445.

[67] A. M. Sherwood, S. E. Williamson, R. S. Crowley, L. M. Abbott, V. W. Day, T. E. Prisinzano, *Org. Lett.* **2017**, *19*, 5414–5417.

[68] J. J. Roach, Y. Sasano, C. L. Schmid, S. Zaidi, V. Katritch, R. C. Stevens, L. M. Bohn, R. A. Shenvi, *ACS Cent. Sci.* **2017**, *3*, 1329–1336.

[69] T. Che, S. Majumdar, S. A. Zaidi, P. Ondachi, J. D. McCorvy, S. Wang, P. D. Mosier, R. Uprety, E. Vardy, …, B. L. Roth, *Cell* **2018**, *172*, 55-67.e15.

[70] K. Puls, G. Wolber, *Molecules* **2023**, *28*, 718.

[71] J. A. Ballesteros, H. Weinstein, Integrated Methods for the Construction of Three-Dimensional Models and Computational Probing of Structure-Function Relations in G Protein-Coupled Receptors, in *Methods in Neurosciences (Volume 25)* (Ed.: S. C. Sealfon), Academic Press, Inc., Cambridge, **1995**, pp. 366–428.

[72] T. E. Prisinzano, R. B. Rothman, *Chem. Rev.* **2008**, *108*, 1732–1743.

[73] R. Li, S. L. Morris-Natschke, K.-H. Lee, *Nat. Prod. Rep.* **2016**, *33*, 1166–1226.

[74] R. R. Neubig, M. Spedding, T. Kenakin, A. Christopoulos, *Pharmacol. Rev.* **2003**, *55*, 597–606.

[75] D. Y. W. Lee, V. V. R. Karnati, M. He, L. Y. Liu-Chen, L. Kondaveti, Z. Ma, Y. Wang, Y. Chen, C. Beguin, …, B. Cohen, *Bioorganic Med. Chem. Lett.* **2005**, *15*, 3744–3747.

[76] K. L. White, J. E. Robinson, H. Zhu, J. F. DiBerto, P. R. Polepally, J. K. Zjawiony, D. E. Nichols, C. J. Malanga, B. L. Roth, *J. Pharmacol. Exp. Ther.* **2015**, *352*, 98–109.

[77] K. L. Mores, B. R. Cummins, R. J. Cassell, R. M. Van Rijn, *Front. Pharmacol.* **2019**, *10*, 1–14.

[78] A. Faouzi, B. R. Varga, S. Majumdar, *Molecules* **2020**, *25*, 4257.

[79] A. P. Riley, C. E. Groer, D. Young, A. W. Ewald, B. M. Kivell, T. E. Prisinzano, *J. Med. Chem.* **2014**, *57*, 10464–10475.

[80] N. Brown et al., *Bioisosteres in Medicinal Chemistry*, Wiley, Weinheim, **2012**.

[81] M. A. M. Subbaiah, N. A. Meanwell, *J. Med. Chem.* **2021**, *64*, 14046–14128.

[82] J. Roach, Y. Sasano, C. Schmid, S. Zaidi, V. Katritch, R. Stevens, L. Bohn, R. Shenvi, *ChemRvix* **2017**, doi:10.26434/chemrxiv.5318188.v2.

[83] T. A. Munro, K. K. Duncan, R. J. Staples, W. Xu, L. Y. Liu-Chen, C. Béguin, W. A. Carlezon, B. M. Cohen, *Beilstein J. Org. Chem.* **2007**, *3*, 1–6.

[84] S. J. Hill, A. U. C. M. Brion, R. A. Shenvi, *Nat. Prod. Rep.* **2020**, *37*, 1478–1496.

[85] Y. E. Bergman, R. Mulder, P. Perlmutter, *J. Org. Chem.* **2009**, *74*, 2589–2591.

[86] S. Hirasawa, M. Cho, T. F. Brust, J. J. Roach, L. M. Bohn, R. A. Shenvi, *Bioorganic Med. Chem. Lett.* **2018**, *28*, 2770–2772.

[87] K. Puls, A. L. Olivé-Marti, S. Hongnak, D. Lamp, M. Spetea, G. Wolber, *J. Med. Chem.* **2024**, *67*, 13788–13801.

[88] X.-Y. Meng, H.-X. Zhang, M. Mezei, M. Cui, *Curr. Comput. Aided-Drug Des.* **2011**, *7*, 146–157.

[89] K. J. Frankowski, M. P. Hedrick, P. Gosalia, K. Li, S. Shi, D. Whipple, P. Ghosh, T. E. Prisinzano, F. J. Schoenen, …, J. Aubé, *ACS Chem. Neurosci.* **2012**, *3*, 221–236.

[90] L. Zhou, K. M. Lovell, K. J. Frankowski, S. R. Slauson, A. M. Phillips, J. M. Streicher, E. Stahl, C. L. Schmid, P. Hodde, …, L. M. Bohn, *J. Biol. Chem.* **2013**, *288*, 36703–36716.

[91] T. C. Beck, T. A. Dix, R. A. Norris, *Trends Endocrinol. Metab.* **2020**, *31*, 801–802.

[92] A. Gupta, I. Gomes, E. N. Bobeck, A. K. Fakira, N. P. Massaro, I. Sharma, A. Cavé, H. E. Hamm, J. Parello, …, S. H. Snyder, *Proc. Natl. Acad. Sci. U. S. A.* **2016**, *113*, 6041–6046.

[93] S. L. Shevick, S. M. Freeman, G. Tong, R. J. Russo, L. M. Bohn, R. A. Shenvi, *ACS Cent. Sci.* **2022**, *8*, 948–954.

[94] C. D. Strader, *J. Med. Chem.* **1996**, *39*, 1.

[95] D. Schaller, D. Šribar, T. Noonan, L. Deng, T. N. Nguyen, S. Pach, D. Machalz, M. Bermudez, G. Wolber, *Wiley Interdiscip. Rev. Comput. Mol. Sci.* **2020**, *10*, 1–20.

[96] M. I. H. Khan, B. J. Sawyer, N. S. Akins, H. V. Le, *Eur. J. Med. Chem.* **2022**, *243*, 114785.

[97] J. De Neve, T. M. A. Barlow, D. Tourwé, F. Bihel, F. Simonin, S. Ballet, *RSC Med. Chem.* **2021**, *12*, 828–870.

[98] C. Joseph, L. Renyu, L. Hoang V., *Transl. Perioper. Pain Med.* **2022**, *9*, 452–457.

[99] S. J. Hill, A. U. C. M. Brion, R. A. Shenvi, *Nat. Prod. Rep.* **2020**, *37*, 1478–1496.

[100] A. R. Lingham, H. M. Hügel, T. J. Rook, *Aust. J. Chem.* **2006**, *59*, 340–348.

[101] J. R. Scheerer, J. F. Lawrence, G. C. Wang, D. A. Evans, *J. Am. Chem. Soc.* **2007**, *129*, 8968–8969.

[102] I. Shiina, M. Kubota, R. Ibuka, *Tetrahedron Lett.* **2002**, *43*, 7535–7539.

[103] A. K. Cheung, R. Murelli, M. L. Snapper, *J. Org. Chem.* **2004**, *69*, 5712–5719.

[104] D. A. Lanfranchi, C. Bour, G. Hanquet, *European J. Org. Chem.* **2011**, 2818–2826.

[105] M. Nozawa, Y. Suka, T. Hoshi, T. Suzuki, H. Hagiwara, *Org. Lett.* **2008**, *10*, 1365–1368.

[106] H. Hagiwara, Y. Suka, T. Nojima, T. Hoshi, T. Suzuki, *Tetrahedron* **2009**, *65*, 4820–4825.

[107] G. M. Rubottom, M. A. Vazquez, D. R. Pelegrina, *Tetrahedron Lett.* **1974**, *15*, 4319–4322.

[108] O. Mitsunobu, M. Yamada, *Bull. Chem. Soc. Jpn.* **1967**, *40*, 2380–2382.

[109] S. Nahm, S. M. Weinreb, *Tetrahedron Lett.* **1981**, *22*, 3815–3818.

[110] H. Hagiwara, T. Nojima, Y. Suka, T. Hoshi, T. Suzuki, *Nat. Prod. Commun.* **2011**, *6*, 333–335.

[111] N. J. Line, A. C. Burns, S. C. Butler, J. Casbohm, C. J. Forsyth, *Chem. Eur. J.* **2016**, *22*, 17983–17986.

[112] M. P. Sibi, L. He, *Org. Lett.* **2004**, *6*, 1749–1752.

[113] J. Boukouvalas, Y. X. Cheng, J. Robichaud, *J. Org. Chem.* **1998**, *63*, 228–229.

[114] S. Zhou, C. R. Chen, H. M. Gau, *Org. Lett.* **2010**, *12*, 48–51.

[115] Q. Li, H. M. Gau, *Chirality* **2011**, *23*, 929–939.

[116] W. P. Griffith, S. V. Ley, G. P. Whitcombe, A. D. White, *J. Chem. Soc. Chem. Commun.* **1987**, 1625–1627.

[117] Y. Wang, P. Metz, *Org. Lett.* **2018**, *20*, 3418–3421.

[118] P. Zimdars, Y. Wang, P. Metz, *Chem. Eur. J.* **2021**, *27*, 7968–7973.

[119] L.-M. Mehl, Totalsynthese von Lingzhiol via radikalischer Cyclisierung sowie Studien zur Synthese der Kernstruktur von Salvinorin A. Doctoral Dissertation, University of Tübingen, **2018**.

[120] M. Halang, Studien zur Totalsynthese des *trans-neo*-Clerodans Salvinorin A. Doctoral Dissertation, University of Tübingen, **2023**.

[121] M. Halang, M. E. Maier, *ChemistryOpen* **2022**, *11*, 1–8.

[122] F. Barabé, P. Levesque, I. Korobkov, L. Barriault, *Org. Lett.* **2011**, *13*, 5580–5583.

[123] H. Tran, P. McGee, L. Barriault, *Chem. Eur. J.* **2023**, *13*, 287–288.

[124] H. M. Tran, Applications of Lewis Acid Gold(I) Catalysis in the Synthesis of Polycyclic Carbocycles and the Total Synthesis of (±)-Salvinorin A. Doctoral Dissertation, University of Ottowa, **2022**.

[125] T. Kocakaya, Erste Versuche der Platin(II)-katalysierten Carbonylylid-Alken-Cyclo-addition zur Darstellung von Oxabicyclo[3.2.1]-Systemen aus Alkeninonen. Master's Thesis, University of Tübingen, **2017**.

[126] H. Kusama, K. Ishida, H. Funami, N. Iwasawa, *Angew. Chem. Int. Ed.* **2008**, *47*, 4903–4905.

[127] K. Ishida, H. Kusama, N. Iwasawa, *J. Am. Chem. Soc.* **2010**, *132*, 8842–8843.

[128] H. Kusama, E. Watanabe, K. Ishida, N. Iwasawa, *Chem. Asian J.* **2011**, *6*, 2273–2277.

[129] P. Muller, *Pure Appl. Chem.* **1994**, *66*, 1077–1184.

[130] H. Kusama, A. Tazawa, K. Ishida, N. Iwasawa, *Chem. Asian J.* **2016**, *11*, 64–67.

[131] T. Groß, P. Metz, *Chem. Eur. J.* **2013**, *19*, 14787–14790.

[132] J. Kang, J. H. Lee, J. Lee, C. H. Oh, *Asian J. Org. Chem.* **2022**, *11*, 6–11.

[133] N. Liaba, J. Lee, C. H. Oh, *Asian J. Org. Chem.* **2023**, *12*, 3–10.

[134] N. Asao, K. Sato, Menggenbateer, Y. Yamamoto, *J. Org. Chem.* **2005**, *70*, 3682–3685.

[135] K. Molawi, N. Delpont, A. M. Echavarren, *Angew. Chem. Int. Ed.* **2010**, *49*, 3517–3519.

[136] Q. Zhou, X. Chen, M. Dawei, *Angew. Chem. Int. Ed.* **2010**, *49*, 3513–3516.

[137] C. H. M. Amijs, V. López-Carrillo, M. Raducan, P. Pérez-Galán, C. Ferrer, A. M. Echavarren, *J. Org. Chem.* **2008**, *73*, 7721–7730.

[138] V. Belting, N. Krause, *Org. Biomol. Chem.* **2009**, *7*, 1221.

[139] Y. Fukuda, H. Shiragami, K. Utimoto, H. Nozaki, *J. Org. Chem.* **1991**, *56*, 5816–5819.

[140] F. Fotakis, Untersuchung eines neuen Syntheseweges zu 2-Methyl-11-dodecen-6-in-3-on. Bachelor's Thesis, University of Tübingen, **2017**.

[141] S. Sewariya, S. Singh, N. Rana, Y. Kumar, R. Chandra, E. A. Anderson, *Eur. J. Med. Chem. Reports* **2023**, *7*, 100101.

[142] V. Navickas, D. B. Ushakov, M. E. Maier, M. Ströbele, H. J. Meyer, *Org. Lett.* **2010**, *12*, 3418–3421.

[143] T. Hanari, N. Shimada, Y. Kurosaki, N. Thrimurtulu, H. Nambu, M. Anada, S. Hashimoto, *Chem. Eur. J.* **2015**, *21*, 11671–11676.

[144] K. C. Nicolaou, Q. Kang, S. Y. Ng, D. Y.-K. Chen, *J. Am. Chem. Soc.* **2010**, *132*, 8219–8222.

[145] C. Reagan, G. Trevitt, K. Tchabanenko, *European J. Org. Chem.* **2019**, *2019*, 1027–1037.

[146] J. B. Hendrickson, J. S. Farina, *J. Org. Chem.* **1980**, *45*, 3359–3361.

[147] J. B. Hendrickson, J. S. Farina, *J. Org. Chem.* **1980**, *45*, 3361–3363.

[148] P. G. Sammes, L. J. Street, *J. Chem. Soc. Chem. Commun.* **1982**, 1056.

[149] P. G. Sammes, L. J. Street, P. Kirby, *J. Chem. Soc. Perkin Trans. 1* **1983**, 2729–2734.

[150] P. G. Sammes, L. J. Street, *J. Chem. Soc. Perkin Trans. 1* **1983**, 1261.

[151] P. G. Sammes, L. J. Street, *J. Chem. Soc., Chem. Commun.* **1983**, *05*, 666–668.

[152] S. M. Bromidge, P. G. Sammes, L. J. Street, *J. Chem. Soc., Perkin Trans. 1* **1985**, 1725–1730.

[153] P. G. Sammes, *Gazz. Chim. Ital.* **1986**, *116*, 109–114.

[154] P. G. Sammes, L. J. Street, R. J. Whitby, *J. Chem. Soc., Perkin Trans. 1* **1986**, 281–289.

[155] D. A. Archer, S. M. Bromidge, P. G. Sammes, *J. Chem. Soc., Perkin Trans. 1* **1988**, *348*, 3223–3228.

[156] P. G. Sammes, A. G. Swanson, R. J. Whitby, *J. Chem. Res.* **1988**, 162–163.

[157] P. A. Wender, H. Y. Lee, R. S. Wilhelm, P. D. Williams, *J. Am. Chem. Soc.* **1989**, *111*, 8954–8957.

[158] P. A. Wender, C. D. Jesudason, H. Nakahira, N. Tamura, A. L. Tebbe, Y. Ueno, S. U. V, R. V July, **1997**, *7863*, 12976–12977.

[159] P. A. Roethle, P. T. Hernandez, D. Trauner, *Org. Lett.* **2006**, *8*, 5901–5904.

[160] B. Tang, C. D. Bray, G. Pattenden, *Tetrahedron Lett.* **2006**, *47*, 6401–6404.

[161] Y. P. Zou, Z. L. Lai, M. W. Zhang, J. Peng, S. Ning, C. C. Li, *J. Am. Chem. Soc.* **2023**, *145*, 10998–11004.

[162] V. Singh, U. Murali Krishna, Vikrant, G. K. Trivedi, *Tetrahedron* **2008**, *64*, 3405–3428.

[163] K. E. O. Ylijoki, J. M. Stryker, *Chem. Rev.* **2013**, *113*, 2244–2266.

[164] H. Pellissier, *Adv. Synth. Catal.* **2018**, *360*, 1551–1583.

[165] L. P. Bejcek, R. P. Murelli, *Tetrahedron* **2018**, *74*, 2501–2521.

[166] P. A. Wender, F. C. Bi, N. Buschmann, F. Gosselin, C. Kan, J.-M. Kee, H. Ohmura, *Org. Lett.* **2006**, *8*, 5373–5376.

[167] P. A. Wender, N. Buschmann, N. B. Cardin, L. R. Jones, C. Kan, J.-M. Kee, J. A. Kowalski, K. E. Longcore, *Nat. Chem.* **2011**, *3*, 615–619.

[168] F. López, L. Castedo, J. L. Mascareñas, *Org. Lett.* **2002**, *4*, 3683–3685.

[169] S. N. Rokey, J. A. Simanis, C. M. Law, S. Pohani, S. Willens Behrends, J. J. Bulandr, G. M. Ferrence, J. R. Goodell, T. Andrew Mitchell, *Tetrahedron Lett.* **2020**, *61*, 152377.

[170] N. Z. Burns, M. R. Witten, E. N. Jacobsen, *J. Am. Chem. Soc.* **2011**, *133*, 14578–14581.

[171] M. R. Witten, E. N. Jacobsen, *Angew. Chem. Int. Ed.* **2014**, *53*, 5912–5916.

[172] H. A. Favre, W. H. Powell, *Nomenclature of Organic Chemistry*, The Royal Society Of Chemistry, London, **2013**.

[173] T. Arenz, M. Vostell, H. Frauenrath, *Synlett* **1991**, *1991*, 23–24.

[174] F. Gaviña, A. M. Costero, M. Rosario Andreu, S. V Luis, *J. Org. Chem.* **1988**, *53*, 6112–6113.

[175] C. Djerassi, *Chem. Rev.* **1948**, *43*, 271–317.

[176] C. B. Wendell, A Study of 2,3-Dimethylbutadiene-1,3 and Related Compounds. Master's Thesis, Massachusetts State College, **1933**.

[177] S. A. Rao, M. Periasamy, *Tetrahedron Lett.* **1988**, *29*, 4313–4314.

[178] A. Basheer, I. Marek, *Beilstein J. Org. Chem.* **2010**, *6*, 1–12.

[179] Y. Shimizu, M. Kanai, *Tetrahedron Lett.* **2014**, *55*, 3727–3737.

[180] D. S. Müller, I. Marek, *Chem. Soc. Rev.* **2016**, *45*, 4552–4566.

[181] S. L. Gwaltney, S. T. Sakata, K. J. Shea, *J. Org. Chem.* **1996**, *61*, 7438–7451.

[182] G. Cahiez, A. Alexakis, J. F. Normant, *Tetrahedron Lett.* **1978**, 3013–3014.

[183] H. Westmijze, H. Kleijn, J. Meijer, P. Vermeer, *Tetrahedron Lett.* **1977**, *18*, 869–872.

[184] J. F. Normant, A. Alexakis, *Synthesis* **1981**, *1981*, 841–870.

[185] H. O. House, D. S. Crumrine, A. Y. Teranishi, H. D. Olmstead, *J. Am. Chem. Soc.* **1973**, *95*, 3310–3324.

[186] M. Gardette, A. Alexakis, J. F. Normant, *Tetrahedron* **1985**, *41*, 5887–5899.

[187] H. Lin, L. A. Paquette, *Synth. Commun.* **1994**, *24*, 2503–2506.

[188] K. V. Baker, J. M. Brown, N. Hughes, A. J. Skarnulis, A. Sexton, *J. Org. Chem.* **1991**, *56*, 698–703.

[189] S. H. Bertz, E. H. Fairchild, I. Denissova, L. Barriault, Copper(I) Bromide, in *Encyclopedia of Reagents for Organic Synthesis*, John Wiley & Sons, Ltd., Chichester, **2004**, pp. 2–5.

[190] P. G. M. Wuts, *Synth. Commun.* **1981**, *11*, 139–140.

[191] H. O. House, C. Y. Chu, J. M. Wilkins, M. J. Umen, *J. Org. Chem.* **1975**, *40*, 1460–1469.

[192] A. B. Theis, C. A. Townsend, *Synth. Commun.* **1981**, *11*, 157–166.

[193] E. Defranq, T. Zesiger, R. Tabacchi, *Helv. Chim. Acta* **1993**, *76*, 425–430.

[194] H. Leicht, I. Göttker-Schnetmann, S. Mecking, *ACS Macro Lett.* **2016**, *5*, 777–780.

[195] S. Chandrasekhar, C. Narsihmulu, V. Jagadeshwar, S. Shameem Sultana, *Arkivoc* **2004**, *2005*, 92–98.

[196] K. Omura, D. Swern, *Tetrahedron* **1978**, *34*, 1651–1660.

[197] H. Gilman, F. K. Cartledge, *J. Organomet. Chem.* **1964**, *2*, 447–454.

[198] O. Achmatowicz, P. Bukowski, B. Szechner, Z. Zwierzchowska, A. Zamojski, *Tetrahedron* **1971**, *27*, 1973–1996.

[199] P. Merino, *Org. React.* **2015**, *87*, 1–256.

[200] A. K. Ghosh, M. Brindisi, *RSC Adv.* **2016**, *6*, 111564–111598.

[201] R. C. M. K. B. Sharpless, *J. Am. Chem. Soc.* **1973**, 6136–6137.

[202] T.-L. Ho, S. G. Sapp, *Synth. Commun.* **1983**, *13*, 207–211.

[203] Y. Gao, K. B. Sharpless, J. M. Klunder, R. M. Hanson, S. Y. Ko, H. Masamune, *J. Am. Chem. Soc.* **1987**, *109*, 5765–5780.

[204] M. Vandichel, K. Leus, P. Van Der Voort, M. Waroquier, V. Van Speybroeck, *J. Catal.* **2012**, *294*, 1–18.

[205] Y. Ji, T. Benkovics, G. L. Beutner, C. Sfouggatakis, M. D. Eastgate, D. G. Blackmond, *J. Org. Chem.* **2015**, *80*, 1696–1702.

[206] C. S. Foote, M. T. Wuesthoff, S. Wexler, I. G. Burstain, R. Denny, G. O. Schenck, K. H. Schulte-Elte, *Tetrahedron* **1967**, *23*, 2583–2599.

[207] F. Richter, C. Maichle-Mössmer, M. E. Maier, *Synlett* **2002**, 1097–1100.

[208] Y. Huang, A. J. Minnaard, B. L. Feringa, *Org. Biomol. Chem.* **2012**, *10*, 29–31.

[209] B. E. Bryant, W. C. Fernelius, D. H. Busch, R. C. Stoufer, W. Stratton, Vanadium(IV) Oxy(acetylacetonate), in *Inorganic Syntheses, Volume V* (Ed.: T. Moeller), McGraw-Hill Book Company, Inc., New York City, **1957**, pp. 113–116.

[210] W. L. F. Armarego, C. L. L. Chai, Purification of Organic Chemicals, in *Purification of Laboratory Chemicals*, Elsevier Inc., Amsterdam, **2009**, pp. 88–444.

[211] M. Kusakabe, Y. Kitano, Y. Kobayashi, F. Sato, *J. Org. Chem.* **1989**, *54*, 2085–2091.

[212] J. G. Hill, B. E. Rossiter, K. B. Sharpless, *J. Org. Chem.* **1983**, *48*, 3607–3608.

[213] F. Vöhringer, Optimierung der Syntheseroute eines Tricyclischen Ketonitril-Intermediats in einer Totalsynthese des Salvinorin A. Bachelor's Thesis, University of Tübingen, **2020**.

[214] O. Diels, K. Alder, *Justus Liebigs Ann. Chem.* **1928**, *460*, 98–122.

[215] K. C. Nicolaou, S. A. Snyder, T. Montagnon, G. Vassilikogiannakis, *Angew. Chem. Int. Ed.* **2002**, *41*, 1668–1698.

[216] E. L. Woodall, J. A. Simanis, C. G. Hamaker, J. R. Goodell, T. A. Mitchell, *Org. Lett.* **2013**, *15*, 3270–3273.

[217] S. Singh, J. P. Grabowski, S. Pohani, C. F. Apuzzo, D. C. Platt, M. A. Jones, T. A. Mitchell, *Molecules* **2020**, *25*, 5461.

[218] R. H. Kaufman, C. M. Law, J. A. Simanis, E. L. Woodall, C. R. Zwick, H. B. Wedler, P. Wendelboe, C. G. Hamaker, J. R. Goodell, …, T. A. Mitchell, *J. Org. Chem.* **2018**, *83*, 9818–9838.

[219] P. Würtz, P. Permi, N. C. Nielsen, O. W. Sørensen, *J. Magn. Reson.* **2008**, *194*, 89–98.

[220] H. Suga, T. Iwai, M. Shimizu, K. Takahashi, Y. Toda, *Chem. Commun.* **2018**, *54*, 1109–1112.

[221] Y. Toda, M. Shimizu, T. Iwai, H. Suga, *Adv. Synth. Catal.* **2018**, *360*, 2377–2381.

[222] K. Utimoto, Y. Wakabayashi, T. Horiie, M. Inoue, Y. Shishiyama, M. Obayashi, H. Nozaki, *Tetrahedron* **1983**, *39*, 967–973.

[223] I. I. Gerus, I. S. Kruchok, V. P. Kukhar, *Tetrahedron Lett.* **1999**, *40*, 5923–5926.

[224] N. Gommermann, P. Knochel, *Org. Synth.* **2009**, 1–10.

[225] T. Nishikawa, M. Yoshikai, K. Obi, M. Isobe, *Tetrahedron Lett.* **1994**, *35*, 7997–8000.

[226] H.-Y. Li, H. Sun, S. G. DiMagno, Tetrabutylammonium Fluoride, in *Encyclopedia of Reagents for Organic Synthesis*, John Wiley & Sons, Ltd., Chichester, **2007**, pp. 459–460.

[227] W. Nagata, M. Yoshioka, *Org. React.* **2005**, 255–476.

[228] C. Agami, J. Levisalles, C. Puchot, *J. Org. Chem.* **1982**, *47*, 3561–3563.

[229] E. Keinan, N. Greenspoon, *Tetrahedron Lett.* **1985**, *26*, 1353–1356.

[230] E. Keinan, N. Greenspoon, *J. Am. Chem. Soc.* **1986**, *108*, 7314–7325.

[231] M. Chandler, Diphenylsilane-Tetrakis(triphenylphosphine)palladium(0)-Zinc Chloride, in *Encyclopedia of Reagents for Organic Synthesis*, John Wiley & Sons, Ltd., Chichester, **2001**, pp. 3–4.

[232] J. L. Hubbard, G. Dake, Lithium Tri-sec-butylborohydride, in *Encyclopedia of Reagents for Organic Synthesis*, John Wiley & Sons, Ltd., Chichester, **2012**, pp. 1–6.

[233] M. T. Reetz, H. Haning, *Tetrahedron Lett.* **1993**, *34*, 7395–7398.

[234] P. Angers, P. Canonne, *Tetrahedron Lett.* **1994**, *35*, 367–370.

[235] G. Stork, P. F. Hudrlik, *J. Am. Chem. Soc.* **1968**, *90*, 4462–4464.

[236] M. Chini, P. Crotti, L. Favero, M. Pineschi, *Tetrahedron Lett.* **1991**, *32*, 7583–7586.

[237] P. Crotti, V. Di Bussolo, L. Favero, M. Pineschi, M. Pasero, *J. Org. Chem.* **1996**, *61*, 9548–9552.

[238] J. Ipaktschi, A. Heydari, *Chem. Ber.* **1993**, *126*, 1905–1912.

[239] I. Kuwajima, E. Nakamura, M. Shimizu, *J. Am. Chem. Soc.* **1982**, *104*, 1025–1030.

[240] I. Kuwajima, E. Nakamura, *Acc. Chem. Res.* **1985**, *18*, 181–187.

[241] C. Defieber, J. T. Mohr, G. A. Grabovyi, B. M. Stoltz, *Synth.* **2018**, *50*, 4359–4368.

[242] L. N. Mander, S. P. Sethi, *Tetrahedron Lett.* **1983**, *24*, 5425–5428.

[243] J. T. Mohr, D. C. Behenna, A. M. Harned, B. M. Stoltz, *Angew. Chem. Int. Ed.* **2005**, *44*, 6924–6927.

[244] B. M. Trost, J. Xu, *J. Org. Chem.* **2007**, *72*, 9372–9375.

[245] S. Hanessian, A. M. Griffin, M. J. Rozema, *Bioorg. Med. Chem. Lett.* **1997**, *7*, 1857–1862.

[246] C. M. Yamada, D. J. Dellinger, M. H. Caruthers, *J. Am. Chem. Soc.* **2006**, *128*, 5251–5261.

[247] P. A. Jacobi, H. G. Selnick, *J. Org. Chem.* **1990**, *55*, 202–209.

[248] W. He, J. Huang, X. Sun, A. J. Frontier, *J. Am. Chem. Soc.* **2008**, *130*, 300–308.

[249] B. M. Trost, M. L. Crawley, *Chem. Rev.* **2003**, *103*, 2921–2943.

[250] B. M. Trost, *Tetrahedron* **2015**, *71*, 5708–5733.

[251] O. Pàmies, J. Margalef, S. Cañellas, J. James, E. Judge, P. J. Guiry, C. Moberg, J. E. Bäckvall, A. Pfaltz, …, M. Diéguez, *Chem. Rev.* **2021**, *121*, 4373–4505.

[252] L. Junk, U. Kazmaier, *ChemistryOpen* **2020**, *9*, 929–952.

[253] B. M. Trost, J. Xu, T. Schmidt, *J. Am. Chem. Soc.* **2009**, *131*, 18343–18357.

[254] A. N. Marziale, D. C. Duquette, R. A. Craig, K. E. Kim, M. Liniger, Y. Numajiri, B. M. Stoltz, *Adv. Synth. Catal.* **2015**, *357*, 2238–2245.

[255] R. A. Craig, S. A. Loskot, J. T. Mohr, D. C. Behenna, A. M. Harned, B. M. Stoltz, *Org. Lett.* **2015**, *17*, 5160–5163.

[256] J. Tsuji, I. Minami, I. Shimizu, *Tetrahedron Lett.* **1983**, *24*, 1793–1796.

[257] D. C. Behenna, B. M. Stoltz, *J. Am. Chem. Soc.* **2004**, *126*, 15044–15045.

[258] J. T. Mohr, D. C. Behenna, A. M. Harned, B. M. Stoltz, *Angew. Chem. Int. Ed.* **2005**, *44*, 6924–6927.

[259] I. Shimizu, T. Yamada, J. Tsuji, *Tetrahedron Lett.* **1980**, *21*, 3199–3202.

[260] T. Tsuda, Y. Chujo, S. Nishi, K. Tawara, T. Saegusa, *J. Am. Chem. Soc.* **1980**, *102*, 6381–6384.

[261] O. Geiseler, M. Müller, J. Podlech, *Tetrahedron* **2013**, *69*, 3683–3689.

[262] Z. X. Zhang, S. C. Chen, L. Jiao, *Angew. Chem. Int. Ed.* **2016**, *55*, 8090–8094.

[263] S. J. Danishefsky, J. J. Masters, W. B. Young, J. T. Link, L. B. Snyder, T. V. Magee, D. K. Jung, R. C. A. Isaacs, W. G. Bornmann, …, M. J. Di Grandi, *J. Am. Chem. Soc.* **1996**, *118*, 2843–2859.

[264] J. H. Rigby, B. Bazin, J. H. Meyer, F. Mohammadi, *Org. Lett.* **2002**, *4*, 799–801.

[265] R. Pappo, D. S. Allen, Jr., R. U. Lemieux, W. S. Johnson, *J. Org. Chem.* **1956**, *21*, 478–479.

[266] W. Yu, Y. Mei, Y. Kang, Z. Hua, Z. Jin, *Org. Lett.* **2004**, *6*, 3217–3219.

[267] K. C. Nicolaou, V. A. Adsool, C. R. H. H. Hale, *Org. Lett.* **2010**, *12*, 1552–1555.

[268] J. Richers, A. Pöthig, E. Herdtweck, C. Sippel, F. Hausch, K. Tiefenbacher, *Chem. Eur. J.* **2017**, *23*, 3178–3183.

[269] Z. K. Yang, Q. H. Chen, F. P. Wang, *Tetrahedron* **2011**, *67*, 4192–4195.

[270] D. A. Carcache, Y. S. Cho, Z. Hua, Y. Tian, Y. M. Li, S. J. Danishefsky, *J. Am. Chem. Soc.* **2006**, *128*, 1016–1022.

[271] A. C. Williams, N. Camp, Product Class 4: Benzopyranones and Benzopyranthiones, in *Science of Synhesis, 14: Category 2, Hetarenes and Related Ring Systems* (Ed.: E. J. Thomas), Georg Thieme Verlag, Stuttgart, **2003**, pp. 347–638.

[272] G. Lin, M. Zhong, *Tetrahedron Lett.* **1996**, *37*, 3015–3018.

[273] D. M. X. Donnelly, D. J. Molloy, J. P. Reilly, J. P. Finet, *J. Chem. Soc. Perkin Trans. 1* **1995**, 2531–2534.

[274] W. C. Still, *J. Org. Chem.* **1976**, *41*, 3063–3064.

[275] M. D. Paredes, R. Alonso, *J. Org. Chem.* **2000**, *65*, 2292–2304.

[276] P. Cuadrado, A. M. Gonzalez, B. Gonzalez, F. J. Pulido, *Synth. Commun.* **1989**, *19*, 275–283.

[277] I. Fleming, R. S. Roberts, S. C. Smith, *J. Chem. Soc. Perkin Trans. 1* **1998**, 1209–1214.

[278] I. Fleming, T. W. Newton, F. Roessler, *J. Chem. Soc. Perkin Trans. 1* **1981**, 2527–2532.

[279] H. C. Brown, E. J. Mead, B. C. Subba Rao, *J. Am. Chem. Soc.* **1955**, *77*, 6209–6213.

[280] G. P. Moss, *Pure Appl. Chem.* **1996**, *68*, 2193–2222.

[281] K. Maruoka, T. Itoh, H. Yamamoto, *J. Am. Chem. Soc.* **1985**, *107*, 4573–4576.

[282] K. Maruoka, M. Sakurai, H. Yamamoto, *Tetrahedron Lett.* **1985**, *26*, 3853–3856.

[283] K. Ohmatsu, K. Maruoka, Bis[2,6-bis(1,1-dimethylethyl)-4-methylphenolato]methyl-aluminum, in *Encyclopedia of Reagents for Organic Synthesis*, John Wiley & Sons, Ltd., Chichester, **2008**, pp. 4–6.

[284] D. B. Ushakov, V. Navickas, M. Ströbele, C. Maichle-Mössmer, F. Sasse, M. E. Maier, *Org. Lett.* **2011**, *13*, 2090–2093.

[285] G.-J. Wu, Y.-H. Zhang, D.-X. Tan, F.-S. Han, *Nat. Commun.* **2018**, *9*, 2148.

[286] J. A. Dodge, J. S. Nissen, M. Presnell, *Org. Synth.* **1996**, *73*, 110.

[287] Y. Torisawa, H. Okabe, S. Ikegami, *Chem. Lett.* **1984**, *13*, 1555–1556.

[288] J. W. Huffman, R. C. Desai, *Synth. Commun.* **1983**, *13*, 553–557.

[289] T. Shimizu, S. Hiranuma, T. Nakata, *Tetrahedron Lett.* **1996**, *37*, 6145–6148.

[290] S. V. Pronin, C. A. Reiher, R. A. Shenvi, *Nature* **2013**, *501*, 195–199.

[291] J. K. Groves, *Chem. Soc. Rev.* **1972**, *1*, 73–97.

[292] J. K. Groves, N. Jones, *J. Chem. Soc. C* **1969**, 608.

[293] M. Yamashita, N. Ohta, T. Shimizu, K. Matsumoto, Y. Matsuura, I. Kawasaki, T. Tanaka, N. Maezaki, S. Ohta, *J. Org. Chem.* **2003**, *68*, 1216–1224.

[294] I. Hachiya, M. Moriwaki, S. Kobayashi, *Bull. Chem. Soc. Jpn.* **1995**, *68*, 2053–2060.

[295] A. Kawada, S. Mitamura, S. Kobayashi, *Chem. Commun.* **1996**, *02*, 183–184.

[296] Y. Di, T. Yoshimura, S. I. Naito, Y. Kimura, T. Kondo, *ACS Omega* **2018**, *3*, 18885–18894.

[297] H. Feng, I. K. Kavrakova, D. A. Pratt, J. Tellinghuisen, N. A. Porter, *J. Org. Chem.* **2002**, *67*, 6050–6054.

[298] C. L. Mero, N. A. Porter, *J. Am. Chem. Soc.* **1999**, *121*, 5155–5160.

[299] K. Ishihara, M. Kubota, H. Kurihara, H. Yamamoto, *J. Am. Chem. Soc.* **1995**, *117*, 4413–4414.

[300] Y. B. Kang, Y. Tang, X. L. Sun, *Org. Biomol. Chem.* **2006**, *4*, 299–301.

[301] D. A. Evans, K. R. Fandrick, H.-J. Song, K. A. Scheidt, R. Xu, *J. Am. Chem. Soc.* **2007**, *129*, 10029–10041.

[302] F. F. Fleming, Q. Wang, O. W. Steward, *J. Org. Chem.* **2001**, *66*, 2171–2174.

[303] J. E. Baldwin, A. V. W. Mayweg, G. J. Pritchard, R. M. Adlington, *Tetrahedron Lett.* **2003**, *44*, 4543–4545.

[304] B. M. Trost, B. R. Taft, J. S. Tracy, C. E. Stivala, *Org. Lett.* **2021**, *23*, 4981–4985.

[305] M. Majewski, D. M. Gleave, *J. Organomet. Chem.* **1994**, *470*, 1–16.

[306] A. X. Gao, S. B. Thomas, S. A. Snyder, Pinacol and Semipinacol Rearrangements in Total Synthesis, in *Molecular Rearrangements in Organic Synthesis* (Ed.: C. M. Rojas), John Wiley & Sons, Inc., Hoboken, **2016**, pp. 1–34.

[307] Z. L. Song, C. A. Fan, Y. Q. Tu, *Chem. Rev.* **2011**, *111*, 7523–7556.

[308] J. S. Kingsbury, E. J. Corey, *J. Am. Chem. Soc.* **2005**, *127*, 13813–13815.

[309] C. H. Heathcock, E. G. DelMar, S. L. Graham, *J. Am. Chem. Soc.* **1982**, *104*, 1907–1917.

[310] M. Betou, L. Male, J. W. Steed, R. S. Grainger, *Chem. Eur. J.* **2014**, *20*, 6505–6517.

[311] A. Baroudi, A. Karton, *Org. Chem. Front.* **2019**, *6*, 725–731.

[312] L. A. Paquette, J. E. Hofferberth, The α-Hydroxy Ketone (α-Ketol) and Related Rearrangements, in *Organic Reactions*, John Wiley & Sons, Inc., Hoboken, **2003**, pp. 477–567.

[313] L. A. Paquette, S. W. Elmore, K. D. Combrink, E. R. Hickey, R. D. Rogers, *Helv. Chim. Acta* **1992**, *75*, 1755–1771.

[314] H. J. M. Gijsen, J. B. P. A. Wijnberg, C. van Ravenswaay, A. de Groot, *Tetrahedron* **1994**, *50*, 4733–4744.

[315] N. Zhao, S. Yin, S. Xie, H. Yan, P. Ren, G. Chen, F. Chen, J. Xu, *Angew. Chem. Int. Ed.* **2018**, *57*, 3386–3390.

[316] M. Tamiya, N. Isaka, T. Kitazawa, A. Hasegawa, K. Ishizawa, M. Ikeda, S. Kawada, M. Ishiguro, *Bull. Chem. Soc. Jpn.* **2019**, *92*, 1474–1494.

[317] E. Jahn, J. Smrček, R. Pohl, I. Císařová, P. G. Jones, U. Jahn, *European J. Org. Chem.* **2015**, *2015*, 7785–7798.

[318] L. E. Overman, R. J. McCready, *Tetrahedron Lett.* **1982**, *23*, 2355–2358.

[319] A. Krasovskiy, P. Knochel, *Angew. Chem. Int. Ed.* **2004**, *43*, 3333–3336.

[320] R. Li-Yuan Bao, R. Zhao, L. Shi, *Chem. Commun.* **2015**, *51*, 6884–6900.

[321] S. Krieck, P. Schüler, J. M. Peschel, M. Westerhausen, *Synth.* **2019**, *51*, 1115–1122.

[322] Z. Peng, J. A. Ragan, R. Colon-Cruz, B. G. Conway, E. M. Cordi, K. Leeman, L. J. Letendre, L. J. Ping, J. E. Sieser, …, S. Taylor, *Org. Process Res. Dev.* **2014**, *18*, 36–44.

[323] T.-L. Ho, *Synth. Commun.* **1979**, *9*, 665–668.

[324] J. A. Profitt, D. S. Watt, E. J. Corey, *J. Org. Chem.* **1975**, *40*, 127–128.

[325] T. Hudlicky, G. Sinai-Zingde, M. G. Natchus, *Tetrahedron Lett.* **1987**, *28*, 5287–5290.

[326] M. Bidar, G. Tokmajyan, F. Nasiri, *Chem. Nat. Compd.* **2013**, *48*, 942–945.

[327] A. C. Wright, Y. E. Du, B. M. Stoltz, *J. Org. Chem.* **2019**, *84*, 11258–11260.

[328] P. Girard, J. L. Namy, B. Kagan, *J. Am. Chem. Soc.* **1980**, *102*, 2693–2698.

[329] K. C. Nicolaou, S. P. Ellery, J. S. Chen, *Angew. Chem. Int. Ed.* **2009**, *48*, 7140–7165.

[330] M. M. Heravi, A. Nazari, *RSC Adv.* **2022**, *12*, 9944–9994.

[331] B. D. J. Procter, R. A. Flowers, T. Skrydstrup, *Organic Synthesis Using Samarium Diiodide: A Practical Guide*, Royal Society Of Chemistry, London, **2009**.

[332] M. Szostak, M. Spain, D. J. Procter, *J. Org. Chem.* **2012**, *77*, 3049–3059.

[333] D. V. Sadasivam, K. A. Choquette, R. A. Flowers, *J. Vis. Exp.* **2013**, e4323, doi:10.3791/4323.

[334] G. A. Molander, C. Kenny, *J. Org. Chem.* **1991**, *56*, 1439–1445.

[335] P. Schröder, J. O. Bauer, C. Strohmann, K. Kumar, H. Waldmann, *J. Org. Chem.* **2016**, *81*, 10242–10255.

[336] D. V. Sadasivam, J. A. Teprovich, D. J. Procter, R. A. Flowers, *Org. Lett.* **2010**, *12*, 4140–4143.

[337] T. K. Hutton, K. W. Muir, D. J. Procter, *Org. Lett.* **2003**, *5*, 4811–4814.

[338] G. A. Molander, G. Hahn, *J. Org. Chem.* **1986**, *51*, 1135–1138.

[339] G. A. Molander, Reductions with Samarium(II) Iodide, in *Organic Reactions (Vol 46)* (Ed.: L. A. Paquette), John Wiley & Sons, Inc., Hoboken, **1994**, pp. 211–367.

[340] J. Inanaga, M. Yamaguchi, K. Kusuda, *Tetrahedron Lett.* **1989**, *30*, 2945–2948.

[341] R. A. Holton, A. D. Williams, *J. Org. Chem.* **1988**, *53*, 5981–5983.

[342] R. J. Linderman, K. P. Cusack, W. R. Kwochka, *Tetrahedron Lett.* **1994**, *35*, 1477–1480.

[343] R. A. Holton, C. Somoza, K.-B. Chai, *Tetrahedron Lett.* **1994**, *35*, 1665–1668.

[344] J. D. White, T. C. Somers, *J. Am. Chem. Soc.* **1987**, *109*, 4424–4426.

[345] R. U. Batwal, N. P. Argade, *Org. Biomol. Chem.* **2015**, *13*, 11331–11340.

[346] G. I. Georg, Z. S. Cheruvallath, *J. Org. Chem.* **1994**, *59*, 4015–4018.

[347] D. S. Hsu, T. Y. Hwang, *European J. Org. Chem.* **2018**, *2018*, 4689–4695.

[348] M. Qian, E. B. Engler-Chiurazzi, S. E. Lewis, N. P. Rath, J. W. Simpkins, D. F. Covey, *Org. Biomol. Chem.* **2016**, *14*, 9790–9805.

[349] C. Wang, N. P. Rath, D. F. Covey, *Tetrahedron* **2007**, *63*, 7977–7984.

[350] E. Hasegawa, D. P. Curran, *J. Org. Chem.* **1993**, *58*, 5008–5010.

[351] Y. Kamochi, T. Kudo, *Chem. Lett.* **1993**, *22*, 1495–1498.

[352] M. Szostak, M. Spain, D. J. Procter, *Chem. Commun.* **2011**, *47*, 10254–10256.

[353] M. Szostak, B. Sautier, M. Spain, D. J. Procter, *Org. Lett.* **2014**, *16*, 1092–1095.

[354] R. Mouselmani, Reduction of Organic Functional Groups Using Hypophosphites. Doctoral Dissertation, Université de Lyon; École Doctorale des Sciences et de Technologie (Beyrouth), **2018**.

[355] F. L. Duecker, R. C. Heinze, S. Steinhauer, P. Heretsch, *Chem. Eur. J.* **2020**, *26*, 9971–9981.

[356] T. Shono, N. Kise, T. Fujimoto, N. Tominaga, H. Morita, *J. Org. Chem.* **1992**, *57*, 7175–7187.

[357] Z. Li, F. C. F. Ip, N. Y. Ip, R. Tong, *Chem. Eur. J.* **2015**, *21*, 11152–11157.

[358] A. J. Fry, Reduction of α-Substituted Carbonyl Compounds CXCO to Carbonyl Compounds CHCO, in *Comprehensive Organic Synthesis: Selectivity, Strategy & Efficiency in Modern Organic Chemistry* (Eds.: B. M. Trost, I. Fleming), Elsevier Ltd., Oxford, **1991**, pp. 983–997.

[359] T. Inokuchi, H. Kawafuchi, S. Torii, *Chem. Lett.* **1992**, *21*, 1895–1896.

[360] M. M. Pichon, D. Hazelard, P. Compain, *European J. Org. Chem.* **2019**, *2019*, 6320–6332.

[361] X. Xu, L. Yan, Z.-K. Zhang, B. Lu, Z. Guo, M. Chen, Z.-Y. Cao, *Molecules* **2022**, *27*, 4675.

[362] G. Lee, I. Youn, E. Choi, H. Lee, G. Yon, H. Yang, C. Pak, *Curr. Org. Chem.* **2005**, *8*, 1263–1287.

[363] F. T. Luo, A. Jeevanandam, *Tetrahedron Lett.* **1998**, *39*, 9455–9456.

[364] A. M. Kelley, J. A. Frost, T. M. Baber, K. C. Youngblood, E. Michishita, S. A. Bain, T. Caleb Lykins, K. S. Petersen, *Tetrahedron Lett.* **2022**, *88*, 153573.

[365] G. Jayachitra, N. Yasmeen, K. Srinivasa Rao, S. L. Ralte, R. Srinivasan, A. K. Singh, *Synth. Commun.* **2003**, *33*, 3461–3466.

[366] H. Kuroiwa, S. Suzuki, K. Irie, C. Tsukano, *J. Am. Chem. Soc.* **2023**, *145*, 14587–14591.

[367] T. Satoh, K. Nanba, S. Suzuki, *Chem. Pharm. Bull.* **1971**, *19*, 817–820.

[368] B. L. Yin, C. B. Cai, J. Q. Lai, Z. R. Zhang, L. Huang, L. W. Xu, H. F. Jiang, *Adv. Synth. Catal.* **2011**, *353*, 3319–3324.

[369] S. Cacchi, E. Morera, G. Ortar, *Tetrahedron Lett.* **1985**, *26*, 1109–1112.

[370] S. Cacchi, P. G. Ciattini, E. Morera, G. Ortar, *Tetrahedron Lett.* **1986**, *27*, 5541–5544.

[371] S. Cacchi, P. G. Ciattini, E. Morera, G. Ortar, *Tetrahedron Lett.* **1986**, *27*, 3931–3934.

[372] W. L. F. Armarego, Purification of Inorganic and Metal-Organic Chemicals, in *Purification of Laboratory Chemicals*, Elsevier Inc., Amsterdam, **2017**, pp. 635–770.

[373] W. C. Still, M. Kahn, A. Mitra, *J. Org. Chem.* **1978**, *43*, 2923–2925.

[374] T. Rundlöf, M. Mathiasson, S. Bekiroglu, B. Hakkarainen, T. Bowden, T. Arvidsson, *J. Pharm. Biomed. Anal.* **2010**, *52*, 645–651.

[375] S. K. Bharti, R. Roy, *Trends Anal. Chem.* **2012**, *35*, 5–26.

[376] L. J. Farrugia, *J. Appl. Crystallogr.* **1999**, *32*, 837–838.

[377] G. M. Sheldrick, *Acta Crystallogr. Sect. A, Found. Crystallogr.* **2008**, *64*, 112–122.

[378] C. B. Hübschle, G. M. Sheldrick, B. Dittrich, *J. Appl. Crystallogr.* **2011**, *44*, 1281–1284.

[379] L. Krause, R. Herbst-Irmer, G. M. Sheldrick, D. Stalke, *J. Appl. Crystallogr.* **2015**, *48*, 3–10.

[380] L. J. Farrugia, *J. Appl. Crystallogr.* **2012**, *45*, 849–854.

[381] A. Dahlén, G. Hilmersson, *Eur. J. Inorg. Chem.* **2004**, 3020–3024.

[382] X. H. Wang, F. H. Yang, C. K. Zhao, L. Gao, C. Li, *Med. Chem. Res.* **2018**, *27*, 406–411.

[383] J. Šrogl, M. Janda, I. Stibor, *Collect. Czechoslov. Chem. Commun.* **1970**, *35*, 3478–3480.

[384] Y. L. Gol'dfarb, M. A. Marakatkina, L. I. Belen'kii, *Chem. Hetereocyclic Compd.* **1970**, *6*, 129–130.

[385] R. Imwinkelried, D. Seebach, *Org. Synth.* **1989**, *67*, 180.

[386] S. H. Kim, H. S. Lee, B. R. Park, J. N. Kim, *Bull. Korean Chem. Soc.* **2011**, *32*, 1725–1728.

CHAPTER 6: APPENDIX

6.1 X-RAY STRUCTURE ANALYSIS

Table 10. Data of crystal structure determinations (1/2). Continuation on the next page.

	Hydroxynitrile **54**	Tetracyclic ether **86-H**	Dioxolane **119.b**	Acyloin **111**
Empirical formula	$C_{17}H_{23}NO_2$	$C_{34}H_{50}Cl_2O_2$	$C_{18}H_{23}NO_4$	$C_{17}H_{21}NO_2$
***M* [g/mol]**	273.36	561.64	317.37	271.35
λ [Å]	0.71073	0.71073	0.71073	0.71073
***T* [K]**	120(2)	120(2)	100(2)	100(2)
Crystal system	orthorhombic	orthorhombic	monoclinic	monoclinic
Space group	*P*bca	$P2_12_12_1$	$P2_1$/n	*C*c
Z	8	2	4	4
***a* [Å]**	13.4977(2)	8.6015(2)	9.45210(10)	12.6586(3)
***b* [Å]**	11.1753(2)	11.8835(3)	10.4145(2)	8.2951(2)
***c* [Å]**	20.0383(3)	14.1534(3)	16.5212(3)	13.7473(3)
α [°]	90	90	90	90
β [°]	90	90	91.4660(10)	91.297(2)
γ [°]	90	90	90	90
***V* [Å^3]**	3022.59(8)	1446.70(6)	1625.80(5)	1443.16(6)
***Dc* [g/cm^3]**	1.201	1.289	1.297	1.249
μ [mm^{-1}]	0.078	0.255	0.091	0.081
F(000)	1184	608	680	584
Crystal size [mm]	0.37×0.33×0.30	0.466×0.340×0.319	0.34×0.29×0.26	0.33×0.29×0.27
θ range [°]	2033 – 28298	2238 – 30513	3140 – 27120	3219 – 28349
Limiting indices	−18 ≤ h ≤ 17	−12 ≤ h ≤ 12	−11 ≤ h ≤ 11	−16 ≤ h ≤ 16
	−14 ≤ k ≤ 14	−16 ≤ k ≤ 16	−13 ≤ k ≤ 13	−11 ≤ k ≤ 9
	−24 ≤ l ≤ 26	−20 ≤ l ≤ 20	−20 ≤ l ≤ 21	−15 ≤ l ≤ 18
Reflections collected	50845	49816	25574	6224
Independent reflexes	3758	4408	3561	2646
R_{int}	0.0200	0.0242	0.0312	0.0226
Completeness [%]	100	100	99.7	99.8
Absorption correction	multi-scan	?	multi-scan	multi-scan
Transmission (max., min.)	0.7457, 0.7111	0.7461, 0.7269	0.7455, 0.7176	0.7457, 0.6978
Parameters/restraints	195/0	177/0	210/0	185/2
$R1$, w$R2$ [$I > 2\sigma(I)$]	0.0461, 0.1202	0.0237, 0.0673	0.0354, 0.0941	0.0298, 0.0784
$R1$, w$R2$ (all data)	0.0514, 0.1254	0.0243, 0.0678	0.0388, 0.0973	0.0309, 0.0796
Goof on F^2	1.070	1.087	1.046	1.034
Peak/hole [$e \cdot$ Å^{-3}]	0.473, −0.282	0.288, −0.174	0.360, −0.220	0.279, −0.170

Table 10. Data of crystal structure determinations (2/2).

	Furyl ketone 6-*epi*-**128**	Lactone **38**	Polycyclic lactone **133**
Empirical formula	$C_{20}H_{21}NO_4$	$C_{20}H_{22}O_5$	$C_{20}H_{22}O_5$
***M* [g/mol]**	339.38	342.37	342.37
***λ* [Å]**	0.71073	0.71073	0.71073
***T* [K]**	293(2)	110(2)	100(2)
Crystal system	triclinic	monoclinic	orthorhombic
Space group	$P\bar{1}$	$P2_1/c$	$P2_12_12_1$
Z	2	4	4
***a* [Å]**	7.0504(2)	13.6629(7)	8.40510(10)
***b* [Å]**	8.6213(3)	6.7532(4)	10.7599(2)
***c* [Å]**	13.9901(4)	18.2978(9)	17.9003(3)
***α* [°]**	88.931(2)	90	90
***β* [°]**	80.5400(10)	92.503(2)	90
***γ* [°]**	77.315(2)	90	90
***V* [Å³]**	818.20(4)	1686.70(16)	1618.87(4)
***Dc* [g/cm³]**	1.378	1.348	1.405
***μ* [mm⁻¹]**	0.096	0.096	0.100
F(000)	360	728	728
Crystal size [mm]	0.32×0.27×0.26	0.31×0.28×0.26	0.32×0.27×0.26
***θ* range [°]**	3002 – 27992	3216 – 25350	2960 – 27707
Limiting indices	$-9 \le h \le 9$	$-16 \le h \le 14$	$-11 \le h \le 10$
	$-11 \le k \le 11$	$-7 \le k \le 8$	$-14 \le k \le 14$
	$-18 \le l \le 18$	$-22 \le l \le 22$	$-22 \le l \le 23$
Reflections collected	19395	13167	20208
Independent reflexes	3928	3041	3780
R_{int}	0.0247	0.0240	0.0396
Completeness [%]	99.6	98.5	99.5
Absorption correction	multi-scan	multi-scan	multi-scan
Transmission (max., min.)	0.7456, 0.7133	0.7459, 0.7013	0.7456, 0.7133
Parameters/restraints	226/180	228/0	230/0
***R*1, w*R*2 [$I > 2\sigma(I)$]**	0.0432, 0.1098	0.0349, 0866	0.0314, 0.0817
***R*1, w*R*2 (all data)**	0.0496, 0.1152	0.0400, 0.0903	0.0335, 0.0836
Goof on F²	1.040	1.030	1.039
Peak/hole [$e \cdot$ Å⁻³]	0.542, –0.403	0.269, –0.223	0.321, –0.179

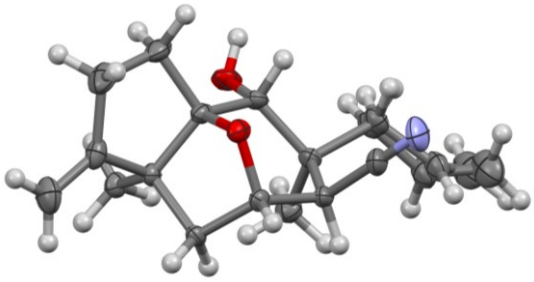

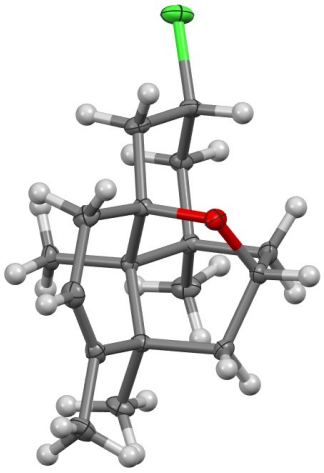

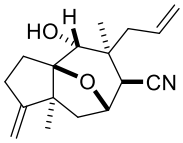

hydroxynitrile **54**

(*cf.* **Figure 22** on page **102**)

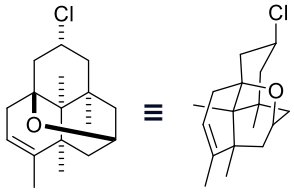

tetracyclic ether **86-H**

(*cf.* **Figure 23** on page **109**)

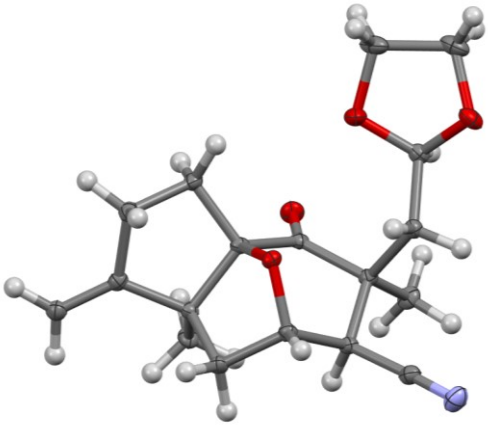

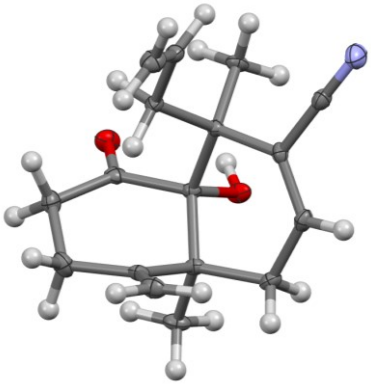

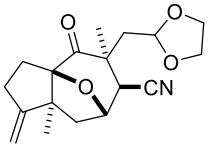

dioxolane **119.b**

(*cf.* **Figure 27** on page **141**)

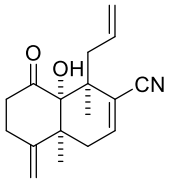

[6,6]-fused acyloin **111**

(*cf.* **Figure 25** on page **132**)

Figure 36. X-Ray crystal structures of hydroxynitrile **54**, dioxolane **119.b**, tetracyclic ether **86-H**, and [6,6]-fused acyloin **111**. The processed structures can be seen in the referred figures.

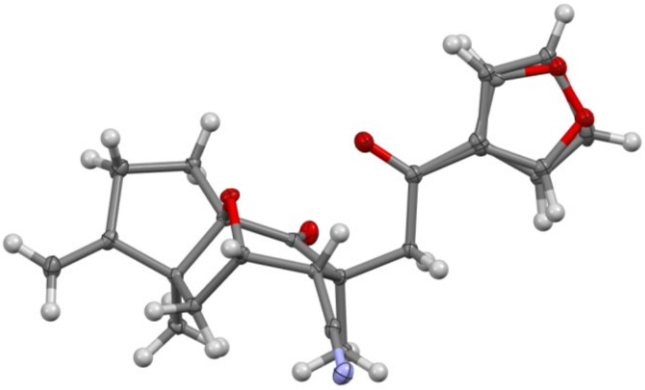

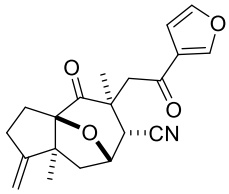

furyl ketone 6-*epi*-**128**

(*cf*. **Figure 33** on page **159**)

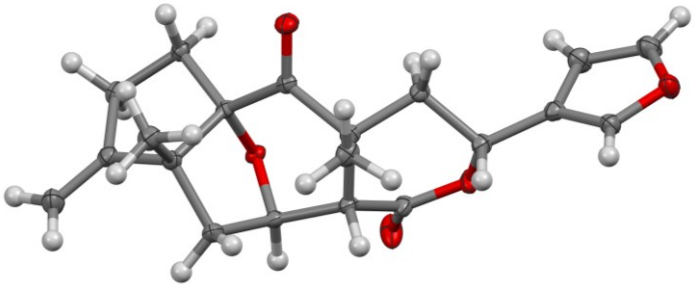

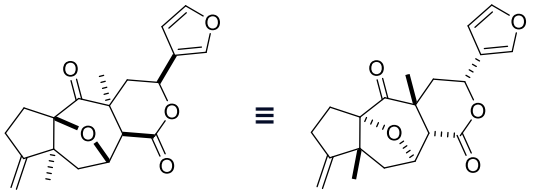

furyl lactone **38**

(*cf*. **Figure 32** (inverted structure) on page **159**)

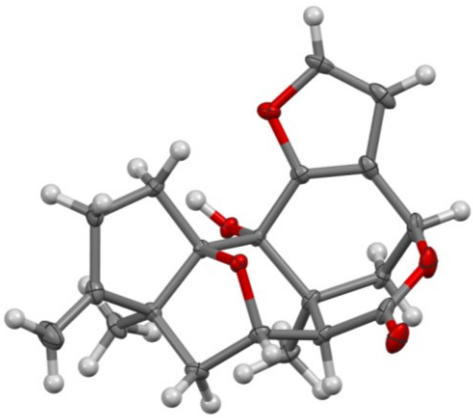

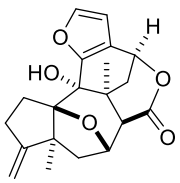

polycyclic lactone **133**

(*cf*. **Figure 34** on page **162**)

Figure 37. X-Ray crystal structures of furyl ketone 6-*epi*-**128**, furyl lactone **38**, and polycyclic lactone **133**. The processed structures can be seen in the referred figures.

6.2 NMR SPECTRA

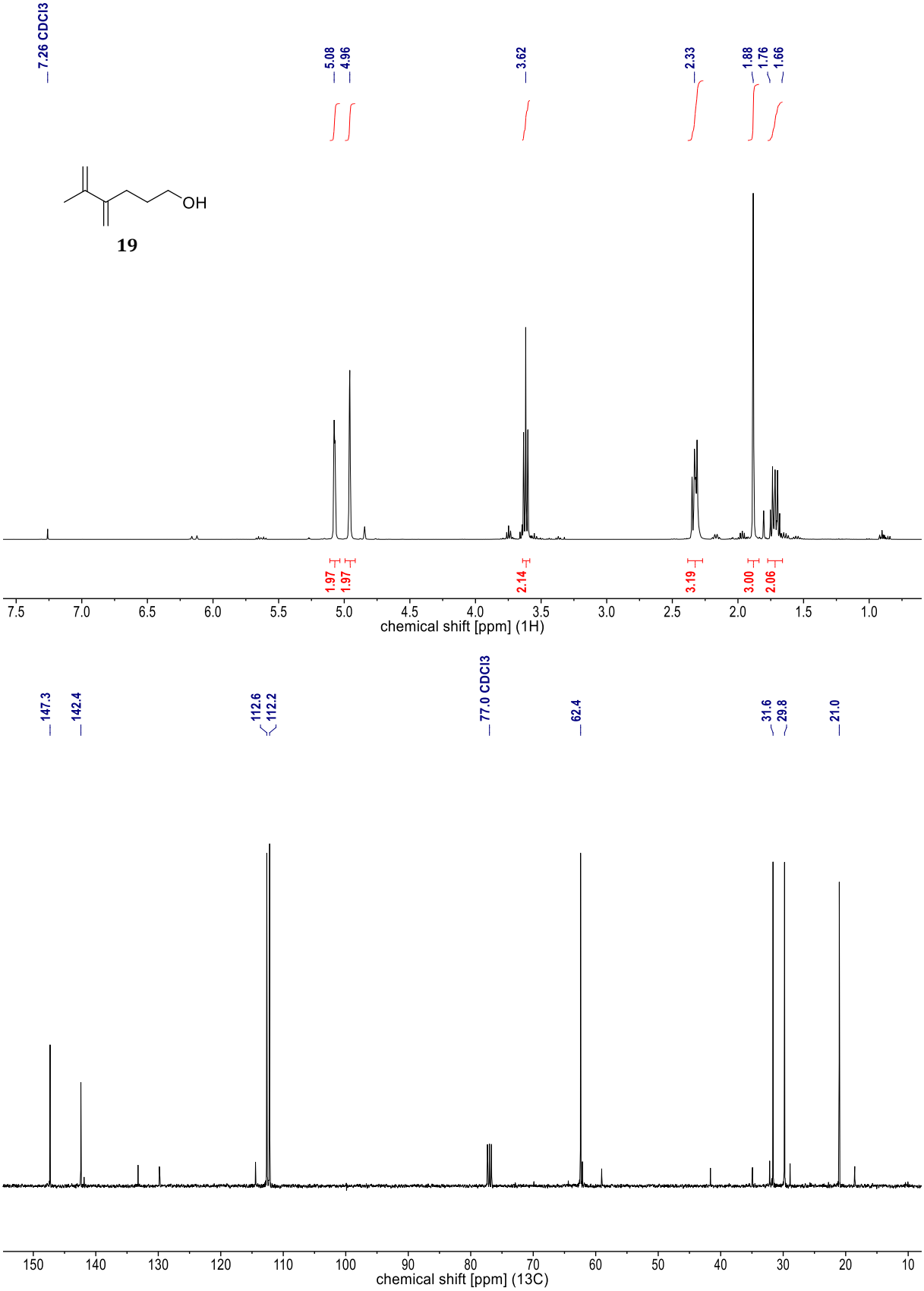

Figure 38. NMR spectra of **19** [^{1}H (400 MHz, $CDCl_3$) & ^{13}C (101 MHz, $CDCl_3$)].

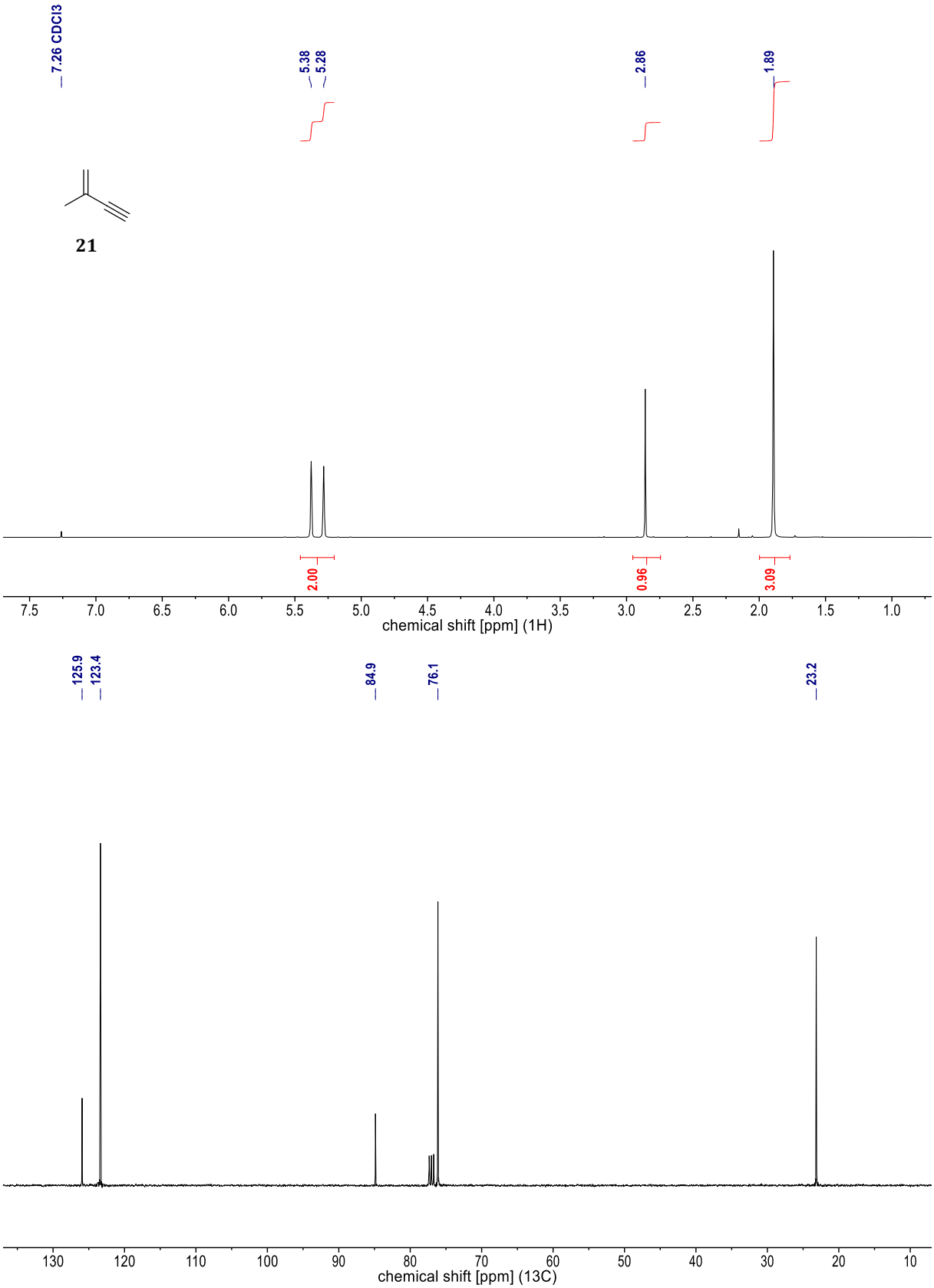

Figure 39. NMR spectra of **21** [^{1}H (400 MHz, $CDCl_3$) & ^{13}C (101 MHz, $CDCl_3$)].

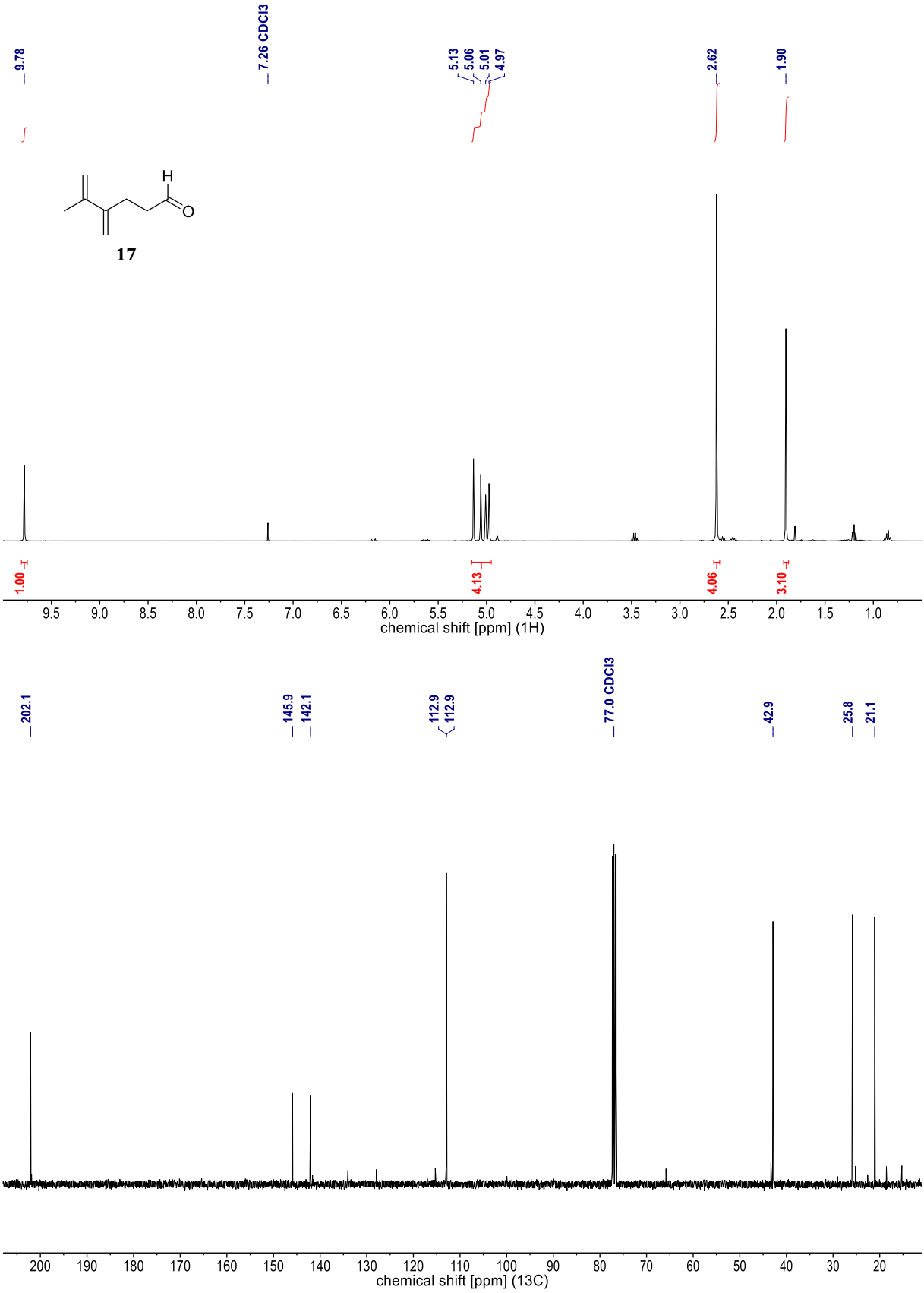

Figure 40. NMR spectra of **17** [^{1}H (400 MHz, $CDCl_3$) & ^{13}C (101 MHz, $CDCl_3$)].

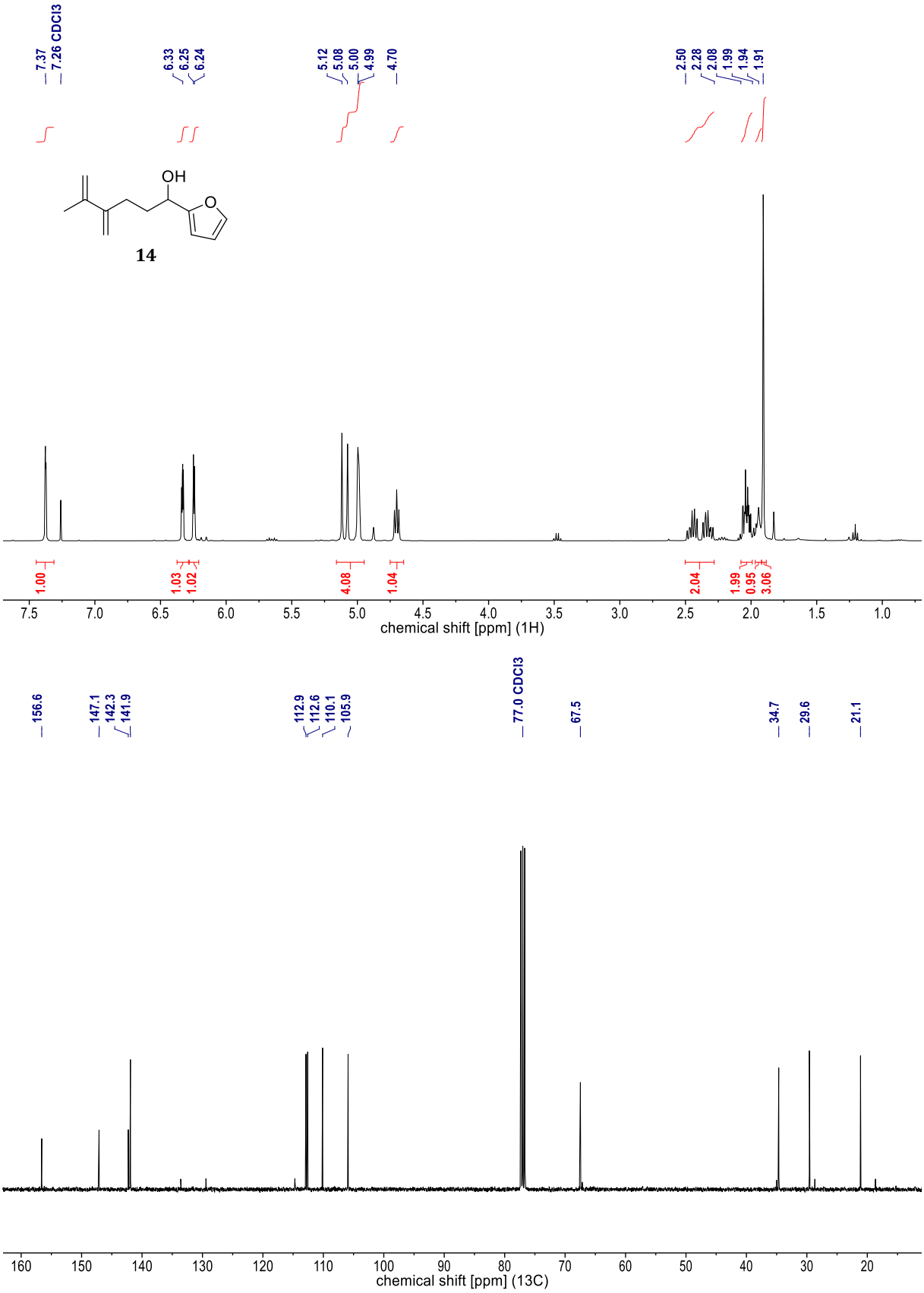

Figure 41. NMR spectra of **14** [^{1}H (400 MHz, $CDCl_3$) & ^{13}C (101 MHz, $CDCl_3$)].

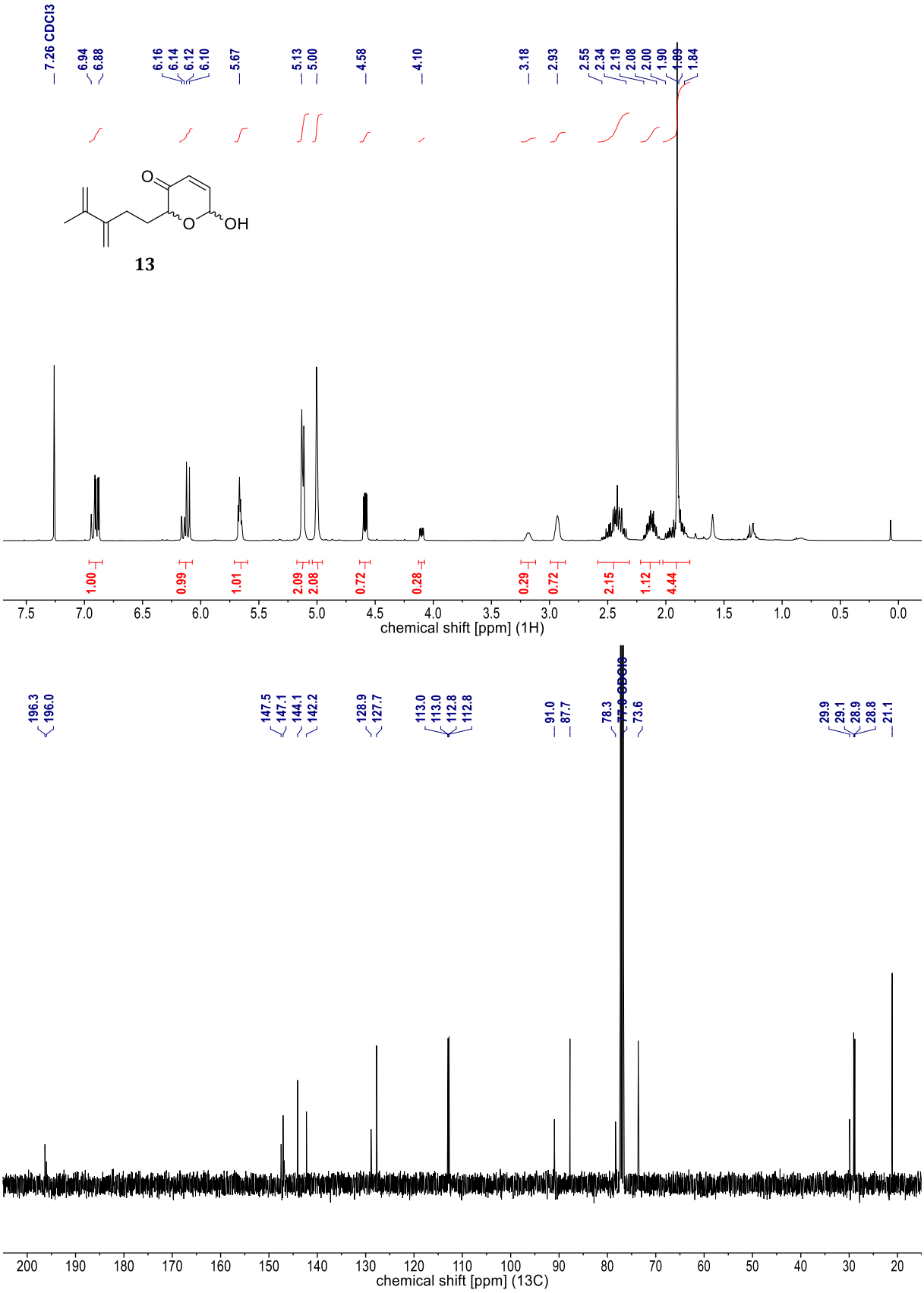

Figure 42. NMR spectra of **13** [^{1}H (400 MHz, $CDCl_3$) & ^{13}C (101 MHz, $CDCl_3$)]. *Diastereomeric mixture*.

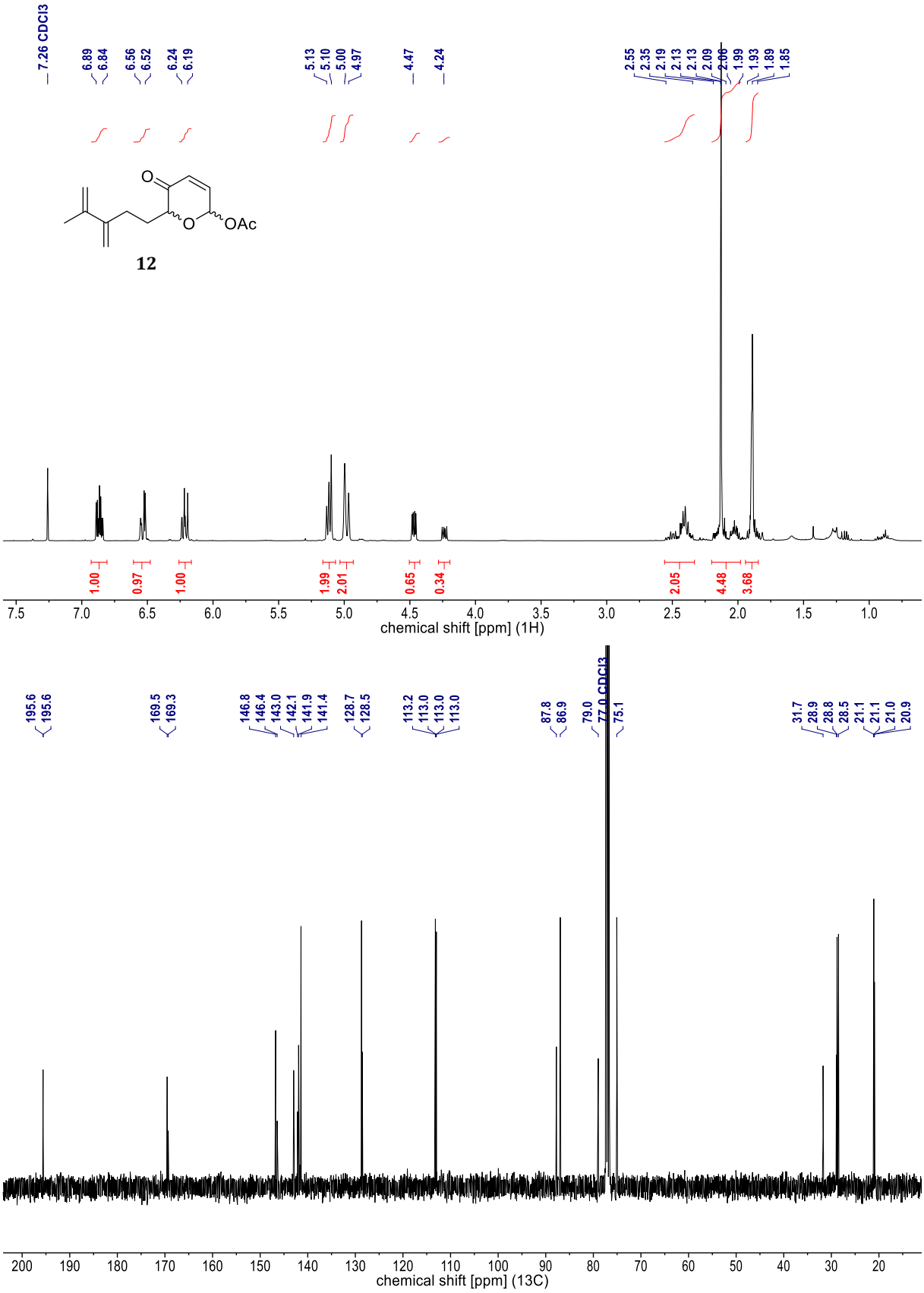

Figure 43. NMR spectra of **12** [^{1}H (400 MHz, $CDCl_3$) & ^{13}C (101 MHz, $CDCl_3$)]. *Diastereomeric mixture*. The NMR spectra of the *less polar DS* can be seen in **Figure 44**.

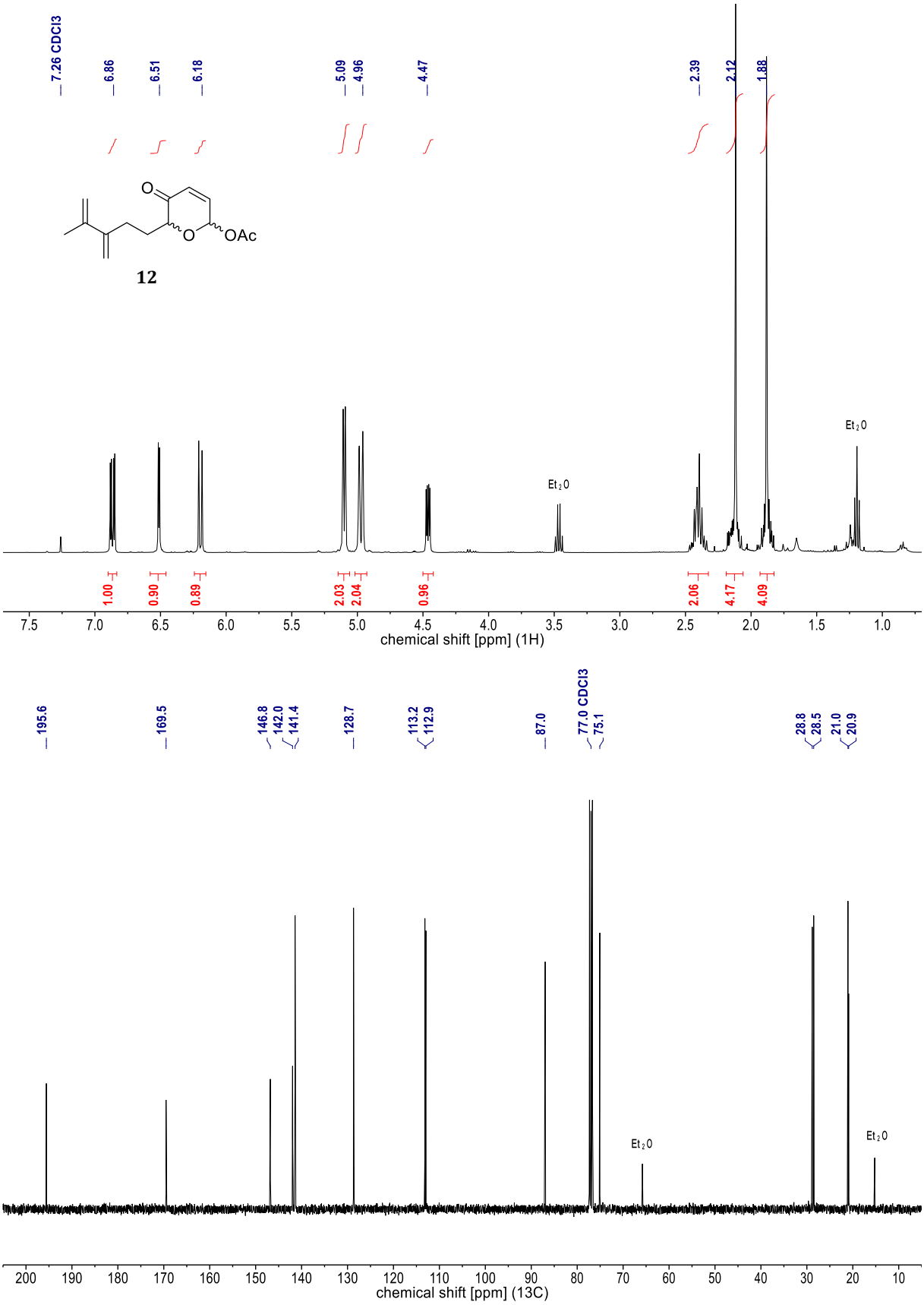

Figure 44. NMR spectra of **12** [^{1}H (400 MHz, $CDCl_3$) & ^{13}C (101 MHz, $CDCl_3$)].
Less polar DS. Some Et_2O is discernible.

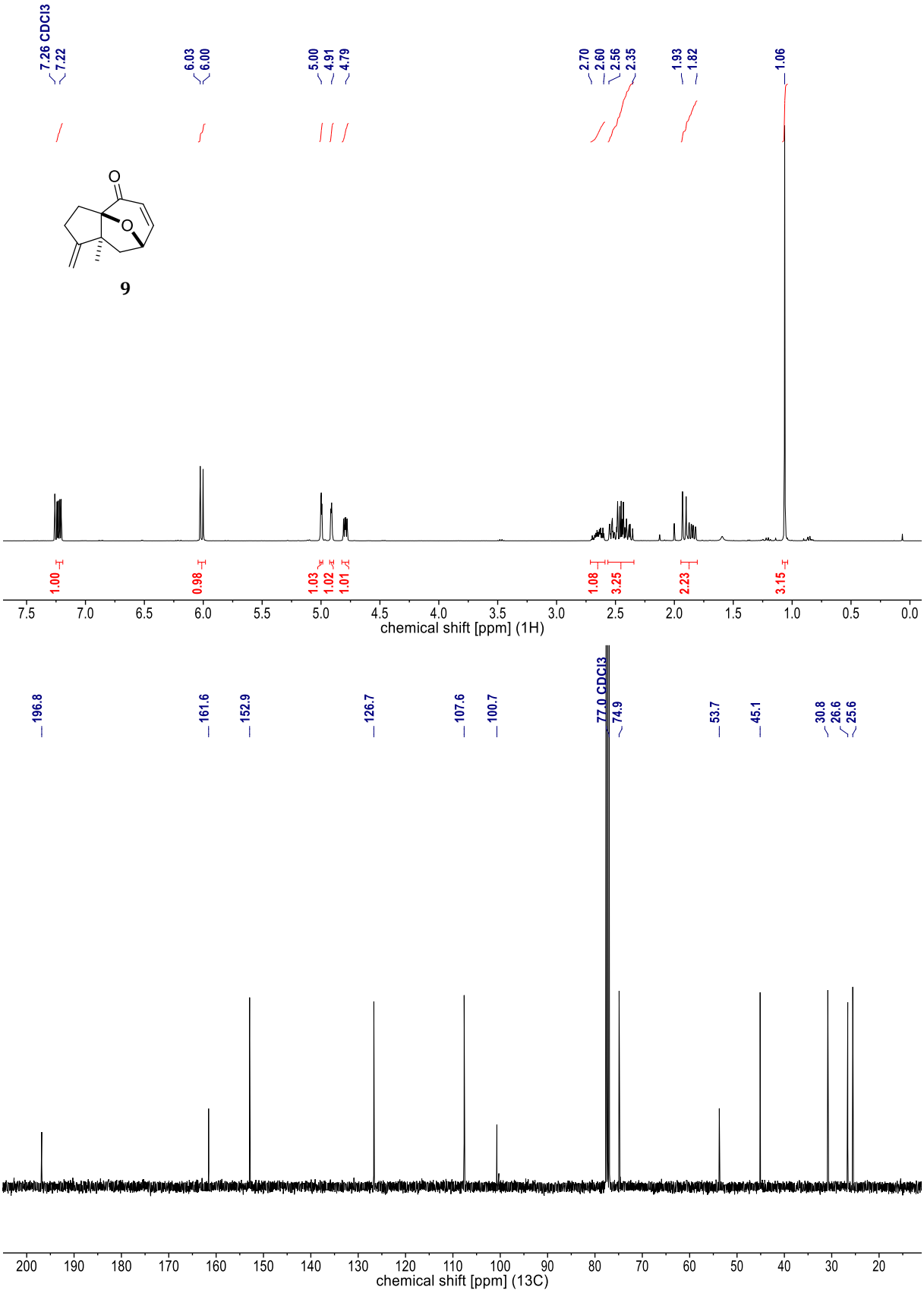

Figure 45. NMR spectra of **9** [^{1}H (400 MHz, **$CDCl_3$**) & ^{13}C (101 MHz, **$CDCl_3$**)].
*NMR Spectra in C_6D_6 can be seen in **Figure 46**.*

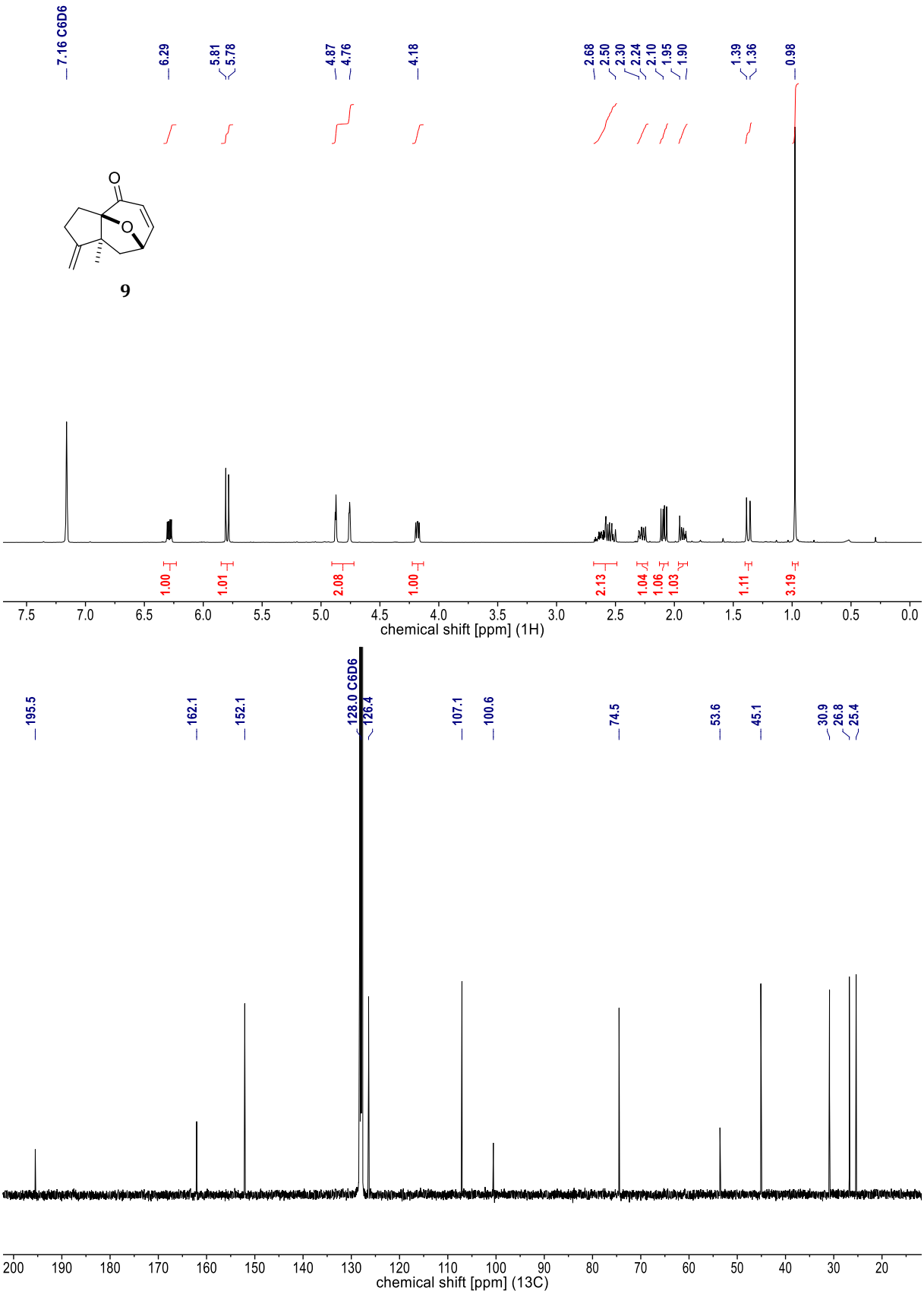

Figure 46. NMR spectra of **9** [^{1}H (400 MHz, $\mathbf{C_6D_6}$) & ^{13}C (101 MHz, $\mathbf{C_6D_6}$)].
NMR Spectra in $CDCl_3$ can be seen in **Figure 45**.

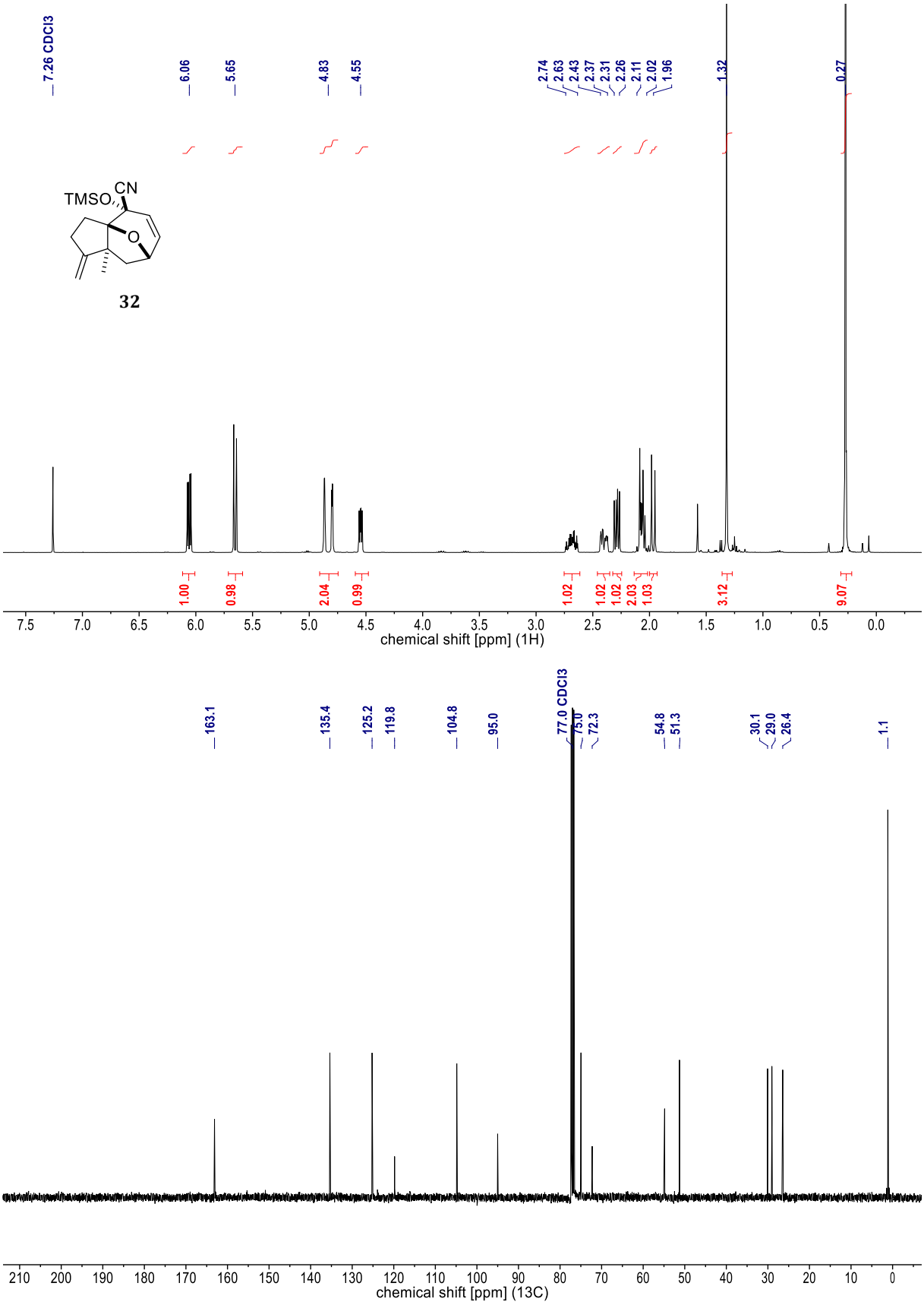

Figure 47. NMR spectra of **32** [^{1}H (400 MHz, $CDCl_3$) & ^{13}C (101 MHz, $CDCl_3$)].

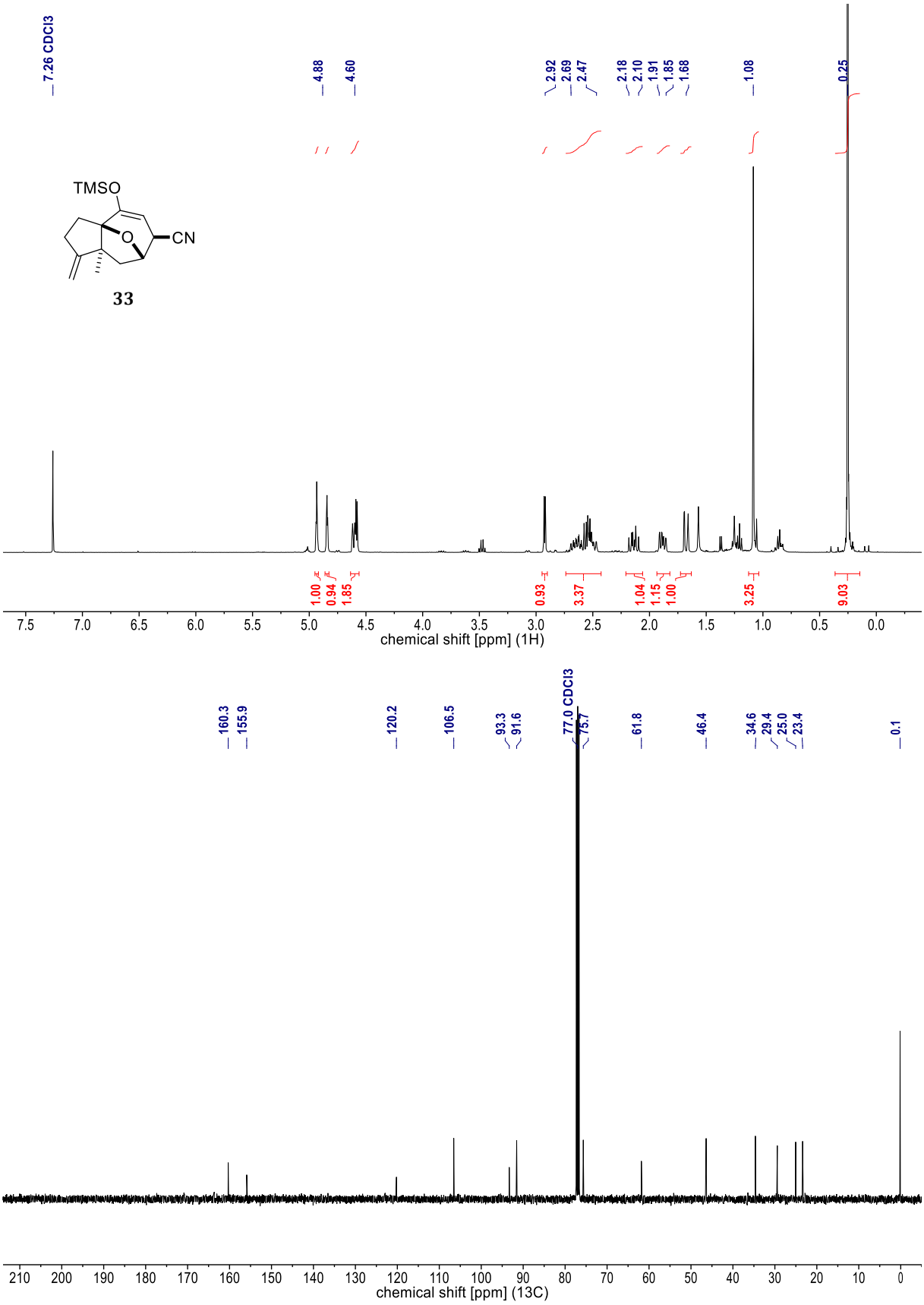

Figure 48. NMR spectra of **33** [^{1}H (400 MHz, $CDCl_3$) & ^{13}C (101 MHz, $CDCl_3$)].

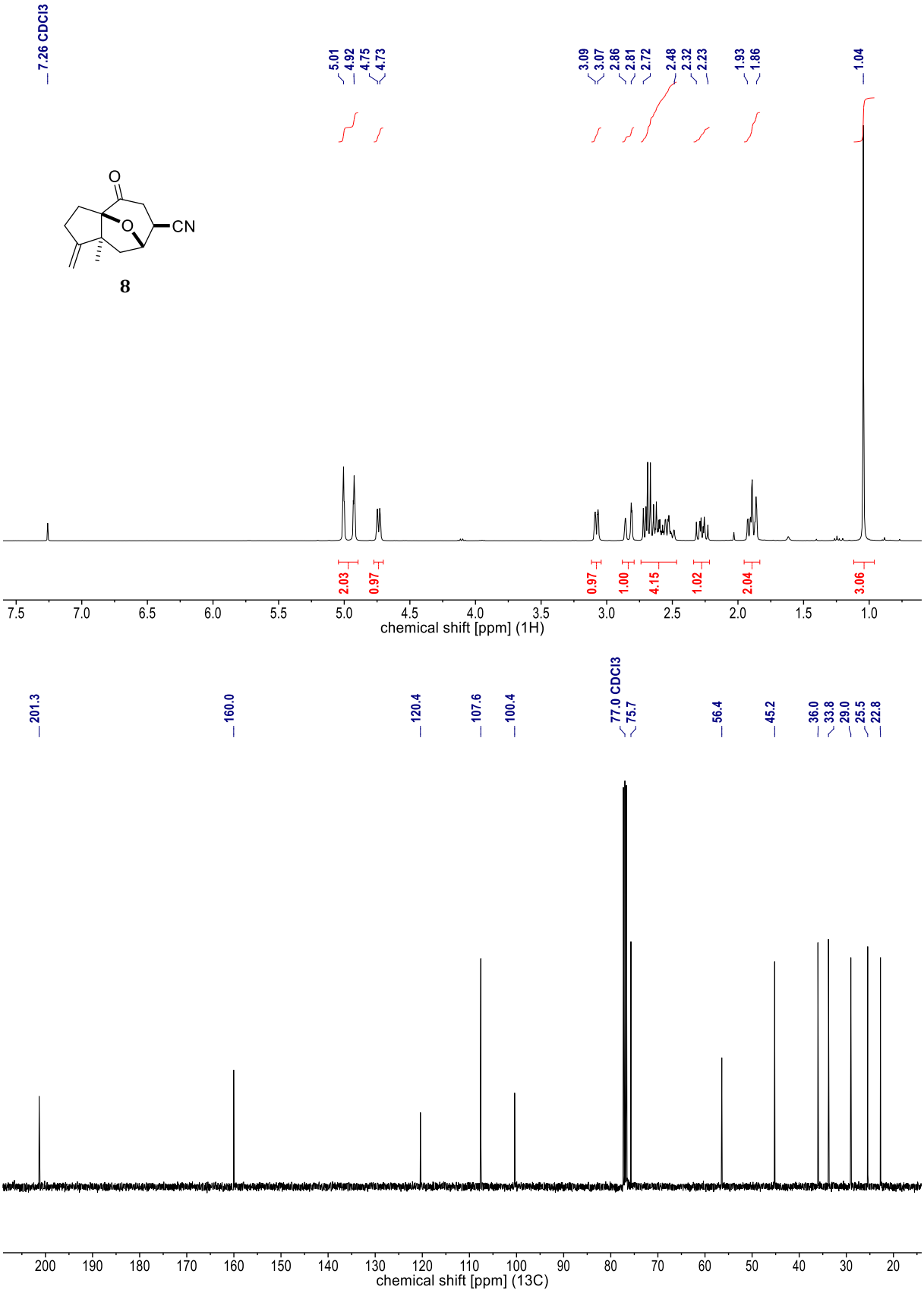

Figure 49. NMR spectra of **8** [^{1}H (400 MHz, $CDCl_3$) & ^{13}C (101 MHz, $CDCl_3$)].

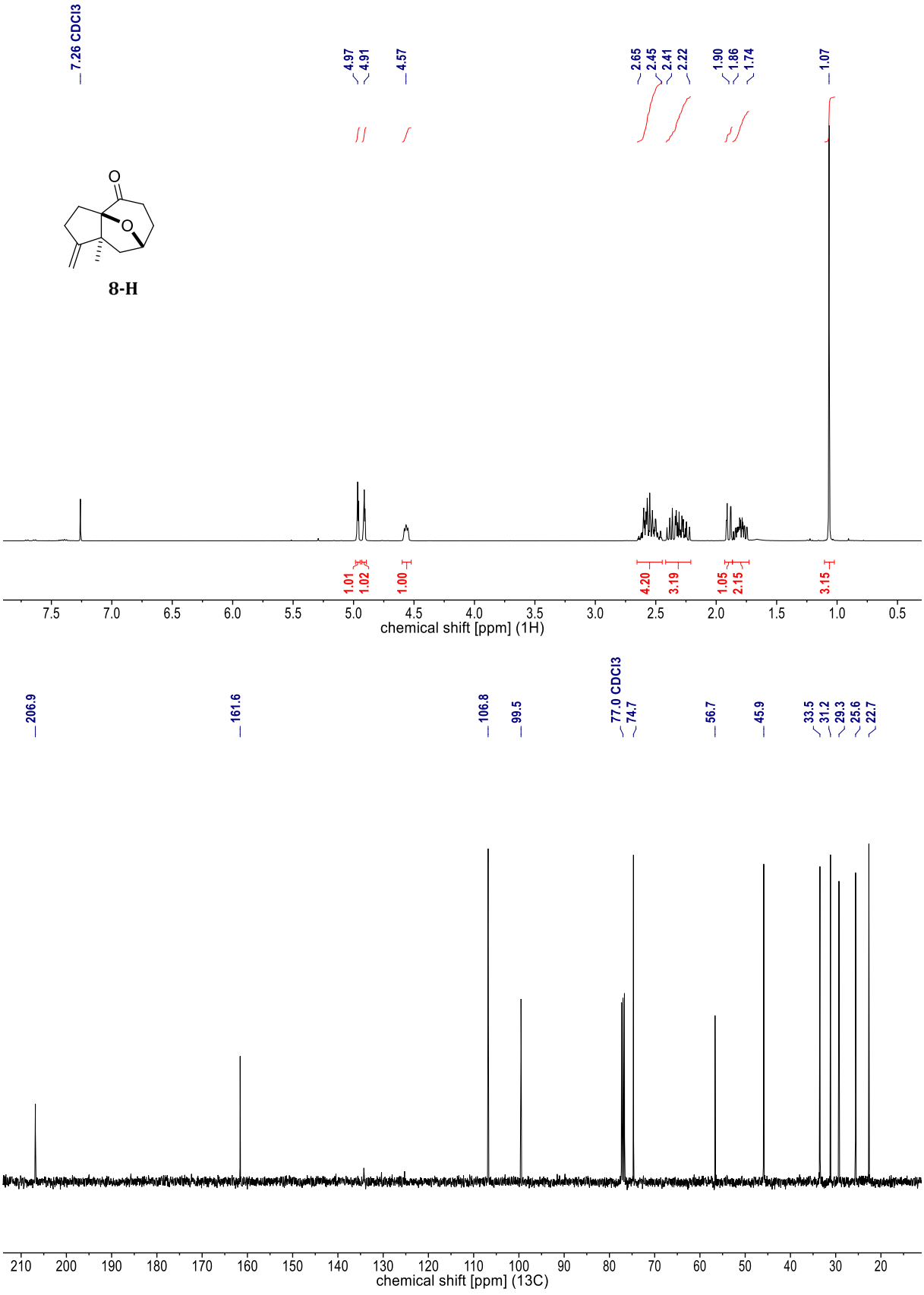

Figure 50. NMR spectra of **8-H** [^{1}H (400 MHz, $CDCl_3$) & ^{13}C (101 MHz, $CDCl_3$)].

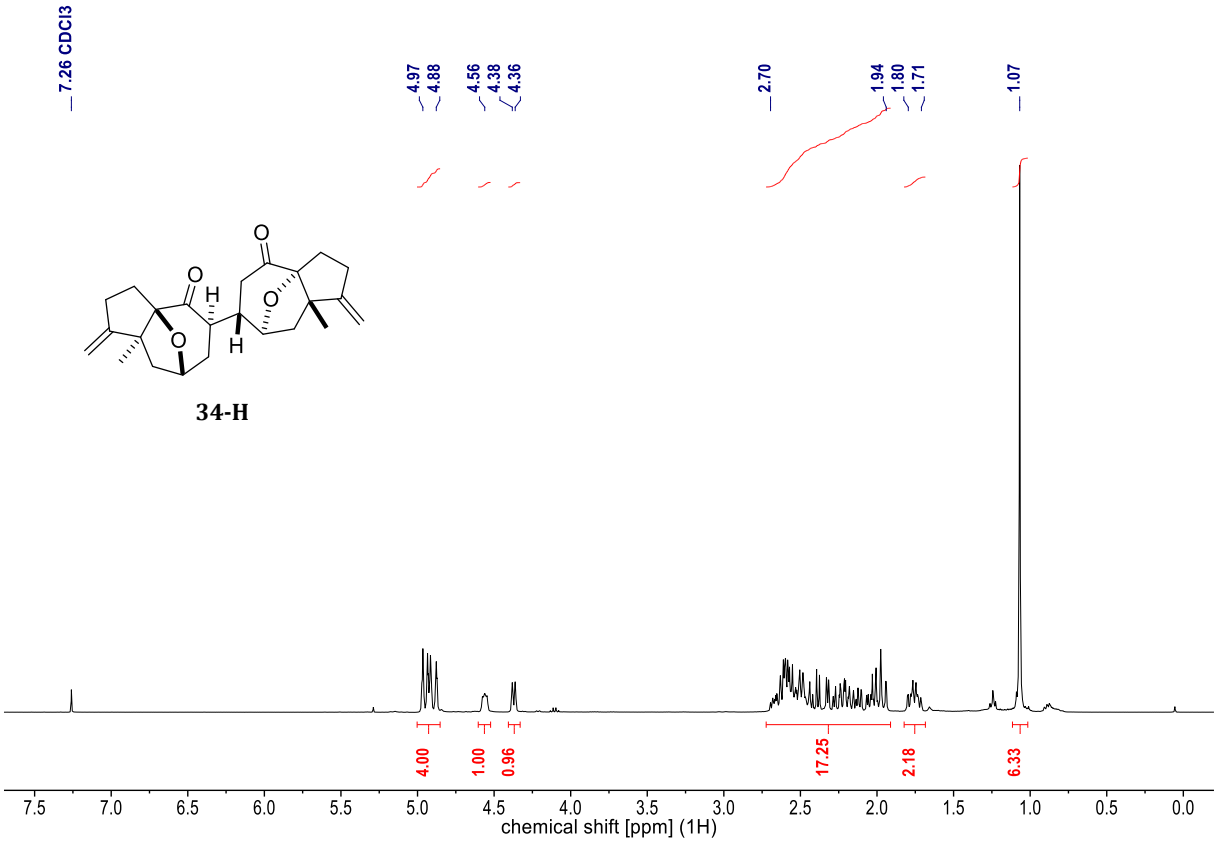

Figure 51. ^{1}H NMR spectrum of **34-H** (400 MHz, $CDCl_3$). *A ^{13}C NMR spectrum was not recorded.*

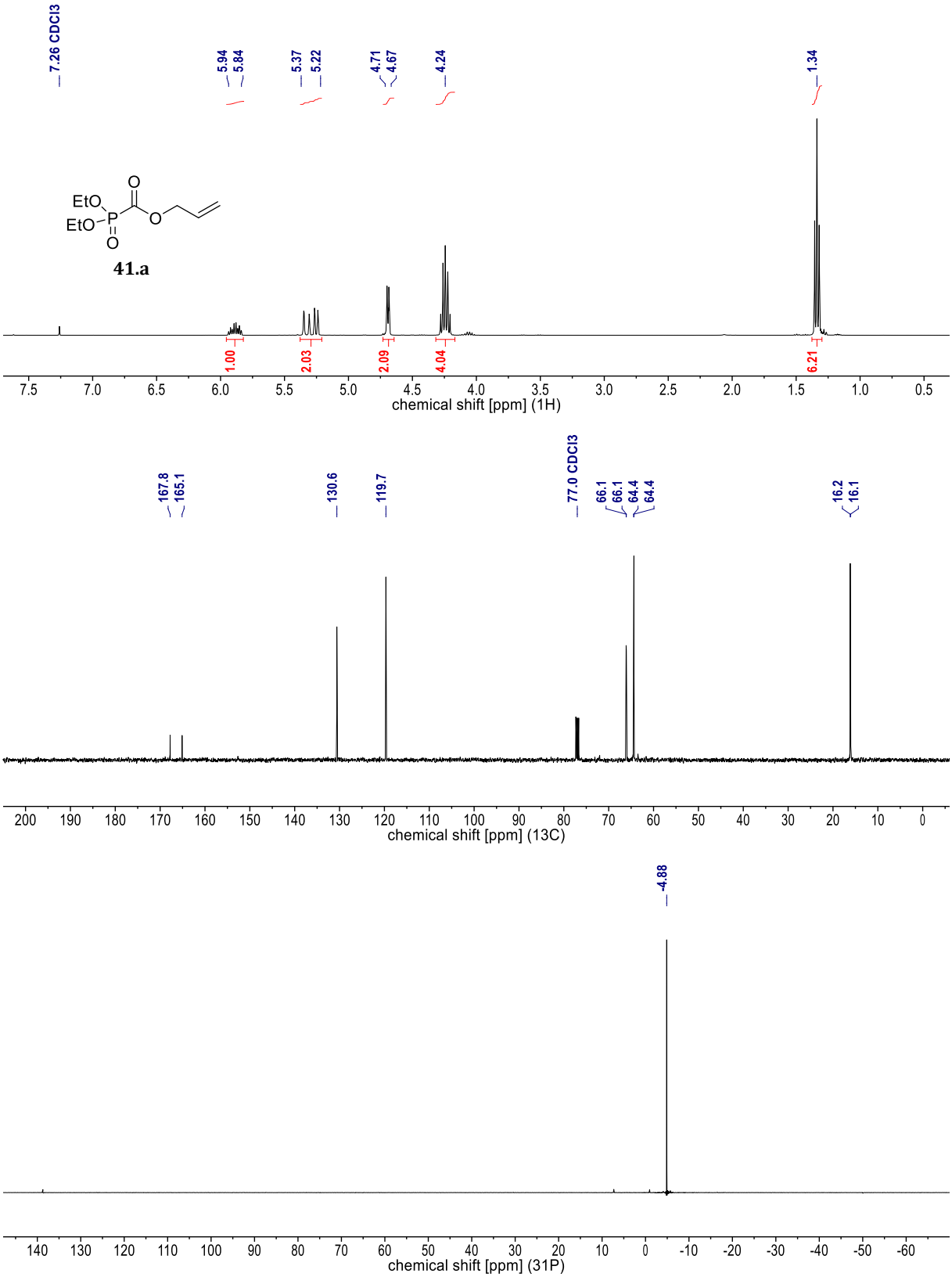

Figure 52. NMR spectra of **41.a** [^{1}H (400 MHz), ^{13}C (101 MHz) & ^{31}P (162 MHz), each in $CDCl_3$].

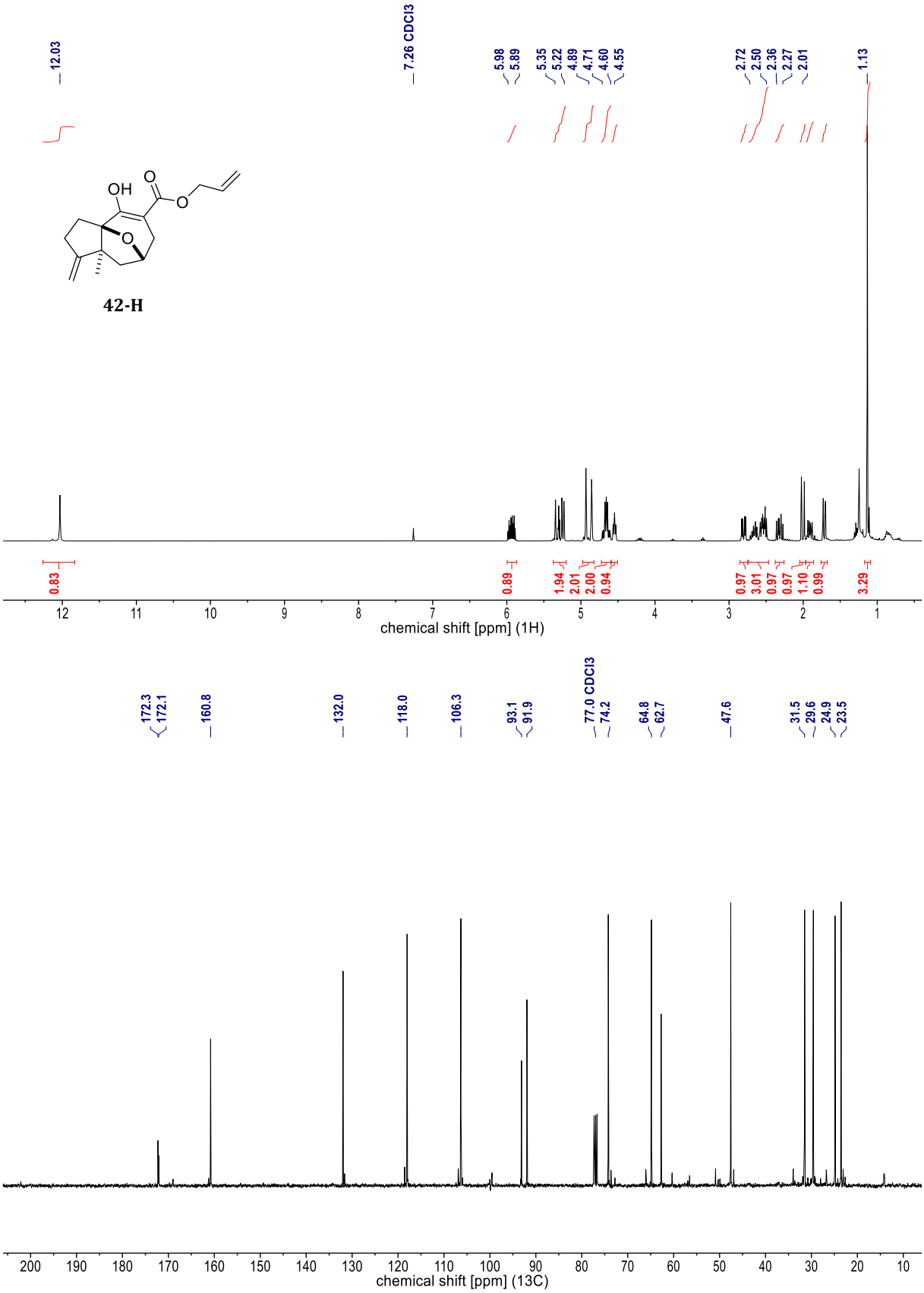

Figure 53. NMR spectra of **42-H** [^{1}H (400 MHz, $CDCl_3$) & ^{13}C (101 MHz, $CDCl_3$)].

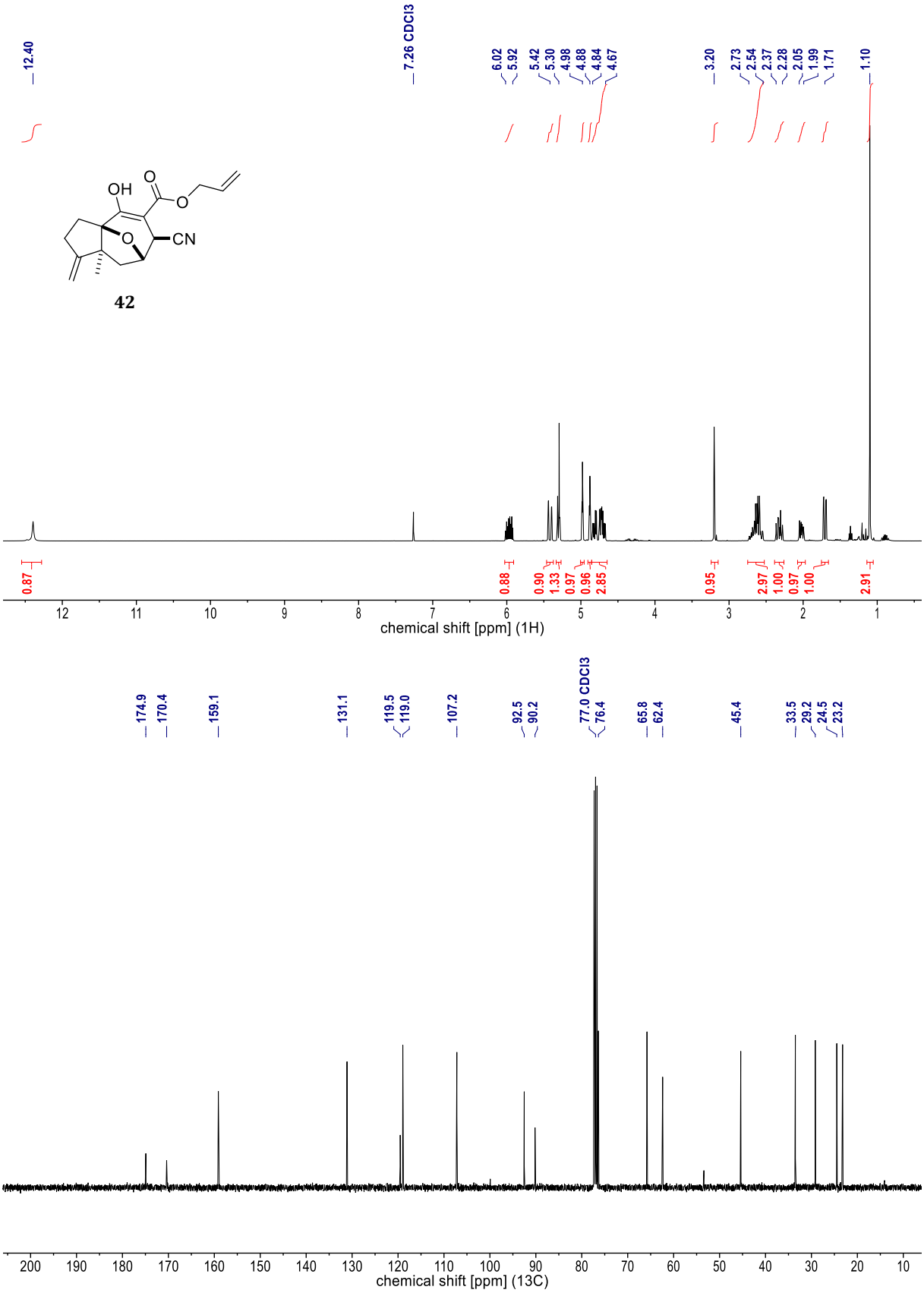

Figure 54. NMR spectra of **42** [^{1}H (400 MHz, $CDCl_3$) & ^{13}C (101 MHz, $CDCl_3$)].

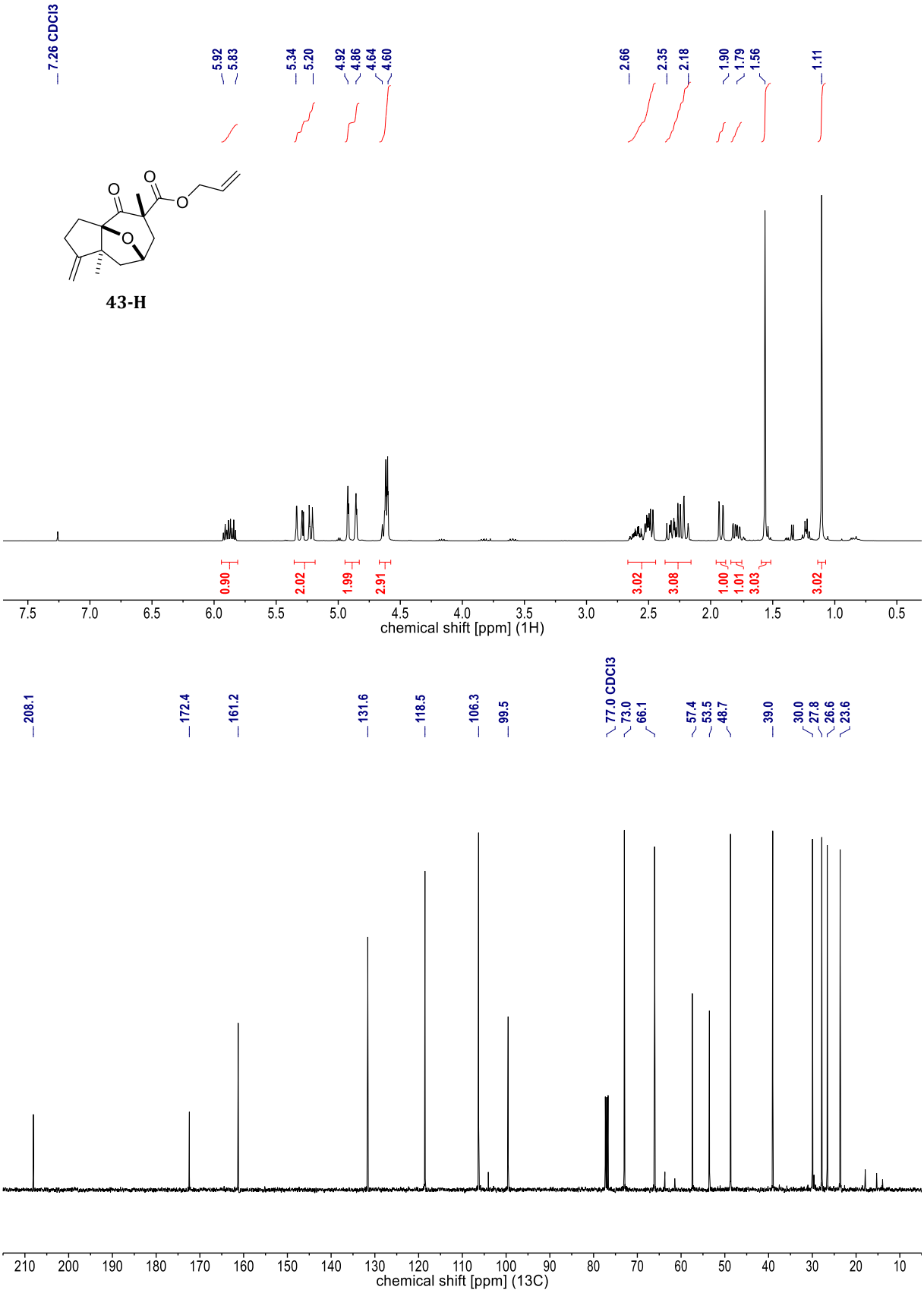

Figure 55. NMR spectra of **43-H** [^{1}H (400 MHz, $CDCl_3$) & ^{13}C (101 MHz, $CDCl_3$)].

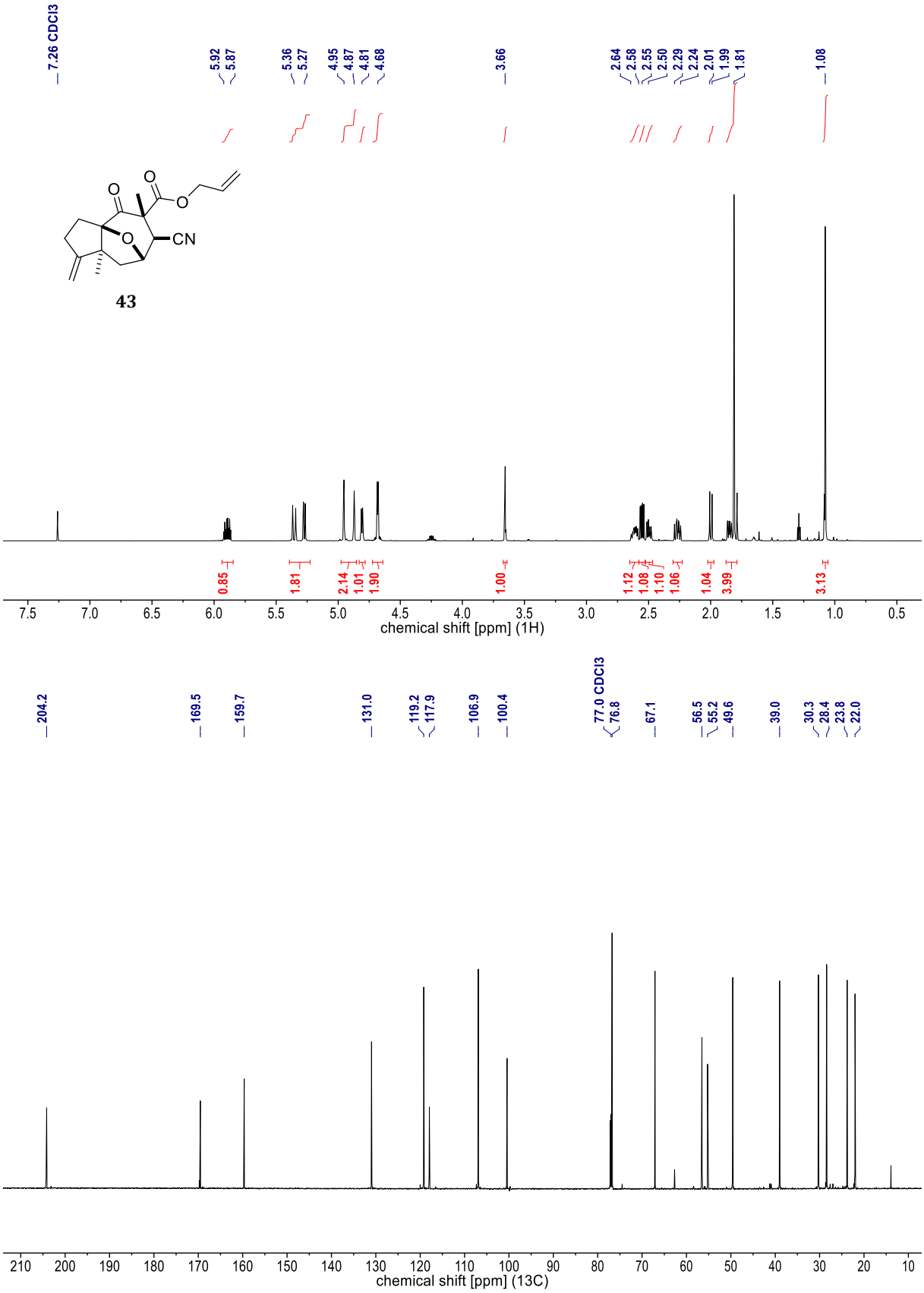

Figure 56. NMR spectra of **43** [^{1}H (700 MHz, $CDCl_3$) & ^{13}C (176 MHz, $CDCl_3$)].

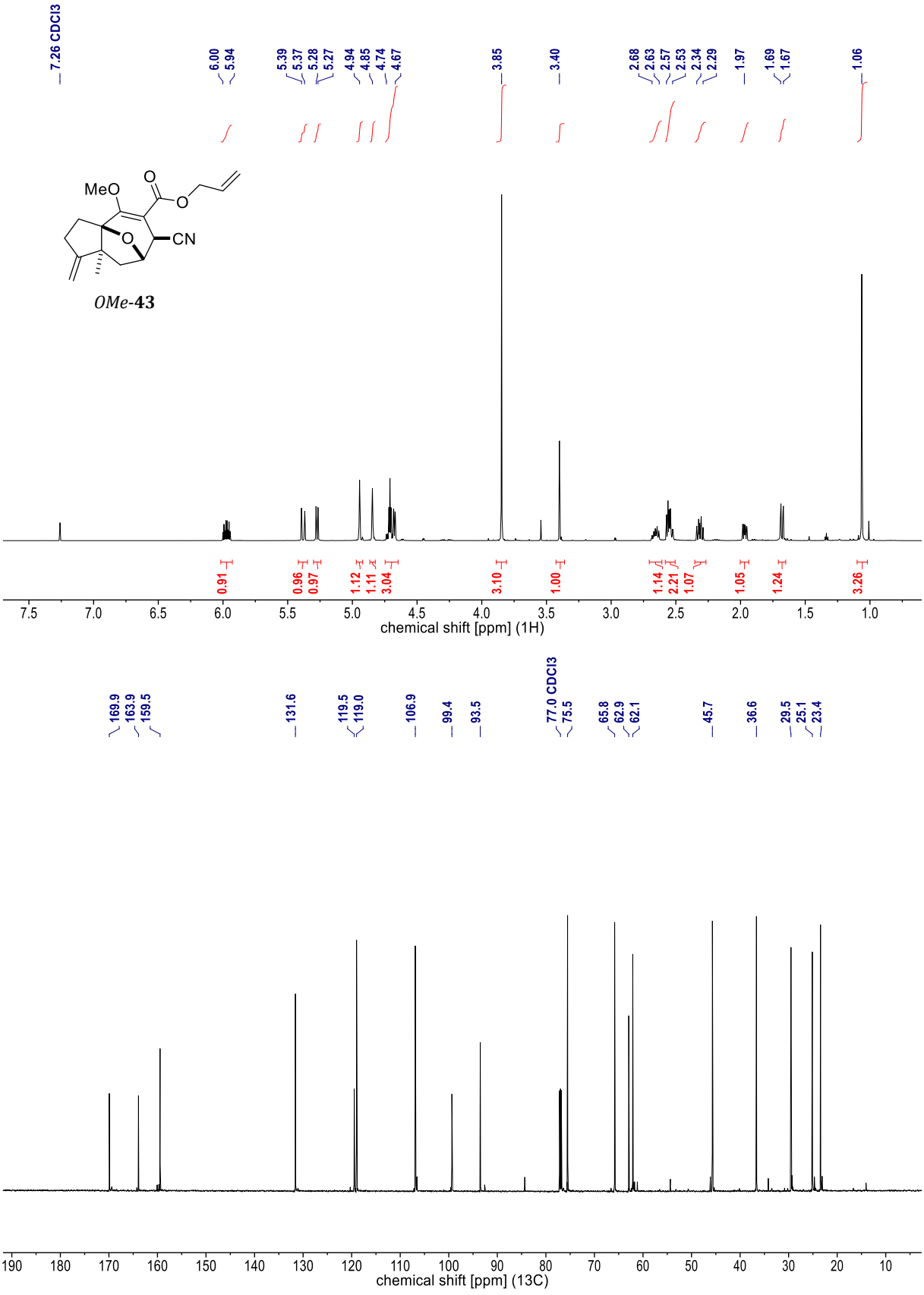

Figure 57. NMR spectra of *OMe*-**43** [^{1}H (700 MHz, $CDCl_3$) & ^{13}C (176 MHz, $CDCl_3$)].

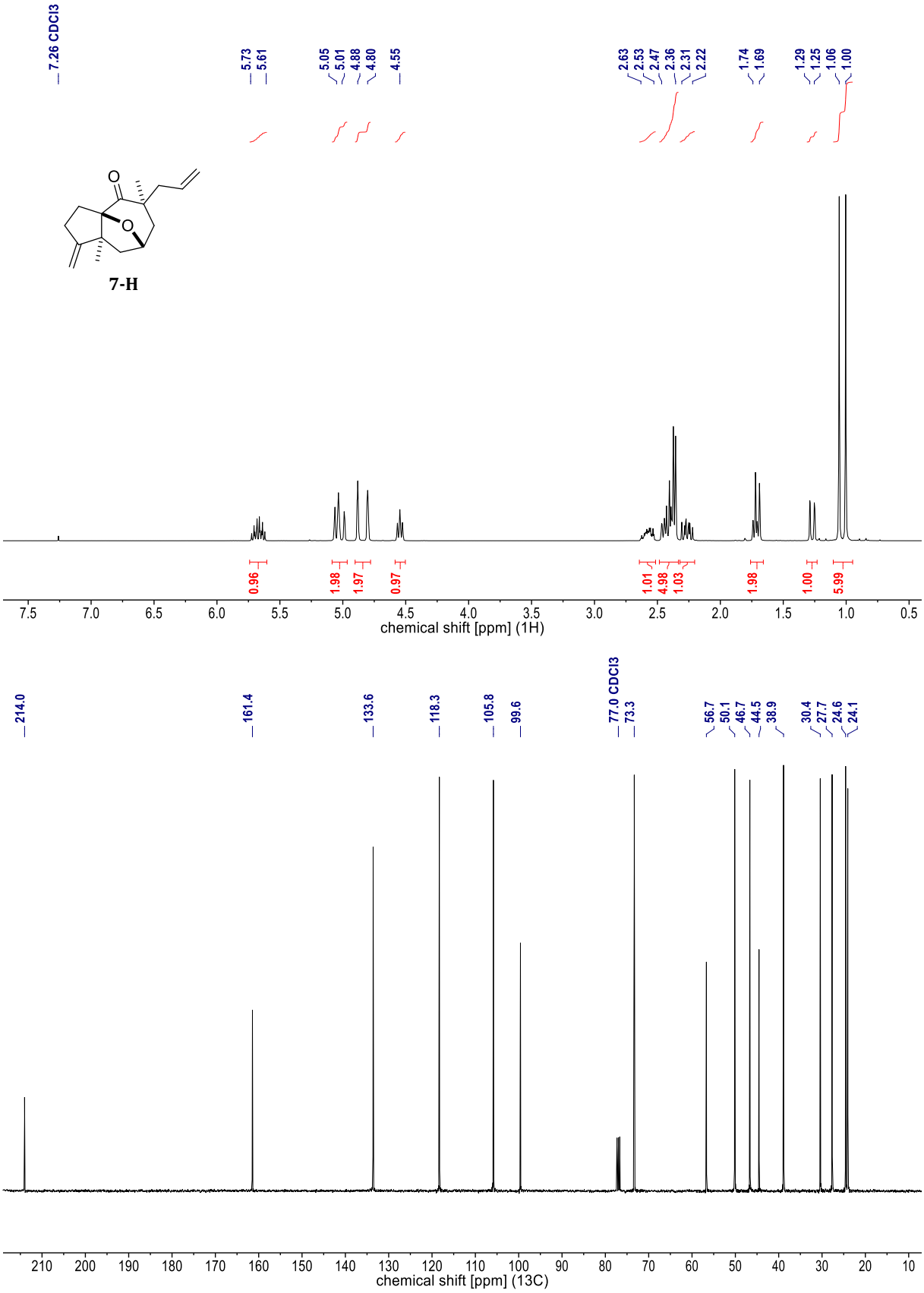

Figure 58. NMR spectra of **7-H** [^{1}H (400 MHz, $CDCl_3$) & ^{13}C (101 MHz, $CDCl_3$)].

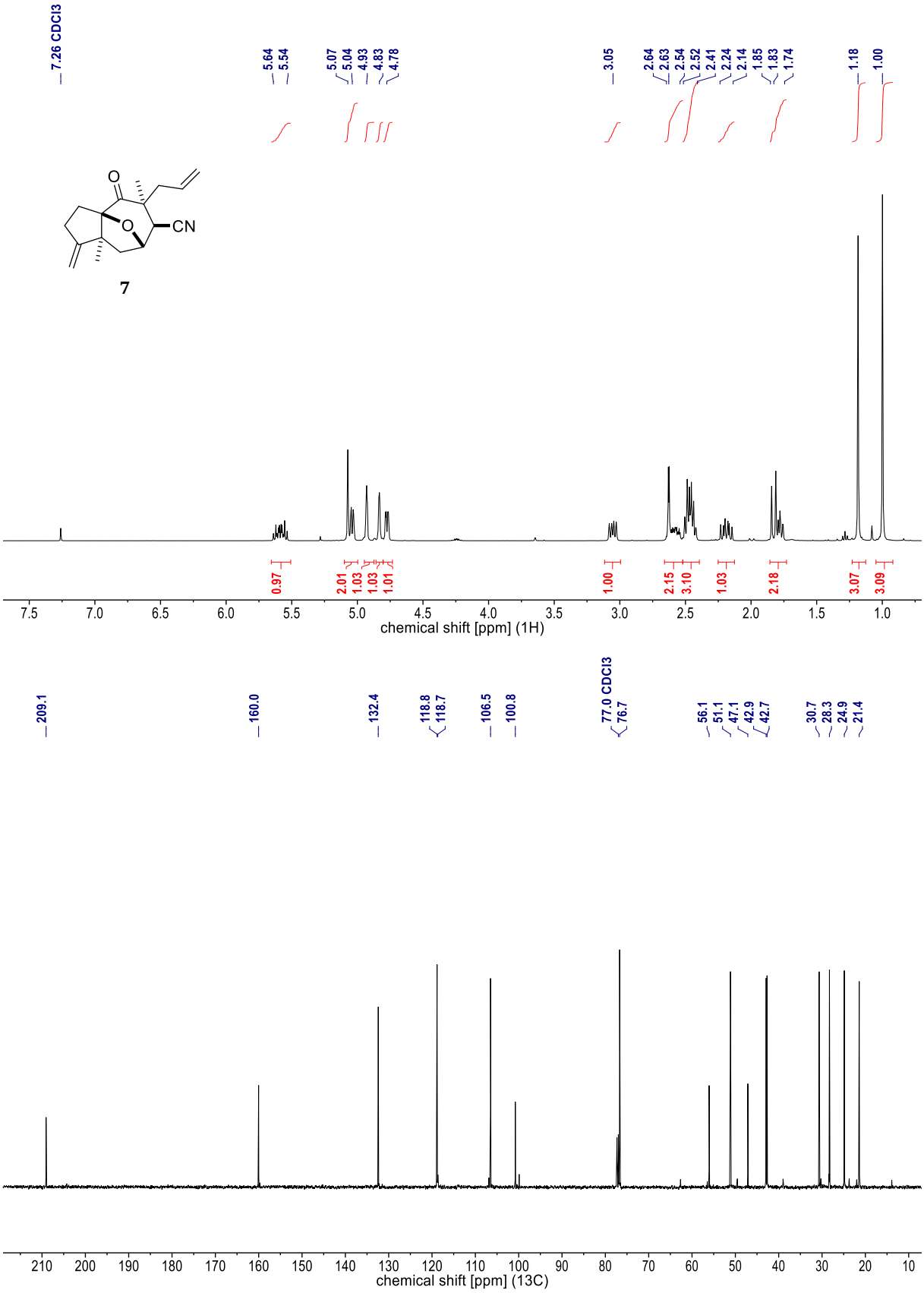

Figure 59. NMR spectra of **7** [^{1}H (400 MHz, $CDCl_3$) & ^{13}C (101 MHz, $CDCl_3$)].

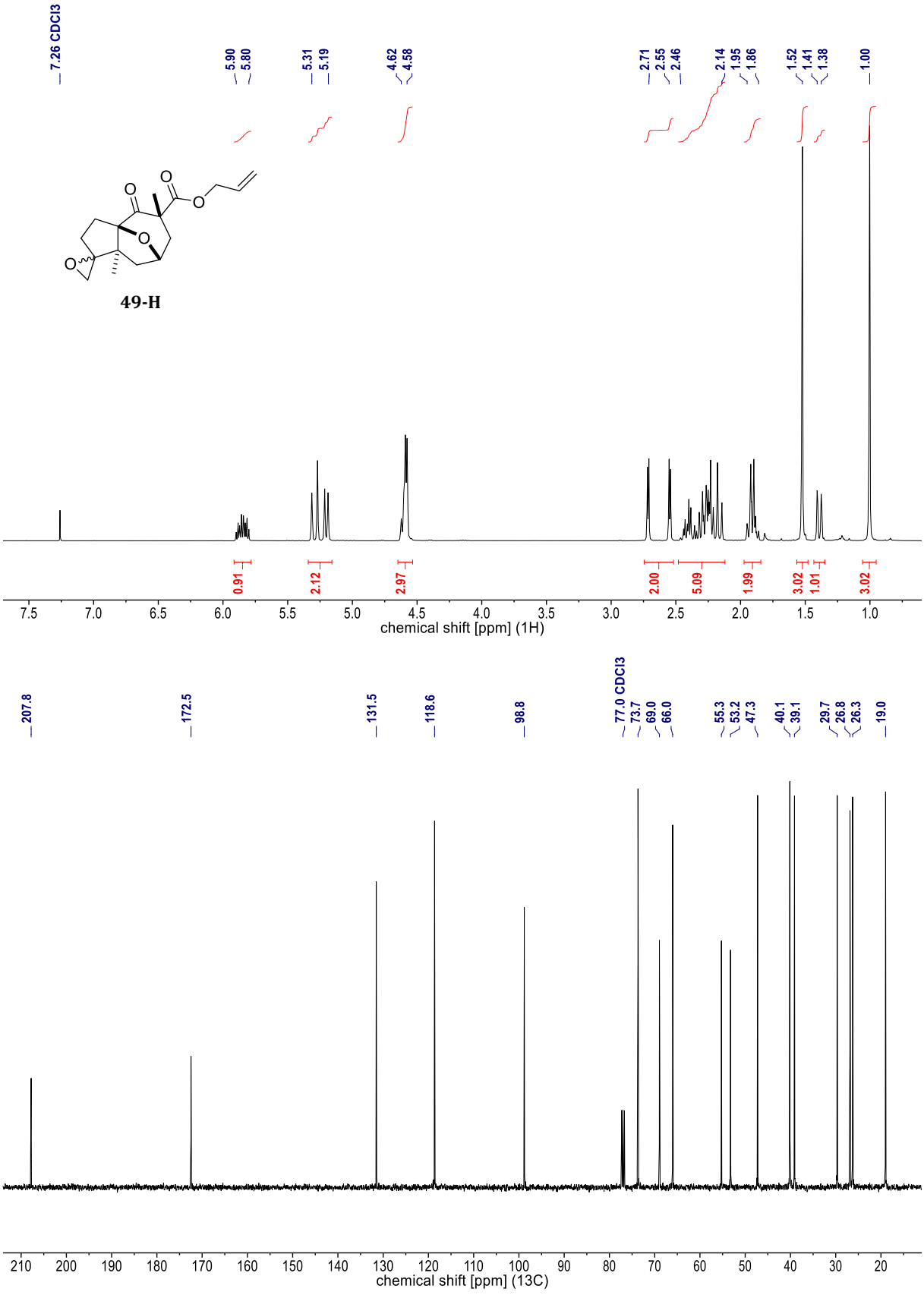

Figure 60. NMR spectra of **49-H** [^{1}H (400 MHz, $CDCl_3$) & ^{13}C (101 MHz, $CDCl_3$)].
Less polar DS.

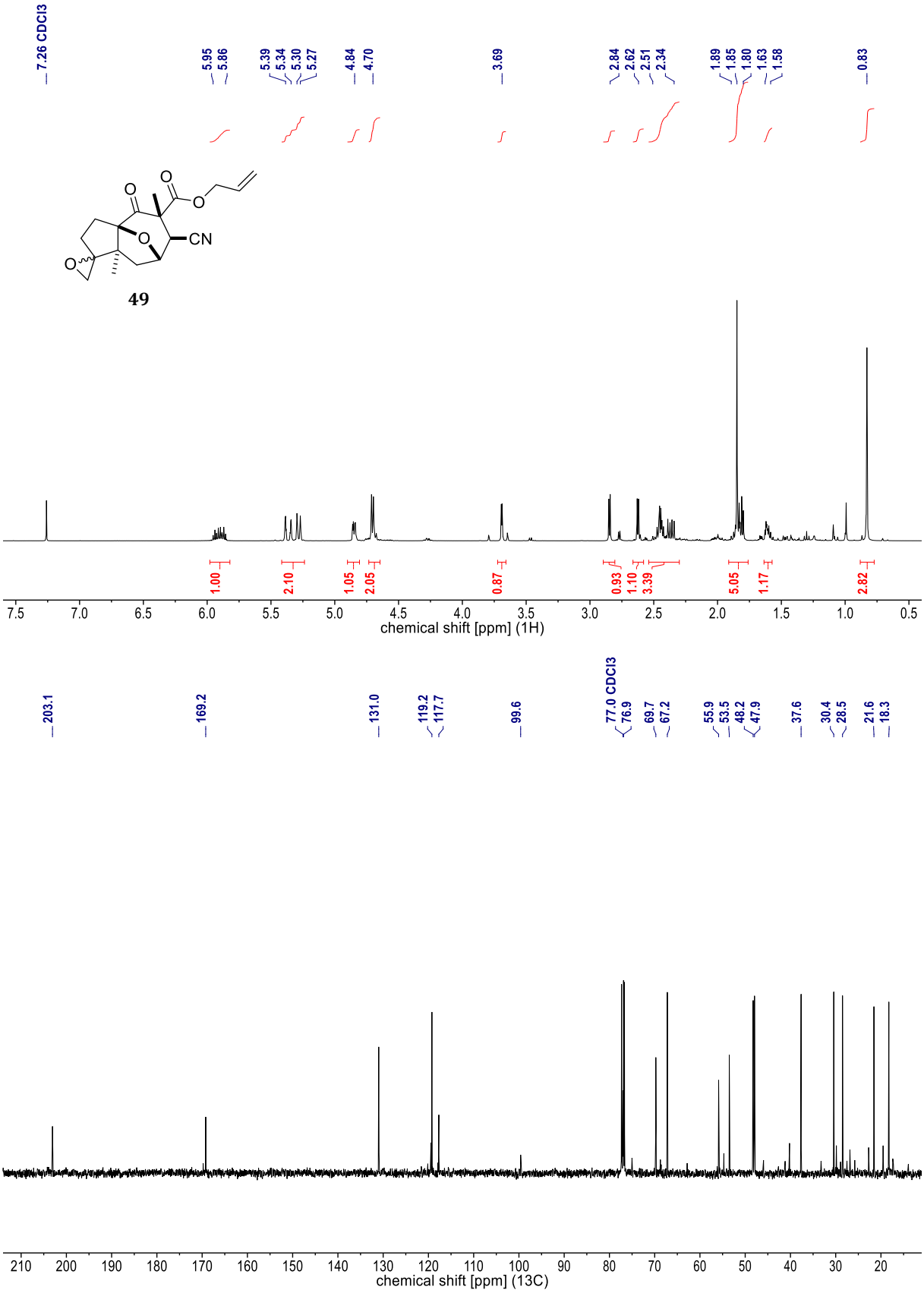

Figure 61. NMR spectra of **49** [^{1}H (400 MHz, $CDCl_3$) & ^{13}C (101 MHz, $CDCl_3$)].
More polar DS.

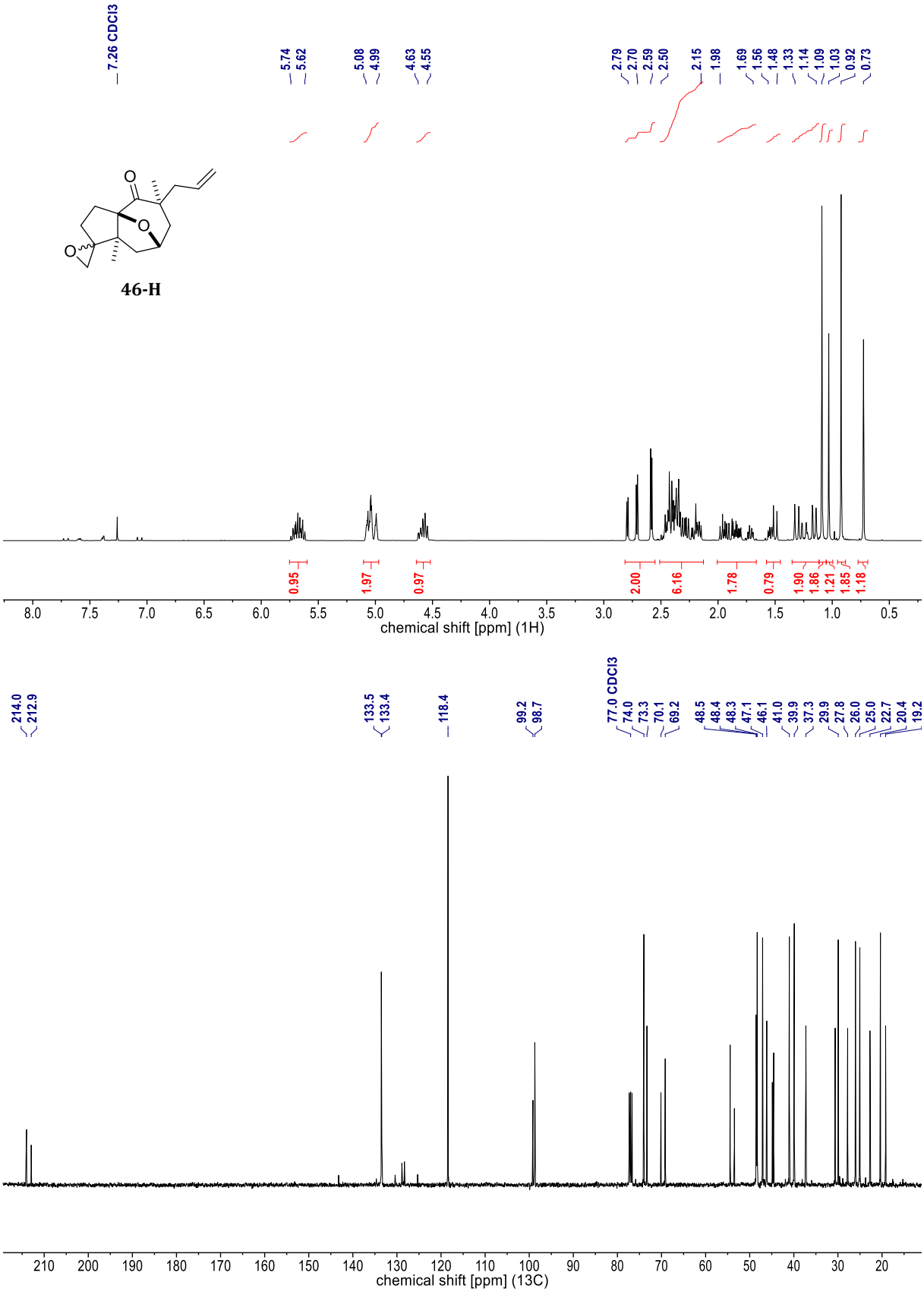

Figure 62. NMR spectra of **46-H** [^{1}H (400 MHz, $CDCl_3$) & ^{13}C (101 MHz, $CDCl_3$)]. *Diastereomeric mixture*.

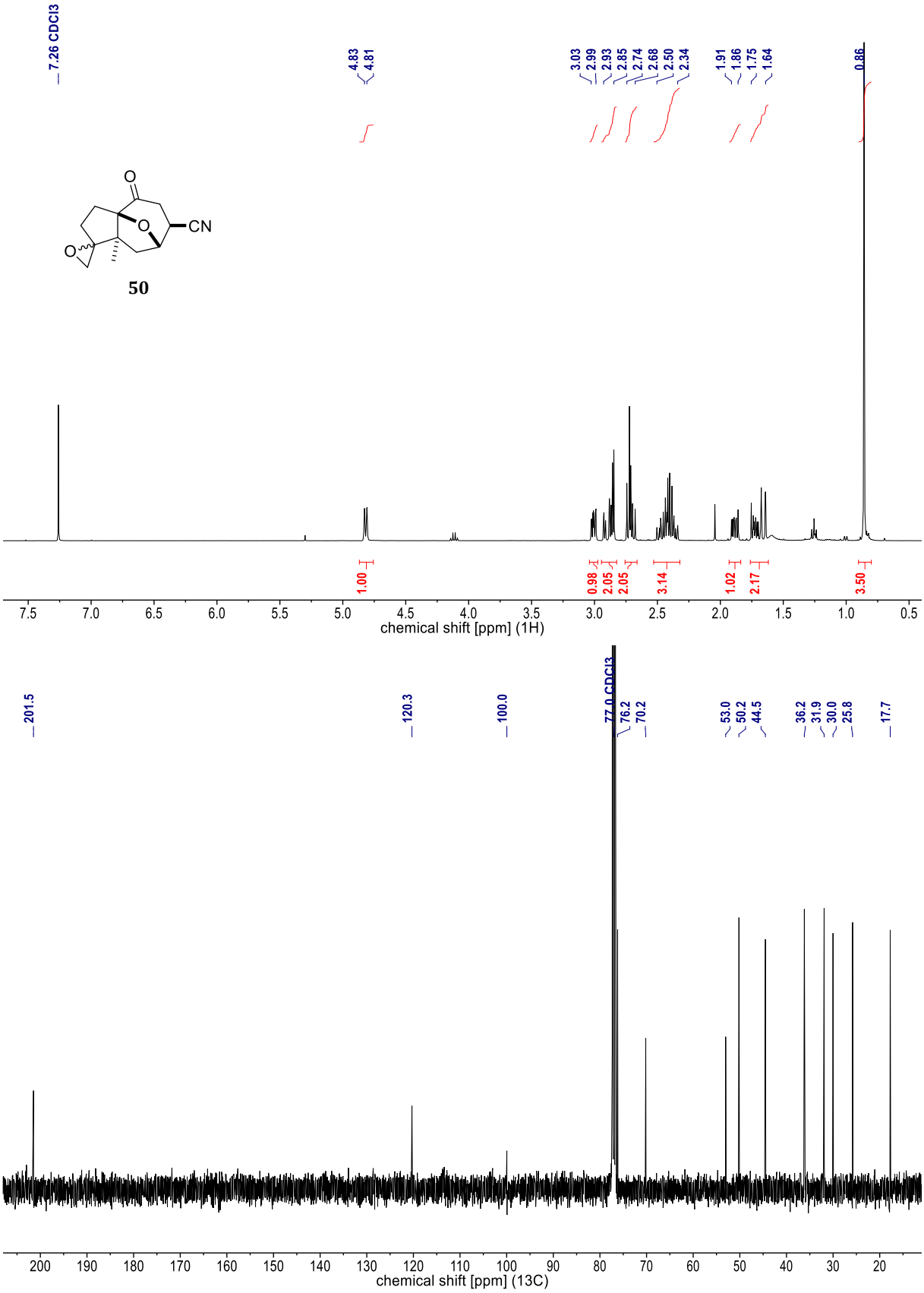

Figure 63. NMR spectra of **50** [^{1}H (400 MHz, $CDCl_3$) & ^{13}C (101 MHz, $CDCl_3$)].
Less polar DS.

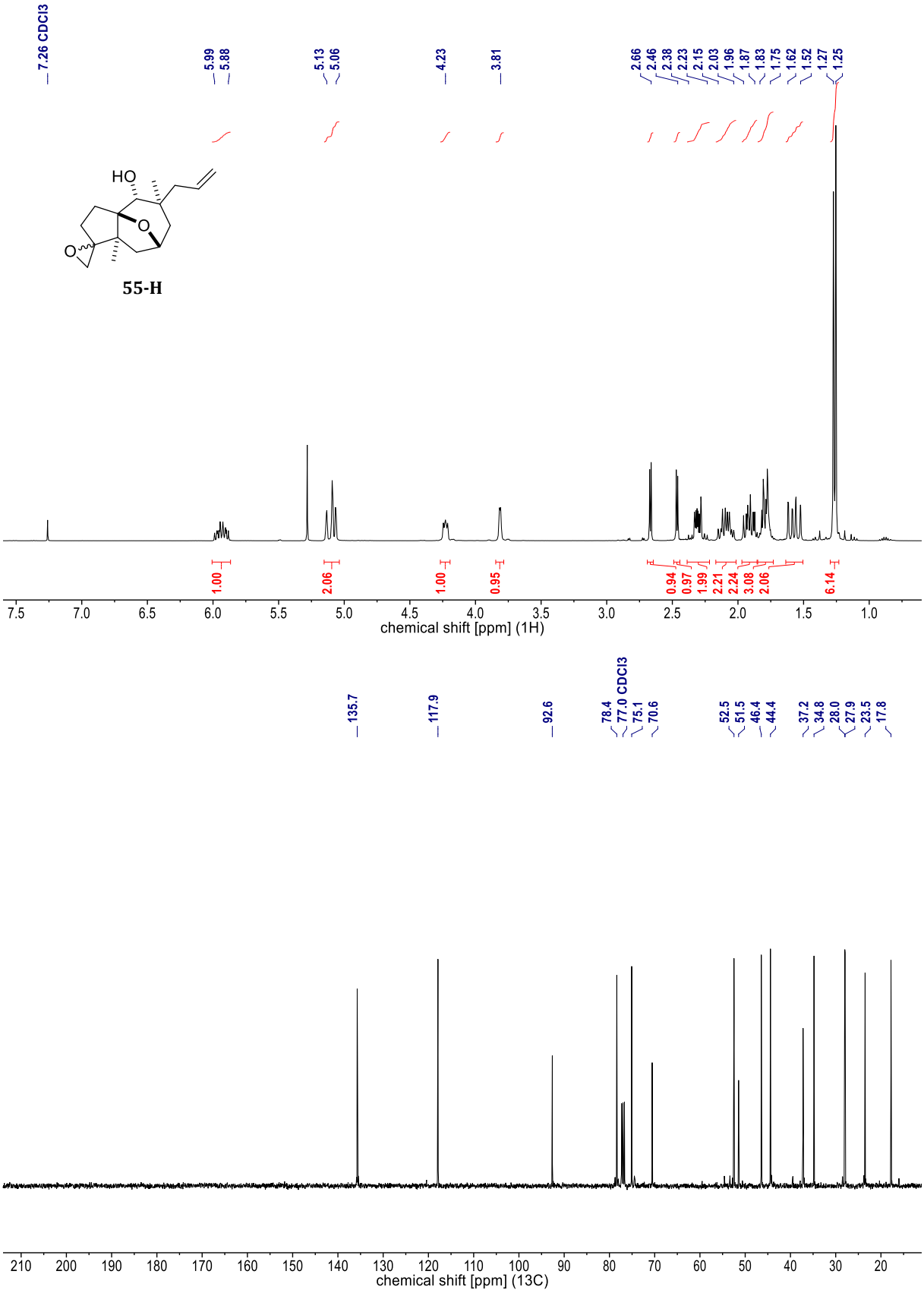

Figure 64. NMR spectra of **55-H** [^{1}H (400 MHz, $CDCl_3$) & ^{13}C (101 MHz, $CDCl_3$)].
More polar DS.

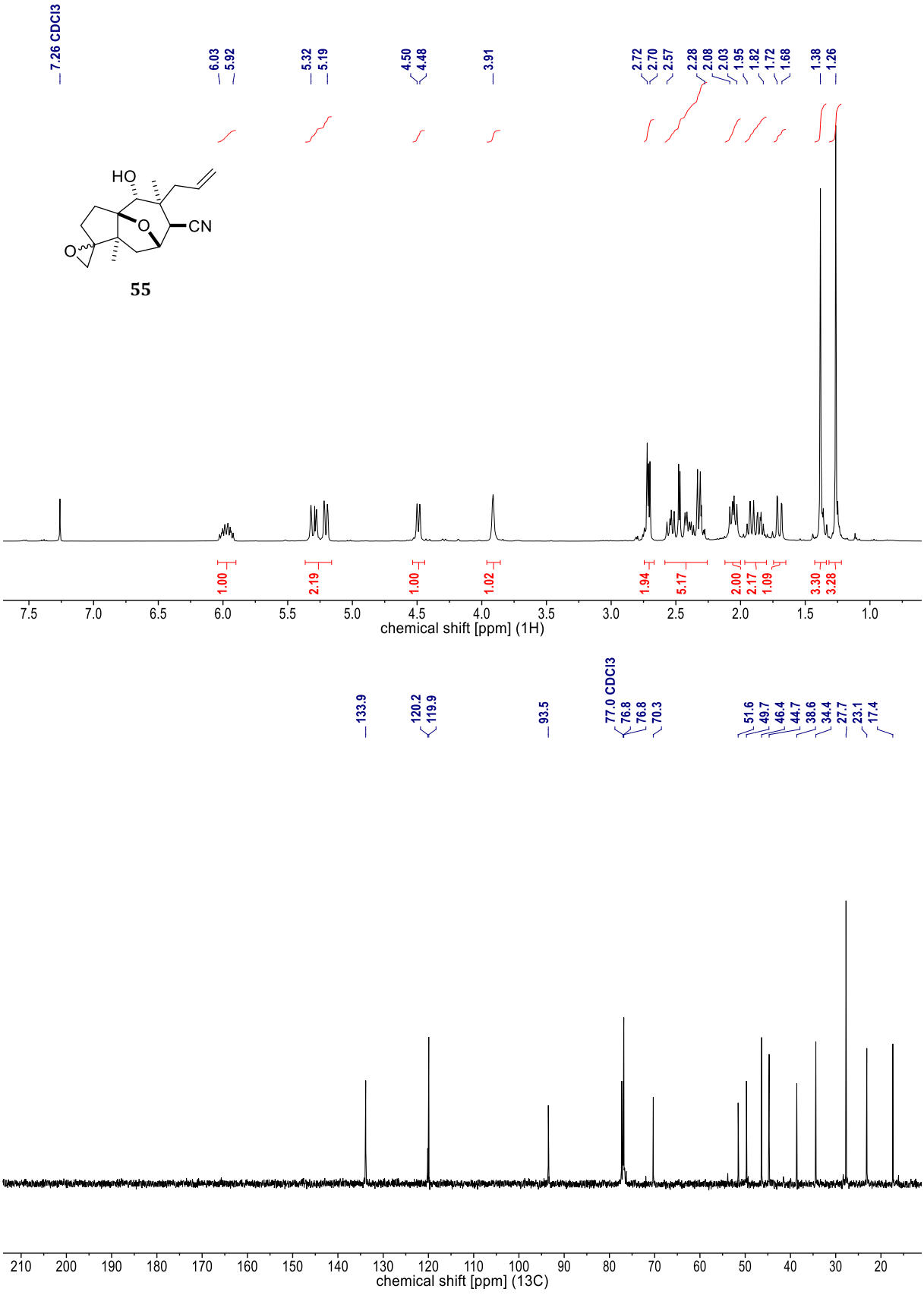

Figure 65. NMR spectra of **55** [^{1}H (400 MHz, $CDCl_3$) & ^{13}C (101 MHz, $CDCl_3$)].
More polar DS.

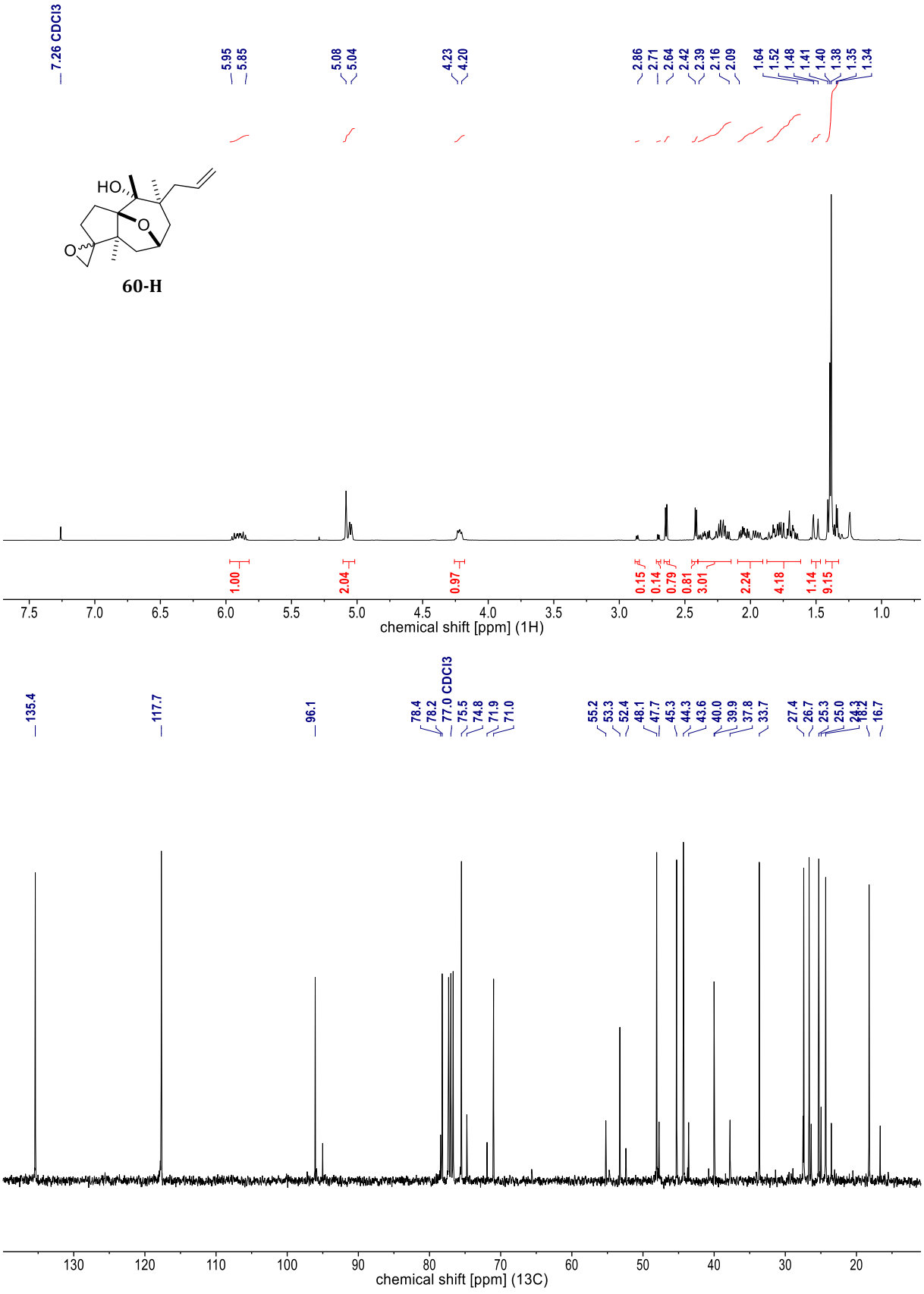

Figure 66. NMR spectra of **60-H** [^{1}H (400 MHz, $CDCl_3$) & ^{13}C (101 MHz, $CDCl_3$)].

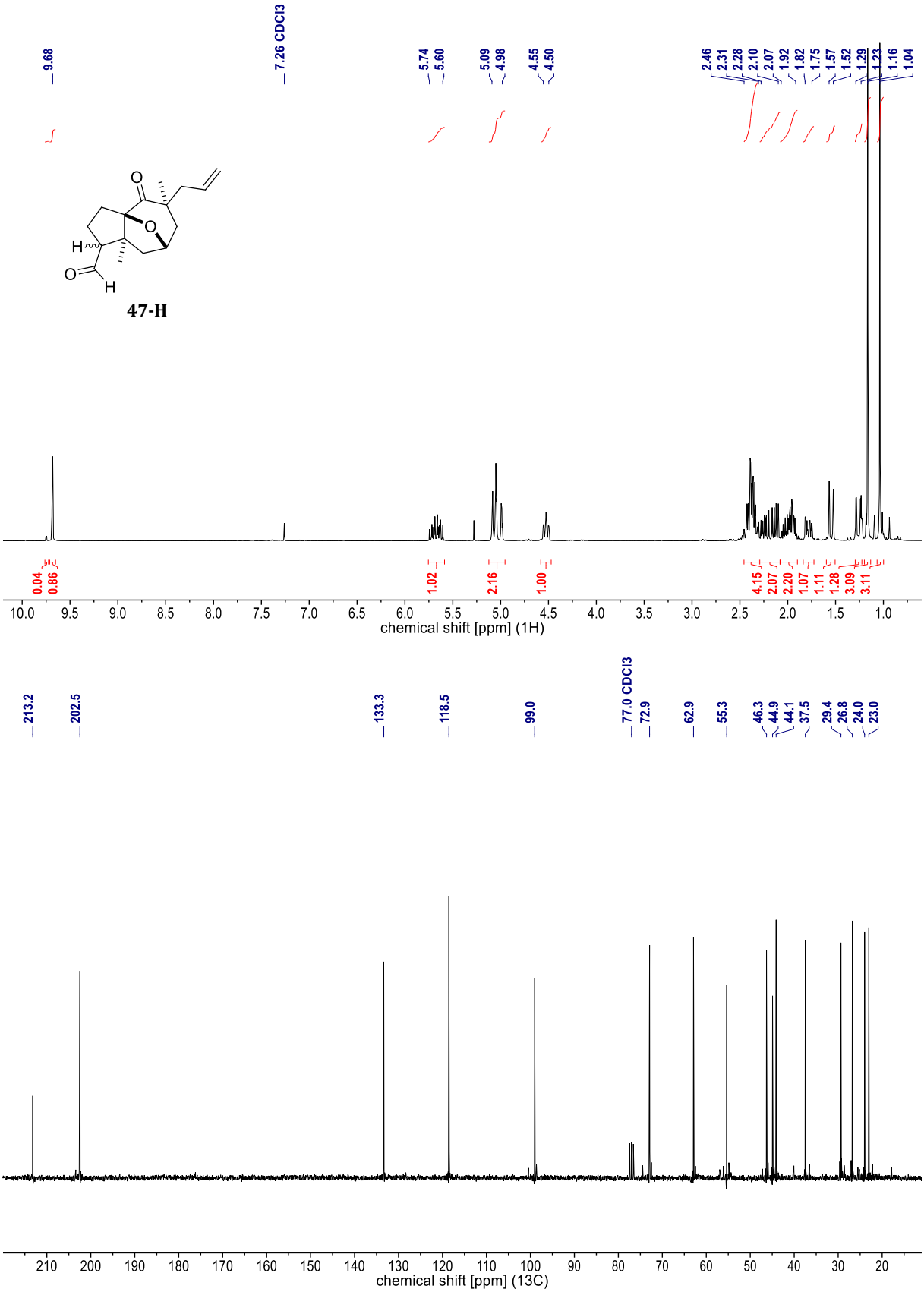

Figure 67. NMR spectra of **47-H** [^{1}H (300 MHz, $CDCl_3$) & ^{13}C (75 MHz, $CDCl_3$)].
Less polar DS.

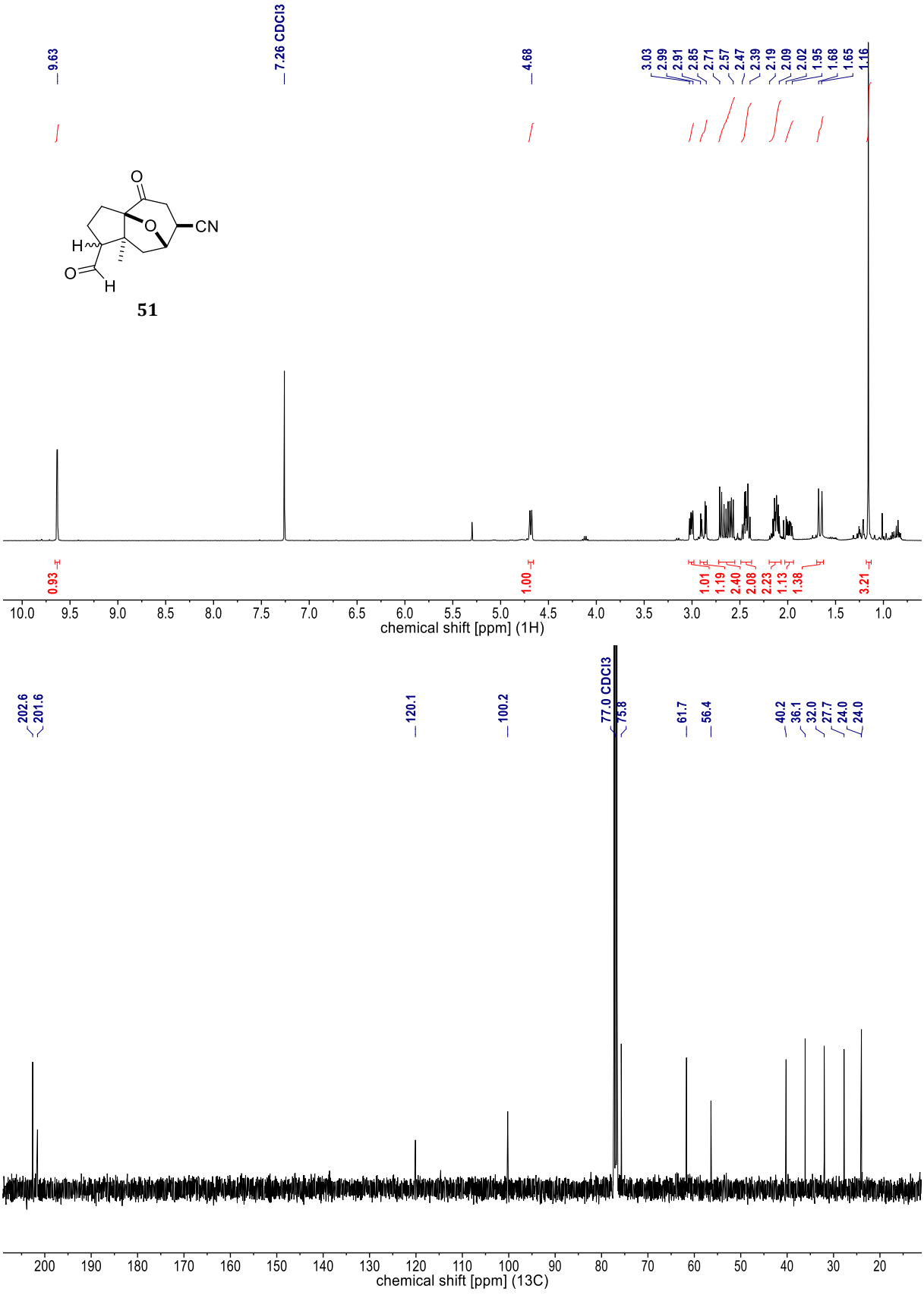

Figure 68. NMR spectra of **51** [^{1}H (400 MHz, $CDCl_3$) & ^{13}C (101 MHz, $CDCl_3$)].
Less polar DS.

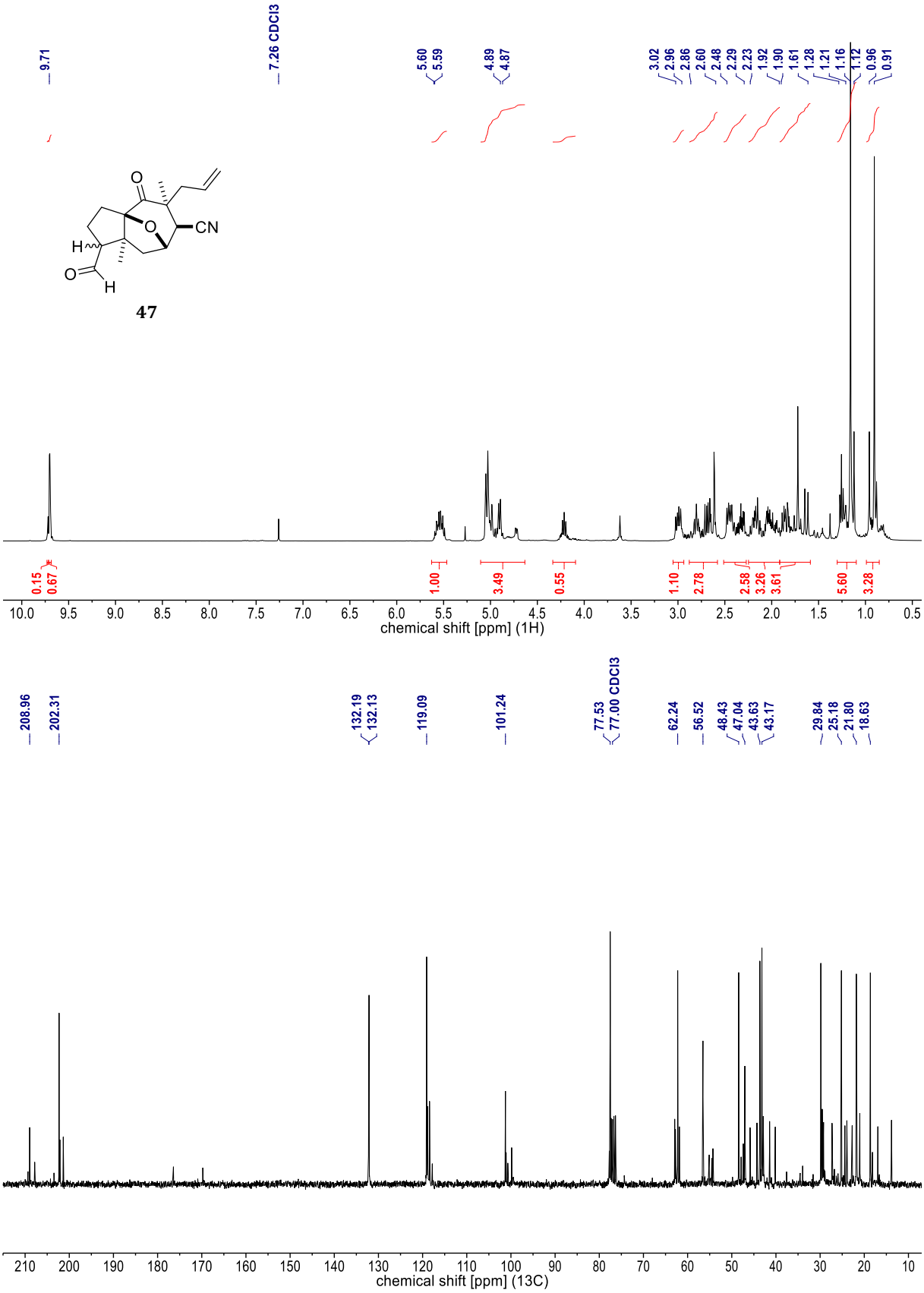

Figure 69. NMR spectra of **47** [^{1}H (400 MHz, $CDCl_3$) & ^{13}C (101 MHz, $CDCl_3$)].
Mostly more polar DS.

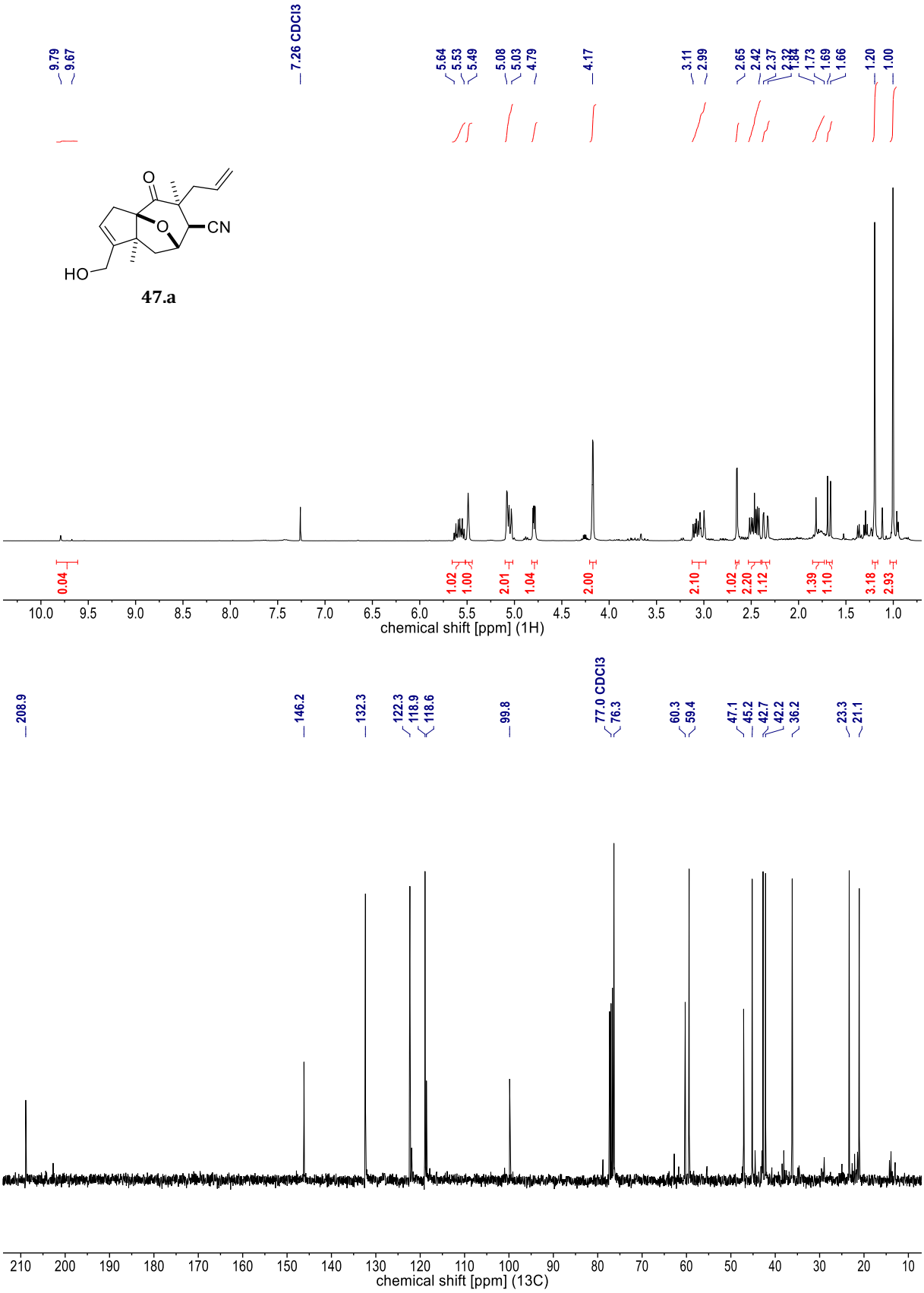

Figure 70. NMR spectra of **47.a** [^{1}H (400 MHz, $CDCl_3$) & ^{13}C (101 MHz, $CDCl_3$)].

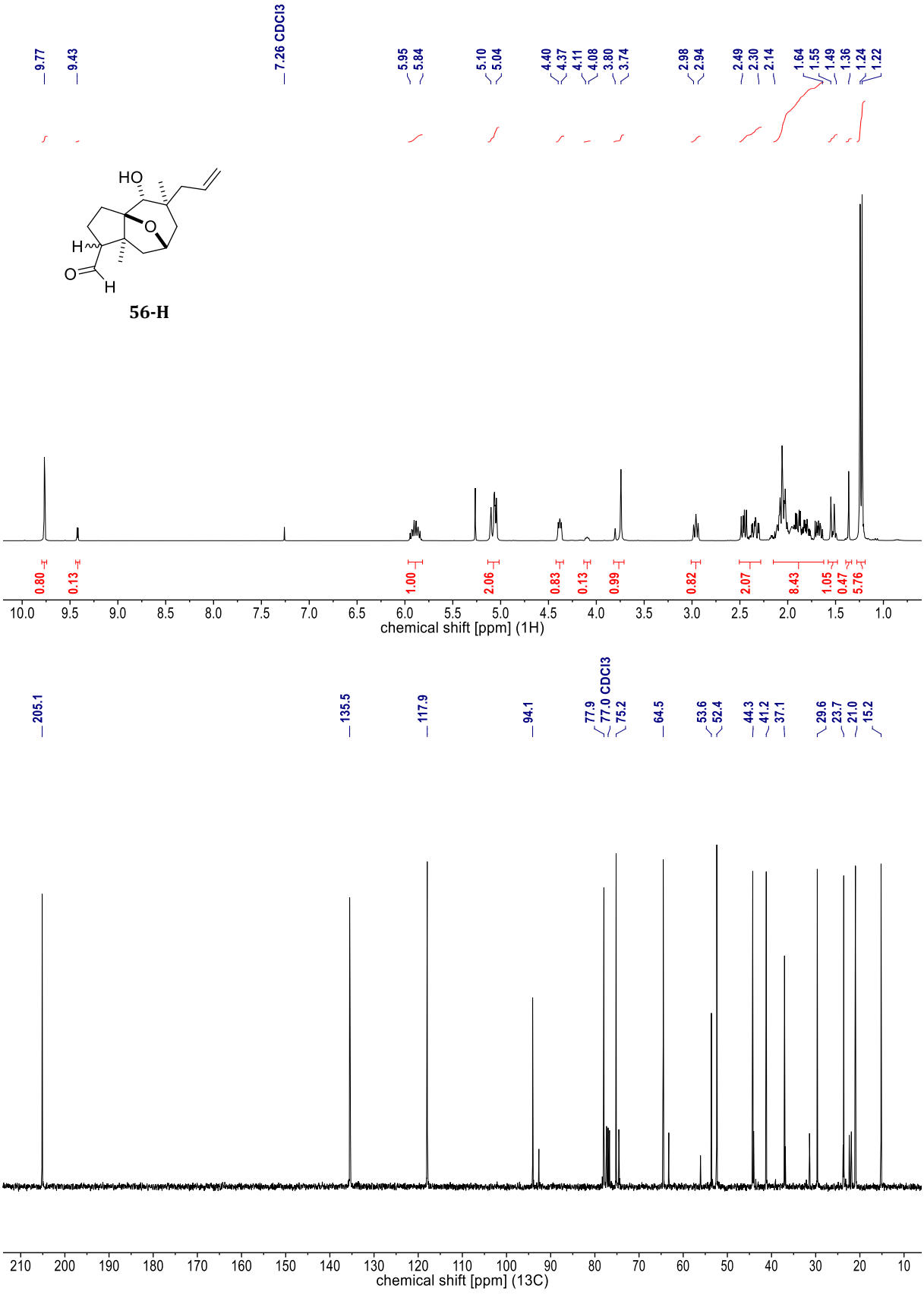

Figure 71. NMR spectra of **56-H** [^{1}H (400 MHz, $CDCl_3$) & ^{13}C (101 MHz, $CDCl_3$)].
Mostly more polar DS.

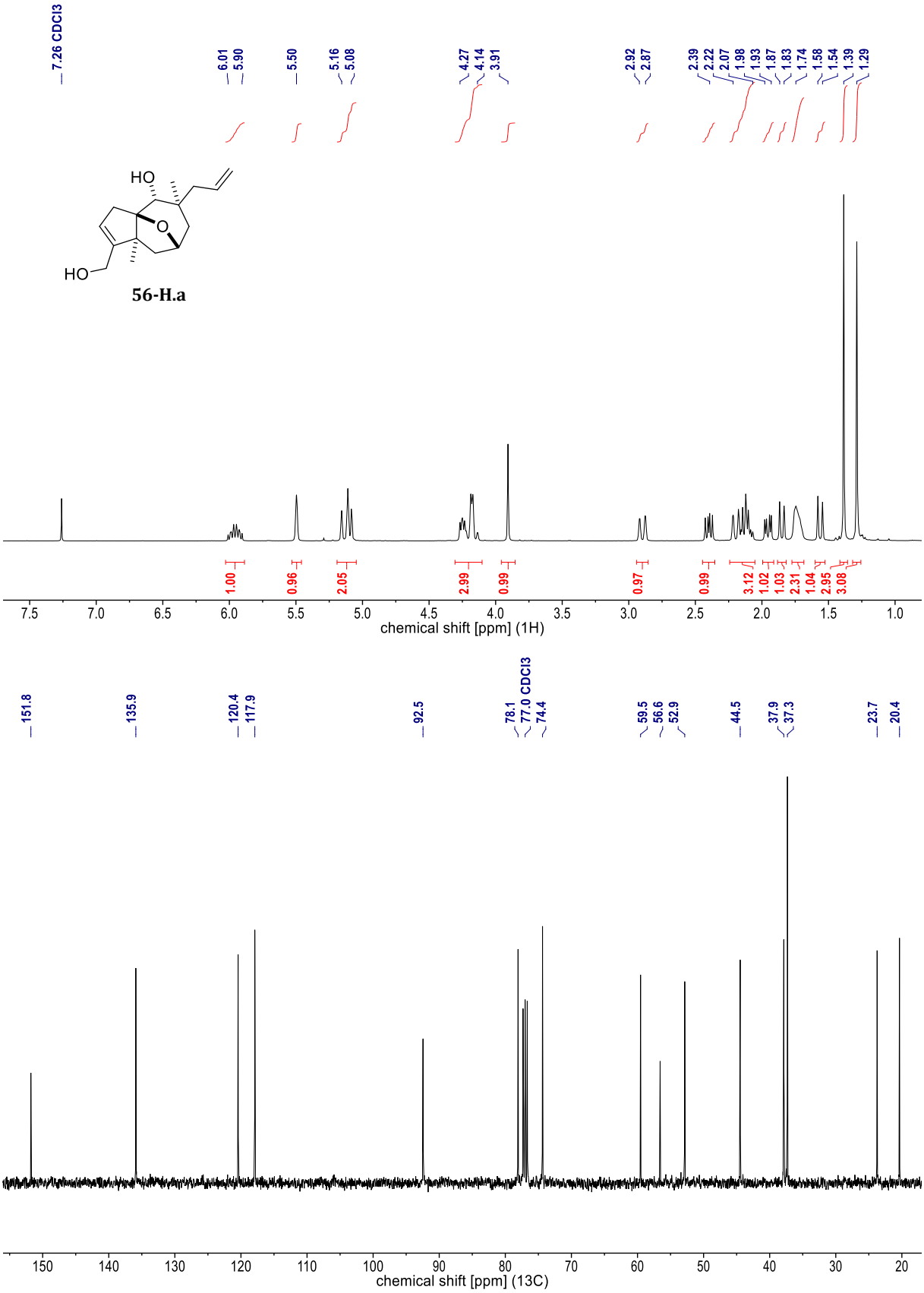

Figure 72. NMR spectra of **56-H.a** [^{1}H (400 MHz, $CDCl_3$) & ^{13}C (101 MHz, $CDCl_3$)].

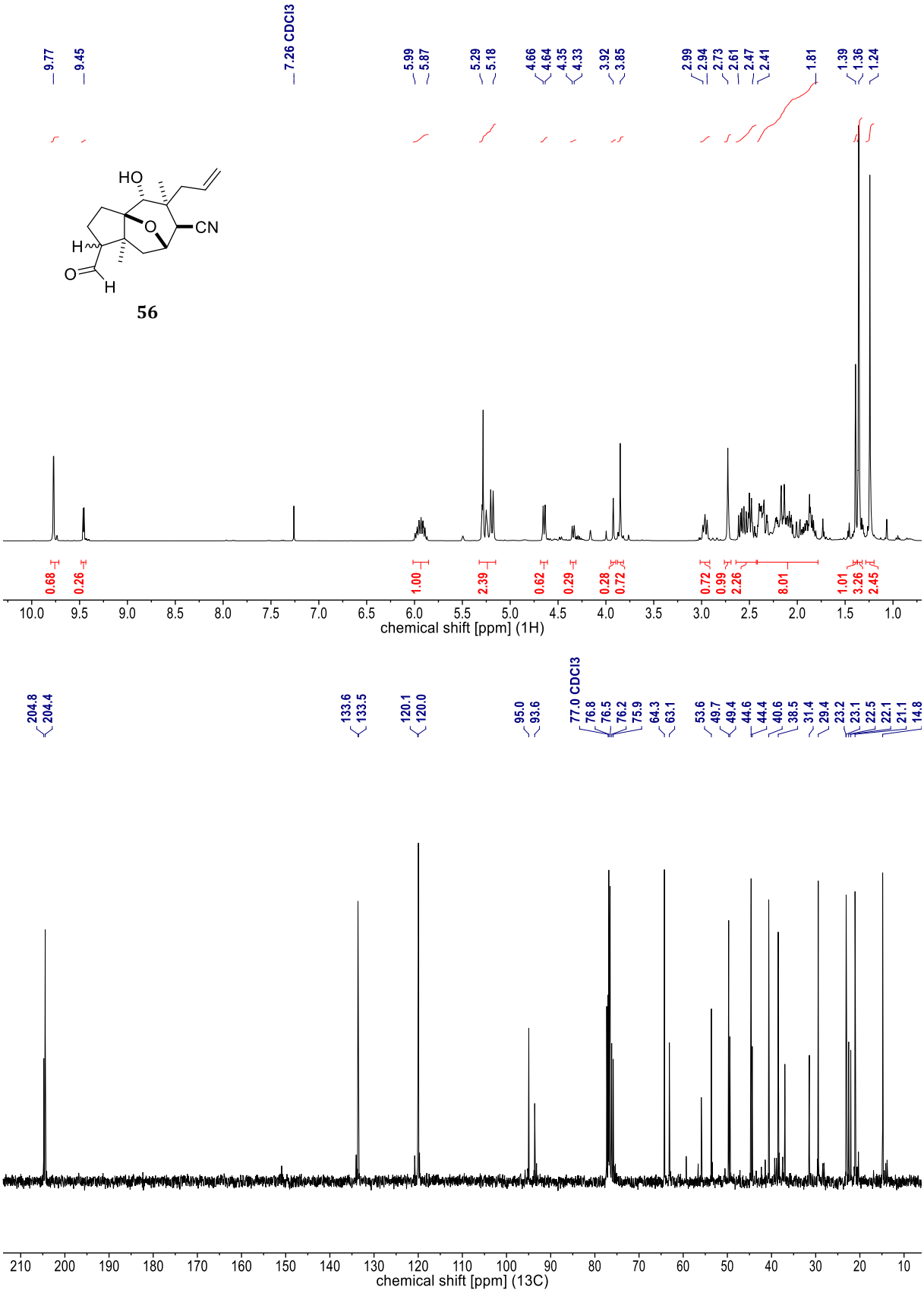

Figure 73. NMR spectra of **56** [^{1}H (400 MHz, $CDCl_3$) & ^{13}C (101 MHz, $CDCl_3$)]. *Diastereomeric mixture*.

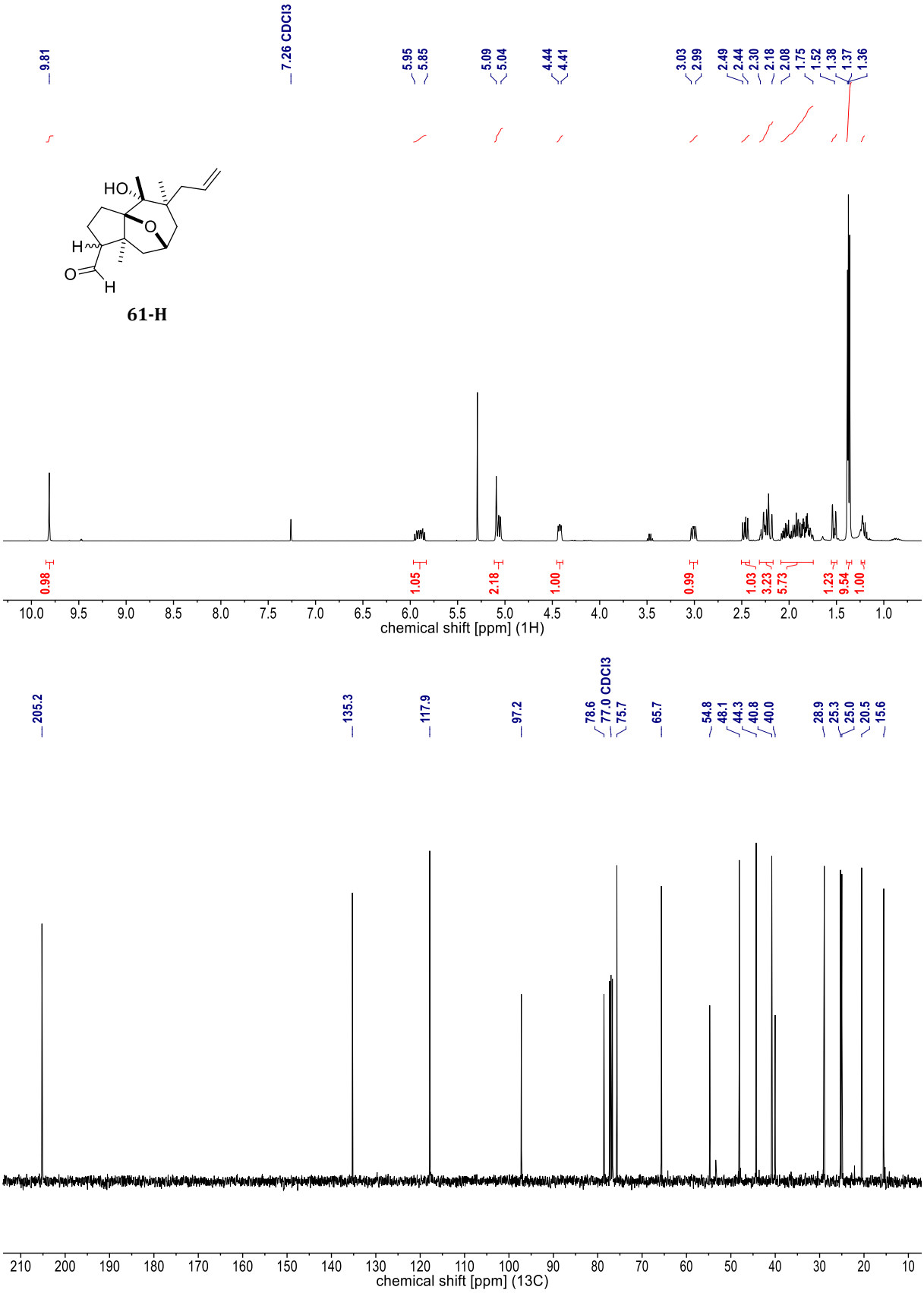

Figure 74. NMR spectra of **61-H** [^{1}H (400 MHz, $CDCl_3$) & ^{13}C (101 MHz, $CDCl_3$)].

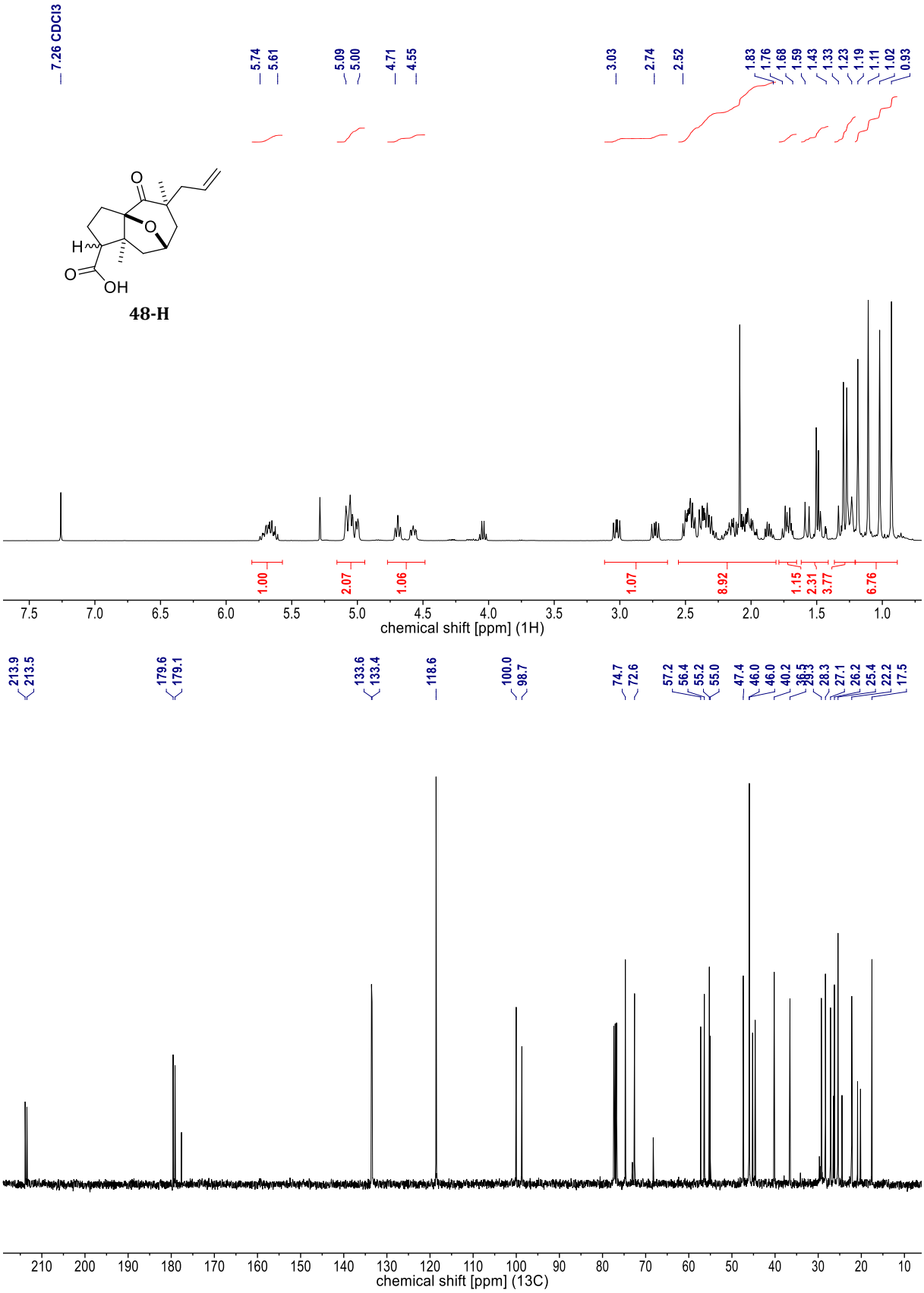

Figure 75. NMR spectra of **48-H** [^{1}H (400 MHz, $CDCl_3$) & ^{13}C (101 MHz, $CDCl_3$)]. *Diastereomeric mixture*.

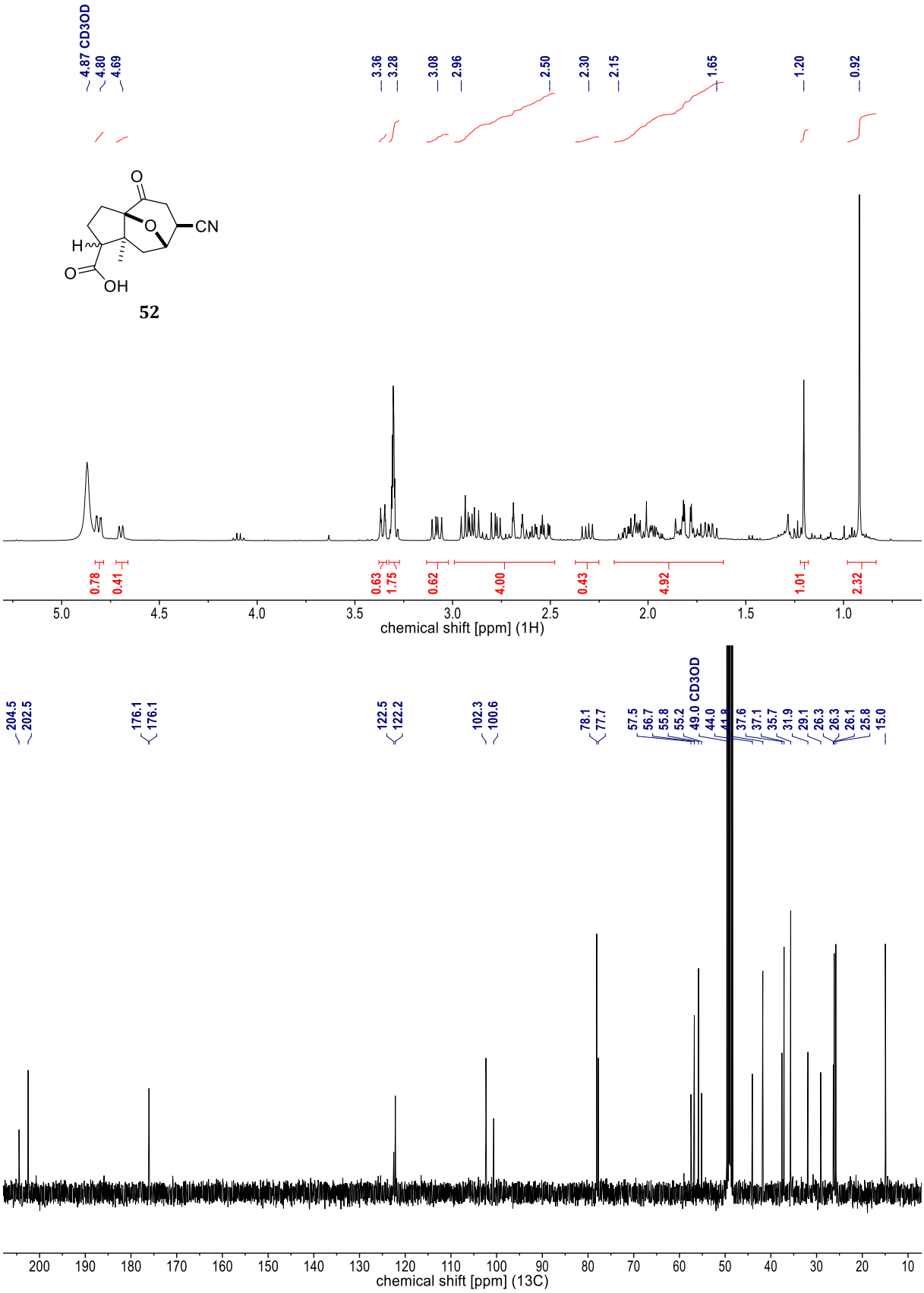

Figure 76. NMR spectra of **52** [^{1}H (400 MHz, CD_3OD) & ^{13}C (101 MHz, CD_3OD)]. *Diastereomeric mixture*.

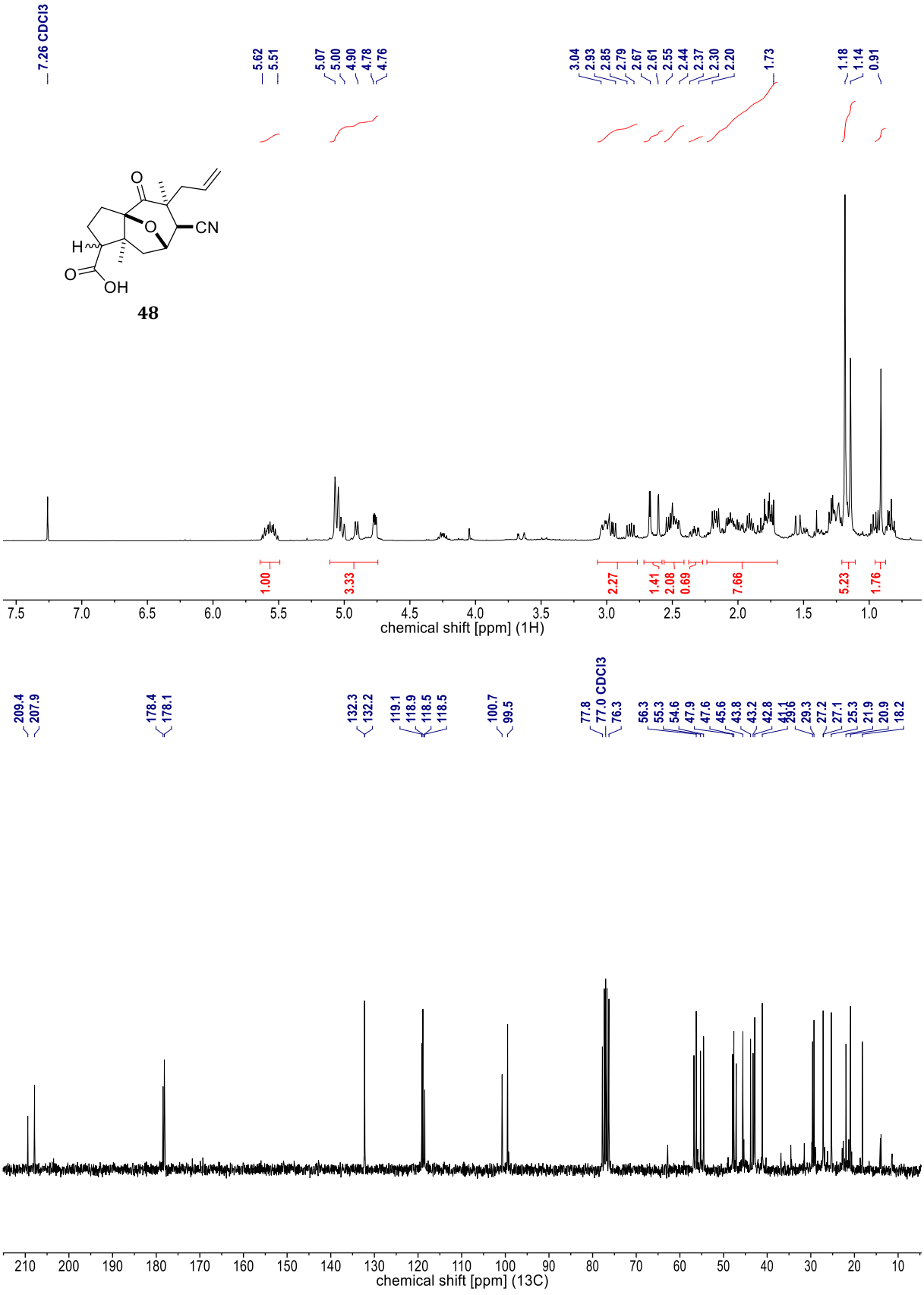

Figure 77. NMR spectra **48** [^{1}H (400 MHz, $CDCl_3$) & ^{13}C (101 MHz, $CDCl_3$)]. *Diastereomeric mixture*.

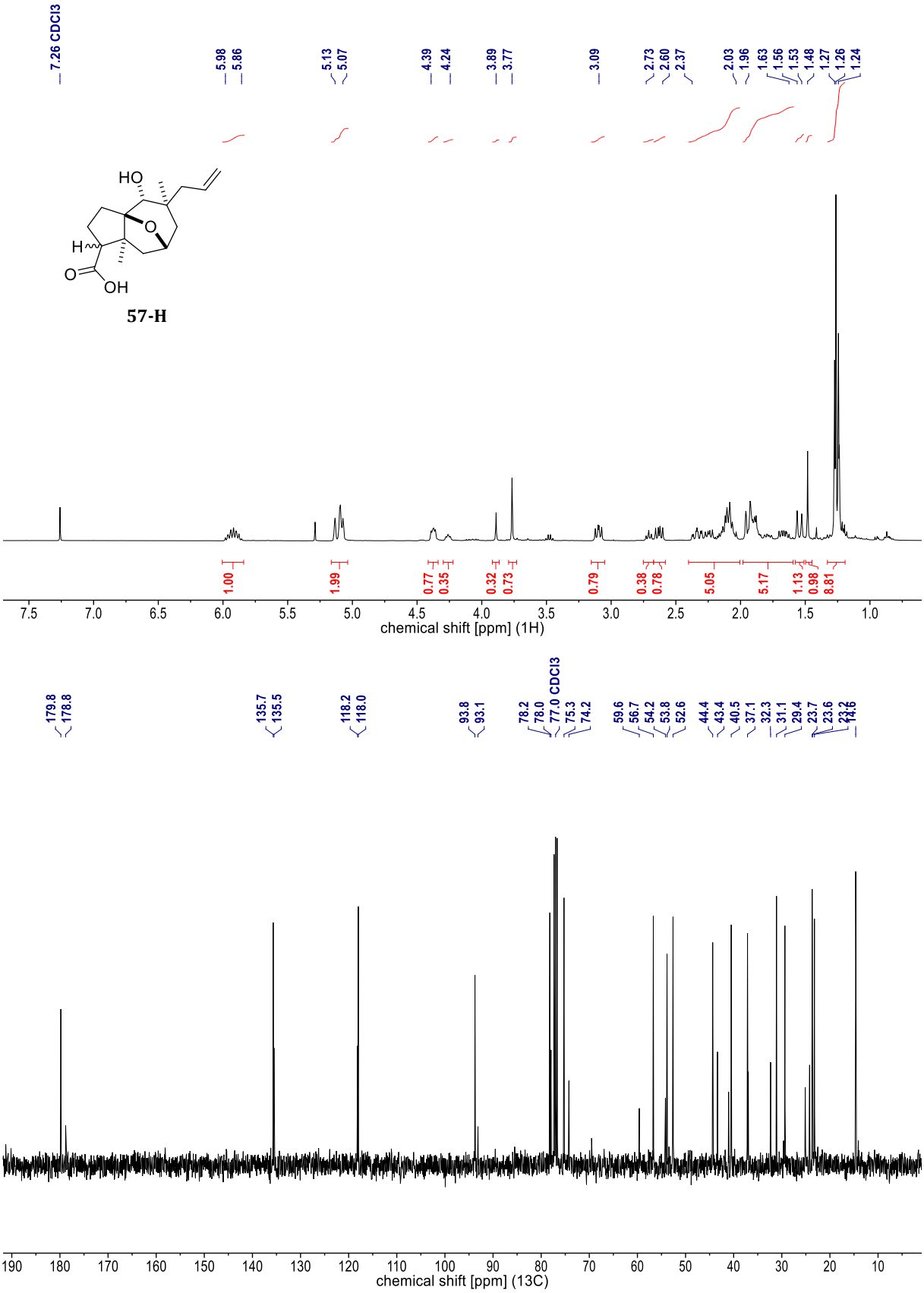

Figure 78. NMR spectra of **57-H** [^{1}H (400 MHz, $CDCl_3$) & ^{13}C (101 MHz, $CDCl_3$)]. *Diastereomeric mixture*.

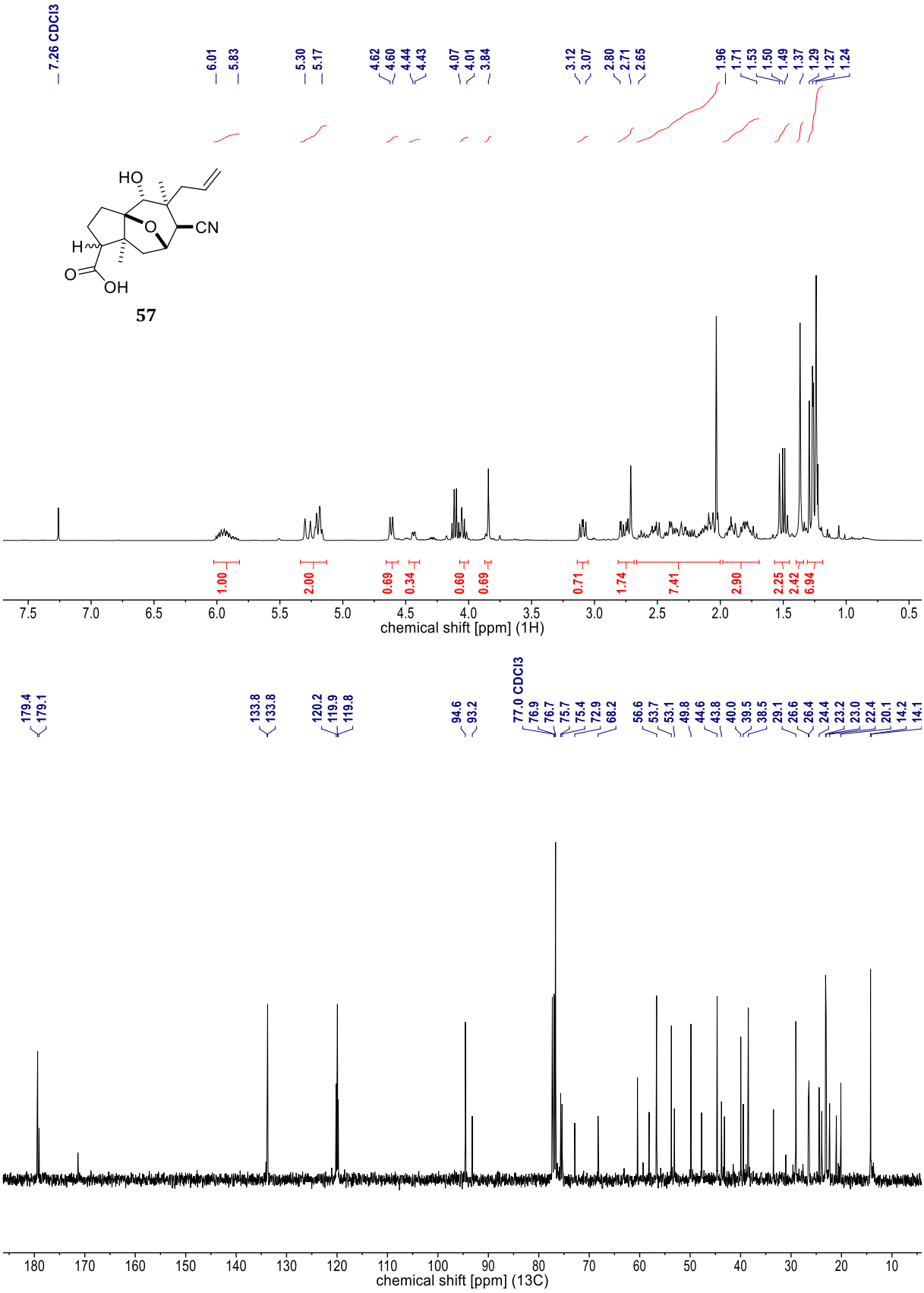

Figure 79. NMR spectra of **57** [^{1}H (400 MHz, $CDCl_3$) & ^{13}C (101 MHz, $CDCl_3$)]. *Diastereomeric mixture*.

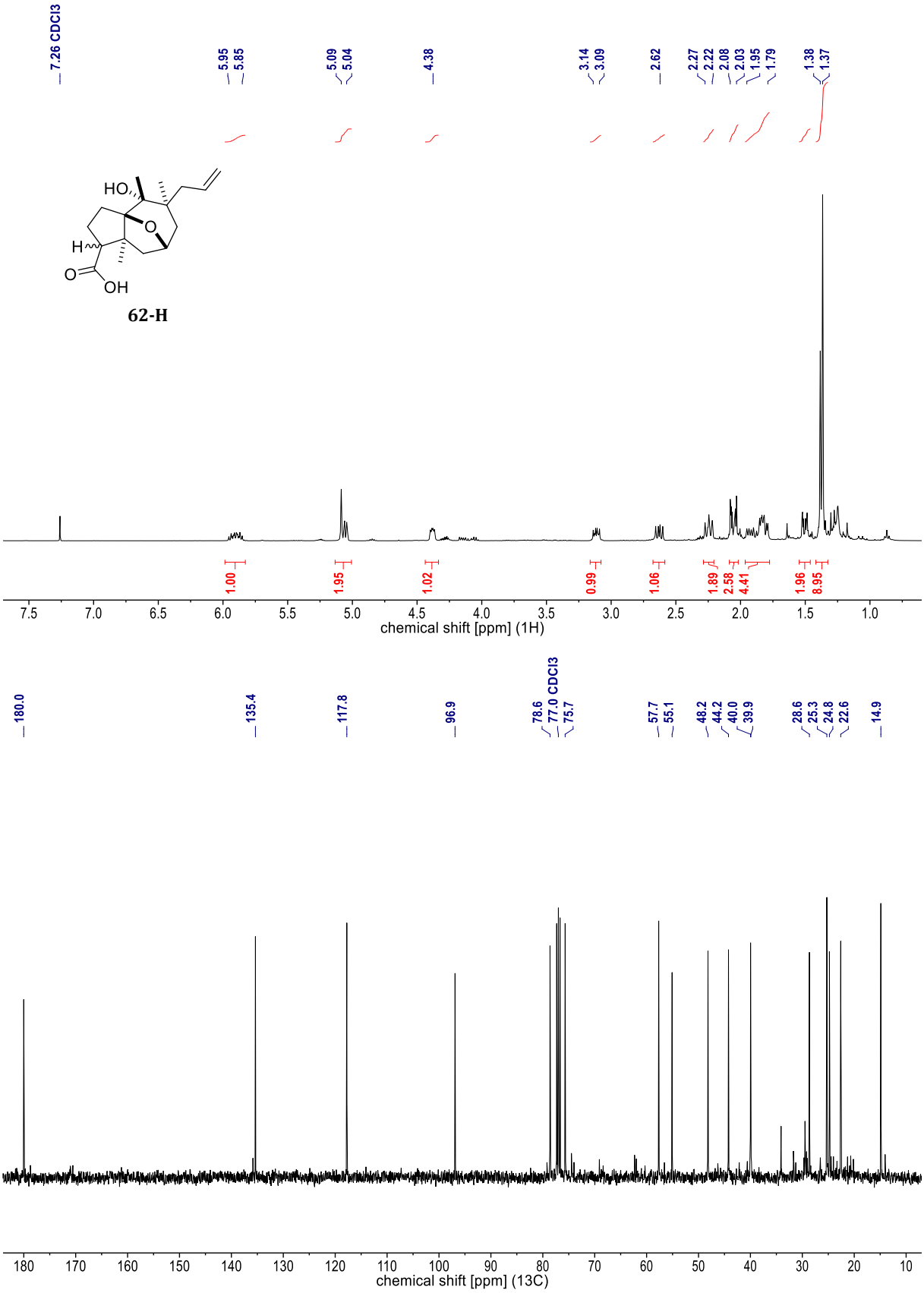

Figure 80. NMR spectra of **62-H** [^{1}H (400 MHz, $CDCl_3$) & ^{13}C (101 MHz, $CDCl_3$)]. *Diastereomeric mixture*.

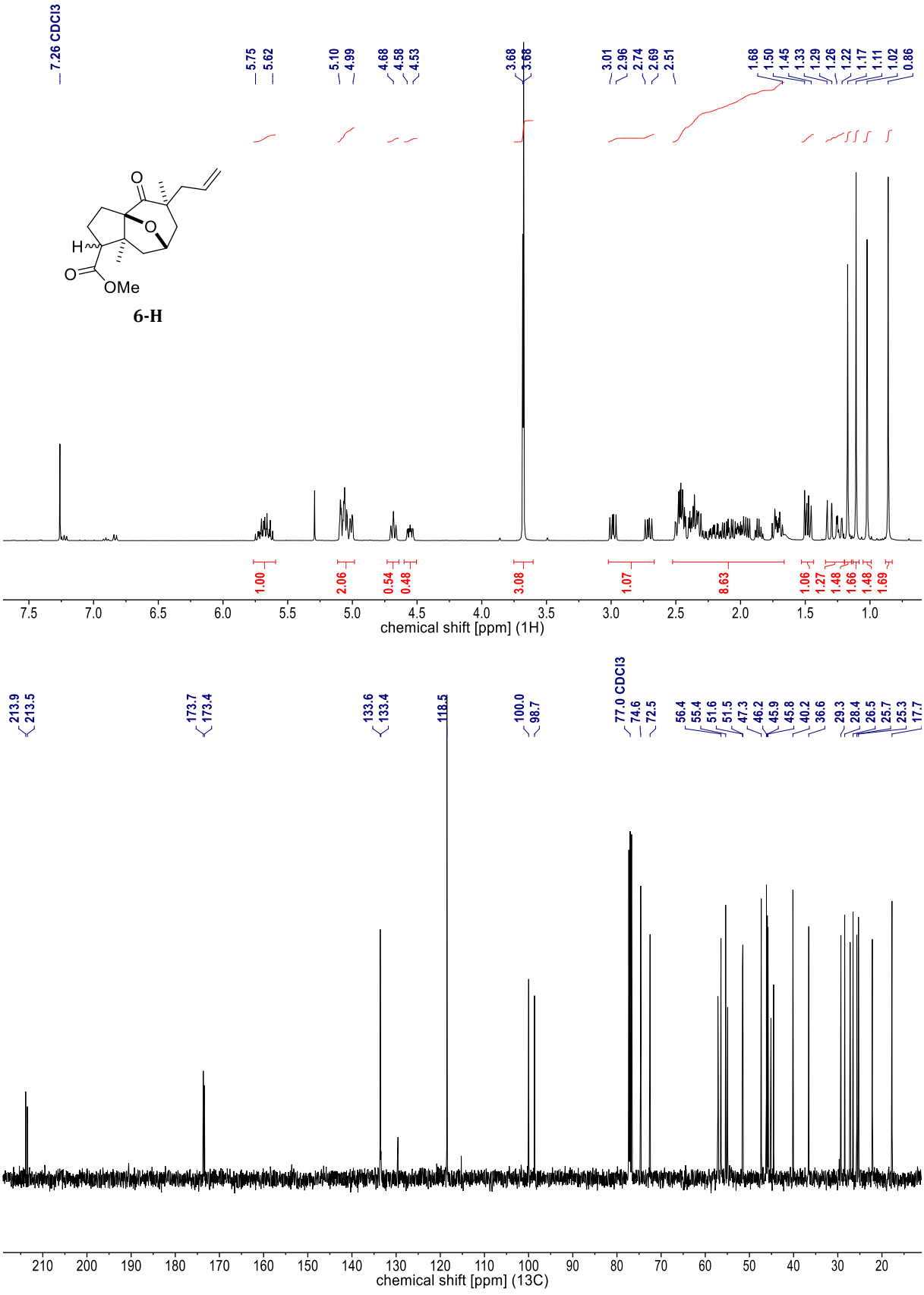

Figure 81. NMR spectra of **6-H** [^{1}H (400 MHz, $CDCl_3$) & ^{13}C (101 MHz, $CDCl_3$)]. *Diastereomeric mixture*.

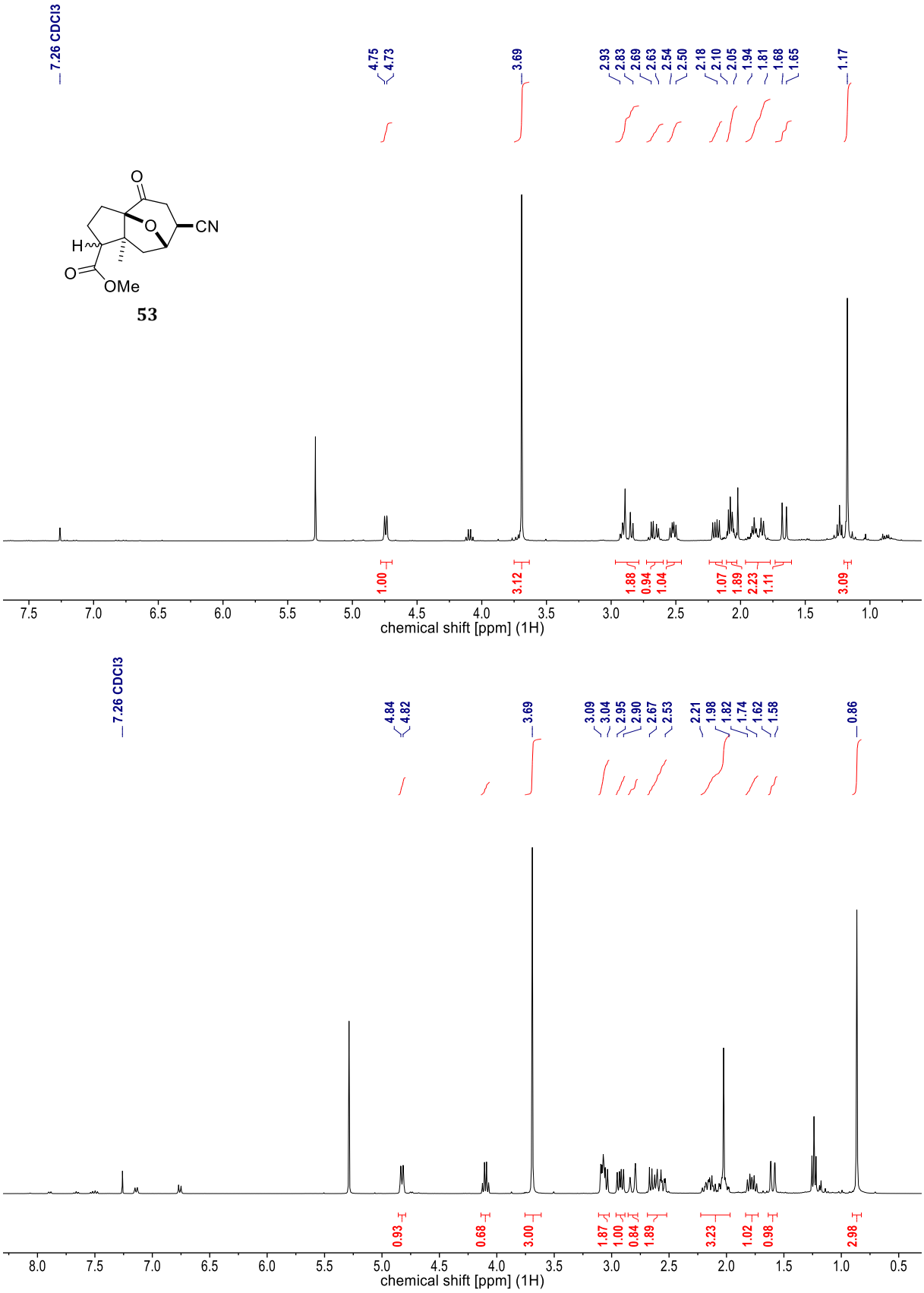

Figure 82. NMR spectra of **53** [^{1}H (400 MHz, $CDCl_3$)].
Upper spectrum: *less polar DS*; lower spectrum: *more polar DS*.
Significant amounts of residual solvents (DCM/EA) are evident.

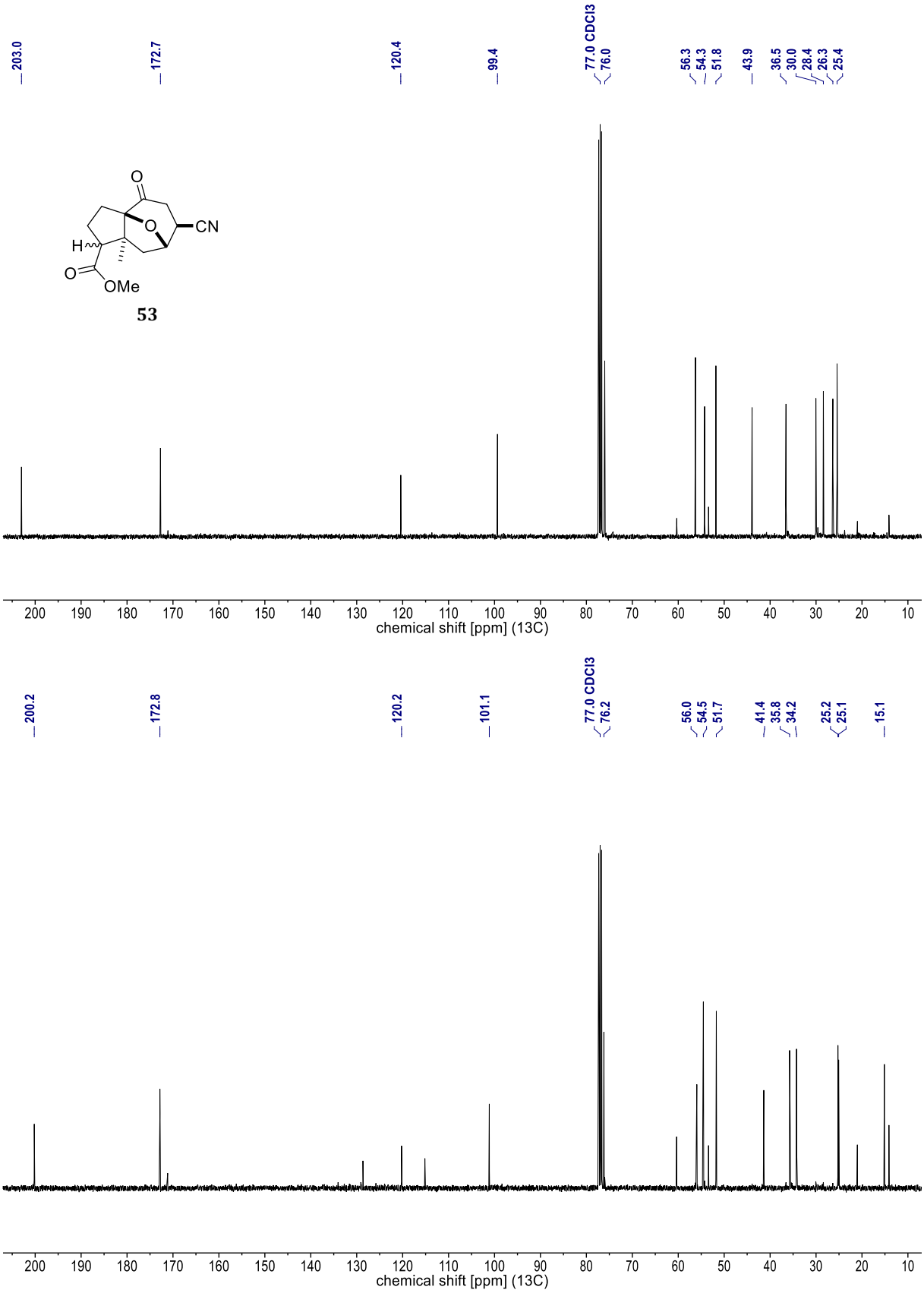

Figure 83. NMR spectra of **53** [^{13}C (101 MHz, $CDCl_3$)].
Upper spectrum: *less polar DS*; lower spectrum: *more polar DS*.
Significant amounts of residual solvents (DCM/EA) are evident.

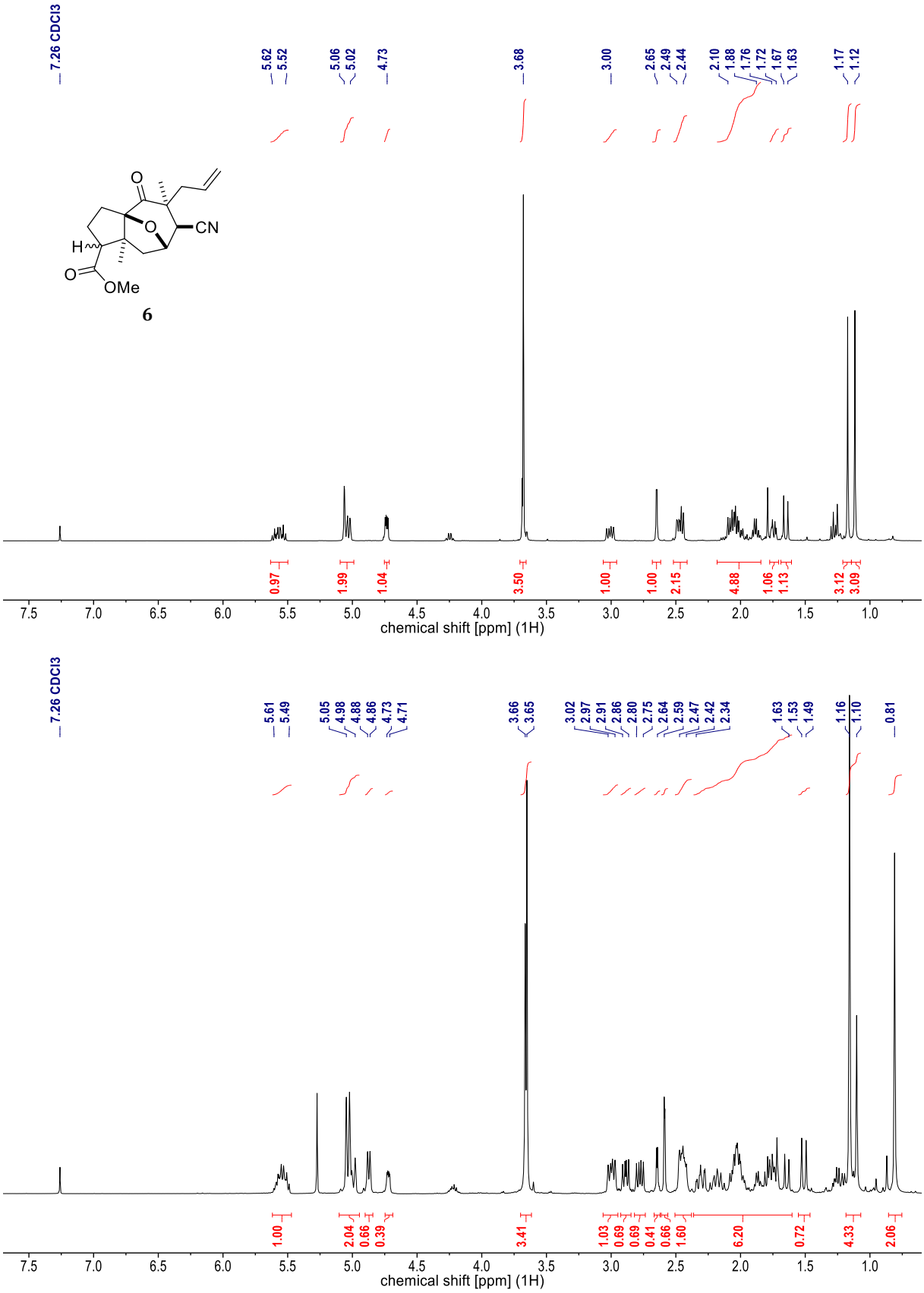

Figure 84. NMR spectra of **6** [^{1}H (400 MHz, $CDCl_3$)].
Upper spectrum: *less polar DS*; lower spectrum: *diastereomeric mixture*.

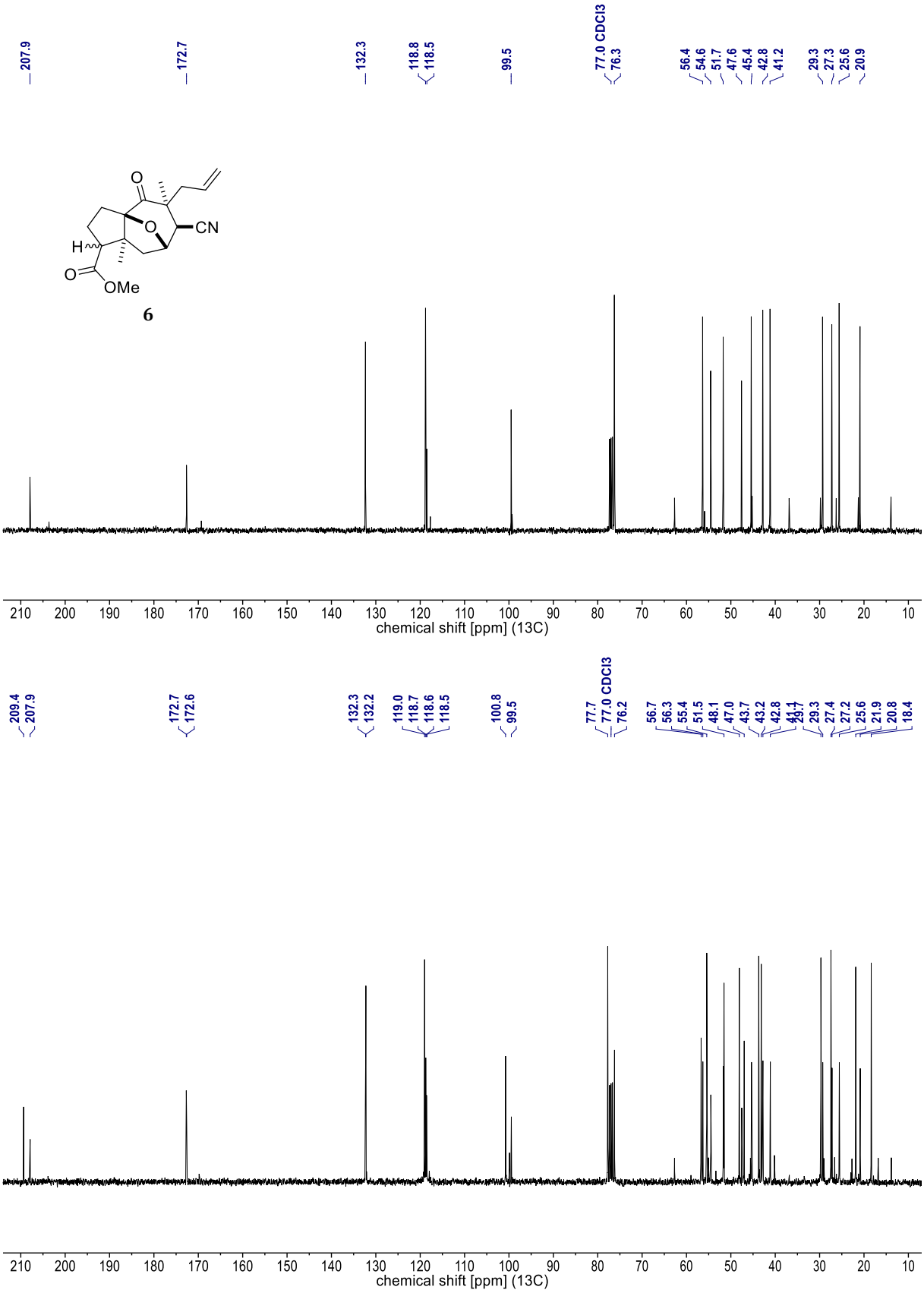

Figure 85. NMR spectra of **6** [^{13}C (101 MHz, $CDCl_3$)].
Upper spectrum: *less polar DS*; lower spectrum: *diastereomeric mixture*.

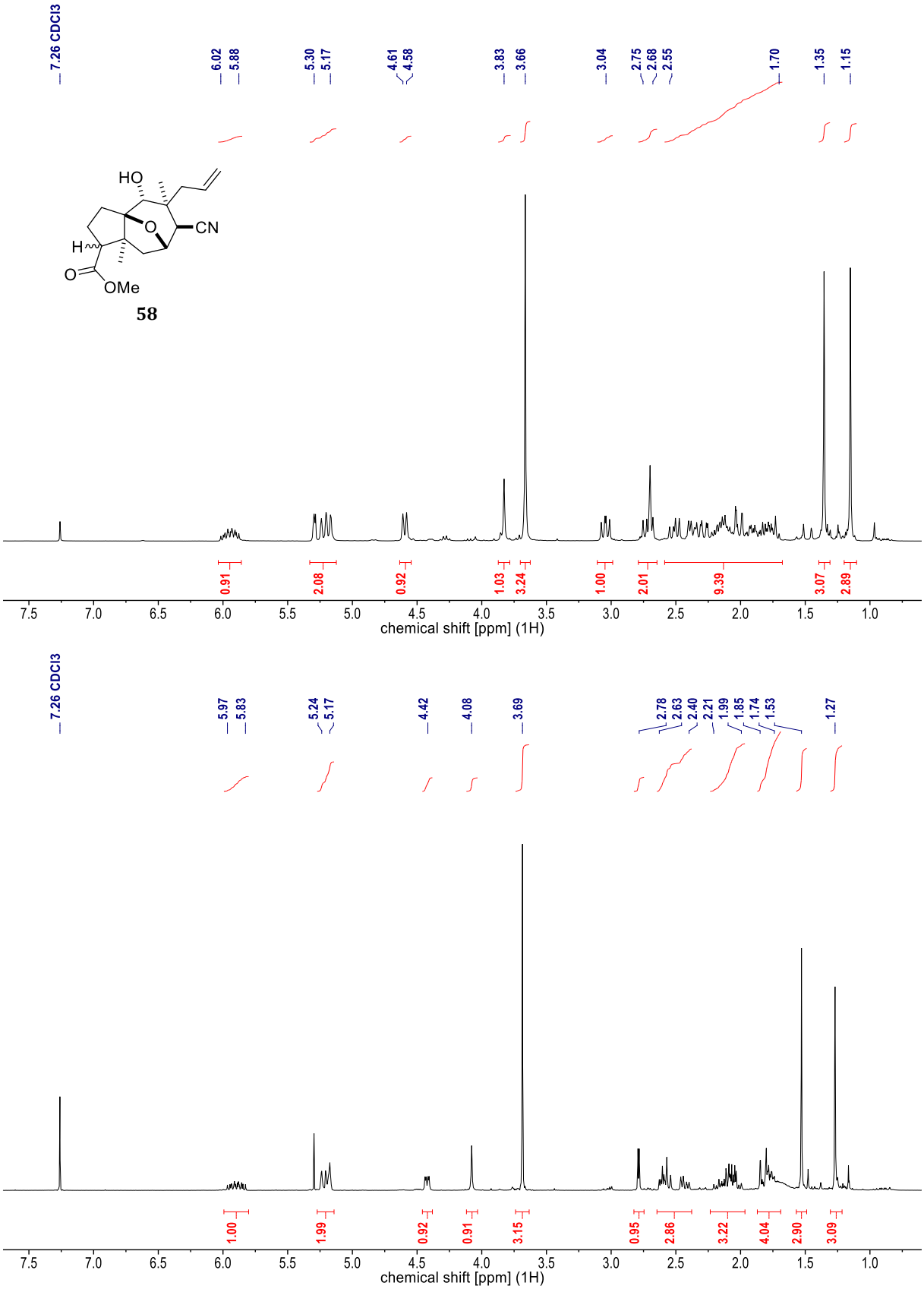

Figure 86. NMR spectra of **58** [^{1}H (300 MHz, $CDCl_3$)].
Upper spectrum: *more polar DS*; lower spectrum: *less polar DS*.

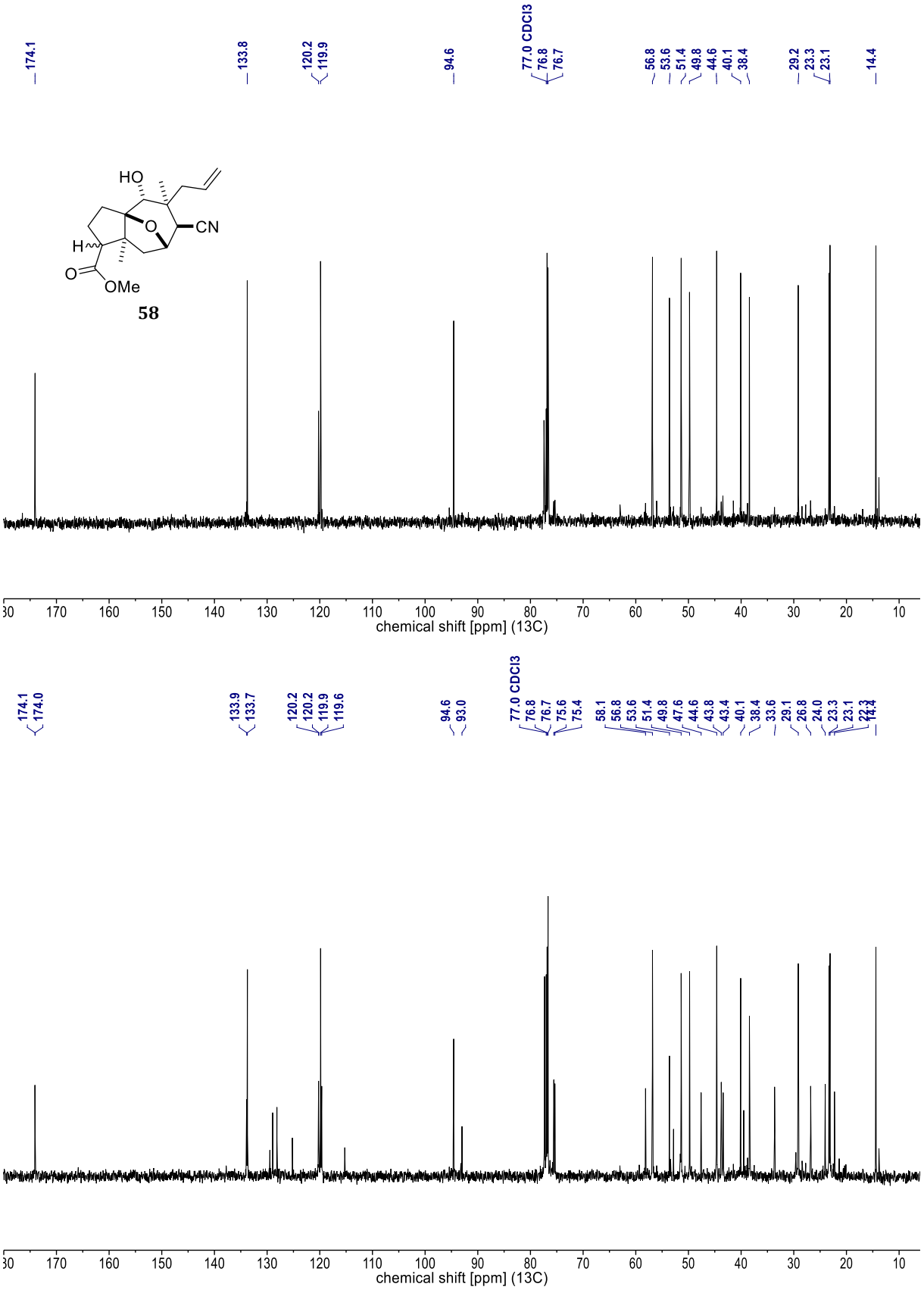

Figure 87. NMR spectra [^{13}C (75 and 101 MHz, $CDCl_3$)] of **58**.
Upper spectrum [75 MHz]: *more polar DS*; lower spectrum: crude product [101 MHz].

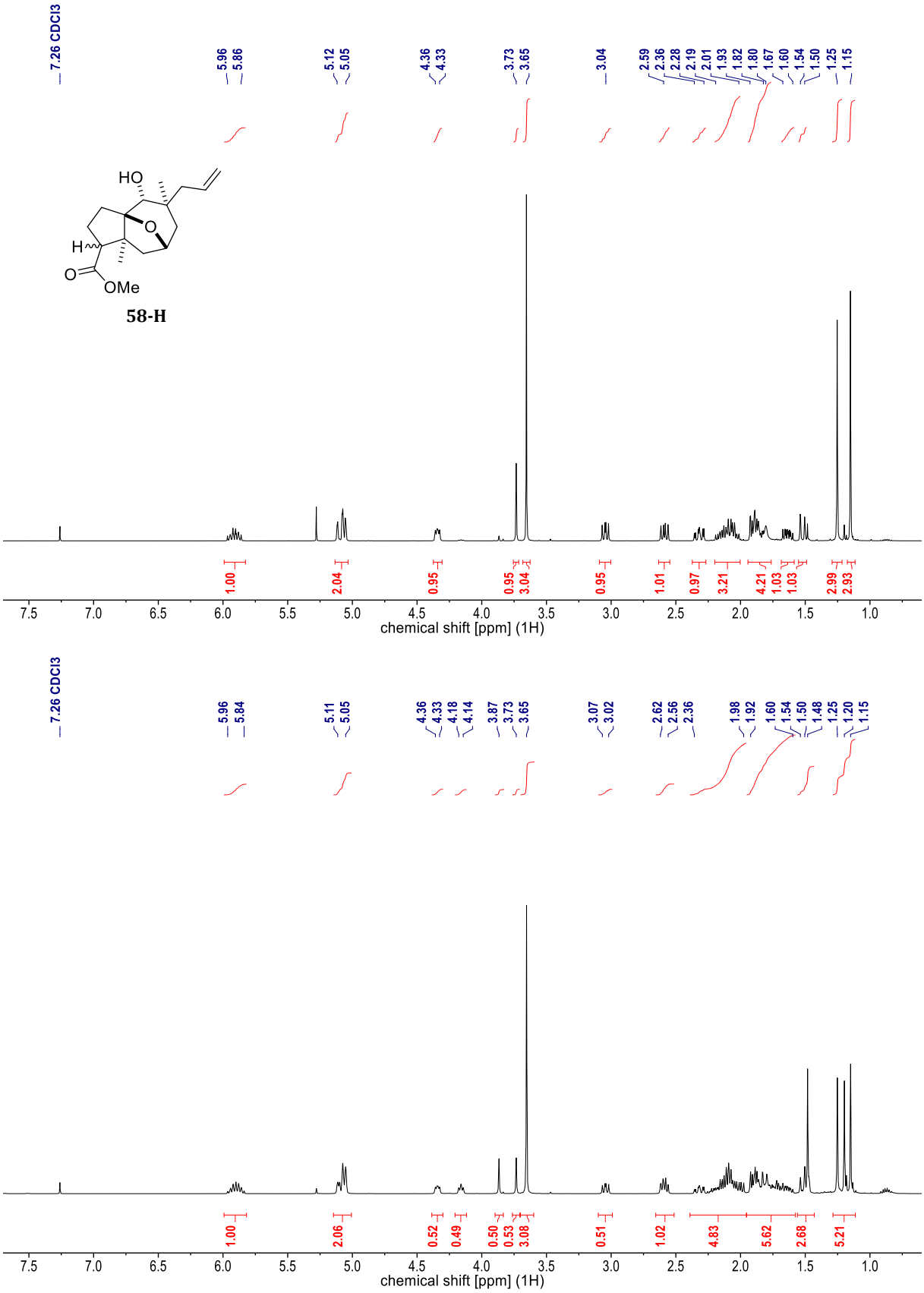

Figure 88. NMR spectra of **58-H** [^{1}H (400 MHz, $CDCl_3$)]
Upper spectrum: *less polar DS*; lower spectrum: *diastereomeric mixture*.

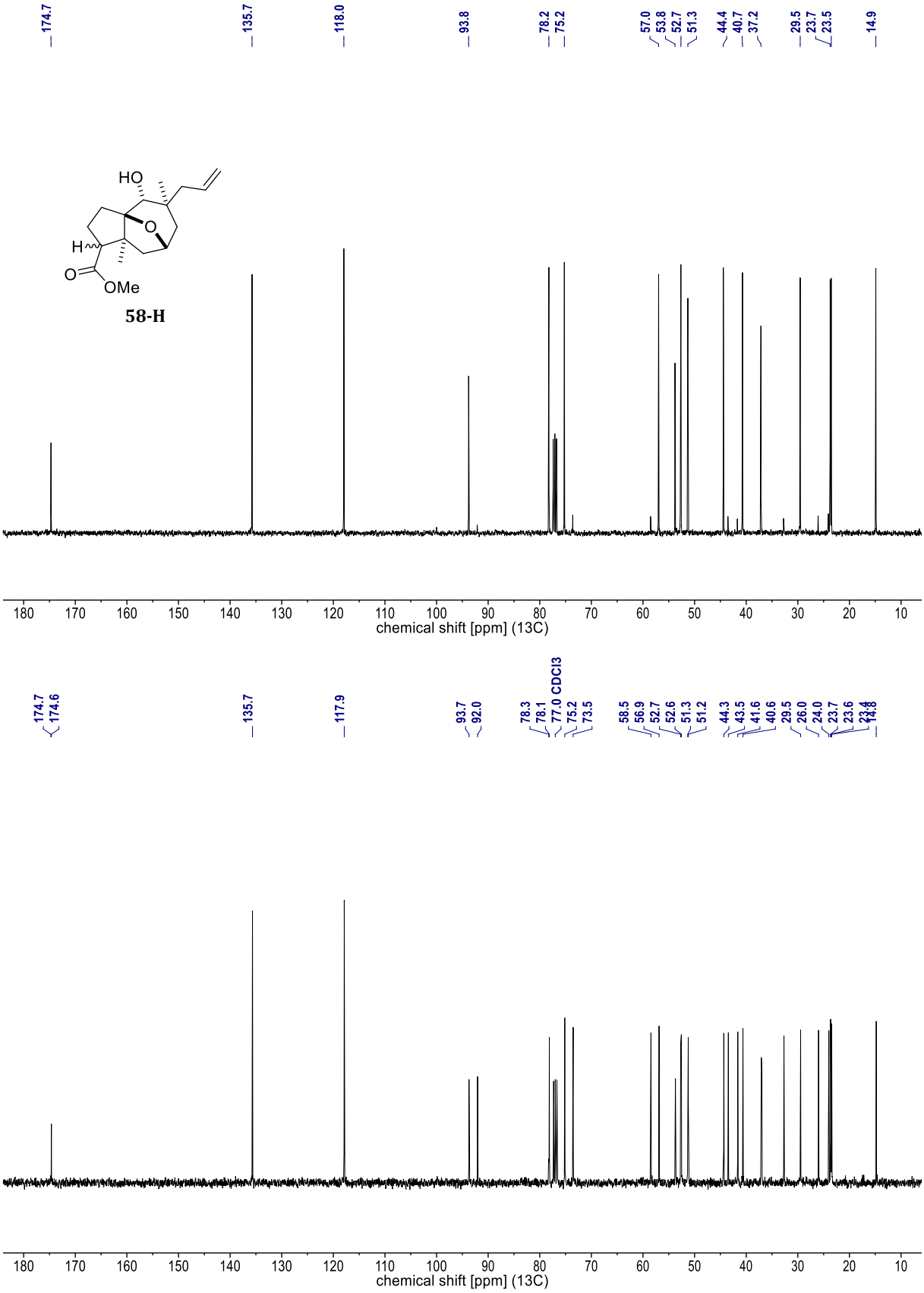

Figure 89. NMR spectra of **58-H** [^{13}C ($CDCl_3$, 101 MHz)].
Upper spectrum: *less polar DS*; lower spectrum: *diastereomeric mixture*.

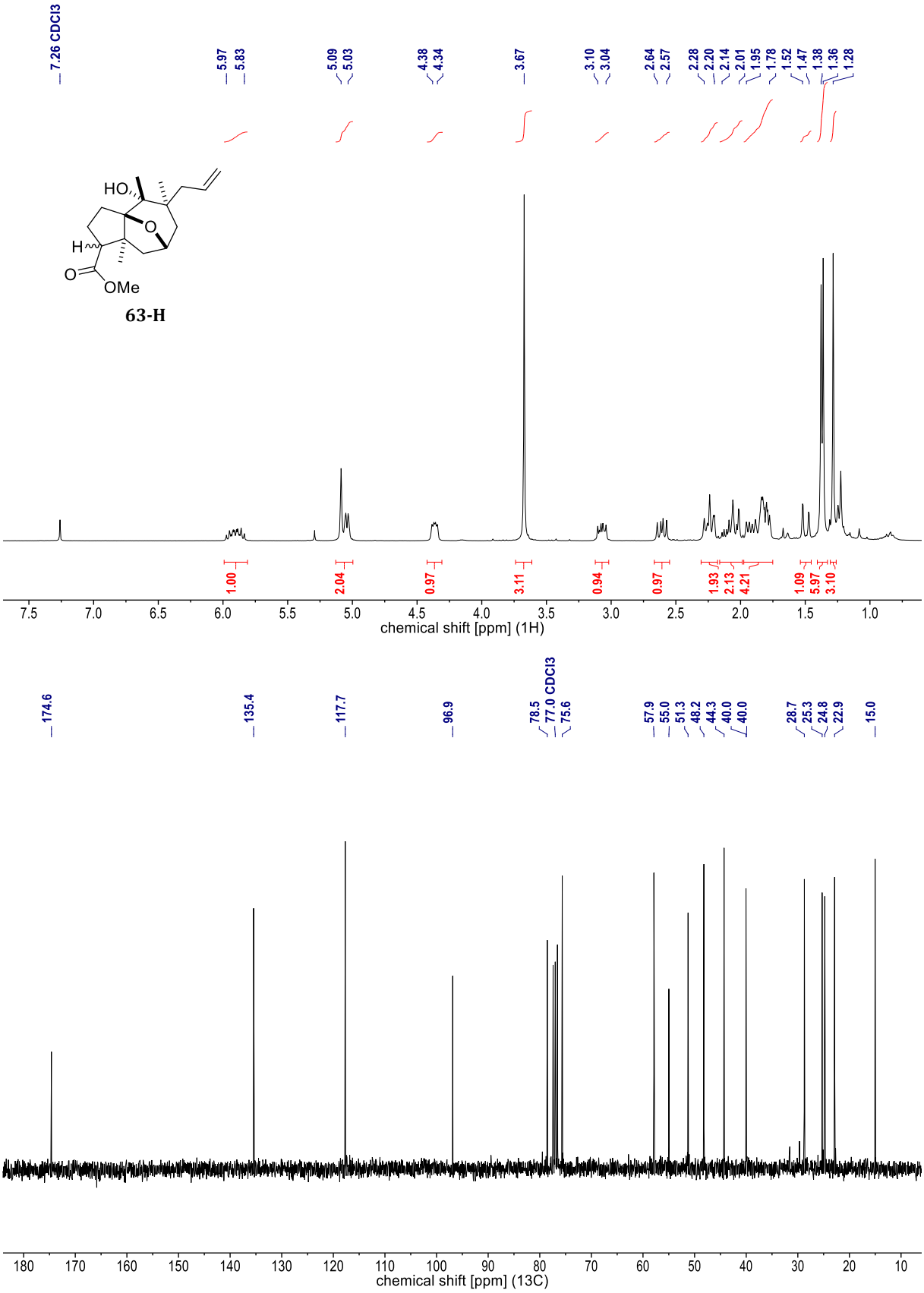

Figure 90. NMR spectra of **63-H** [^{1}H (300 MHz, $CDCl_3$) & ^{13}C (75 MHz, $CDCl_3$)].
Major, less polar DS.

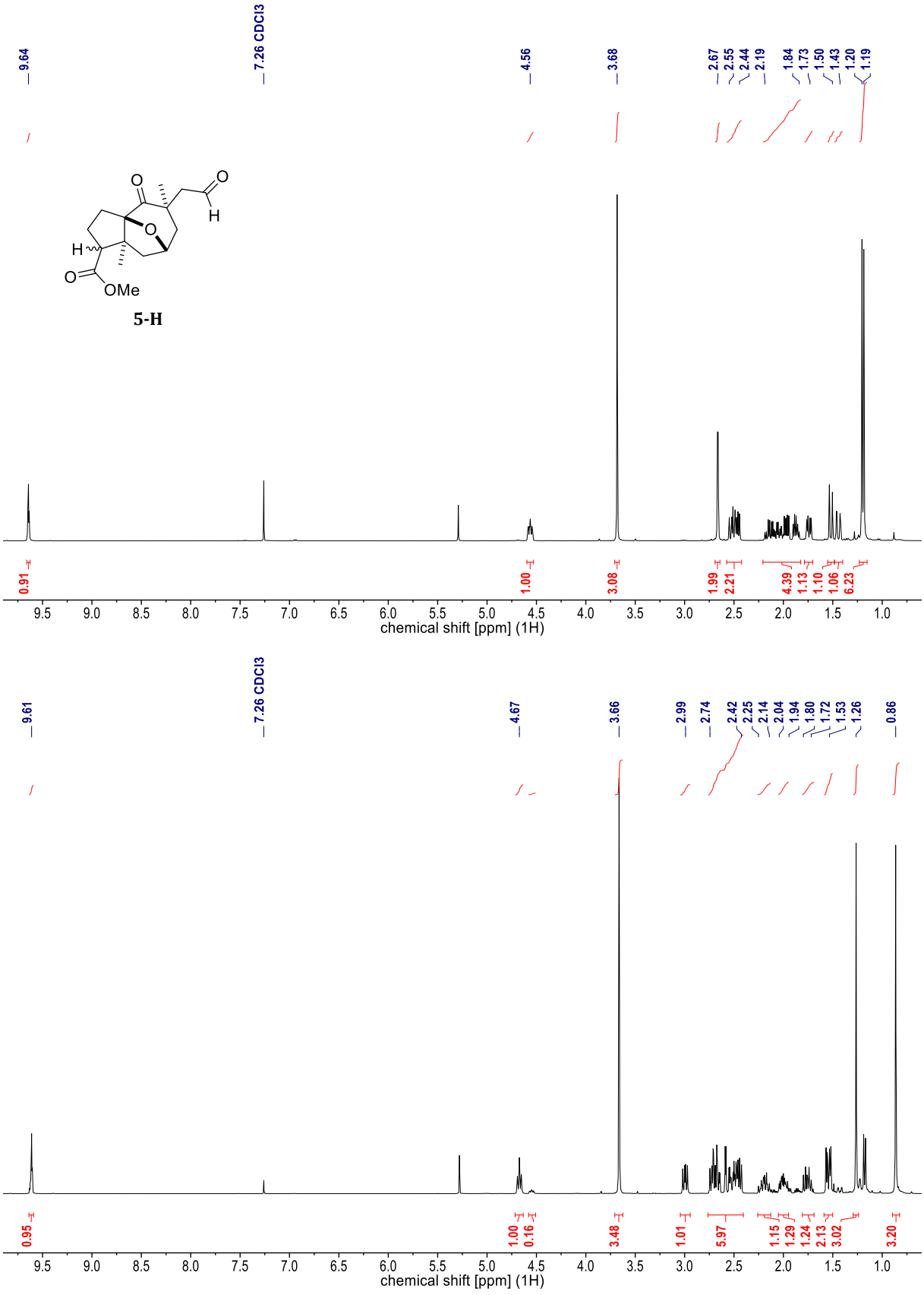

Figure 91. NMR spectra of **5-H** [^{1}H (400 MHz, $CDCl_3$)].
Upper spectrum: *minor, less polar DS*; lower spectrum: *major, more polar DS*.

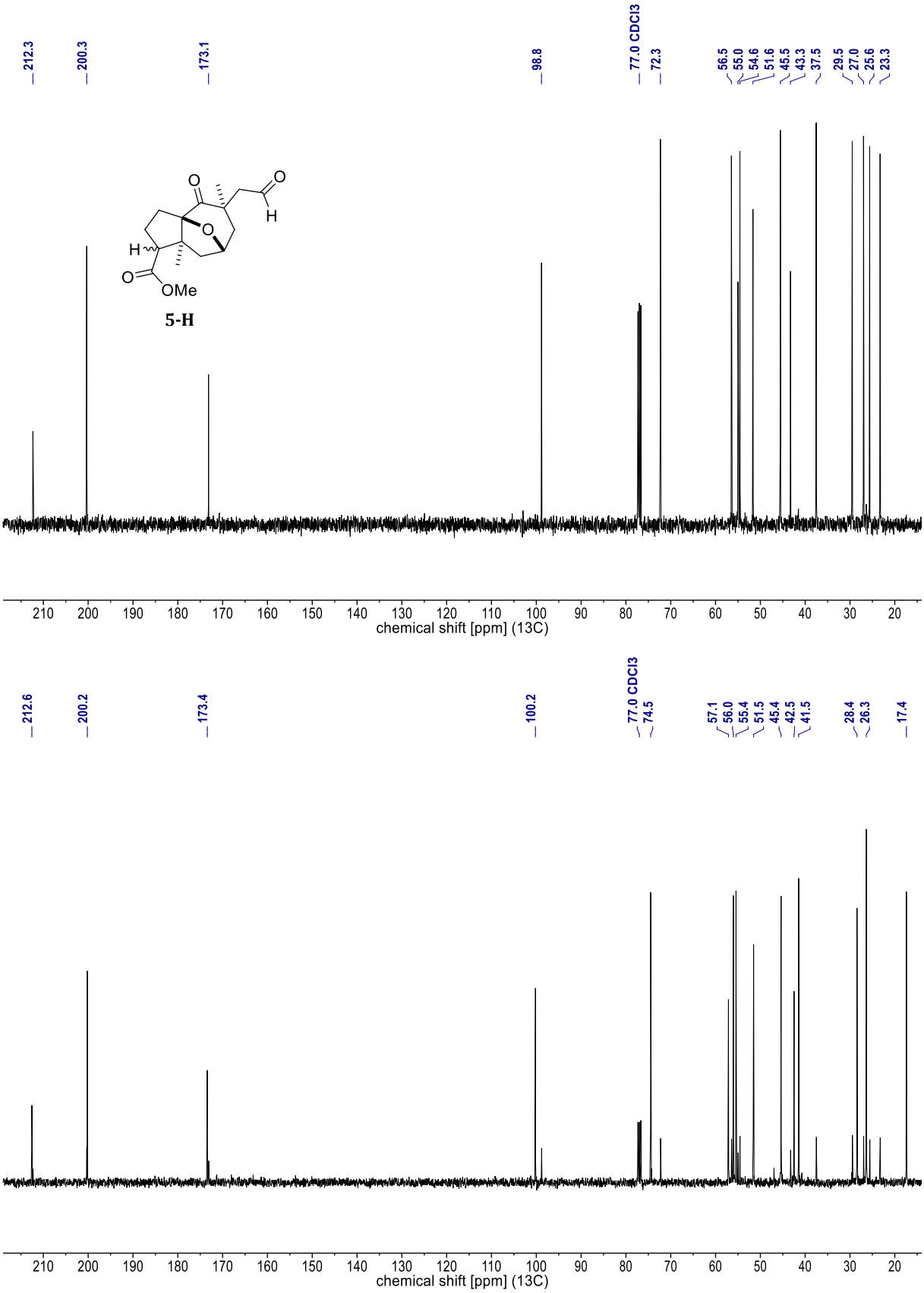

Figure 92. NMR spectra of **5-H** [^{13}C (101 MHz, $CDCl_3$)].
Upper spectrum: *minor, less polar DS*; lower spectrum: *major, more polar DS*.

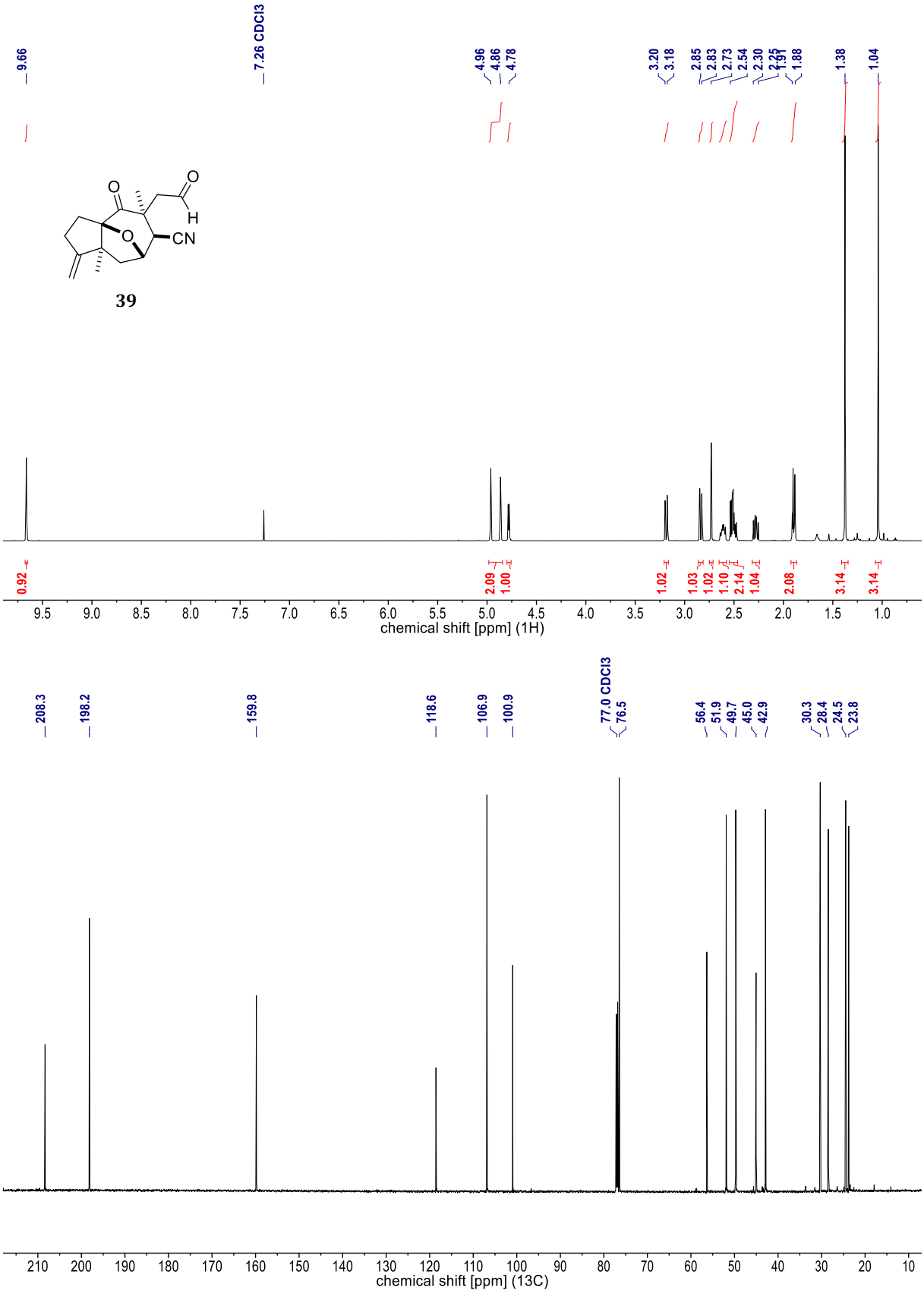

Figure 93. NMR spectra of **39** [^{1}H (700 MHz, $CDCl_3$) & ^{13}C (176 MHz, $CDCl_3$)].

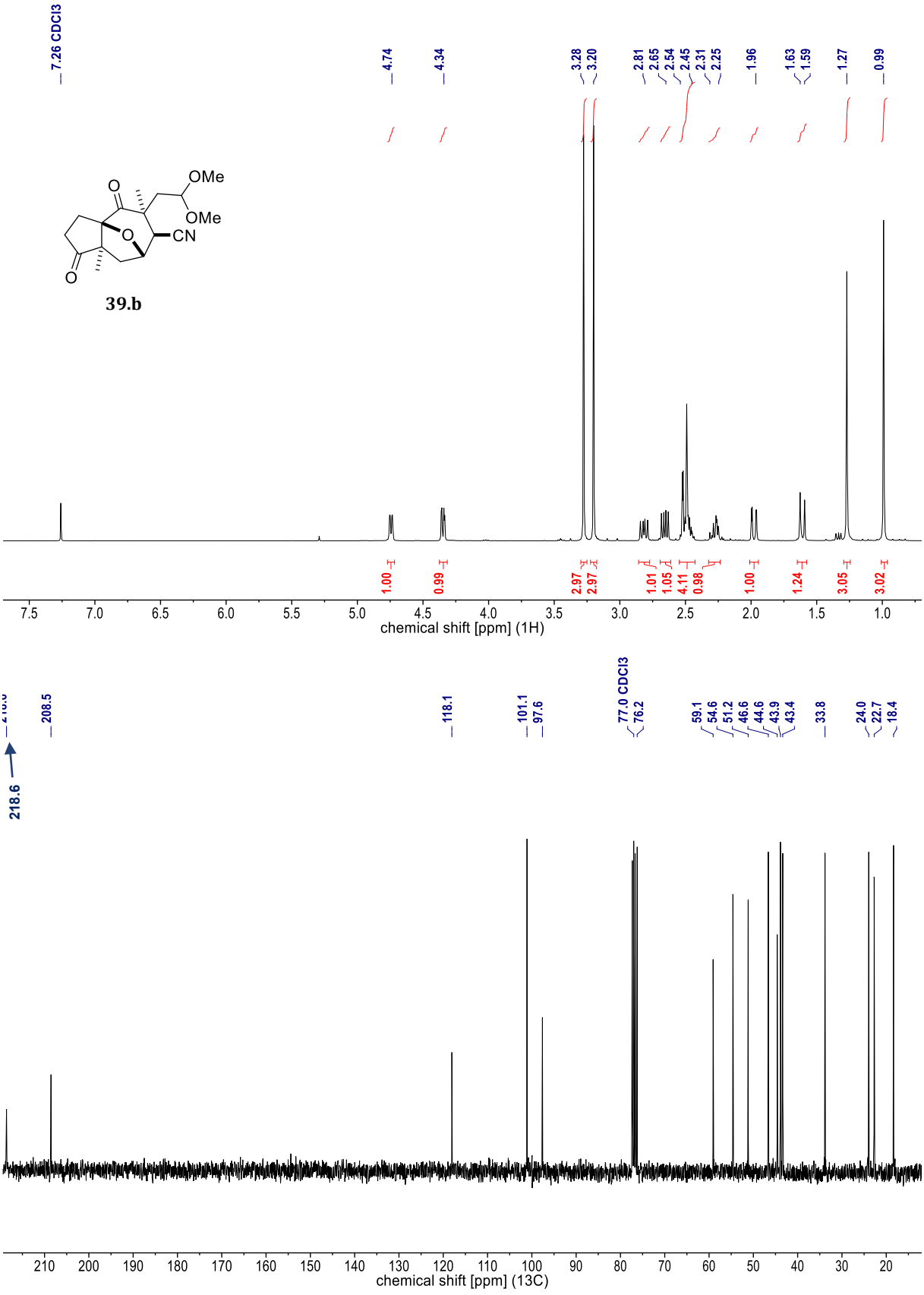

Figure 94. NMR spectra of **39.b** [^{1}H (400 MHz, $CDCl_3$) & ^{13}C (101 MHz, $CDCl_3$)].
The ^{13}C signal at δ = 218.6 ppm almost falls out of range (recorded scan width up to 219.4 ppm).

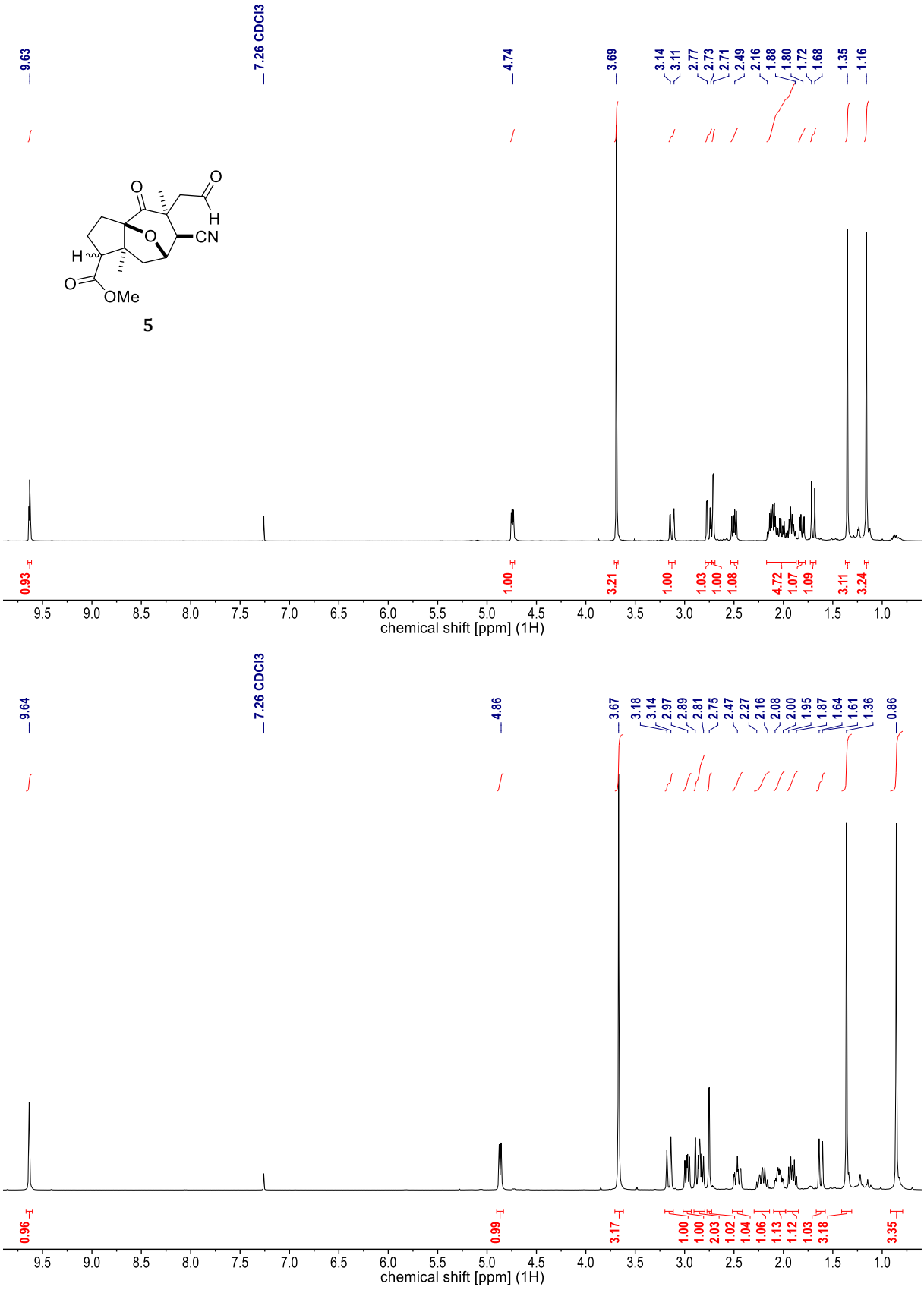

Figure 95. NMR spectra of **5** [^{1}H (400 MHz, $CDCl_3$)].
Upper spectrum: *minor, less polar DS*; lower spectrum: *major, more polar DS*.

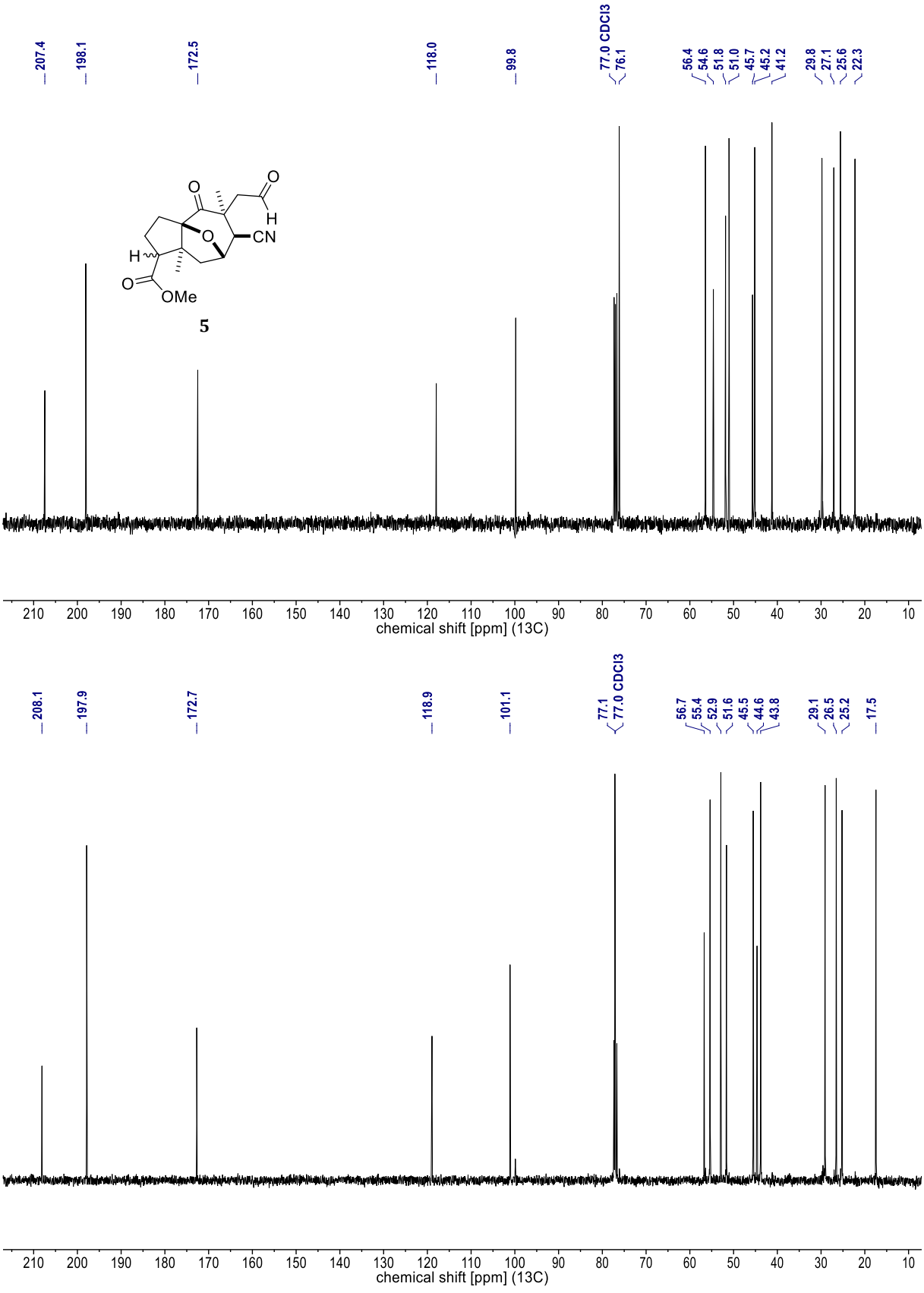

Figure 96. NMR spectra of **5** [^{13}C (101 MHz, $CDCl_3$)].
Upper spectrum: *minor, less polar DS*; lower spectrum: *major, more polar DS*.

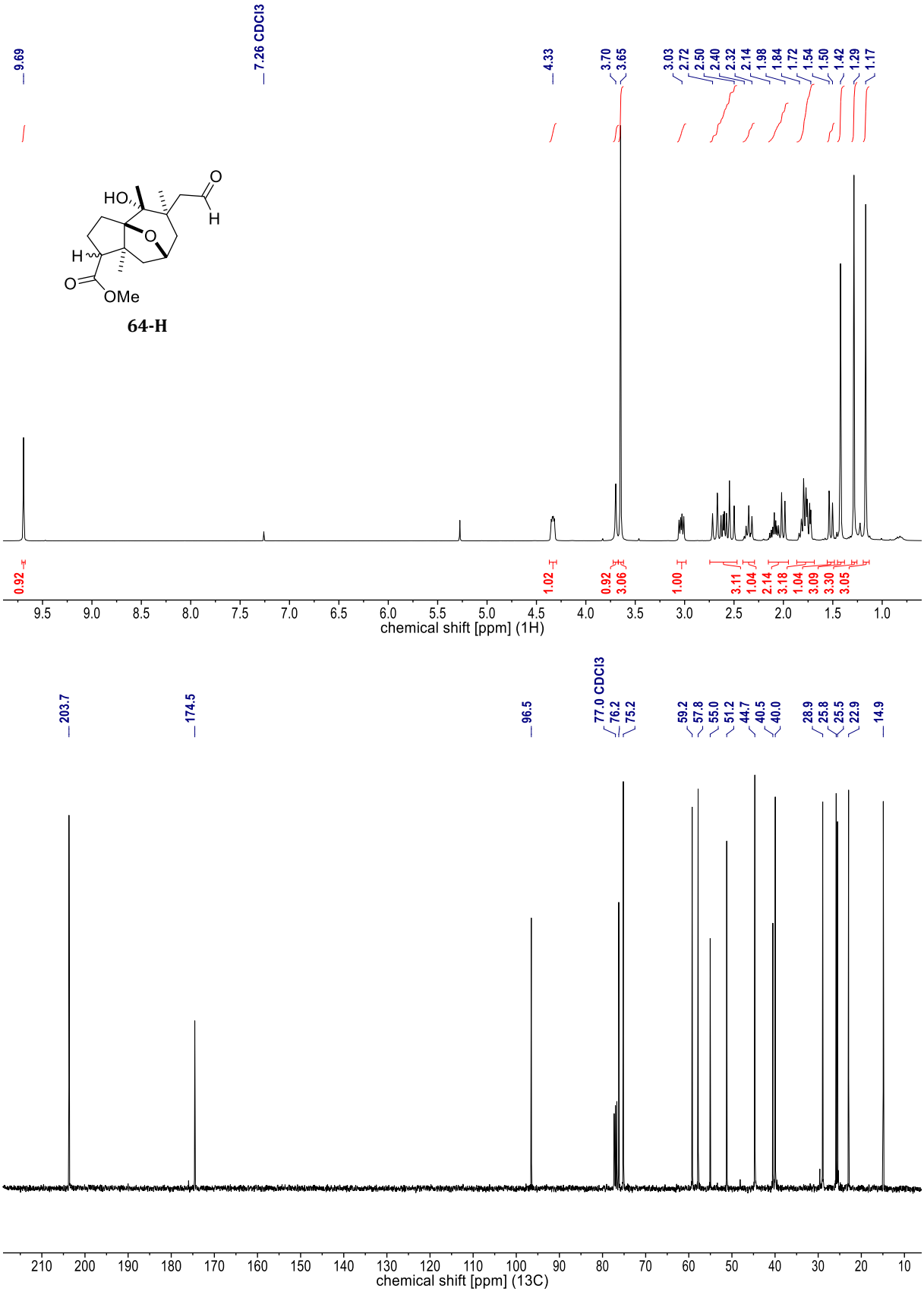

Figure 97. NMR spectra of **64-H** [^{1}H (400 MHz, $CDCl_3$) & ^{13}C (101 MHz, $CDCl_3$)].

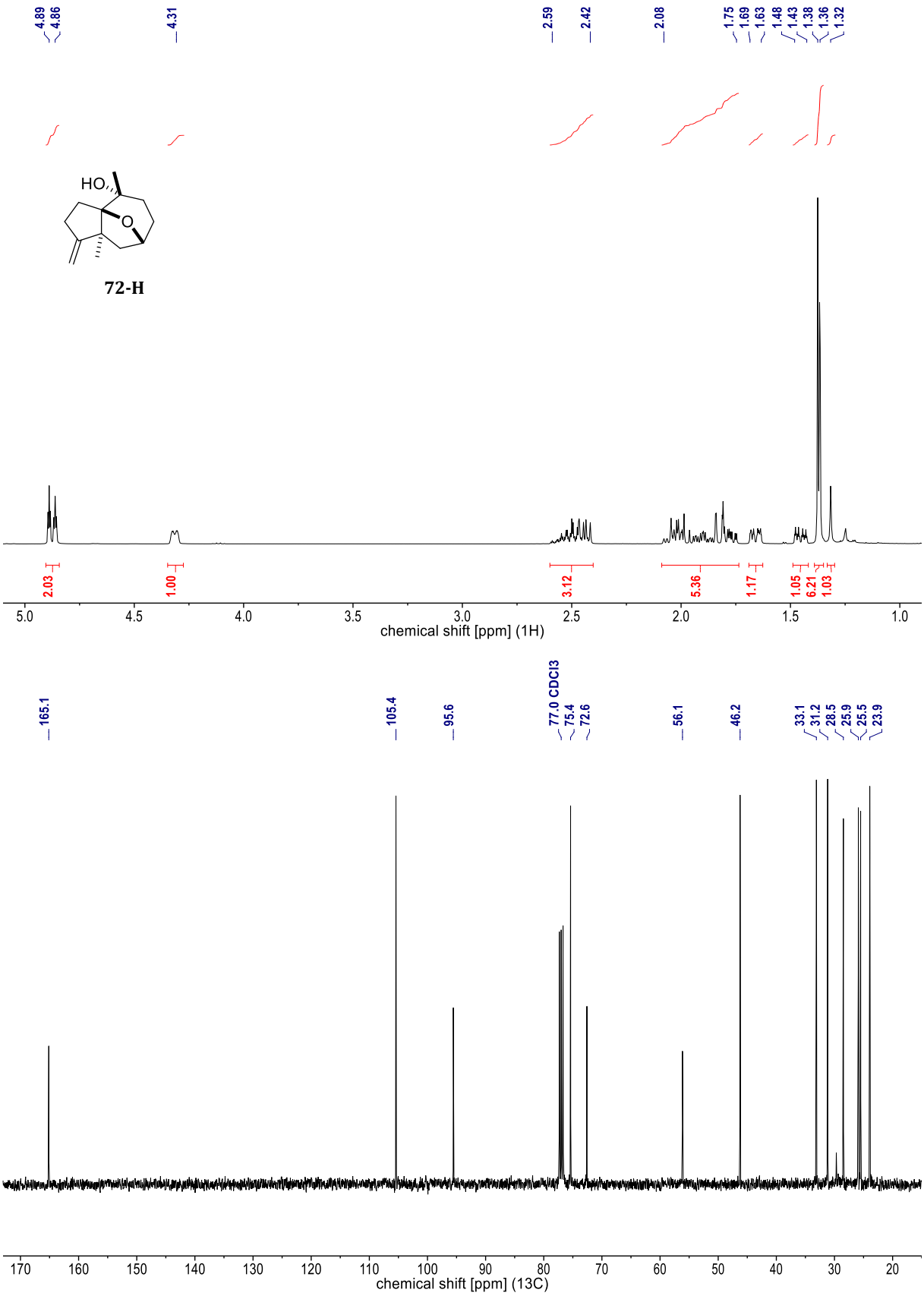

Figure 98. NMR spectra of **72-H** [^{1}H (400 MHz, $CDCl_3$) & ^{13}C (101 MHz, $CDCl_3$)].

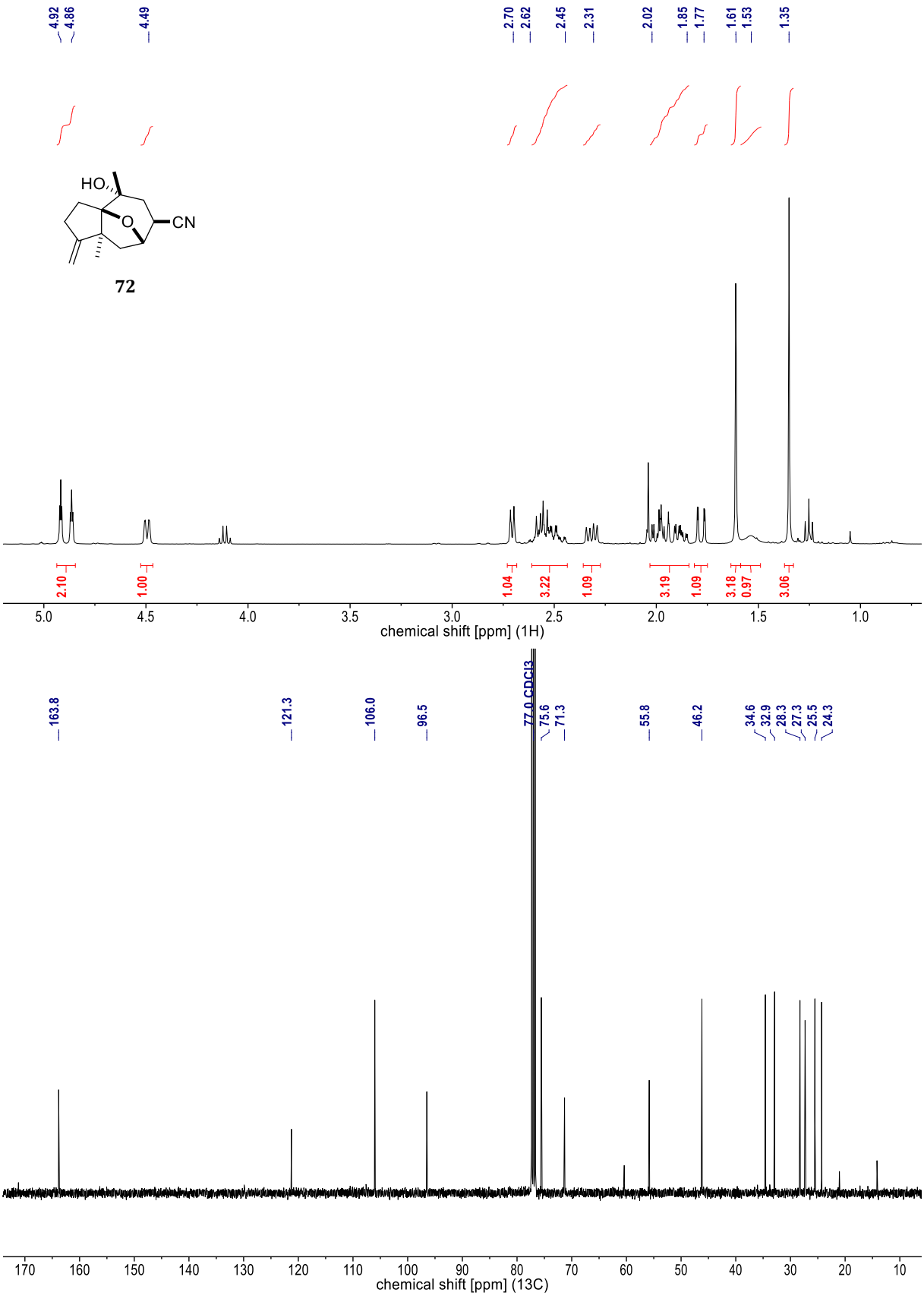

Figure 99. NMR spectra of **72** [^{1}H (400 MHz, $CDCl_3$) & ^{13}C (101 MHz, $CDCl_3$)].

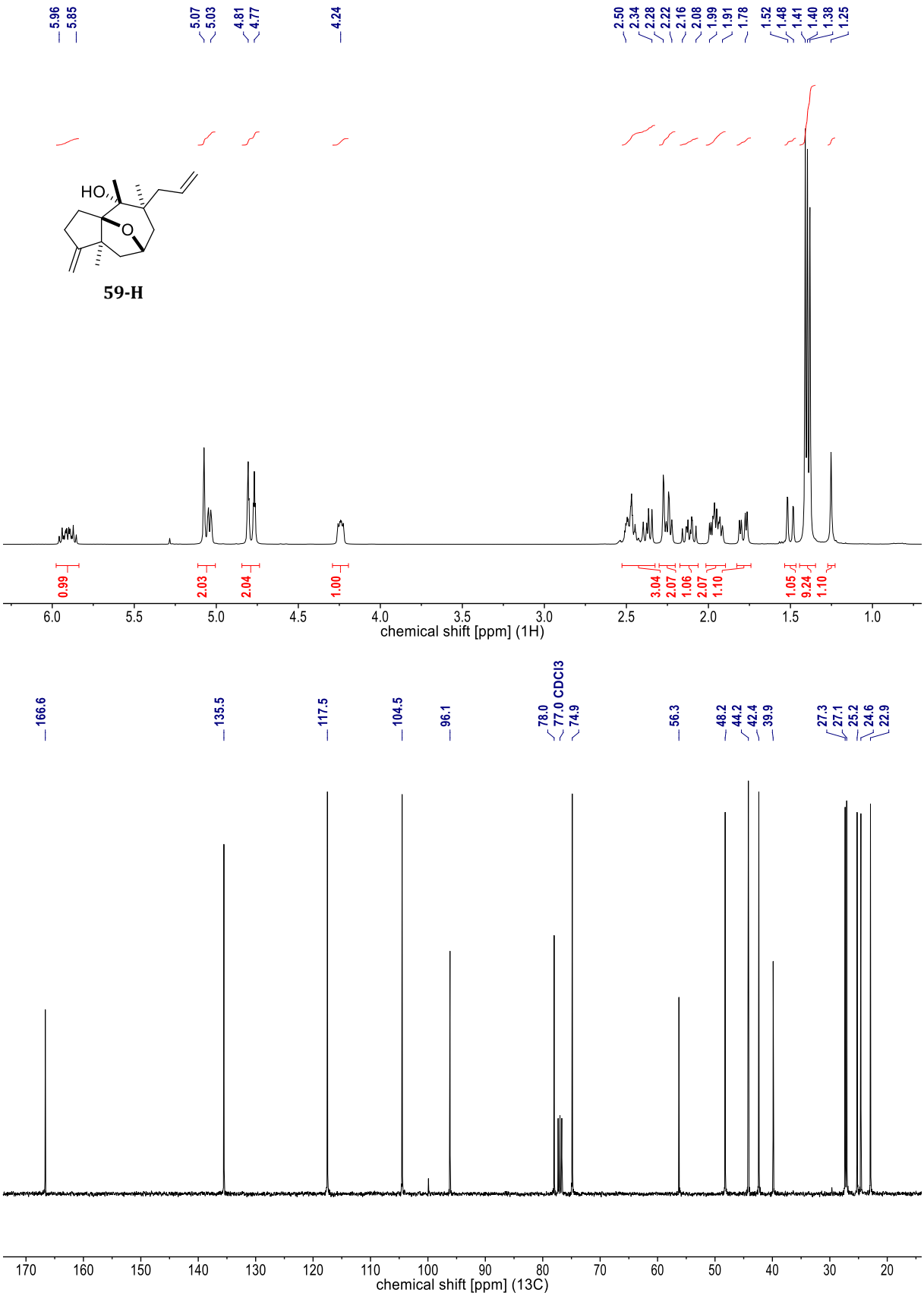

Figure 100. NMR spectra of **59-H** [^{1}H (400 MHz, $CDCl_3$) & ^{13}C (101 MHz, $CDCl_3$)].

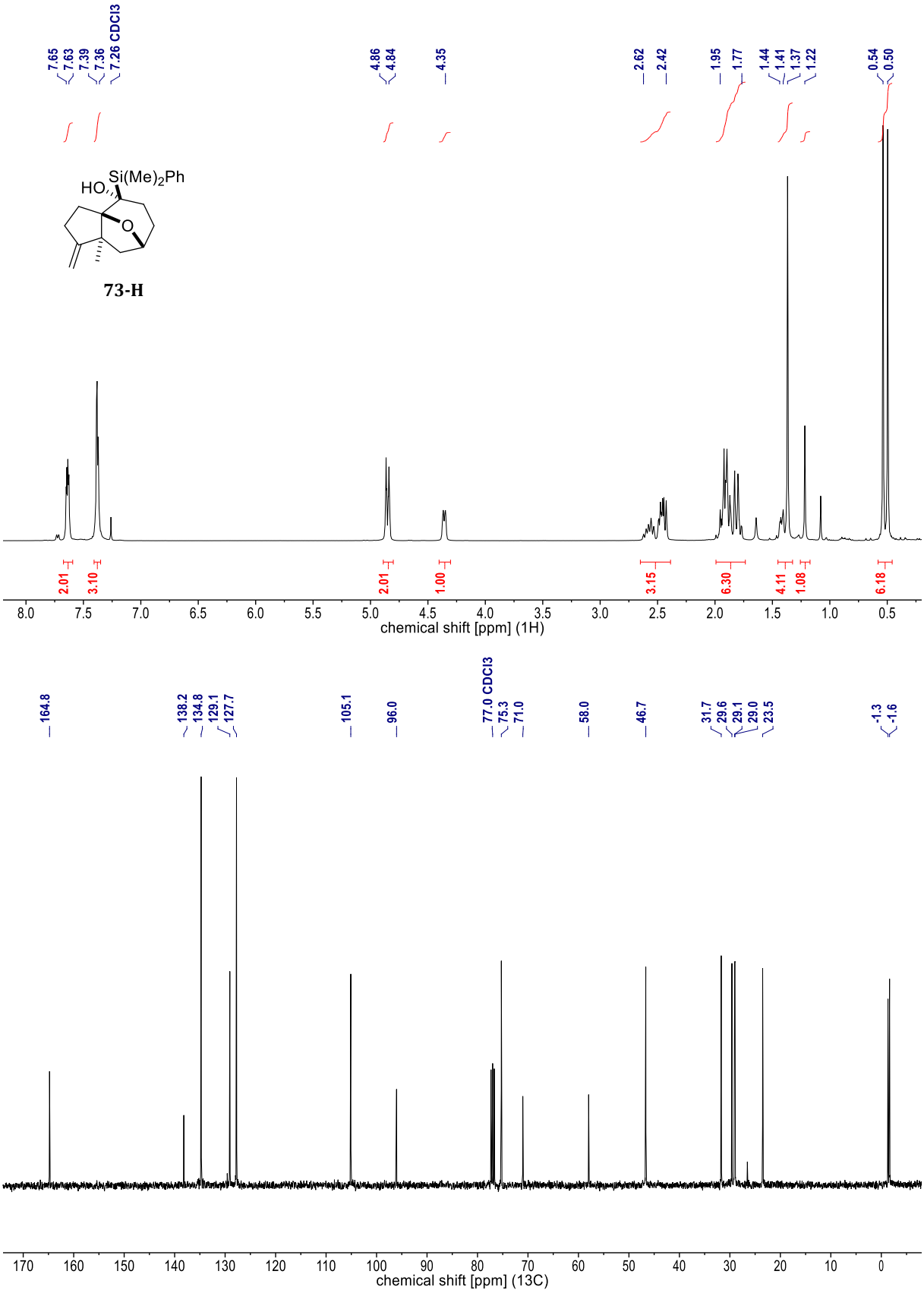

Figure 101. NMR spectra of **73-H** [^{1}H (400 MHz, $CDCl_3$) & ^{13}C (101 MHz, $CDCl_3$)].

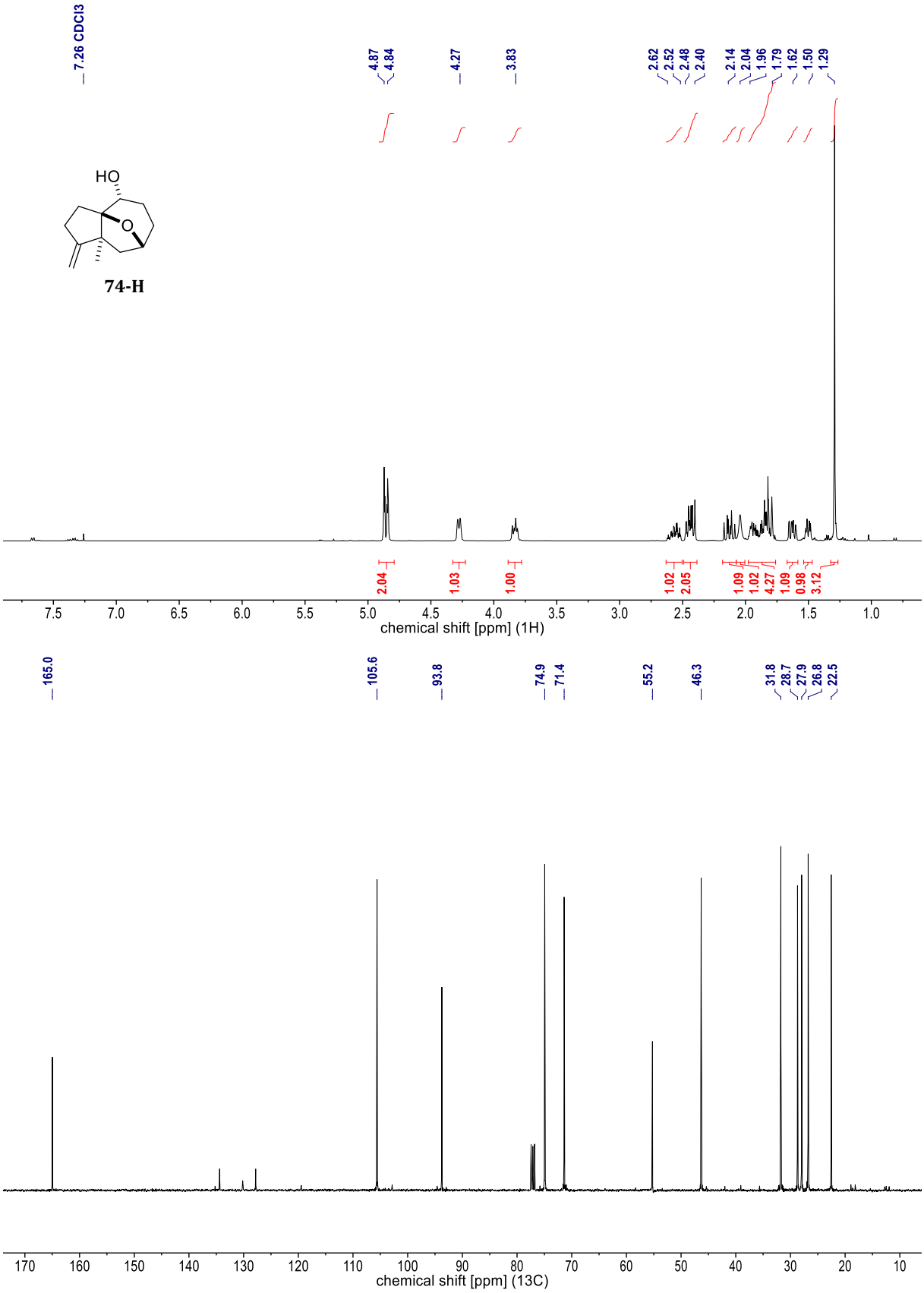

Figure 102. NMR spectra of **74-H** [^{1}H (400 MHz, $CDCl_3$) & ^{13}C (101 MHz, $CDCl_3$)].
*Some aromatic impurities due to concomitant reduction of dba (from slightly impure substrate, ketone **8-H**) are discernible.*

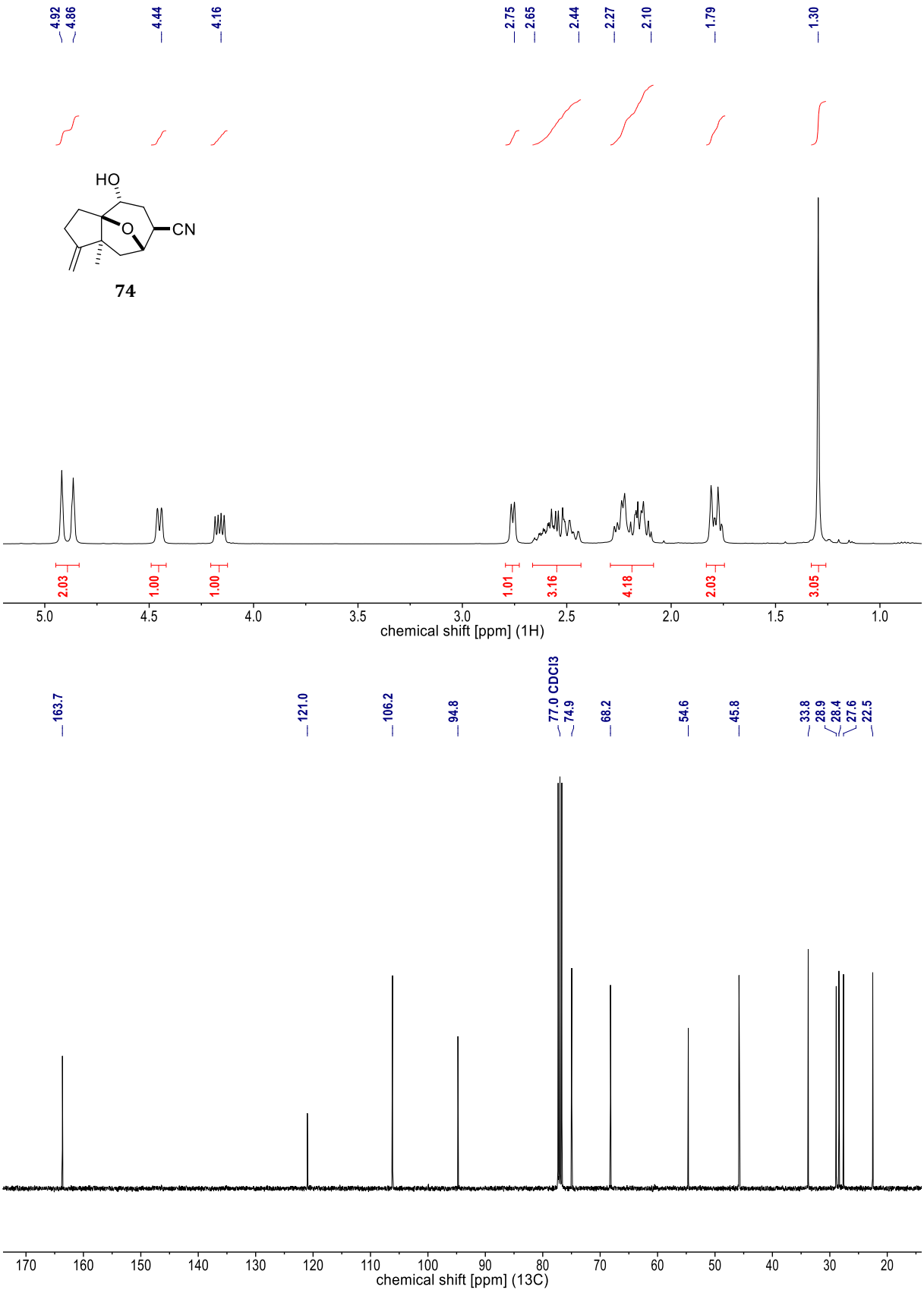

Figure 103. NMR spectra of **74** [^{1}H (400 MHz, $CDCl_3$) & ^{13}C (101 MHz, $CDCl_3$)].

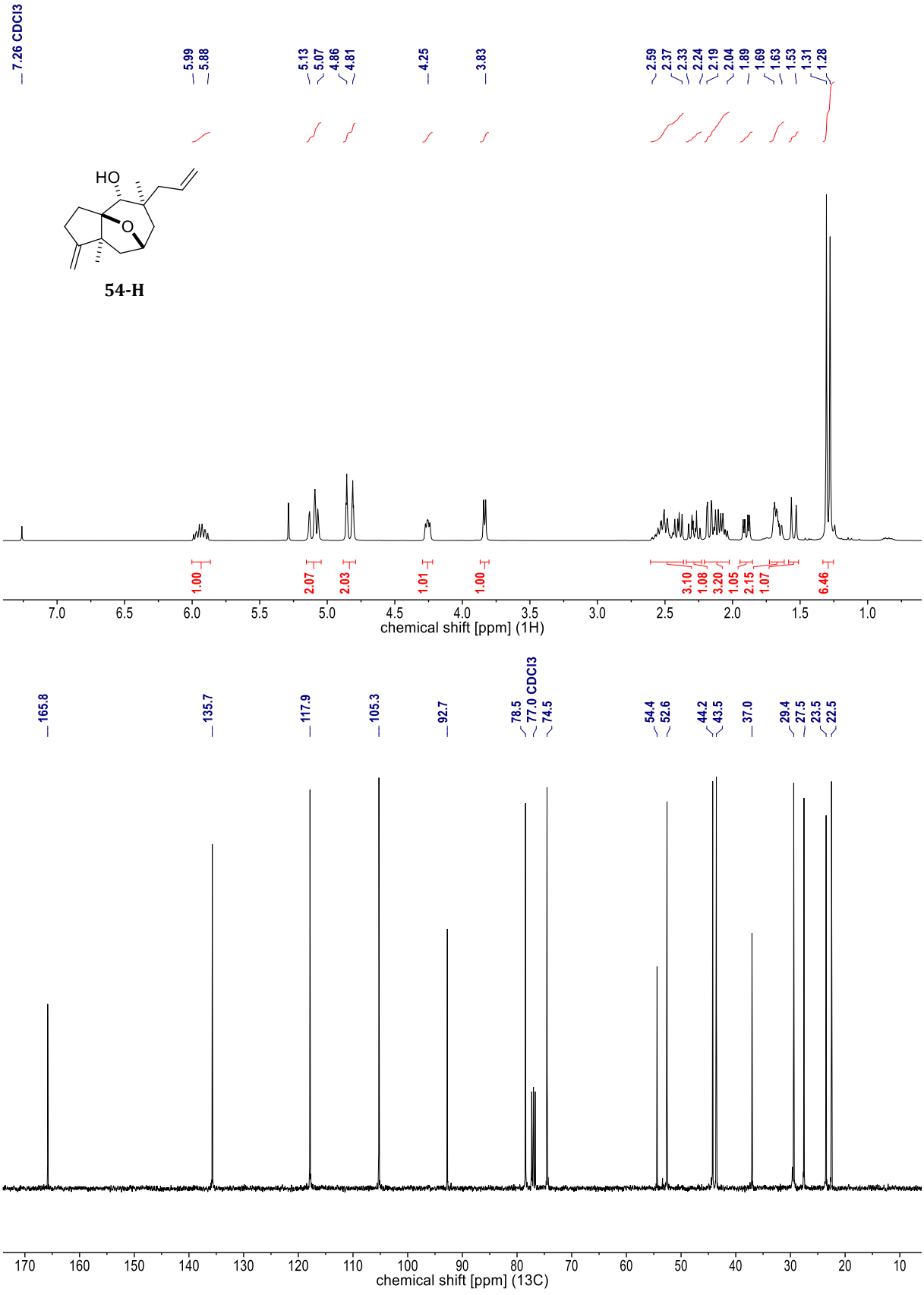

Figure 104. NMR spectra of **54-H** [^{1}H (400 MHz, $CDCl_3$) & ^{13}C (101 MHz, $CDCl_3$)].

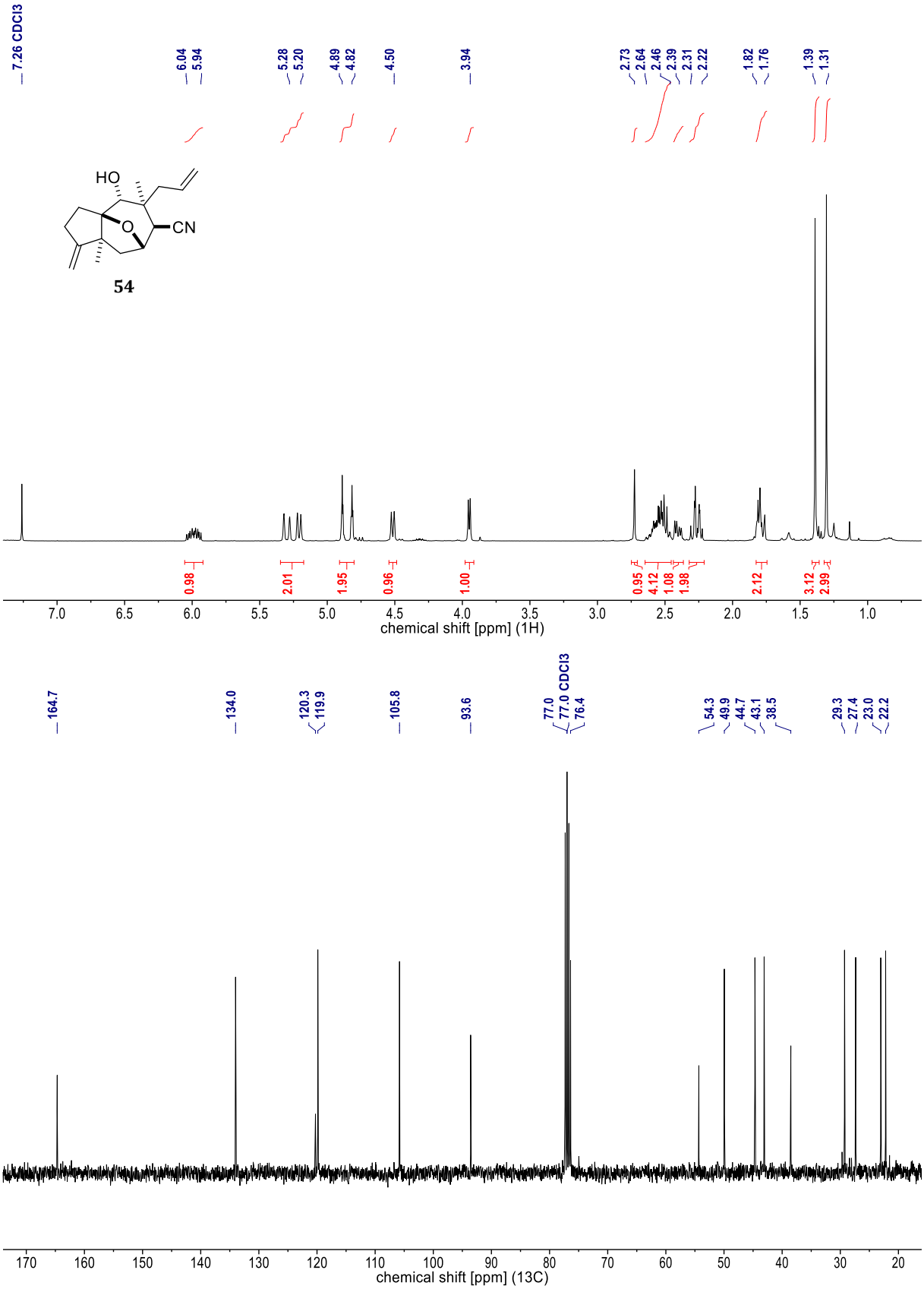

Figure 105. NMR spectra of **54** [^{1}H (400 MHz, $CDCl_3$) & ^{13}C (101 MHz, $CDCl_3$)].

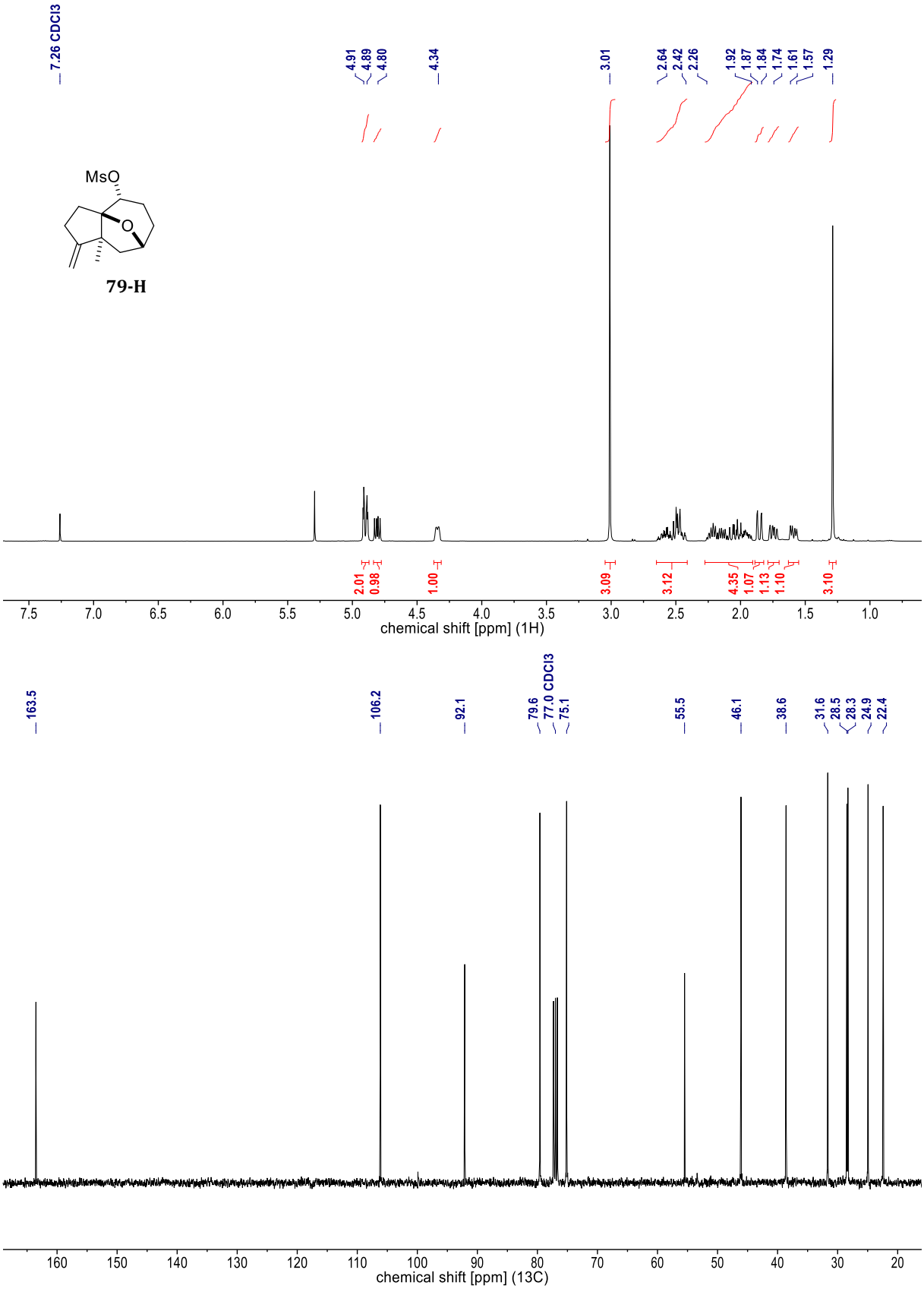

Figure 106. NMR spectra of **79-H** [^{1}H (400 MHz, $CDCl_3$) & ^{13}C (101 MHz, $CDCl_3$)].

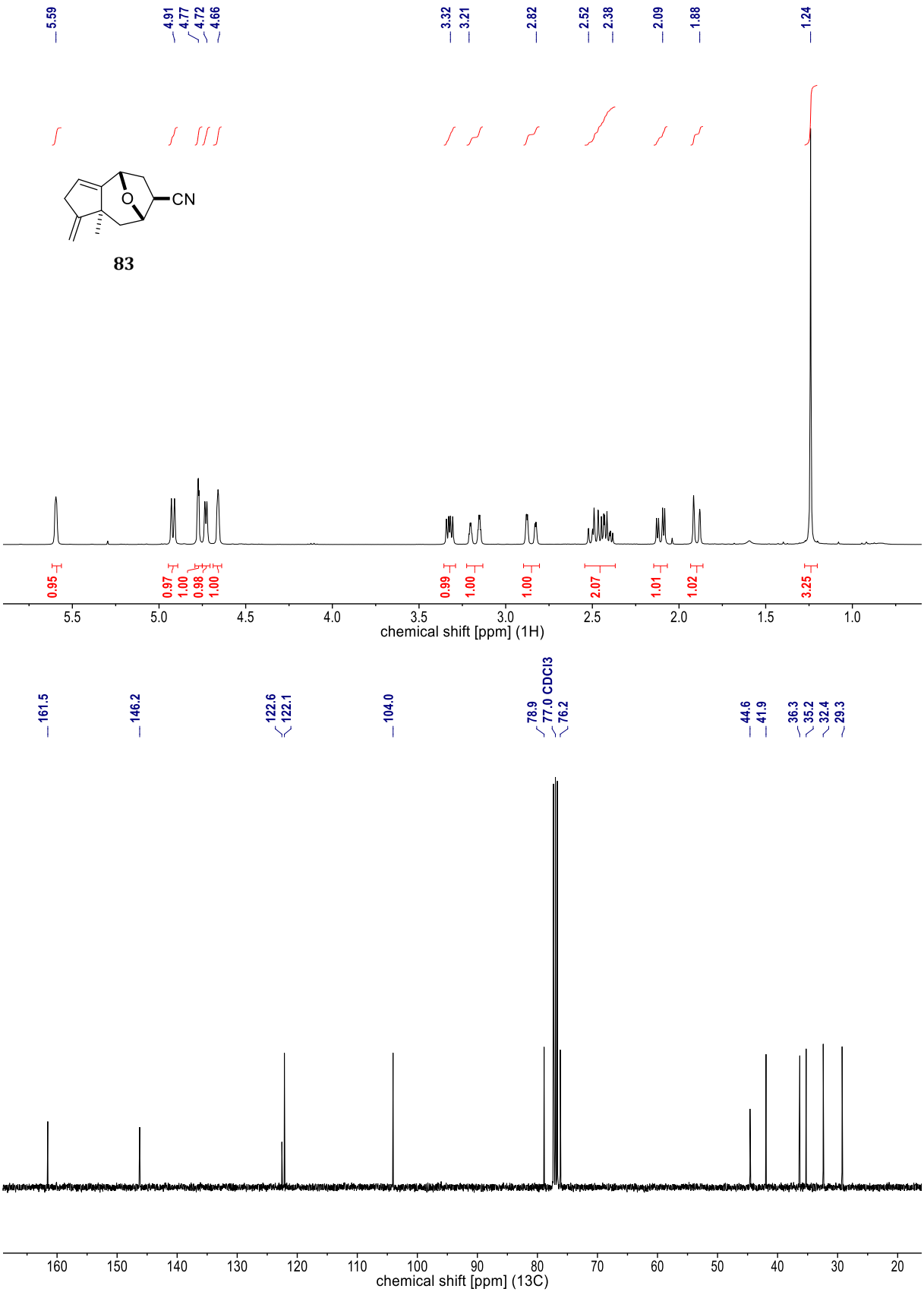

Figure 107. NMR spectra of **83** [^{1}H (400 MHz, $CDCl_3$) & ^{13}C (101 MHz, $CDCl_3$)].

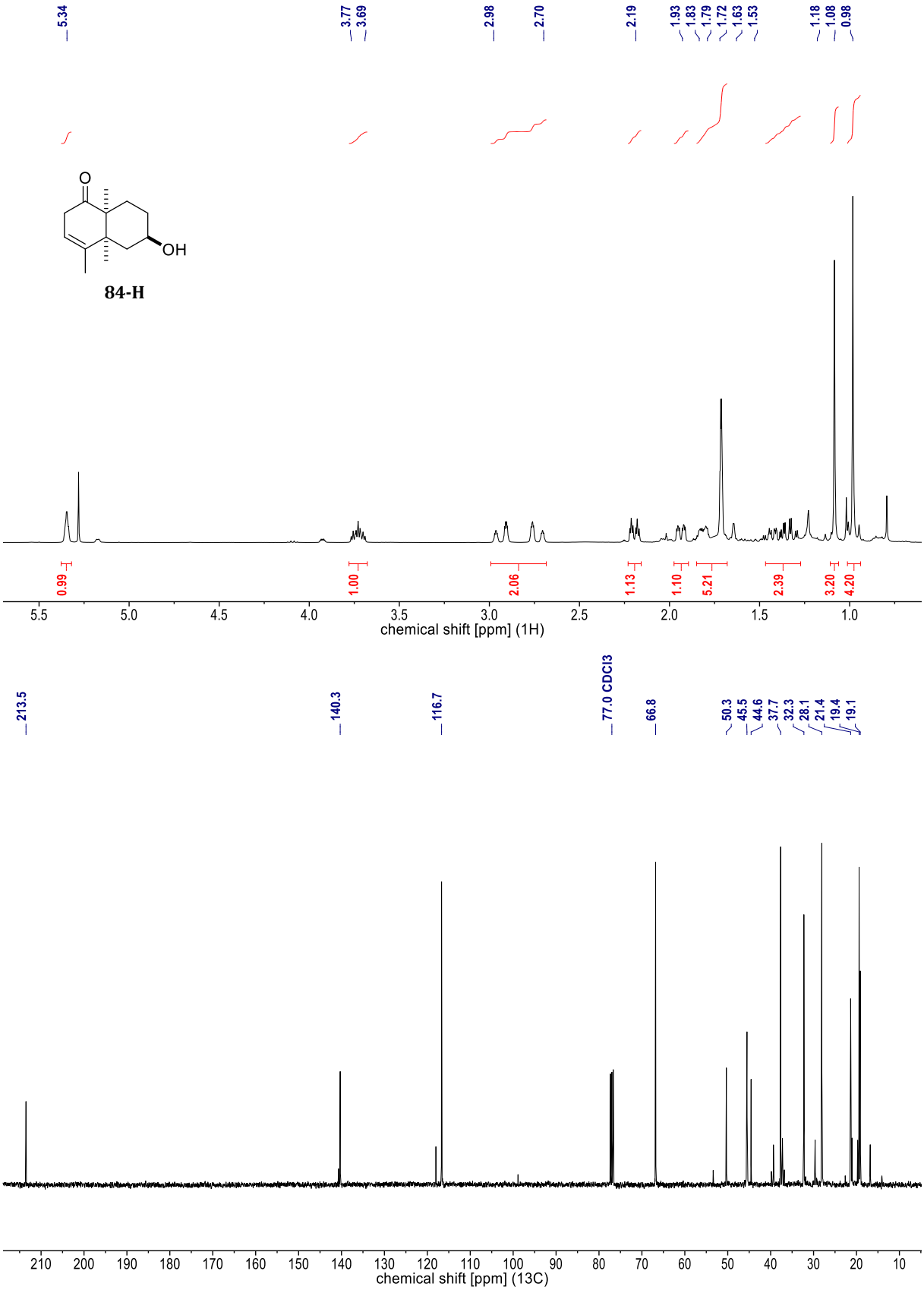

Figure 108. NMR spectra of **84-H** [^{1}H (400 MHz, $CDCl_3$) & ^{13}C (101 MHz, $CDCl_3$)].

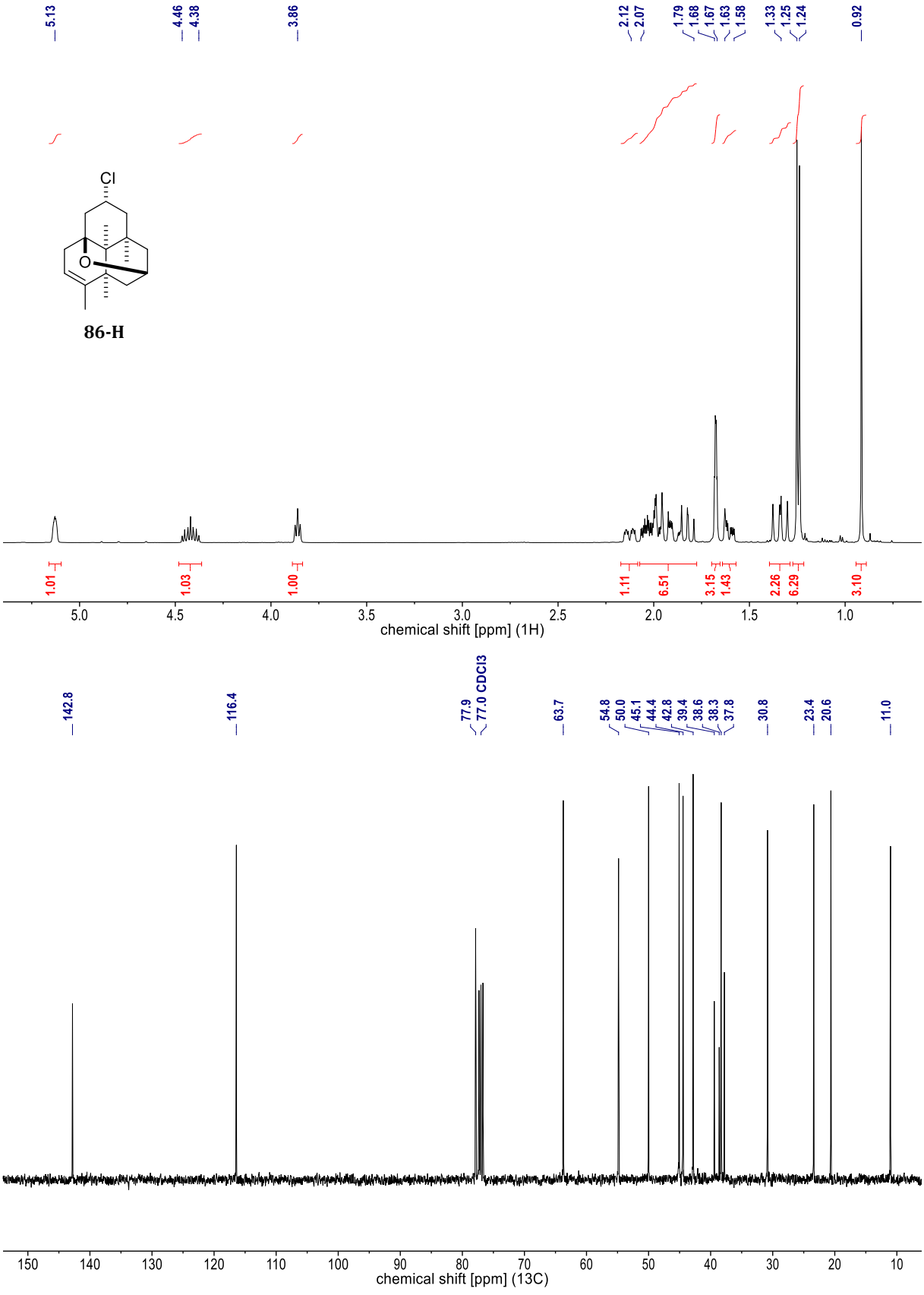

Figure 109. NMR spectra of **86-H** [^{1}H (400 MHz, $CDCl_3$) & ^{13}C (101 MHz, $CDCl_3$)].

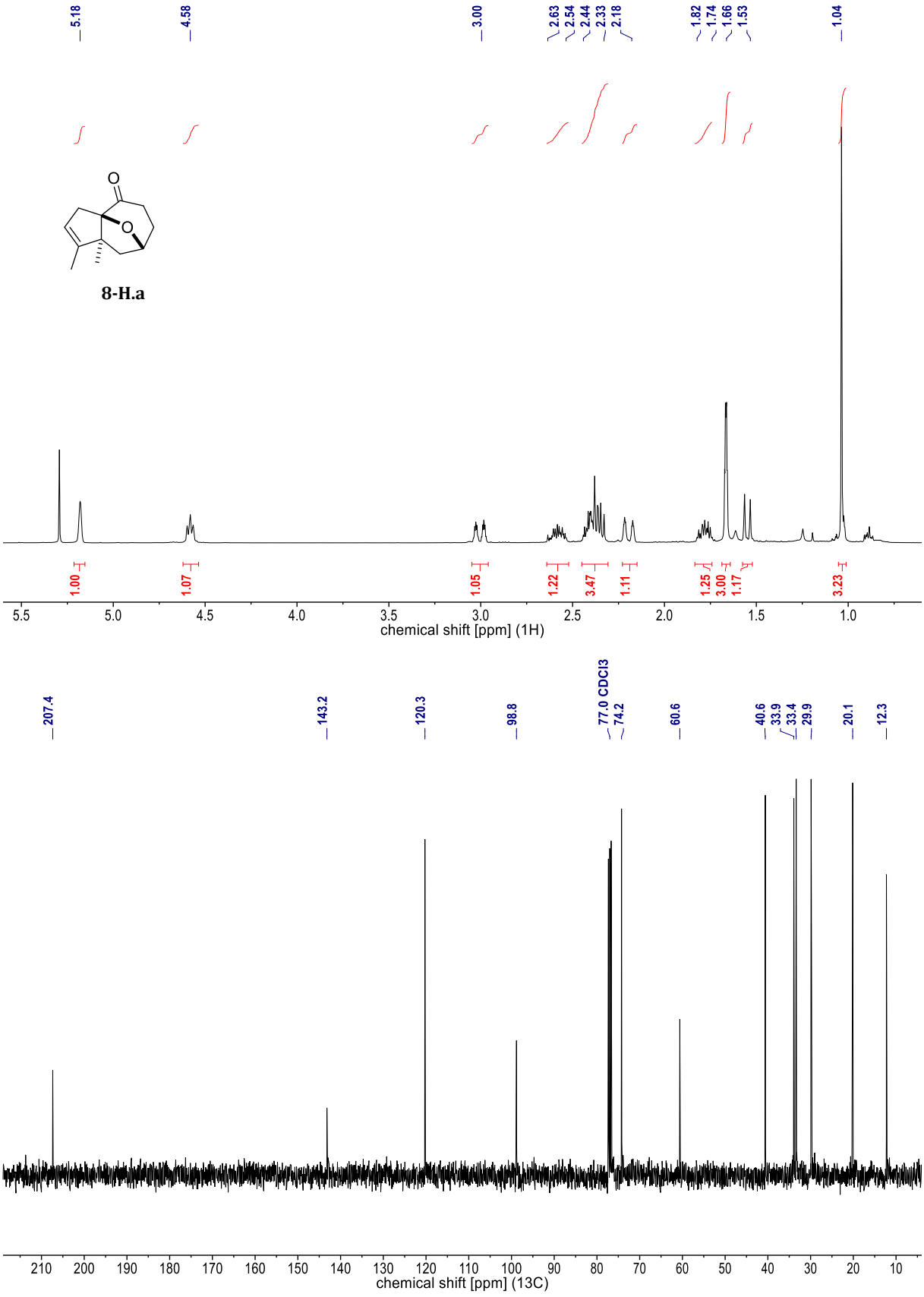

Figure 110. NMR spectra of **8-H.a** [^{1}H (400 MHz, $CDCl_3$) & ^{13}C (101 MHz, $CDCl_3$)].

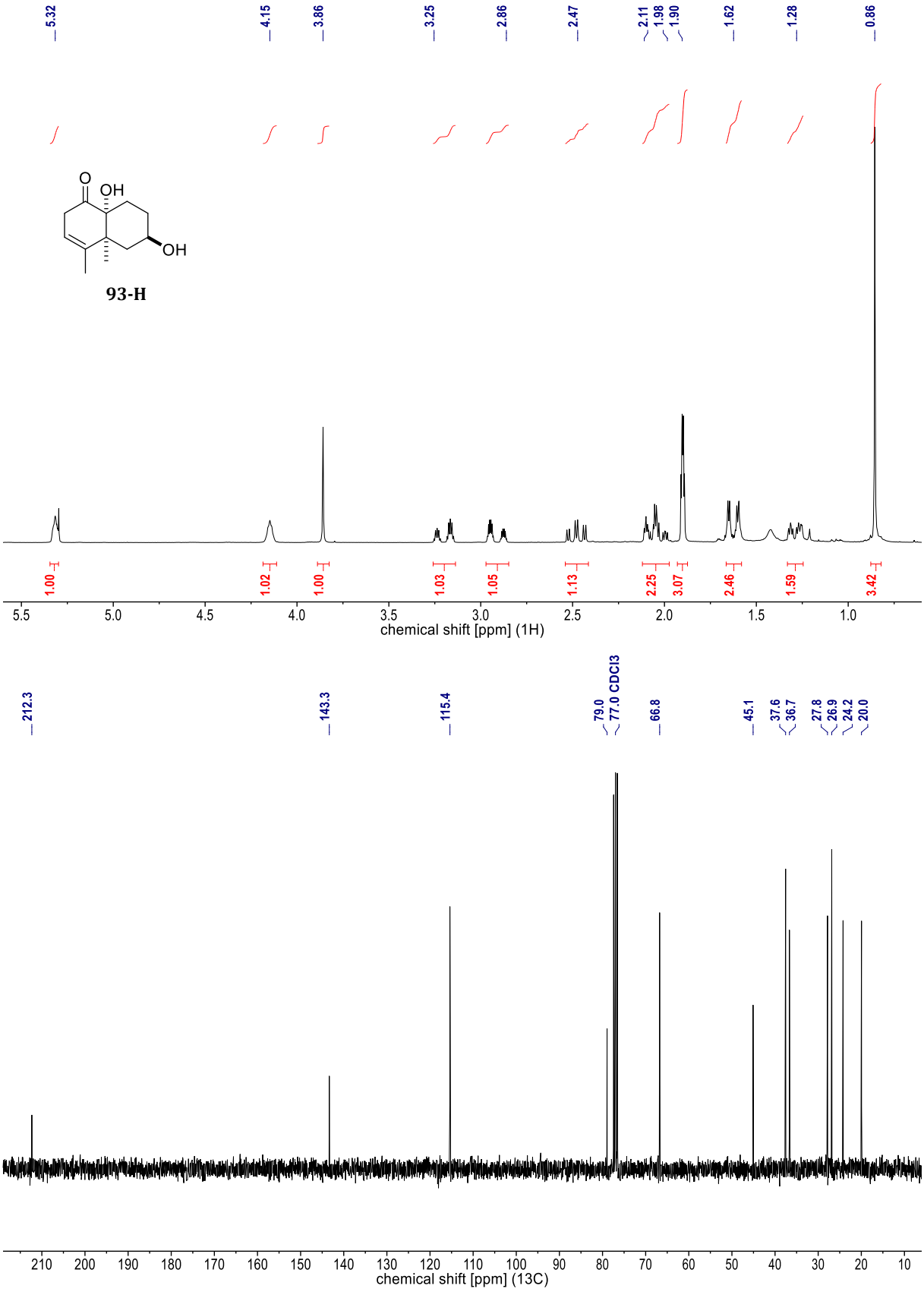

Figure 111. NMR spectra of **93-H** [^{1}H (300 MHz, $CDCl_3$) & ^{13}C (76 MHz, $CDCl_3$)].

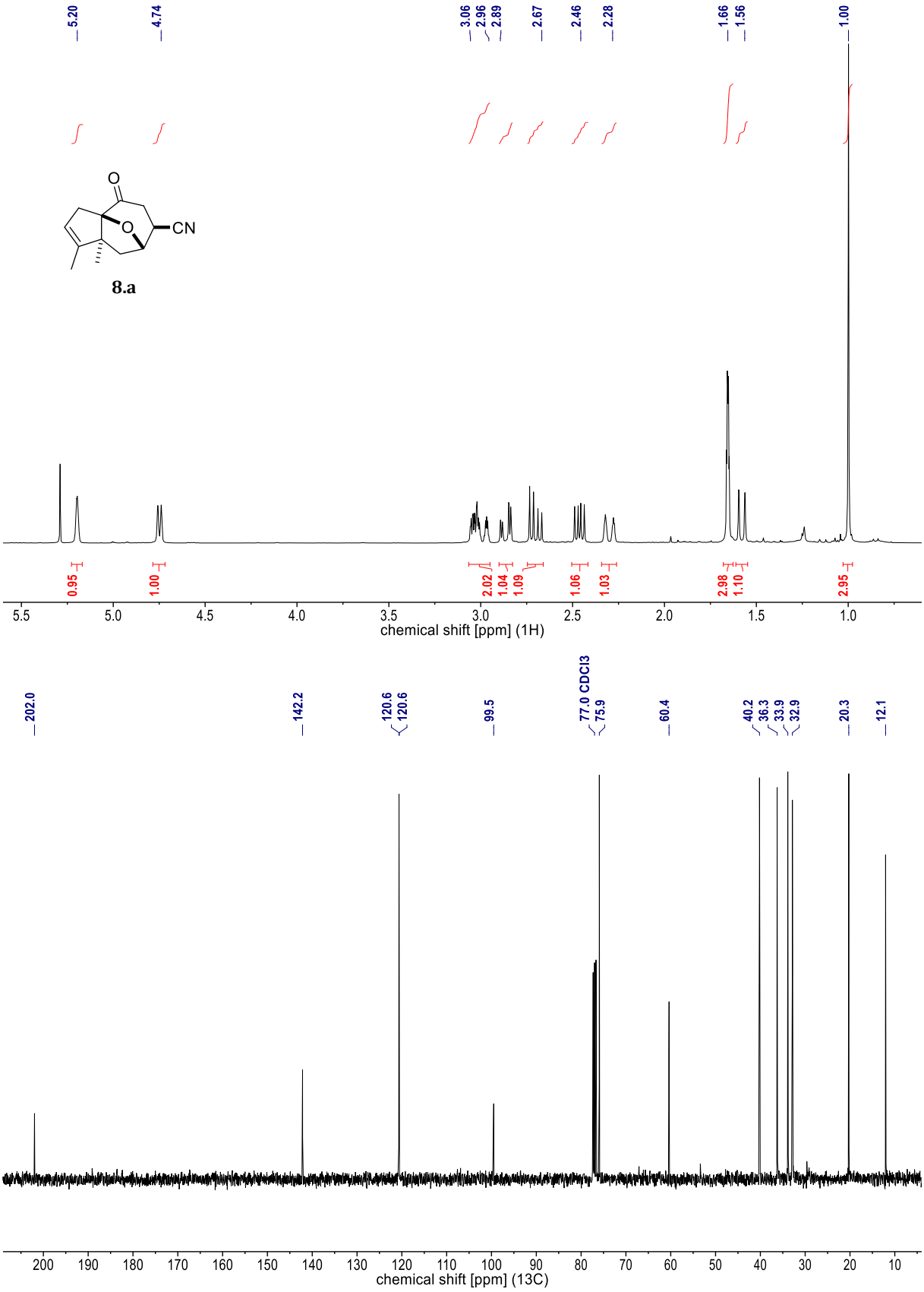

Figure 112. NMR spectra of **8.a** [^{1}H (300 MHz, $CDCl_3$) & ^{13}C (76 MHz, $CDCl_3$)].

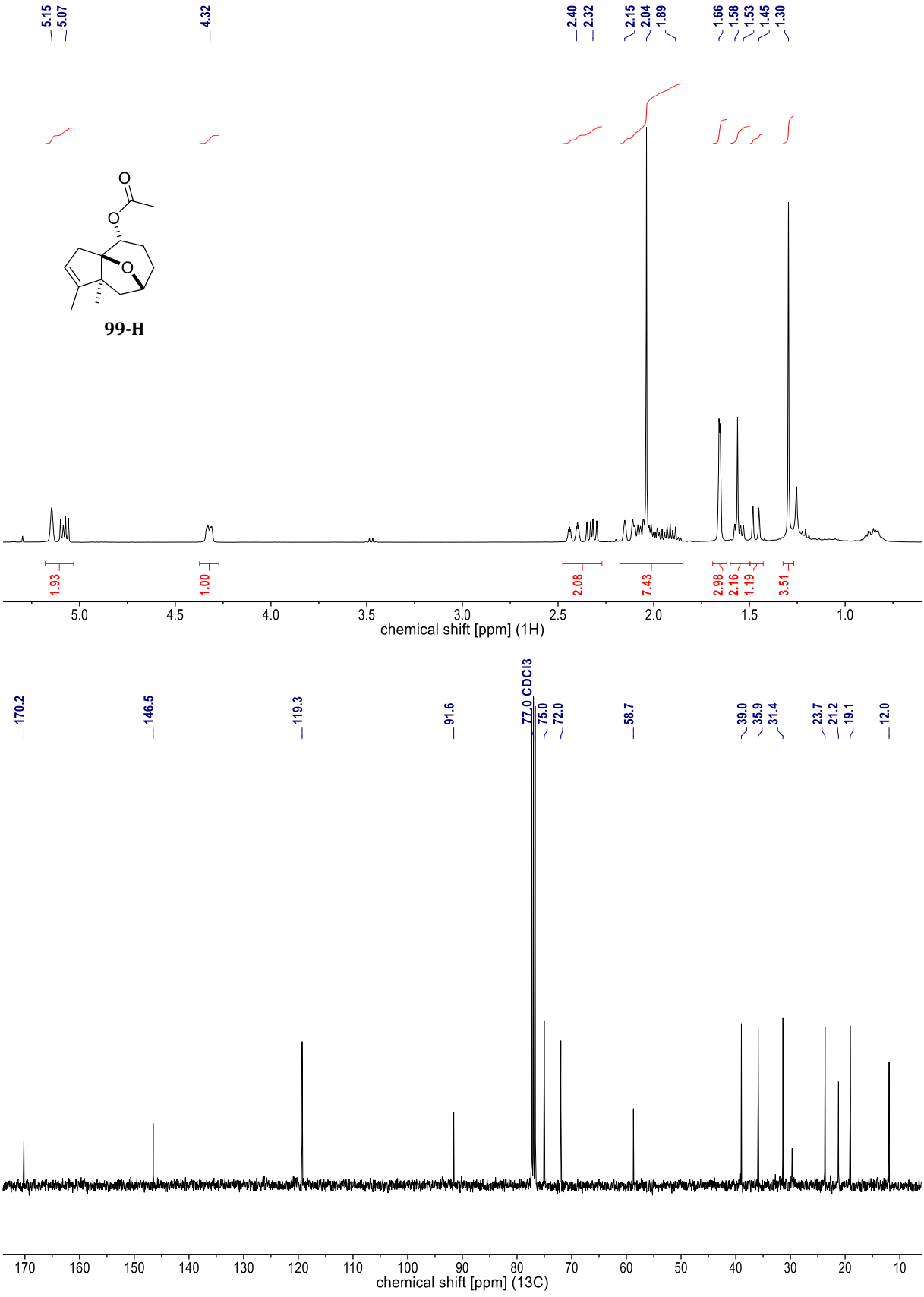

Figure 113. NMR spectra of **99-H** [^{1}H (400 MHz, $CDCl_3$) & ^{13}C (101 MHz, $CDCl_3$)].

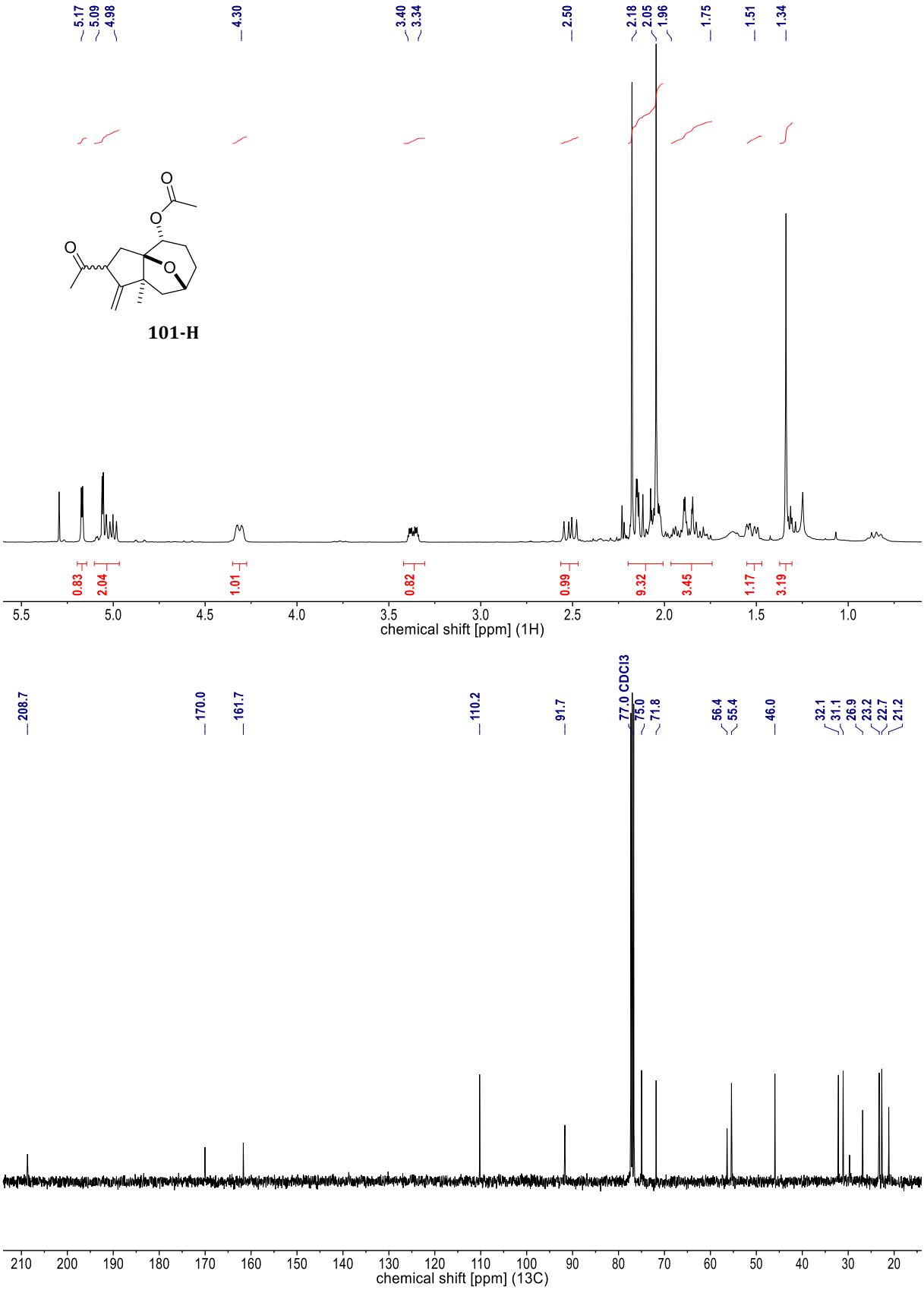

Figure 114. NMR spectra of **101-H** [^{1}H (400 MHz, $CDCl_3$) & ^{13}C (101 MHz, $CDCl_3$)].

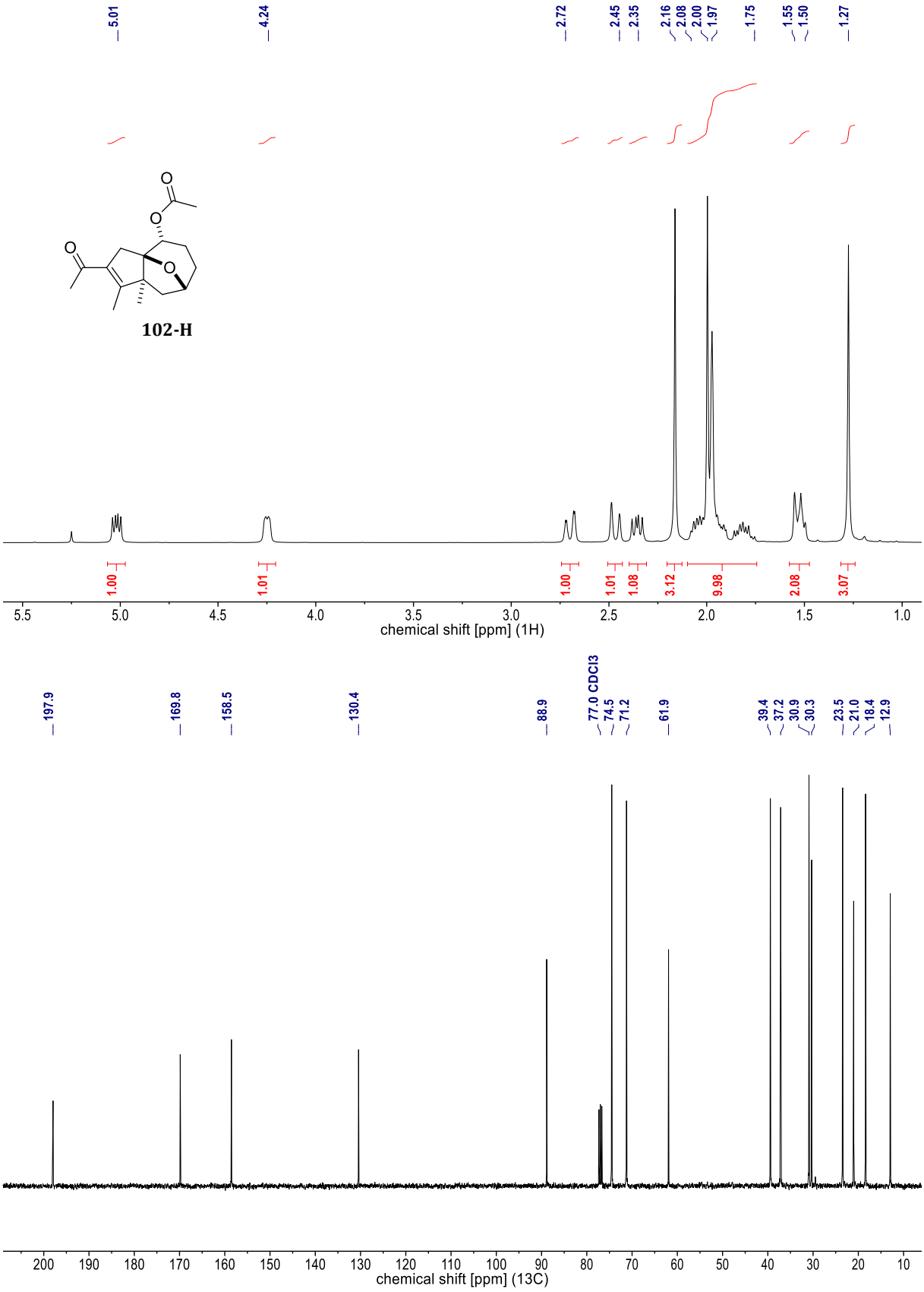

102-H

Figure 115. NMR spectra of **102-H** [^{1}H (400 MHz, $CDCl_3$) & ^{13}C (101 MHz, $CDCl_3$)].

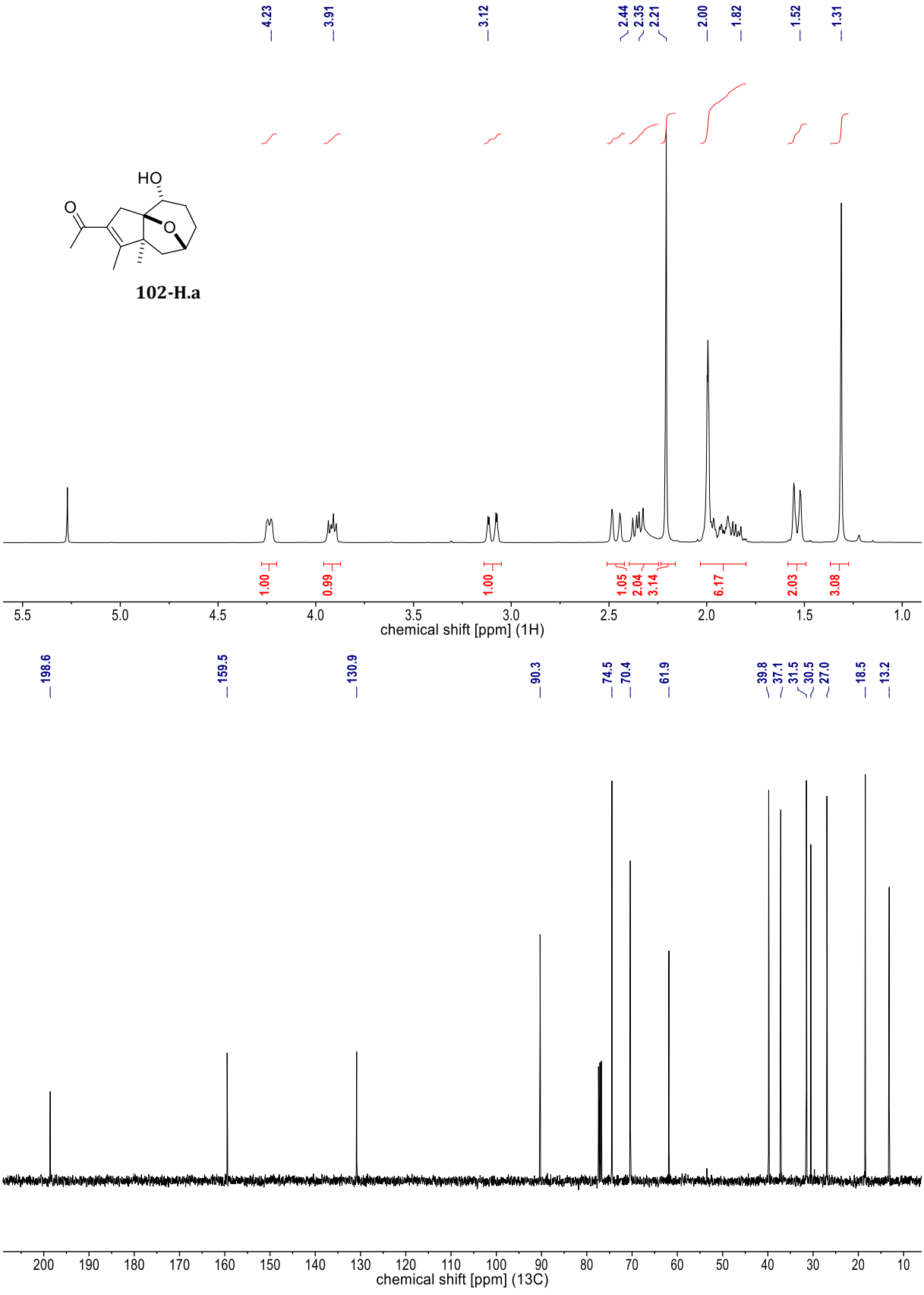

102-H.a

Figure 116. NMR spectra of **102-H.a** [^{1}H (400 MHz, $CDCl_3$) & ^{13}C (101 MHz, $CDCl_3$)].

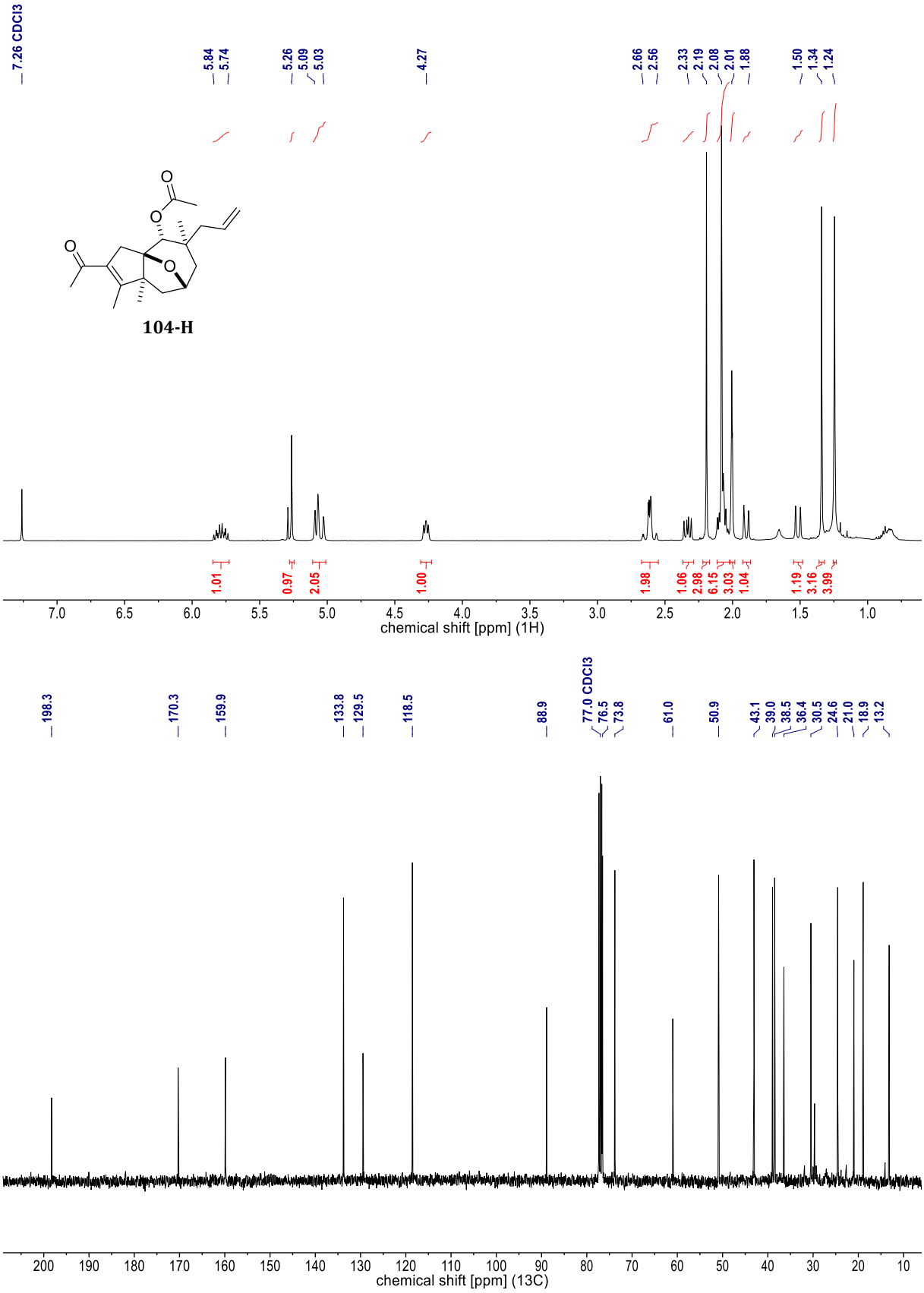

Figure 117. NMR spectra of **104-H** [^{1}H (400 MHz, $CDCl_3$) & ^{13}C (101 MHz, $CDCl_3$)].

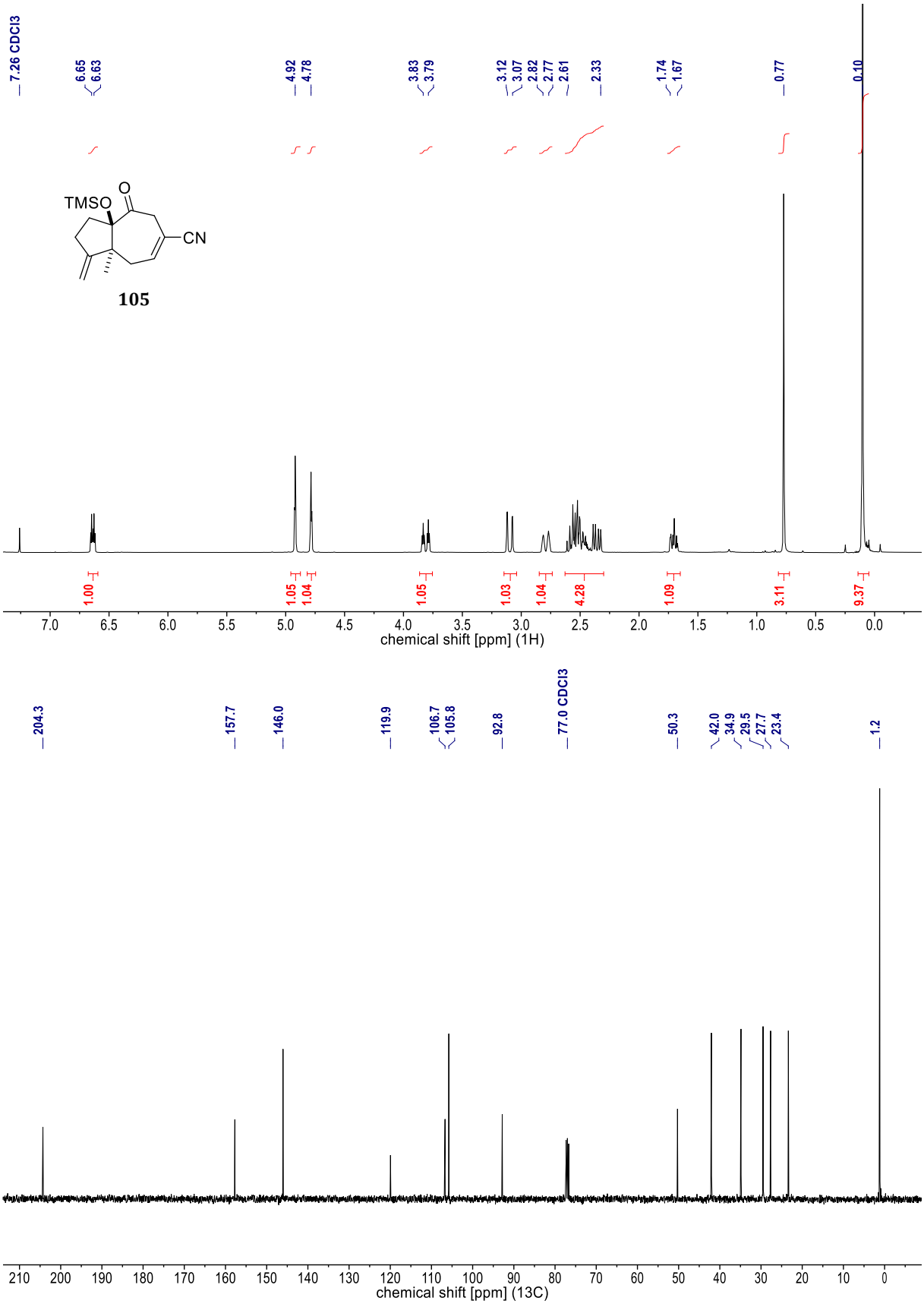

Figure 118. NMR spectra of **105** [^{1}H (400 MHz, $CDCl_3$) & ^{13}C (101 MHz, $CDCl_3$)].

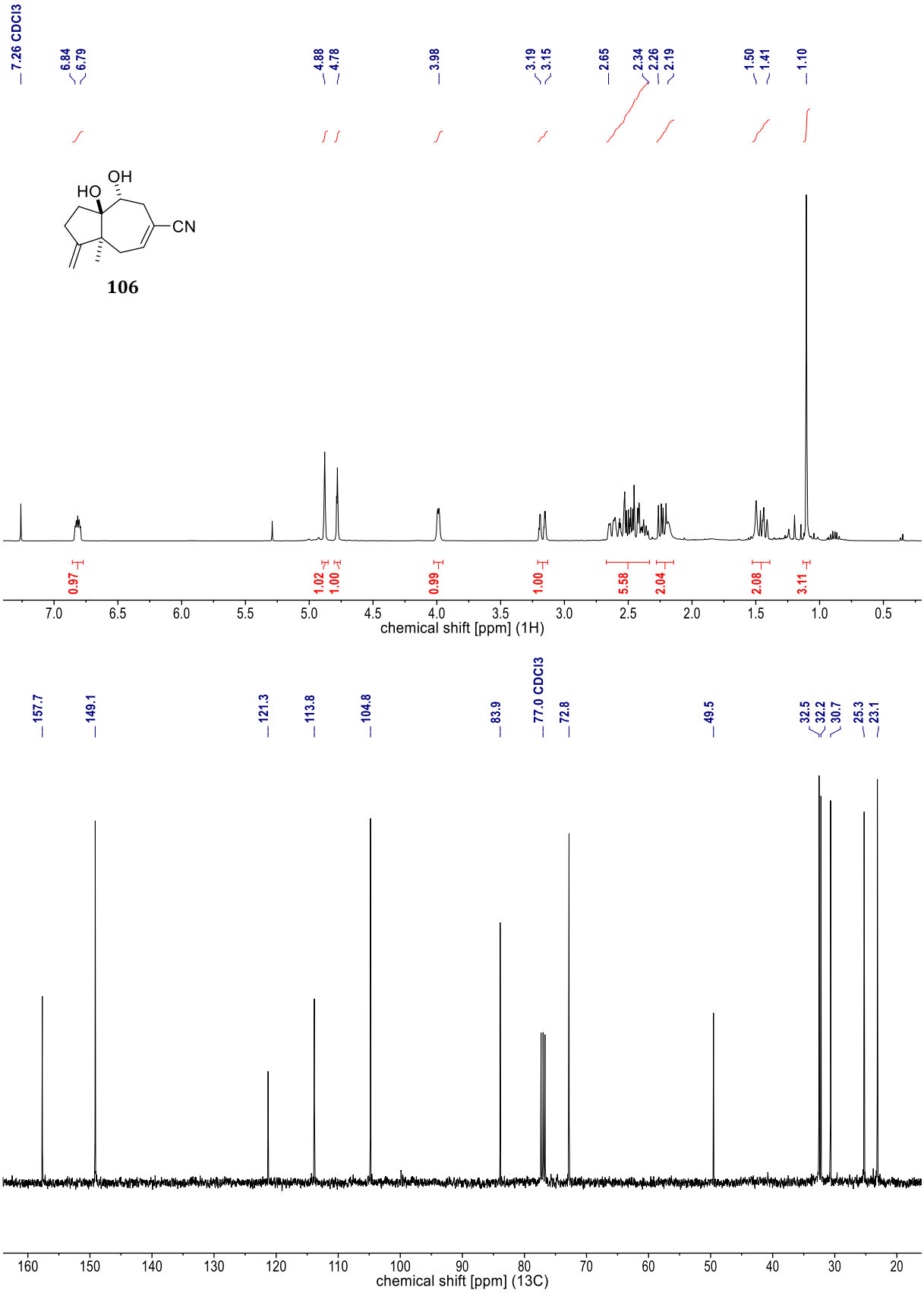

Figure 119. NMR spectra of **106** [^{1}H (400 MHz, $CDCl_3$) & ^{13}C (101 MHz, $CDCl_3$)].

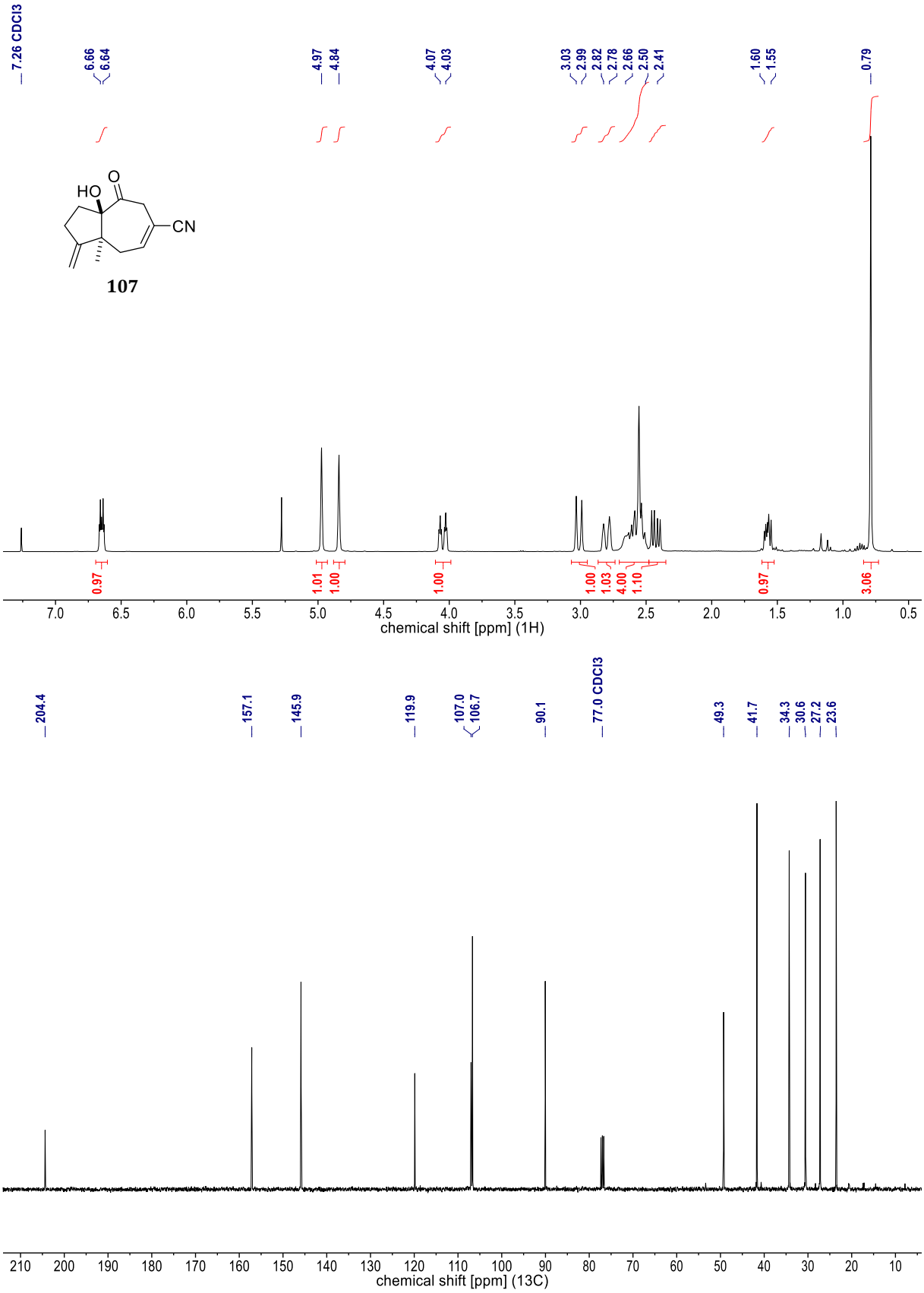

Figure 120. NMR spectra of **107** [^{1}H (400 MHz, $CDCl_3$) & ^{13}C (101 MHz, $CDCl_3$)].

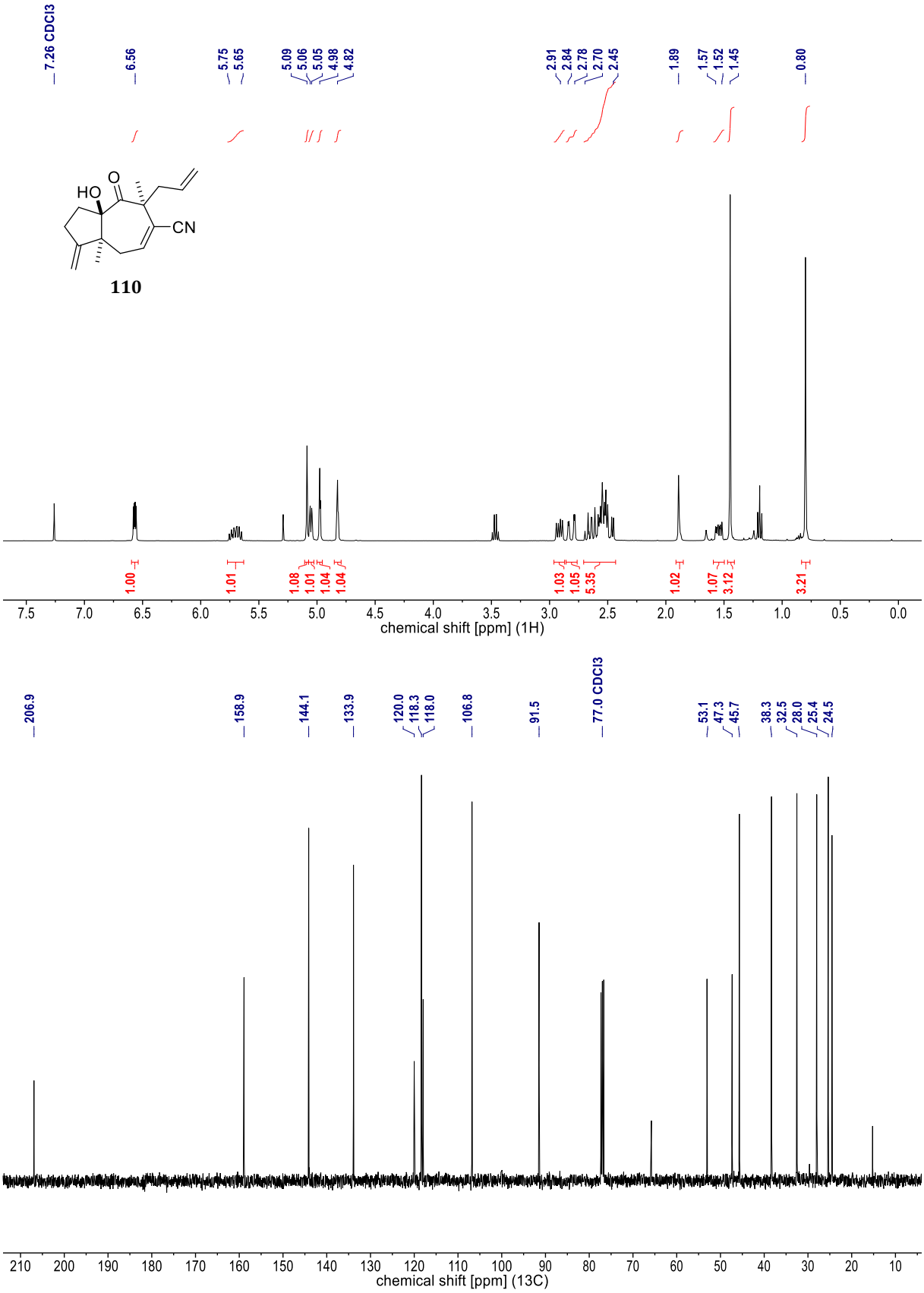

Figure 121. NMR spectra of **110** [^{1}H (400 MHz, $CDCl_3$) & ^{13}C (101 MHz, $CDCl_3$)].

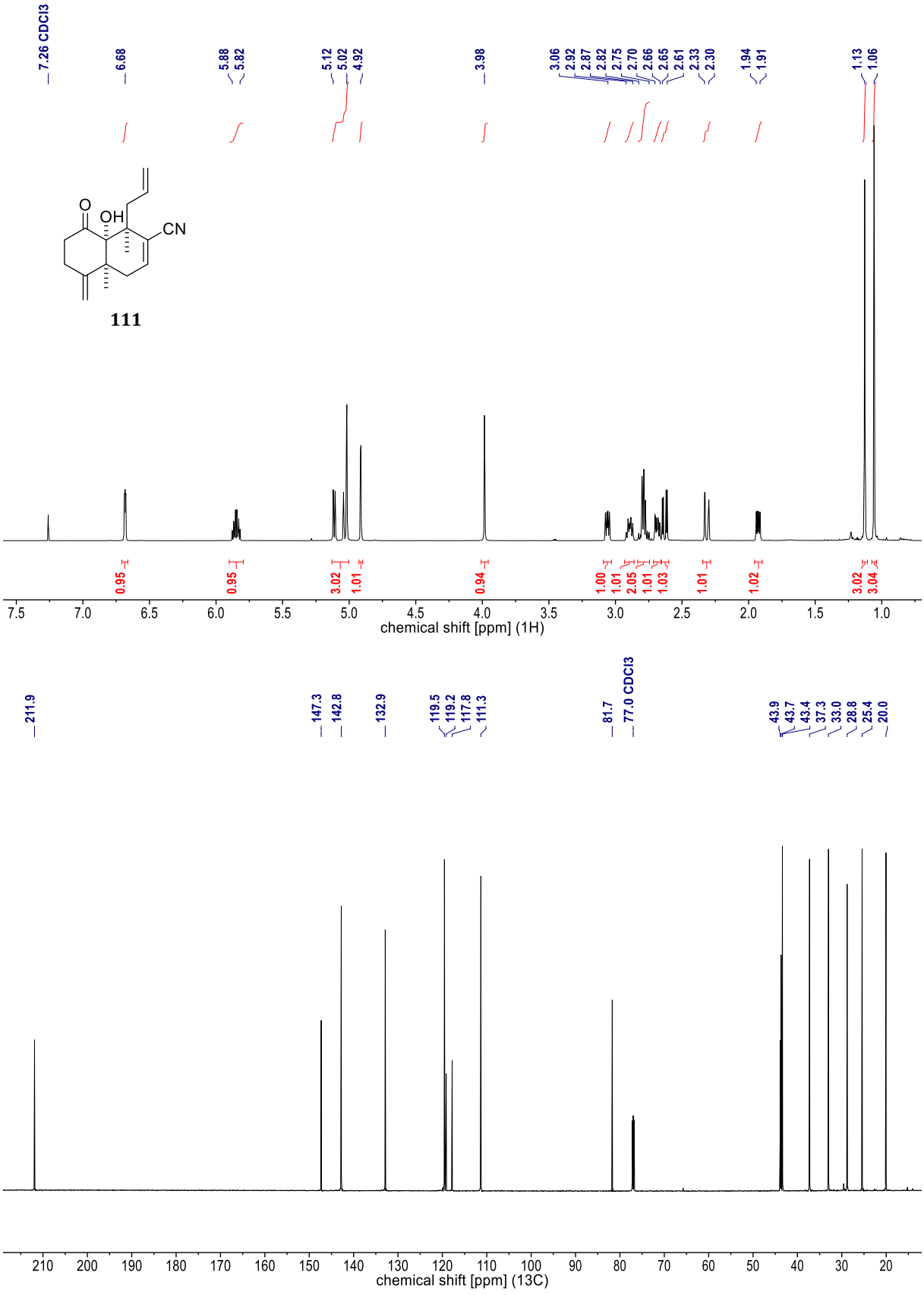

Figure 122. NMR spectra of **111** [^{1}H (700 MHz, $CDCl_3$) & ^{13}C (176 MHz, $CDCl_3$)].

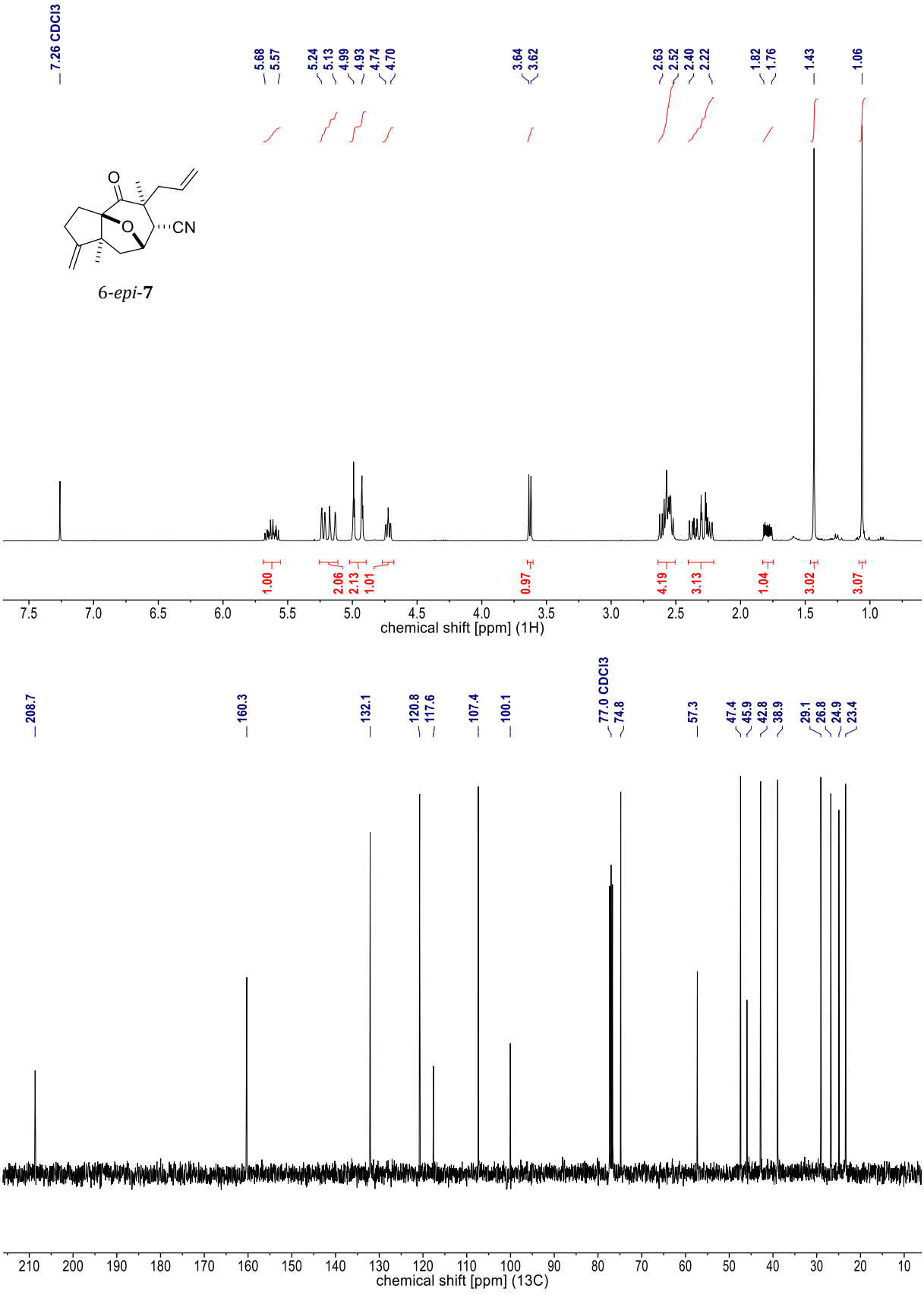

Figure 123. NMR spectra of 6-*epi*-**7** [^{1}H (400 MHz, $CDCl_3$) & ^{13}C (101 MHz, $CDCl_3$)].

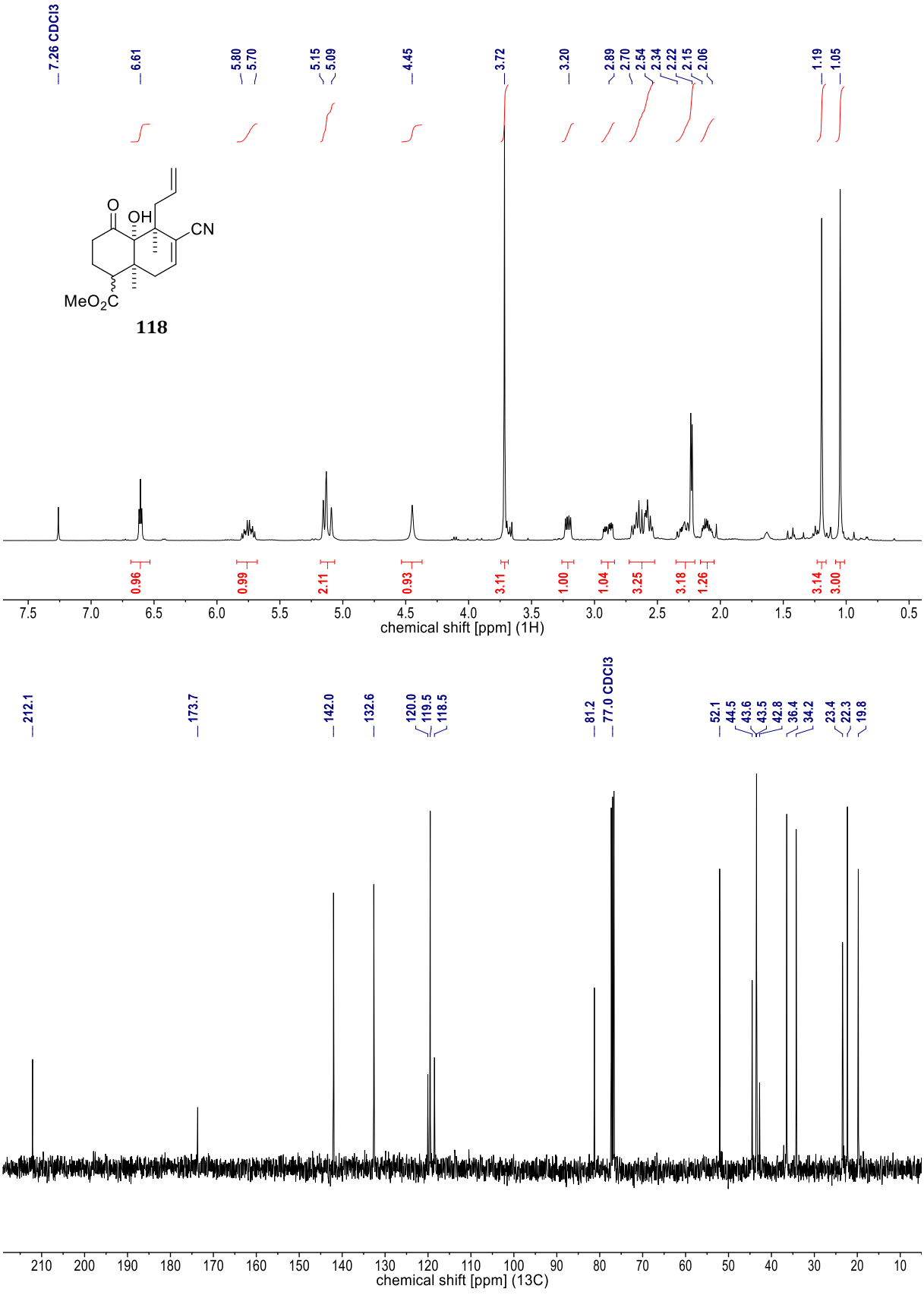

Figure 124. NMR spectra of **118** [^{1}H (400 MHz, $CDCl_3$) & ^{13}C (101 MHz, $CDCl_3$)].

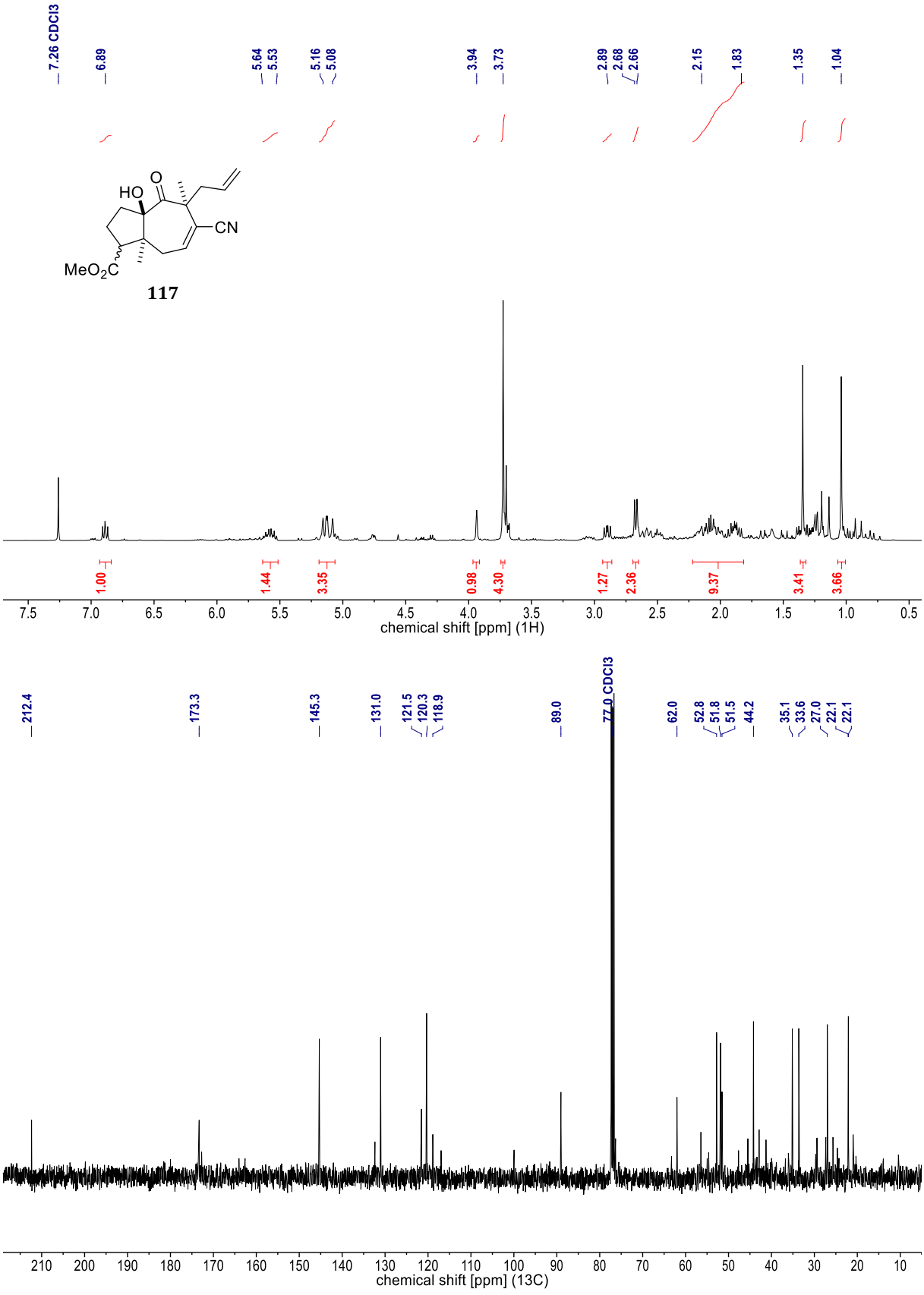

Figure 125. NMR spectra of impure **117** [^{1}H (400 MHz, $CDCl_3$) & ^{13}C (101 MHz, $CDCl_3$)].

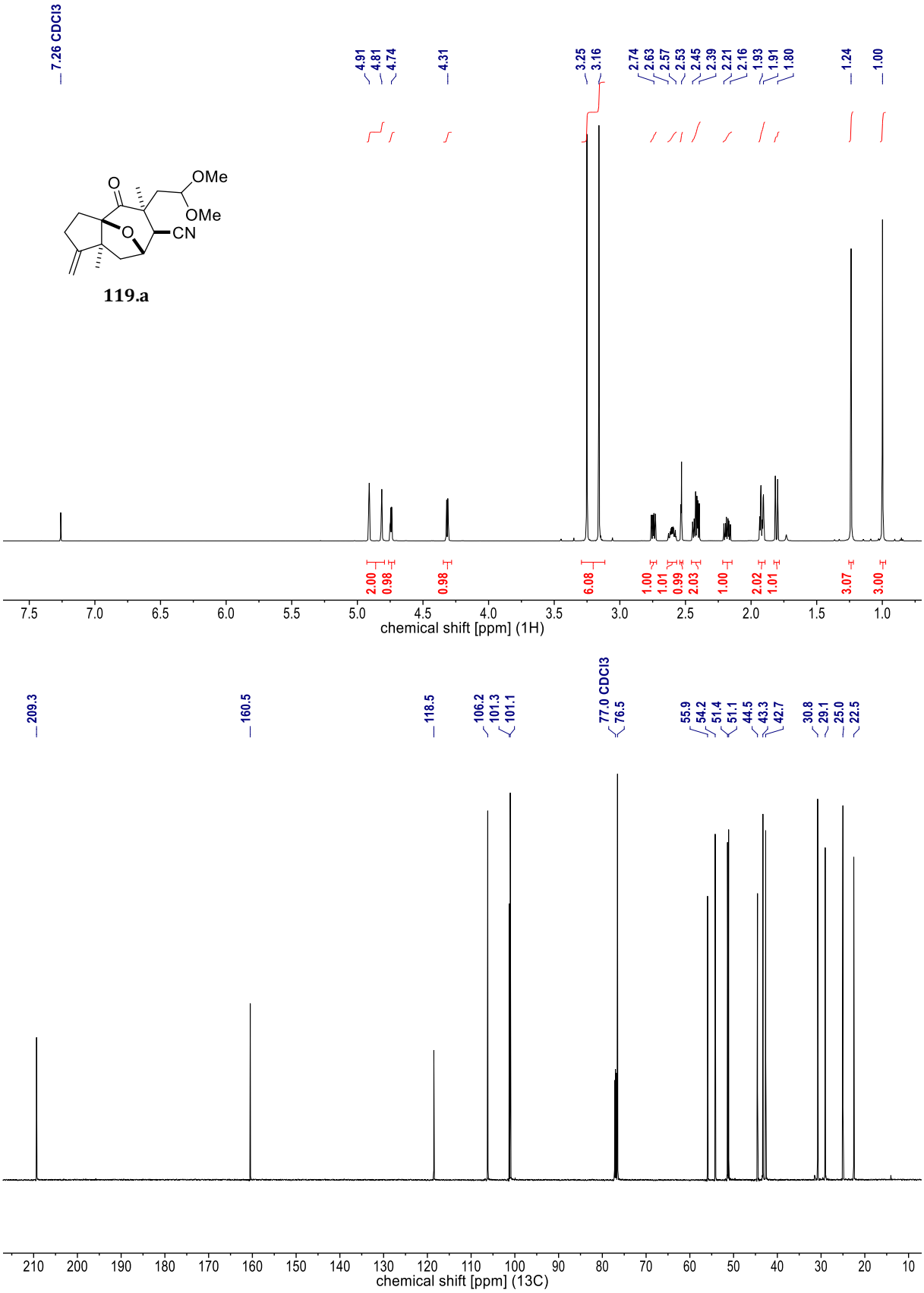

Figure 126. NMR spectra of **119.a** [^{1}H (700 MHz, $CDCl_3$) & ^{13}C (176 MHz, $CDCl_3$)].

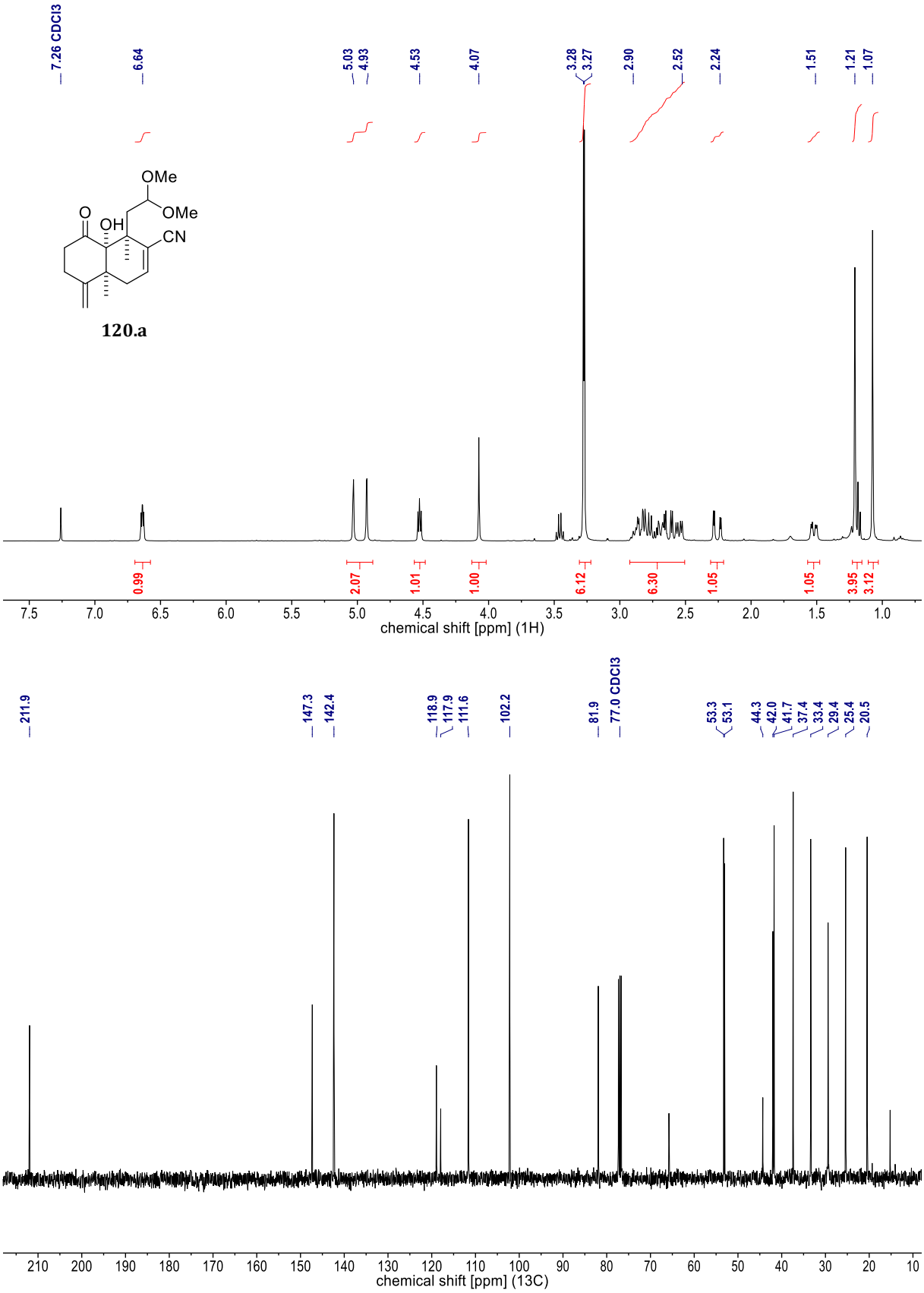

Figure 127. NMR spectra of **120.a** [^{1}H (400 MHz, $CDCl_3$) & ^{13}C (101 MHz, $CDCl_3$)].

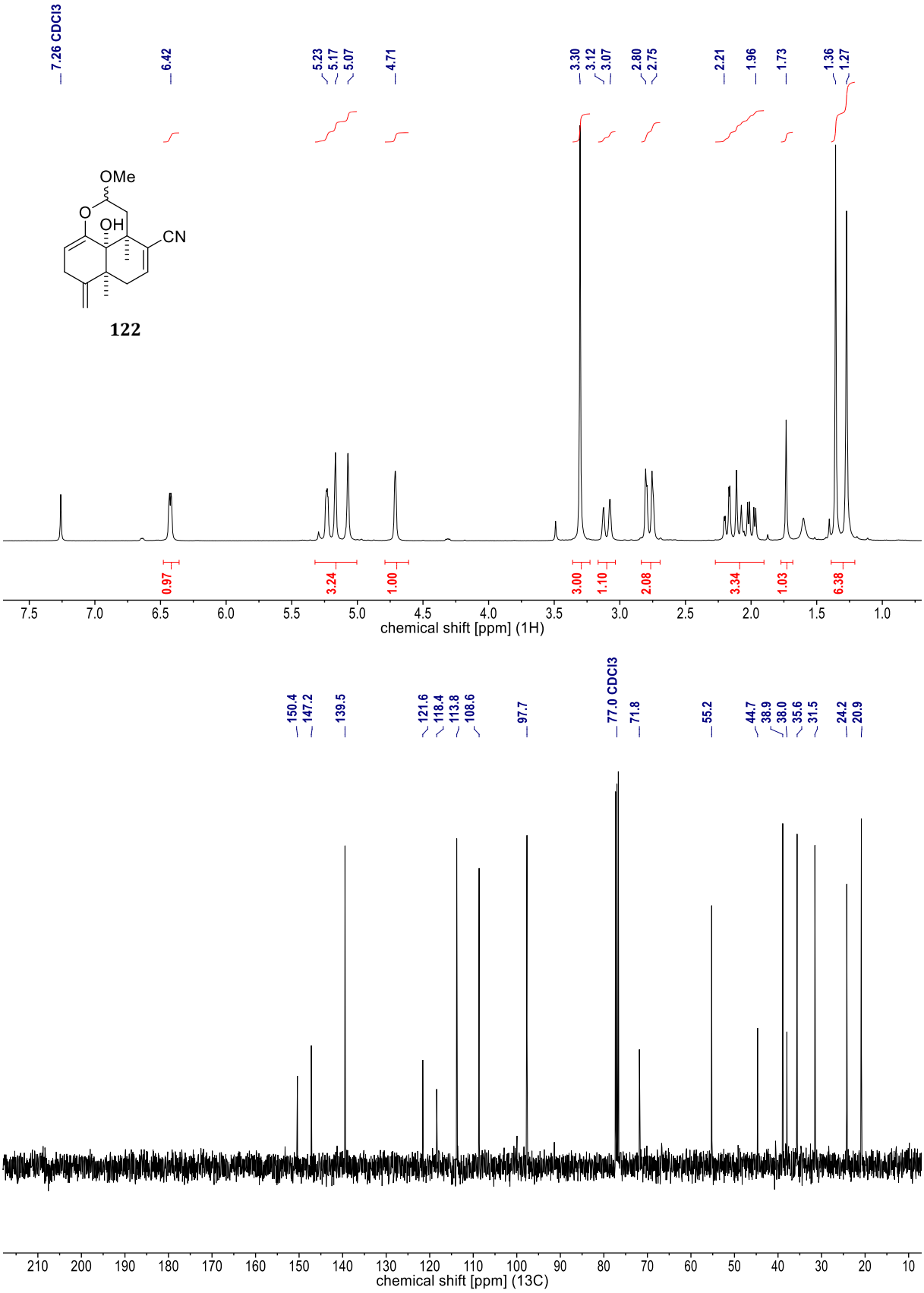

Figure 128. NMR spectra of **122** [^{1}H (400 MHz, $CDCl_3$) & ^{13}C (101 MHz, $CDCl_3$)].

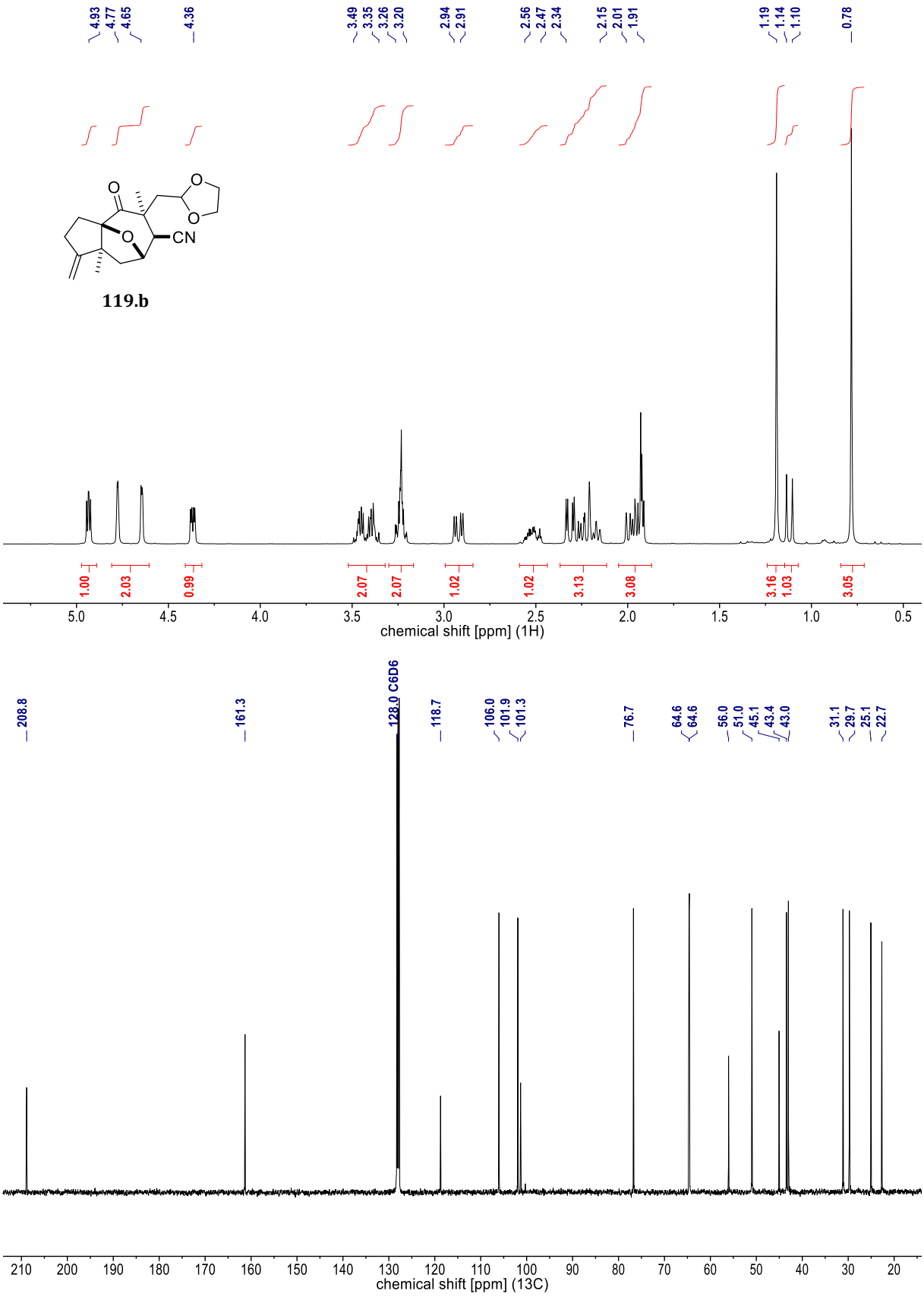

119.b

Figure 129. NMR spectra of **119.b** [^{1}H (400 MHz, C_6D_6) & ^{13}C (101 MHz, C_6D_6)].

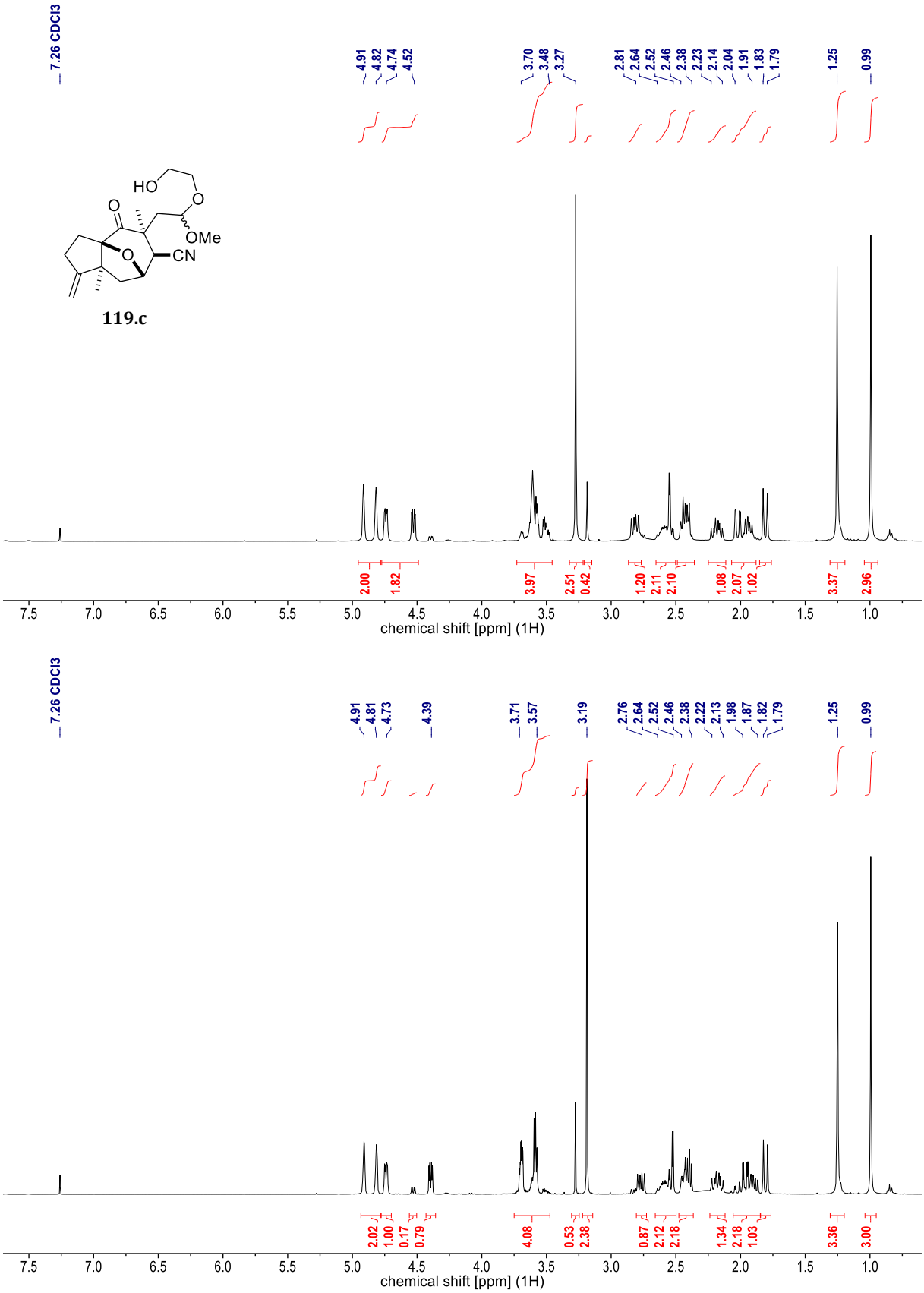

Figure 130. ^{1}H NMR spectra of **119.c** (400 MHz, $CDCl_3$).
Upper spectrum: *less polar DS*; lower spectrum: *more polar DS*.

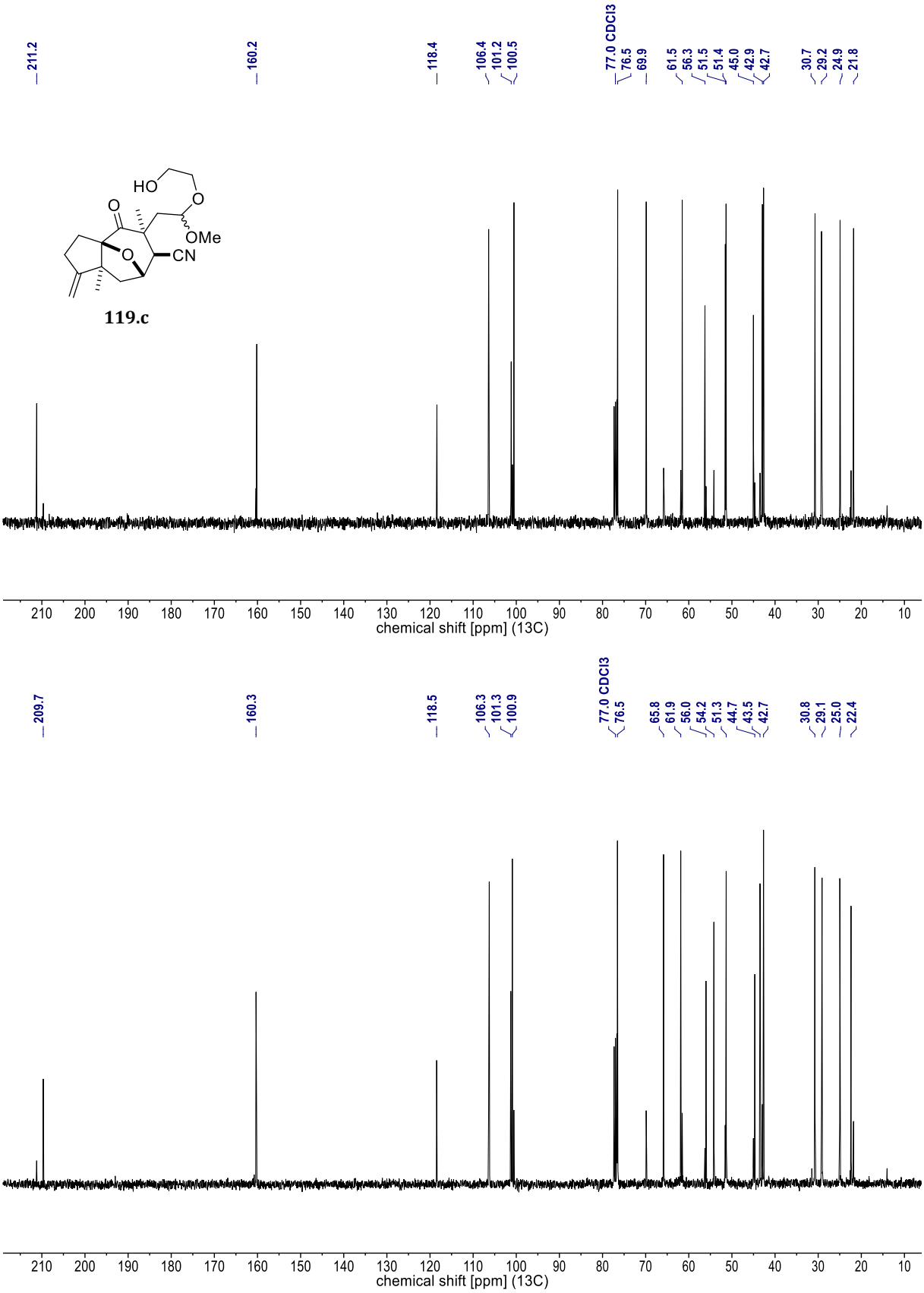

Figure 131. ^{13}C NMR spectra of **119.c** (101 MHz, $CDCl_3$).
Upper spectrum: *less polar DS*; lower spectrum: *more polar DS*.

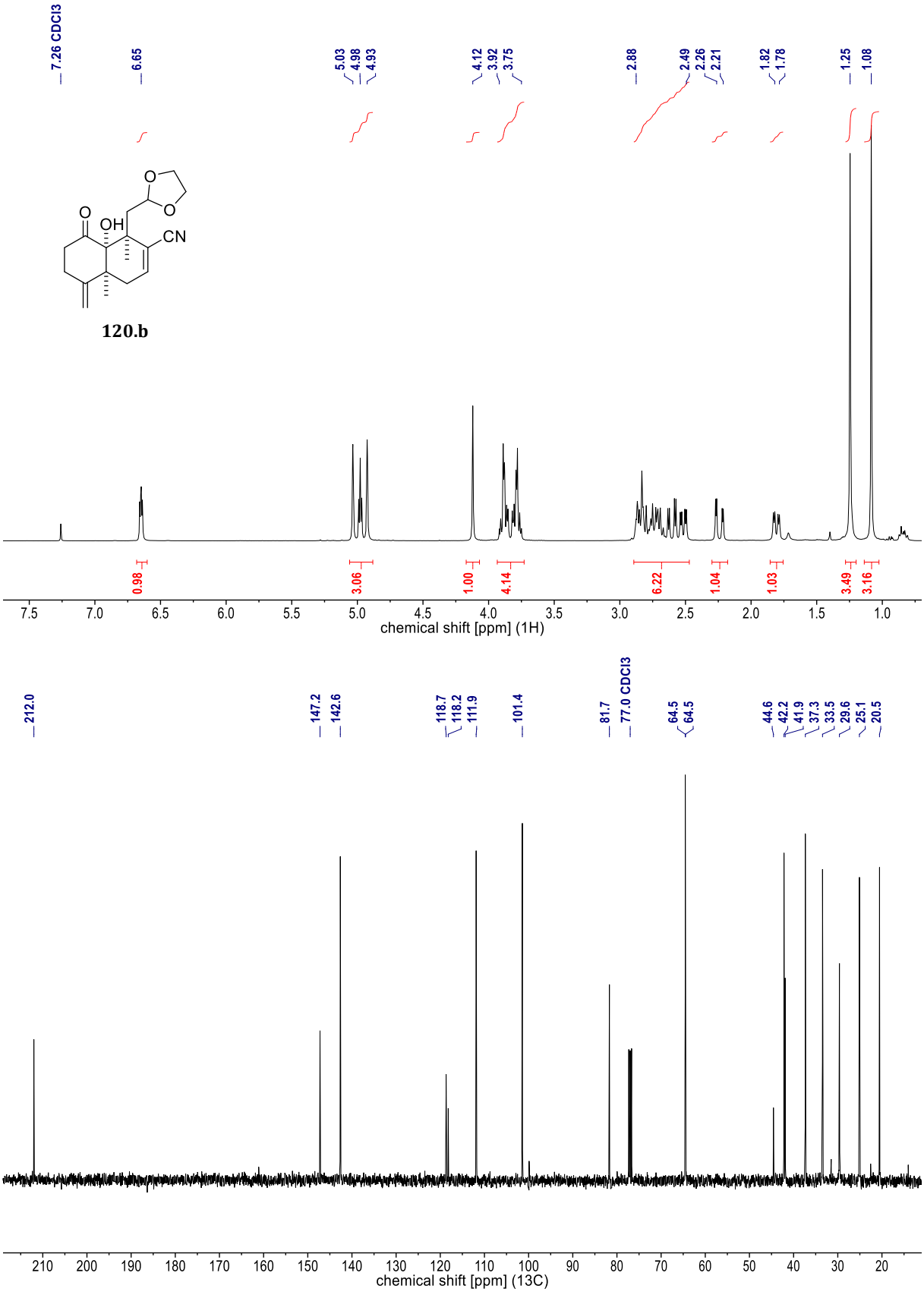

Figure 132. NMR spectra of **120.b** [^{1}H (400 MHz, $CDCl_3$) & ^{13}C (101 MHz, $CDCl_3$)].

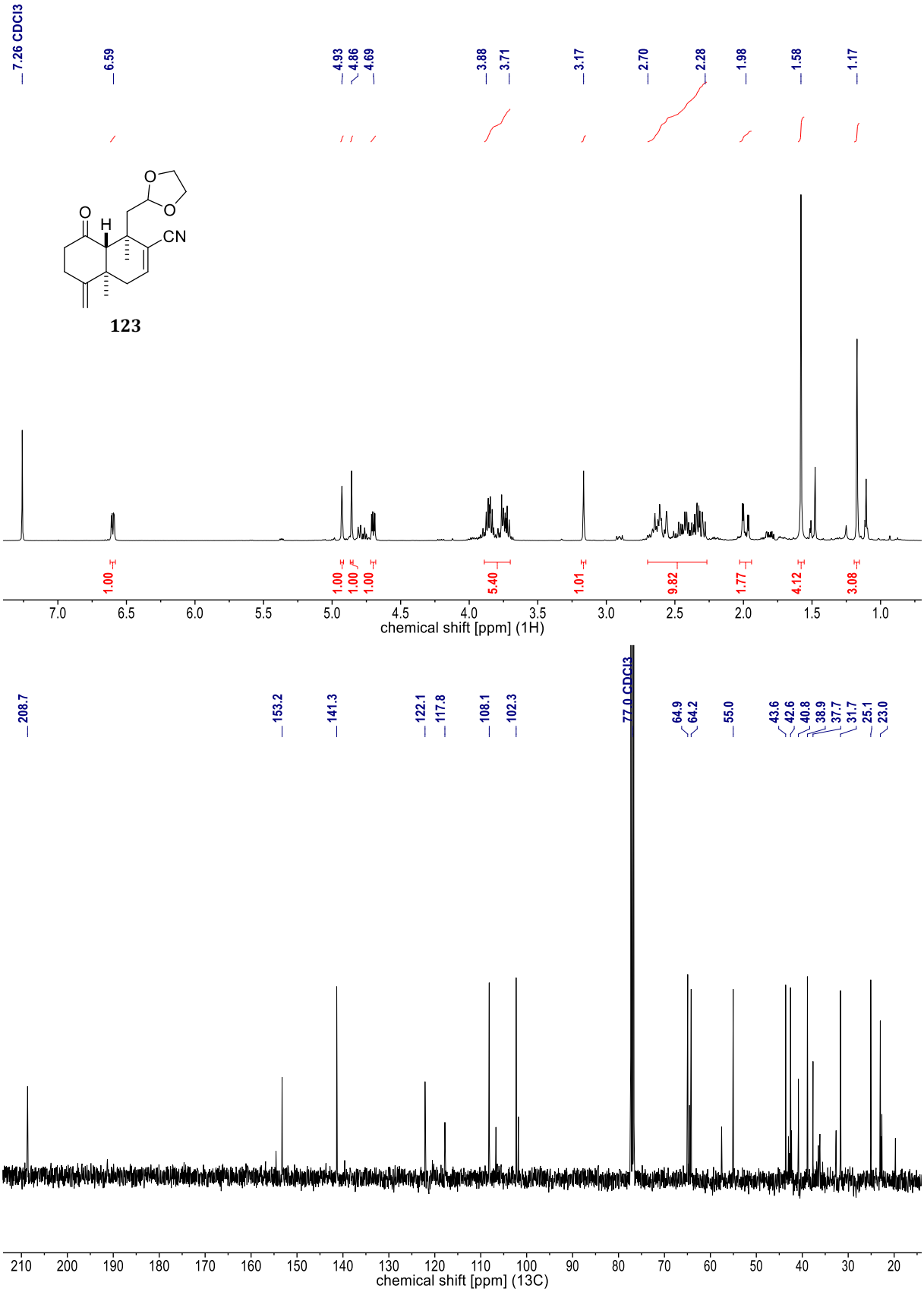

Figure 133. NMR spectra of **123** [^{1}H (400 MHz, $CDCl_3$) & ^{13}C (101 MHz, $CDCl_3$)].
The presence of another compound is evident (presumably the respective alcohol).

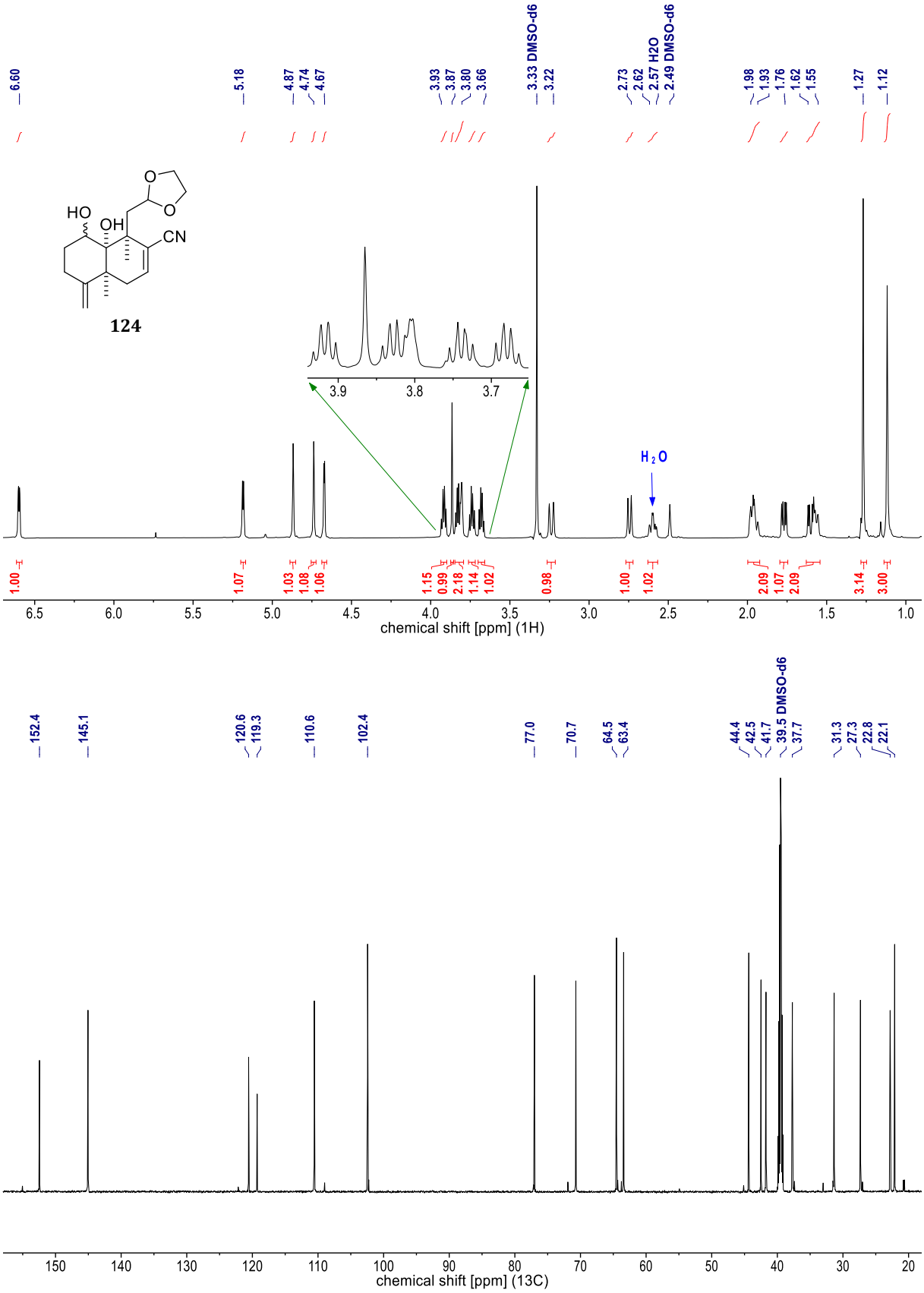

Figure 134. NMR spectra of **124** [^{1}H (700 MHz, DMSO-d_6) & ^{13}C (176 MHz, DMSO-d_6)].

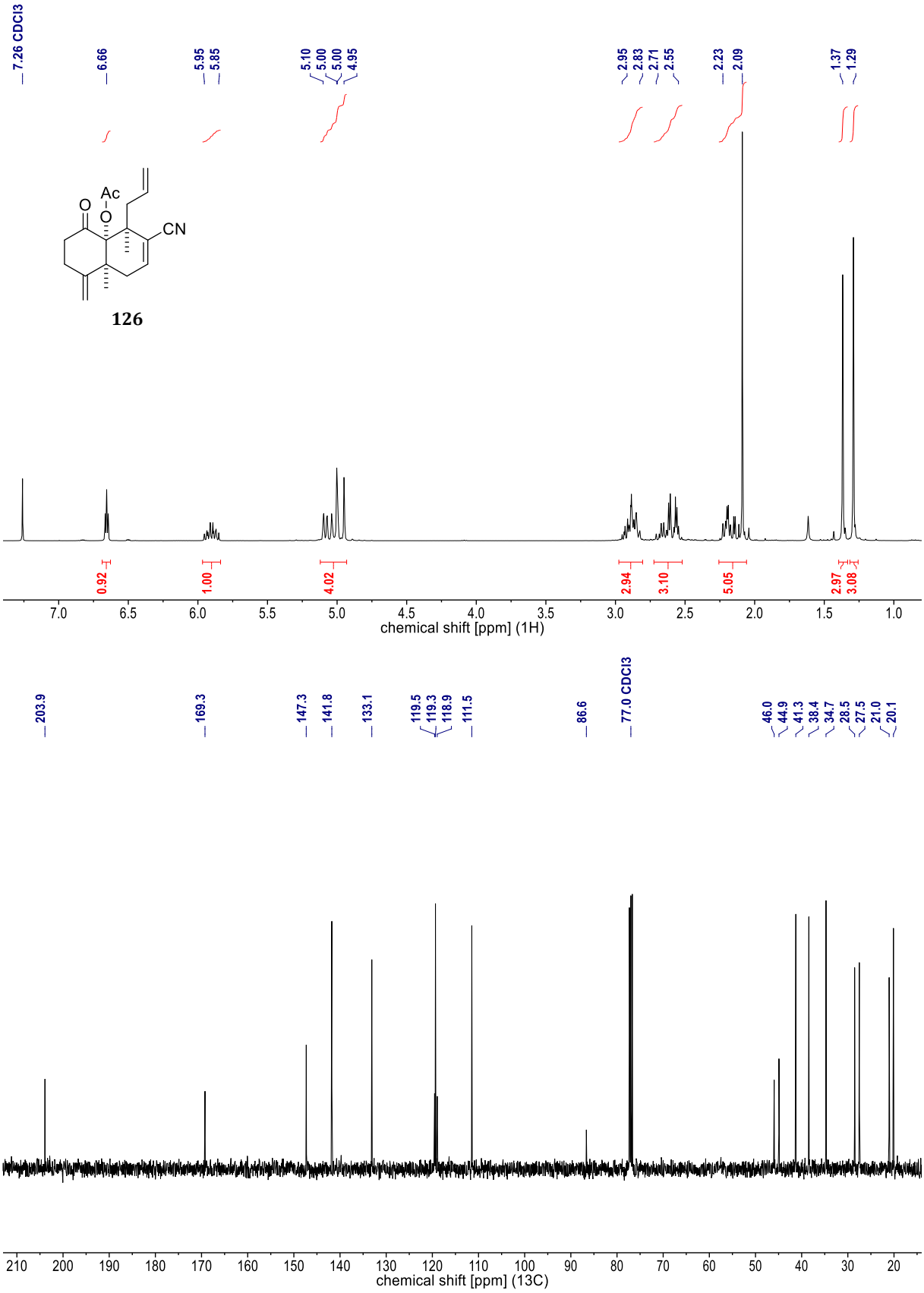

Figure 135. NMR spectra of **126** [^{1}H (400 MHz, $CDCl_3$) & ^{13}C (101 MHz, $CDCl_3$)].

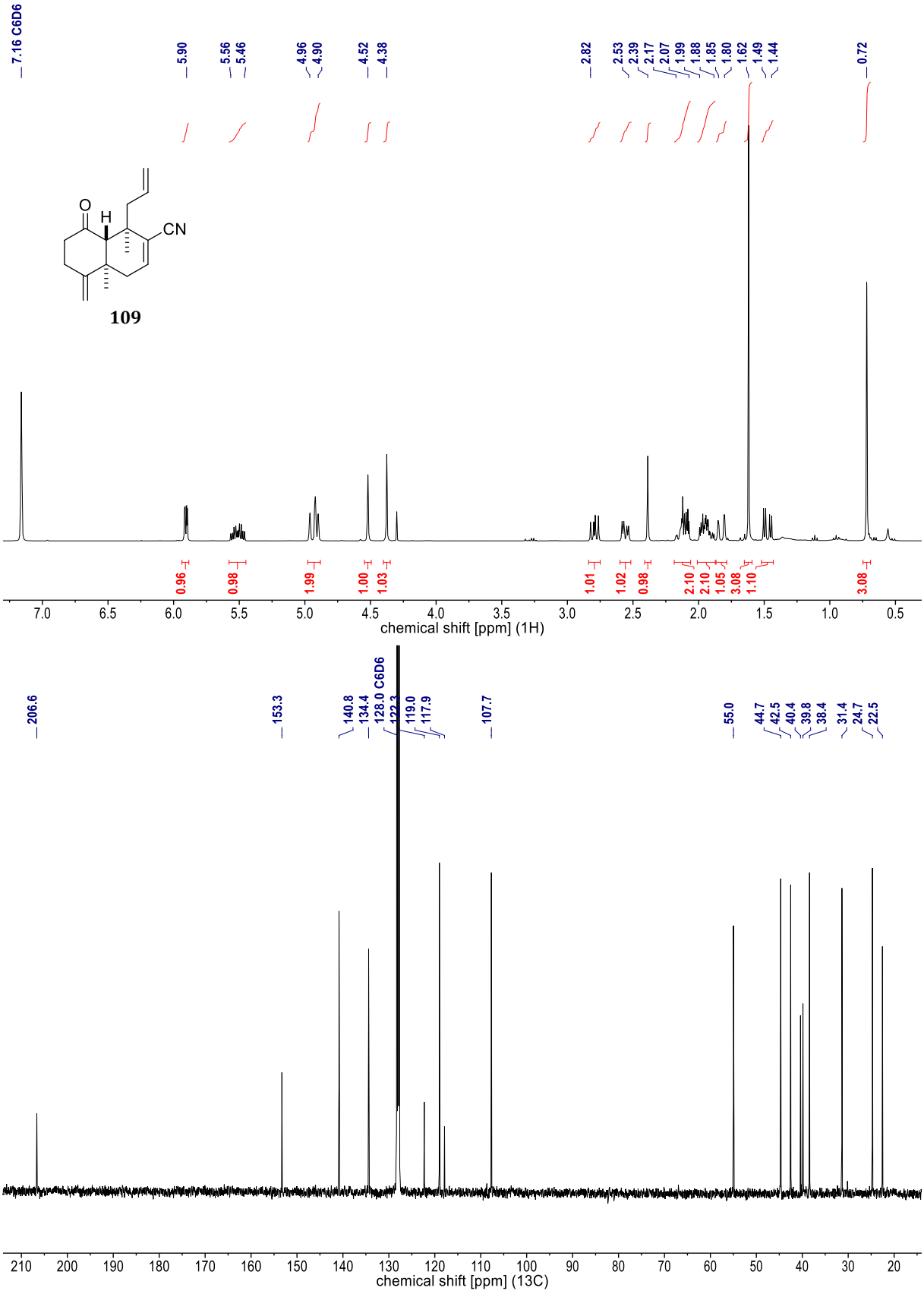

Figure 136. NMR spectra of **109** [^{1}H (400 MHz, C_6D_6) & ^{13}C (101 MHz, C_6D_6)]; *cf.* **Figure 137**.

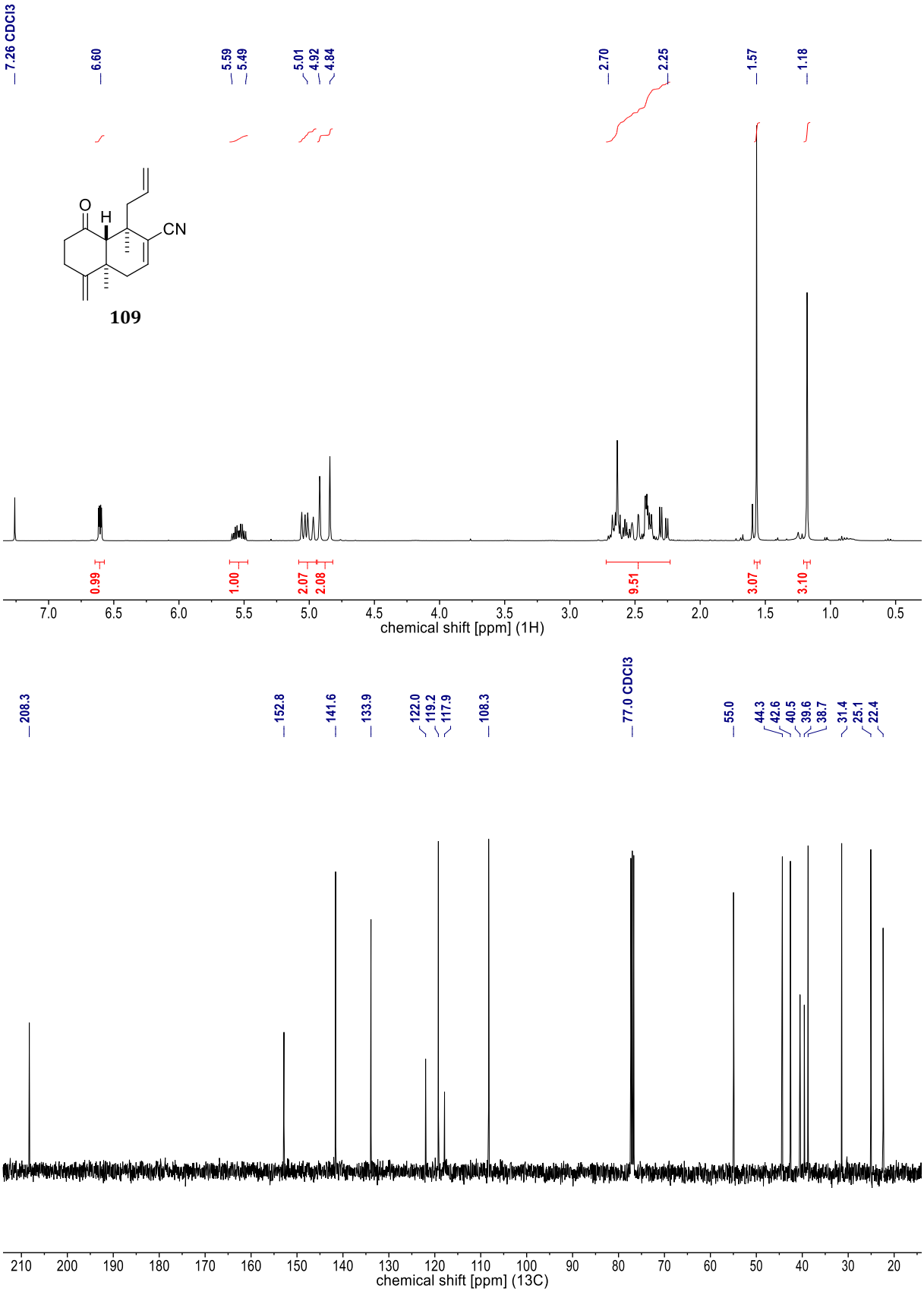

Figure 137. NMR spectra of **109** [^{1}H (400 MHz, $CDCl_3$) & ^{13}C (101 MHz, $CDCl_3$)]; *cf.* **Figure 136**.

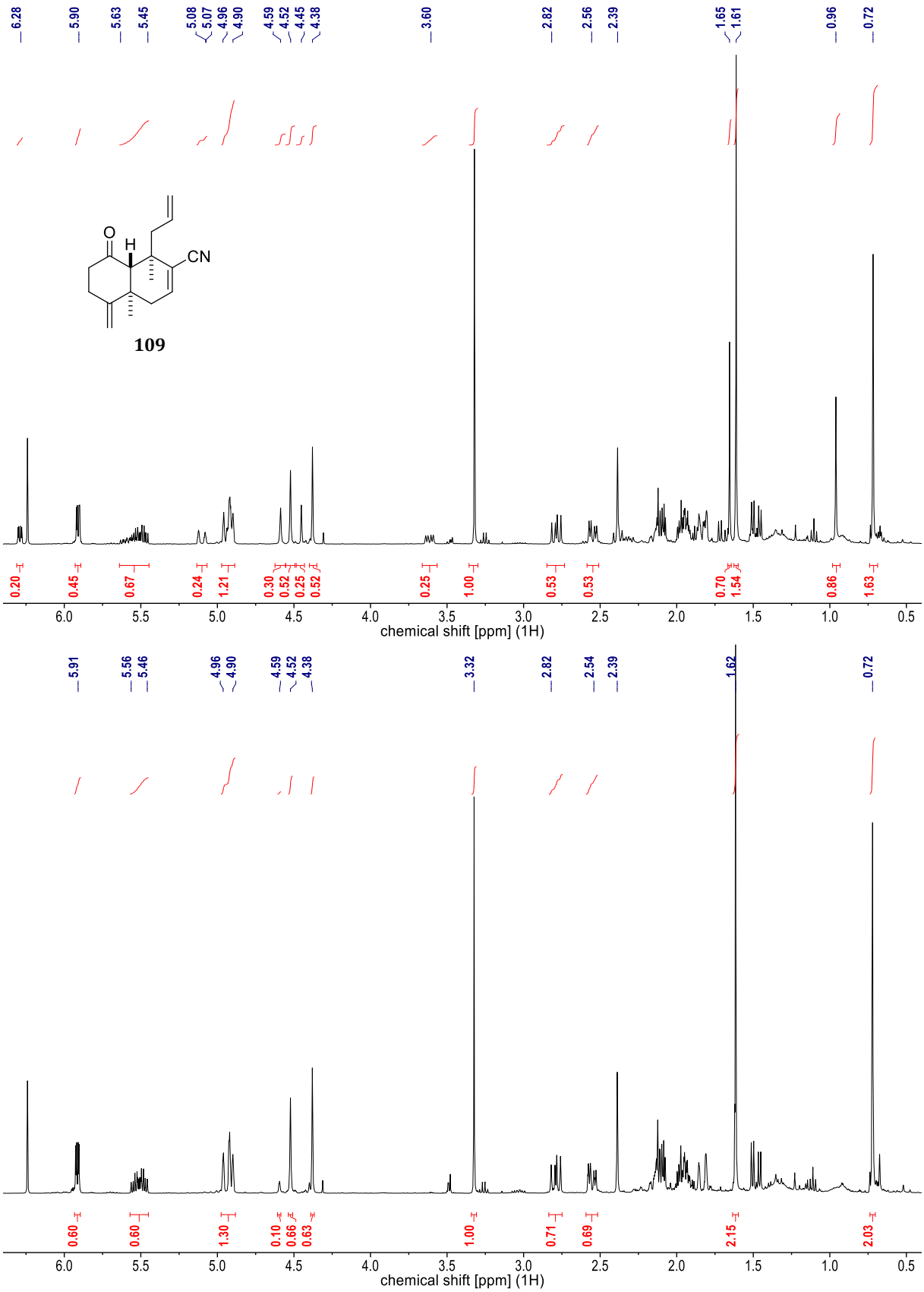

Figure 138. ^{1}H NMR spectra [400 MHz, C_6D_6] of a crude product, in which the ongoing conversion of the *unidentified compound* to **109** could be observed. Upper spectrum: 'immediately' after removal of solvents; lower spectrum: after letting the same NMR solution stand overnight. Distinct signals were picked, integrated, and referenced to the internal standard TMOB (3.32 ppm).

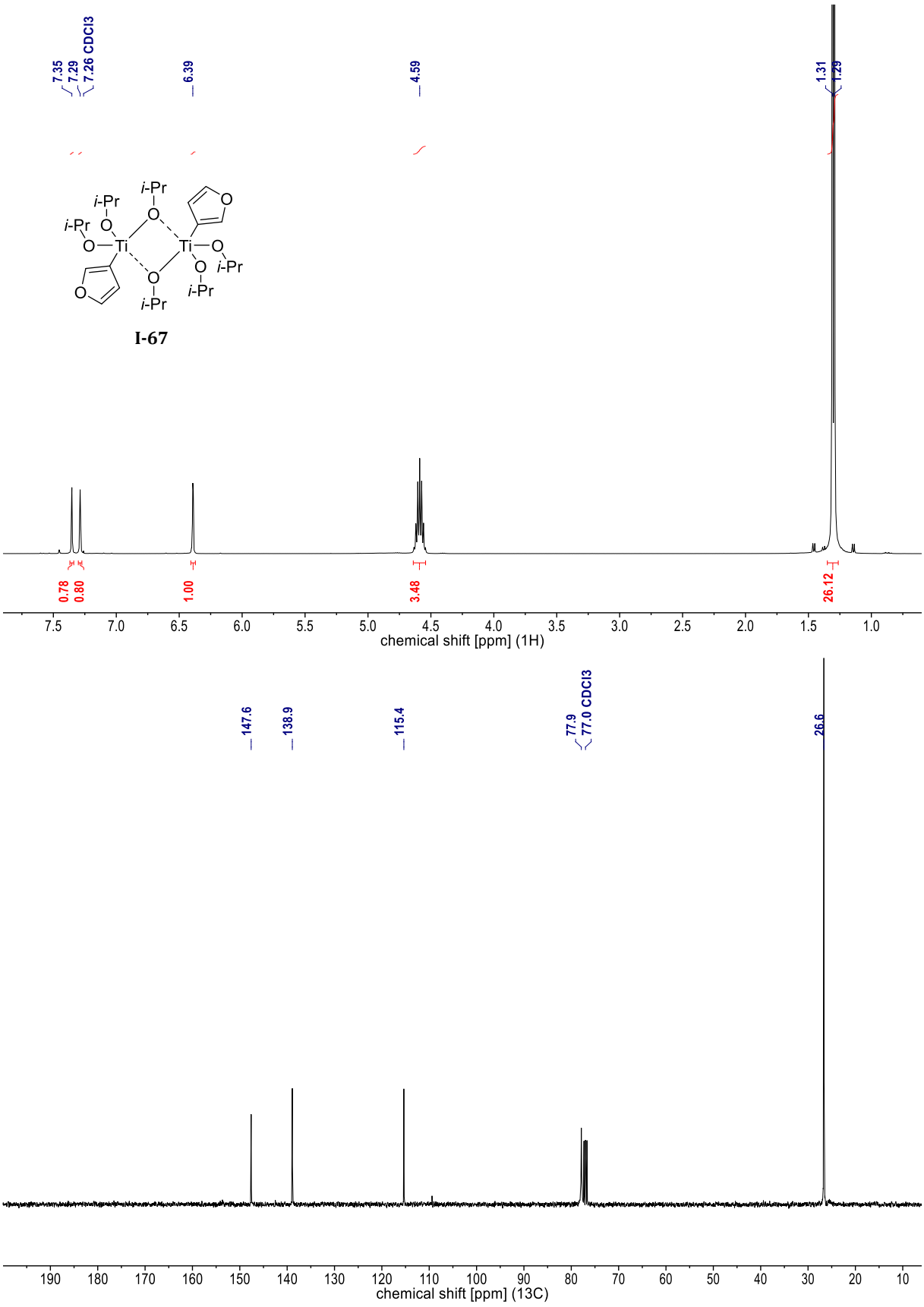

I-67

Figure 139. NMR spectra of **I-67** [^{1}H (400 MHz, $CDCl_3$) & ^{13}C (101 MHz, $CDCl_3$)].

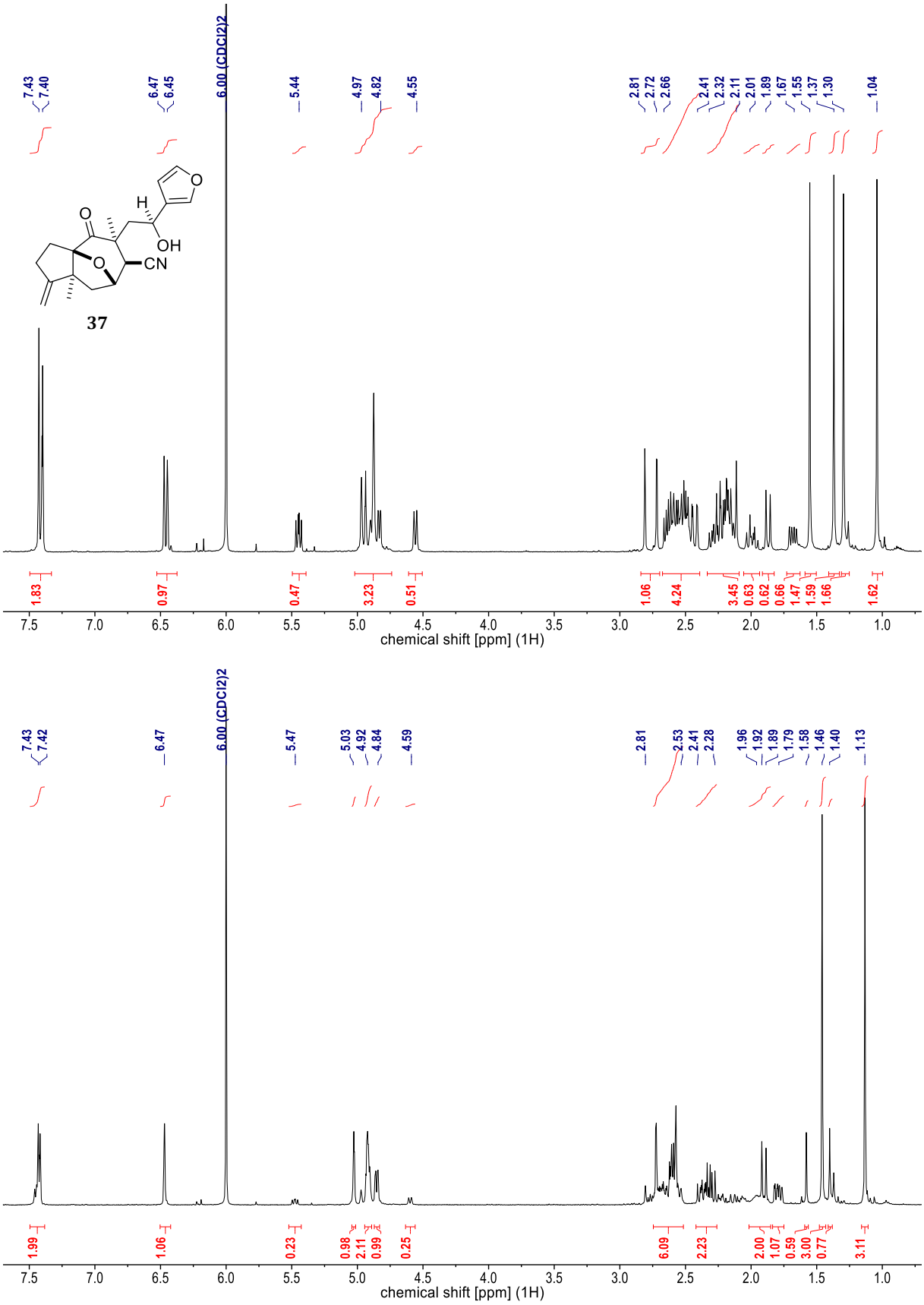

Figure 140. ^{1}H NMR spectra of **37** (400 MHz, 1,1,2,2-tetrachloroethane-d_2, *4 Å MS in NMR tube*). Upper spectrum recorded at 298 K; lower spectrum recorded at 403 K.

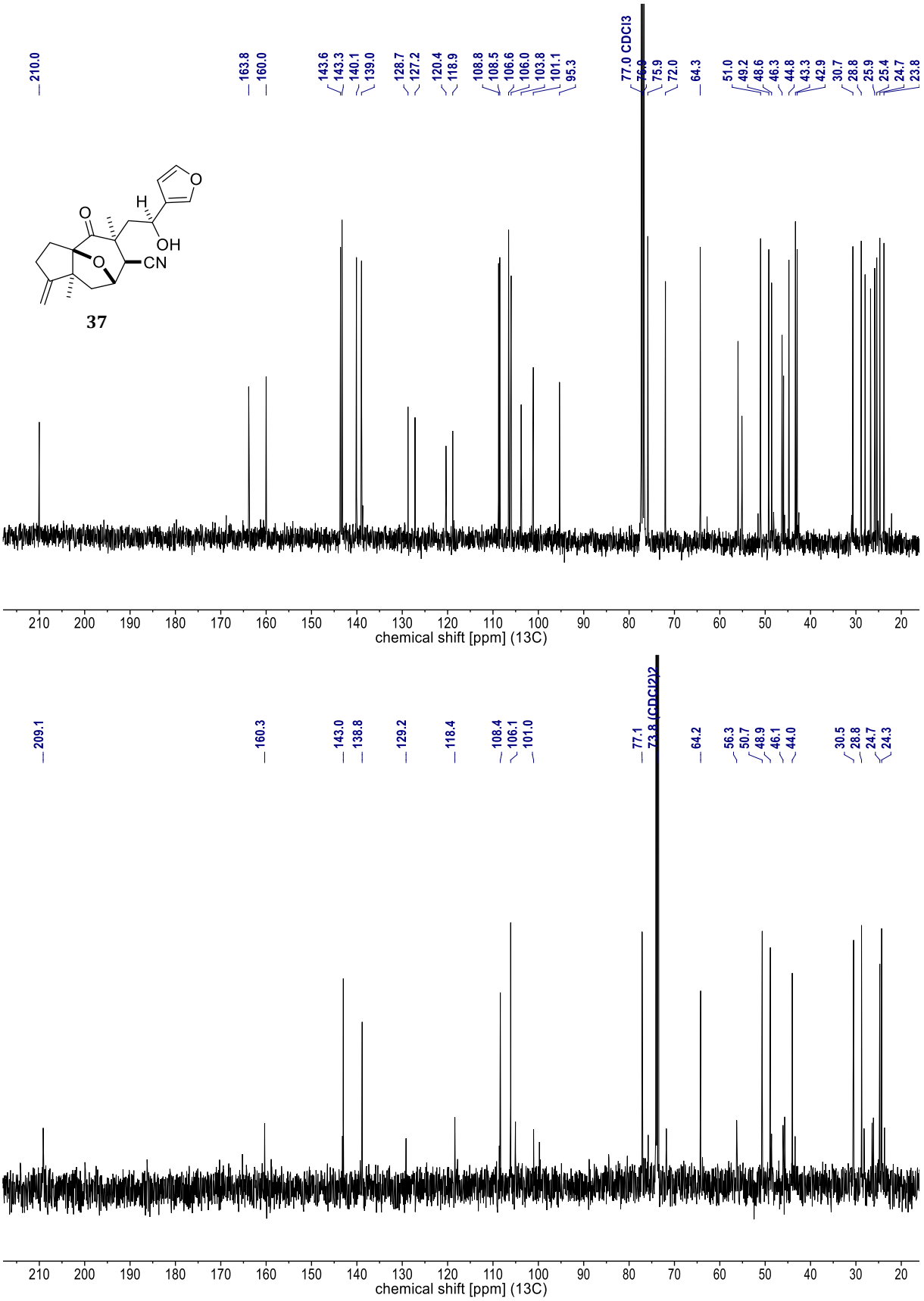

Figure 141. ^{13}C NMR spectra of **37**. Upper spectrum: 101 MHz, $CDCl_3$, recorded at 298 K; lower spectrum: 101 MHz, 1,1,2,2-tetrachloroethane-d_2, *4 Å MS in NMR tube*, recorded at 403 K. *A ^{13}C NMR spectrum in 1,1,2,2-tetrachloroethane was not recorded at 298 K.*

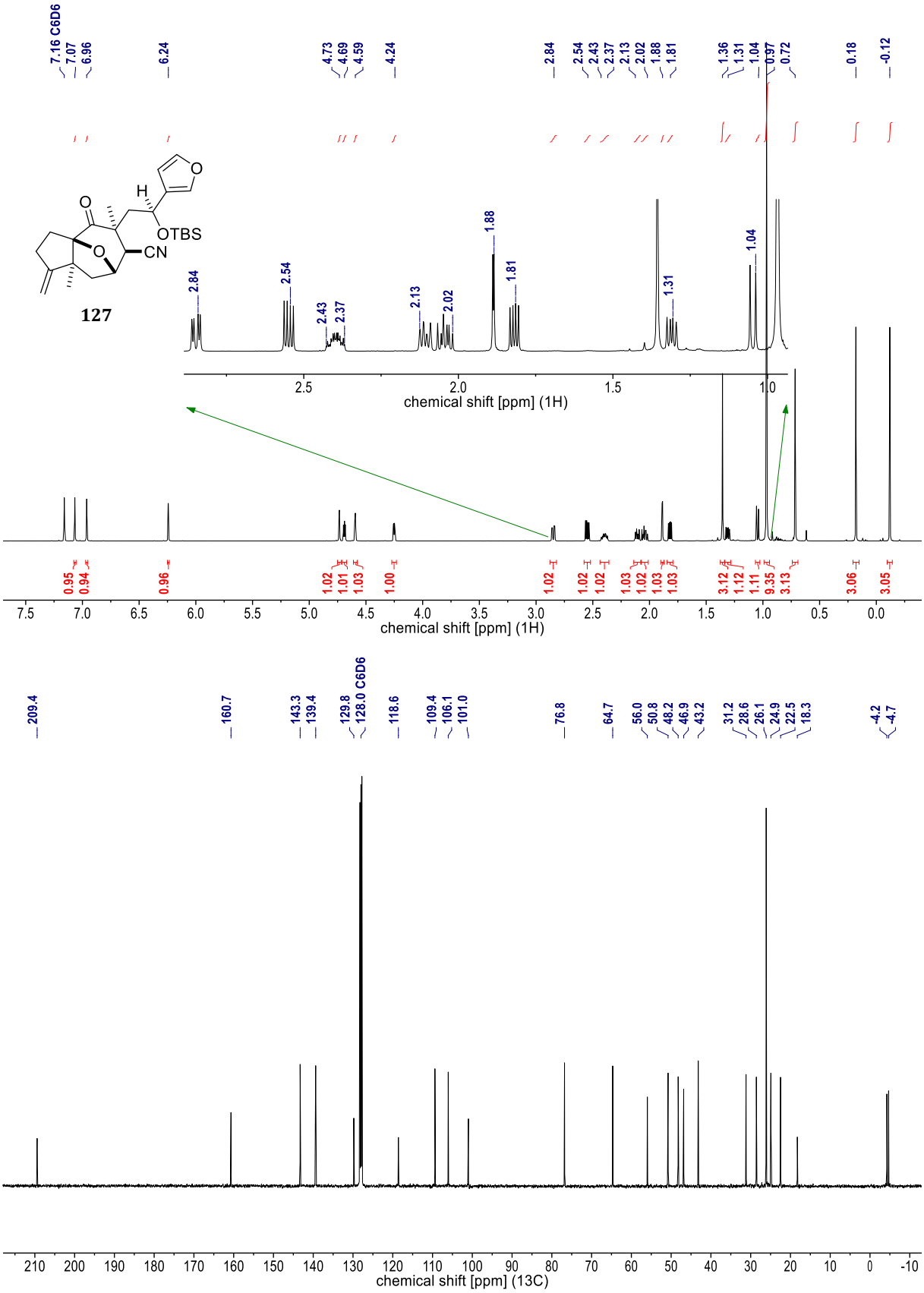

Figure 142. NMR spectra of **127** [^{1}H (700 MHz, C_6D_6) & ^{13}C (101 MHz, C_6D_6)].

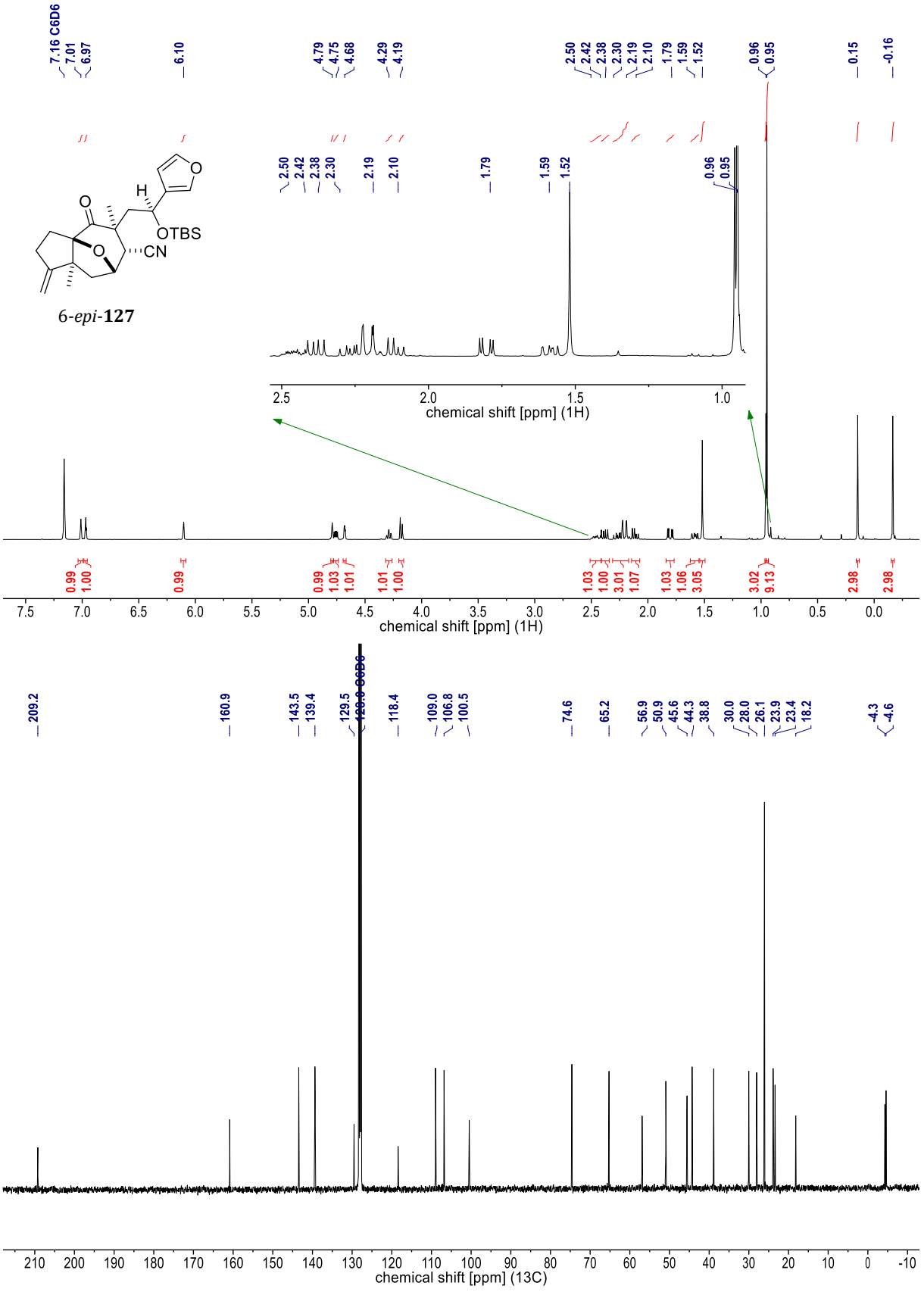

Figure 143. NMR spectra of 6-*epi*-**127** [^{1}H (400 MHz, C_6D_6) & ^{13}C (101 MHz, C_6D_6)].

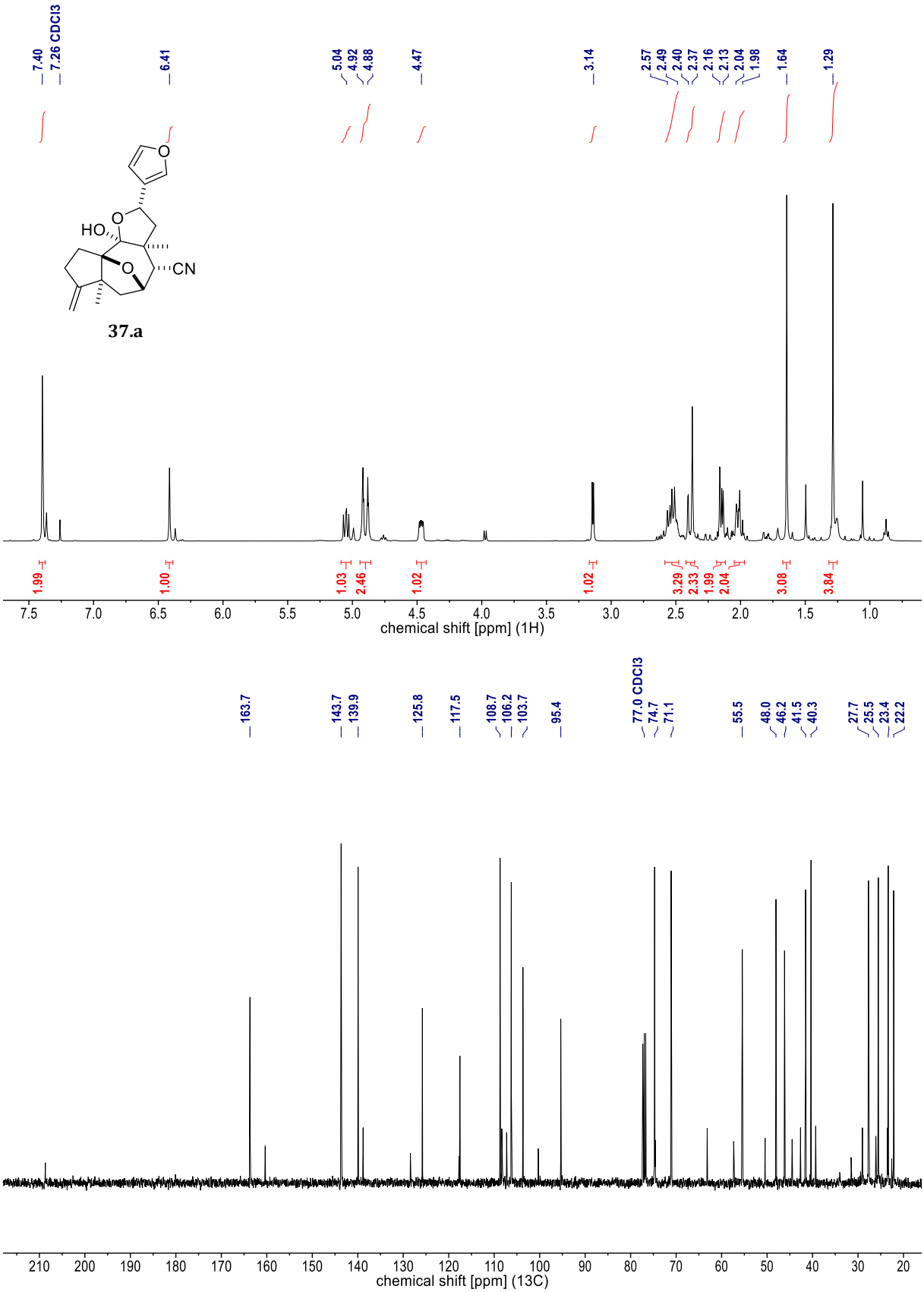

Figure 144. NMR spectra of **37.a** [^{1}H (400 MHz, $CDCl_3$) & ^{13}C (101 MHz, $CDCl_3$)].

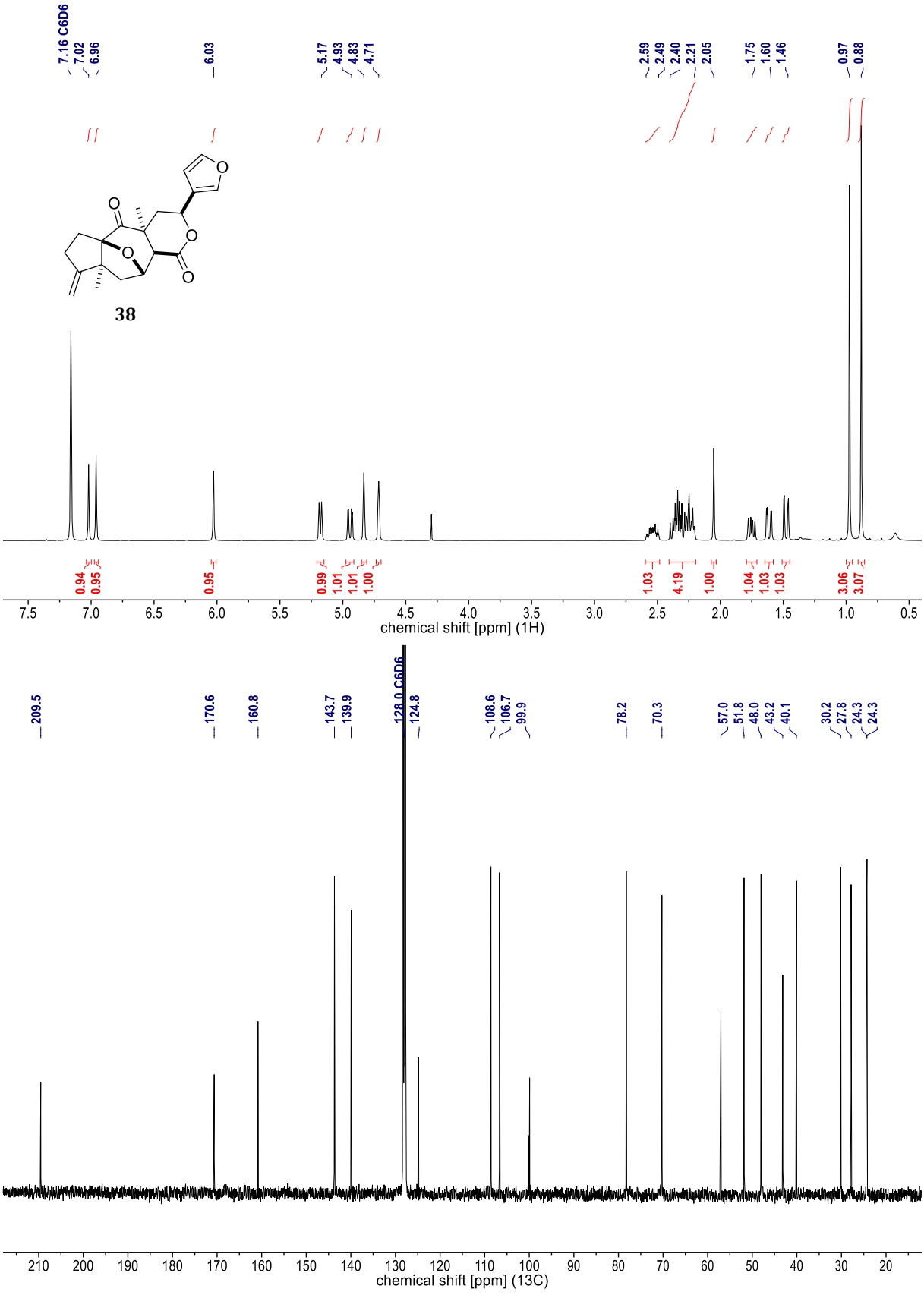

Figure 145. NMR spectra of **38** [^{1}H (400 MHz, C_6D_6) & ^{13}C (101 MHz, C_6D_6)].

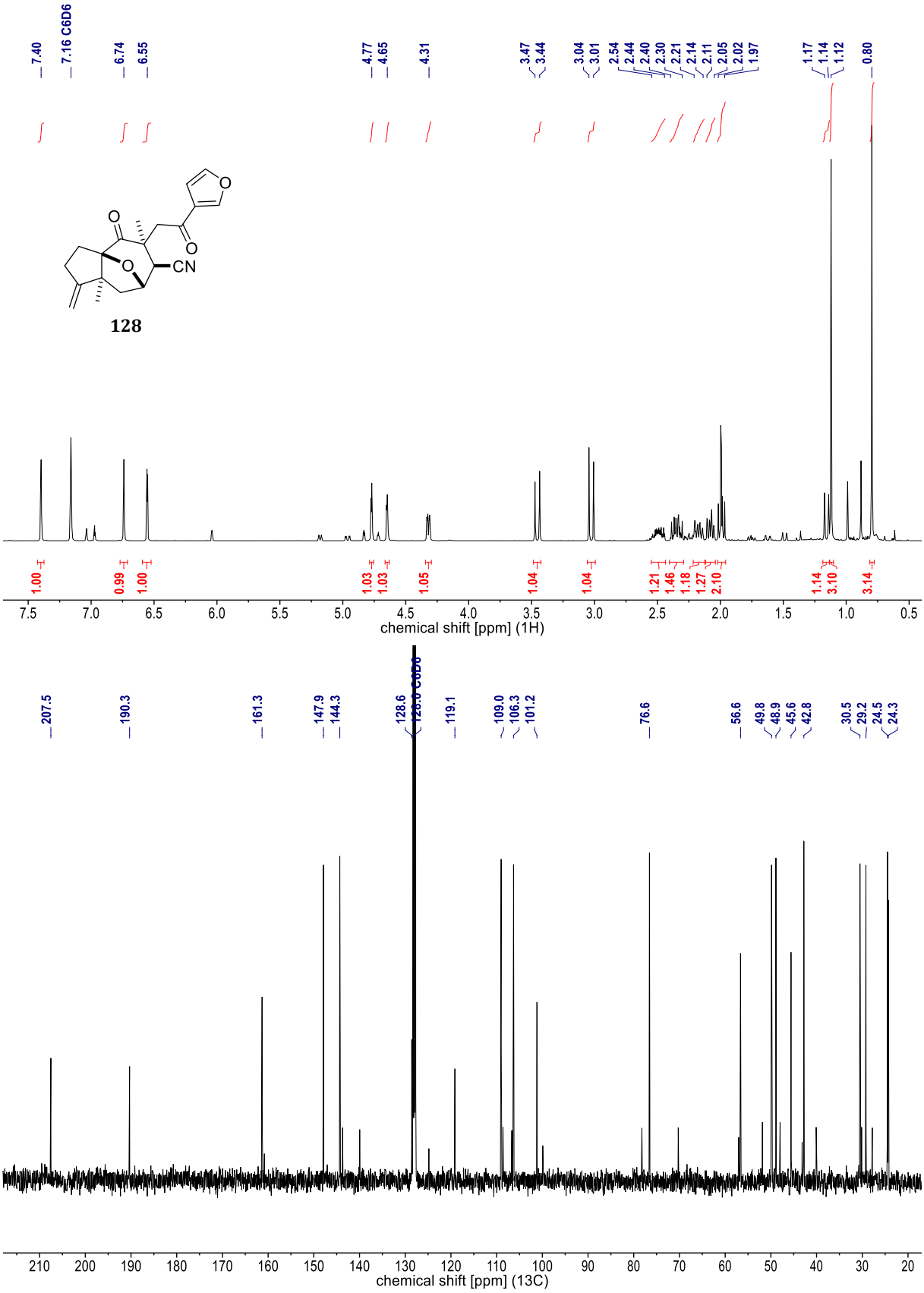

Figure 146. NMR spectra of **128** [^{1}H (400 MHz, C_6D_6) & ^{13}C (101 MHz, C_6D_6)].
*Some lactone **38** is discernible.*

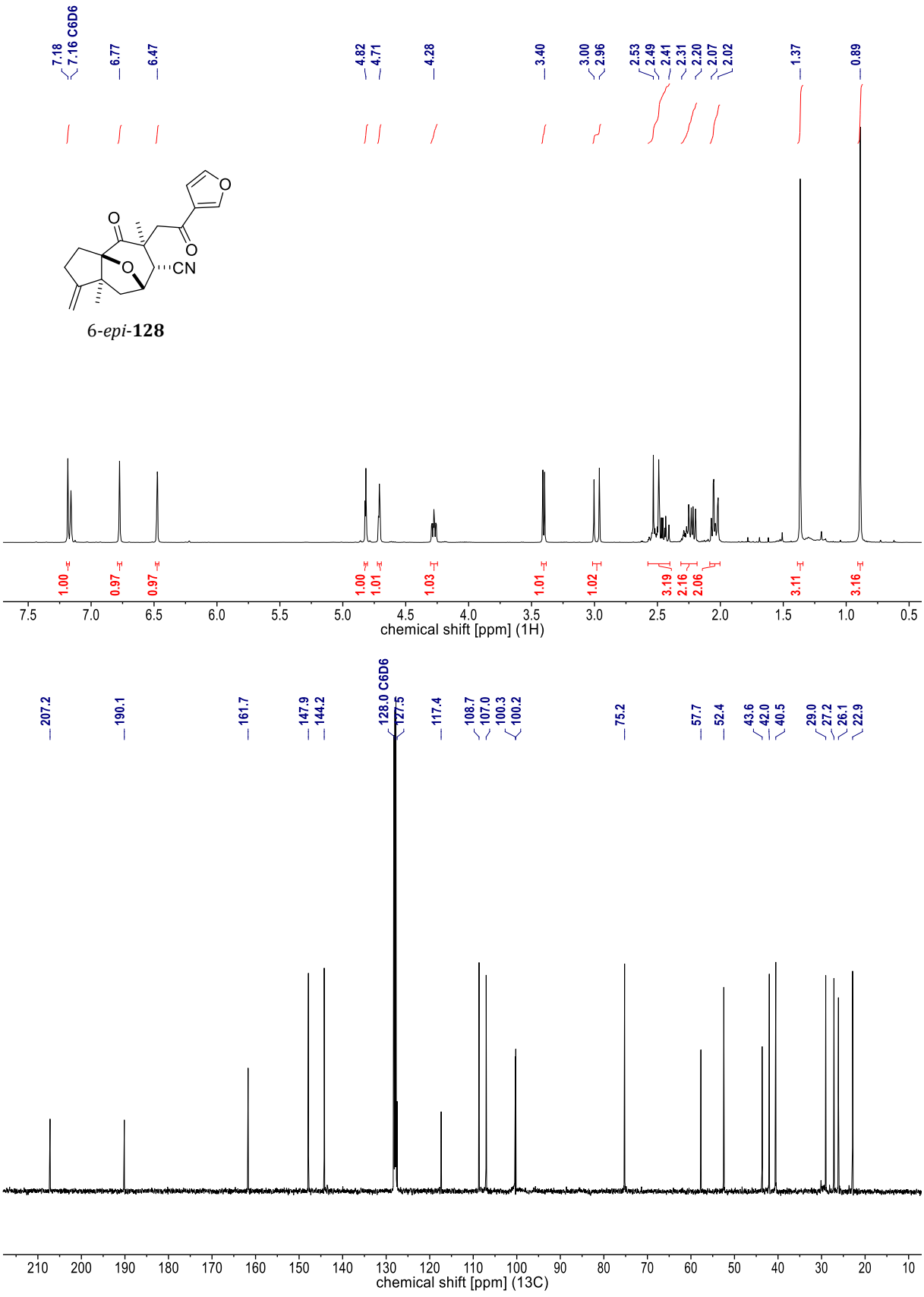

6-*epi*-**128**

Figure 147. NMR spectra of 6-*epi*-**128** [^{1}H (400 MHz, C_6D_6) & ^{13}C (101 MHz, C_6D_6)].

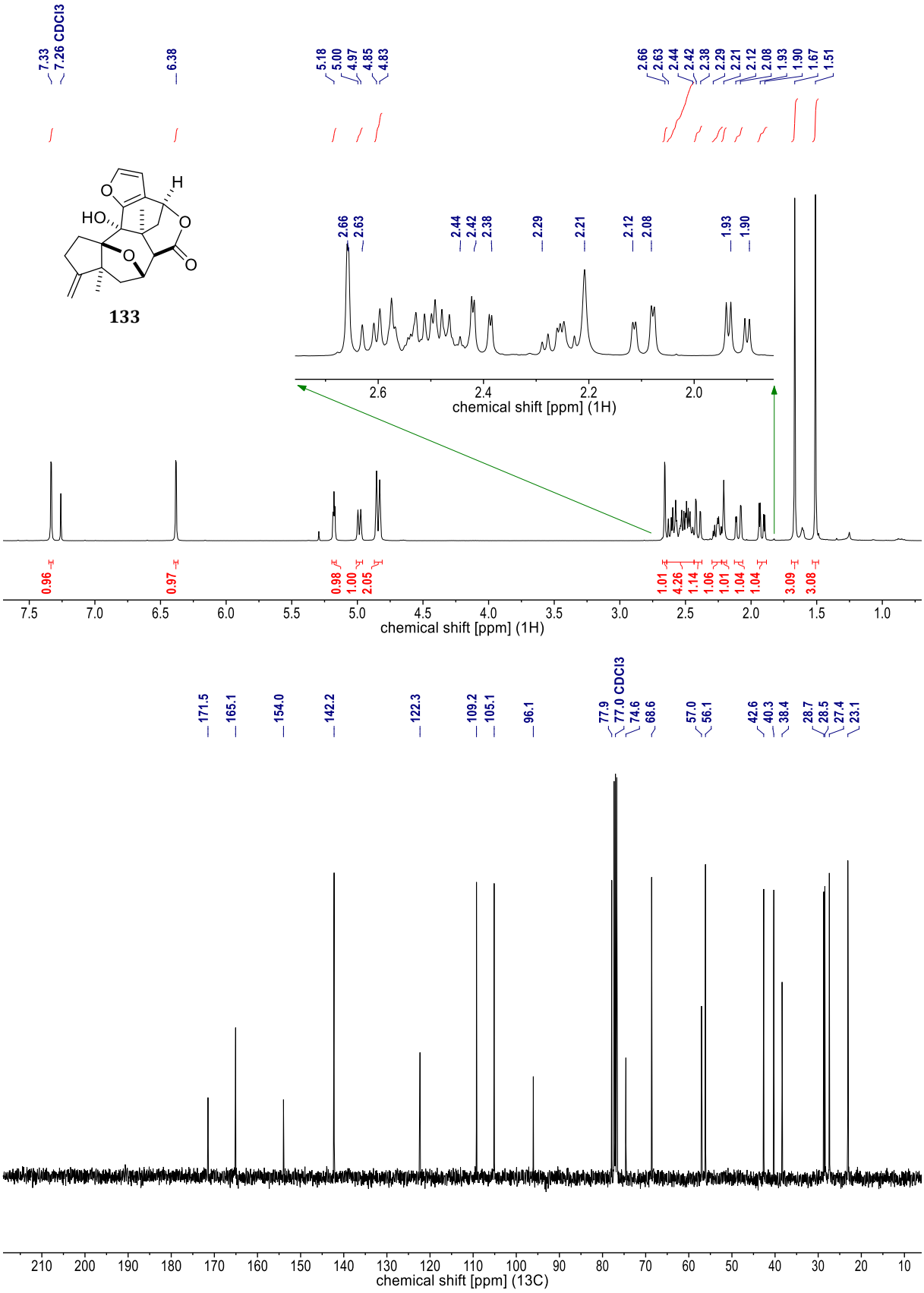

Figure 148. NMR spectra of **133** [^{1}H (400 MHz, $CDCl_3$) & ^{13}C (101 MHz, $CDCl_3$)].

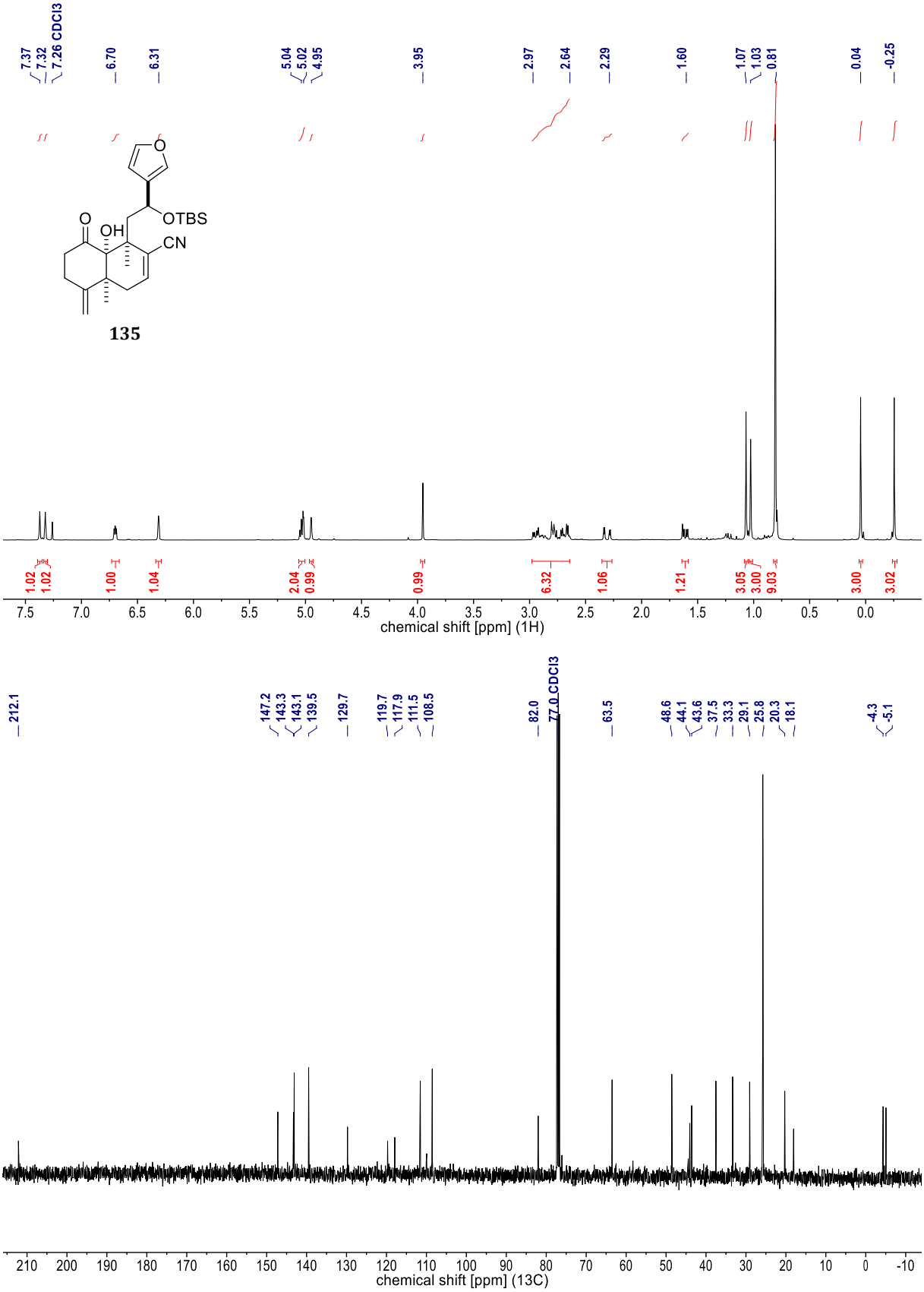

Figure 149. NMR spectra of **135** [^{1}H (400 MHz, $CDCl_3$) & ^{13}C (101 MHz, $CDCl_3$)].

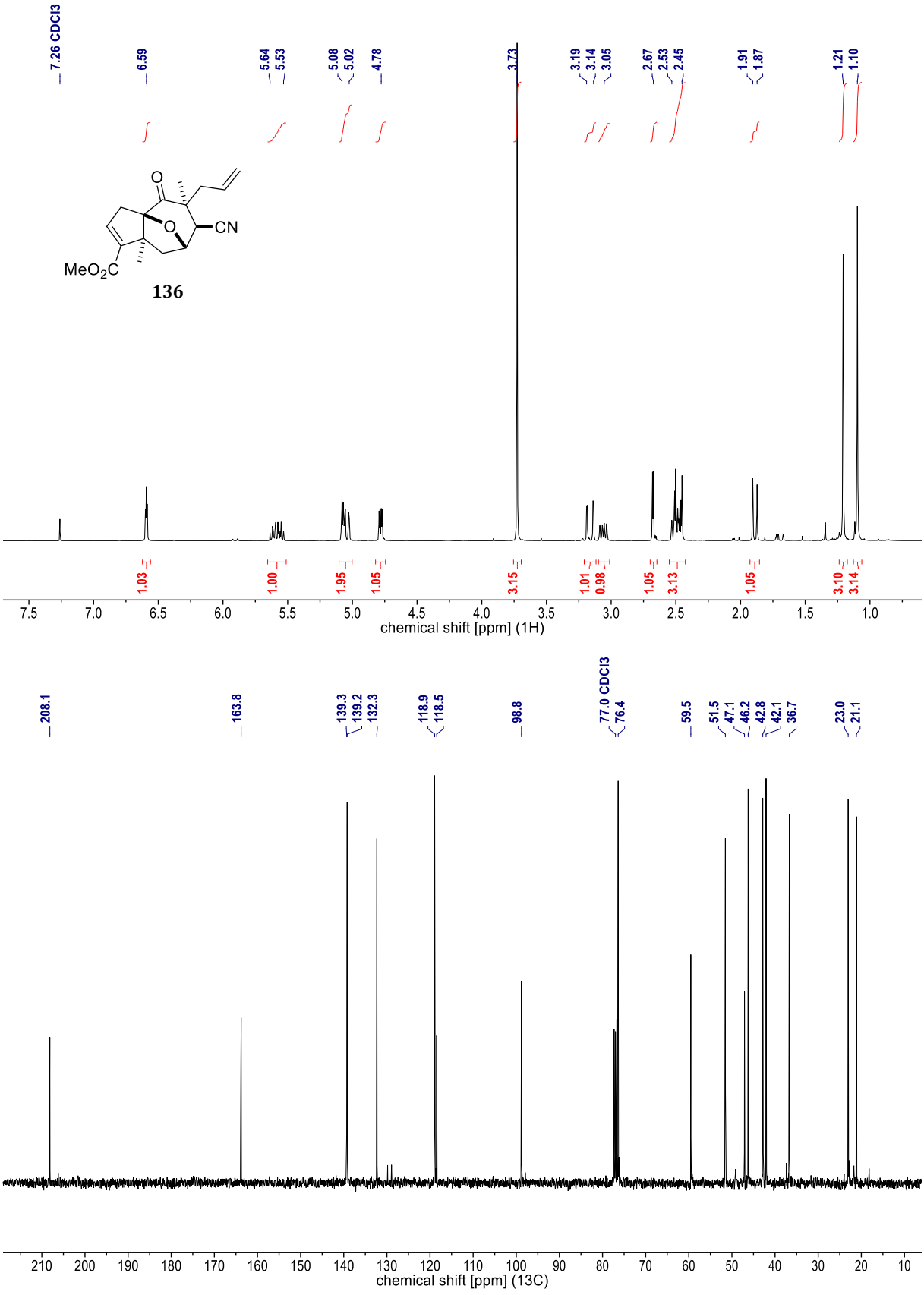

Figure 150. NMR spectra of **136** [^{1}H (400 MHz, $CDCl_3$) & ^{13}C (101 MHz, $CDCl_3$)].

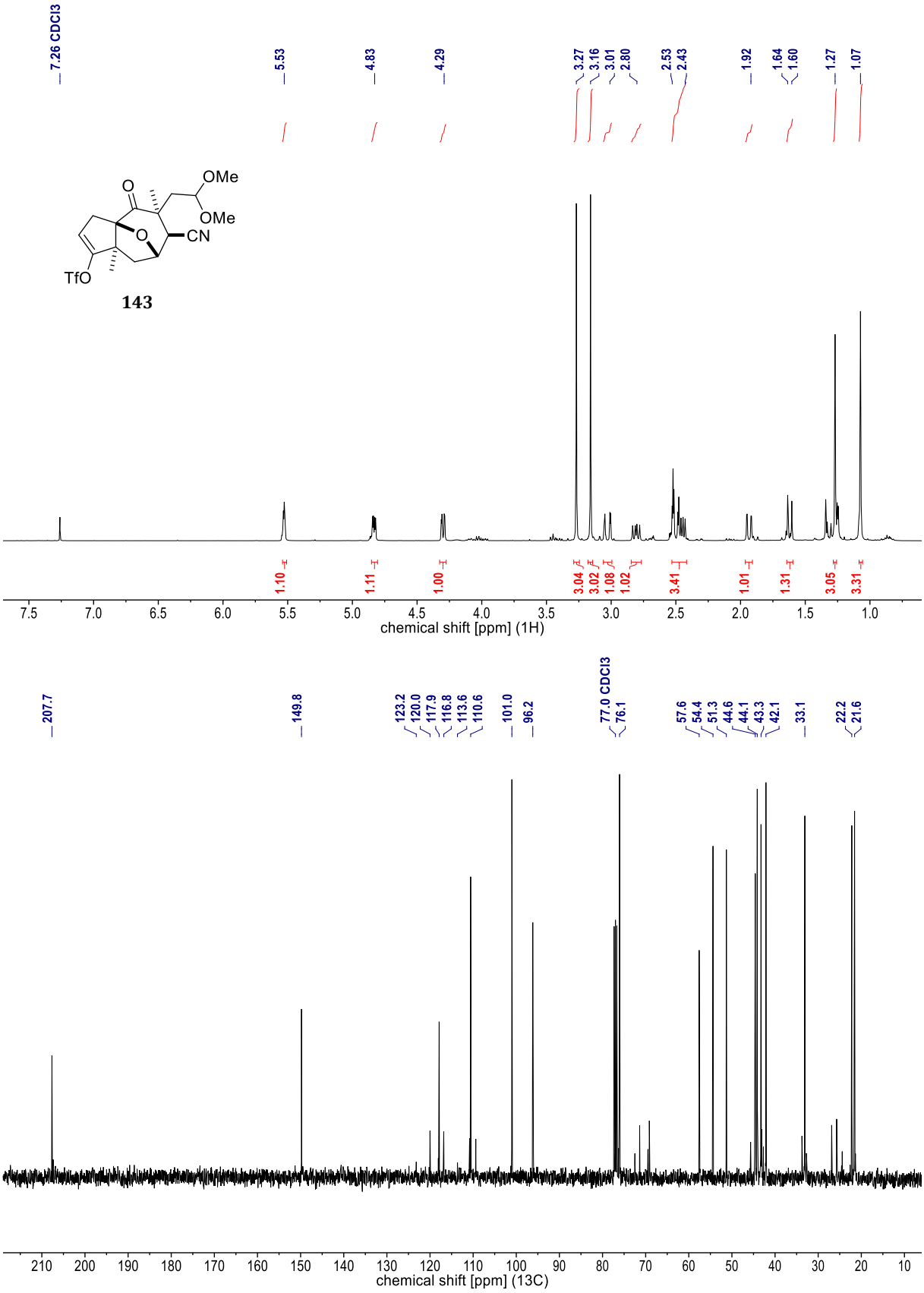

Figure 151. NMR spectra of **143** [^{1}H (400 MHz, $CDCl_3$) & ^{13}C (101 MHz, $CDCl_3$)].
The C-F coupling of the trifluoromethyl group is discernible (132.2, 120.02, 116.8 & 113.6 ppm).

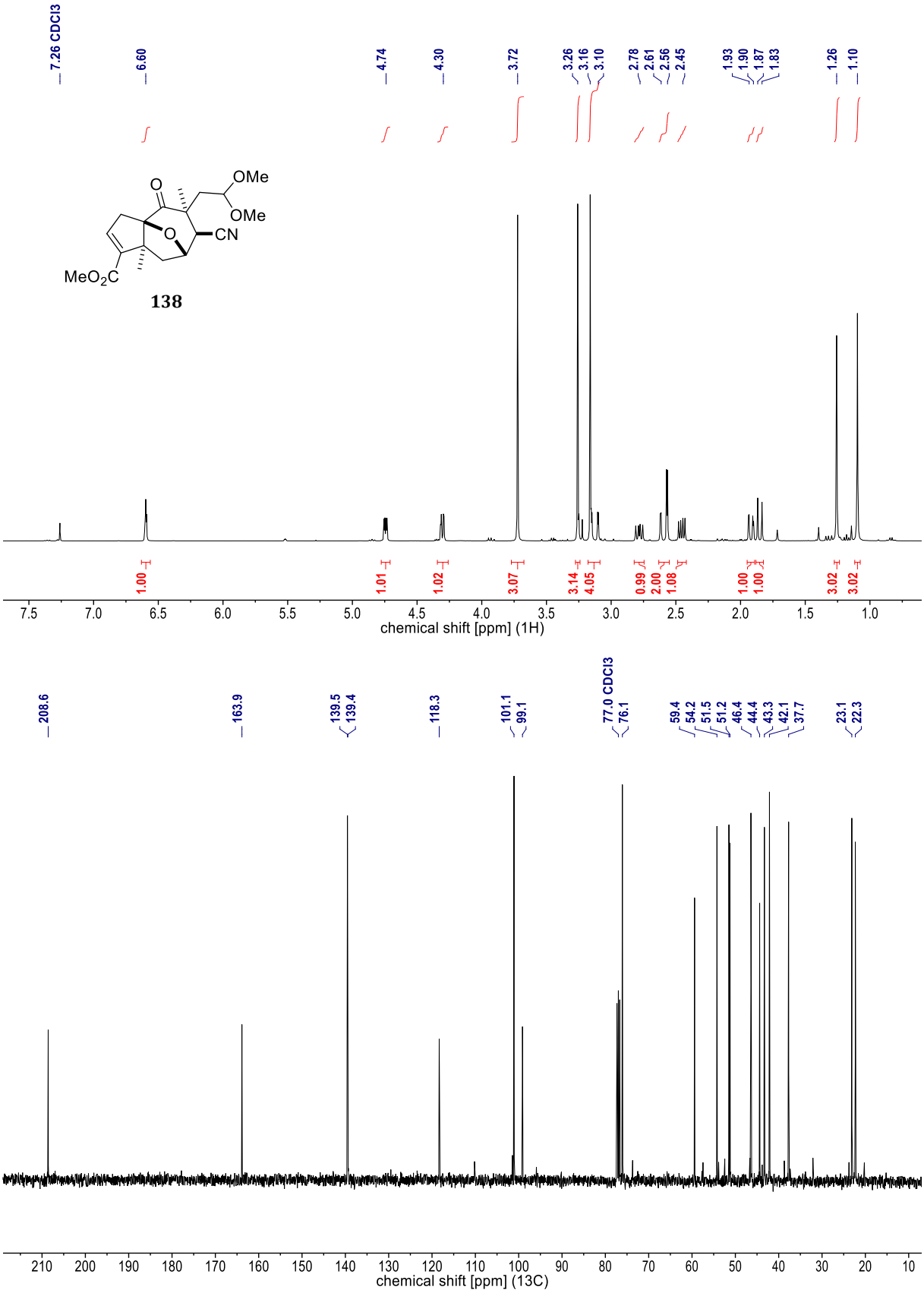

Figure 152. NMR spectra of **138** [^{1}H (400 MHz, $CDCl_3$) & ^{13}C (101 MHz, $CDCl_3$)].

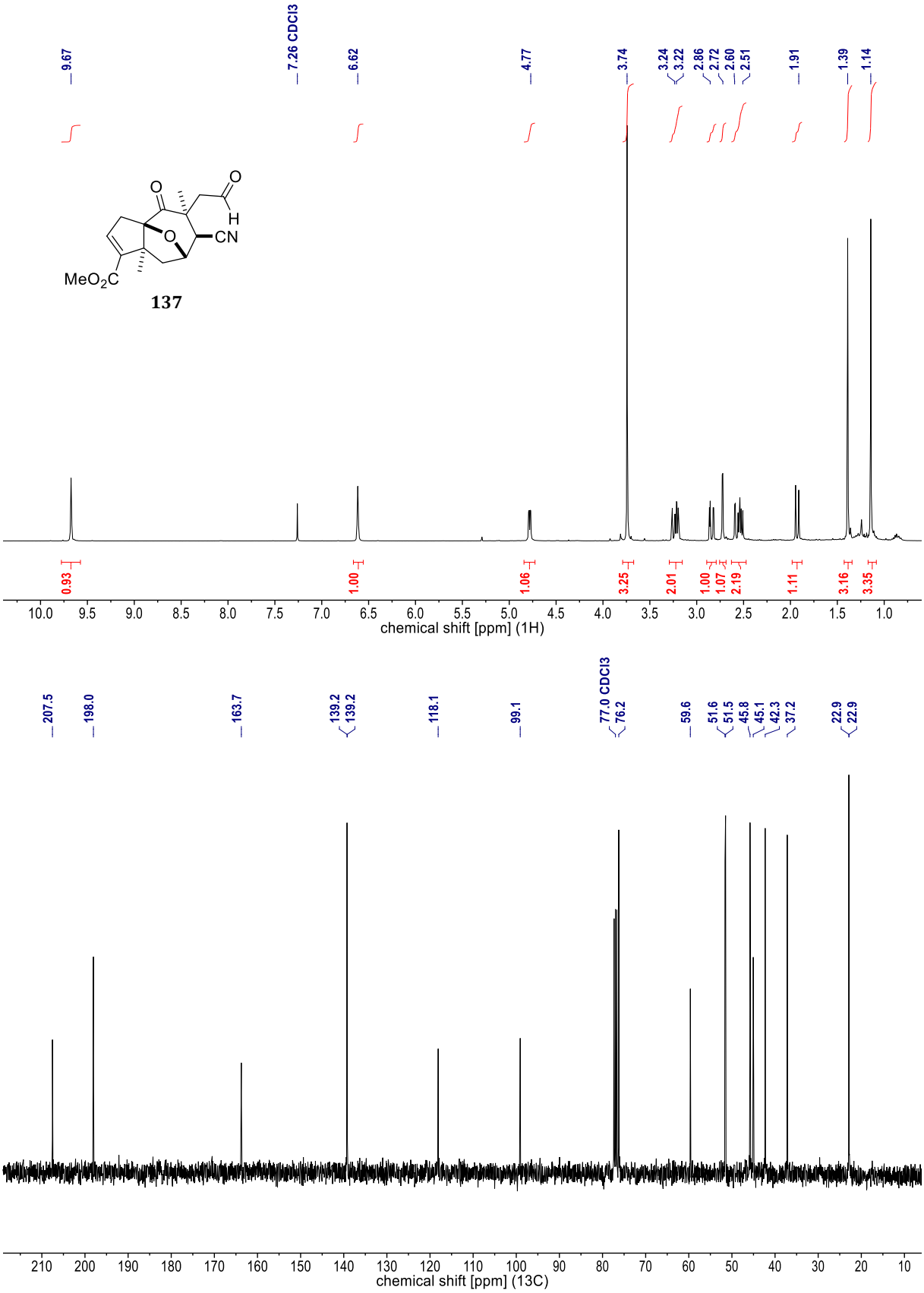

Figure 153. NMR spectra of **137** [^{1}H (400 MHz, $CDCl_3$) & ^{13}C (101 MHz, $CDCl_3$)].

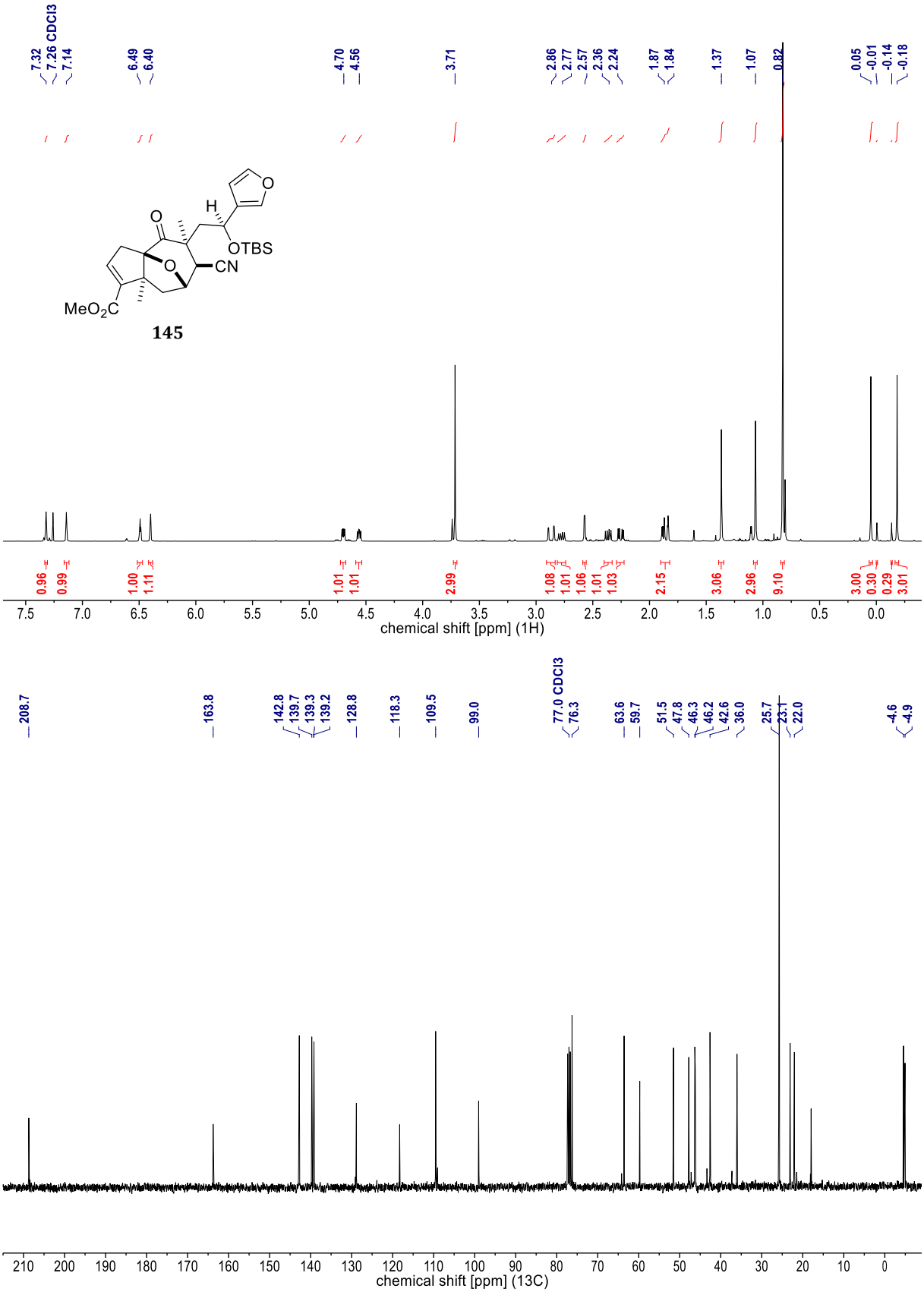

Figure 154. NMR spectra of **145** [^{1}H (400 MHz, $CDCl_3$) & ^{13}C (101 MHz, $CDCl_3$)].

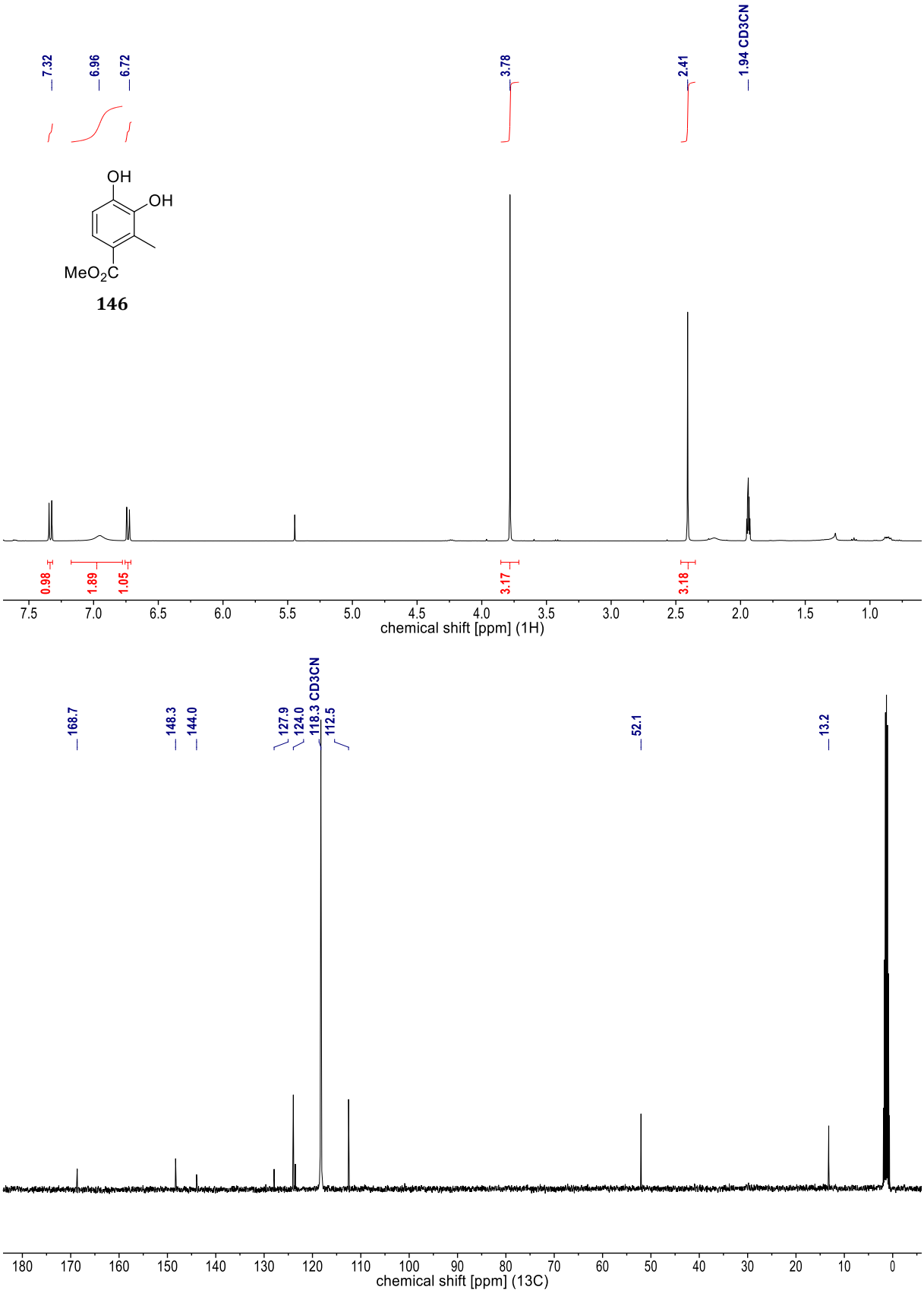

Figure 155. NMR spectra of **146** [^{1}H (400 MHz, CD_3CN) & ^{13}C (101 MHz, CD_3CN)].

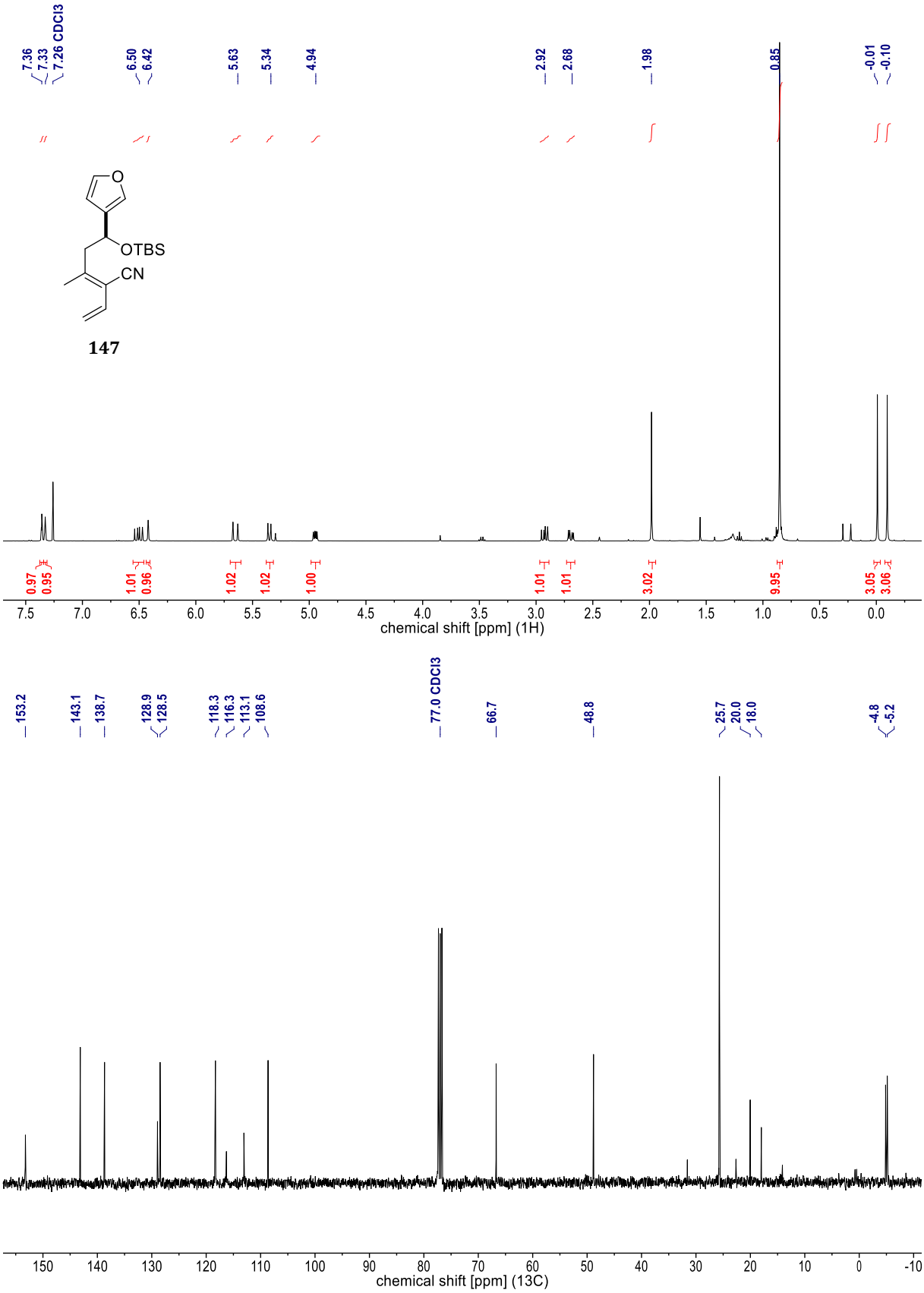

Figure 156. NMR spectra of **147** [^{1}H (400 MHz, $CDCl_3$) & ^{13}C (101 MHz, $CDCl_3$)].

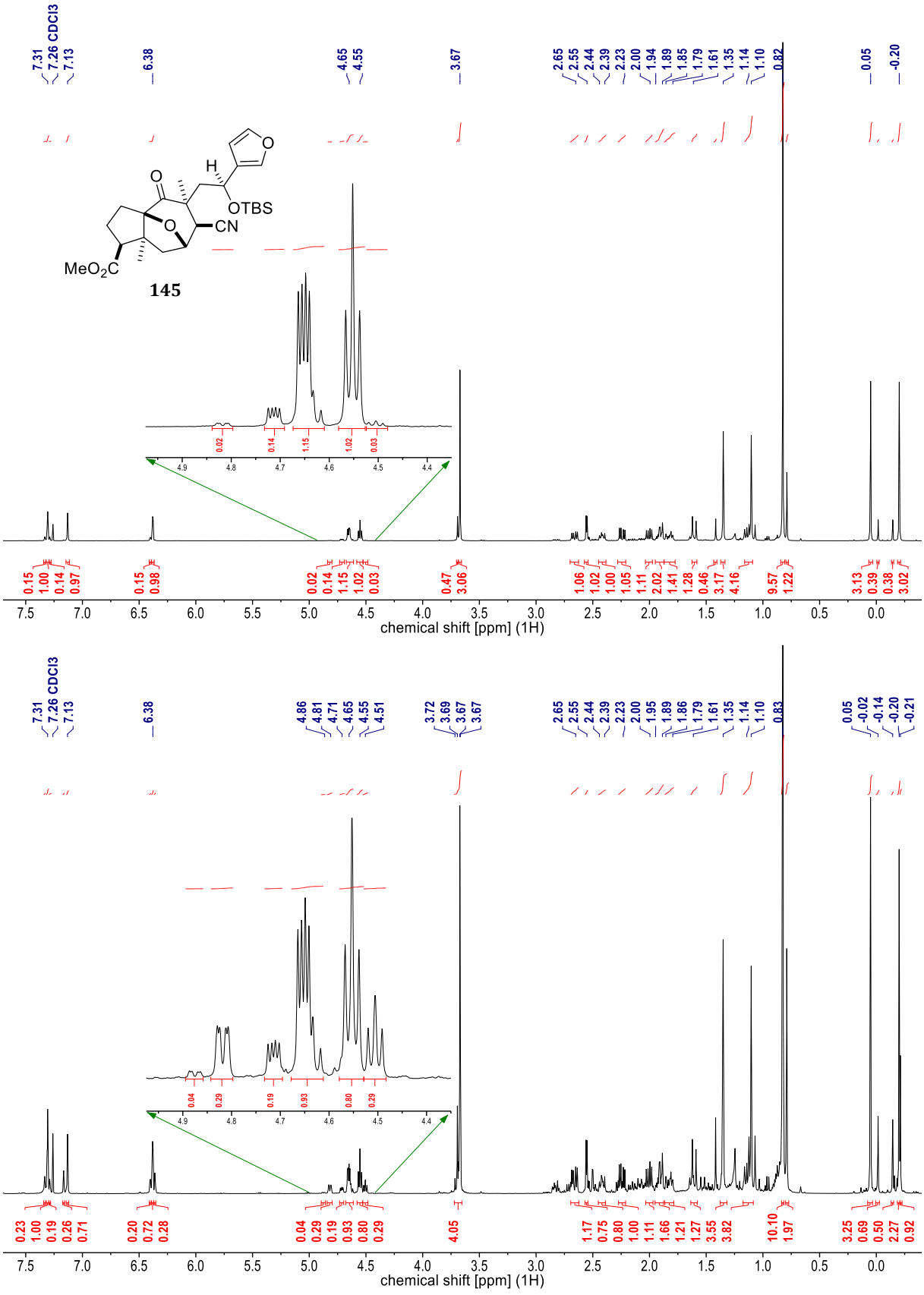

Figure 157. ^{1}H NMR spectra of **145** (400 MHz, $CDCl_3$).
Upper spectrum: *middle product fraction tubes*;
lower spectrum: *remaining product fraction tubes*.

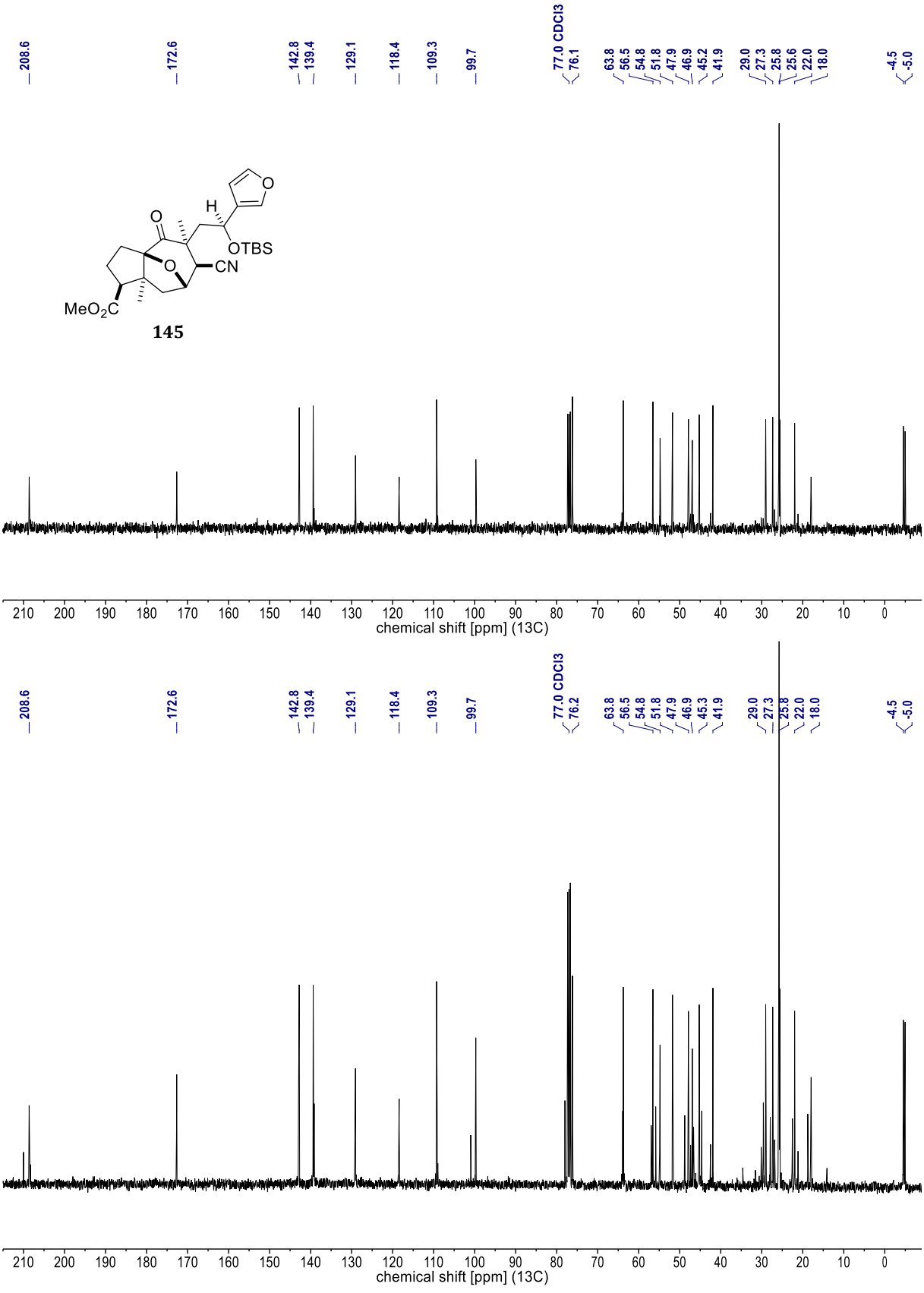

Figure 158. ^{13}C NMR spectra of **145** (101 MHz, $CDCl_3$).
Upper spectrum: *middle product fraction tubes*;
lower spectrum: *remaining product fraction tubes*.

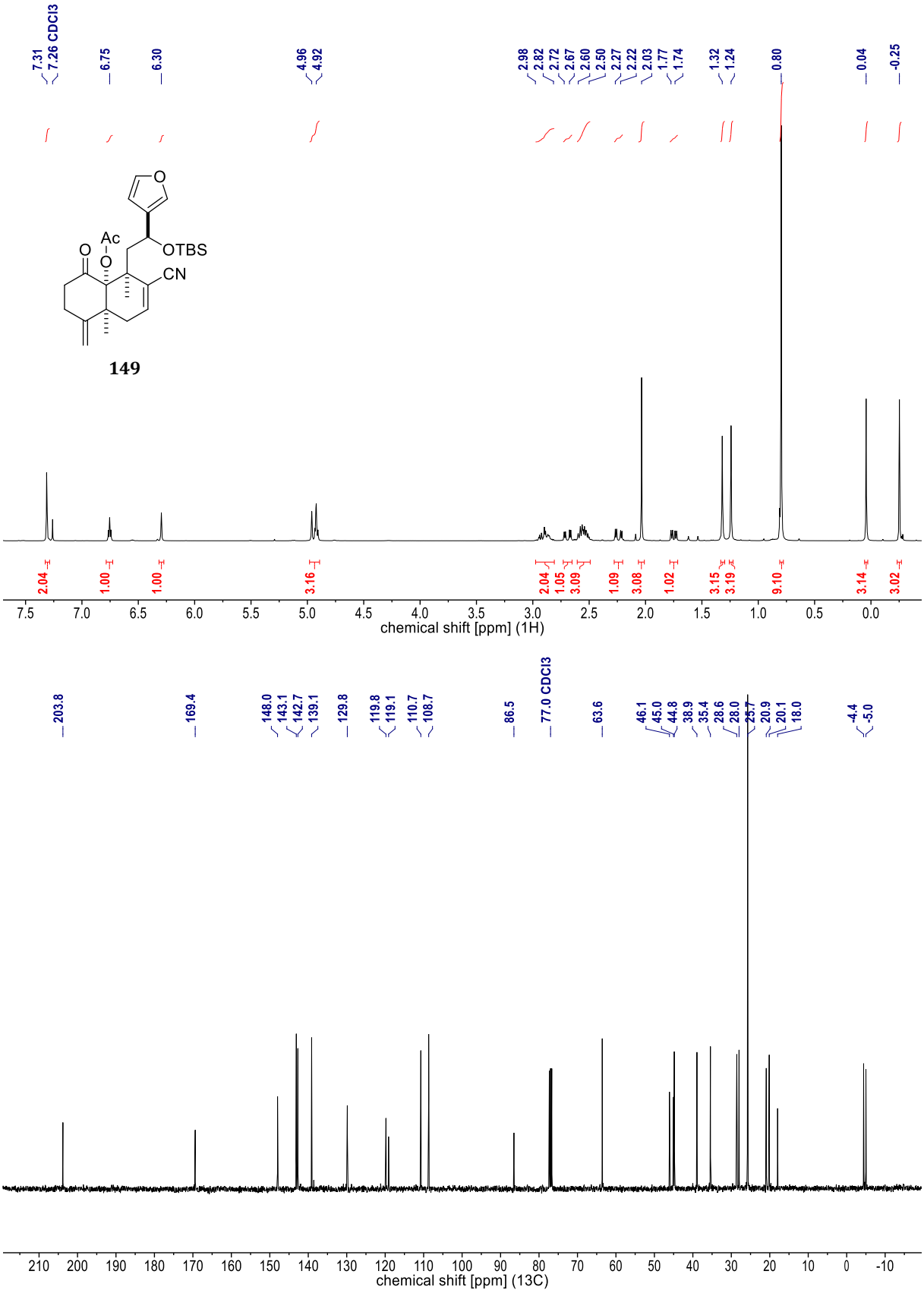

Figure 159. NMR spectra of **149** [^{1}H (400 MHz, $CDCl_3$) & ^{13}C (101 MHz, $CDCl_3$)].

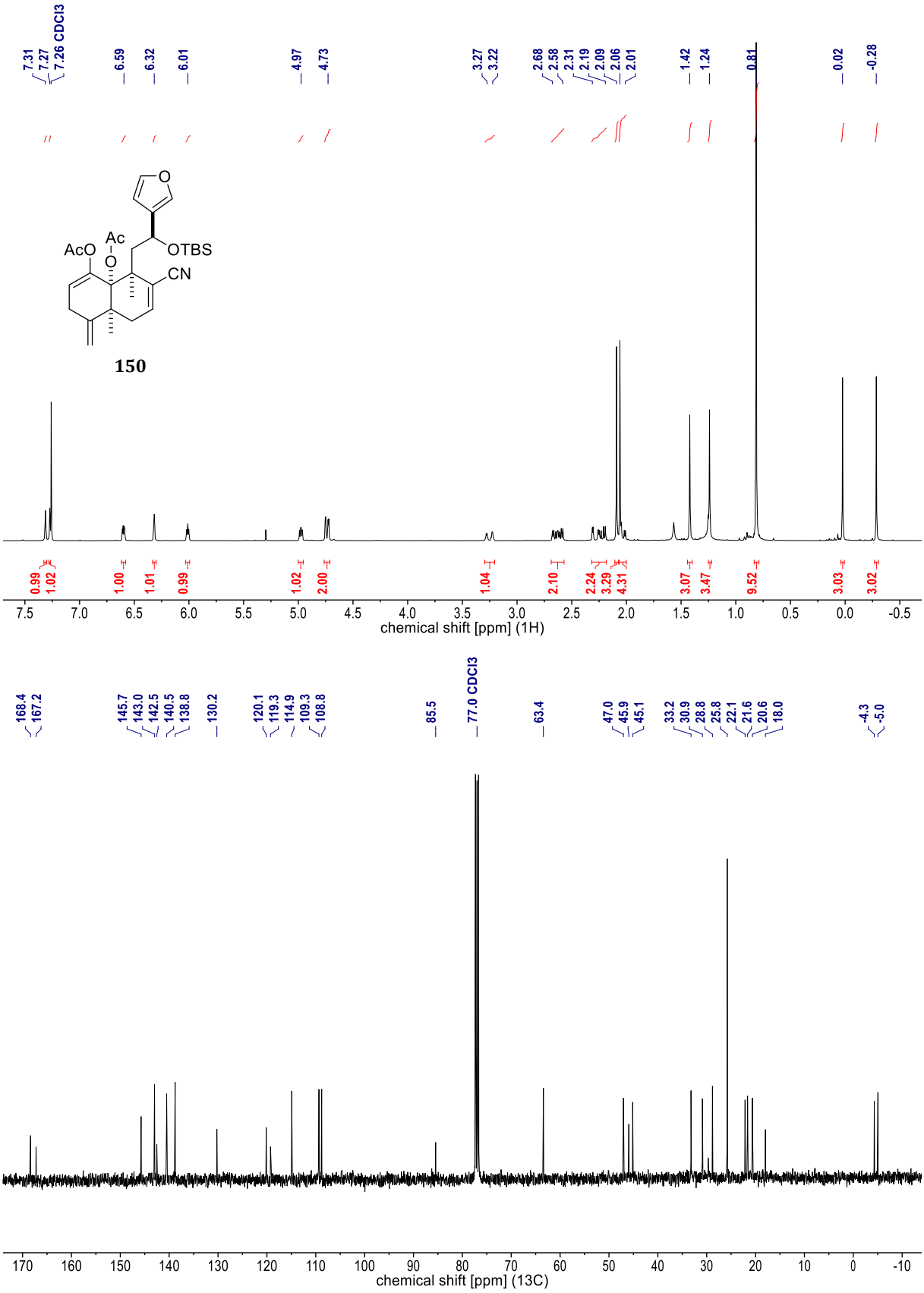

Figure 160. NMR spectra of **150** [^{1}H (400 MHz, $CDCl_3$) & ^{13}C (101 MHz, $CDCl_3$)].

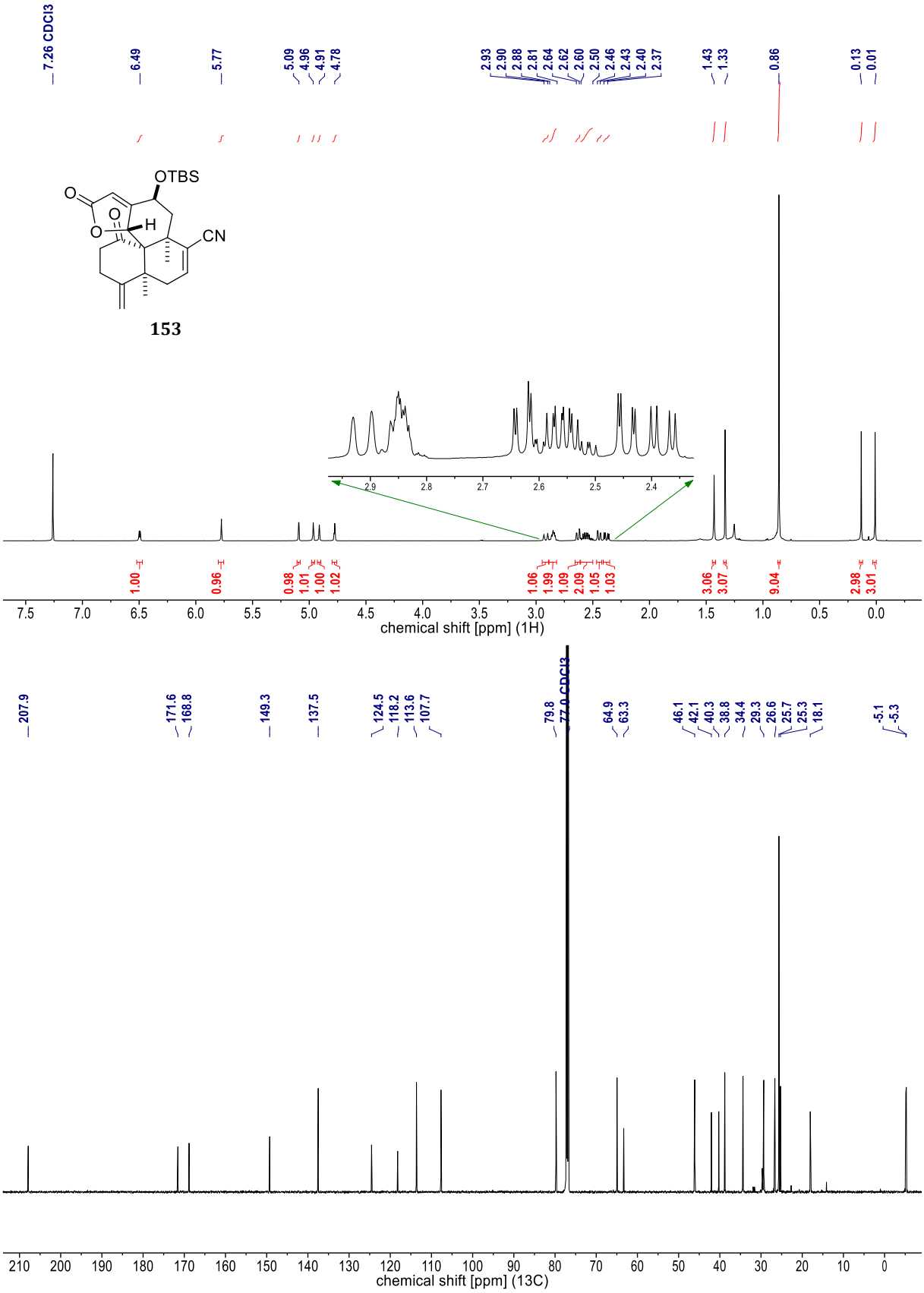

Figure 161. NMR spectra of **153** [^{1}H (600 MHz, $CDCl_3$) & ^{13}C (151 MHz, $CDCl_3$)].

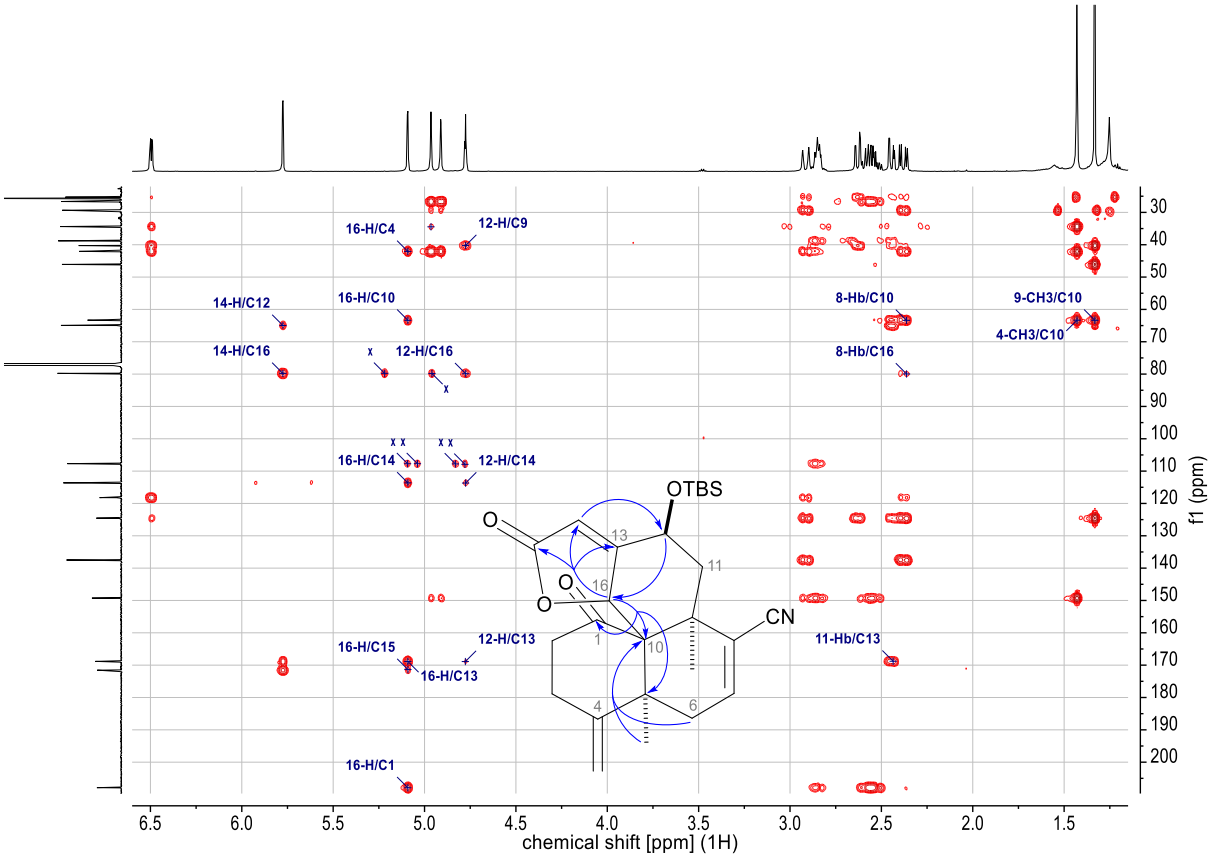

Figure 162. ^{1}H-^{13}C HMBC spectrum of **153** ($CDCl_3$, 600 MHz/151 MHz). Crucial HMBC correlations are shown as blue arrows in the structure and annotated in the spectrum. To prevent misinterpretation, some *one-bond artifacts* are annotated as 'x.'

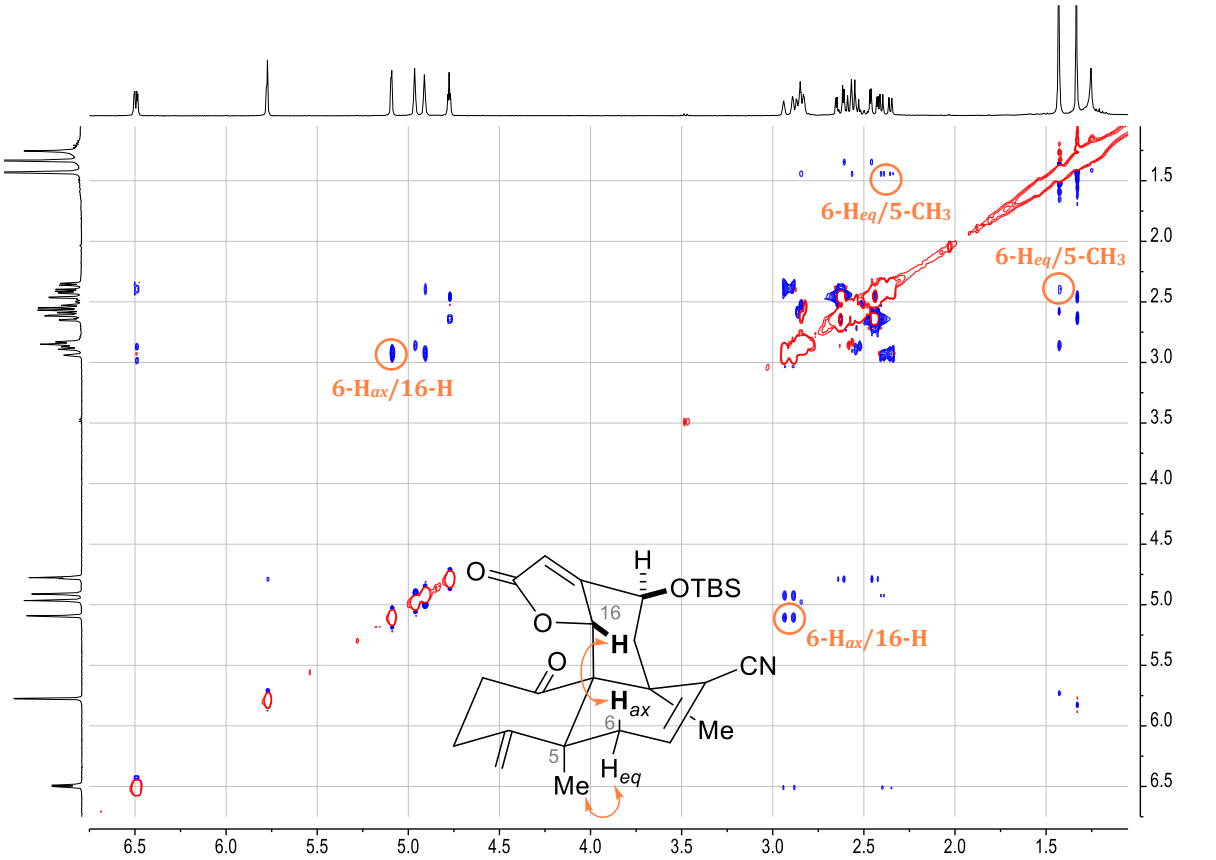

Figure 163. ^{1}H-^{1}H NOESY spectrum of **153** ($CDCl_3$, 400 MHz). The most revealing NOE signals are highlighted in orange. The structure was adapted to a *simplified all-chair system* in order to better represent the structural relations in the 'true' structure.

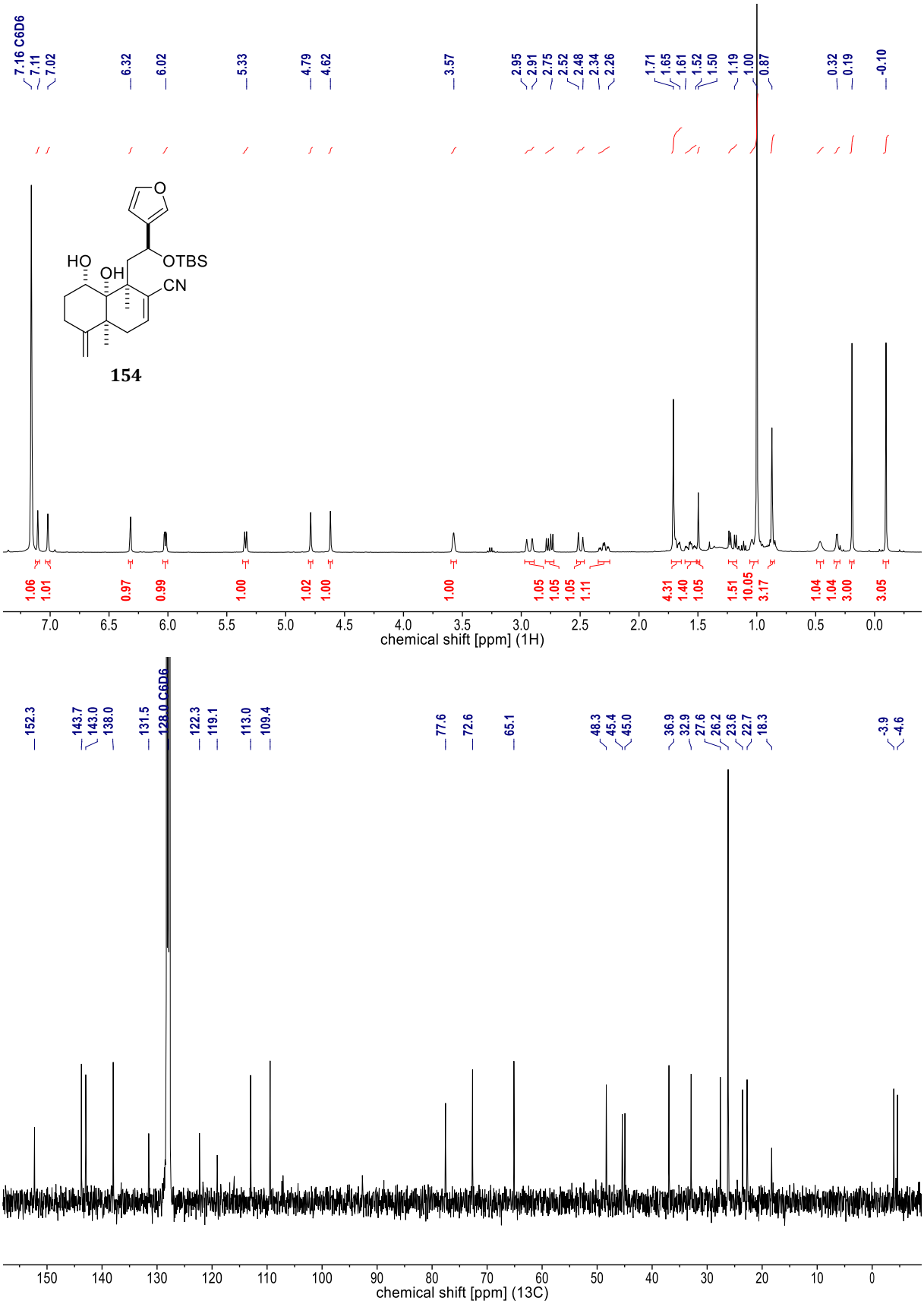

Figure 164. NMR spectra of **154** [^{1}H (400 MHz, C_6D_6) & ^{13}C (101 MHz, C_6D_6)].

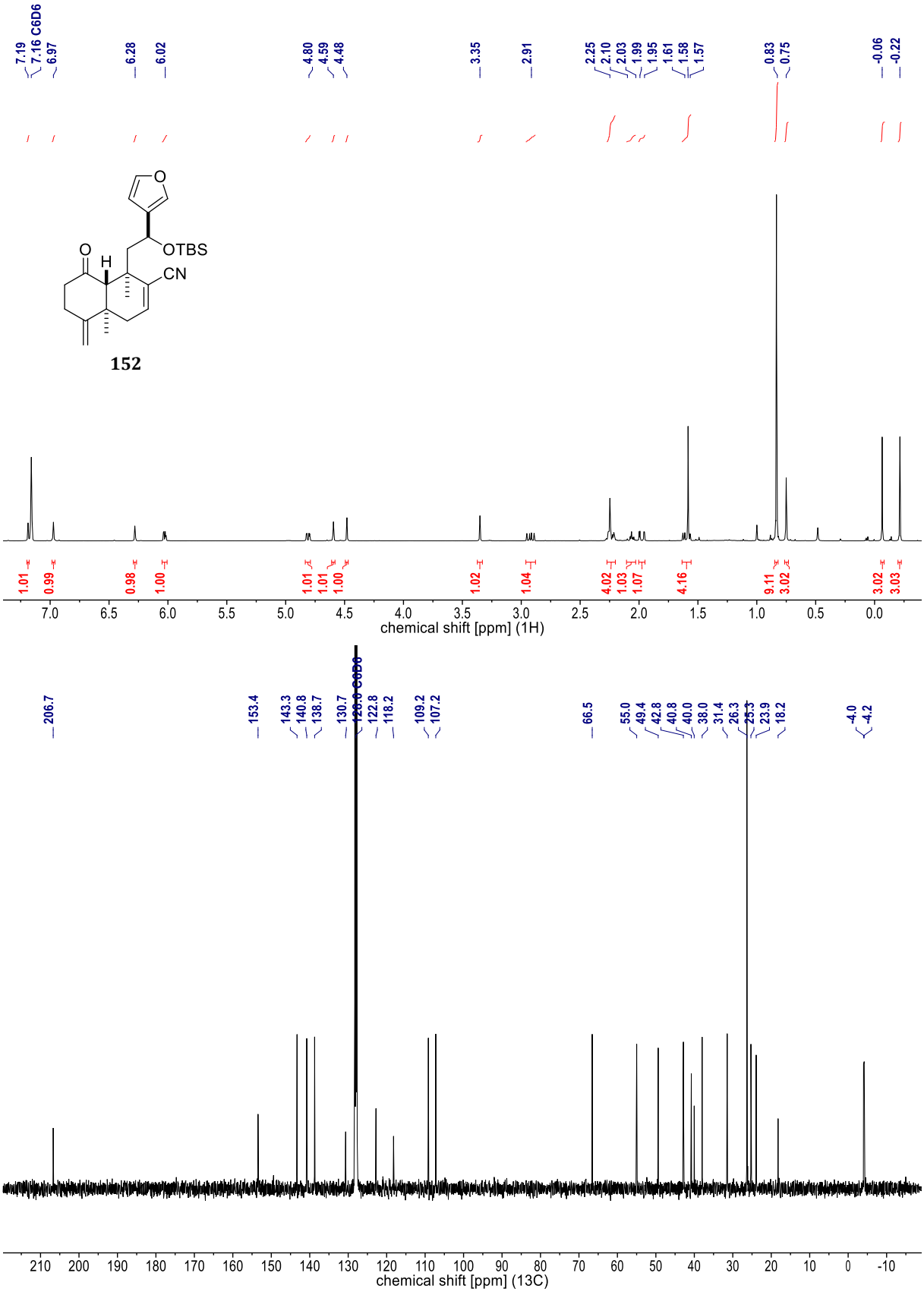

Figure 165. NMR spectra of **152** [^{1}H (400 MHz, C_6D_6) & ^{13}C (101 MHz, C_6D_6)].

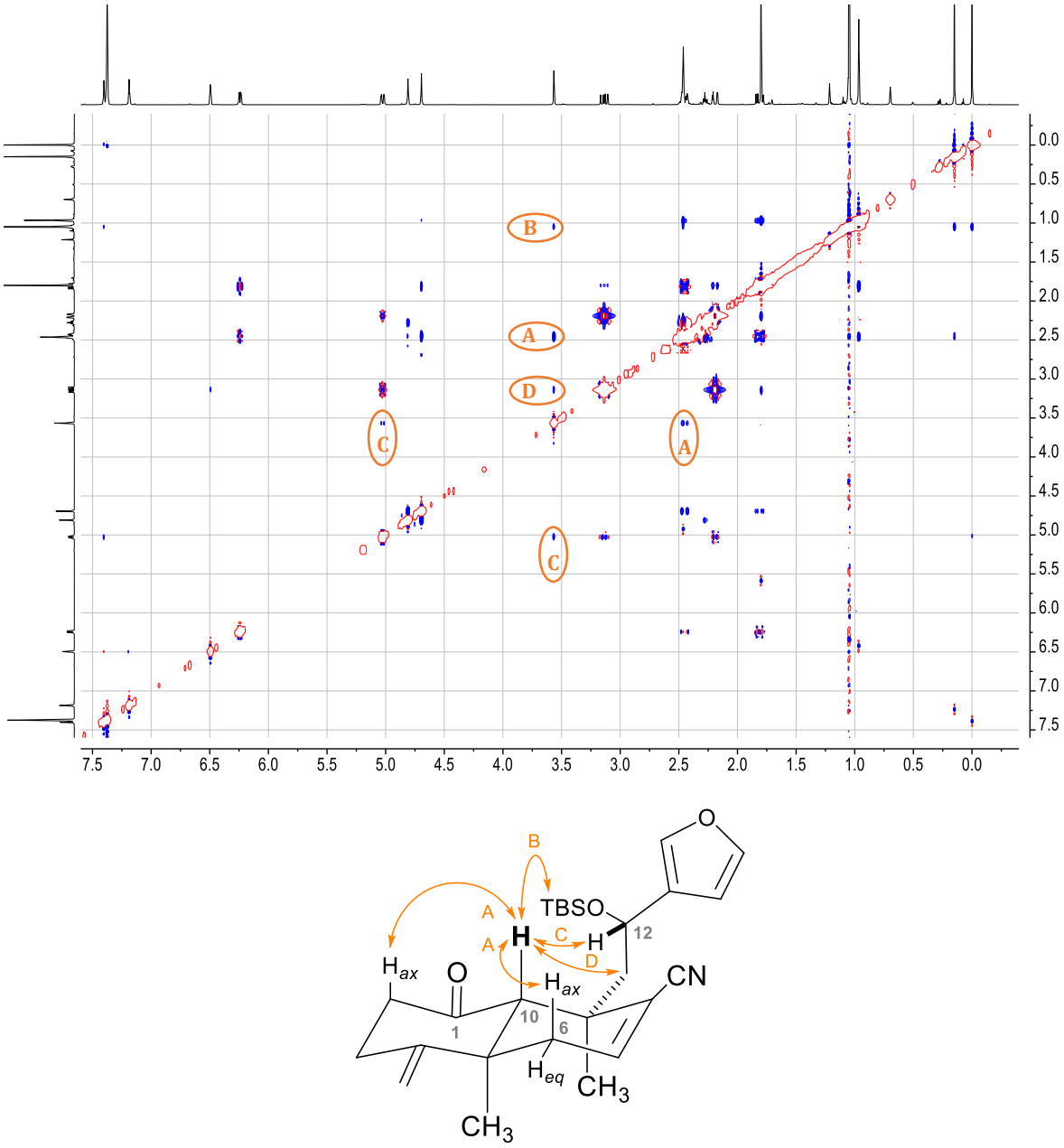

Figure 166. ^{1}H-^{1}H NOESY spectrum of **152** (C_6D_6, 400 MHz).

Crucial NOE signals are highlighted in orange in the spectrum and in the more appropriate (*but simplified*) structural depiction, which does not include potential effects of the sp^2-hybridized carbon centers on the decalone core. The expectedly low intensities of the NOE signals **B**, **C** and **D** necessitate lowering the intensity threshold to a level, at which *t1 noise* of the TBS group is rather pronounced.